NEW TECHNOLOGIES FOR WOMEN'S HEALTH

EDITED BY: Lana McClements, Vesna Garovic and Dunja Aksentijevic
PUBLISHED IN: Frontiers in Bioengineering and Biotechnology

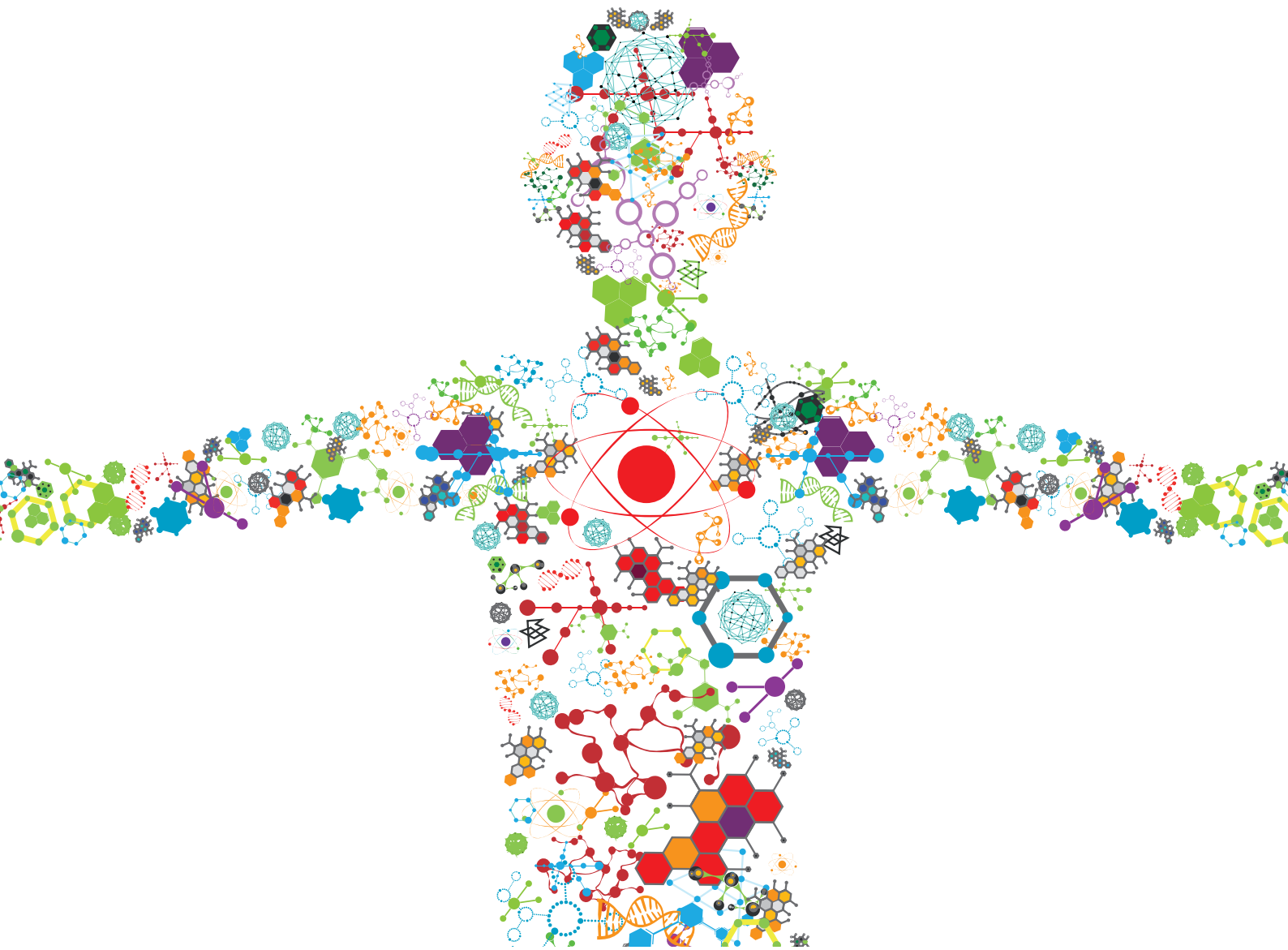

frontiers Research Topics

frontiers

ISSN 1664-8714
ISBN 978-2-88976-738-0
DOI 10.3389/978-2-88976-738-0

About Frontiers

Frontiers is more than just an open-access publisher of scholarly articles: it is a pioneering approach to the world of academia, radically improving the way scholarly research is managed. The grand vision of Frontiers is a world where all people have an equal opportunity to seek, share and generate knowledge. Frontiers provides immediate and permanent online open access to all its publications, but this alone is not enough to realize our grand goals.

Frontiers Journal Series

The Frontiers Journal Series is a multi-tier and interdisciplinary set of open-access, online journals, promising a paradigm shift from the current review, selection and dissemination processes in academic publishing. All Frontiers journals are driven by researchers for researchers; therefore, they constitute a service to the scholarly community. At the same time, the Frontiers Journal Series operates on a revolutionary invention, the tiered publishing system, initially addressing specific communities of scholars, and gradually climbing up to broader public understanding, thus serving the interests of the lay society, too.

Dedication to Quality

Each Frontiers article is a landmark of the highest quality, thanks to genuinely collaborative interactions between authors and review editors, who include some of the world's best academicians. Research must be certified by peers before entering a stream of knowledge that may eventually reach the public - and shape society; therefore, Frontiers only applies the most rigorous and unbiased reviews.
Frontiers revolutionizes research publishing by freely delivering the most outstanding research, evaluated with no bias from both the academic and social point of view. By applying the most advanced information technologies, Frontiers is catapulting scholarly publishing into a new generation.

What are Frontiers Research Topics?

Frontiers Research Topics are very popular trademarks of the Frontiers Journals Series: they are collections of at least ten articles, all centered on a particular subject. With their unique mix of varied contributions from Original Research to Review Articles, Frontiers Research Topics unify the most influential researchers, the latest key findings and historical advances in a hot research area! Find out more on how to host your own Frontiers Research Topic or contribute to one as an author by contacting the Frontiers Editorial Office: frontiersin.org/about/contact

NEW TECHNOLOGIES FOR WOMEN'S HEALTH

Topic Editors:
Lana McClements, University of Technology Sydney, Australia
Vesna Garovic, Mayo Clinic, United States
Dunja Aksentijevic, Queen Mary University of London, United Kingdom

Citation: McClements, L., Garovic, V., Aksentijevic, D., eds. (2022). New Technologies for Women's Health. Lausanne: Frontiers Media SA. doi: 10.3389/978-2-88976-738-0

Table of Contents

frontiers | Frontiers in Bioengineering and Biotechnology

EDITORIAL
published: 13 July 2022
doi: 10.3389/fbioe.2022.969389

Editorial: New Technologies for Women's Health

Lana McClements[1]*, *Dunja Aksentijevic*[2] and *Vesna Garovic*[3,4]

[1]School of Life Sciences, Faculty of Science, University of Technology Sydney, Sydney, NSW, Australia, [2]Centre for Biochemical Pharmacology, William Harvey Research Institute, Barts and the London School of Medicine and Dentistry, Queen Mary University of London, London, United Kingdom, [3]Division of Nephrology and Hypertension, Department of Internal Medicine, Mayo Clinic College of Medicine, Rochester, MN, United States, [4]Division of Nephrology and Hypertension, Department of Obstetrics and Gynaecology, Mayo Clinic College of Medicine, Rochester, MN, United States

Keywords: women's health, preeclampsia, ovarian cancer, pregnancy, 3D bio printing, biomarkers, miRNA, placenta

Editorial on the Research Topic

New Technologies for Women's Health

INTRODUCTION

Over the last decade, sex differences have been widely explored and have demonstrated the importance of understanding women's and men's health in the context of population health as a whole. These differences start *in-utero*, where male foetuses are larger by the second semester, whilst maternal immune response is stronger towards a male foetus creating a more pronounced pro-inflammatory environment compared to a female foetus. Male foetuses are also at higher risk of infection that can lead to premature birth (Inkster et al., 2021). In this Research Topic "*New Technologies for Women's Health*," we focused on emerging technologies and discoveries specific to women's health that includes eleven articles divided into four themes: ovarian cancer (2), pregnancy (4), preeclampsia (3) and digital technologies (2).

Ovarian Cancer (2)

Two articles have been published related to ovarian cancer research. One describes innovative three D (3D) cellular technologies for modelling of ovarian cancer, which can be used to accelerate discovery towards implementation of personalized medicine Yee et al. Ovarian cancer is a heterogenous disease with different subtypes, some of them, such as high grade serous ovarian cancer, poorly responding to currently available therapies. 3D modelling systems of ovarian cancer can recapitulate cell-cell and cell-microenvironment interactions better than 2D, hence improving chances of successful translation of emerging treatments and improving responses of particular ovarian cancer subtypes to available therapies. The second article Hossain et al. outlines novel approaches to biomarker discovery for early diagnosis of ovarian cancer, which is an area of unmet clinical need. Potential candidates were discussed including circulating miRNA and cell-free DNA (cf-DNA), exosomes, and Chloride Intracellular Ion Channels (CLIC) family of proteins.

Pregnancy-Related Research and Technologies (4)

This sub-theme covers a wide range of research during pregnancy. For example, Bertini et al. is a systematic review of machine learning approaches for prediction of complications in pregnancy. The data collection methods included electronic medical records, medical images, biological markers, and to a lesser extent, sensors and foetal heart rate. They concluded that the machine learning approach

OPEN ACCESS

Edited and reviewed by:
Andrea Banfi,
University of Basel, Switzerland

***Correspondence:**
Lana McClements
lana.mcclements@uts.edu.au

Specialty section:
This article was submitted to Preclinical Cell and Gene Therapy, a section of the journal Frontiers in Bioengineering and Biotechnology

Received: *14 June 2022*
Accepted: *22 June 2022*
Published: *13 July 2022*

Citation:
McClements L, Aksentijevic D and Garovic V (2022) Editorial: New Technologies for Women's Health. Front. Bioeng. Biotechnol. 10:969389. doi: 10.3389/fbioe.2022.969389

was the most effective when using medical images for prediction of preterm birth and neonatal mortality.

Ghamrawi et al. compared methylation status in pregnancy using buffy coat DNA vs. DNA isolated from polymorphonuclear (PMN) and lymphocytic fractions obtained within 24 h prior to delivery from 29 normotensive pregnant women. Their study determined that buffy coat DNA rather than lymphocytic DNA is more representative of methylation patterns in white blood cells during normal pregnancy.

A retrospective cohort study reported on the effectiveness of fetoscopic laser coagulation in ameliorating the metabolomic alteration caused by twin-twin transfusion syndrome in placental tissue and cord plasma Liu et al. They also state that these altered metabolites are involved mainly in fatty acid and lipid-like molecule metabolism and that certain lipids and lipid-like molecules are correlated with neonatal birth weight or ejection fraction.

Novel therapeutic strategies involving an anti-oxidant and anti-inflammatory agent, dendrimer-based N-acetyl cysteine (DNAC), were evaluated in Liu et al. in terms of its ability to ameliorate placental inflammation, as a key cause of preterm birth and post-pregnancy adverse health consequences. The results of this *in vivo* study demonstrated that DNAC reduced the M1 pro-inflammatory macrophage cell subpopulation whilst increasing M2 anti-inflammatory macrophages, hence improving the placental immune profile in the intrauterine inflammation model.

Preeclampsia (3)

Preeclampsia is the leading cause of mortality and morbidity in pregnancy, yet currently this pregnancy-specific hypertensive disorder does not have a cure (Thornton et al., 2013). Better understanding of the pathogenic mechanisms leading to preeclampsia, particularly those affecting placental health, is key to developing better management strategies for preeclampsia. In this meta-analysis, Cirkovic et al. using publically available data, a number of placental miRNAs were identified as having the most promising role in the pathogenesis of preeclampsia. These included placental miRNA-16, miRNA-20b, miRNA-23a, miRNA-29b, miRNA-155 and miRNA-210, miRNA-376c, and peripheral blood miRNA-155 and miRNA-16; the vast majority of these were increased except for miRNA-376c and miRNA-16, which were found to be decreased in preeclampsia.

On the other hand, another study Freimane et al. performed a systematic review that identified the most promising biomarker candidates for early pregnancy prediction of preeclampsia risk in women with type 1 diabetes mellitus (T1DM). Pregnant women with T1DM have a four-fold increased risk of developing preeclampsia (Weissgerber and Mudd, 2015). This important review discussed 32 biomarkers, suggesting that first trimester HbA1c, urinary albumin, neutrophil gelatinase-associated lipocalin and adipokines likely have the best potential for prediction of preeclampsia in women with T1DM. These biomarkers are reflective of glycaemic control, insulin resistance and renal function.

Given that there are no effective treatments for preeclampsia, the research community has been focused on developing potential therapeutic strategies. In this review Murray et al. discussed an immunomodulatory treatment strategy that targets the $CD4^+$ T cell mechanism. This mechanism-based approach associated with preeclampsia targets placental inflammation (Aneman et al., 2020), which, if ameliorated, could improve spiral artery invasion, placentation, and maternal tolerance.

Digital Technologies for Women's Health (2)

Digital health and remote monitoring technologies are rapidly emerging for women's health application and could be useful particularly for high-risk pregnancies requiring close surveillance. One such application includes the management of gestational diabetes mellitus, which affects around 1 in 8 pregnant women (Hod et al., 2015). This systematic review Bertini et al. outlines the benefits of remote monitoring technologies including: improved glycaemic control, increased satisfaction and acceptability, maternal confidence, decreased gestational weight gain, knowledge of gestational diabetes mellitus, and improved medical team time management.

An article Hurst B. S. et al. in our Research Topic also reported the accuracy of a novel skin-worn sensor and its associated algorithm in determining the fertile window and absence of ovulation in 80 women. This innovative skin-sensor was compared directly to a vaginal sensor and its algorithm, showing that it could be a useful tool for women with ovarian dysfunction who are trying to conceive.

CONCLUSION

In summary, this Research Topic on "*New Technologies for Women's Health*" presents articles on different types of conditions affecting women, from challenges with conception to pregnancy complications and ovarian cancer. These articles describe breakthrough science and innovative technologies that could improve the health of women globally.

AUTHOR CONTRIBUTIONS

LM wrote the manuscript. DA and VG edited the manuscript. All authors read and approved the final version.

REFERENCES

Aneman, I., Pienaar, D., Suvakov, S., Simic, T. P., Garovic, V. D., and McClements, L. (2020). Mechanisms of Key Innate Immune Cells in Early- and Late-Onset Preeclampsia. *Front. Immunol.* 11, 1864. Front Immunol [Internet]Available from: https://www.frontiersin.org/article/10.3389/fimmu.2020.01864/full. doi:10.3389/fimmu.2020.01864

Hod, M., Kapur, A., Sacks, D. A., Hadar, E., Agarwal, M., Di Renzo, G. C., et al. (2015). The International Federation of Gynecology and Obstetrics (FIGO)

Initiative on Gestational Diabetes Mellitus: A Pragmatic Guide for Diagnosis, Management, and Care. *Int. J. Gynaecol. Obstet.* [Internet][cited 2017 Aug 21]; 131 Suppl 3:S173-211. Available from: http://doi.wiley.com/10.1016/S0020-7292(15)30007-2.

Inkster, A. M., Fernández-Boyano, I., and Robinson, W. P. (2021). Sex Differences Are Here to Stay: Relevance to Prenatal Care. *Jcm* 10 (13), 3000. Available from: https://www.mdpi.com/2077-0383/10/13/3000. doi:10.3390/jcm10133000

Thornton, C., Dahlen, H., Korda, A., and Hennessy, A. (2013). The Incidence of Preeclampsia and Eclampsia and Associated Maternal Mortality in Australia from Population-Linked Datasets: 2000-2008. *Am. J. Obstet. Gynecol.* 208 (6), 476.e1–5. Available from: https://linkinghub.elsevier.com/retrieve/pii/S0002937813002378. doi:10.1016/j.ajog.2013.02.042

Weissgerber, T. L., and Mudd, L. M. (2015). Preeclampsia and Diabetes, [Internet]. *Curr. Diab Rep.* 15 (3), 9. Available from: http://www.ncbi.nlm.nih.gov/pubmed/25644816. doi:10.1007/s11892-015-0579-4

Conflict of Interest: The authors declare that the research was conducted in the absence of any commercial or financial relationships that could be construed as a potential conflict of interest.

frontiers in Bioengineering and Biotechnology

SYSTEMATIC REVIEW
published: 24 December 2021
doi: 10.3389/fbioe.2021.782845

Preeclamptic Women Have Disrupted Placental microRNA Expression at the Time of Preeclampsia Diagnosis: Meta-Analysis

Andja Cirkovic[1†], Dejana Stanisavljevic[1†], Jelena Milin-Lazovic[1], Nina Rajovic[1], Vedrana Pavlovic[1], Ognjen Milicevic[1], Marko Savic[1], Jelena Kostic Peric[2], Natasa Aleksic[3], Nikola Milic[4], Tamara Stanisavljevic[4], Zeljko Mikovic[5], Vesna Garovic[6] and Natasa Milic[1,6]*

[1]Institute for Medical Statistics and Informatics, Faculty of Medicine, University of Belgrade, Belgrade, Serbia, [2]Institute of Molecular Genetics and Genetic Engineering, University of Belgrade, Belgrade, Serbia, [3]Center for Molecular Biology, University of Vienna, Vienna, Austria, [4]Faculty of Medicine, University of Belgrade, Belgrade, Serbia, [5]Clinic for Gynecology and Obstetrics Narodni Front, Belgrade, Serbia, [6]Division of Nephrology and Hypertension, Mayo Clinic, Rochester, MN, United States

OPEN ACCESS

Edited by:
Umberto Galderisi,
University of Campania Luigi Vanvitelli, Italy

Reviewed by:
Liv Cecilie Vestrheim Thomsen,
University of Bergen, Norway
Martin Mueller,
University Hospital Bern, Switzerland

***Correspondence:**
Vesna Garovic
garovic.vesna@mayo.edu

[†]These authors share first authorship

Specialty section:
This article was submitted to Preclinical Cell and Gene Therapy, a section of the journal Frontiers in Bioengineering and Biotechnology

Received: 24 September 2021
Accepted: 22 November 2021
Published: 24 December 2021

Citation:
Cirkovic A, Stanisavljevic D, Milin-Lazovic J, Rajovic N, Pavlovic V, Milicevic O, Savic M, Kostic Peric J, Aleksic N, Milic N, Stanisavljevic T, Mikovic Z, Garovic V and Milic N (2021) Preeclamptic Women Have Disrupted Placental microRNA Expression at the Time of Preeclampsia Diagnosis: Meta-Analysis. Front. Bioeng. Biotechnol. 9:782845. doi: 10.3389/fbioe.2021.782845

Introduction: Preeclampsia (PE) is a pregnancy-associated, multi-organ, life-threatening disease that appears after the 20th week of gestation. The aim of this study was to perform a systematic review and meta-analysis to determine whether women with PE have disrupted miRNA expression compared to women who do not have PE.

Methods: We conducted a systematic review and meta-analysis of studies that reported miRNAs expression levels in placenta or peripheral blood of pregnant women with vs. without PE. Studies published before October 29, 2021 were identified through PubMed, EMBASE and Web of Science. Two reviewers used predefined forms and protocols to evaluate independently the eligibility of studies based on titles and abstracts and to perform full-text screening, data abstraction and quality assessment. Standardized mean difference (SMD) was used as a measure of effect size.

Results: 229 publications were included in the systematic review and 53 in the meta-analysis. The expression levels in placenta were significantly higher in women with PE compared to women without PE for miRNA-16 (SMD = 1.51,95%CI = 0.55–2.46), miRNA-20b (SMD = 0.89, 95%CI = 0.33–1.45), miRNA-23a (SMD = 2.02, 95%CI = 1.25–2.78), miRNA-29b (SMD = 1.37, 95%CI = 0.36–2.37), miRNA-155 (SMD = 2.99, 95%CI = 0.83–5.14) and miRNA-210 (SMD = 1.63, 95%CI = 0.69–2.58), and significantly lower for miRNA-376c (SMD = –4.86, 95%CI = –9.51 to –0.20). An increased level of miRNK-155 expression was found in peripheral blood of women with PE (SMD = 2.06, 95%CI = 0.35–3.76), while the expression level of miRNA-16 was significantly lower in peripheral blood of PE women (SMD = –0.47, 95%CI = –0.91 to –0.03). The functional roles of the presented miRNAs include control of trophoblast proliferation, migration, invasion, apoptosis, differentiation, cellular metabolism and angiogenesis.

Conclusion: miRNAs play an important role in the pathophysiology of PE. The identification of differentially expressed miRNAs in maternal blood creates an opportunity to define an easily accessible biomarker of PE.

Keywords: epigenetics, miRNA, preeclampsia, pathophysiology, meta-analysis

INTRODUCTION

Preeclampsia (PE) has been shown to affect 1–7.5% of all pregnancies, making it one of the leading causes of maternal and fetal morbidity and mortality worldwide (Abalos et al., 2013; Witcher, 2018; Garovic et al., 2020). PE is a multi-factorial, multi-systemic pregnancy specific condition found typically after 20 weeks of gestation or early post-delivery (American College of Obstetricians and Gynecologists, 2019). Although clinical symptoms appear relatively late in pregnancy, PE pathology begins early, making the identification of potential biomarkers during the first trimester a possible strategy for identifying predictors of PE (McElrath et al., 2020). Several potential biomarkers already have been evaluated: C reactive protein (CRP), cytokines (IL-6, IL-8, TNF-α), microparticle proteins (C1RL, GP1BA, VTNC, and ZA2G), oxidative stress markers (malondialdehyde - MDA), and genetic factors (PAI-1 4G/5G polymorphism) (Black and Horowitz, 2018; Giannakou et al., 2018; Taravati and Tohidi, 2018; McElrath et al., 2020). There are few known biomarkers, however, that can accurately predict the risk for PE. The use of combinations of several biomarkers previously has been proposed as a diagnostic or predictive parameter, such as the ratio of soluble fms-like tyrosine kinase-1 to placental growth factor ratio (sFlt-1/PlGF) (Lecarpentier and Tsatsaris, 2016). A study by Garovic et al. reported podocyturia, defined as the presence of podocin-positive cells in urine sampled ≤24 h of delivery, as a 100% sensitive and specific diagnostic marker for PE (Garovic et al., 2007).

Significant progress has been made in the past decade in the assessment of epigenetic mechanisms that might be involved in the pathophysiology of PE, and which aim to identify potential diagnostic and/or predictive epigenetic markers of PE. More specifically, short non-coding microRNAs (miRNAs) are involved in post-transcriptional gene expression and play a role in numerous diseases, modulating regulatory pathways that control development, differentiation, and organ function. MiRNAs are single-stranded RNA molecules consisting of 19–24 nucleotides, and their mode of action is primarily by degrading targeted mRNA transcripts or inhibiting translation of mRNA into a protein product (Hombach and Kretz, 2016). It is also known that miRNA molecules are involved in the physiological regulation of major processes of placentation (Mouillet et al., 2015). It might therefore be anticipated that dysfunction of miRNA expression could be important for the development of PE. Studies recently published explored a possible causal relationship between miRNA expression and PE (Youssef and Marei, 2019; Hemmatzadeh et al., 2020). It has been demonstrated that expression levels of miRNAs in different tissues play a role in physiological pregnancy as regulators of trophoblast proliferation, migration, invasion, apoptosis, differentiation, cellular metabolism and placental angiogenesis (Hayder et al., 2018). The placenta is one of the main sources of miRNAs, but they also can be found in the circulation (Mouillet et al., 2015). Placental miRNA-210 expression has been the most studied in PE and other pregnancy related complications, and increased levels have been demonstrated (Muralimanoharan et al., 2012; Awamleh and Han, 2020). Results from evaluations of other frequently analyzed miRNAs, such as miRNA-155, -223, -126, -183, -182, -281b, -154, -139-5p, -29b, -181a, -15b (Mayor-Lynn et al., 2011; Yang et al., 2011; Zhao et al., 2013; Sheikh et al., 2016; Hemmatzadeh et al., 2020), suggest that miRNA expression differs according to the severity of PE (Jairajpuri et al., 2017), and also differs throughout the course of normal pregnancy (Cai et al., 2017). While some research has been done to investigate the association between miRNA expression levels and PE, there is still a lack of evidence to support the common use of miRNAs as functional biomarkers related to PE. The aim of this study was to perform a systematic review and meta-analysis to determine whether women with PE have disrupted miRNA expressions compared to women without PE.

MATERIALS AND METHODS

This systematic review was performed in accordance with the Preferred Reporting Items for Systematic Reviews and Meta-Analyses (PRISMA) and MOOSE guidelines (Stroup et al., 2000; Liberati et al., 2009).

Study Selection

Publications were screened for inclusion in the systematic review in two phases, and all disagreements were resolved by discussion at each stage with inclusion of a third reviewer. We included studies that compared miRNA expression levels between women with and without PE. Studies were eligible for inclusion if the miRNA expression levels were measured in both groups. Studies were excluded if they: 1) investigated other outcomes, 2) did not make comparisons between PE and control groups, 3) examined other populations (animal, cell lines), 4) assessed other epigenetic markers, 5) were abstracts, or 6) were not original articles.

Database Search

Two biostatisticians with expertise in conducting systematic reviews and meta-analyses (NM, AC) developed the search strategy. A systematic review of peer-reviewed publications was performed through searches of PubMed, Web of Science (WoS) and embase electronic databases until October 29, 2021. Search queries differed according to the database. Key words for the PubMed search were: preeclampsia and (epigenetic or epigenetics or miRNA or microRNA or DNA methylation or DNA methylation or long non coding RNA); for Wos: TS = *eclampsia and TS= (epigenetic* or microRNA or DNA methylation or gene imprinting or long non coding RNA), and for embase: preeclampsia and (epigenetics or microRNA or DNA methylation or genome imprinting or long untranslated RNA). Only publications in English were considered. In addition, reference lists of articles identified through electronic retrieval were manually searched, as well as relevant reviews and editorials. Experts in the field were contacted to identify other potentially relevant articles.

Authors of relevant articles were contacted to obtain missing data. Studies with combined data of gestational hypertension and/or chronic hypertension in pregnancy and PE were only

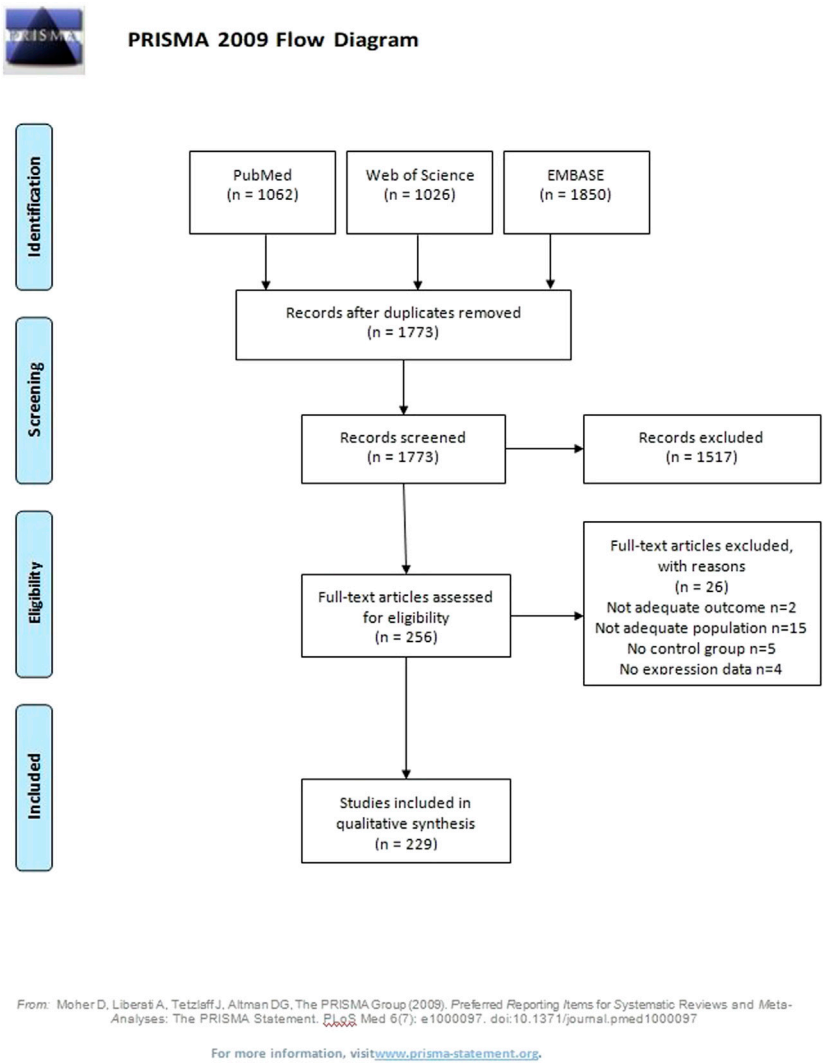

FIGURE 1 | Flow diagram.

eligible if data for the subset of women who developed preeclampsia were available.

Article Screening and Selection

Two reviewers (AC, JML) independently evaluated the eligibility of all titles and abstracts. Studies were included in the full text screening if either reviewer identified the study as being potentially eligible, or if the abstract and title did not include sufficient information. Studies were eligible for full text screening if they included comparisons of miRNA expression levels between women with and without PE. Preeclampsia included more severe, less severe, and not specified forms. The same reviewers independently performed full text screening to select articles for inclusion according to the criteria listed under Inclusion and Exclusion Criteria. Disagreements were resolved by consensus (AC, JML) or arbitration (NM, DS).

Data Abstraction and Quality Assessment

Two reviewers independently abstracted the following data: author(s), country of research, year of publication, study design, sample size, study population, maternal age, preeclampsia definitions, disease severity (more severe, less severe or not-specified PE), inclusion and exclusion criteria used in the original articles, sample type and time of sampling, matching, evaluated miRNAs, method for miRNA expression quantification, miRNA expression value, housekeeping gene for internal control, conclusion in original article. Each reviewer independently evaluated the quality of selected manuscripts using an adapted version of the Newcastle-Ottawa tool for observational studies (Wells et al., 2014). Reviewers used a standardized previously defined miRNA protocol when selecting and abstracting data. All detailed information about quality assessment, data extraction, variables, miRNA expression

TABLE 1 | Systematic review.

Author year* Country	Study design	Sample size		Maternal age[a] PE vs. Controls (years)	Sample	Time of sampling	Controls/Unexposed	Matching	Inclusion criteria		
		n PE	n Controls						All primiparas	All non-smokers	No chronic hypertension
Pineles 2007* (Pineles et al., 2007) United States	Not clear (cross-sectional, case-control study)	9	9	28 (19–39) vs. 24 (18–37)	placenta	NR	pregnant women with presence of regular uterine contractions at a frequency of at least 2 contractions every 10 min that were associated with cervical changes and resulted in delivery at 37 completed weeks of gestation who delivered normal infants with birthweights appropriate for gestational age (10th–90th percentile) matched for gestational age at delivery (within 2 weeks)	Gestational age	NR	no	yes
Hu 2009* (Hu et al., 2009) China	Cross-sectional	24	26	28.1 ± 1.3 vs. 28.7 ± 1.1	placenta (chorion)	at the time of delivery	pregnant women with normal term pregnancy, without chronic hypertension, cardiovascular disease, renal disease, hepatitis, diabetes, any evidence of intrapartum infection or other pregnancy complications, such as fetal anomalies or chromosomal abnormalities	Maternal age and gestational age	no	NR	yes
Zhu 2009* (Zhu et al., 2009) China	Cross-sectional	23 Total 8 mPE 15 sPE	11	31.9 ± 3.8 (sPE); 29.5 ± 5.3 (mPE) vs. 31.8 ± 3.7	placenta (villi)	NR	normal pregnancies	Gestational age	all nulliparous	NR	yes
Zhang 2010* (Zhang et al., 2010) China	Case-control	20	20	NR	placenta (chorion)	at the time of delivery	normotensive pregnancies with gestational age matched groups	Gestational age	NR	NR	yes
Cheng 2011 (Cheng et al., 2011) China	Cross-sectional	5	5	33 ± 3 (25–40) vs. 29 ± 1 (27–33)	UC HUVECs	at the time of delivery	Healthy women	NR	NR	NR	NR
Enquobahrie 2011 (Enquobahrie et al., 2011) United States	Not clear (participants were selected from cohort and case-control studies)	20	20	32.8 ± 7.4) vs. 30.4 ± 5.6)	placenta	at the time of delivery	normotensive pregnancies uncomplicated by proteinuria matched for parity, maternal race/ethnicity, and labor status	Parity, maternal race/ethnicity and labor status	no	NR	yes
Gunel 2011 (Gunel et al., 2011) Turkey	Cross-sectional	20	20	NR	MPB (plasma)	NR	healthy pregnant women	NR	NR	NR	NR
Guo 2011 (Guo et al., 2011) China	Cross-sectional	NR	NR	NR	placenta	NR	normal pregnant women	NR	NR	NR	NR
Mayor-Lynn 2011* (Mayor-Lynn et al., 2011) United States	Cross-sectional	6	10 Total 5 term controls 5 preterm controls	23.8 (20–26) vs. 28.3 (21–38)	placenta (villi)	at the time of delivery	term controls - pregnancies who delivered normal infants at term without labor via elective Caesarean section preterm controls - presence of preterm regular uterine contractions of at least 3 contractions in 10 min that were associated with cervical changes that resulted in delivery at ≤35 completed weeks of gestation	NR	no	no	NR
Yang 2011 (Yang et al., 2011) China	Cross-sectional	4 Total 2 mPE 2 sPE	1	Individual data sPE: 28; 34 mPE: 26; 27 Control: 28 years	MPB (serum)	before delivery (during 3rd trimester)	normal pregnant women	NR	all nulliparous	NR	NR
Bai 2012*(Bai et al., 2012) China	Cross-sectional	15	17	27.5 ± 4.3 vs. 29.7 ± 2.6	placenta	at the time of delivery	normal pregnant women defined as a single gestation in	Gestational age	no	NR	yes

(Continued on following page)

TABLE 1 | (*Continued*) Systematic review.

Author year* Country	Study design	Sample size		Maternal age[a] PE vs. Controls (years)	Sample	Time of sampling	Controls/Unexposed	Matching	Inclusion criteria		
		n PE	n Controls						All primiparas	All non-smokers	No chronic hypertension
							a previously normotensive woman who did not suffer from high blood pressure and proteinuria during pregnancy, and delivered a healthy neonate with a weight adequate for gestational age after 37 weeks of pregnancy				
Hromadnikova 2012 (Hromadnikova et al., 2012) Czech Republic	Not clear (retrospective, cohort)	16 + 7 who later developed PE	50	NR	MPB (plasma)	NR	normal progression of pregnancy defined as those without medical, obstetric, or surgical complications at the time of the study and who subsequently delivered full-term, singleton, healthy infants weighing >2,500 g after 37 completed weeks of gestation	Gestational age	NR	NR	NR
Ishibashi 2012 (Takizawa et al., 2012) China	Cross-sectional	8	10	Individual data for PE patients: 28, 28, 29, 31, 31, 32, 32, 36; NR for controls	placenta	NR	normal pregnancies	Gestational age	NR	NR	NR
Lazar 2012 (Lázár et al., 2012) Hungary	Not clear (prospective study)	31	28	29 (18–39) vs. 28 (20–41)	placenta	at the time of delivery	normotensive pregnant women	NR	no	NR	NR
Liu 2012*(Liu et al., 2012) China	Cross-sectional	11	16	NR	UC-MSCs placenta (decidua)	NR NR	women with normal pregnancy	NR	NR	NR	NR
Muralimanoharan 2012*(Muralimanoharan et al., 2012) United States	Cross-sectional	6	6	32.6 ± 3.6 vs. 28.6 ± 2.6	placenta (villi)	at the time of delivery	uncomplicated pregnancies	NR	NR	NR	NR
Wang 2012*(Wang et al., 2012a) United States	Cross-sectional	10	10	23 ± 1.2 vs. 23 ± 1.2	placenta	at the time of delivery	normotensive term pregnancies	NR	NR	yes	NR
Wang 2012*(Wang et al., 2012b) China	Cross-sectional	20	20	30.81 ± 0.74 vs. 30.50 ± 0.76	placenta (decidua MSCs)	at the time of delivery	maternal age and gestational age at delivery matched normotensive controls	NR	NR	NR	yes
Wu 2012*(Wu et al., 2012) China	Case-control	10	9	29.9 ± 3.1 vs. 30.4 ± 1.3	MPB (plasma)	NR	term matched normal pregnancies	Yes (no variable)	no	yes	NR
Zhang 2012 (Zhang et al., 2012) China	Case-control	30 Total 15 mPE 15 sPE	15	30.9 ± 4.1 (sPE) 31.6 ± 3.6 (mPE) vs. 29.7 ± 3.6	MPB (plasma)	NR	healthy pregnant controls who had had normal blood pressure with the absence of medical and obstetrical complications matched for age, gestational age, parity, and body mass index (BMI) at the time of blood sampling	Maternal age, gestational age, parity, and BMI at the time of sampling	NR	NR	yes
Anton* 2013 (Anton et al., 2013) United States	Case-control	40 (PE + GHTA)	33	25.5 ± 7.5 vs. 26.2 ± 6.7	MPB (serum)	before delivery (during 3rd trimester)	women without hypertension-related complications who presented for delivery at term (≥37 gestational weeks)	NR	no	NR	NR
	Nested case-control	41 (PE + GHTA)	56	31.2 ± 7.5 vs. 29.7 ± 6.6	MPB (serum)	before delivery (15–20 gw)	randomly selected from the cohort	NR	no	no	yes
Betoni 2013*(Betoni et al., 2013) United States	Case-control	16	12	26.0 ± 5.9 vs. 30.9 ± 5.8	placenta	NR	patients without PE matched for maternal age and ethnicity, as well as for type of delivery, gestational age, birth weight and sex of the child	Gestational age	no	no	yes
Choi 2013 (Choi et al., 2013) China	Cross-sectional	11	10	31.0 ± 5.3 vs. 30.7 ± 3.9	placenta	NR	normotensive pregnancies uncomplicated by proteinuria	NR	no	NR	yes

(Continued on following page)

TABLE 1 | (*Continued*) Systematic review.

Author year* Country	Study design	Sample size		Maternal age[a] PE vs. Controls (years)	Sample	Time of sampling	Controls/Unexposed	Matching	Inclusion criteria		
		n PE	n Controls						All primiparas	All non-smokers	No chronic hypertension
Fu, 2013*(Fu et al., 2013) China	Cross-sectional	15	22 term controls	30.8 ± 1.9 (preterm PE) 34.8 ± 2.2 (term PE) Vs. 32.0 ± 1.23 (preterm controls) 33.4 ± 0.7 (term controls)	placenta	at the time of delivery (36–40 gw)	normal pregnancies	Gestational age	NR	NR	NR
	Cross-sectional	29 Total 13 preterm PE 16 term PE	44 Total 13 preterm controls 31 term controls	29.8 ± 0.7 (preterm PE) Vs. 29.5 ± 0.8 (preterm controls) 29.2 ± 1.0 (term PE) Vs. 31.7 ± 0.6 (term controls)	MPB (plasma)	before delivery (15-18 gw and 36-40 gw)	normal pregnancies	NR	NR	NR	NR
	Cross-sectional	37 Total 16 preterm PE 11 term PE	23 preterm controls 25 term controls	NR	placenta	at the time of delivery (25-35 gw and 36–40 gw)	normal pregnancies	NR	NR	NR	NR
Guo 2013 (Guo et al., 2013) United States	Cross-sectional	16	29	NR	placenta	NR	control group	NR	no	NR	yes
Hromadnikova 2013 (Hromadnikova et al., 2013) Czech Republic	Cohort	63 Total 24 mPE 39 sPE 24 EOPE 39 LOPE	55	NR	MPB (plasma)	NR	pregnant women without complications who delivered full term, singleton, healthy infants weighting >2,500 g after 37 completed gw	Gestational age	NR	NR	no
Kumar 2013 (Kumar et al., 2013) China	Cross-sectional	8	8	NR	placenta	at the time of delivery	term gestation-matched normotensive pregnant women	Gestational age	NR	NR	yes
Li 2013 (Li et al., 2013a) China	Cross-sectional	4 mPE +4 sPE profiling study 16 mPE +22 sPE validation study	4 in profiling study 32 in validation study	34 (28–39) (sPE) 29 (23–36) (mPE) vs. 28 (26–30) in profiling study 33 (24–43) (sPE) 31 (26–39) (mPE) vs. 29 (25–36) in validation study	MPB (plasma)	before delivery	normal pregnancies, age, gestational week and gravidity matched with PE	Maternal age, gestational age, and gravidity	yes	NR	yes
Li 2013*(Li et al., 2013b) China	Cross-sectional	24	26	28.1 ± 1.3 vs. 28.7 ± 1.1	placenta (chorion)	at the time of delivery	normal term pregnancies without chronic hypertension, cardiovascular disease, renal disease, hepatitis, diabetes, any evidence of intrapartum infection or other pregnancy complications, such as fetal anomalies or chromosomal abnormalities	NR	no	NR	NR
Yan 2013 (Yan et al., 2013a) China	Case-control	12	12	31.4 ± 4.03 vs. 30.3 ± 3.67	placenta	NR	normotensive and nonproteinuric during pregnancy and delivered healthy infants of appropriate weight	Maternal age, BMI, and gestational age	NR	yes	yes
Campos 2014 (Campos et al., 2014) Brasil	Cross-sectional	19	14	26 ± 6 vs. 27 ± 6	MPB (plasma)	before delivery (at the time of clinical attendance)	healthy pregnant women	NR	no	yes	yes
Chen 2014 (Chen et al., 2014) China	Cross-sectional	20 Total 15 mPE 5 sPE	40	27 (24–34) vs. 25 (25–30)	placenta	NR	normal deliveries	NR	NR	NR	NR
Doridot 2014 (Doridot et al., 2014) France	Cross-sectional	5	8	NR	placenta	NR	Women who underwent Caesarean surgery without suffering any disease during pregnancy	NR	NR	NR	NR
Hong 2014 (Hong et al., 2014) China	Case-control	115	115	NR	placenta	at the time of delivery	gestational age matched normotensive pregnancies	Gestational age	NR	NR	yes
Lalevee 2014*(Lalevée et al., 2014) Switzerland		15	14	36.1 (22.6–44.5) vs. 33.3 (26.5–37.2)	placenta	at the time of delivery	controls	NR	no	NR	NR

(Continued on following page)

TABLE 1 | (*Continued*) Systematic review.

Author year* Country	Study design	Sample size		Maternal age[a] PE vs. Controls (years)	Sample	Time of sampling	Controls/Unexposed	Matching	Inclusion criteria		
		n PE	n Controls						All primiparas	All non-smokers	No chronic hypertension
	Not clear (prospective case–control study)										
Li 2014 (Li et al., 2014a) China	Case-control	13	26	29.58 ± 0.68 vs. 29.56 ± 0.48	Placenta (basal plate and chorionic plate)	at the time of delivery	gestation-week-matched pregnant healthy controls without renal disease, cardiovascular disease, transient hypertension in pregnancy, gestational diabetes mellitus, hepatitis. Any evidence of spontaneous abortion, intrauterine fetal death, fetal chromosomal or other pregnancy complications were excluded from this study	Gestational age	no	NR	yes
Li 2014*(Li et al., 2014b) China	Cross-sectional	19	22	27.6 ± 4.2 vs. 28.2 ± 4.5	placenta	at the time of delivery	normal pregnant women defined as previously and currently normotensive female during pregnancy who delivered a healthy neonate following 37 weeks of gestation	NR	NR	NR	yes
Luo 2014*(Luo et al., 2014) China	Case-control	15	26	29.3 ± 1.3 vs. 31.6 ± 0.9	placenta (chorionic villi) placenta (chorionic plate and basal plate)	after abortion/ elective termination (7–8 gw) at the time of delivery	normal pregnant women defined as gestation in a previously normotensive woman who did not suffer from any complications during pregnancy and who delivered a healthy neonate with a weight adequate for a gestational age of more than 37 weeks of pregnancy	Gestational age	NR	NR	yes
Luque 2014 (Luque et al., 2014) Spain	Nested case-control	31	44	32.6 ± 6.6 vs. 32.3 ± 5.6	MPB (serum)	before delivery (11 + 0, 13 + 6 gw)	normotensive pregnancies without proteinuria	NR	no	no	yes
Ura 2014 (Ura et al., 2014) Italy	Not clear (retrospective study)	24	24	34.4 (33.0–36.8) vs. 33.7 (30.3–36.1)	MPB (serum)	before delivery (12–14 gw)	normal pregnancies	NR	no	no	NR
Wang 2014 (Wang et al., 2014) China	Not clear	NR	NR	NR	placenta	NR	normal pregnancies	NR	NR	NR	NR
Weedon-Fekjaer 2014 (Weedon-Fekjær et al., 2014) Norway	Cross-sectional	49 Total 23 EOPE 26 LOPE	23	NR	placenta	at the time of delivery	uncomplicated pregnancies delivered at term (37–41 gw)	NR	NR	NR	yes
Winger 2014 (Winger et al., 2014) United States	Not clear (retrospective study)	12 Total 7LOPE 5EOPE	19	43.7 ± 8.7 vs. 37.6 ± 5.1	MPB	before delivery (1st trimester)	delivery of a singleton normal karyotype baby with the following pregnancy criteria: (i) delivered at 37- to 40-weeks of gestation, (ii) birthweight of ≥6 lbs, (iii) normal maternal blood pressure throughout pregnancy or (iv) twin delivery with gestational age ≥35 weeks with birthweights of ≥5.1 lbs and (v) no other pregnancy or delivery complications	NR	NR	NR	NR
	Case-control	14	33	NR				Gestational age	NR	NR	NR

(Continued on following page)

TABLE 1 | (*Continued*) Systematic review.

Author year* Country	Study design	Sample size		Maternal age[a] PE vs. Controls (years)	Sample	Time of sampling	Controls/Unexposed	Matching	Inclusion criteria		
		n PE	n Controls						All primiparas	All non-smokers	No chronic hypertension
Xu 2014*(Xu et al., 2014) China	Case-control	20	20	NR	placenta (chorionic plate and basal plate) MPB (plasma)	at the time of delivery before delivery (15–19 gw) at the time of delivery (35–39 gw)	gestational week matched normal pregnant women gestational week matched normal pregnant women	Gestational age	NR	NR	NR
Zhao 2014*(Zhao et al., 2014) China	Case-control	20	20	28.9 ± 1.2 vs. 29.2 ± 1.4	Placenta (decidual MSCs)	at the time of delivery	age matched normotensive controls	Maternal age	no	NR	yes
Zou 2014 (Zou et al., 2014) China	Cross-sectional	30	30	30.2 ± 5.7 vs. 30.6 ± 3.5	placenta	at the time of delivery (immediately after placental delivery)	normal pregnant women defined as not having PE or any other complications (including maternal history of hypertension and/or renal disease, maternal infection, smoking, alcoholism, chemical dependency, and fetal congenital anomalies)	NR	yes	no	NR
Akehurst 2015*(Akehurst et al., 2015) Scotland	Not clear (prospective study)	18	18	31 ± 5.3 vs. 31 ± 5.4	MPB (plasma)	before delivery (16–18 gw)	matched for age, BMI, and parity	Maternal age, BMI, and parity	no	no	NR
	Case-control	19	19	29 ± 5.4 vs. 30 ± 4.6	placenta	at the time of delivery	normotensive individuals matched for age, BMI, and parity	Maternal age, BMI, and parity	no	no	NR
	Not clear	2	9 term	NR	myometrium	at the time of delivery	normotensive women	Maternal age, BMI, and parity	NR	NR	NR
Anton 2015 (Anton et al., 2015) United States	Case-control	31 Total 18 term PE 13 preterm PE	14	28.1 ± 7.7 (total) 28.3 ± 8.2 (term PE) 27.8 ± 7.3 (preterm PE) vs. 27.0 ± 7.2	placenta	at the time of delivery	women without hypertension-related complications that presented for delivery at term (37 gestational weeks)	NR	NR	NR	NR
Chen 2015 (Chen et al., 2015) China	Cross-sectional	5	10	NR	placenta (decidua MSCs)	at the time of delivery	healthy pregnancies	NR	NR	NR	NR
Ding 2015 (Ding et al., 2015) China	Case-control	18	21	28.44 ± 0.95 vs. 30.05 ± 0.72	placenta	at the time of delivery	normal pregnancy defined as patients with no history of hypertension or proteinuria during weeks 35–40 of pregnancy who delivered healthy neonates via Caesarean section	Maternal age, gestational age	yes	NR	yes
Hromadnikova 2015a (Hromadnikova et al., 2015a) Czech Republic	Cohort	80	20	33 (30–36) vs. 30 (26.5–33)	placenta	NR	without medical, obstetrical, or surgical complications at the time of the study and who subsequently delivered full term, singleton healthy infants weighing >2,500 g after 37 completed weeks of gestation	NR	NR	NR	yes
Hromadnikova 2015b (Hromadnikova et al., 2015b) Czech Republic	Cohort	63	42	31.7 ± 5.0 vs. 30.6 ± 4.4	placenta	NR	those without medical, obstetrical, or surgical complications at the time of the study and who subsequently delivered full-term, singleton healthy infants weighing >2,500 g after 37 completed weeks of gestation	NR	NR	NR	yes
Hu 2015 (Hu et al., 2015) China	Cross-sectional	24 Total 17 7	24 Total 17 7	27.42 ± 3.89 vs. 27.11 ± 3.18	umbilical cord vein UC-MSC	NR	normal pregnancies delivered after 34 weeks	NR	NR	NR	NR
	Cross-sectional	20	20	28.1 ± 4.8 vs. 26.3 ± 5.2	placenta	NR		NR	NR	NR	yes

(Continued on following page)

TABLE 1 | (*Continued*) Systematic review.

Author year* Country	Study design	Sample size		Maternal age[a] PE vs. Controls (years)	Sample	Time of sampling	Controls/Unexposed	Matching	Inclusion criteria		
		n PE	n Controls						All primiparas	All non-smokers	No chronic hypertension
Jiang 2015 (Jiang et al., 2015) China							previously and currently normotensive pregnant female, who delivered a healthy neonate following 37 weeks of gestation				
Lasabova 2015*(Lasabová et al., 2015) Slovak Republic	Case-control	11	7	27.6 ± 4.9 vs. 26.6 ± 2.8	placenta	at the time of delivery	normotensive healthy singleton pregnancies with no history of cigarette smoking, diabetes autoimmune disease, or thrombophilia	NR	NR	NR	yes
Li 2015*(LI et al., 2015) China	Case-control	60 Total 12 - 1st trimester 20 - 2nd trimester 28 - 3rd trimester	60 Total 12 - 1st trimester 20 - 2nd trimester 28 - 3rd trimester	28.7 ± 3.6 vs. 28.1 ± 3.8	MPB (serum)	before delivery (after ≥8 h fasting)	healthy pregnant women without complications	Maternal age at delivery within 1-year-old gap and gestational age of blood sampling	NR	NR	NR
Miura 2015 (Miura et al., 2015) Japan	Case-control	20 Total 6 sEOPE 14 sLOPE	20	31.9 ± 2.9 sEOPE 30.2 ± 4.4 sLOPE vs. 32.8 ± 4.0	MPB (plasma)	before delivery (27–34 gw)	Uncomplicated gestational age matched pregnant women	Gestational	NR	NR	NR
Murphy 2015 (Murphy et al., 2015) Canada	Cohort	13 Total 7 mPE 6 sPE	17	30.4 ± 7.3 (total) 32.4 ± 6.9 (mPE) 28.0 ± 7.6 (sPE) vs. 28.2 ± 4.1	MPB (plasma)	at the time of delivery (peripartum) after delivery (1 year postpartum)	Uncomplicated pregnancies	Time	NR	NR	NR
Sun 2015 (Sun et al., 2015) China	Cross-sectional	20	20	29 ± 3.7 vs. 28.9 ± 2.5	placenta	at the time of delivery	Healthy pregnancies	NR	NR	NR	NR
Winger 2015 (Winger et al., 2015) United States	Cross-sectional	12 Total 7 LOPE 5 EOPE 5 preconceptional PEs 5 1st trimester	20 Total 11 pre-conception controls 9 Controls for 1st trimester	36.7 ± 3.5 (total) 37.7 ± 3.8 (LOPE) 35.2 ± 2.8 (EOPE) vs. 36.3 ± 4.7	MPB	before delivery (pre-conception and 1st trimester)	Healthy pregnant women in healthy pregnancies	NR	NR	NR	NR
Yang 2015 (Yang et al., 2015) China	Cross-sectional	4	1	PE patients' individual data mPE: 27, 26 sPE: 34, 28 vs. Controls NR	MPB (plasma) placenta	before delivery at the time of delivery	Pregnant women without complications	NR	NR	NR	NR
Zhang 2015*(Zhang et al., 2015) China	Cross-sectional	3	3	29.58 ± 0.68 vs. 29.56 ± 0.48	placenta (basal plate and chorionic plate)	at the time of delivery	Normal pregnant controls without any complications	Yes (no variable)	NR	NR	NR
Hromadnikova 2016*(Hromadnikova et al., 2016) Czech Republic	Not clear (retrospective study from prospective cohort)	68 Total 32 mPE 36 sPE 24 EOPE 44 LOPE	20	33 (30–36) vs. 30 (26.5–33)	MPB (whole peripheral blood)	NR	Normal pregnancies defined as those without medical, obstetrical, or surgical complications at the time of the study and who subsequently delivered full term, singleton healthy infants weighing >2,500 g after 37 completed weeks of gestation	NR	NR	NR	no
Hu 2016 (Hu et al., 2016) China	Cross-sectional	19	23	27.42 ± 3.89 vs. 27.11 ± 3.18	placenta	NR	healthy pregnant women at term	NR	no	NR	yes
Munaut 2016*(Munaut et al., 2016) Belgium	Not clear (retrospective study from prospective cohort)	23	44	29 (19–44) vs. 30 (19–38)	MPB (serum)	before delivery	pregnant women presenting, at 24 to <37 weeks' gestation, clinical suspicion of, but not manifesting preeclampsia/ eclampsia/HELLP syndrome	NR	no	no	no
Ospina-Prieto (Ospina-Prieto et al., 2016) 2016 Germany	Cross-sectional	11	13	27.0 ± 2.8 (total) 28.0 mean EOPE 26.4 mean LOPE vs. 29.5 ± 5.8	placenta (villi)	at the time of delivery (immediately after delivery)	NR	Maternal age		yes	
Sandrim 2016a (Sandrim et al., 2016a) Brasil	Case-control	7	10	24 ± 6 vs. 28 ± 6	MPB (plasma)	at the time of delivery	healthy pregnancies matched for gestational age at sampling, maternal age, and BMI	Gestational age, maternal age, and BMI	NR	NR	NR
Sandrim 2016b (Sandrim et al., 2016b) Brasil	Case-control	19	14	26 ± 5 vs. 27 ± 6	MPB (plasma)	before delivery	healthy pregnant women	NR	no	yes	yes
	Nested case-control	8	8	NR	MPB (plasma)		healthy pregnant women	NR	no	yes	NR

(Continued on following page)

TABLE 1 | (*Continued*) Systematic review.

Author year* Country	Study design	Sample size		Maternal age[a] PE vs. Controls (years)	Sample	Time of sampling	Controls/Unexposed	Matching	Inclusion criteria		
		n PE	n Controls						All primiparas	All non-smokers	No chronic hypertension
Vashukova 2016 (Vashukova et al., 2016) Russia	Cross-sectional	5	6	35.0 ± 2.4 vs. 29.3 ± 0.6	placenta	before delivery (35 + 1 and 35 + 5 gw) at the time of delivery	normal pregnancies	NR	NR	NR	yes
Wang 2016 (Wang et al., 2016a) United States	Cross-sectional	5	5	26 ± 5 (20–33) vs. 29 ± 7 (20–37)	Maternal subcutaneous fat tissue endothelial cells	at the time of delivery	normal pregnancies defined as pregnancy with blood pressure (<140/90 mm Hg), absence of proteinuria, and obstetrical and medical complications	NR	NR	yes	NR
Wang 2016 (Wang et al., 2016b) China	Case-control	34 Total 13 PE age 21–29 years 13 PE age >30 years 8 PE with complications (chronic HTA and GDM)	13	25.69 ± 1.31 vs. 29.08 ± 2.60	MPB	NR	normal pregnant women	NR	no	NR	NR
Yang 2016 (Yang et al., 2016) China	Cross-sectional	17	40	28.85 ± 2.02 vs. 28.96 ± 4.11	placenta (chorionic plate, basal plate) MPB (plasma)	at the time of delivery NR	normal pregnant women	NR	no	NR	NR
Zhou 2016*(Zhou et al., 2016) China	Cross-sectional	31 Total 9 discovery set 22 validation set	29 Total 9 discovery set 20 validation set	Discovery set 32.1 ± 6.9 vs. 28.3 ± 1.4 Validation set 30.4 ± 4.7 vs. 30.5 ± 4.4	placenta (chorionic plate)	at the time of delivery	normal pregnant women	NR	NR	NR	NR
Adel 2017*(Adel et al., 2017) Egypt	Cross-sectional	35 Total 25 mPE 10 sPE	35	24 (18–40) vs. 25 (19–35)	placenta (villi)	at the time of delivery	primigravid normotensive throughout gestation with no excess albumin in urine	NR	NR	NR	NR
Azizi 2017*(Azizi et al., 2017) Iran	Case-control	59	40	27.42 ± 6.7 vs. 23.78 ± 4.15	placenta (chorion)	at the time of delivery	gestational age-matched normotensive pregnancies	Gestational age	all nulliparous	NR	yes
Fang 2017 (Fang et al., 2017) China	Cross-sectional	12	12	NR	placenta (trophoblast cells)	at the time of delivery	normal pregnancies	NR	NR	NR	NR
Gan 2017 (Gan et al., 2017) China	Case-control	20	20	28.95 ± 4.16 vs. 30.05 ± 4.22	MPB (serum) urine	before delivery before delivery	healthy pregnant women without complications were selected as the control based on similar maternal age at delivery and the similar weight at delivery	Maternal age and maternal weight at delivery	NR	NR	NR
Gao 2017 (Gao et al., 2017) China	Cross-sectional	26	18	30.8 ± 5.2 vs. 29.6 ± 4.6	MPB (plasma)placenta	before delivery (16, 20, 24, 30 gw) NR	normal pregnancies were defined as those without medical, obstetric or surgical complications at the time of the study and who subsequently delivered full term, singleton healthy infants weighing >2,500 g after 37 completed weeks of gestation	NR	NR	NR	NR
Gunel 2017 (Gunel et al., 2017) Turkey	Case-control	18	18	NR	MPB (plasma)	at the time of delivery	matched for age, gestational week, and gravidity healthy pregnancies 37-40 gw	Maternal age, gestational age, and gravidity	yes	NR	NR
Guo 2017 (Guo et al., 2017) China	Cross-sectional	29	26	32.14 ± 1.17 vs. 29.64 ± 1.00	placenta	at the time of delivery	healthy pregnant women	NR	NR	no	yes
Han 2017 (Han et al., 2017) China	Cross-sectional	40	20	30.25 ± 5.16 vs. 29.74 ± 4.16	placenta	at the time of delivery	women in normal late pregnancy	NR	NR	yes	NR
Hromadnikova 2017 (Hromadnikova et al., 2017) Czech Republic	Not clear (retrospective study)	56 Total 15 mPE 41 sPE 19 EOPE 37 LOPE	44	33 (22–43) vs. 32 (20–39)	UC blood	NR	Normal pregnancies defined as those without medical, obstetrical, or surgical complications at the time of the study and who subsequently delivered full term, singleton healthy infants weighing	NR	no	NR	no

(Continued on following page)

TABLE 1 | (*Continued*) Systematic review.

Author year* Country	Study design	Sample size		Maternal age[a] PE vs. Controls (years)	Sample	Time of sampling	Controls/Unexposed	Matching	Inclusion criteria		
		n PE	n Controls						All primiparas	All non-smokers	No chronic hypertension
							>2,500 g after 37 completed weeks of gestation				
Hu 2017 (Hu et al., 2017) China	Cross-sectional	19	23	NR	placenta	at the time of delivery	healthy pregnant women at term	NR	NR	NR	NR
Huang 2017 (Zhang et al., 2017) China	Nested case-control	26	52	28.3 ± 3.8 vs. 28.1 ± 4.4	MPB (plasma)	before delivery (12–20 gw)	healthy pregnant women who had no relevant disease over the same period	gestational age and maternal age	no	no	yes
Jairajpuri 2017 (Jairajpuri et al., 2017) Kingdom of Bahrain	Cross-sectional	15	7	30 (25–38) (mPE) 34 (28–39) (sPE) vs. 29 (23–36)	MPB (plasma)	NR	no previous history of hypertension, cardiovascular disease, hepatitis, kidney disease, diabetes, and any evidence of intrapartum infection or other complications of pregnancy such as fetal anomalies or chromosomal abnormalities	Maternal age and BMI	yes	NR	no
Jiang 2017 (Jiang et al., 2017) China	Case-control	19	19	31.3 ± 5.8 vs. 30.9 ± 5.6	MPB (serum)	1st trimester 10-14 gw 2nd trimester 20-24 gw 3rd trimester 30-34 gw	healthy pregnant women without complications	maternal age (±1 year) at delivery and gestational age	NR	NR	yes
Jin 2017*(Jin et al., 2017) China	Cross-sectional	15	15	NR	Placenta MPB	NR NR	normal pregnancies	NR	NR	NR	NR
Korkes 2017*(Korkes et al., 2017) United States	Cross-sectional	11	11	31.6 ± 1.63 vs. 34.36 ± 1.5	placenta	NR	normal pregnancies	NR	NR	NR	yes
Li 2017a*(Li et al., 2017a) China	Cross-sectional	NR	NR	NR	placenta	at the time of delivery	Normal pregnancy without preeclampsia or any other complications	NR	NR	NR	NR
Li 2017b (Li et al., 2017b) China	Case-control	32 Total 24 (UC tissue) 8 (UC-MSCs)	30 Total 24 (UC tissue) 6 (UC-MSCs)	29.5 ± 0.9 vs. 28.9 ± 0.5 (UC tissue) 29.6 ± 0.2 vs. 28.7 ± 0.9 (UC-MCSs)	UC tissue UC-MSCs	at the time of delivery	healthy pregnancies who underwent Caesarean section	NR	no	NR	yes
Lu 2017 (Lu et al., 2017) China	Cross-sectional	84 Total 38 mPE 46 sPE	50	28.5 ± 1.6 (mPE) 29.2 ± 2.1 (sPE) vs. 28.6 ± 1.3	placenta	at the time of delivery	normal pregnancy	NR	NR	no	NR
Luo 2017 (Luo et al., 2017a) NR	Cross-sectional	16	16	NR	placenta	NR	NR	NR	NR	NR	NR
Luo 2017 (Luo et al., 2017b) China	Case-control	23	15	30.6 ± 1.0 vs. 28.1 ± 0.9	placenta	at the time of delivery	healthy women not having preeclampsia or any other complications, such as maternal history of hypertension and/or renal or cardiac disease, maternal infection, multiple pregnancies, premature rupture of membranes or fetal anomalies	NR	NR	NR	NR
Meng 2017 (Meng et al., 2017) Inner Mongolia (China)	Cross-sectional	20	10	28.9 ± 0.15 vs. 28.3 ± 0.21	placenta	at the time of delivery	normal pregnancy	NR	all nulliparous	NR	NR
Nizyaeva 2017*(Nizyaeva et al., 2017) NR	Cross-sectional	10 Total 5 EOPE 5 LOPE	8 Total 4 preterm 4 full-term	23–40 for all respondents	Placenta (syncytiotrophoblast and syncytial knots)	NR	preterm controls - women without clinical manifestations of hypertensive disorders and without inflammatory diseases (no inflammatory infiltration was confirmed by results of histological analysis) term controls - uterine scar after the previously surgery, severe myopia, and anatomically narrow pelvis	NR	NR	NR	NR
					MPB (plasma exosomes)			Gestational age	NR	yes	yes

(Continued on following page)

TABLE 1 | (*Continued*) Systematic review.

Author year* Country	Study design	Sample size		Maternal age[a] PE vs. Controls (years)	Sample	Time of sampling	Controls/Unexposed	Matching	Inclusion criteria		
		n PE	n Controls						All primiparas	All non-smokers	No chronic hypertension
Salomon 2017 (Salomon et al., 2017) Chile	Not clear (retrospectively stratified case-control experimental design)	45 Total 15 11–14 gw 15 22–24 gw 15 32–36 gw	96 Total 32 11–14 gw 32 22–24 gw 32 32–36 gw	29 ± 1.6 (18–40) vs. 25 ± 1.2 (18–36)		11–14 gw 22–24 gw 32–36 gw	healthy subjects without pregnancy complications or chronic medical problems, and did not differ in racial origin from PE patients				
Shao 2017 (Shao et al., 2017) China	Case-control	24 Total sEOPE 10 sLOPE 14	43 10 Preterm controls 33 Term controls	29.8 ± 6.5 (total) 30.3 ± 6.2 (sEOPE) 28.8 ± 5.3 (sLOPE) vs. 29.2 ± 5.6 (preterm controls) 28.6 ± 4.7 (normal pregnancy)	placenta	at the time of delivery	Term controls - gestation in a previously healthy woman who did not experience any complications during pregnancy and who delivered a healthy neonate with a weight adequate for a gestational age of longer than 37 weeks Preterm controls - unexplained preterm labor defined as labor of unknown causes earlier than 34 weeks, but without any other diagnosable pregnancy problems	Gestational age	NR	NR	yes
Singh 2017 (Singh et al., 2017) United States	Cross-sectional	4	4	NR	placenta (chorionic villi)	before delivery (11–12 gw)	healthy pregnancies who delivered at term matched for gestational age at CVS (+/- 6 days), fetal sex, parity with PE women	Gestational age (+/- 6 days), fetal sex and parity	NR	yes	yes
Truong 2017 (Truong et al., 2017) United States	Case-control	6	6	32 ± 4.3 (28 ± 33) vs. 31 ± 2.9 (29 ± 35)	MPB (plasma exosomes)	before delivery (before 20 gw)	women without chronic medical conditions or obstetric complications	NR	NR	NR	yes
Tsai 2017 (Tsai et al., 2017) Taiwan	Case-control	31	60	33.83 ± 5.77 vs. 31.33 ± 4.31	MPB (plasma) fetal cord blood (plasma) placenta	before delivery - within hours to 2 days before delivery at the time of delivery	healthy controls	Gestational age	NR	NR	yes
Wang 2017 (Wang et al., 2017) China	Cross-sectional	25	25	20–35 for all respondents	placenta	at the time of delivery	healthy controls	NR	NR	NR	yes
Wei 2017 (Wei et al., 2017) New Zealand	Cross-sectional	7	4	28.0 ± 5.78 vs. 32 ± 4.99	placenta (trophoblast debris)	at the time of delivery	normotensive term pregnancies	NR	NR	NR	yes
Xiao 2017 (Xiao et al., 2017) China	Cross-sectional	30	30	28.34 ± 4.12 vs. 28.81 ± 4.94	placenta	at the time of delivery	healthy pregnancies who underwent Caesarean section	NR	NR	NR	NR
Xu 2017 (Xu and Zhang, 2017) China	Cross-sectional	25	25	NR	placenta	NR	normal pregnancies	NR	NR	NR	NR
Yang 2017*(Yang et al., 2017) China	Cross-sectional	60	20	NR	MPB (serum) placenta	at the time of delivery	subjects who were normotensive during pregnancy and who, both previously and presently, had delivered a healthy neonate after 37 weeks of gestation	NR	NR	NR	yes
Brkic 2018 (Brkić et al., 2018) China	Cross-sectional	15	15	36.67 ± 0.27 vs. 37.56 ± 0.2	Placenta (chorionic plate and basal plate)	at the time of delivery	previously normotensive women who did not suffer from complications during pregnancy and who delivered a healthy neonate with a weight adequate for a gestational age	Gestational age	NR	NR	yes
	Case-control	9 Term PE	69 Total 13 1st trimester 9 2nd trimester 23 preterm control 24 term control	32 ± 1.17 (term PE) vs. (preterm control) 33 ± 0.76 (term control)	placenta (trophoblast cells)	at the time of delivery	1st and 2nd trimester - healthy patients undergoing elective termination of pregnancy Preterm controls – spontaneous preterm labor delivered either by Caesarean	NR	NR	NR	NR

(Continued on following page)

TABLE 1 | (*Continued*) Systematic review.

Author year* Country	Study design	Sample size		Maternal age[a] PE vs. Controls (years)	Sample	Time of sampling	Controls/Unexposed	Matching	Inclusion criteria		
		n PE	n Controls						All primiparas	All non-smokers	No chronic hypertension
							section for fetal distress or vaginal delivery Term controls - vaginal delivery or elective Caesarean sections with Appropriate for Gestation Age babies				
Chi 2018 (Chi and Zhang, 2018) China	Cross-sectional	30	30	25–35 for all respondents	placenta (placental villi)	NR	age matched healthy controls	Maternal age	NR	NR	NR
Dai 2018 (Dai and Cai, 2018) China	Cross-sectional	63 Total 55 sEOPE 8 sLOPE	65	29.7 ± 4.2 vs. 30.8 ± 3.9	placenta (trophoblast cells)	NR	pregnancies free of any pregnancy complications that terminated between 34 and 40 gestational weeks	Maternal age, BMI and gestational age	no	NR	NR
Fang 2018 (Fang et al., 2018) China	Cross-sectional	50	50	29.8 ± 4.2 vs. 30.5 ± 3.2	Placenta	NR	normal pregnant women	NR	NR	NR	NR
Gao 2018 (Gao et al., 2018a) China	Cross-sectional	42	42	30.12 ± 3.98 vs. 32.36 ± 4.87	Placenta	at the time of delivery	normal pregnancy	NR	NR	NR	NR
Gao 2018 (Gao et al., 2018b) China	Cross-sectional	29	35	28.3 ± 4.2 vs. 27.2 ± 3.1	Placenta	at the time of delivery	pregnant women without PE or any other complications, such as premature rupture of membranes, fetal anomalies, maternal history of hypertension and/or renal or cardiac disease, maternal infection, or smoking	NR	NR	NR	NR
Gunel 2018 (Gunel et al., 2020) Turkey	Cross-sectional	10	10	30.7 ± 2.3 vs. 31.75 ± 3.92	MPB (plasma) placenta	just before delivery at the time of delivery	healthy women	NR	NR	NR	NR
Guo 2018 (Guo et al., 2018) China	Cross-sectional	20	20	28.6 ± 3.1 vs. 27.1 ± 2.6	MPB (plasma and serum)	at the time of delivery	healthy pregnant women	NR	NR	NR	NR
Khaliq 2018*(Khaliq et al., 2018) South Africa	Cross-sectional	28	32	Not clear	MPB (serum) placenta	NR at the time of delivery	normotensives with no obstetrical or medical complications	NR	NR	NR	yes
Kim 2018 (Kim et al., 2018) Republic of Korea	Cross-sectional	17	17	NR	MPB (serum)	NR	normal pregnant women	NR	NR	NR	NR
Li 2018*(Li et al., 2018) China	Cross-sectional	91 Total 40 mPE 51 sPE	67	29.4 ± 2.8 vs. 28.4 ± 3.5	MPB (plasma) placenta	during the treatment at the time of delivery	normal pregnant women	NR	NR	NR	yes
Liu 2018 (Liu et al., 2018) China	Cross-sectional	18	20	30.3 ± 4.6 vs. 29.5 ± 4.3	Placenta	at the time of delivery	normal pregnant women	NR	NR	NR	NR
Lou 2018 (Lou et al., 2018) China	Case-control	28	34	NR	Placenta	at the time of delivery	age matched healthy controls	Maternal age	NR	NR	NR
Lykoudi 2018 (Lykoudi et al., 2018) Greece	Cross-sectional	16 Total 11 EOPE 5 LOPE	8	35.1 (28–45) EOPE 28.4 (20–35) LOPE vs. 35.7 (35–39)	Placenta	at the time of delivery	uncomplicated term pregnancies	NR	NR	NR	NR
Martinez-Fierro 2018 (Martinez-Fierro et al., 2018) Mexico	Nested case–control study	45 in total 6 at 12 gw 10 at 16 gw 14 at 20 gw 15 at the time of diagnosis	18	23.5 ± 5.1 vs. 23.4 ± 5.8	MPB (serum)	before delivery (12th, 16th and/or 20th gw) at enrolment and PE patients at the time of diagnosis	matched healthy pregnancies without complications (normotensive controls)	NR	no	yes	yes
Motawi 2018 (Motawi et al., 2018) Egypt	Case-control	100 Total 23 EOPE 77 LOPE	100 Total 20 early pregnancy controls 80 late pregnancy controls	28.77 ± 5.72 vs. 28.06 ± 5.65	MPB (plasma exosomes)	NR	uncomplicated pregnancy: (1) gestational age at venipuncture between 20 – 42 weeks; (2) no medical, obstetrical, or surgical complications; (3) absence of labor at the time of venipuncture; and (4) delivery of a normal term (≥37 weeks)	Maternal age	NR	NR	yes

(Continued on following page)

TABLE 1 | (*Continued*) Systematic review.

Author year* Country	Study design	Sample size		Maternal age[a] PE vs. Controls (years)	Sample	Time of sampling	Controls/Unexposed	Matching	Inclusion criteria		
		n PE	n Controls						All primiparas	All non-smokers	No chronic hypertension
							neonate whose birth weight was between the 10th and 90th percentile for gestational age. Divided into early (<20 gw) and late (>20 gw) pregnancy control groups				
Niu 2018* (Niu et al., 2018) China	Cross-sectional	25	20	27.9 ± 2.9 vs. 28.1 ± 3.2	Placenta	at the time of delivery	healthy pregnant women	NR	NR	yes	yes
Nizyaeva 2018*(Nizyaeva et al., 2018) Russia	Cross-sectional	22 Total 12 EOPE 10 LOPE	15 Total 10 late normal 5 early normal	NR	placenta (syncytiotrophoblast) endothelium	at the time of delivery	Late normal pregnancies defined as women with physiological course of pregnancy and full-term gestational age. Early normal pregnancies defined as women with preterm operative delivery at 26–31 gw	NR	NR	NR	NR
Shen 2018 (Shen et al., 2018) China	Case-control	10	10	29.11 ± 5.01 vs. 27.56 ± 3.21	MPB (serum exosomes)	before delivery (prior to treatment)	gestational age-matched normal pregnant women	Gestational age	NR	NR	yes
Timofeeva 2018 (Timofeeva et al., 2018) Russia	Cohort	28 Total 16 EOPE 2 moderate EOPE 14 severe EOPE 12 LOPE 11 moderate LOPE 1 severe LOPE	26 Total 16 full term 10 indicated for Caesarean	NR	Placenta MPB (plasma)	at the time of delivery	women with full term physiological pregnancy (37–40 gw) and pregnant women with an indication for an emergency Caesarean section due to the lack of prolonging the pregnancy because of cervical insufficiency, placental abruption, or premature rupture of the fetal membrane without clinical manifestations of PE	NR	NR	NR	NR
	Cohort	6 sEOPE	10	NR	MPB (plasma exosomes)	before delivery (11-13 gw, 24–26 gw and 30–32 gw)	women with physiological pregnancy	NR	NR	NR	NR
Wang 2018 (Wang and Yan, 2018) China	Cross-sectional	20	20	29.7 ± 2.4 vs. 28.6 ± 3.2	Placenta	at the time of delivery	pregnant women with normal term pregnancy (without PE or other complications)	NR	NR	NR	NR
Wang 2018 (Wang et al., 2018a) China	Cross-sectional	9	8	34.8 ± 1.4 vs. 34.3 ± 2.2	MPB (plasma)	at the time of delivery	preterm labor control defined an uniparous gestation in a previously normotensive woman who did not exhibit any gestational complication and delivered a healthy newborn of gestational age before 37 weeks of pregnancy	Gestational age	no	NR	yes
Wang 2018*(Wang et al., 2018b) China	Case-control	10	10	31.3 ± 4.84 vs. 30.5 ± 4.37	Placenta	NR	normal pregnancies	NR	NR	NR	NR
Wang 2018 (Wang et al., 2018c) Australia	Case-control	16 Total 8 EOPE 8 LOPE	48 Total 8 term controls 7 at 10–11 gw 8 at 14.3–17.8 gw 8 preterm controls	NR	Placenta	at the time of delivery	Term controls defined as uncomplicated singleton pregnancies delivering at term (38.2–40.4 weeks gestation) by elective Caesarean section in the absence of labor. Women treated with non-steroidal anti-inflammatory drugs or who had a history of infection, chorioamnionitis, PE, or who were undergoing induction of labor, were excluded from this group. Women undergoing	Gestational age	NR	NR	NR

(Continued on following page)

TABLE 1 | (*Continued*) Systematic review.

Author year* Country	Study design	Sample size		Maternal age[a] PE vs. Controls (years)	Sample	Time of sampling	Controls/Unexposed	Matching	Inclusion criteria		
		n PE	n Controls						All primiparas	All non-smokers	No chronic hypertension
							elective terminations of pregnancy at 10–11 gw or 14.3–17.8 gw. Preterm controls defined as equivalent gestational age women who delivered preterm (at 31.6–35.1 gestational weeks) after spontaneous labor/rupture of membranes and vaginal delivery with no evidence of hypertension				
Winger 2018 (Winger et al., 2018) United States	Not clear (retrospective study)	4	20	30.9 ± 8.8 vs. 33.3 ± 6.5	MPB (buffy coat)	before delivery (11–13 gw)	Normal delivery defined as the delivery of a singleton, normal karyotype baby with the following pregnancy criteria: delivery at 38 ± 42 weeks gestation, baby weight within the normal range for gestational age and maternal BMI <30	NR	NR	NR	NR
Zou 2018 (Zou et al., 2018) China	Cross-sectional	15	18	NR	placenta (basal plate) placenta (chorionic plate)	NR	normal pregnant women	NR	NR	NR	NR
Awamleh 2019 (Awamleh et al., 2019) Canada	Case-control	19	20	28.6 ± 7.0 vs. 28.2 ± 5.0	placenta (villi)	at the time of delivery	gestational age- matched patients with preterm labor and no other complications before 34 weeks of gestation	Gestational age	NR	NR	yes
Biro 2019*(Biró et al., 2019) Hungary	Cross-sectional	21 Total 8 13	15 Total 8 7	33.43 ± 6.48 vs. 31.25 ± 5.80	MPB (plasma) placenta	before delivery (3rd trimester) at the time of delivery	normotensive group with the exclusion of women with history of pregnancy-related or other forms of hypertension, spontaneous abortion, preterm birth, and intrauterine growth restriction	NR	NR	NR	NR
Chen 2019*(Chen et al., 2019) China	Cross-sectional	29	27	31 ± 7 vs. 26 ± 6	Placenta	at the time of delivery	pregnant women with normal uncomplicated pregnancies (≥36 weeks of gestation)	NR	no	NR	yes
Devor 2019 (Devor et al., 2020) United States	Case-control	4	5	35.8 ± 2.8 vs. 29.2 ± 2.1	MPB (plasma exosomes)	before delivery (in each trimester)	matched healthy controls who underwent a normal spontaneous vaginal delivery	Yes (no variable)	NR	NR	NR
Dong 2019*(Dong et al., 2019) China	Case-control	40 Total 20 EOPE 20 LOPE	40 Total 20 early control 20 late control	29.10 ± 6.03 (EOPE) 29.15 ± 5.13 (LOPE) vs. 29.6 ± 4.88 (early controls) 30.05 ± 4.91 (late controls)	MPB (plasma)	before delivery (prior to any surgery) at the time of delivery (for PE patients)	Early controls defined as 20–34 gestational week normal pregnant women who underwent routine outpatient antenatal examinations and did not develop preeclampsia. Late controls defined as 34–41 gestational week normal pregnant women who underwent routine outpatient antenatal examinations and did not develop preeclampsia	Gestational age	no	yes	yes
Eghbal-Fard 2019 (Eghbal-Fard et al., 2019) Iran	Case-control	50	50	33.2 ± 5.1 vs. 31.8 ± 3.4	MPB (mononuclear cells)	before delivery	healthy gestational matched pregnant women	Gestational age	NR	NR	NR
Hocaoglu 2019*(Hocaoglu et al., 2019) Turkey	Case-control	23 Total 6 mEOPE 6 sEOPE 5 mLOPE 6 sLOPE	28	29.8 ± 5.9 (Total) vs. 28.1 ± 5.8	MPB (leukocytes)	before delivery	no obstetrical or medical complications whose gestational weeks were matched	Gestational age	no	no	yes
			89		MPB		normal gestation	NR	no	no	NR

(Continued on following page)

TABLE 1 | (*Continued*) Systematic review.

Author year* Country	Study design	Sample size		Maternal age[a] PE vs. Controls (years)	Sample	Time of sampling	Controls/Unexposed	Matching	Inclusion criteria		
		n PE	n Controls						All primiparas	All non-smokers	No chronic hypertension
Hromadnikova 2019a*(Hromadnikova et al., 2019b) Czech Republic	Not clear (cohort case-control study)	101 Total 24 mPE 77 sPE		32 (21–44) at delivery 38 (28–52) at follow-up vs. 32 (25–43) at delivery 38 (29–50) at follow-up		after delivery (3–11 years postpartum)					
Hromadnikova 2019b (Hromadnikova et al., 2019a) Czech Republic	Nested case-control	43 Total 13 mPE 30 sPE 10 EOPE 33 LOPE	102 Total 50 control 1 52 control 2	32.34 ± 0.73 Total vs. 31.88 ± 0.56 (control 1) 31.21 ± 0.56 (control 2)	MPB (plasma exosomes)	before delivery (10–13 gw)	normal pregnancies without complications delivering full term, healthy infants after 37 weeks of gestation weighting >2,500 g, were selected for equal gestational age, equal age of women at the time of sampling and equal plasma sample storage times	NR	no	NR	NR
Hu 2019 (Hu et al., 2019) China	Cross-sectional	25	25	29.24 ± 4.05 vs. 28.04 ± 3.09	Placenta	NR	normal pregnancy	NR	NR	NR	NR
Huang 2019 (Huang et al., 2019) China	Cross-sectional	20	20	29.6 (5.8) vs. 31.3 (4.6)	Placenta	at the time of delivery	normotensive pregnant women	NR	yes	NR	NR
Li 2019 (Li et al., 2019) China	Cross-sectional	10	10	27.92 ± 3.94 (23–34) vs. 28.00 ± 3.54 (22–34)	Placenta	at the time of delivery	healthy controls	NR	NR	NR	NR
Liu 2019 (Liu et al., 2019a) China	Cross-sectional	20	20	NR	Placenta	at the time of delivery	normal pregnant women	NR	NR	NR	NR
Liu 2019 (Liu et al., 2019b) China	Cross-sectional	39	42	NR	Placenta	NR	normal pregnant women	NR	NR	NR	NR
Liu 2019 (Liu et al., 2019c) China	Cross-sectional	30	30	27.07 ± 2.53 vs. 28.67 ± 2.78	Placenta	at the time of delivery	normal pregnant women	NR	NR	NR	yes
Ma 2019 (Ma et al., 2019) China	Not clear (prospective study)	89	70	27.25 vs. 26.81	MPB (serum)	before delivery (20 gw)	pregnant women with no evident anomalies detected during physical examinations	NR	NR	no	yes
Martinez-Fierro 2019 (Martinez-Fierro et al., 2019) Mexico	Nested case-control	30 Total 6 12 gw 10 16 gw 14 20 gw	18	23.5 ± 5.1 vs. 23.4 ± 5.8	MPB (serum)	before delivery (at the time of PE diagnosis, and at the 12th, 16th and/or 20th gw)	healthy pregnancies without complications matched by age, nulliparity, body mass index (BMI), and a personal and family history of PE	Maternal age, nulliparity, BMI and personal and family history of PE	no	yes	NR
Mei 2019 (Mei et al., 2019) China	Cross-sectional	20	20	NR	Placenta	at the time of delivery	normal pregnant women	NR	NR	NR	NR
Nejad 2019 (Nejad et al., 2019) Iran	Case-control	20	20	29 ± 1.1 vs. 28 ± 0.92	MPB (plasma)	NR	healthy controls matched for BMI (body mass index, 29–39 kg/m2), ethnicity (Iranian), smoking (non-smoker)	BMI (29–39 kg/m^2), ethnicity (Iranian), smoking (non-smoker)	NR	yes	yes
Pillay 2019 (Pillay et al., 2019) South Africa	Case-control	30 Total 15 EOPE 15 LOPE	15 Preterm controls (≤33 gw) 15 Term controls (≥34 gw)	25.25 ± 5.13 (EOPE) 27.11 ± 5.23 (LOPE) vs. 28.43 ± 2.23 (≤33 gw) 26.12 ± 3.62 (>34 gw)	MPB (plasma exosomes)	before delivery (at the time of clinical diagnosis of PE)	Gestationally matched normotensive pregnant woman (blood pressure of 120 ± 10/80 ± 5 (systolic/diastolic mm Hg) with absent proteinuria as detected by a rapid urine dipstick test)	Gestational age	NR	NR	NR
Sekar 2019 (Sekar et al., 2019) India	Cross-sectional	NR	NR	NR	MPB	NR	Normotensives	NR	NR	NR	NR
Shi 2019 (Shi et al., 2019) China	Cross-sectional	15	15	29.5 ± 2.8 vs. 28.3 ± 3.7	placenta	at the time of delivery	Normal-term pregnancies without PE or any other complications	NR	NR	NR	NR
Tang 2019 (Tang et al., 2019) China	Case-control	30	30	27.8 (24.5–31.0) vs. 27.3 (25.0–28.0)	placenta	at the time of delivery	healthy pregnant women with uncomplicated pregnancies	Gestational age	no	yes	yes
Wang 2019 (Wang et al., 2019a) Taiwan	Case-control	33	55	34.02 ± 5.57 vs. 31.33 ± 4.31	MPB (plasma)	before delivery (prepartum after hospital admittance for delivery)	healthy controls	NR	no	NR	NR
	Cross-sectional	20	20		Placenta MPB (serum)		normal controls	NR	NR	NR	NR

(Continued on following page)

TABLE 1 | (*Continued*) Systematic review.

Author year* Country	Study design	Sample size		Maternal age[a] PE vs. Controls (years)	Sample	Time of sampling	Controls/Unexposed	Matching	Inclusion criteria		
		n PE	n Controls						All primiparas	All non-smokers	No chronic hypertension
Wang 2019 (Wang et al., 2019b) China				Individual data 29.00 ± 3.82 vs. 27.50 ± 3.35		at the time of delivery					
Wang 2019 (Wang et al., 2019e) China	Cross-sectional	42	39	28.9 ± 2.1 vs. 29.1 ± 1.9	Placenta MPB (serum exosomes)	NR	normal pregnancies	NR	NR	NR	NR
Wang 2019*(Wang et al., 2019c) China	Case-control	17	17	28.1 ± 0.8 vs. 29.7 ± 1.2	placenta	at the time of delivery	normotensive healthy nulliparous and nonproteinuric during pregnancy matched for age and BMI	Maternal age and BMI	NR	yes	NR
Wang 2019 (Wang et al., 2019d) China	Cross-sectional	30	30	28.2 ± 3.2 vs. 28.9 ± 3.0	placenta	at the time of delivery	healthy pregnant women	NR	NR	NR	yes
Xiaobo 2019 (Xiaobo et al., 2019) China	Cross-sectional	15 Total 10 EOPE 5 LOPE	15	30.2 ± 5.4 vs. 29.3 ± 4.7	placenta	at the time of delivery	healthy pregnant women	NR	NR	NR	yes
Xie 2019 (Xie et al., 2019) Chin	Cross-sectional	57	57	27.12 ± 4.11 vs. 26.37 ± 3.29	placenta	NR	healthy patients	NR	NR	NR	NR
Xue 2019 (Xue et al., 2019) China	Case-control	20	20	28.55 ± 0.83 vs. 27.00 ± 0.68	Placenta MPB (serum)	at the time of delivery NR	women without renal disease, cardiovascular disease, transient hypertension in pregnancy, gestational diabetes mellitus, hepatitis, any evidence of spontaneous abortion, intrauterine fetal death, fetal chromosomal or other pregnancy complications	Maternal age and gestational age	no	NR	NR
Yang 2019*(Yang et al., 2019a) China	Cross-sectional	57 Total preterm PE 12 term PE 14 31 plasma	32 Total preterm age matched control 11 term age matched control 12 9 plasma	31.57 ± 2.98 vs. 32.83 ± 3.19	Placenta MPB (plasma)	at the time of delivery	Early trimester controls – patients undergoing terminated pregnancies through dilation and curettage procedure	Maternal age	no	NR	NR
Yang 2019a (Yang and Guo, 2019) China	Cross-sectional	30	30	28.63 ± 2.24 vs. 28.83 ± 2.42	placenta	at the time of delivery	control group	NR	NR	NR	yes (essential HTA)
Yang 2019b (Yang and Meng, 2019) China	Cross-sectional	30	30	27.80 ± 2.10 vs. 28.20 ± 1.50	placenta	at the time of delivery	normal group	NR	NR	yes	yes
Yang 2019a (Yang et al., 2019b) China	Cross-sectional	40	40	30.5 ± 5.3 vs. 30.9 ± 4.6	placenta	at the time of delivery	healthy controls	NR	NR	NR	NR
Yang 2019b (Yang et al., 2019c) China	Cross-sectional	57	70	73.8 ± 3.3 vs. 67.2 ± 2.6	placenta	at the time of delivery	normal controls	NR	yes	NR	yes
Youssef 2019*(Youssef and Marei, 2019) Egypt	Cross-sectional	30 Total mPE 12 sPE 18	20	31.77 ± 3.16 vs. 29.75 ± 4.24	MPB (serum)	before delivery	healthy pregnant women without any pregnancy complications who came for delivery between 38 and 40 weeks of gestation	NR	no	NR	yes
Zhong 2019 (Zhong et al., 2019) China	Cross-sectional	3	3	NR	MPB (plasma)	before delivery	normal pregnancies	NR	NR	NR	NR
Ayoub 2019* (Ayoub et al., 2019) Egypt	Cross-sectional	80	80	30.5 (21–41) vs. 32 (19.42)	MPB (serum)	At the time of diagnosis of PE	Normal pregnancies	No	NR	Yes	Yes
Cao 2019 (Cao et al., 2019) China	Cross-sectional	25	28	29.78 ± 5.25 vs. 30.45 ± 4.62	Placenta MPB (plasma)	NR	Normal pregnancies	No	NR	NR	NR
Demirer 2019 (Demirer et al., 2020) Turkey	Not clear (prospective study)	96 total 48 EOPE 48 LOPE	23 + 3 early stage 3 late stage	30.12 ± 5.7 Total 31.0 ± 5.5 EOPE 29.4 ± 5.8 LOPE	MPB	Before delivery	Healthy pregnant women with no obstetrical or medical complications	No	No	No	Yes
Lip 2019 (Lip et al., 2020) Netherlands	Cross-sectional	10 EOPE	10	31.5 ± 5.7 vs. 28.0 ± 4.4	MPB (plasma)	At the time of PE diagnosis	Healthy pregnant women	Gestational age at sampling	NR	No	Yes
Lv 2019 (Lv et al., 2019) China	Cross-sectional	18	18	32.94 ± 4.64 vs. 31.06 ± 4.02	Placenta	At the time of delivery	Normal singleton pregnant women by Caesarean	No	NR	NR	Yes
Qian 2019 (Qian and Liu, 2019) China	Cross-sectional	16	16	29.3 ± 2.5 vs. 28.4 ± 3.1	Placenta (villi)	At the time of delivery	Normal pregnant women	No	NR	NR	NR
Xu 2019 (Xu et al., 2019) United States	Cross-sectional	6	6	29 ± 6 vs. 29 ± 7	Maternal subcutaneous adipose tissue	At the time of delivery	Normal pregnant women	No	NR	Yes	NR
	Case-control	30	30		Placenta		Normal full term pregnancy	No	Yes	Yes	Yes

(Continued on following page)

TABLE 1 | (*Continued*) Systematic review.

Author year* Country	Study design	Sample size		Maternal age[a] PE vs. Controls (years)	Sample	Time of sampling	Controls/Unexposed	Matching	Inclusion criteria		
		n PE	n Controls						All primiparas	All non-smokers	No chronic hypertension
Yang 2019 (Yang and Meng, 2020) China				28.30 ± 2.07 vs. 29.00 ± 1.55		At the time of delivery					
Yuan 2019* (Yuan et al., 2020) China	Cross-sectional	30	30	27.8 ± 2.8 vs. 26.52 ± 4.9	Placenta	At the time of delivery	Normal pregnancies	No	NR	NR	NR
Zhang 2019 (Zhang et al., 2019b) China	Cross-sectional	30	30	28.36 ± 4.78 vs. 24.34 ± 2.87	MPB (serum)	At the time of delivery	Healthy pregnancies	No	NR	NR	NR
Akgor 2020* (Akgör et al., 2021) Turkey	Cross-sectional	31	32	29.9 ± 6.66 vs. 29.47 ± 6.33	MPB (plasma)	Before delivery	Term-matched healthy pregnancies	Gestational age, BMI, additional comorbities, parities, age	No	NR	NR
Devor 2020 (Devor et al., 2020) United States	Case-control	4 LOPE	5	35.8 ± 2.8 vs. 29.2 ± 2.1	MPB (plasma)	Before delivery (1st trimester -before 13 GW 2nd trimester -13-26 GW 3rd trimester -26-40 GW)	Matched healthy controls	Mmaternal age, BMI	NR	NR	Yes
Dong 2020*(Dong et al., 2020) China	Cross-sectional	20	20	31.7 ± 3.2 vs. 29.7 ± 2.3	MPB Placenta	Before delivery At the time of delivery	Women without PE	No	NR	NR	Yes
Fan 2020* (Fan et al., 2020) China	Cross-sectional	25	25	27.92 ± 2.81 vs. 26.84 ± 2.30	Placenta	At the time of delivery	Normal pregnant women without any other complications, such as premature rupture of membranes, fetal anomalies, maternal history of hypertension and/or renal or cardiac disease, maternal infection, or smoking	No	NR	Yes	Yes
Gong 2020 (Gong et al., 2020) China	Cross-sectional	8	8	31 ± 4.3 vs. 30 ± 4.5	Placenta	At the time of delivery	Healthy pregnancies	No	NR	NR	Yes
Han 2020 (Han et al., 2021) China	Cross-sectional	60 Total 30 severe EOPE 30 mild EOPE 20 PE	30 20	31.56 ± 4.76 Severe EOPE vs. 30.34 ± 4.28 Mild EOPE 31.18 ± 4.16 vs. 30.86 ± 4.72	MPB (serum) UCB Placenta	At the time of delivery	Normal pregnancies	Gestational age, maternal age	NR	Yes	Yes
Huang 2020 (Huang et al., 2020) China	Cross-sectional	46 sPE	57	29.6 ± 3.9 vs. 28.5 ± 4.1	Placenta	At the time of delivery	pregnant women without any pregnancy complications (34–40 gestational weeks)	Gestational age, BMI, maternal age	NR	NR	Yes
Jelena 2020 (Jelena et al., 2020) Serbia	Case-control	19	17	34 (20–51) vs. 32 (22–40)	MPB (plasma)	At the time of delivery	Healthy pregnant women	No	NR	No	Yes
Kim 2020 (Kim et al., 2020) South Korea	Case-control	92	92	32.73 ± 0.54 vs. 31.49 ± 0.50	MPB (serum)	Before delivery	Normotensive pregnant women selected at random	No	NR	NR	Yes
Li W 2020 (Li et al., 2020d) China	Cross-sectional	30	30	NR	Placenta	At the time of delivery	Healthy	No	NR	NR	NR
Li T 2020* (Li et al., 2020c) China	Case-control	30 sPE	20	25.45 ± 3.03 vs. 25.27 ± 3.19	Placenta	At the time of delivery	Healthy pregnant women	No	yes	NR	Yes
Li Q 2020 (Li et al., 2020b) China	Nested case-control	15	29	31.13 ± 1.24 vs. 30.62 ± 0.72	MPB (plasma) Placenta	Before delivery (between 12 + 0 and 13 + 6 GW) At the time of delivery	Gestational age matched healthy pregnancies without any other complications during pregnancy	Gestational age	NR	NR	Yes
Li H 2020 (Li et al., 2020a) China	Cross-sectional	24	24	NR	Placenta	At the time of delivery	Healthy Pregnancies	No	NR	NR	Yes
Licini 2020 (Licini et al., 2021)li Russia	Nested case-control	13 10	18 20	33 (31; 34) 36.9 ± 5.25 vs. 30.2 ± 7.59 1st trimester 32.6 ± 4.05 3rd trimester	MPB (plasma) Placenta	Before delivery (12th GW) At the time of delivery	Healthy pregnant women (normal uterine and umbilical Doppler flow velocimetry during gestation and where the foetus was appropriate for the gestational age (newborns _10th _ 90th percentile for gender and gestational age	Gestational age	NR	No	Yes

(Continued on following page)

TABLE 1 | (*Continued*) Systematic review.

Author year* Country	Study design	Sample size		Maternal age[a] PE vs. Controls (years)	Sample	Time of sampling	Controls/Unexposed	Matching	Inclusion criteria		
		n PE	n Controls						All primiparas	All non-smokers	No chronic hypertension
							according to Italian charts) Voluntary terminations in the 1st trimester, and healthy term prgnancies				
Ma 2020 (Ma et al., 2020) China	Cross-sectional	36	30	NR	Placental monocytes MPB (serum exosomes)	NR	Normal pregnant volunteers	No	NR	NR	NR
Mavreli 2020 (Mavreli et al., 2020) Greece	Case-control	17 LOPE 5 for NGS 12 for qRT-PCR	17 5 for NGS 12 for qRT-PCR	31.81 (21.2–39.50) vs. 33.19 (26.75–41.27)	MPB (plasma)	Before delivery (1st trimester)	Uncomplicated pregnancies delivered at 38–42 GW, chromosomally normal baby weighing within the normal range for gestational age, matched for maternal age, gestational age and duration of storage of plasma samples	Maternal age, gestational age, duration of storage plasma samples	NR	No	Yes
Sheng 2020 (Sheng et al., 2020) China	Case-control	200	200	31.19 ± 4.84 vs. 31.02 ± 4.26	MPB (plasma)	NR	Healthy pregnant women	No	NR	Yes	Yes
Song 2020 (Song et al., 2020) China	Cross-sectional	24	24	NR	Placenta	At the time of delivery	Healthy pregnant women	No	NR	NR	NR
Tao 2020 (Tao et al., 2020) China	Cross-sectional	35	35	28.31 ± 2.86 vs. 28.66 ± 3.0	Placenta	At the time of delivery	Normal pregnancies	No	NR	NR	NR
Wang 2020 (Wang et al., 2020) China	Cross-sectional	24	24	NR	Placenta	At the time of delivery	Healthy pregnancies	No	NR	NR	NR
Whigham 2020 (Whigham et al., 2020) Australia	Case-control	34 PE 36 GW 43 PE 28 GW 32 sEOPE 34 LOPE	196 Controls 36 GW 91 Controls 28 GW 22 gestation matched preterm 12 gestation matched term	28 GW 31 (36–34) vs. 32 (29–34.8) 36 GW 31 (28–33) vs. 31 (26.5–36.3)	MPB (whole blood) Placenta	Before delivery (28 GW) At the time of delivery	Pre-term controls - pre-term rupture of membranes, placenta praevia or antepartum haemorrhage without any evidence of infection (histopathological examination of the placentas), hypertensive disease or maternal comorbidities. Term controls – healthy pregnancies matched fo gestational age	Gestational age	NR	NR	Yes
Wu 2020 (Wu et al., 2020a) China	Cross-sectional	30	30	31.2 ± 4.8 vs. 28.6 ± 5.7	Placenta	At the time of delivery	Healthy pregnant women	No	NR	NR	Yes
Wu 2020 (Wu et al., 2020b) China	Cross-sectional	64 Total 26 mPE 28 sPE	35	NR	Placenta	At the time of delivery	Healthy pregnant women	No	NR	NR	NR
Xueya 2020 (Xueya et al., 2020) China	Cross-sectional	18	20	32.5 ± 1.25 vs. 32.1 ± 0.75	UCB (exosomes) MPB (plasma exosomes) Placenta	After childbirth After PE diagnosis At the time of delivery	Healthy donors	No	NR	NR	NR
Yang 2020 (Yang et al., 2021) China	Cross-sectional	20	20	NR	Placenta UCMSC	At the time of delivery	Normotensive pregnant women	No	NR	NR	Yes
Zhao 2020 (Zhao et al., 2020) China	Case-control	30	30	NR	Placenta	At the time of delivery	Normal pregnancies	No	NR	NR	NR
Zheng W 2020 (Zheng et al., 2020) China	Cross-sectional	30 sPE	20	28.2 ± 2.1 vs. 27.3 ± 1.9	Placenta MPB (serum)	At the time of delivery	Healthy pregnant women	No	NR	NR	Yes
Zhou 2020 (Zhou et al., 2020) China	Cross-sectional	32	28	32 ± 4.6 vs. 33 ± 3.9	MPB (serum) Placenta	At the time of delivery	Normal pregnant women	Maternal age, gestational age, pre-pregnancy indices	NR	NR	NR
Zhu 2020 (Zhu et al., 2020) China	Cross-sectional	30	30	NR	Placenta	At the time of delivery	Normal full term pregnancies	No	Yes	NR	NR
Ali 2021 (Ali et al., 2021) Pakistan	Cross-sectional	27	27	26 (23–30) vs. 25 (22–28)	MPB (serum)	At the time of delivery	Healthy pregnant women with normal blood pressure (BP) and comparable age in the final trimester (28–40 weeks)	Maternal age, gestational age	NR	Yes	Yes
Brodowski 2021 (Brodowski et al., 2021) Germany	Cross-sectional	12 (6 UCB +6 MPB samples)	9 (6 UCB +6 MPB samples)	UCB ECFC 31.5 ± 3.7 vs. 32.8 ± 5.2 MPB	UCB (endothelial colony forming cells) MPB	Before delivery	Healthy uncomplicated pregnancies	Gestational age at delivery, BMI, and maternal age	No	NR	Yes

(Continued on following page)

TABLE 1 | (*Continued*) Systematic review.

Author year* Country	Study design	Sample size		Maternal age[a] PE vs. Controls (years)	Sample	Time of sampling	Controls/Unexposed	Matching	Inclusion criteria		
		n PE	n Controls						All primiparas	All non-smokers	No chronic hypertension
				ECFC30.8 ± 5.5 vs. 31.7 ± 7.4	(endothelial colony forming cells)						
Cai 2021 (Cai et al., 2021) China	Cross-sectional	40	40	29.95 ± 2.67 vs. 28.00 ± 3.20	Placenta	At the time of delivery	Normal pregnancies defined as blood pressure or urine protein in the normal range within 35–40 weeks of pregnancy, followed by Caesarean delivery of healthy infants	No	NR	NR	Yes
Chu 2021 (Chu et al., 2021) China	Cross-sectional	18	28	28 ± 8 vs. 29 ± 6	Placenta	At the time of delivery After selective pregnancy termination (1st and 2nd trimester controls)	Normal term pregnancies 1st trimester (6–8 GW) controls 2nd trimester (18–21 GW) controls	No	No	NR	NR
Hayder 2021 (Hayder et al., 2021) Canada	Case-control	18 Total 14 Pre-term PE 4 Term PE	30 Total 13 Pre-term 17 Term	Pre-term 30.27 ± 0.36 vs. 29.83 ± 0.51 Term 37.25 ± 0.25 vs. 38.32 ± 0.14	Placenta	At the time of delivery	Pre-term controls 26–36 GW Term controls 37–40 GW	No	NR	NR	NR
Jairajpuri 2021 (Jairajpuri et al., 2021) Bahrain	Case-control	30 15 mPE 15 sPE	15	32 (29–35) mPE 33 (29–37) sPE vs. 30 (25–35)	MPB (plasma)	At the time of delivery	Healthy controls with no previous history of hypertension, cardiovascular disease, hepatitis, kidney disease, diabetes, and any evidence of intrapartum infection or other complications of pregnancy such as fetal anomalies or chromosomal abnormalities in the third trimester	No	NR	Yes	Yes
Liu 2021 (Liu et al., 2021) China	Cross-sectional	30 EOPE	30	30.77 ± 5.75 vs. 32.10 ± 4.96	Placenta	At the time of delivery	Helathy pregnancies who had chosen Caesarean section because of abnormal fetal position, pelvic stenosis, or social factorsetc.	No	No	NR	NR
Kamali Simsek, 2021 (Kamali Simsek et al., 2021) Turkey	Cross-sectional	7	7	31.3 ± 5.02 vs. 28.2 ± 4.7	Placenta (hDMSC)	At the time of delivery	Healthy pregnant women	Gestational age	NR	NR	NR
Kolkova 2021 (Kolkova et al., 2021) Slovakia	Case-control	27 Total 13 mPE 11 sPE 7 EOPE 17 LOPE	32 (29 used for miRNA analysis)	27 (21–50) vs. 30 (25–37)	MPB (plasma)	Before delivery	Normal pregnancies with no pregnancy complications, such as artificial insemination, threatened abortion, premature rupture of membranes and/or premature birth, placenta praevia, and foetal macrosomia	No	NR	NR	Yes
Liao 2021 (Liao et al., 2021) China	Case-control	70 EOPE 33 sEOPE 37 mEOPE	35	28.6 ± 2.2 sEOPE 27.9 ± 3.1 mEOPE vs. 28.2 ± 2.9	MPB (serum)	Before delivery	Normal pregnant women	No	NR	NR	Yes
Luizon 2021 (Luizon et al., 2021) Brasil	Nested case-control	5 sPE	5	29.8 ± 2.0 vs. 28.8 ± 2.6	MPB (plasma)	Before delivery	Healthy pregnancies	No	NR	NR	Yes
Mao 2021 (Mao et al., 2021) China	Case-control	24	21	32.21 ± 4.51 Vs. 34.23 ± 3.29	Placenta	At the time of delivery	Normal pregnancies	Maternal age, maternal weight, systolic blood pressure mmHg, diastolic blood pressure mmHg, proteinuria g/day, body weight of infant g, Gestational age	NR	Yes	NR

(Continued on following page)

TABLE 1 | (*Continued*) Systematic review.

Author year* Country	Study design	Sample size		Maternal age[a] PE vs. Controls (years)	Sample	Time of sampling	Controls/Unexposed	Matching	Inclusion criteria		
		n PE	n Controls						All primiparas	All non-smokers	No chronic hypertension
Martinez-Fierro 2021 (Martinez-Fierro and Garza-Veloz, 2021) Mexico	Nested case-control	16	18	23.5 ± 5.1 vs. 23.4 ± 5.8	MPB (serum)	Before delivery (12, 16, 20 GW) At the time of PE diagnosis	Healthy pregnancies without complications	No	No	NR	Yes
Peng 2021 (Peng et al., 2021) China	Cross-sectional	30	30	30.2 ± 5.1 vs. 30.5 ± 4.8	Placenta	At the time of delivery	Normal pregnant women	No	NR	NR	Yes
Witvrouwen 2021* (Witvrouwen et al., 2021) Belgium	Cross-sectional	24 EOPE	30	28.5 (26.7–30.9) vs. 29.2 (27.4–32.5)	MPB (plasma)	At the time of PE diagnosis (22–36 GW)	Healthy pregnancies free from medication and did not have a history of PE, (pregnancy-induced) hypertension, cardiovascular disease or other chronic conditions	No	No	No	No
Xu 2021 (Xu et al., 2021) China	Cross-sectional	35 Total 20 EOPE 15 sPE	38	30.92 ± 1.89 EOPE 31.27 ± 3.85 sPE vs. 30.67 ± 2.56	Placenta	At the time of delivery	Healthy pregnant women	No	NR	NR	NR
Yu 2021 (Yu et al., 2021) China	Case-control	40 sPE	40	NR	Placenta	At the time of delivery	Control pregnancies	No	NR	NR	Yes
Zhao X 2021a* (Zhao et al., 2021a) China	Cross-sectional	10	10	29.73 ± 4.2 vs. 28.85 ± 3.9	Placenta	At the time of delivery	normal pregnant women were: 1) healthy subjects; 2) successful pregnancy, normal blood pressure and negative proteinuria	No	NR	NR	Yes
Zhao X 2021b (Zhao et al., 2021b) China	Case-control	25	25	28.91 ± 5.42 vs. 26.73 ± 4.34	Placenta	At the time of delivery	Normal pregnant women	No	NR	NR	Yes
Zhu 2021 (Zhu and Liu, 2021) China	Cross-sectional	21	21	34.1 ± 5 vs. 33.5 ± 4	MPB (serum)	NR	Normal pregnant women defined as i) Healthy subjects; ii) delivery after 37 weeks; iii) successful pregnancy without any complications, normal blood pressure and negative proteinuria	No	NR	NR	Yes
Zolfaghari 2021 (Zolfaghari et al., 2021) Iran	Case-control	25	25	29.2 ± 4.38 vs. 28.12 ± 3.84	MPB (mononuclear cells)	Before delivery	Healthy age-matched pregnant women at 28–38 weeks of gestation with no sign of historical disorders were engaged for this study	Maternal age	NR	NR	Yes

[a]*Expressed as mean ± sd, mean ± sd (min-max), mean (min-max), mean ± se, med (min-max), med (25–75 percentile), med (Q1; Q3), or as individual data, as stated in the original article.*

GW, gestational week; mPE, mild PE; sPE, severe PE; MPB, maternal peripheral blood; mEOPE, mild early onset PE; sEOPE, severe early onset PE; mLOPE, mild late onset PE; sLOPE, severe late onset PE; BMI, body mass index; MSC, mesenchymal stem cells; UC, umbilical cord; NR, not reported; UCMSC, umbilical cord mesenchymal stem cells; UCB, umbilical cord blood; hDMSC, decidual derived mesenchymal stem cells; GHTA, gestational hypertension; Lbs, pounds; HELLP, Hemolysis, elevated Liver enzymes and Low Platelets; HTA, hypertension; GDM, gestational diabetes mellitus; CVS, chorionic villus sampling.

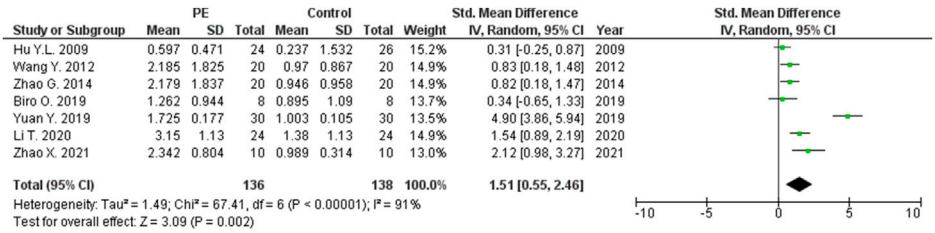

FIGURE 2 | Meta-analysis of differences in expression level of miRNA-16 in placenta between women with vs. without preeclampsia.

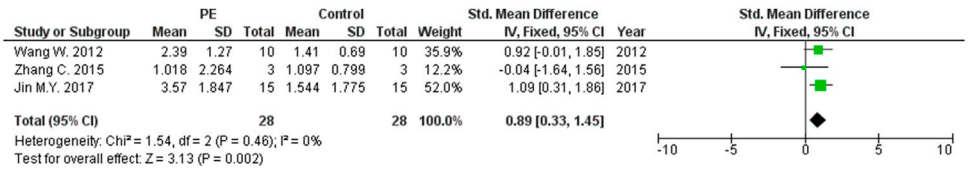

FIGURE 3 | Meta-analysis of differences in expression level of miRNA-20b in placenta between women with vs. without preeclampsia.

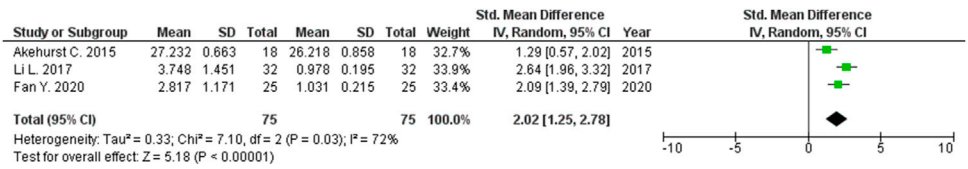

FIGURE 4 | Meta-analysis of differences in expression level of miRNA-23a in placenta between women with vs. without preeclampsia.

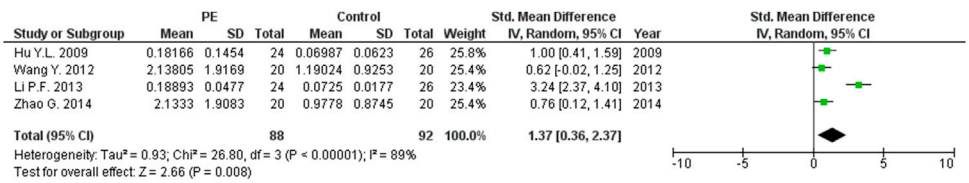

FIGURE 5 | Meta-analysis of differences in expression level of miRNA-29b in placenta between women with vs. without preeclampsia.

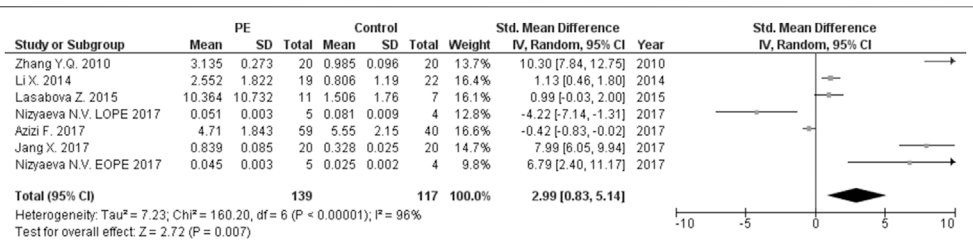

FIGURE 6 | Meta-analysis of differences in expression level of miRNA-155 in placenta between women with vs. without preeclampsia.

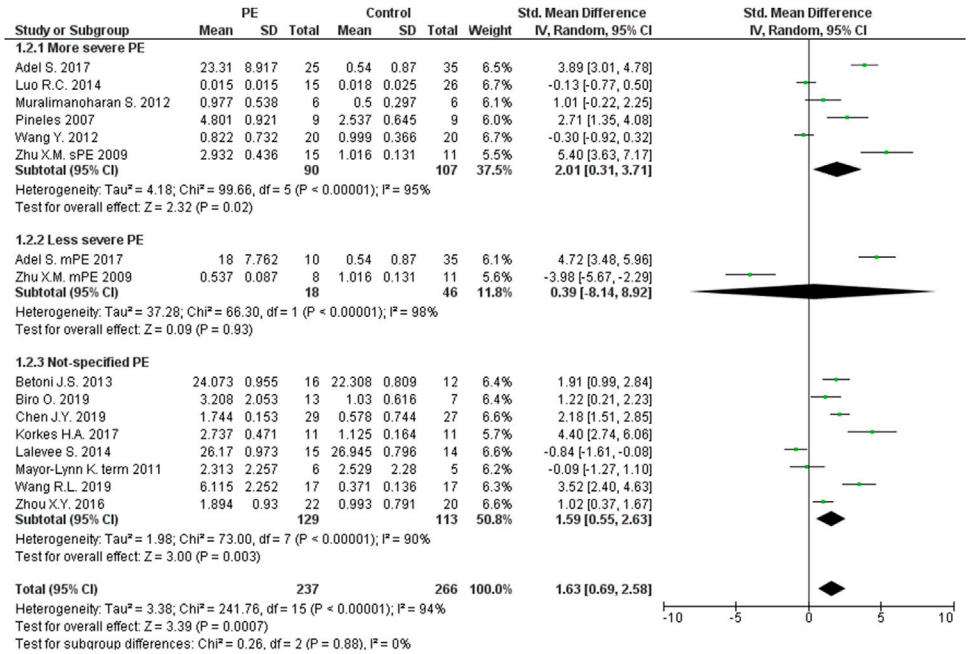

FIGURE 7 | Meta-analysis of differences in expression level of miRNA-210 in placenta between women with vs. without preeclampsia.

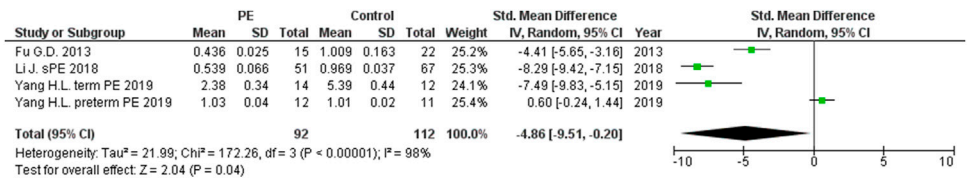

FIGURE 8 | Meta-analysis of differences in expression level of miRNA-376c in placenta between women with vs. without preeclampsia.

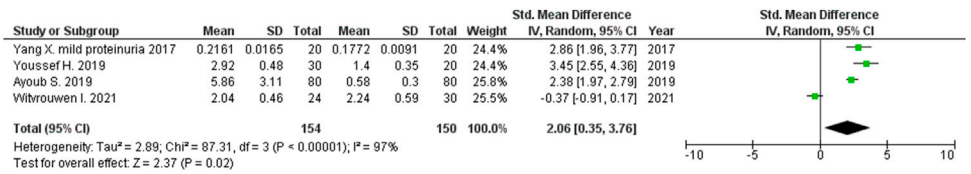

FIGURE 9 | Meta-analysis of differences in expression level of miRNA-155 in peripheral blood between women with vs. without preeclampsia.

quantification methods and housekeeping gene for internal normalization are available at https://osf.io/g42ze/.

Statistical Analysis

The primary outcome was expression levels of miRNAs, presented as means with standard deviation. GetData Graph Digitizer version 2.26.0.20 was used to read miRNA values when figures presenting miRNA expression levels were available (Digitize graphs and plots, 2013). Median was used as an approximation of the arithmetic mean, and IQR/1.35 was used as an approximation of standard deviation. If standard error was used in the original article, standard deviation was calculated as $sd = se^* \sqrt{n}$, and if the range was presented, standard deviation was estimated as (max-min)/4.

Methodologies for measuring miRNA expression levels varied; therefore, the standardized mean difference (SMD) was used as a measure of effect size to examine differences between the preeclampsia and non-preeclampsia groups. SMD expresses

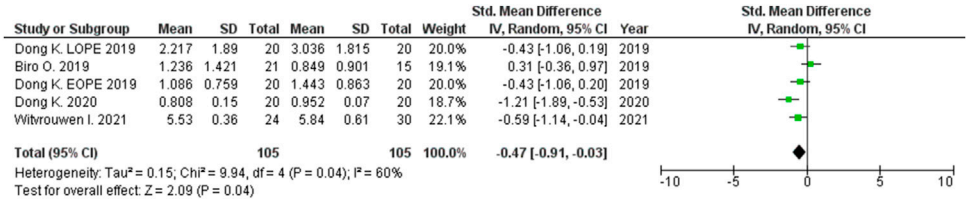

FIGURE 10 | Meta-analysis of differences in expression level of miRNA-16 in peripheral blood between women with vs. without preeclampsia.

the difference between group means in units of standard deviation and was estimated by pooling individual trial results using random-effects models via the Der Simonian-Laird method. Heterogeneity was assessed using the Chi-square Q and I2 statistic. I2 presents the inconsistency between the study results and quantifies the proportion of observed dispersion that is real, i.e., due to between-study differences and not due to random error. The categorization of heterogeneity was based on the Cochrane Handbook (Higgins et al., 2019) and states that I2<30%, 30–60% or >60%, correspond to low, moderate and high heterogeneity, respectively. Forest plots were constructed for each analysis showing the SMD (box), 95% confidence interval (lines), and weight (size of box) for each trial. The overall effect size was represented by a diamond. Meta-analysis was performed for all miRNAs with available data from at least three relevant studies.

Sensitivity analyses were conducted to examine the effects of: 1) replacement of studies that measured miRNA expression levels in the chorionic plate with studies exploring the basal plate, 2) inclusion of measurements performed in more severe, less severe or not-specified PE forms only (instead of all PE forms), 3) replacement of miRNA expression levels obtained in term controls with miRNA expression levels in preterm controls, 4) inclusion of studies exploring miRNA expression levels in moderate or mild proteinuria PE groups, instead of severe proteinuria as in the PE group in the first analysis. A p value < 0.05 was statistically significant. Analyses were performed using Review Manager Version 5.4 (Cochrane, 2021).

RESULTS

Systematic Review

A total of 1773 potentially eligible articles were found. 1,517 articles were excluded because they were duplicates, not original articles, were without PE as the outcome, did not compare PE and control groups, examined populations other than women (animals, cell lines), did not explore miRNA expression levels, or were abstracts. Of the 256 reviewed full text articles, 229 were selected for inclusion in the systematic review. A flow diagram illustrating this selection process is presented in **Figure 1**.

Characteristics of all 229 publications included in the systematic review are presented in detail in **Table 1**. They were published between 2007 and 2021, with a total of 13043 participants; 6,459 women with and 6584 without PE. The minimum sample size of the PE group was four, and a minimum of one for the control group. The maximum sample size was 200 in PE and 321 in the control group. Four publications did not report the number of participants. 139 studies were cross-sectional, 64 were case-control, 11 were nested case-control studies, while only six were prospectively followed cohorts. Five studies included two or three sub-studies with the same or different study designs. In eighteen publications, the study design was not clearly stated. Most studies were from China (138), United States (19), and Czech Republic (8). Study groups were matched in 73 (32%) of all articles, and gestational age at the time of delivery was the most used variable for matching (in 53 of 73 publications). Maternal age at the time of delivery was used for matching in 35 publications. Other matching variables were BMI at the time of delivery, parity, race and/or ethnicity, gravidity, delivery, fetal gender, family history of PE, smoking history, additional comorbidities, systolic blood pressure at the time of inclusion, diastolic blood pressure at the time of inclusion, proteinuria at the time of inclusion, infant weight, pre-pregnancy indices, duration of storage of plasma samples, and maternal body weight at the time of delivery. Regression analysis was used to account for confounders in 14 publications. Ethnicity was reported in eight and race in eleven publications. Fetal gender was reported in 25 publications. The expression levels of miRNA were explored according to fetal gender in just three studies, and a regression model was adjusted for fetal gender in one publication. The most examined source of miRNAs was placenta, reported in 155/229 publications. Ninety-eight studies used maternal peripheral blood: plasma in 46, serum in 28, plasma exosomes in 9, mononuclear cells in 2, serum exosomes in 2, whole blood in 2, and leukocytes and buffy coat in one study each. Twelve studies analyzed miRNA expression levels in umbilical cord cell populations: mesenchymal stem cells in 4, and HUVECs, vein cells, maternal blood, exosomes, endothelial progenitor cells, serum, fetal blood, and umbilical cord tissue in one study each. Other rarely sampled tissues were myometrium, urine, maternal subcutaneous fat tissue endothelium, and placental blood vessel endothelium. Tissue was sampled at the time of delivery in 149 (65%) studies. In 60 studies, sampling was done prior to delivery and, in two studies, after delivery; 1 year after (Murphy et al., 2015), and 3–11 years after delivery (Hromadnikova et al., 2019b). Time of sampling was not reported in 34 (15%) publications. Most articles did not differentiate the type of PE (70%). Inclusion and exclusion criteria were not reported in most studies assessing miRNA in preeclamptic pregnancies. Only primiparous women were included in six studies, only non-smokers in 17, and only

TABLE 2 | Functional roles of significant miRNAs.

miRNA	Placenta	Maternal peripheral blood	Role
16	↑	↓	https://www.genecards.org/cgi-bin/carddisp.pl?gene=MIR16-1
20b	↑	NA	https://www.genecards.org/cgi-bin/carddisp.pl?gene=MIR20B&keywords=miRNA-20b
23a	↑	NA	https://www.genecards.org/cgi-bin/carddisp.pl?gene=MIR23A&keywords=miRNA-23a
29b	↑	NA	https://www.genecards.org/cgi-bin/carddisp.pl?gene=MIR29B1&keywords=miRNA-29b
155	↑	↑	https://www.genecards.org/cgi-bin/carddisp.pl?gene=MIR155&keywords=miRNA-155
210	↑	NA	https://www.genecards.org/cgi-bin/carddisp.pl?gene=MIR210&keywords=miRNA-210
376c	↓	NA	https://www.genecards.org/cgi-bin/carddisp.pl?gene=MIR376C&keywords=miRNA-376c

women without chronic hypertension in 89 publications. Detailed additional inclusion and exclusion criteria are presented in **Supplementary Table S1**. The presence of renal disease was the most common (50/229). The presence of diabetes mellitus (49/229) and the presence of cardiovascular disease (32/229) were reported less often. The presence of obesity was reported in six and preeclampsia in the previous gestation in five publications.

Disease severity was reported in 70/229 publications. Details regarding PE definitions and the diagnostic criteria used in the original articles are presented in **Supplementary Tables S2, S3**. qRT-PCR as the detection method with U6 as an internal control was utilized in almost all studies, and the details regarding quantification methods and housekeeping genes used are presented in **Supplementary Table S4**. A list of all explored miRNAs from the included publications according to PE severity (more severe, less severe, and not-specified PE) is presented in **Supplementary Tables S5–S7**.

Meta-Analysis

A meta-analysis was performed for the following fourteen miRNAs: miRNA-16, miRNA-17, miRNA-17-5p, miRNA-20b, miRNA-23a, miRNA-29a-3p, miRNA-29b, miRNA-30a-3p, miRNA-155, miRNA-155-5p, miRNA-181a, miRNA-195, miRNA-210, and miRNA-376c.

The expression levels were significantly higher in the placentas of women with PE compared to women without PE for miRNA-16 (SMD = 1.51, 95%CI = 0.55–2.46, p = 0.002) (**Figure 2**), miRNA-20b (SMD = 0.89, 95%CI = 0.33–1.45, p = 0.002) (**Figure 3**), miRNA-23a (SMD = 2.02, 95%CI = 1.25–2.78, p < 0.001) (**Figure 4**), miRNA-29b (SMD = 1.37, 95%CI = 0.36–2.37, p = 0.008) (**Figure 5**), miRNA-155 (SMD = 2.99, 95%CI = 0.83–5.14, p = 0.007) (**Figure 6**) and miRNA-210 (SMD = 1.63, 95%CI = 0.69–2.58, p < 0.001) (**Figure 7**). Subgroup analysis showed increased levels of miRNA-210 expression in placentas of women with more severe (SMD = 2.01, 95%CI = 0.31–3.71, p = 0.020), but not in women with a less severe form of PE (SMD = 0.39, 95%CI = –8.14 = 8.92, p = 0.930), compared to women without PE (**Figure 7**). The expression levels in placenta were significantly lower in women with PE compared to women without PE for miRNA-376c (SMD = –4.86, 95%CI = –9.51 to –0.20, p = 0.040) (**Figure 8**).

The expression level was significantly higher in the maternal peripheral blood of women with PE compared to women without PE for miRNA-155 (SMD = 2.06, 95CI = 0.35–3.76, p = 0.020) (**Figure 9**), but it was lower for miRNA-16 (SMD = –0.47, 95%CI = –0.91 to –0.03, p = 0.040) (**Figure 10**).

The functional roles of all significant miRNAs are presented in detail in **Table 2**. Although the roles of the evaluated miRNAs are confusing, special emphasis should be placed on the interpretation of the miRNAs known roles in controlling trophoblast proliferation, migration, invasion, apoptosis, differentiation, cellular metabolism, and angiogenesis.

Placental expression levels were not significantly different in women with PE compared to women without PE for miRNA-17 (SMD = 0.22, 95%CI = -1.35 to –1.79, p = 0.790) (**Supplementary Figure S1**), miRNA-30a-3p (SMD = 1.00, 95%CI = –0.50–2.50, p = 0.190) (**Supplementary Figure S2**), miRNA-181a (SMD = 0.05, 95%CI = –0.99–1.08, p = 0.930) (**Supplementary Figure S3**), and miRNA-195 (SMD = –0.16, 95%CI = –1.35–1.02, p = 0.780) (**Supplementary Figure S4**). The expression level was not significantly different in maternal peripheral blood in women with PE compared to women without PE for miRNA-17-5p (SMD = 0.08, 95%CI = –0.74–0.90, p = 0.850) (**Supplementary Figure S5**), miRNA-29a-3p (SMD = –0.29, 95%CI = –1.22–0.64, p = 0.540) (**Supplementary Figure S6**), miRNA-155-5p (SMD = –0.37, 95%CI = –1.07–0.33, p = 0.300) (**Supplementary Figure S7**), miRNA-181a (SMD = 0.22, 95%CI = –0.42–0.86, p = 0.500) (**Supplementary Figure S8**), and miRNA-210 (SMD = 0.48, 95%CI = –0.66–1.62, p = 0.410) (**Supplementary Figure S9**).

The same results were obtained when sensitivity analyses were performed to exclude studies with unspecified types of PE, to replace expression data obtained from the chorionic plate with those obtained from the basal plate, including/excluding different forms (more/less severe) of PE where possible (**Supplementary Figures S10–S22**).

DISCUSSION

We identified in this study seven differentially expressed miRNAs in the placentas of women with vs without PE. miRNA-16, miRNA-20b, miRNA-23a, miRNA-29b, miRNA-155, and miRNA-210 were significantly increased in the placentas of PE women, while the levels of miRNA-376c were significantly decreased in PE placentas. We found no differences in the expression levels of miRNA-17, miRNA-30a-3p, miRNA-181a, and miRNA-195 in placentas of PE vs. non-PE women. A meta-analysis of the miRNA expression levels in the peripheral blood of PE women compared to women without PE was performed for miRNA-16, miRNA-17-5p, miRNA-29a-3p, miRNA-155, miRNA-155-5p, miRNA-181a and miRNA-210. A significant

decrease in miRNA-16 expression levels in maternal peripheral blood of PE women was found, and no differences were found for other evaluated miRNAs. A sensitivity analysis did not change the results of the primary analysis.

Placentation is thought to be the basis for normal physiological pregnancy and is required for fetal growth and development, as well as the expectation of term labor. Several sensitive, precisely dictated, vascular processes involving angiogenesis at the fetal-maternal interface and adequate cytotrophoblast invasion with spiral-artery remodeling are essential for placentation (Weedon-Fekjær et al., 2014). At the very beginning of a pregnancy in which PE will develop, the transformation of proliferative endothelium into invasive endothelium is absent, and the expected extensive invasion of cytotrophoblasts into the spiral arteries does not occur. This results in pathologic remodeling of the placental arterioles, which become narrow, with reduced flow and sclerotic changes in the arteriolar walls (Mouillet et al., 2015). Placental ischemia promotes an inflammatory state that is characterized by increased production of inflammatory cytokines by pro-inflammatory T cells, and a decrease in regulatory and anti-inflammatory cytokines (Hanna et al., 2000). Decreased levels of anti-inflammatory cytokines (IL-10, IL-4) and increased pro-inflammatory cytokines (TNF-α, IL-6) in the circulation and placental tissue support the inflammatory background of preeclampsia (Keiser et al., 2009; Spence et al., 2021). These processes lead to placental malnutrition, and subsequent development of PE. The placenta is known to be an organ in which a large number of miRNAs are expressed (Mouillet et al., 2015). Several miRNAs contribute to the processes of trophoblast proliferation, invasion, and differentiation. miRNA-125b-1-3p and miRNA-210 inhibit trophoblast proliferation and invasion, while miRNA-155 inhibits trophoblast invasion only. In contrast, miRNA-376c enhances trophoblast proliferation and invasion (Mouillet et al., 2015). Fu et al. demonstrated that miR-376c promotes trophoblast cell proliferation, survival, migration, and invasion, and postulated that inhibition of Nodal and TGF-β signaling by miR-376c is important for adequate placentation (Fu et al., 2013). Primate-specific C19MC miRNAs, which are almost exclusively expressed in placenta, were described as important factors influencing adequate trophoblast invasion and arterial remodeling (Hromadnikova et al., 2013; Mouillet et al., 2015). As knowledge of the functional importance of miRNAs in adequate placentation and the development of PE increases (Hayder et al., 2018), it becomes important to determine whether miRNA expression levels are disrupted in PE, and which specific miRNA contributes predominantly to disease pathogenesis.

Meta-analysis in this study revealed significantly higher miRNA-16 expression in the placentas of women with PE compared to those without PE. Confirmation of the possible association between altered expression of miRNA-16 and PE was first described by Hu et al. who showed that there is increased expression of miRNA-16 in the placentas of women with severe PE (Hu et al., 2009). This was followed by Vu et al. who found increased expression of miRNA-16 in the sera of women with PE compared with healthy controls (Wu et al., 2012). The pathologic significance of miRNA-16 lies in its function in regulating the cell cycle. Liu et al. have shown that miRNA-16 stops the cell cycle in G1 phase by regulating the expressions of the CCND3, CCNE1 and CDK6 genes. Based on these physiological roles, it is supposed that miRNA-16 acts as a tumor suppressor (Yan X. et al., 2013). It also is known that the target of miRNA-16 is the Vascular Endothelial Growth Factor (VEGF) gene, whose product is an extremely important protein that initiates vasculogenesis in the placenta and induces proliferation and migration of endothelial cells in blood vessels (Wang and Zhao, 2010). In a study by Wang et al., miRNA-16 was found to have the potential to inhibit proliferation, migration and angiogenesis in mesenchymal stem cells (Wang Y. et al., 2012). The significantly lower miRNA-16 expression levels in the maternal peripheral blood of women with PE compared to those without PE led epigenetic analysis in another direction. It is proposed, but not proven, that miRNA-16 plays a significant role in the progression of human cardiac cell injury in ischemic dilated cardiomyopathy through endoplasmic reticulum stress, inflammation, autophagy, and apoptosis (Calderon-Dominguez et al., 2021). Down regulation of this miRNA, known as an anti-apoptotic factor, also was registered in ischemic myocardial cells, as a reaction to hypoxia in order to protect the tissue (Zhang H. J. et al., 2019). Therefore, miRNA-16 may play a role in both ischemic cardiomyopathy and preeclampsia, which similarly represent hypoxia induced pathological states. Original research articles have reported differing results regarding miRNA-16 levels in pregnancy complications. miRNA-16 levels were elevated in fetal macrosomia, but decreased in severe preeclampsia (Wu et al., 2012; Ge et al., 2015).

Increased expressions of miRNA-20b and miRNA-29b in the placentas of women with PE compared to women without PE were also found in our study. It is well known that the target gene for both miRNA-20 and miRNA-16 is VEGF, thus affecting placental vasculogenesis (Hayder et al., 2018). miRNA-20b binds to the Ephrin Type-B Receptor 4 (EPHB4) and Ephrin Type-B Receptor 2 (EPHB2), important receptors for intercellular communication, which have functions in the regulation of cellular morphology, binding, migration, proliferation, differentiation, and survival. These processes are assumed to be involved in the miRNA-20b contribution to placental blood vessel remodeling (Pasquale, 2005; Lisabeth et al., 2013). miRNA-29b is involved in the processes of trophoblast proliferation and invasion (Harapan and Andalas, 2015). miRNA-29b contributes to preeclampsia through dysregulation of the extracellular signal-regulated protein kinase and focal adhesion kinase (ERK/FAK) signaling pathway that allows the expression of matrix metalloproteinase-2 (MMP2), which is in turn an important factor for migration and invasion of trophoblast cells. Increased expression of miRNA-29b in severe PE has been previously shown to be associated with reduced expressions of MMP2 and integrin β1(ITGβ1) (Li H. et al., 2013).

The increased miRNA-23a levels in PE placentas support previously reported results that the level of this miRNA is upregulated in conditions related to abnormal angiogenesis (Chhabra et al., 2010). The main role of miRNA-23a, as part of the miR-23a~27a~24–2 cluster, is to mediate blood vessel genesis. It is included, except in PE, in pathological states such as

muscle atrophy, cardiac hypertrophy, and cancers (Chhabra et al., 2010). Data *in vitro*, as well as *in vivo*, indicate that miRNA-23a and miR-23b may have opposite roles, with the former regulating angiogenesis and cellular junctions, and hence inhibiting vascular permeability, while miRNA-23b promotes permeability (Li et al., 2016).

MiRNA-155 expression levels were significantly increased in the placentas and maternal peripheral blood of women with PE compared to those without PE. The increased expression of miRNA-155 and resultant lower levels of cysteine-rich protein 61 (CYR61) and cyclin D1, have been associated with the inhibition of trophoblast invasion (Zhang et al., 2010; Dai et al., 2012). It also has been previously demonstrated that a significant increase in miRNA-155 decreases endothelial nitric oxide synthase (eNOS) expression and thus contributes to development of severe PE (Li X. et al., 2014). This result is consistent with findings from previous studies (Zhang et al., 2010; Gan et al., 2017). This immunomodulatory miRNA, induced in activated T lymphocytes, B lymphocytes and macrophages (Bernstein et al., 2003), is also disrupted in maternal peripheral blood. Its increased expression level was associated with a decreased level of pro-angiogenic factor, VEGF, in an experimental rat model of PE (Cheng et al., 2011). Newly performed studies have reported significantly higher levels of miRNA-155 in the maternal peripheral blood of women with compared to women without PE (Ayoub et al., 2019; Youssef and Marei, 2019; Witvrouwen et al., 2021).

MiRNA-210 has been the most evaluated small non-coding RNA. It is known that miRNA-210 is induced under hypoxic conditions which exist prior to, as well as during the clinical manifestations of PE. Hypoxia stimulates the production of NF-kB 1 (nuclear factor kappa-B 1) and HIF-1A (hypoxia inducible factor 1 α), which induce the expression of miRNA-210 (Muralimanoharan et al., 2012). Previous research has confirmed significantly increased expression of miRNA-210 in both the placentas and sera of women with PE and suggests that miRNA-210 obtained from serum may be a useful biomarker even months before diagnosis (Anton et al., 2013). Micro RNA-210 plays a role in several processes, such as inhibition of cytotrophoblast migration and invasion, differentiation, apoptosis, inflammation, angiogenesis, as well as in the regulation of cellular metabolism. miRNA-210 partially inhibits trophoblast invasion via the ERK/MAPK signaling pathway (Anton et al., 2012). Cell metabolism is dictated by miRNA-210 in that increased expression leads to decreased mitochondrial respiration and vice versa (Hayder et al., 2018). miRNA-210 also plays a role as a suppressor of EFNA3, a member of the ephrin ligand family which is important for cell migration, and HOXA9, an important angiogenesis regulator (Zhang et al., 2012; Luo et al., 2014). Overall, inadequate trophoblast invasion and impaired cellular metabolism are confirmed factors that can lead to the development of PE. Anton et al. found that for each 5-U increase in miR-210 in sera of previously healthy women at the beginning of the second trimester, the odds of PE development later in pregnancy increased fourfold (Anton et al., 2013).

MiRNA-376c plays a role in trophoblast proliferation and differentiation (Hayder et al., 2018). We found significantly lower levels of expression in the placentas of women with PE compared to women without PE, which is consistent with the findings of other studies (Fu et al., 2013; Yang H.-l. et al., 2019). Only Yang et al. showed no significant difference in the levels of miRNA-376c expression in the placentas of women with preterm preeclampsia and gestational age matched controls without PE (Yang H.-l. et al., 2019). Fu at al. showed that a decrease in miR-376c expression results in excessive apoptosis, insufficient cell proliferation, and shallow invasion of trophoblasts in the uterus in preeclampsia (Fu et al., 2013).

In summary, our results clearly identify a subset of miRNAs that are dysregulated in preeclampsia and clearly point towards the underlying mechanisms that may be contributing to the pathophysiology of preeclampsia. Our results set the stage for several venues for future research with an overall goal to facilitate early diagnosis and optimize fetal and maternal outcomes. First, given the clinical heterogeneity of preeclampsia (severe vs. mild, late vs. early, and "placental" vs. "maternal"), adequately designed and powered studies may detect differences in miRNA and related specific underlying mechanisms responsible for specific clinical subtypes. Second, clinical studies may identify a marker (or set of markers) with either predictive or diagnostic role. Third, further discovery of signaling pathways affected by miRNA may lead to mechanism-based therapies.

Our study has several limitations. They originate from the unavailability of all/some data from the original publications, uninformative figures presented in the articles, and selection of the housekeeping gene used for internal controls. The consequences of the data unavailability are possible exclusion of relevant data and a smaller number of included studies, as well as miRNAs, in the meta-analysis that may lead to an overestimation/underestimation of the effects of miRNA expression level on PE development. The importance of adequate selection of the housekeeping gene should be emphasized to standardize miRNA evaluation methodology and to provide comparability between studies. The definition of PE is not the same in each of the included studies which may lead to inclusion of heterogeneous cases that can change the assessment of the effect. Through the systematic review, it was realized that cases and controls were rarely matched for gestational age at the time of sampling. It is necessary to highlight the importance of comparing matched groups because it is known that there are physiological changes in miRNAs expression levels throughout pregnancy. The miRNA source in plasma may be maternal, fetal, or both, yet only a small number of studies reported these data.

CONCLUSION

MiRNAs play an important role in the pathophysiology of PE. The functional roles of the microRNAs found to be disrupted in preeclamptic pregnancies include control of trophoblast proliferation, migration, invasion, apoptosis, differentiation, cellular metabolism, and angiogenesis. The identification of differentially expressed miRNAs in maternal blood creates an opportunity to define an easily accessible biomarker of PE. A better understanding of the role of microRNAs in the

development of PE offers great potential for developing diagnostic and therapeutic targets for PE.

DATA AVAILABILITY STATEMENT

The original contributions presented in the study are included in the article/**Supplementary Material**, further inquiries can be directed to the corresponding authors.

AUTHOR CONTRIBUTIONS

Conceptualization: AC, VG, ZM, DS, NM; Data curation: AC, JM, MS, NR, JK, NA, TS, VP, DS, NM; Formal analysis: AC, JM, MS, NR, DS, NM; Investigation: AC, VG, JM, OM, MS, NR, JK, NA, NM, TS, VP, DS, NM; Methodology: AC, VG, JM, DS, NM; Project administration: VG, DS, NM; Supervision: VG, DS, NM; Visualization: AC, JM, MS, DS, NM; Writing – original draft: AC, VG, JM, OM, MS, NR, NA, TS, JK, VP, DS, NM; Writing – review & editing: AC, VG, JM, OM, MS, NR, NA, NM, TS, JK, VP, DS, NM. All authors read and approved the final manuscript.

FUNDING

Funding: NIH R01-HL136348 (VG).

SUPPLEMENTARY MATERIAL

The Supplementary Material for this article can be found online at: https://www.frontiersin.org/articles/10.3389/fbioe.2021.782845/full#supplementary-material

REFERENCES

Abalos, E., Cuesta, C., Grosso, A. L., Chou, D., and Say, L. (2013). Global and Regional Estimates of Preeclampsia and Eclampsia: A Systematic Review. *Eur. J. Obstet. Gynecol. Reprod. Biol.* 170, 1–7. doi:10.1016/j.ejogrb.2013.05.005

Adel, S., Mansour, A., Louka, M., Matboli, M., Elmekkawi, S. F., and Swelam, N. (2017). Evaluation of MicroRNA-210 and Protein Tyrosine Phosphatase, Non-receptor Type 2 in Pre-eclampsia. *Gene* 596, 105–109. doi:10.1016/j.gene.2016.10.014

Akehurst, C., Small, H. Y., Sharafetdinova, L., Forrest, R., Beattie, W., Brown, C. E., et al. (2015). Differential Expression of microRNA-206 and its Target Genes in Preeclampsia. *J. Hypertens.* 33, 2068–2074. doi:10.1097/HJH.0000000000000656

Akgör, U., Ayaz, L., and Çayan, F. (2021). Expression Levels of Maternal Plasma microRNAs in Preeclamptic Pregnancies. *J. Obstet. Gynaecol.* 41, 910–914. doi:10.1080/01443615.2020.1820465

Ali, Z., Zafar, U., Zaki, S., Ahmad, S., Khaliq, S., and Lone, K. P. (2021). Expression Levels of MiRNA-16, SURVIVIN and TP53 in Preeclamptic and Normotensive Women. *J. Pak. Med. Assoc.* 71, 2208–2213. doi:10.47391/JPMA.1171

American College of Obstetricians and Gynecologists (2019). ACOG Practice Bulletin No. 202: Gestational Hypertension and Preeclampsia. *Obstet. Gynecol.* 133, e1. doi:10.1097/AOG.0000000000003018

Anton, L., Brown, A. G., Parry, S., and Elovitz, M. A. (2012). Lipopolysaccharide Induces Cytokine Production and Decreases Extravillous Trophoblast Invasion through a Mitogen-Activated Protein Kinase-Mediated Pathway: Possible Mechanisms of First Trimester Placental Dysfunction. *Hum. Reprod.* 27, 61–72. doi:10.1093/humrep/der362

Anton, L., Olarerin-George, A. O., Hogenesch, J. B., and Elovitz, M. A. (2015). Placental Expression of miR-517a/b and miR-517c Contributes to Trophoblast Dysfunction and Preeclampsia. *PLoS One* 10, e0122707. doi:10.1371/journal.pone.0122707

Anton, L., Olarerin-George, A. O., Schwartz, N., Srinivas, S., Bastek, J., Hogenesch, J. B., et al. (2013). MiR-210 Inhibits Trophoblast Invasion and Is a Serum Biomarker for Preeclampsia. *Am. J. Pathol.* 183, 1437–1445. doi:10.1016/j.ajpath.2013.07.021

Awamleh, Z., Gloor, G. B., and Han, V. K. M. (2019). Placental microRNAs in Pregnancies with Early Onset Intrauterine Growth Restriction and Preeclampsia: Potential Impact on Gene Expression and Pathophysiology. *BMC Med. Genomics* 12, 91. doi:10.1186/s12920-019-0548-x

Awamleh, Z., and Han, V. K. M. (2020). Identification of miR-210-5p in Human Placentae from Pregnancies Complicated by Preeclampsia and Intrauterine Growth Restriction, and its Potential Role in the Pregnancy Complications. *Pregnancy Hypertens.* 19, 159–168. doi:10.1016/j.preghy.2020.01.002

Ayoub, S. E., Shaker, O. G., Abdelwahed, M. Y., Ahmed, N. A., Abdelhameed, H. G., Bosilah, A. H., et al. (2019). Association of MicroRNA-155rs767649 Polymorphism with Susceptibility to Preeclampsia. *Int. J. Mol. Cel Med* 8, 247–257. doi:10.22088/IJMCM.BUMS.8.4.247

Azizi, F., Saleh Gargari, S., Asadi Shahmirzadi, S., Dodange, F., Amiri, V., Mirfakhraie, R., et al. (2017). Evaluation of Placental Mir-155-5p and Long Non-coding RNA sONE Expression in Patients with Severe Pre-eclampsia. *Int. J. Mol. Cel Med* 6, 22–30.

Bai, Y., Yang, W., Yang, H.-x., Liao, Q., Ye, G., Fu, G., et al. (2012). Downregulated miR-195 Detected in Preeclamptic Placenta Affects Trophoblast Cell Invasion via Modulating ActRIIA Expression. *PLoS One* 7, e38875. doi:10.1371/journal.pone.0038875

Bernstein, E., Kim, S. Y., Carmell, M. A., Murchison, E. P., Alcorn, H., Li, M. Z., et al. (2003). Dicer Is Essential for Mouse Development. *Nat. Genet.* 35, 215–217. doi:10.1038/ng1253

Betoni, J. S., Derr, K., Pahl, M. C., Rogers, L., Muller, C. L., Packard, R. E., et al. (2013). MicroRNA Analysis in Placentas from Patients with Preeclampsia: Comparison of New and Published Results. *Hypertens. Pregnancy* 32, 321–339. doi:10.3109/10641955.2013.807819

Biró, O., Fóthi, Á., Alasztics, B., Nagy, B., Orbán, T. I., and Rigó, J. (2019). Circulating Exosomal and Argonaute-Bound microRNAs in Preeclampsia. *Gene* 692, 138–144. doi:10.1016/j.gene.2019.01.012

Black, K. D., and Horowitz, J. A. (2018). Inflammatory Markers and Preeclampsia. *Nurs. Res.* 67, 242–251. doi:10.1097/NNR.0000000000000285

Brkić, J., Dunk, C., O'Brien, J., Fu, G., Nadeem, L., Wang, Y.-l., et al. (2018). MicroRNA-218-5p Promotes Endovascular Trophoblast Differentiation and Spiral Artery Remodeling. *Mol. Ther.* 26, 2189–2205. doi:10.1016/j.ymthe.2018.07.009

Brodowski, L., Schröder-Heurich, B., von Hardenberg, S., Richter, K., von Kaisenberg, C. S., Dittrich-Breiholz, O., et al. (2021). Microrna Profiles of Maternal and Neonatal Endothelial Progenitor Cells in Preeclampsia. *Ijms* 22, 5320. doi:10.3390/ijms22105320

Cai, H., Li, D., Wu, J., and Shi, C. (2021). MiR-519d Downregulates LEP Expression to Inhibit Preeclampsia Development. *Open Med.* 16, 1215–1227. doi:10.1515/med-2021-0244

Cai, M., Kolluru, G. K., and Ahmed, A. (2017). Small Molecule, Big Prospects: MicroRNA in Pregnancy and its Complications. *J. Pregnancy* 2017, 1–15. doi:10.1155/2017/6972732

Calderon-Dominguez, M., Mangas, A., Belmonte, T., Quezada-Feijoo, M., Ramos, M., and Toro, R. (2021). Ischemic Dilated Cardiomyopathy Pathophysiology through microRNA-16-5p. *Revista Española de Cardiología (English Edition)* 74, 740–749. doi:10.1016/j.rec.2020.08.012

Campos, C. B., Marques, T. M., Pereira, R. W., and Sandrim, V. C. (2014). Reduced Circulating miR-196b Levels Is Associated with Preeclampsia. *Pregnancy Hypertens. Int. J. Women's Cardiovasc. Health* 4, 11–13. doi:10.1016/j.preghy.2013.10.002

Cao, G., Cui, R., Liu, C., and Zhang, Z. (2019). MicroRNA Regulation of Transthyretin in Trophoblast Biofunction and Preeclampsia. *Arch. Biochem. Biophys.* 676, 108129. doi:10.1016/j.abb.2019.108129

Chen, J., Zhao, L., Wang, D., Xu, Y., Gao, H., Tan, W., et al. (2019). Contribution of Regulatory Tcells to Immune Tolerance and Association of microRNA-210 and Foxp3 in P-reeclampsia. *Mol. Med. Rep.* 19, 1150–1158. doi:10.3892/mmr.2018.9733

Chen, S., Zhao, G., Miao, H., Tang, R., Song, Y., Hu, Y., et al. (2015). MicroRNA-494 Inhibits the Growth and Angiogenesis-Regulating Potential of Mesenchymal Stem Cells. *FEBS Lett.* 589, 710–717. doi:10.1016/j.febslet.2015.01.038

Chen, Y.-S., Shen, L., Mai, R.-Q., and Wang, Y. (2014). Levels of microRNA-181b and Plasminogen Activator Inhibitor-1 Are Associated with Hypertensive Disorders Complicating Pregnancy. *Exp. Ther. Med.* 8, 1523–1527. doi:10.3892/etm.2014.1946

Chhabra, R., Dubey, R., and Saini, N. (2010). Cooperative and Individualistic Functions of the microRNAs in the miR-23a~27a~24-2 Cluster and its Implication in Human Diseases. *Mol. Cancer* 9, 232. doi:10.1186/1476-4598-9-232

Chi, Z., and Zhang, M. (2018). Exploration of the Regulation and Control Mechanisms of miR-145 in T-rophoblast C-ell P-roliferation and I-nvasion. *Exp. Ther. Med.* 16, 5298–5304. doi:10.3892/etm.2018.6890

Choi, S.-Y., Yun, J., Lee, O.-J., Han, H.-S., Yeo, M.-K., Lee, M.-A., et al. (2013). MicroRNA Expression Profiles in Placenta with Severe Preeclampsia Using a PNA-Based Microarray. *Placenta* 34, 799–804. doi:10.1016/j.placenta.2013.06.006

Chu, X., Gu, Y., Sheng, W., Sun, J., Morgan, J. A., Lewis, D. F., et al. (2021). Downregulation of miR-126-3p Expression Contributes to Increased Inflammatory Response in Placental Trophoblasts in Preeclampsia. *J. Reprod. Immunol.* 144, 103281. doi:10.1016/j.jri.2021.103281

Cochrane (2021). RevMan 5 Download | Cochrane Training. Available at: https://training.cochrane.org/online-learning/core-software-cochrane-reviews/revman/revman-5-download (Accessed August 26, 2021).

Dai, X., and Cai, Y. (2018). Retracted: Down-regulation of microRNA Let-7d Inhibits the Proliferation and Invasion of Trophoblast Cells in Preeclampsia. *J. Cel. Biochem.* 119, 1141–1151. doi:10.1002/jcb.26282

Dai, Y., Qiu, Z., Diao, Z., Shen, L., Xue, P., Sun, H., et al. (2012). MicroRNA-155 Inhibits Proliferation and Migration of Human Extravillous Trophoblast Derived HTR-8/SVneo Cells via Down-Regulating Cyclin D1. *Placenta* 33, 824–829. doi:10.1016/j.placenta.2012.07.012

Demirer, S., Hocaoglu, M., Turgut, A., Karateke, A., and Komurcu-Bayrak, E. (2020). Expression Profiles of Candidate microRNAs in the Peripheral Blood Leukocytes of Patients with Early- and Late-Onset Preeclampsia versus normal Pregnancies. *Pregnancy Hypertens.* 19, 239–245. doi:10.1016/j.preghy.2019.11.003

Devor, E., Santillan, D., Scroggins, S., Warrier, A., and Santillan, M. (2020). Trimester-specific Plasma Exosome microRNA Expression Profiles in Preeclampsia. *J. Maternal-Fetal Neonatal Med.* 33, 3116–3124. doi:10.1080/14767058.2019.1569614

Digitize graphs and plots (2013). GetData Graph Digitizer - Graph Digitizing Software - Download. Available at: http://getdata-graph-digitizer.com/download.php (Accessed August 26, 2021).

Ding, J., Huang, F., Wu, G., Han, T., Xu, F., Weng, D., et al. (2015). MiR-519d-3p Suppresses Invasion and Migration of Trophoblast Cells via Targeting MMP-2. *PLoS One* 10, e0120321. doi:10.1371/journal.pone.0120321

Dong, D., Khoong, Y., Ko, Y., and Zhang, Y. (2020). microRNA-646 I-nhibits A-ngiogenesis of E-ndothelial P-rogenitor C-ells in P-re-eclamptic P-regnancy by T-argeting the VEGF-A/HIF-1α axis. *Exp. Ther. Med.* 20, 1879–1888. doi:10.3892/etm.2020.8929

Dong, K., Zhang, X., Ma, L., Gao, N., Tang, H., Jian, F., et al. (2019). Downregulations of Circulating miR-31 and miR-21 Are Associated with Preeclampsia. *Pregnancy Hypertens.* 17, 59–63. doi:10.1016/j.preghy.2019.05.013

Doridot, L., Houry, D., Gaillard, H., Chelbi, S. T., Barbaux, S., and Vaiman, D. (2014). miR-34A Expression, Epigenetic Regulation, and Function in Human Placental Diseases. *Epigenetics* 9, 142–151. doi:10.4161/epi.26196

Eghbal-Fard, S., Yousefi, M., Heydarlou, H., Ahmadi, M., Taghavi, S., Movasaghpour, A., et al. (2019). The Imbalance of Th17/Treg axis Involved in the Pathogenesis of Preeclampsia. *J. Cel. Physiol.* 234, 5106–5116. doi:10.1002/jcp.27315

Enquobahrie, D. A., Abetew, D. F., Sorensen, T. K., Willoughby, D., Chidambaram, K., and Williams, M. A. (2011). Placental microRNA Expression in Pregnancies Complicated by Preeclampsia. *Am. J. Obstet. Gynecol.* 204, 178e12–178. e21. doi:10.1016/j.ajog.2010.09.004

Fan, Y., Dong, Z., Zhou, G., Fu, J., Zhan, L., Gao, M., et al. (2020). Elevated miR-23a Impairs Trophoblast Migration and Invasiveness through HDAC2 Inhibition and NF-Kb Activation. *Life Sci.* 261, 118358. doi:10.1016/j.lfs.2020.118358

Fang, M., Du, H., Han, B., Xia, G., Shi, X., Zhang, F., et al. (2017). Hypoxia-inducible microRNA-218 Inhibits Trophoblast Invasion by Targeting LASP1: Implications for Preeclampsia Development. *Int. J. Biochem. Cel Biol.* 87, 95–103. doi:10.1016/j.biocel.2017.04.005

Fang, Y., Huang, Z., Tan, W., Zhang, Q., and Wu, J. (2018). High Expression of miR-182-5p Promotes Preeclampsia Progression. *Eur. Rev. Med. Pharmacol. Sci.* 22, 6583–6590. doi:10.26355/eurrev_201810_16132

Fu, G., Ye, G., Nadeem, L., Ji, L., Manchanda, T., Wang, Y., et al. (2013). MicroRNA-376c Impairs Transforming Growth Factor-β and Nodal Signaling to Promote Trophoblast Cell Proliferation and Invasion. *Hypertension* 61, 864–872. doi:10.1161/HYPERTENSIONAHA.111.203489

Gan, L., Liu, Z., Wei, M., Chen, Y., Yang, X., Chen, L., et al. (2017). MIR-210 and miR-155 as Potential Diagnostic Markers for Pre-eclampsia Pregnancies. *Med. (United States* 96, e7515. doi:10.1097/MD.0000000000007515

Gao, S., Wang, Y., Han, S., and Zhang, Q. (2017). Up-regulated microRNA-300 in Maternal Whole Peripheral Blood and Placenta Associated with Pregnancy-Induced Hypertension and Preeclampsia. *Int. J. Clin. Exp. Pathol.* 10, 4232–4242.

Gao, X., Li, H., and Wei, J. X. (2018a). MiR-4421 Regulates the Progression of Preeclampsia by Regulating CYP11B2. *Eur. Rev. Med. Pharmacol. Sci.* 22, 1533–1540. doi:10.26355/eurrev_201803_14557

Gao, Y., She, R., Wang, Q., Li, Y., and Zhang, H. (2018b). Up-regulation of miR-299 Suppressed the Invasion and Migration of HTR-8/SVneo Trophoblast Cells Partly via Targeting HDAC2 in Pre-eclampsia. *Biomed. Pharmacother.* 97, 1222–1228. doi:10.1016/j.biopha.2017.11.053

Garovic, V. D., Wagner, S. J., Turner, S. T., Rosenthal, D. W., Watson, W. J., Brost, B. C., et al. (2007). Urinary Podocyte Excretion as a Marker for Preeclampsia. *Am. J. Obstet. Gynecol.* 196, 320e1–320. e7. doi:10.1016/j.ajog.2007.02.007

Garovic, V. D., White, W. M., Vaughan, L., Saiki, M., Parashuram, S., Garcia-Valencia, O., et al. (2020). Incidence and Long-Term Outcomes of Hypertensive Disorders of Pregnancy. *J. Am. Coll. Cardiol.* 75, 2323–2334. doi:10.1016/j.jacc.2020.03.028

Ge, Q., Zhu, Y., Li, H., Tian, F., Xie, X., and Bai, Y. (2015). Differential Expression of Circulating miRNAs in Maternal Plasma in Pregnancies with Fetal Macrosomia. *Int. J. Mol. Med.* 35, 81–91. doi:10.3892/ijmm.2014.1989

Giannakou, K., Evangelou, E., and Papatheodorou, S. I. (2018). Genetic and Non-genetic Risk Factors for Pre-eclampsia: Umbrella Review of Systematic Reviews and Meta-Analyses of Observational Studies. *Ultrasound Obstet. Gynecol.* 51, 720–730. doi:10.1002/uog.18959

Gong, F., Chai, W., Wang, J., Cheng, H., Shi, Y., Cui, L., et al. (2020). miR-214-5p Suppresses the Proliferation, Migration and Invasion of Trophoblast Cells in Pre-eclampsia by Targeting Jagged 1 to Inhibit Notch Signaling Pathway. *Acta Histochem.* 122, 151527. doi:10.1016/j.acthis.2020.151527

Gunel, T., Hosseini, M. K., Gumusoglu, E., Kisakesen, H. I., Benian, A., and Aydinli, K. (2017). Expression Profiling of Maternal Plasma and Placenta microRNAs in Preeclamptic Pregnancies by Microarray Technology. *Placenta* 52, 77–85. doi:10.1016/j.placenta.2017.02.019

Gunel, T., Kamali, N., Hosseini, M. K., Gumusoglu, E., Benian, A., and Aydinli, K. (2020). Regulatory Effect of miR-195 in the Placental Dysfunction of Preeclampsia. *J. Maternal-Fetal Neonatal Med.* 33, 901–908. doi:10.1080/14767058.2018.1508439

Gunel, T., Zeybek, Y. G., Akçakaya, P., Kalelioglu, I., Benian, A., Ermis, H., et al. (2011). Serum microRNA Expression in Pregnancies with Preeclampsia. *Genet. Mol. Res.* 10, 4034–4040. doi:10.4238/2011.November.8.5

Guo, L., Liu, Y., Guo, Y., Yang, Y., and Chen, B. (2018). MicroRNA-423-5p Inhibits the Progression of Trophoblast Cells via Targeting IGF2BP1. *Placenta* 74, 1–8. doi:10.1016/j.placenta.2018.12.003

Guo, L., Tsai, S. Q., Hardison, N. E., James, A. H., Motsinger-Reif, A. A., Thames, B., et al. (2013). Differentially Expressed microRNAs and Affected Biological Pathways Revealed by Modulated Modularity Clustering (MMC) Analysis of

Human Preeclamptic and IUGR Placentas. *Placenta* 34, 599–605. doi:10.1016/j.placenta.2013.04.007

Guo, L., Yang, Q., Lu, J., Li, H., Ge, Q., Gu, W., et al. (2011). A Comprehensive Survey of miRNA Repertoire and 3′ Addition Events in the Placentas of Patients with Pre-eclampsia from High-Throughput Sequencing. *PLoS One* 6, e21072. doi:10.1371/journal.pone.0021072

Guo, M., Zhao, X., Yuan, X., and Li, P. (2017). Elevated microRNA-34a Contributes to Trophoblast Cell Apoptosis in Preeclampsia by Targeting BCL-2. *J. Hum. Hypertens.* 31, 815–820. doi:10.1038/jhh.2017.65

Han, L., Luo, Q. q., Peng, M. g., Zhang, Y., and Zhu, X. h. (2021). miR -483 Is D Ownregulated in Pre-eclampsia via Targeting Insulin-like Growth Factor 1 (IGF1) and Regulates the PI3K/Akt/mTOR Pathway of Endothelial Progenitor Cells. *J. Obstet. Gynaecol. Res.* 47, 63–72. doi:10.1111/jog.14412

Han, L., Zhao, Y., Luo, Q. Q., Liu, X. X., Lu, S. S., and Zou, L. (2017). The Significance of miR-145 in the Prediction of Preeclampsia. *Bll* 118, 523–528. doi:10.4149/BLL_2017_101

Hanna, N., Hanna, I., Hleb, M., Wagner, E., Dougherty, J., Balkundi, D., et al. (2000). Gestational Age-dependent Expression of IL-10 and its Receptor in Human Placental Tissues and Isolated Cytotrophoblasts. *J. Immunol.* 164, 5721–5728. doi:10.4049/jimmunol.164.11.5721

Harapan, H., and Andalas, M. (2015). The Role of microRNAs in the Proliferation, Differentiation, Invasion, and Apoptosis of Trophoblasts during the Occurrence of Preeclampsia-A Systematic Review. *Tzu Chi Med. J.* 27, 54–64. doi:10.1016/j.tcmj.2015.05.001

Hayder, H., Fu, G., Nadeem, L., O'Brien, J. A., Lye, S. J., and Peng, C. (2021). Overexpression of Mir-210-3p Impairs Extravillous Trophoblast Functions Associated with Uterine Spiral Artery Remodeling. *Ijms* 22, 3961. doi:10.3390/ijms22083961

Hayder, H., O'Brien, J., Nadeem, U., and Peng, C. (2018). MicroRNAs: Crucial Regulators of Placental Development. *Reproduction* 155, R259–R271. doi:10.1530/REP-17-0603

Hemmatzadeh, M., Shomali, N., Yousefzadeh, Y., Mohammadi, H., Ghasemzadeh, A., and Yousefi, M. (2020). MicroRNAs: Small Molecules with a Large Impact on Pre-eclampsia. *J. Cel. Physiol.* 235, 3235–3248. doi:10.1002/jcp.29286

Higgins, J. P., Thomas, J., Chandler, J., Cumpston, M., Li, T., Page, M. J., et al. (2019). *Cochrane Handbook for Systematic Reviews of Interventions*. John Wiley & Sons. doi:10.1002/9781119536604

Hocaoglu, M., Demirer, S., Senturk, H., Turgut, A., and Komurcu-Bayrak, E. (2019). Differential Expression of Candidate Circulating microRNAs in Maternal Blood Leukocytes of the Patients with Preeclampsia and Gestational Diabetes Mellitus. *Pregnancy Hypertens.* 17, 5–11. doi:10.1016/j.preghy.2019.04.004

Hombach, S., and Kretz, M. (2016). Non-coding RNAs: Classification, Biology and Functioning. *Adv. Exp. Med. Biol.* 937, 3–17. doi:10.1007/978-3-319-42059-2_1

Hong, F., Li, Y., and Xu, Y. (2014). Decreased Placental miR-126 Expression and Vascular Endothelial Growth Factor Levels in Patients with Pre-eclampsia. *J. Int. Med. Res.* 42, 1243–1251. doi:10.1177/0300060514540627

Hromadnikova, I., Dvorakova, L., Kotlabova, K., and Krofta, L. (2019a). The Prediction of Gestational Hypertension, Preeclampsia and Fetal Growth Restriction via the First Trimester Screening of Plasma Exosomal C19MC microRNAs. *Ijms* 20, 2972. doi:10.3390/ijms20122972

Hromadnikova, I., Kotlabova, K., Doucha, J., Dlouha, K., and Krofta, L. (2012). Absolute and Relative Quantification of Placenta-specific MicroRNAs in Maternal Circulation with Placental Insufficiency-Related Complications. *J. Mol. Diagn.* 14, 160–167. doi:10.1016/j.jmoldx.2011.11.003

Hromadnikova, I., Kotlabova, K., Dvorakova, L., and Krofta, L. (2019b). Postpartum Profiling of microRNAs Involved in Pathogenesis of Cardiovascular/cerebrovascular Diseases in Women Exposed to Pregnancy-Related Complications. *Int. J. Cardiol.* 291, 158–167. doi:10.1016/j.ijcard.2019.05.036

Hromadnikova, I., Kotlabova, K., Hympanova, L., and Krofta, L. (2015a). Cardiovascular and Cerebrovascular Disease Associated microRNAS Are Dysregulated in Placental Tissues Affected with Gestational Hypertension, Preeclampsia and Intrauterine Growth Restriction. *PLoS One* 10, e0138383. doi:10.1371/journal.pone.0138383

Hromadnikova, I., Kotlabova, K., Hympanova, L., and Krofta, L. (2016). Gestational Hypertension, Preeclampsia and Intrauterine Growth Restriction Induce Dysregulation of Cardiovascular and Cerebrovascular Disease Associated microRNAs in Maternal Whole Peripheral Blood. *Thromb. Res.* 137, 126–140. doi:10.1016/j.thromres.2015.11.032

Hromadnikova, I., Kotlabova, K., Ivankova, K., Vedmetskaya, Y., and Krofta, L. (2017). Profiling of Cardiovascular and Cerebrovascular Disease Associated microRNA Expression in Umbilical Cord Blood in Gestational Hypertension, Preeclampsia and Fetal Growth Restriction. *Int. J. Cardiol.* 249, 402–409. doi:10.1016/j.ijcard.2017.07.045

Hromadnikova, I., Kotlabova, K., Ondrackova, M., Kestlerova, A., Novotna, V., Hympanova, L., et al. (2013). Circulating C19MC MicroRNAs in Preeclampsia, Gestational Hypertension, and Fetal Growth Restriction. *Mediators Inflamm.* 2013, 1–12. doi:10.1155/2013/186041

Hromadnikova, I., Kotlabova, K., Ondrackova, M., Pirkova, P., Kestlerova, A., Novotna, V., et al. (2015b). Expression Profile of C19MC microRNAs in Placental Tissue in Pregnancy-Related Complications. *DNA Cel Biol.* 34, 437–457. doi:10.1089/dna.2014.2687

Hu, E., Ding, L., Miao, H., Liu, F., Liu, D., Dou, H., et al. (2015). MiR-30a Attenuates Immunosuppressive Functions of IL-1β-elicited Mesenchymal Stem Cells via Targeting TAB3. *FEBS Lett.* 589, 3899–3907. doi:10.1016/j.febslet.2015.11.001

Hu, S., Li, J., Tong, M., Li, Q., Chen, Y., Lu, H., et al. (2019). MicroRNA-144-3p M-ay P-articipate in the P-athogenesis of P-reeclampsia by T-argeting Cox-2. *Mol. Med. Rep.* 19, 4655–4662. doi:10.3892/mmr.2019.10150

Hu, T.-X., Guo, X., Wang, G., Gao, L., He, P., Xia, Y., et al. (2017). MiR133b Is Involved in Endogenous Hydrogen Sulfide Suppression of sFlt-1 Production in Human Placenta. *Placenta* 52, 33–40. doi:10.1016/j.placenta.2017.02.012

Hu, T.-X., Wang, G., Guo, X.-J., Sun, Q.-Q., He, P., Gu, H., et al. (2016). MiR 20a,-20b and -200c Are Involved in Hydrogen Sulfide Stimulation of VEGF Production in Human Placental Trophoblasts. *Placenta* 39, 101–110. doi:10.1016/j.placenta.2016.01.019

Hu, Y., Li, P., Hao, S., Liu, L., Zhao, J., and Hou, Y. (2009). Differential Expression of microRNAs in the Placentae of Chinese Patients with Severe Pre-eclampsia. *Clin. Chem. Lab. Med.* 47, 923–929. doi:10.1515/CCLM.2009.228

Huang, J., Zheng, L., Kong, H., Wang, F., Su, Y., and Xin, H. (2020). miR-139-5p Promotes the Proliferation and Invasion of Trophoblast Cells by Targeting sFlt-1 in Preeclampsia. *Placenta* 92, 37–43. doi:10.1016/j.placenta.2020.02.003

Huang, X., Wu, L., Zhang, G., Tang, R., and Zhou, X. (2019). Elevated MicroRNA-181a-5p Contributes to Trophoblast Dysfunction and Preeclampsia. *Reprod. Sci.* 26, 1121–1129. doi:10.1177/1933719118808916

Ishibashi, O., Ohkuchi, A., Ali, M. M., Kurashina, R., Luo, S.-S., Ishikawa, T., et al. (2012). Hydroxysteroid (17-β) Dehydrogenase 1Is Dysregulated byMir-210andMir-518cThat Are Aberrantly Expressed in Preeclamptic Placentas. *Hypertension* 59, 265–273. doi:10.1161/HYPERTENSIONAHA.111.180232

Jairajpuri, D. S., Malalla, Z. H., Mahmood, N., and Almawi, W. Y. (2017). Circulating microRNA Expression as Predictor of Preeclampsia and its Severity. *Gene* 627, 543–548. doi:10.1016/j.gene.2017.07.010

Jairajpuri, D. S., Malalla, Z. H., Sarray, S., and Mahmood, N. (2021). Analysis of Differential Expression of Hypoxia-Inducible microRNA-210 Gene Targets in Mild and Severe Preeclamptic Patients. *Non-coding RNA Res.* 6, 51–57. doi:10.1016/j.ncrna.2021.03.001

Jelena, M., Sopić, M., Joksić, I., Zmrzljak, U. P., Karadžov-Orlić, N., Košir, R., et al. (2020). Placenta-specific Plasma miR518b Is a Potential Biomarker for Preeclampsia. *Clin. Biochem.* 79, 28–33. doi:10.1016/j.clinbiochem.2020.02.012

Jiang, F., Li, J., Wu, G., Miao, Z., Lu, L., Ren, G., et al. (2015). Upregulation of microRNA-335 and microRNA-584 Contributes to the Pathogenesis of Severe Preeclampsia through Downregulation of Endothelial Nitric Oxide Synthase. *Mol. Med. Rep.* 12, 5383–5390. doi:10.3892/mmr.2015.4018

Jiang, L., Long, A., Tan, L., Hong, M., Wu, J., Cai, L., et al. (2017). Elevated microRNA-520g in Pre-eclampsia Inhibits Migration and Invasion of Trophoblasts. *Placenta* 51, 70–75. doi:10.1016/j.placenta.2017.02.001

Jin, M., Li, H., Xu, H., Huo, G., and Yao, Y. (2017). MicroRNA-20b Inhibits Trophoblast Cell Migration and Invasion by Targeting MMP-2. *Int. J. Clin. Exp. Pathol.* 10, 10901–10909.

Kamali Simsek, N., Benian, A., Sevgin, K., Ergun, Y., Goksever Celik, H., Karahuseyinoglu, S., et al. (2021). Microrna Analysis of Human Decidua Mesenchymal Stromal Cells from Preeclampsia Patients. *Placenta* 115, 12–19. doi:10.1016/j.placenta.2021.09.004

Keiser, S. D., Veillon, E. W., Parrish, M. R., Bennett, W., Cockrell, K., Fournier, L., et al. (2009). Effects of 17-Hydroxyprogesterone on Tumor Necrosis Factor-

-Induced Hypertension during Pregnancy. *Am. J. Hypertens.* 22, 1120–1125. doi:10.1038/ajh.2009.149

Khaliq, O. P., Murugesan, S., Moodley, J., and Mackraj, I. (2018). Differential Expression of miRNAs Are Associated with the Insulin Signaling Pathway in Preeclampsia and Gestational Hypertension. *Clin. Exp. Hypertens.* 40, 744–751. doi:10.1080/10641963.2018.1431257

Kim, S., Lee, K.-S., Choi, S., Kim, J., Lee, D.-K., Park, M., et al. (2018). NF-κB-responsive miRNA-31-5p Elicits Endothelial Dysfunction Associated with Preeclampsia via Down-Regulation of Endothelial Nitric-Oxide Synthase. *J. Biol. Chem.* 293, 18989–19000. doi:10.1074/jbc.RA118.005197

Kim, S., Park, M., Kim, J.-Y., Kim, T., Hwang, J., Ha, K.-S., et al. (2020). Circulating miRNAs Associated with Dysregulated Vascular and Trophoblast Function as Target-Based Diagnostic Biomarkers for Preeclampsia. *Cells* 9, 2003. doi:10.3390/cells9092003

Kolkova, Z., Holubekova, V., Grendar, M., Nachajova, M., Zubor, P., Pribulova, T., et al. (2021). Association of Circulating Mirna Expression with Preeclampsia, its Onset, and Severity. *Diagnostics* 11, 476. doi:10.3390/diagnostics11030476

Korkes, H. A., De Oliveira, L., Sass, N., Salahuddin, S., Karumanchi, S. A., and Rajakumar, A. (2017). Relationship between Hypoxia and Downstream Pathogenic Pathways in Preeclampsia. *Hypertens. Pregnancy* 36, 145–150. doi:10.1080/10641955.2016.1259627

Kumar, P., Luo, Y., Tudela, C., Alexander, J. M., and Mendelson, C. R. (2013). The C-Myc-Regulated MicroRNA-17~92 (miR-17~92) and miR-106a~363 Clusters Target hCYP19A1 and hGCM1 to Inhibit Human Trophoblast Differentiation. *Mol. Cel. Biol.* 33, 1782–1796. doi:10.1128/MCB.01228-12

Lalevée, S., Lapaire, O., and Bühler, M. (2014). MiR455 Is Linked to Hypoxia Signaling and Is Deregulated in Preeclampsia. *Cell Death Dis* 5, e1408. doi:10.1038/cddis.2014.368

Lasabová, Z., Vážan, M., Zibolenová, J., Švecová, I., and Lasabová, A. Z. (2015). Overexpression of miR-21 and miR-122 in Preeclamptic Placentas. *Neuro Endocrinol. Lett.* 36, 695–699.

Lázár, L., Nagy, B., Molvarec, A., Szarka, A., and Rigó, J. (2012). Role of Hsa-miR-325 in the Etiopathology of Preeclampsia. *Mol. Med. Rep.* 6, 597–600. doi:10.3892/mmr.2012.954

Lecarpentier, E., and Tsatsaris, V. (2016). Angiogenic Balance (sFlt-1/PlGF) and Preeclampsia. *Ann. d'Endocrinologie* 77, 97–100. doi:10.1016/j.ando.2016.04.007

Li, H., Ge, Q., Guo, L., and Lu, Z. (2013a). Maternal Plasma miRNAs Expression in Preeclamptic Pregnancies. *Biomed. Res. Int.* 2013, 1–9. doi:10.1155/2013/970265

Li, H. Q., Fan, J. J., Li, X. H., and Bao, D. (2020a). MiR-507 Inhibits the Growth and Invasion of Trophoblasts by Targeting CAMK4. *Eur. Rev. Med. Pharmacol. Sci.* 24, 5856–5862. doi:10.26355/eurrev_202006_21477

Li, J., Du, J., Wang, Z., Wang, C., Bai, J., and Zhang, S. (2018). Expression of miR-376 in B-lood of P-regnant W-omen with P-reeclampsia and its E-ffect on 25-hydroxyvitamin D. *Exp. Ther. Med.* 16, 1701–1706. doi:10.3892/etm.2018.6394

Li, J., Zhao, Y., Lu, Y., Ritchie, W., Grau, G., Vadas, M. A., et al. (2016). The Poly-Cistronic miR-23-27-24 Complexes Target Endothelial Cell Junctions: Differential Functional and Molecular Effects of miR-23a and miR-23b. *Mol. Ther. - Nucleic Acids* 5, e354. doi:10.1038/mtna.2016.62

Li, L., Hou, A., Gao, X., Zhang, J., Zhang, L., Wang, J., et al. (2017a). Lentivirus-mediated miR-23a Overexpression Induces Trophoblast Cell Apoptosis through Inhibiting X-Linked Inhibitor of Apoptosis. *Biomed. Pharmacother.* 94, 412–417. doi:10.1016/j.biopha.2017.07.082

Li, P., Guo, W., Du, L., Zhao, J., Wang, Y., Liu, L., et al. (2013b). MicroRNA-29b Contributes to Pre-eclampsia through its Effects on Apoptosis, Invasion and Angiogenesis of Trophoblast Cells. *Clin. Sci.* 124, 27–40. doi:10.1042/CS20120121

Li, Q., Han, Y., Xu, P., Yin, L., Si, Y., Zhang, C., et al. (2020b). Elevated microRNA-125b Inhibits Cytotrophoblast Invasion and Impairs Endothelial Cell Function in Preeclampsia. *Cell Death Discov.* 6, 35. doi:10.1038/s41420-020-0269-0

Li, Q., Long, A., Jiang, L., Cai, L., Xie, L., Gu, J. A., et al. (2015). Quantification of Preeclampsia-Related microRNAs in Maternal Serum. *Biomed. Rep.* 3, 792–796. doi:10.3892/br.2015.524

Li, Q., Pan, Z., Wang, X., Gao, Z., Ren, C., and Yang, W. (2014a). MiR-125b-1-3p Inhibits Trophoblast Cell Invasion by Targeting Sphingosine-1-Phosphate Receptor 1 in Preeclampsia. *Biochem. Biophysical Res. Commun.* 453, 57–63. doi:10.1016/j.bbrc.2014.09.059

Li, R., Wang, N., Xue, M., Long, W., Cheng, C., Mi, C., et al. (2019). A Potential Regulatory Network Among WDR86-AS1, miR-10b-3p, and LITAF Is Possibly Involved in Preeclampsia Pathogenesis. *Cell Signal.* 55, 40–52. doi:10.1016/j.cellsig.2018.12.006

Li, T., Zhou, B., He, Y., Liu, J., and Li, Y. (2020c). Expression and Clinical Diagnostic Value of miR-383 in Patients with Severe Preeclampsia. *Cel Mol Biol (Noisy-le-grand)* 66, 92–100. doi:10.14715/cmb/2020.66.3.14

Li, W., Yu, N., Fan, L., Chen, S.-H., and Wu, J.-L. (2020d). Circ_0063517 Acts as ceRNA, Targeting the miR-31-5p-ETBR axis to Regulate Angiogenesis of Vascular Endothelial Cells in Preeclampsia. *Life Sci.* 244, 117306. doi:10.1016/j.lfs.2020.117306

Li, X., Li, C., Dong, X., and Gou, W. (2014b). MicroRNA-155 Inhibits Migration of Trophoblast Cells and Contributes to the Pathogenesis of Severe Preeclampsia by Regulating Endothelial Nitric Oxide Synthase. *Mol. Med. Rep.* 10, 550–554. doi:10.3892/mmr.2014.2214

Li, X., Song, Y., Liu, D., Zhao, J., Xu, J., Ren, J., et al. (2017b). MiR-495 Promotes Senescence of Mesenchymal Stem Cells by Targeting Bmi-1. *Cell. Physiol. Biochem.* 42, 780–796. doi:10.1159/000478069

Liao, G., Cheng, D., Li, J., and Hu, S. (2021). Clinical Significance of microRNA-320a and Insulin-like Growth Factor-1 Receptor in Early-Onset Preeclampsia Patients. *Eur. J. Obstet. Gynecol. Reprod. Biol.* 263, 164–170. doi:10.1016/j.ejogrb.2021.06.032

Liberati, A., Altman, D. G., Tetzlaff, J., Mulrow, C., Gøtzsche, P. C., Ioannidis, J. P. A., et al. (2009). The PRISMA Statement for Reporting Systematic Reviews and Meta-Analyses of Studies that Evaluate Health Care Interventions: Explanation and Elaboration. *Plos Med.* 6, e1000100. doi:10.1371/journal.pmed.1000100

Licini, C., Avellini, C., Picchiassi, E., Mensà, E., Fantone, S., Ramini, D., et al. (2021). Pre-eclampsia Predictive Ability of Maternal miR-125b: a Clinical and Experimental Study. *Translational Res.* 228, 13–27. doi:10.1016/j.trsl.2020.07.011

Lip, S. V., Boekschoten, M. V., Hooiveld, G. J., van Pampus, M. G., Scherjon, S. A., Plösch, T., et al. (2020). Early-onset Preeclampsia, Plasma microRNAs, and Endothelial Cell Function. *Am. J. Obstet. Gynecol.* 222, 497e1–497. e12. doi:10.1016/j.ajog.2019.11.1286

Lisabeth, E. M., Falivelli, G., and Pasquale, E. B. (2013). Eph Receptor Signaling and Ephrins. *Cold Spring Harbor Perspect. Biol.* 5, a009159. doi:10.1101/cshperspect.a009159

Liu, B., Liu, L., Cui, S., Qi, Y., and Wang, T. (2021). Expression and Significance of microRNA -126 and VCAM -1 in Placental Tissues of Women with Early-onset Preeclampsia. *J. Obstet. Gynaecol. Res.* 47, 2042–2050. doi:10.1111/jog.14732

Liu, E., Liu, Z., Zhou, Y., Chen, M., Wang, L., and Li, J. (2019a). MicroRNA-142-3p I-nhibits T-rophoblast C-ell M-igration and I-nvasion by D-isrupting the TGF-β1/Smad3 S-ignaling P-athway. *Mol. Med. Rep.* 49, 3775–3782. doi:10.3892/mmr.2019.9997

Liu, F., Wu, K., Wu, W., Chen, Y., Wu, H., Wang, H., et al. (2018). miR-203 C-ontributes to P-re-eclampsia via I-nhibition of VEGFA E-xpression. *Mol. Med. Rep.* 17, 5627–5634. doi:10.3892/mmr.2018.8558

Liu, J. J., Zhang, L., Zhang, F. F., Luan, T., Yin, Z. M., Rui, C., et al. (2019b). Influence of miR-34a on Preeclampsia through the Notch Signaling Pathway. *Eur. Rev. Med. Pharmacol. Sci.* 23, 923–931. doi:10.26355/eurrev_201902_16978

Liu, L., Wang, Y., Fan, H., Zhao, X., Liu, D., Hu, Y., et al. (2012). MicroRNA-181a Regulates Local Immune Balance by Inhibiting Proliferation and Immunosuppressive Properties of Mesenchymal Stem Cells. *Stem Cells* 30, 1756–1770. doi:10.1002/stem.1156

Liu, W., Liu, T., Jiang, F., Liu, C., Zhao, X., Gao, Y., et al. (2011). microRNA-155 Regulates Angiotensin II Type 1 Receptor Expression in Umbilical Vein Endothelial Cells from Severely Pre-eclamptic Pregnant Women. *Int. J. Mol. Med.* 27, 393–399. doi:10.3892/ijmm.2011.598

Liu, Z., Zhao, X., Shan, H., Gao, H., and Wang, P. (2019c). microRNA-520c-3p Suppresses NLRP3 Inflammasome Activation and Inflammatory cascade in Preeclampsia by Downregulating NLRP3. *Inflamm. Res.* 68, 643–654. doi:10.1007/s00011-019-01246-8

Lou, C. X., Zhou, X. T., Tian, Q. C., Xie, H. Q., and Zhang, J. Y. (2018). Low Expression of microRNA-21 Inhibits Trophoblast Cell Infiltration through Targeting PTEN. *Eur. Rev. Med. Pharmacol. Sci.* 22, 6181–6189. doi:10.26355/eurrev_201810_16023

Lu, T.-M., Lu, W., and Zhao, L.-J. (2017). MicroRNA-137 Affects Proliferation and Migration of Placenta Trophoblast Cells in Preeclampsia by Targeting ERRα. *Reprod. Sci.* 24, 85–96. doi:10.1177/1933719116650754

Luizon, M. R., Conceição, I. M. C. A., Viana-Mattioli, S., Caldeira-Dias, M., Cavalli, R. C., and Sandrim, V. C. (2021). Circulating MicroRNAs in the Second Trimester from Pregnant Women Who Subsequently Developed Preeclampsia: Potential Candidates as Predictive Biomarkers and Pathway Analysis for Target Genes of miR-204-5p. *Front. Physiol.* 12, 678184. doi:10.3389/fphys.2021.678184

Luo, R., Shao, X., Xu, P., Liu, Y., Wang, Y., Zhao, Y., et al. (2014). MicroRNA-210 Contributes to Preeclampsia by Downregulating Potassium Channel Modulatory Factor 1. *Hypertension* 64, 839–845. doi:10.1161/HYPERTENSIONAHA.114.03530

Luo, S., Cao, N., Tang, Y., and Gu, W. (2017a). Identification of Key microRNAs and Genes in Preeclampsia by Bioinformatics Analysis. *PLoS One* 12, e0178549. doi:10.1371/journal.pone.0178549

Luo, S., Li, H., Cao, N., Tang, Y., and Gu, W. (2017b). MicroRNA-148a Affects Functions of Placental Trophoblast Cells in Preeclampsia by Regulating HLA-G. *Int. J. Clin. Exp. Pathol.* 10, 5205–5212.

Luque, A., Farwati, A., Crovetto, F., Crispi, F., Figueras, F., Gratacós, E., et al. (2014). Usefulness of Circulating microRNAs for the Prediction of Early Preeclampsia at First-Trimester of Pregnancy. *Sci. Rep.* 4, 4882. doi:10.1038/srep04882

Lv, Y., Lu, X., Li, C., Fan, Y., Ji, X., Long, W., et al. (2019). miR-145-5p Promotes Trophoblast Cell Growth and Invasion by Targeting FLT1. *Life Sci.* 239, 117008. doi:10.1016/j.lfs.2019.117008

Lykoudi, A., Kolialexi, A., Lambrou, G. I., Braoudaki, M., Siristatidis, C., Papaioanou, G. K., et al. (2018). Dysregulated Placental microRNAs in Early and Late Onset Preeclampsia. *Placenta* 61, 24–32. doi:10.1016/j.placenta.2017.11.005

Ma, H. Y., Cu, W., Sun, Y. H., and Chen, X. (2020). MiRNA-203a-3p Inhibits Inflammatory Response in Preeclampsia through Regulating IL24. *Eur. Rev. Med. Pharmacol. Sci.* 24, 5223–5230. doi:10.26355/eurrev_202005_21304

Ma, R., Lu, Y., Dou, C., and Gu, Q. (2019). Clinical Significance of miR-133a and miR-206 in Pregnant Women with Preeclampsia and Correlation with Pregnancy Outcomes. *Int. J. Clin. Exp. Med.* 12, 7383–7391.

Mao, Y., Hou, B., Shan, L., Sun, X., and Wang, L. (2021). Aberrantly Up-Regulated miR-142-3p Inhibited the Proliferation and Invasion of Trophoblast Cells by Regulating FOXM1. *Placenta* 104, 253–260. doi:10.1016/j.placenta.2021.01.002

Martinez-Fierro, M. L., Carrillo-Arriaga, J. G., Luevano, M., Lugo-Trampe, A., Delgado-Enciso, I., Rodriguez-Sanchez, I. P., et al. (2019). Serum Levels of miR-628-3p and miR-628-5p during the Early Pregnancy Are Increased in Women Who Subsequently Develop Preeclampsia. *Pregnancy Hypertens.* 16, 120–125. doi:10.1016/j.preghy.2019.03.012

Martinez-Fierro, M. L., and Garza-Veloz, I. (2021). Analysis of Circulating Microrna Signatures and Preeclampsia Development. *Cells* 10, 1003. doi:10.3390/cells10051003

Martinez-Fierro, M. L., Garza-Veloz, I., Gutierrez-Arteaga, C., Delgado-Enciso, I., Barbosa-Cisneros, O. Y., Flores-Morales, V., et al. (2018). Circulating Levels of Specific Members of Chromosome 19 microRNA Cluster Are Associated with Preeclampsia Development. *Arch. Gynecol. Obstet.* 297, 365–371. doi:10.1007/s00404-017-4611-6

Mavreli, D., Lykoudi, A., Lambrou, G., Papaioannou, G., Vrachnis, N., Kalantaridou, S., et al. (2020). Deep Sequencing Identified Dysregulated Circulating MicroRNAs in Late Onset Preeclampsia. *In Vivo* 34, 2317–2324. doi:10.21873/invivo.12044

Mayor-Lynn, K., Toloubeydokhti, T., Cruz, A. C., and Chegini, N. (2011). Expression Profile of microRNAs and mRNAs in Human Placentas from Pregnancies Complicated by Preeclampsia and Preterm Labor. *Reprod. Sci.* 18, 46–56. doi:10.1177/1933719110374115

McElrath, T. F., Cantonwine, D. E., Gray, K. J., Mirzakhani, H., Doss, R. C., Khaja, N., et al. (2020). Late First Trimester Circulating Microparticle Proteins Predict the Risk of Preeclampsia. *Sci. Rep.* 10, 17353. doi:10.1038/s41598-020-74078-w

Mei, Z., Huang, B., Zhang, Y., Qian, X., Mo, Y., and Deng, N. (2019). Histone Deacetylase 6 Negatively Regulated microRNA-199a-5p Induces the Occurrence of Preeclampsia by Targeting VEGFA *In Vitro*. *Biomed. Pharmacother.* 114, 108805. doi:10.1016/j.biopha.2019.108805

Meng, H.-X., Xu, L.-N., Jing, G., Qian, L., and Qi, M.-G. (2017). MiR-223 Promotes Trophoblast Cell Survival and Invasion by Targeting STAT3 in Preeclampsia. *Int. J. Clin. Exp. Med.* 10, 6577–6585.

Miura, K., Higashijima, A., Murakami, Y., Tsukamoto, O., Hasegawa, Y., Abe, S., et al. (2015). Circulating Chromosome 19 miRNA Cluster microRNAs in Pregnant Women with Severe Pre-eclampsia. *J. Obstet. Gynaecol. Res.* 41, 1526–1532. doi:10.1111/jog.12749

Motawi, T. M. k., Sabry, D., Maurice, N. W., and Rizk, S. M. (2018). Role of Mesenchymal Stem Cells Exosomes Derived microRNAs; miR-136, miR-494 and miR-495 in Pre-eclampsia Diagnosis and Evaluation. *Arch. Biochem. Biophys.* 659, 13–21. doi:10.1016/j.abb.2018.09.023

Mouillet, J.-F., Ouyang, Y., Coyne, C. B., and Sadovsky, Y. (2015). MicroRNAs in Placental Health and Disease. *Am. J. Obstet. Gynecol.* 213, S163–S172. doi:10.1016/j.ajog.2015.05.057

Munaut, C., Tebache, L., Blacher, S., Noël, A., Nisolle, M., and Chantraine, F. (2016). Dysregulated Circulating miRNAs in Preeclampsia. *Biomed. Rep.* 5, 686–692. doi:10.3892/br.2016.779

Muralimanoharan, S., Maloyan, A., Mele, J., Guo, C., Myatt, L. G., and Myatt, L. (2012). MIR-210 Modulates Mitochondrial Respiration in Placenta with Preeclampsia. *Placenta* 33, 816–823. doi:10.1016/j.placenta.2012.07.002

Murphy, M. S.-Q., Casselman, R. C., Tayade, C., and Smith, G. N. (2015). Differential Expression of Plasma microRNA in Preeclamptic Patients at Delivery and 1 Year Postpartum. *Am. J. Obstet. Gynecol.* 213, 367e1–367.e9. doi:10.1016/j.ajog.2015.05.013

Nejad, R. M. A., Saeidi, K., Gharbi, S., Salari, Z., and Saleh-Gohari, N. (2019). Quantification of Circulating miR-517c-3p and miR-210-3p Levels in Preeclampsia. *Pregnancy Hypertens.* 16, 75–78. doi:10.1016/j.preghy.2019.03.004

Niu, Z.-r., Han, T., SunluanLuanxia, X., Luan, L.-x., Gou, W.-l., and Zhu, X.-m. (2018). MicroRNA-30a-3p Is Overexpressed in the Placentas of Patients with Preeclampsia and Affects Trophoblast Invasion and Apoptosis by its Effects on IGF-1. *Am. J. Obstet. Gynecol.* 218, 249e1–249. e12. doi:10.1016/j.ajog.2017.11.568

Nizyaeva, N. V., Kulikova, G. V., Nagovitsyna, M. N., Kan, N. E., Prozorovskaya, K. N., and Shchegolev, A. I. (2018). Change in OncomicroRNA Expression in the Placenta during Preeclampsia. *Bull. Exp. Biol. Med.* 165, 793–797. doi:10.1007/s10517-018-4267-7

Nizyaeva, N. V., Kulikova, G. V., Nagovitsyna, M. N., Kan, N. E., Prozorovskaya, K. N., Shchegolev, A. I., et al. (2017). Expression of MicroRNA-146a and MicroRNA-155 in Placental Villi in Early- and Late-Onset Preeclampsia. *Bull. Exp. Biol. Med.* 163, 394–399. doi:10.1007/s10517-017-3812-0

Ospina-Prieto, S., Chaiwangyen, W., Herrmann, J., Groten, T., Schleussner, E., Markert, U. R., et al. (2016). MicroRNA-141 Is Upregulated in Preeclamptic Placentae and Regulates Trophoblast Invasion and Intercellular Communication. *Translational Res.* 172, 61–72. doi:10.1016/j.trsl.2016.02.012

Pasquale, E. B. (2005). Eph Receptor Signalling Casts a Wide Net on Cell Behaviour. *Nat. Rev. Mol. Cel Biol.* 6, 462–475. doi:10.1038/nrm1662

Peng, P., Song, H., Xie, C., Zheng, W., Ma, H., Xin, D., et al. (2021). miR-146a-5p-mediated Suppression on Trophoblast Cell Progression and Epithelial-Mesenchymal Transition in Preeclampsia. *Biol. Res.* 54, 30. doi:10.1186/s40659-021-00351-5

Pillay, P., Vatish, M., Duarte, R., Moodley, J., and Mackraj, I. (2019). Exosomal microRNA Profiling in Early and Late Onset Preeclamptic Pregnant Women Reflects Pathophysiology. *Ijn* 14, 5637–5657. doi:10.2147/IJN.S208865

Pineles, B. L., Romero, R., Montenegro, D., Tarca, A. L., Han, Y. M., Kim, Y. M., et al. (2007). Distinct Subsets of microRNAs Are Expressed Differentially in the Human Placentas of Patients with Preeclampsia. *Am. J. Obstet. Gynecol.* 196, 261e1–261. e6. doi:10.1016/j.ajog.2007.01.008

Qian, S., and Liu, R. (2019). miR-30b Facilitates Preeclampsia through Targeting MXRA5 to Inhibit the Viability, Invasion and Apoptosis of Placental Trophoblast Cells. *Int. J. Clin. Exp. Pathol.* 12, 4057–4065.

Salomon, C., Guanzon, D., Scholz-Romero, K., Longo, S., Correa, P., Illanes, S. E., et al. (2017). Placental Exosomes as Early Biomarker of Preeclampsia: Potential Role of Exosomal MicroRNAs across Gestation. *J. Clin. Endocrinol. Metab.* 102, 3182–3194. doi:10.1210/jc.2017-00672

Sandrim, V. C., Dias, M. C., Bovolato, A. L. d. C., Tanus-Santos, J. E., Deffune, E., and Cavalli, R. C. (2016a). Plasma from Pre-eclamptic Patients Induces the Expression of the Anti-angiogenic miR-195-5p in Endothelial Cells. *J. Cel. Mol. Med.* 20, 1198–1200. doi:10.1111/jcmm.12767

Sandrim, V., Luizon, M., Palei, A., Tanus-Santos, J., and Cavalli, R. (2016b). Circulating microRNA Expression Profiles in Pre-eclampsia: Evidence of Increased miR-885-5p Levels. *Bjog: Int. J. Obstet. Gy* 123, 2120–2128. doi:10.1111/1471-0528.13903

Sekar, D., Lakshmanan, G., Mani, P., and Biruntha, M. (2019). Methylation-dependent Circulating microRNA 510 in Preeclampsia Patients. *Hypertens. Res.* 42, 1647–1648. doi:10.1038/s41440-019-0269-8

Shao, X., Liu, Y., Liu, M., Wang, Y., Yan, L., Wang, H., et al. (2017). Testosterone Represses Estrogen Signaling by Upregulating miR-22. *Hypertension* 69, 721–730. doi:10.1161/HYPERTENSIONAHA.116.08468

Sheikh, A. M., Small, H. Y., Currie, G., and Delles, C. (2016). Systematic Review of Micro-RNA Expression in Pre-eclampsia Identifies a Number of Common Pathways Associated with the Disease. *PLoS One* 11, e0160808. doi:10.1371/journal.pone.0160808

Shen, L., Li, Y., Li, R., Diao, Z., Yany, M., Wu, M., et al. (2018). Placenta-associated S-erum E-xosomal miR-155 D-erived from P-atients with P-reeclampsia I-nhibits eNOS E-xpression in H-uman U-mbilical V-ein E-ndothelial C-ells. *Int. J. Mol. Med.* 41, 1731–1739. doi:10.3892/ijmm.2018.3367

Sheng, C., Zhao, Y., and Zhu, L. (2020). Down-regulation of EDN1 Gene Expression by Circulating miR-206 Is Associated with Risk of Preeclampsia. *Medicine (Baltimore)* 99, e20319. doi:10.1097/MD.0000000000020319

Shi, Z., She, K., Li, H., Yuan, X., Han, X., and Wang, Y. (2019). MicroRNA-454 Contributes to Sustaining the Proliferation and Invasion of Trophoblast Cells through Inhibiting Nodal/ALK7 Signaling in Pre-eclampsia. *Chemico-Biological Interactions* 298, 8–14. doi:10.1016/j.cbi.2018.10.012

Singh, K., Williams, J., Brown, J., Wang, E. T., Lee, B., Gonzalez, T. L., et al. (2017). Up-regulation of microRNA-202-3p in First Trimester Placenta of Pregnancies Destined to Develop Severe Preeclampsia, a Pilot Study. *Pregnancy Hypertens.* 10, 7–9. doi:10.1016/j.preghy.2017.04.002

Song, H., Wang, X., Li, J. C., and Lv, Y. H. (2020). MiR-655-3p Inhibits Growth and Invasiveness of Trophoblasts via Targeting PBX3 and Thus Deteriorates Preeclampsia. *Eur. Rev. Med. Pharmacol. Sci.* 24, 10346–10351. doi:10.26355/eurrev_202010_23383

Spence, T., Allsopp, P. J., Yeates, A. J., Mulhern, M. S., Strain, J. J., and McSorley, E. M. (2021). Maternal Serum Cytokine Concentrations in Healthy Pregnancy and Preeclampsia. *J. Pregnancy* 2021, 1–33. doi:10.1155/2021/6649608

Stroup, D. F., Berlin, J. A., Morton, S. C., Olkin, I., Williamson, G. D., Rennie, D., et al. (2000). Meta-analysis of Observational Studies in EpidemiologyA Proposal for Reporting. *JAMA* 283, 2008–2012. doi:10.1001/jama.283.15.2008

Sun, M., Chen, H., Liu, J., Tong, C., and Meng, T. (2015). MicroRNA-34a Inhibits Human Trophoblast Cell Invasion by Targeting MYC. *BMC Cel Biol* 16, 21. doi:10.1186/s12860-015-0068-2

Tang, Q., Gui, J., Wu, X., and Wu, W. (2019). Downregulation of miR-424 in Placenta Is Associated with Severe Preeclampsia. *Pregnancy Hypertens.* 17, 109–112. doi:10.1016/j.preghy.2019.05.017

Tao, J., Xia, L.-Z., Liang, L., Chen, Y., Wei, D., Meng, J., et al. (2020). MiR-124-3p Promotes Trophoblast Cell HTR-8/SVneo Pyroptosis by Targeting Placental Growth Factor. *Placenta* 101, 176–184. doi:10.1016/j.placenta.2020.08.011

Taravati, A., and Tohidi, F. (2018). Comprehensive Analysis of Oxidative Stress Markers and Antioxidants Status in Preeclampsia. *Taiwanese J. Obstet. Gynecol.* 57, 779–790. doi:10.1016/j.tjog.2018.10.002

Timofeeva, A. V., Gusar, V. A., Kan, N. E., Prozorovskaya, K. N., Karapetyan, A. O., Bayev, O. R., et al. (2018). Identification of Potential Early Biomarkers of Preeclampsia. *Placenta* 61, 61–71. doi:10.1016/j.placenta.2017.11.011

Truong, G., Guanzon, D., Kinhal, V., Elfeky, O., Lai, A., Longo, S., et al. (2017). Oxygen Tension Regulates the miRNA Profile and Bioactivity of Exosomes Released from Extravillous Trophoblast Cells - Liquid Biopsies for Monitoring Complications of Pregnancy. *PLoS One* 12, e0174514. doi:10.1371/journal.pone.0174514

Tsai, P.-Y., Li, S.-H., Chen, W.-N., Tsai, H.-L., and Su, M.-T. (2017). Differential miR-346 and miR-582-3p Expression in Association with Selected Maternal and Fetal Complications. *Ijms* 18, 1570. doi:10.3390/ijms18071570

Ura, B., Feriotto, G., Monasta, L., Bilel, S., Zweyer, M., and Celeghini, C. (2014). Potential Role of Circulating microRNAs as Early Markers of Preeclampsia. *Taiwanese J. Obstet. Gynecol.* 53, 232–234. doi:10.1016/j.tjog.2014.03.001

Vashukova, E. S., Glotov, A. S., Fedotov, P. V., Efimova, O. A., Pakin, V. S., Mozgovaya, E. V., et al. (2016). Placental microRNA Expression in Pregnancies Complicated by Superimposed Pre-eclampsia on Chronic Hypertension. *Mol. Med. Rep.* 14, 22–32. doi:10.3892/mmr.2016.5268

Wang, C. Y., Tsai, P. Y., Chen, T. Y., Tsai, H. L., Kuo, P. L., and Su, M. T. (2019a). Elevated miR-200a and miR-141 Inhibit Endocrine Gland-derived Vascular Endothelial Growth Factor Expression and Ciliogenesis in Preeclampsia. *J. Physiol.* 597, 3069–3083. doi:10.1113/JP277704

Wang, F., and Yan, J. (2018). MicroRNA-454 Is Involved in Regulating Trophoblast Cell Proliferation, Apoptosis, and Invasion in Preeclampsia by Modulating the Expression of Ephrin Receptor B4. *Biomed. Pharmacother.* 107, 746–753. doi:10.1016/j.biopha.2018.08.055

Wang, H., Zhang, L., Guo, X., Bai, Y., Li, Y.-X., Sha, J., et al. (2018a). MiR-195 Modulates Oxidative Stress-Induced Apoptosis and Mitochondrial Energy Production in Human Trophoblasts via Flavin Adenine Dinucleotide-dependent Oxidoreductase Domain-Containing Protein 1 and Pyruvate Dehydrogenase Phosphatase Regulatory Subunit. *J. Hypertens.* 36, 306–318. doi:10.1097/HJH.0000000000001529

Wang, N., Feng, Y., Xu, J., Zou, J., Chen, M., He, Y., et al. (2018b). miR-362-3p Regulates Cell Proliferation, Migration and Invasion of Trophoblastic Cells under Hypoxia through Targeting Pax3. *Biomed. Pharmacother.* 99, 462–468. doi:10.1016/j.biopha.2018.01.089

Wang, N., Li, R., and Xue, M. (2019b). Potential Regulatory Network in the PSG10P/miR-19a-3p/IL1RAP Pathway Is Possibly Involved in Preeclampsia Pathogenesis. *J. Cel. Mol. Med.* 23, 852–864. doi:10.1111/jcmm.13985

Wang, R., Liu, W., Liu, X., Liu, X., Tao, H., Wu, D., et al. (2019c). MicroRNA-210 Regulates Human Trophoblast Cell Line HTR-8/SVneo Function by Attenuating Notch1 Expression: Implications for the Role of microRNA-210 in Pre-eclampsia. *Mol. Reprod. Dev.* 86, 896–907. doi:10.1002/mrd.23154

Wang, S., Wang, X., Weng, Z., Zhang, S., Ning, H., and Li, B. (2017). Expression and Role of microRNA 18b and Hypoxia Inducible Factor-1α in P-lacental T-issues of P-reeclampsia P-atients. *Exp. Ther. Med.* 14, 4554–4560. doi:10.3892/etm.2017.5067

Wang, W., Feng, L., Zhang, H., Hachy, S., Satohisa, S., Laurent, L. C., et al. (2012a). Preeclampsia up-regulates angiogenesis-associated microRNA (i.e., miR-17, -20a, and -20b) that target ephrin-B2 and EPHB4 in human placenta. *J. Clin. Endocrinol. Metab.* 97, E1051–E1059. doi:10.1210/jc.2011-3131

Wang, Y., Cheng, K., Zhou, W., Liu, H., Yang, T., Hou, P., et al. (2019d). miR-141-5p Regulate ATF2 via Effecting MAPK1/ERK2 Signaling to Promote Preeclampsia. *Biomed. Pharmacother.* 115, 108953. doi:10.1016/j.biopha.2019.108953

Wang, Y., Dong, Q., Gu, Y., and Groome, L. J. (2016a). Up-regulation of miR-203 Expression Induces Endothelial Inflammatory Response: Potential Role in Preeclampsia. *Am. J. Reprod. Immunol.* 76, 482–490. doi:10.1111/aji.12589

Wang, Y., Fan, H., Zhao, G., Liu, D., Du, L., Wang, Z., et al. (2012b). MiR-16 Inhibits the Proliferation and Angiogenesis-Regulating Potential of Mesenchymal Stem Cells in Severe Pre-eclampsia. *FEBS J.* 279, 4510–4524. doi:10.1111/febs.12037

Wang, Y., Lumbers, E. R., Arthurs, A. L., De Meaultsart, C. C., Mathe, A., Avery-Kiejda, K. A., et al. (2018c). Regulation of the Human Placental (Pro)renin Receptor-Prorenin-Angiotensin System by microRNAs. *Mol. Hum. Reprod.* 24, 453–464. doi:10.1093/molehr/gay031

Wang, Y. P., Zhao, P., Liu, J. Y., Liu, S. M., and Wang, Y. X. (2020). MicroRNA-132 Stimulates the Growth and Invasiveness of Trophoblasts by Targeting DAPK-1. *Eur. Rev. Med. Pharmacol. Sci.* 24, 9837–9843. doi:10.26355/eurrev_202010_23193

Wang, Y., Yang, X., Yang, Y., Wang, W., Zhao, M., Liu, H., et al. (2016b). High-throughput Deep Screening and Identification of Four Peripheral Leucocyte microRNAs as Novel Potential Combination Biomarkers for Preeclampsia. *J. Perinatol.* 36, 263–267. doi:10.1038/jp.2015.192

Wang, Y., Zhang, Y., Wang, H., Wang, J., Zhang, Y., Wang, Y., et al. (2014). Aberrantly Up-Regulated miR-20a in Pre-eclampsic Placenta Compromised the Proliferative and Invasive Behaviors of Trophoblast Cells by Targeting Forkhead Box Protein A1. *Int. J. Biol. Sci.* 10, 973–982. doi:10.7150/ijbs.9088

Wang, Y., and Zhao, S. (2010). Vascular Biology of the Placenta. *Review*. doi:10.4199/C00016ED1V01Y201008ISP009

Wang, Z., Wang, P., Wang, Z., Qin, Z., Xiu, X., Xu, D., et al. (2019e). MiRNA-548c-5p Downregulates Inflammatory Response in Preeclampsia via Targeting PTPRO. *J. Cel. Physiol.* 234, 11149–11155. doi:10.1002/jcp.27758

Weedon-Fekjær, M. S., Sheng, Y., Sugulle, M., Johnsen, G. M., Herse, F., Redman, C. W., et al. (2014). Placental miR-1301 Is Dysregulated in Early-Onset Preeclampsia and Inversely Correlated with Maternal Circulating Leptin. *Placenta* 35, 709–717. doi:10.1016/j.placenta.2014.07.002

Wei, J., Blenkiron, C., Tsai, P., James, J. L., Chen, Q., Stone, P. R., et al. (2017). Placental Trophoblast Debris Mediated Feto-Maternal Signalling via Small RNA Delivery: Implications for Preeclampsia. *Sci. Rep.* 7, 14681. doi:10.1038/s41598-017-14180-8

Wells, G., Shea, B., O'connell, D., Peterson, J., and Welch, V. (2014). *The Newcastle-Ottawa Scale (NOS) for Assessing the Quality of Nonrandomised Studies in Meta-Analyses*.

Whigham, C.-A., MacDonald, T. M., Walker, S. P., Hiscock, R., Hannan, N. J., Pritchard, N., et al. (2020). MicroRNAs 363 and 149 Are Differentially Expressed in the Maternal Circulation Preceding a Diagnosis of Preeclampsia. *Sci. Rep.* 10, 18077. doi:10.1038/s41598-020-73783-w

Winger, E. E., Reed, J. L., and Ji, X. (2014). First Trimester Pbmc Microrna Predicts Adverse Pregnancy Outcome. *Am. J. Reprod. Immunol.* 72, 515–526. doi:10.1111/aji.12287

Winger, E. E., Reed, J. L., and Ji, X. (2015). First-trimester Maternal Cell microRNA Is a superior Pregnancy Marker to Immunological Testing for Predicting Adverse Pregnancy Outcome. *J. Reprod. Immunol.* 110, 22–35. doi:10.1016/j.jri.2015.03.005

Winger, E. E., Reed, J. L., Ji, X., and Nicolaides, K. (2018). Peripheral Blood Cell microRNA Quantification during the First Trimester Predicts Preeclampsia: Proof of Concept. *PLoS One* 13, e0190654. doi:10.1371/journal.pone.0190654

Witcher, P. M. (2018). Preeclampsia: Acute Complications and Management Priorities. *AACN Adv. Crit. Care* 29, 316–326. doi:10.4037/aacnacc2018710

Witvrouwen, I., Mannaerts, D., Ratajczak, J., Boeren, E., Faes, E., van Craenenbroeck, A. H., et al. (2021). MicroRNAs Targeting VEGF Are Related to Vascular Dysfunction in Preeclampsia. *Biosci. Rep.* 41, BSR20210874. doi:10.1042/BSR20210874

Wu, D., Shi, L., Hong, L., Chen, X., and Cen, H. (2020a). MiR-135a-5p Promotes the Migration and Invasion of Trophoblast Cells in Preeclampsia by Targeting β-TrCP. *Placenta* 99, 63–69. doi:10.1016/j.placenta.2020.07.028

Wu, G.-M., Jin, Y., Cao, Y.-M., and Li, J.-Y. (2020b). The Diagnostic Value and Regulatory Mechanism of miR-200a Targeting ZEB1 in Pregnancy-Induced Hypertension. *Hypertens. Pregnancy* 39, 243–251. doi:10.1080/10641955.2020.1757700

Wu, L., Zhou, H., Lin, H., Qi, J., Zhu, C., Gao, Z., et al. (2012). Circulating microRNAs Are Elevated in Plasma from Severe Preeclamptic Pregnancies. *Reproduction* 143, 389–397. doi:10.1530/REP-11-0304

Xiao, J., Tao, T., Yin, Y., Zhao, L., Yang, L., and Hu, L. (2017). miR-144 May Regulate the Proliferation, Migration and Invasion of Trophoblastic Cells through Targeting PTEN in Preeclampsia. *Biomed. Pharmacother.* 94, 341–353. doi:10.1016/j.biopha.2017.07.130

Xiaobo, Z., Qizhi, H., Zhiping, W., and Tao, D. (2019). Down-regulated miR-149-5p Contributes to Preeclampsia via Modulating Endoglin Expression. *Pregnancy Hypertens.* 15, 201–208. doi:10.1016/j.preghy.2019.01.002

Xie, N., Jia, Z., and Li, L. (2019). miR-320a U-pregulation C-ontributes to the D-evelopment of P-reeclampsia by I-nhibiting the G-rowth and I-nvasion of T-rophoblast C-ells by T-argeting I-nterleukin 4. *Mol. Med. Rep.* 20, 3256–3264. doi:10.3892/mmr.2019.10574

Xu, H., and Zhang, X. (2017). Abnormal Expression of microRNA-370 Regulates Endoglin Expression in Preeclampsia. *Int. J. Clin. Exp. Med.* 10, 4943–4949.

Xu, J., Gu, Y., Lewis, D. F., Cooper, D. B., McCathran, C. E., and Wang, Y. (2019). Downregulation of Vitamin D Receptor and miR-126-3p Expression Contributes to Increased Endothelial Inflammatory Response in Preeclampsia. *Am. J. Reprod. Immunol.* 82, e13172. doi:10.1111/aji.13172

Xu, P., Zhao, Y., Liu, M., Wang, Y., Wang, H., Li, Y.-x., et al. (2014). Variations of MicroRNAs in Human Placentas and Plasma from Preeclamptic Pregnancy. *Hypertension* 63, 1276–1284. doi:10.1161/HYPERTENSIONAHA.113.02647

Xu, Q., Song, Y., and Lu, L. (2021). Overexpression of Let-7d Explains Down-regulated KDM3A and ENO2 in the Pathogenesis of Preeclampsia. *J. Cel. Mol. Med.* 25, 8127–8139. doi:10.1111/jcmm.16299

Xue, F., Yang, J., Li, Q., and Zhou, H. (2019). Down-regulation of microRNA-34a-5p Promotes Trophoblast Cell Migration and Invasion via Targetting Smad4. *Biosci. Rep.* 39, BSR20181631. doi:10.1042/BSR20181631

Xueya, Z., Yamei, L., Sha, C., Dan, C., Hong, S., Xingyu, Y., et al. (2020). Exosomal Encapsulation of miR-125a-5p Inhibited Trophoblast Cell Migration and Proliferation by Regulating the Expression of VEGFA in Preeclampsia. *Biochem. Biophysical Res. Commun.* 525, 646–653. doi:10.1016/j.bbrc.2020.02.137

Yan, T., Liu, Y., Cui, K., Hu, B., Wang, F., and Zou, L. (2013a). MicroRNA-126 Regulates EPCs Function: Implications for a Role of miR-126 in Preeclampsia. *J. Cel. Biochem.* 114, 2148–2159. doi:10.1002/jcb.24563

Yan, X., Liang, H., Deng, T., Zhu, K., Zhang, S., Wang, N., et al. (2013b). The Identification of Novel Targets of miR-16 and Characterization of Their Biological Functions in Cancer Cells. *Mol. Cancer* 12, 1–11. doi:10.1186/1476-4598-12-92

Yang, H.-l., Zhang, H.-z., Meng, F.-r., Han, S.-y., and Zhang, M. (2019a). Differential Expression of microRNA-411 and 376c Is Associated with Hypertension in Pregnancy. *Braz. J. Med. Biol. Res.* 52, e7546. doi:10.1590/1414-431X20197546

Yang, Q., Lu, J., Wang, S., Li, H., Ge, Q., and Lu, Z. (2011). Application of Next-Generation Sequencing Technology to Profile the Circulating microRNAs in the Serum of Preeclampsia versus normal Pregnant Women. *Clinica Chim. Acta* 412, 2167–2173. doi:10.1016/j.cca.2011.07.029

Yang, S., Li, H., Ge, Q., Guo, L., and Chen, F. (2015). Deregulated microRNA Species in the Plasma and Placenta of Patients with Preeclampsia. *Mol. Med. Rep.* 12, 527–534. doi:10.3892/mmr.2015.3414

Yang, W., Wang, A., Zhao, C., Li, Q., Pan, Z., Han, X., et al. (2016). MiR-125b Enhances IL-8 Production in Early-Onset Severe Preeclampsia by Targeting Sphingosine-1-Phosphate Lyase 1. *PLoS One* 11, e0166940. doi:10.1371/journal.pone.0166940

Yang, X., and Guo, F. (2019). miR-342-3p S-uppresses C-ell M-igration and I-nvasion in P-reeclampsia by T-argeting P-latelet-derived G-rowth F-actor R-eceptor α. *Mol. Med. Rep.* 20, 1772–1780. doi:10.3892/mmr.2019.10372

Yang, X., and Meng, T. (2019). MicroRNA-431 Affects Trophoblast Migration and Invasion by Targeting ZEB1 in Preeclampsia. *Gene* 683, 225–232. doi:10.1016/j.gene.2018.10.015

Yang, X., and Meng, T. (2020). miR-215-5p Decreases Migration and Invasion of Trophoblast Cells through Regulating CDC6 in Preeclampsia. *Cell Biochem. Funct.* 38, 472–479. doi:10.1002/cbf.3492

Yang, X., Zhang, J., and Ding, Y. (2017). Association of microRNA-155, Interleukin 17A, and Proteinuria in Preeclampsia. *Med. (United States* 96, e6509. doi:10.1097/MD.0000000000006509

Yang, Y., Li, H., Ma, Y., Zhu, X., Zhang, S., and Li, J. (2019b). MiR-221-3p Is Down-Regulated in Preeclampsia and Affects Trophoblast Growth, Invasion and Migration Partly via Targeting Thrombospondin 2. *Biomed. Pharmacother.* 109, 127–134. doi:10.1016/j.biopha.2018.10.009

Yang, Y., Xi, L., Ma, Y., Zhu, X., Chen, R., Luan, L., et al. (2019c). The lncRNA Small Nucleolar RNA Host Gene 5 Regulates Trophoblast Cell Proliferation, Invasion, and Migration via Modulating miR-26a-5p/N-cadherin axis. *J. Cel. Biochem.* 120, 3173–3184. doi:10.1002/jcb.27583

Yang, Z., Shan, N., Deng, Q., Wang, Y., Hou, Y., Mei, J., et al. (2021). Extracellular Vesicle-derived microRNA-18b Ameliorates Preeclampsia by Enhancing Trophoblast Proliferation and Migration via Notch2/TIM3/mTORC1 axis. *J. Cel. Mol. Med.* 25, 4583–4595. doi:10.1111/jcmm.16234

Youssef, H. M. G., and Marei, E. S. (2019). Association of MicroRNA-210 and MicroRNA-155 with Severity of Preeclampsia. *Pregnancy Hypertens.* 17, 49–53. doi:10.1016/j.preghy.2019.05.010

Yu, Z., Zhang, Y., Zheng, H., Gao, Q., and Wang, H. (2021). LncRNA SNHG16 Regulates Trophoblast Functions by the miR-218-5p/LASP1 axis. *J. Mol. Histol.* 52, 1021–1033. doi:10.1007/s10735-021-09985-x

Yuan, Y., Wang, X., Sun, Q., Dai, X., and Cai, Y. (2020). MicroRNA-16 Is Involved in the Pathogenesis of Pre-eclampsia via Regulation of Notch2. *J. Cel. Physiol.* 235, 4530–4544. doi:10.1002/jcp.29330

Zhang, C., Li, Q., Ren, N., Li, C., Wang, X., Xie, M., et al. (2015). Placental miR-106a~363 Cluster Is Dysregulated in Preeclamptic Placenta. *Placenta* 36, 250–252. doi:10.1016/j.placenta.2014.11.020

Zhang, H. J., Zhang, Y. N., and Teng, Z. Y. (2019a). Downregulation of miR-16 P-rotects H9c2(2-1) C-ells against H-ypoxia/reoxygenation D-amage by T-argeting CIAPIN1 and R-egulating the NF-κB P-athway. *Mol. Med. Rep.* 20, 3113–3122. doi:10.3892/mmr.2019.10568

Zhang, W. M., Cao, P., Xin, L., Zhang, Y., Liu, Z., Yao, N., et al. (2019b). Effect of miR-133 on Apoptosis of Trophoblasts in Human Placenta Tissues via Rho/ROCK Signaling Pathway. *Eur. Rev. Med. Pharmacol. Sci.* 23, 10600–10608. doi:10.26355/eurrev_201912_19755

Zhang, Y., Diao, Z., Su, L., Sun, H., Li, R., Cui, H., et al. (2010). MicroRNA-155 Contributes to Preeclampsia by Down-Regulating CYR61. *Am. J. Obstet. Gynecol.* 202, 466e1–466. e7. doi:10.1016/j.ajog.2010.01.057

Zhang, Y., Fei, M., Xue, G., Zhou, Q., Jia, Y., Li, L., et al. (2012). Elevated Levels of Hypoxia-Inducible microRNA-210 in Pre-eclampsia: New Insights into Molecular Mechanisms for the Disease. *J. Cel. Mol. Med.* 16, 249–259. doi:10.1111/j.1582-4934.2011.01291.x

Zhang, Y., Huang, G., Zhang, Y., Yang, H., Long, Y., Liang, Q., et al. (2017). MiR-942 Decreased before 20 Weeks Gestation in Women with Preeclampsia and Was Associated with the Pathophysiology of Preeclampsia *In Vitro*. *Clin. Exp. Hypertens.* 39, 108–113. doi:10.1080/10641963.2016.1210619

Zhao, G., Zhou, X., Chen, S., Miao, H., Fan, H., Wang, Z., et al. (2014). Differential Expression of microRNAs in Decidua-Derived Mesenchymal Stem Cells from Patients with Pre-eclampsia. *J. Biomed. Sci.* 21, 81. doi:10.1186/s12929-014-0081-3

Zhao, X., Liu, F., Zhang, J., Zhang, J., Zhang, L., and Chen, L. (2021a). LINC01128 - miR-16 Interaction Regulates the Migration and Invasion of Human Chorionic Trophoblast Cells. *Hypertens. Pregnancy* 40, 152–161. doi:10.1080/10641955.2021.1917602

Zhao, X., Zhang, X., Wu, Z., Mei, J., Li, L., and Wang, Y. (2021b). Up-regulation of microRNA-135 or Silencing of PCSK6 Attenuates Inflammatory Response in Preeclampsia by Restricting NLRP3 Inflammasome. *Mol. Med.* 27, 82. doi:10.1186/s10020-021-00335-x

Zhao, Y.-H., Liu, Y.-L., Fei, K.-L., and Li, P. (2020). Long Non-coding RNA HOTAIR Modulates the Progression of Preeclampsia through Inhibiting miR-106 in an EZH2-dependent Manner. *Life Sci.* 253, 117668. doi:10.1016/j.lfs.2020.117668

Zhao, Z., Moley, K. H., and Gronowski, A. M. (2013). Diagnostic Potential for miRNAs as Biomarkers for Pregnancy-specific Diseases. *Clin. Biochem.* 46, 953–960. doi:10.1016/j.clinbiochem.2013.01.026

Zheng, W., Chen, A., Yang, H., and Hong, L. (2020). MicroRNA-27a I-nhibits T-rophoblast C-ell M-igration and I-nvasion by T-argeting SMAD2: Potential R-ole in P-reeclampsia. *Exp. Ther. Med.* 20, 2262–2269. doi:10.3892/etm.2020.8924

Zhong, Y., Zhu, F., and Ding, Y. (2019). Differential microRNA Expression Profile in the Plasma of Preeclampsia and normal Pregnancies. *Exp. Ther. Med.* 18, 826–832. doi:10.3892/etm.2019.7637

Zhou, F., Sun, Y., Gao, Q., and Wang, H. (2020). microRNA-21 R-egulates the P-roliferation of P-lacental C-ells via FOXM1 in P-reeclampsia. *Exp. Ther. Med.* 20, 1871–1878. doi:10.3892/etm.2020.8930

Zhou, X., Li, Q., Xu, J., Zhang, X., Zhang, H., Xiang, Y., et al. (2016). The Aberrantly Expressed miR-193b-3p Contributes to Preeclampsia through Regulating Transforming Growth Factor-β Signaling. *Sci. Rep.* 6, 19910. doi:10.1038/srep19910

Zhu, H., Niu, X., Li, Q., Zhao, Y., Chen, X., and Sun, H. (2020). Circ_0085296 Suppresses Trophoblast Cell Proliferation, Invasion, and Migration via Modulating miR-144/e-Cadherin axis. *Placenta* 97, 18–25. doi:10.1016/j.placenta.2020.06.002

Zhu, L., and Liu, Z. (2021). Serum from Patients with Hypertension Promotes Endothelial Dysfunction to Induce Trophoblast Invasion through the miR-27b-3p/ATPase P-lasma M-embrane Ca2+ T-ransporting 1 axis. *Mol. Med. Rep.* 23, 319. doi:10.3892/mmr.2021.11958

Zhu, X.-m., Han, T., Sargent, I. L., Yin, G.-w., and Yaoqing, Y.-q. (2009). Differential Expression Profile of microRNAs in Human Placentas from Preeclamptic Pregnancies vs normal Pregnancies. *Am. J. Obstet. Gynecol.* 200, 661e1–661. e7. doi:10.1016/j.ajog.2008.12.045

Zolfaghari, M. A., Motavalli, R., Soltani-Zangbar, M. S., Parhizkar, F., Danaii, S., Aghebati-Maleki, L., et al. (2021). A New Approach to the Preeclampsia Puzzle; MicroRNA-326 in CD4+ Lymphocytes Might Be as a Potential Suspect. *J. Reprod. Immunol.* 145, 103317. doi:10.1016/j.jri.2021.103317

Zou, A.-X., Chen, B., Li, Q.-X., and Liang, Y.-C. (2018). MiR-134 Regulates the Progression of Preeclampsia. *Eur. Rev. Med. Pharmacol. Sci.* 22, 2199–2206. doi:10.26355/eurrev_201803_14557

Zou, Y., Jiang, Z., Yu, X., Zhang, Y., Sun, M., Wang, W., et al. (2014). MiR-101 Regulates Apoptosis of Trophoblast HTR-8/SVneo Cells by Targeting Endoplasmic Reticulum (ER) Protein 44 during Preeclampsia. *J. Hum. Hypertens.* 28, 610–616. doi:10.1038/jhh.2014.35

Conflict of Interest: The authors declare that the research was conducted in the absence of any commercial or financial relationships that could be construed as a potential conflict of interest.

Publisher's Note: All claims expressed in this article are solely those of the authors and do not necessarily represent those of their affiliated organizations, or those of the publisher, the editors and the reviewers. Any product that may be evaluated in this article, or claim that may be made by its manufacturer, is not guaranteed or endorsed by the publisher.

frontiers in Bioengineering and Biotechnology

ORIGINAL RESEARCH
published: 05 January 2022
doi: 10.3389/fbioe.2021.782843

Buffy Coat DNA Methylation Profile Is Representative of Methylation Patterns in White Blood Cell Types in Normal Pregnancy

*Ranine Ghamrawi[1†], Igor Velickovic[2†], Ognjen Milicevic[2], Wendy M. White[3,4], Lillian Rosa Thistlethwaite[5], Julie M. Cunningham[6], Aleksandar Milosavljevic[5], Natasa M. Milic[1,2] and Vesna D. Garovic[1,3]**

[1]Division of Nephrology and Hypertension, Department of Medicine, Mayo Clinic, Rochester, MN, United States, [2]Department of Medical Statistics and Informatics, Medical Faculty University of Belgrade, Belgrade, Serbia, [3]Department of Obstetrics and Gynecology, Mayo Clinic, Rochester, MN, United States, [4]Department of Perinatology, Olmsted Medical Center, Rochester, MN, United States, [5]Department of Molecular and Human Genetics, Baylor College of Medicine, Houston, TX, United States, [6]Department of Laboratory Medicine and Pathology, Mayo Clinic, Rochester, MN, United States

OPEN ACCESS

Edited by:
Umberto Galderisi,
University of Campania Luigi Vanvitelli, Italy

Reviewed by:
Ying Cai,
Albert Einstein College of Medicine, United States
Jing-Woei Li,
Prince of Wales Hospital, China

***Correspondence:**
Vesna D. Garovic
garovic.vesna@mayo.edu

[†]These authors share first authorship

Specialty section:
This article was submitted to Preclinical Cell and Gene Therapy, a section of the journal Frontiers in Bioengineering and Biotechnology

Received: 24 September 2021
Accepted: 09 December 2021
Published: 05 January 2022

Citation:
Ghamrawi R, Velickovic I, Milicevic O, White WM, Thistlethwaite LR, Cunningham JM, Milosavljevic A, Milic NM and Garovic VD (2022) Buffy Coat DNA Methylation Profile Is Representative of Methylation Patterns in White Blood Cell Types in Normal Pregnancy. Front. Bioeng. Biotechnol. 9:782843. doi: 10.3389/fbioe.2021.782843

Background: We aimed to assess the extent to which the buffy coat DNA methylome is representative of methylation patterns in constitutive white blood cell (WBC) types in normal pregnancy.

Methods: A comparison of differential methylation of buffy coat DNA vs DNA isolated from polymorphonuclear (PMN) and lymphocytic fractions was performed for each blood sample obtained within 24 h prior to delivery from 29 normotensive pregnant women. Methylation profiles were obtained using an Illumina Human Methylation 450 BeadChip and CHaMP bioinformatics pipeline. A subset of differentially methylated probes (DMPs) showing discordant methylation were further investigated using statistical modeling and enrichment analysis.

Results: The smallest number of DMPs was found between the buffy coat and the PMN fraction (2.96%). Pathway enrichment analysis of the DMPs identified biological pathways involved in the particular leukocyte lineage, consistent with perturbations during isolation. The comparisons between the buffy coat and the isolated fractions as a group using linear modeling yielded a small number of probes (~29,000) with discordant methylation. Demethylation of probes in the buffy coat compared to derived cell lines was more common and was prevalent in shelf and open sea regions.

Conclusion: Buffy coat is representative of methylation patterns in WBC types in normal pregnancy. The differential methylations are consistent with perturbations during isolation of constituent cells and likely originate *in vitro* due to the physical stress during cell separation and are of no physiological relevance. These findings help the interpretation of DNA methylation profiling in pregnancy and numerous other conditions.

Keywords: buffy coat, DNA methylation, epigenetics, white blood cells, pregnancy

INTRODUCTION

DNA methylation, the addition of a 5-methyl group to a cytosine nucleotide at a cytosine-phosphate-guanine (CpG) site, is an essential epigenetic modification implicated in switching on and off genes that control early mammalian embryogenesis, including development, differentiation, imprinting, and cellular function (Straussman et al., 2009; Portela and Esteller, 2010; Hodges et al., 2011; Jones, 2012). Many CpG sites are clustered in CpG islands which are flanked by shores and shelves (up to 2, and 2–4 kb from CpG islands, respectively) and are separated by "open sea" regions, which represent the rest of the genome. Tissue-specific DNA methylation tends to be observed within CpG shores rather than islands (Doi et al., 2009). DNA methylation frequently affects a gene promoter leading to gene silencing, while DNA methylation of the gene body indicates active transcription (Hellman and Chess, 2007).

Altered DNA methylation of regulatory regions has been shown to contribute to the control of proliferative, invasive, and immune tolerance mechanisms involved in oncogenesis (Klutstein et al., 2016; Kuss-Duerkop et al., 2018)— a disease process with many parallels to that of normal pregnancy—with the common goal of providing a nutrient supply and immune tolerance to a growing tumor and fetus, respectively. In our previous studies, we described a transient state of hypomethylation in maternal leukocyte DNA occurring in normal early pregnancy (White et al., 2012). We also have demonstrated that in preeclampsia—a pregnancy-specific hypertensive disorder clinically characterized by multisystem involvement and, commonly, proteinuria—maternal leukocyte DNA showed genome-wide differential methylation favoring hypermethylation compared with normotensive pregnant controls (White et al., 2013; White et al., 2016). Similar to other investigators, we have performed our studies on buffy coat, a mixed leukocyte cell population, which is obtained after centrifuging whole anticoagulated blood at low speeds (Houseman et al., 2015). The scientific rigor of such results critically depends on the ability to discern any experimentally introduced methylation changes.

The buffy coat of a healthy, non-pregnant individual contains white blood cells, leukocytes, which are comprised of 70% polymorphonuclear (PMN) leukocytes, also referred to as granulocytes (0.5–1% basophils, ~65% neutrophils and 2–4% eosinophils), and roughly 30% mononuclear cells (3–8% monocytes, and 20–25% lymphocytes). Consequently, buffy coat comparisons may be confounded by shifts in cell type composition, which occur both in physiological conditions and during disease processes. This may be of particular importance for pregnancy, when an increase in the number of PMN leukocytes and monocytes, together with a decrease in the number of lymphocytes, dendritic cells, and natural killer (NK) cells occurs (Naccasha et al., 2001; Luppi et al., 2002a; Luppi et al., 2002b). Preeclampsia has been shown to be associated with an increase in the number of neutrophils (Järemo et al., 2000), along with activation of other PMN leukocytes and monocytes (Sacks et al., 1999). These shifts in white blood cell composition that occur both in normotensive and preeclamptic pregnancies could affect the DNA methylation results found in the buffy coat (Adalsteinsson et al., 2012). As methylation can vary at specific loci among individual cell types, the shifts in buffy coat cell composition, rather than shifts in cell-intrinsic methylation patterns, may cause methylation differences between buffy coat samples.

To date, limited work has addressed the stability and correlation of DNA methylation patterns in buffy coat compared with the different leukocyte fractions. Given our research focus on pregnancy and its complications, the objective of the current study was to assess to what extent the buffy coat methylome is representative of, or different from, the distinct cell types that it contains, namely PMN leukocytes and lymphocytes. To that end, we compared genome-wide methylation patterns in buffy coat to those of the PMN and lymphocytic fractions in the same pregnant individuals from blood samples collected within 24 h prior to delivery.

MATERIALS AND METHODS

Sources for Cases and Blood Samples

Pregnant women were recruited prospectively at Mayo Clinic in Rochester, MN, United States A convenience sample of 30 ml of blood was drawn into an EDTA tube from normotensive pregnant women admitted for delivery and within the 24 h prior to giving birth. In each of 29 cases, the leukocytes were separated into three groups within 2 hours of collection. Using typical slow centrifugation, a buffy coat was made and immediately frozen. The remaining sample was further subdivided into a PMN and a lymphocytic fraction using a Ficoll gradient and subsequently frozen.

Clinical Data

The medical records were abstracted for data including age, ethnicity, gravidity, body mass index (BMI), and gestational age (GA) at the time of delivery.

DNA Extraction and Processing

In the buffy coat and PMN fraction, DNA was extracted using the AutoGenFlex DNA purification kit. In order to enrich the yield, manual extraction of DNA was performed for the lymphocytic fraction. Genomic DNA was quantified using a NanoDrop spectrophotometer, normalized with standard Pico Green methodology and plated. Bisulfite modification was performed using the EZ DNA Methylation Kit (Zymo Research).

Methylation Assay

Plate maps were generated to determine the random location for each sample on the plate, as well as the samples that were run in duplicate. All samples were run in a single batch. Bisulfite-treated DNA was hybridized and imaged on an Illumina Infinium Human Methylation 450 K BeadChip that can detect methylation levels at 486,685 CpG dinucleotides across the genome and covers 96% of the CpG islands in the human genome.

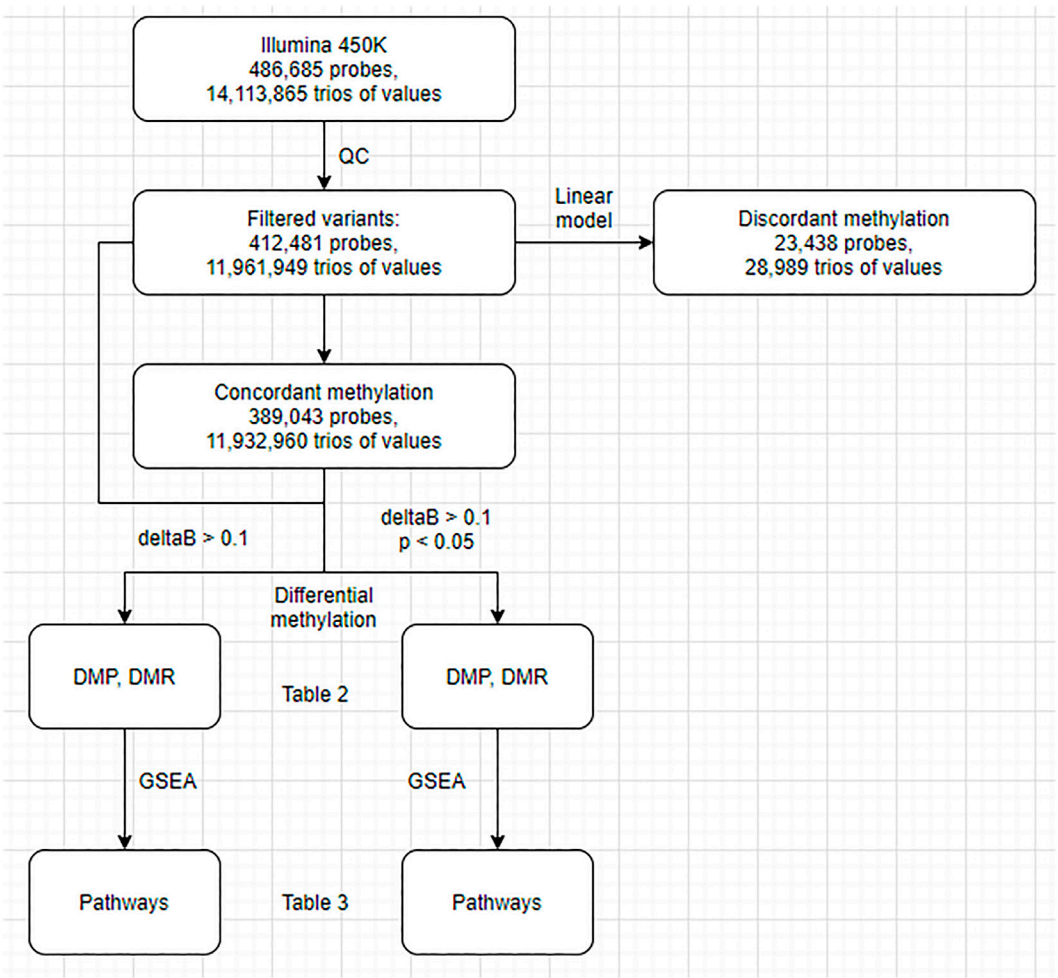

FIGURE 1 | Flowchart of the analysis. DMP, differentially methylated probes; DMR, differentially methylated regions; GSEA, gene set enrichment analysis.

Quality Control

The samples were processed and then scanned using Illumina's iScan instrumentation. The raw data were then analyzed using Illumina's Genome Studio software (version 2011.1), with methylation module (version 1.9.0). Quality assessment of the array was conducted using the "Control Dashboard" in the Genome Studio software package, which includes a graphical inspection of the 10 types of embedded control probes: staining, extension, hybridization, target removal, bisulfite conversion, G/T mismatch, specificity, non-polymorphic controls, negative controls, and restoration controls.

Overall sample performance was determined by the total number of detected CpGs, the average detection *p* value across all CpG sites, and the distribution of average beta values for all CpGs. Call rates for each CpG site and sample were determined. Methylation sites and samples were excluded if the unreliable call rate (detection *p*-value) was greater than 5%. Technical replicate reproducibility was estimated by the Pearson correlation coefficient.

While all samples were bisulfite modified and run concurrently to avoid batch effects, multiple BeadChips were used, and may have variations in assay integrity leading to the "chip" effect. Thus, data were examined using principal components analysis and subsequent unsupervised hierarchical clustering of obtained components.

Statistical Analysis

First, we conducted a standard differential methylation analysis to examine DNA methylation differences between the buffy coat and its PMN and lymphocytic fractions. Second, we aimed to differentiate between true differential methylation and discordant methylation, the latter being defined as methylation of specific CPGs in the buffy coat that did not match their methylation status in derived (PMN and lymphocytic) fractions (**Figure 1**). We used linear modeling to determine whether the linear combination of methylation profiles from PMN and lymphocytic fractions predicts the methylation profile of the buffy coat. Assuming that the methylation status of each CPG

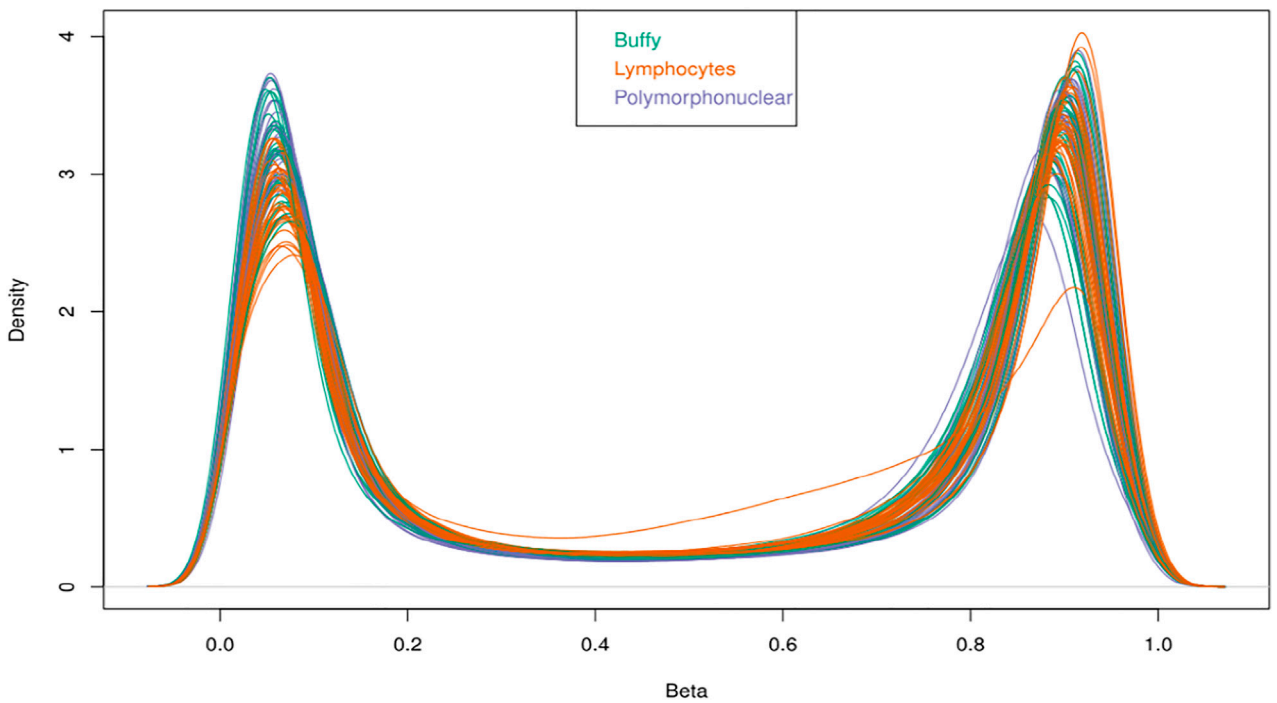

FIGURE 2 | Density plot of samples raw beta distributions (412,481 probes); the buffy coat, polymorphonuclear leukocytes and lymphocytes showed a similar distribution of beta values. All the probes show an expected bimodal grouping at extreme ends.

site in the buffy coat will agree with the methylation status in the derived fractions, we identified concordant (the presence of prediction/agreement) and discordant (the lack of prediction/agreement) CpGs. Third, we attempted to investigate the factors predicting discordance (e.g., presence of nearby SNPs, GC composition of probes, presence of motifs).

Analysis of the differential methylation at the individual CpG probe level (DMP) was performed using the Limma package (version 3.30.13) (Smyth, 2004). To adjust for multiple comparisons, we used the Benjamini-Hochberg procedure of multiple testing, with $\alpha = 0.05$. Analysis of the differentially methylated regions (DMR) as aggregates of individual probes was performed using the DMRcate package (Peters et al., 2015). In DMRcate, a default false discovery rate (FDR) cutoff of 0.05 was used for CpG sites. The data generated by DMR and DMP were used as an input for **Figure 2**. Gene set enrichment analysis (GSEA) was performed using the Gometh method to avoid probes-per-gene bias (Young et al., 2010; Geeleher et al., 2013; Phipson et al., 2016). Another filtering criterion, in addition to statistical significance, was differences in beta (delta beta) larger than 0.1. For the purposes of enrichment and correlation analyses, we used the GRCh37 reference build. The mappability and uniqueness of probes was calculated using Bismap (Karimzadeh et al., 2018). Normalized beta values and sample annotations are available to the public at https://osf.io/324ak/?view_only = 5c1c7cf5b77a40d3bb29b7d9c418f763.

TABLE 1 | Study population demographics.

Demographics	All patients (*n* = 29)
Age, yrs (mean ± SD)	29.2 ± 6.0
White, *n* (%)	24 (82.8)
Gravida, *n* (%)	
1	13 (44.8)
>1	16 (55.2)
Parity, *n* (%)	
0	14 (48.3)
1	4 (13.8)
>1	11 (37.9)
BMI, (kg/m^2), (mean ± SD)	29.3 ± 7.7
GA at delivery, weeks, (mean ± SD)	39.9 ± 1.4

BMI, body mass index; GA, gestational age; SD, standard deviation.

RESULTS

Clinical Characteristics

The blood samples of 29 normotensive pregnancies were collected and analyzed. Patients were predominantly white, and the mean gestational age at delivery was 39.9 ± 1.4 weeks. Demographic and clinical characteristics are listed in **Table 1**.

Differential Methylation

A total of 412,481 probes passed all the filters (**Figure 3**). A pairwise comparison between the buffy coat, PMN leukocytes,

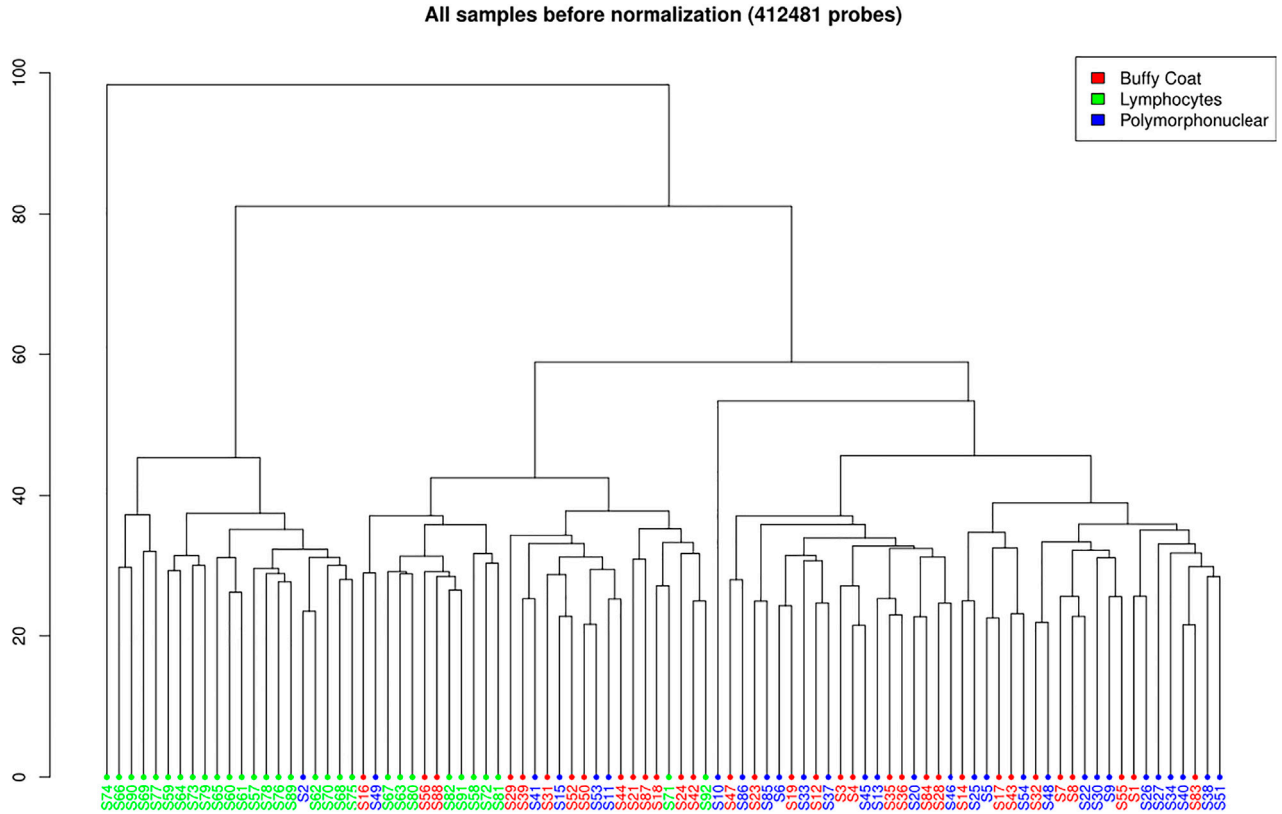

FIGURE 3 | Hierarchal clustering of all samples before normalization (412,481 probes) on Illumina 450K data.

TABLE 2 | Number of differentially methylated probes and regions.

Differentially methylated	Significance filters	Original analysis			Without violating probe trios[a]		
		BP	BL	PL	BP	BL	PL
DMP	$p < 0.05$	12,207	125,962	143,097	13,926	124,251	143,048
	$p < 0.05$ and $\Delta\beta > 0.1$	2,450	20,271	26,334	2,963	20,303	26,495
DMR	$p < 0.05$	596	5,270	6,086	627	5,209	6,120
	$p < 0.05$ and $\Delta\beta > 0.1$	0	164	25	0	157	24
GSEA-DMP	$p < 0.05$	15	0	0	14	0	0
	$p < 0.05$ and $\Delta\beta > 0.1$	11	32	17	12	31	23
GSEA-DMR	$p < 0.05$	0	10	19	0	14	23
	$p < 0.05$ and $\Delta\beta > 0.1$	0	1	1	0	0	0

[a]*Analysis of differentially methylated probes after elimination of outliers.*

DMP, differentially methylated probes; DMR, differentially methylated regions; GSEA, gene set enrichment analysis.

BP, Comparison of buffy coat to polymorphonuclear leukocytes; BL, comparison of buffy coat to lymphocytes; PL, comparison of polymorphonuclear leukocytes to lymphocytes.

and lymphocytes was performed to identify differentially methylated probes (DMP). When considering the $\alpha = 0.05$ significance level with Benjamini-Hochberg multiple testing corrections, the greatest number of differentially methylated sites was found between PMN and lymphocytes (143,097; 34.69%), and the smallest between the buffy coat and PMN (12,207; 2.96%), as represented in **Table 2**. This finding is not unexpected, considering that the buffy coat contains predominantly PMN leukocytes, so in this case only a small proportion of other cells (mainly lymphocytes) was present and contributed to differential signals. The opposite rationale can be drawn for the comparison of buffy coat and lymphocyte fractions. Clustering in **Figure 3** corroborates this with a clearly distinct lymphocyte fraction and an overlap of the other two fractions. The analysis was subsequently repeated for differentially methylated regions (DMR), but these results have moderate interpretability due to the variable sizes of a region, and they primarily served as an input for gene set enrichment analysis

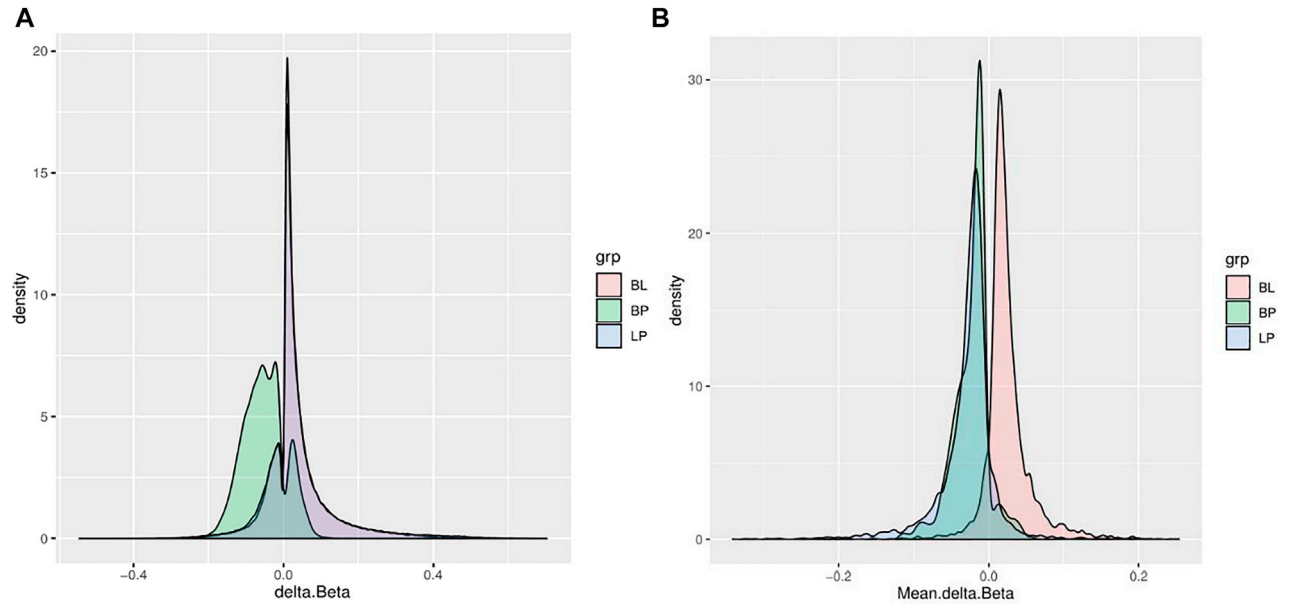

FIGURE 4 | Probability density functions for the effect size between groups. These distributions are useful for selecting cutoffs for differential methylation. **(A)** Differences in beta values for differentially methylated probes. **(B)** Differences in mean delta beta for differentially methylated regions. BP, Comparison of buffy coat to polymorphonuclear leukocytes: BL, Comparison of buffy coat to lymphocytes; PL, Comparison of polymorphonuclear leukocytes to lymphocytes.

(GSEA). The magnitudes of differences for both the DMP and DMR analyses are shown in **Figure 4A** (delta beta) and 4 B (mean beta fold change). In addition, the number of differentially methylated probes/regions between the groups are shown when the applied threshold for delta beta was 0.1 (Original Analysis in **Table 2**).

Gene Set Enrichment Analysis

Gene set enrichment analysis (GSEA) was performed using either only $p < 0.05$, or by combining $p < 0.05$ with delta beta >0.1. When using only *p*-values, DMPs give enriched gene sets only for the buffy coat to polymorphonuclear leukocytes (BP) pairing, where the least differences in methylation are expected. Matching DMR analyses give opposite (and expected) results with no gene sets for the BP and a larger number of sets in the polymorphonuclear leukocytes to lymphocyte (PL) pairing. The pathways identified tended to be general in nature, e.g., *gene silencing by miRNA, mRNA binding involved in post-transcriptional gene silencing,* and *micro-ribonucleoprotein complex* (**Table 2**). In contrast, when we used delta beta values as an additional filter, GSEA generated several pathways for DMP and virtually no pathways for DMR, and the resulting pathways were indicative of the leukocyte lineages, e.g., *innate immune response, inflammatory response,* and *neutrophil degranulation* (**Table 3**).

Consistency of Results Between Leukocyte Fractions and the Buffy Coat

Under the assumption that the buffy coat is mostly the weighted sum of PMN and lymphocytes, buffy coat methylations are essentially estimated twice. We took advantage of the redundant methylation information to test whether we could extract the ratio of PMN and lymphocytes in the peripheral blood. Without additional constraints, we fit the model *buffy coat ~ lymphocytes + PMN leukocytes + error* for each subject and obtained coefficients for both lymphocytes and PMN summing to 0.98–0.99. This shows that the model is valid and reflects the physiological setup. The coefficients were interpreted as the differential blood count, with an expectancy of 20–40% lymphocytes and 40–80% PMN leukocytes.

We next performed linear modeling to determine whether the weighted combination of methylation profiles from isolated cellular fractions predicts the methylation profile of the buffy coat and identified the discordant CpG probes where the weighted combination deviates from methylation measured on the buffy coat. We applied the fitted model to each probe and each trio of samples and calculated the residuals (**Figure 5**). Although most probes centered around zero in a unimodal distribution, there was a prominent peak around the negative extreme (**Figure 6**), which corresponds to CpGs that are less methylated in the buffy coat than predicted from the relatively high CpG methylation in constituent fractions. Positive residuals correspond to methylated loci in buffy coat for which either of the fractions is hypomethylated and we can see several clusters between 0.3 and 0.8. Notably, the negative peak at the far left is dominant and has no matching positive counterpart. These discordant values with absolute residuals larger than expected could be a consequence of random probe errors or may be a result of physical/chemical stress occurring during cell separation, thus leading to methylation in isolated cellular fractions of

TABLE 3 | Gene sets obtained.

Method	Sig. Filters	Original analysis			Without violating probe trios*		
		BP	BL	PL	BP	BL	PL
GSEA-DMP	$p < 0.05$	1.neutrophil degranulation 2.specific granule membrane 3.specific granule lumen 4.signal transduction 5.tertiary granule membrane 6.external side of plasma membrane 7.inflammatory response 8.cellular response to lipopolysaccharide 9.humoral immune response 10.innate immune response 11.positive regulation of interleukin-10 production 12.actin binding 13.plasma membrane 14.antimicrobial humoral response 15.tertiary granule lumen			1.neutrophil degranulation 2.specific granule membrane 3.tertiary granule membrane 4.external side of plasma membrane 5.actin binding 6.immune response 7.signal transduction 8.specific granule lumen 9.innate immune response 10.positive regulation of interleukin-10 production 11.humoral immune response 12.tertiary granule lumen 13.positive regulation of I-kappaB kinase/ NF-kappaB signaling 14.cellular response to lipopolysaccharide		
	$p < 0.05$ & $\Delta\beta > 0.1$	1.neutrophil degranulation 2.specific granule lumen 3.specific granule membrane 4.antimicrobial humoral response 5.innate immune response 6.tertiary granule lumen 7.cytosol 8.tertiary granule membrane 9.defense response to bacterium 10.azurophil granule lumen 11.protein binding	1.neutrophil degranulation 2.inflammatory response 3.specific granule membrane 4.innate immune response 5.cytokine-mediated signaling pathway 6.immune response 7.signal transduction 8.specific granule lumen 9.tertiary granule membrane 10.lipopolysaccharide-mediated signaling pathway 11.positive regulation of GTPase activity 12.B cell receptor signaling pathway	1.neutrophil degranulation 2.inflammatory response 3.specific granule membrane 4.innate immune response 5.signal transduction 6.cytokine-mediated signaling pathway 7.immune response 8.lipopolysaccharide-mediated signaling pathway 9.tertiary granule membrane 10.external side of plasma membrane 11.chemotaxis 12.signaling receptor activity	1.neutrophil degranulation 2.specific granule lumen 3.specific granule membrane 4.cytosol 5.antimicrobial humoral response 6.tertiary granule lumen 7.innate immune response 8.defense response to bacterium 9.protein binding 10.azurophil granule lumen 11.tertiary granule membrane 12.endoribonuclease activity	1.neutrophil degranulation 2.inflammatory response 3.specific granule membrane 4.innate immune response 5.cytokine-mediated signaling pathway 6.signal transduction 7.immune response 8.specific granule lumen 9.lipopolysaccharide-mediated signaling pathway 10.tertiary granule membrane 11.positive regulation of GTPase activity 12.positive regulation of I-kappaB kinase/ NF-kappaB signaling	1.neutrophil degranulation 2.inflammatory response 3.innate immune response 4.specific granule membrane 5.signal transduction 6.cytokine-mediated signaling pathway 7.immune response 8.lipopolysaccharide-mediated signaling pathway 9.tertiary granule membrane 10.cellular response to lipopolysaccharide 11.external side of plasma membrane 12.positive regulation of I-kappaB kinase/ NF-kappaB signaling

(Continued on following page)

TABLE 3 | (*Continued*) Gene sets obtained.

Method	Sig. Filters	Original analysis			Without violating probe trios*		
		BP	BL	PL	BP	BL	PL
			13.cellular response to lipopolysaccharide	13.cellular response to lipopolysaccharide		13.cellular response to lipopolysaccharide	13.B cell receptor signaling pathway
			14.positive regulation of I-kappaB kinase/NF-kappaB signaling	14.positive regulation of GTPase activity		14.B cell receptor signaling pathway	14.positive regulation of interleukin-2 biosynthetic process
			15.secretory granule membrane	15.positive regulation of I-kappaB kinase/ NF-kappaB signaling		15.secretory granule membrane	15.cell surface
			16.cell surface	16.secretory granule membrane		16.T cell activation	16.signaling receptor activity
			17.T cell activation	17.T cell activation		17.chemotaxis	17.chemotaxis
			18.perinuclear region of cytoplasm			18.cell surface	18.secretory granule membrane
			19.chemotaxis			19.negative regulation of tumor necrosis factor production	19.cell-cell adhesion
			20.Golgi apparatus			20.tertiary granule lumen	20.T cell activation
			21.negative regulation of tumor necrosis factor production			21.cellular defense response	21.positive regulation of GTPase activity
			22.tertiary granule lumen			22.T cell costimulation	22.focal adhesion
			23.cellular defense response			23.adaptive immune response	23.negative regulation of tumor necrosis factor production
			24.T cell costimulation			24.cytosol	
			25.adaptive immune response			25.platelet activation	
			26.platelet activation			26.GTPase activator activity	
			27.regulation of immune response			27.Golgi apparatus	
			28.GTPase activator activity			28.regulation of immune response	
			29.cytosol			29.perinuclear region of cytoplasm	
			30.external side of plasma membrane			30.extracellular exosome	
			31.Golgi membrane			31.Golgi membrane	
			32.extracellular exosome				
GSEA-DMR	$p <$ 0.05		1.mRNA binding involved in posttranscriptional gene silencing	1.gene silencing by miRNA		1.mRNA binding involved in posttranscriptional gene silencing	1.gene silencing by miRNA
			2.micro-ribonucleoprotein complex	2.mRNA binding involved in posttranscriptional gene silencing		2.micro-ribonucleoprotein complex	2.mRNA binding involved in posttranscriptional gene silencing
			3.gene silencing by miRNA	3.micro-ribonucleoprotein complex		3.gene silencing by miRNA	3.micro-ribonucleoprotein complex
			4.extracellular space	4.extracellular space		4.extracellular space	4.extracellular space
			5.DNA-binding transcription activator activity, RNA polymerase II-specific	5.DNA-binding transcription activator activity, RNA polymerase II-specific		5.DNA-binding transcription activator activity, RNA polymerase II-specific	5.extracellular region
			6.uterus development	6.extracellular region		6.extracellular region	6.DNA-binding transcription activator activity, RNA polymerase II-specific

(Continued on following page)

TABLE 3 | (*Continued*) Gene sets obtained.

Method	Sig. Filters	Original analysis			Without violating probe trios*		
		BP	BL	PL	BP	BL	PL
			7.DNA-binding transcription factor activity, RNA polymerase II-specific	7.integral component of plasma membrane		7.uterus development	7.integral component of plasma membrane
			8.extracellular region	8.collagen-containing extracellular matrix		8.embryonic forelimb morphogenesis	8.collagen-containing extracellular matrix
			9.odontogenesis	9.DNA-binding transcription factor activity, RNA polymerase II-specific		9.odontogenesis	9.sequence-specific DNA binding
			10.embryonic forelimb morphogenesis	10.embryonic forelimb morphogenesis		10.positive regulation of neuron differentiation	10.DNA-binding transcription factor activity, RNA polymerase II-specific
				11.dopaminergic neuron differentiation		11.collagen-containing extracellular matrix	11.embryonic forelimb morphogenesis
				12.homophilic cell adhesion via plasma membrane adhesion molecules		12.dopaminergic neuron differentiation	12.homophilic cell adhesion via plasma membrane adhesion molecules
				13.sequence-specific DNA binding		13.integral component of plasma membrane	13.dopaminergic neuron differentiation
				14.uterus development		14.DNA-binding transcription factor activity, RNA polymerase II-specific	14.uterus development
				15.negative regulation of sprouting angiogenesis			15.negative regulation of sprouting angiogenesis
				16.calcium ion binding			16.chemical synaptic transmission
				17.extracellular matrix organization			17.cell junction
				18.neuropeptide signaling pathway			18.neuropeptide signaling pathway
				19.cell junction			19.extracellular matrix organization
							20.pancreas development
							21.calcium ion binding
							22.DNA-binding transcription factor activity
							23.growth factor activity
	$p <$ 0.05 & Δβ>0.1		1.neutrophil degranulation	1.neutrophil degranulation			

particular site(s), which were not methylated in the initial, pre-separation analysis of the buffy coat.

For subsequent analysis, we calculated the $p < 0.05$ cutoff using Bonferroni correction (z-score 5.29) and labeled as discordant all probes that fell outside of this range as outliers when standardized. The total number of discordant probe trios was 28,989 (0.24%) out of n*412,481 (n = 29) included in the model. These values were filtered out of the data from all three types of samples. All analyses were then repeated with the new "filtered" dataset (called without discordant probes) to determine whether the differentially methylated regions or probes were actually false positives. We found that, regardless of the filtering criteria used, the changes were minor in terms of DMP and DMR (**Table 2** left, without discordant probes) and did not seem to affect the top scoring GSEA sites (**Table 2** right).

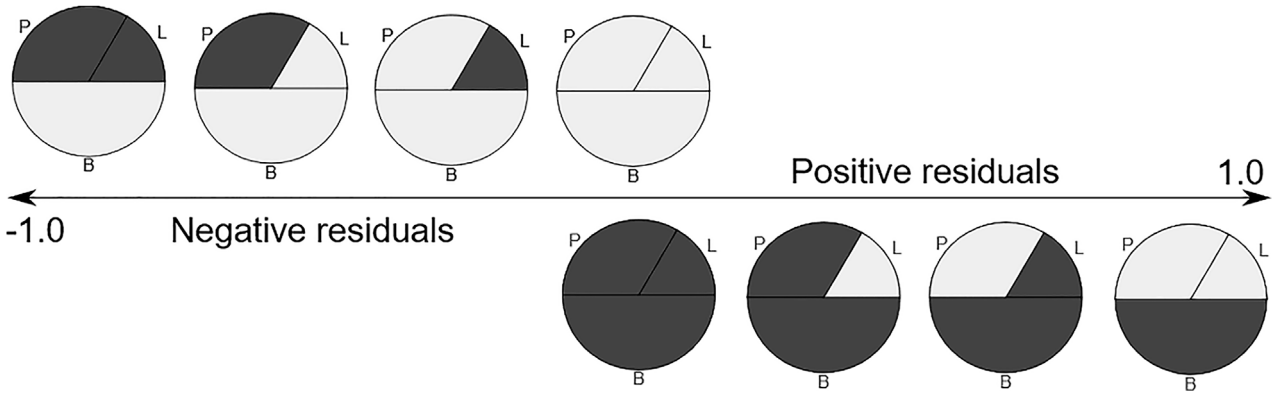

FIGURE 5 | The expected residuals of the linear model based on the methylation state of each fraction. Methylated regions are shown in dark gray. P-polymorphonuclears, L-lymphocytes, B-buffy coat.

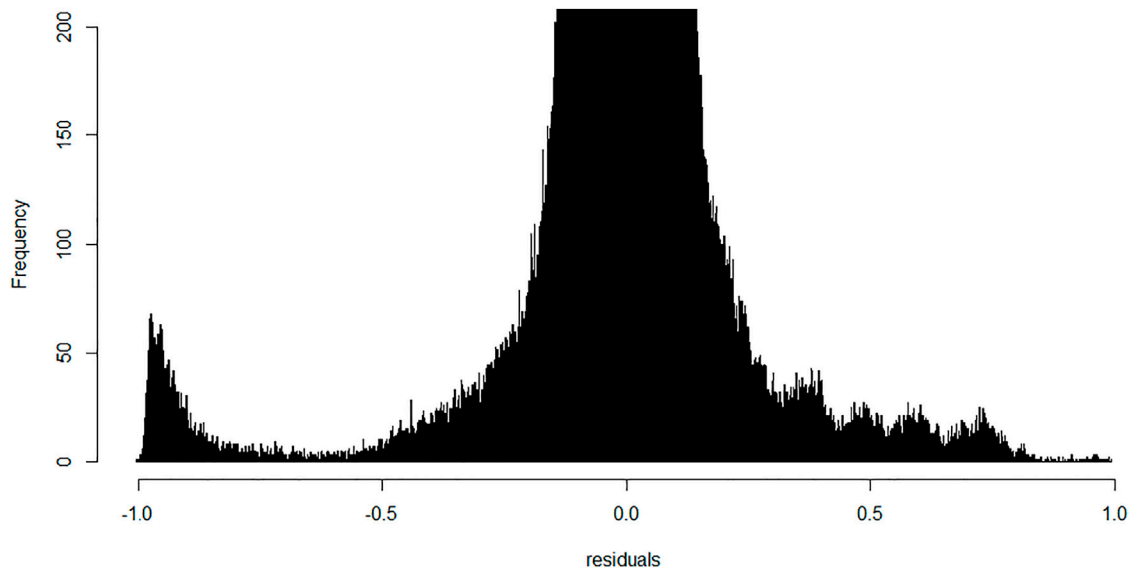

FIGURE 6 | Frequency of probes generated residuals after application of the fitted linear model; bin width is 0.001. Y-range is limited from 0–200 to allow visualization of important minority groups. Most of the probes centered around zero with a small peak in the furthest negative region indicative of a cluster of probes methylated in polymorphonuclears and lymphocytes but not in the original buffy coat.

Analysis of Discordant Probes

The number of discordant probes for which prediction of the methylation in the buffy coat was discordant from the prediction based on constituent fractions (PMN leukocytes and lymphocytes) was 23,438 (4.83% of probes). The remaining 389,043 probes that passed filters were labeled as "concordant." We hypothesized that there would be something in the design or location of those probes that would predict discordance. We downloaded the Illumina 450K manifest and analyzed the properties that differed between the two datasets.

After intersecting the locations of discordant probes with the unique Bismap ranges, only 11 of 23,438 discordant probes proved to map to non-unique segments in the bisulfite-converted reference, which are expected to yield more reliable results. On the other hand, 212 of 389,043 concordant probes proved to be multi-mapped in the concordant probes. Both types of probes had identical uniqueness (99.95%) rounded to four significant digits, suggesting that systematic mis-mapping does not explain discordance. Interestingly, 11,730 of 73,031 (16.06%) probes that were filtered out by ChAMP default QC mapped to non-unique 50-mers according to this methodology. This high uniqueness of virtually all the probes that passed filters indicates that the probes are hybridizing with the expected sequences and that the discordance is an *in-vitro*, pre-measurement phenomenon.

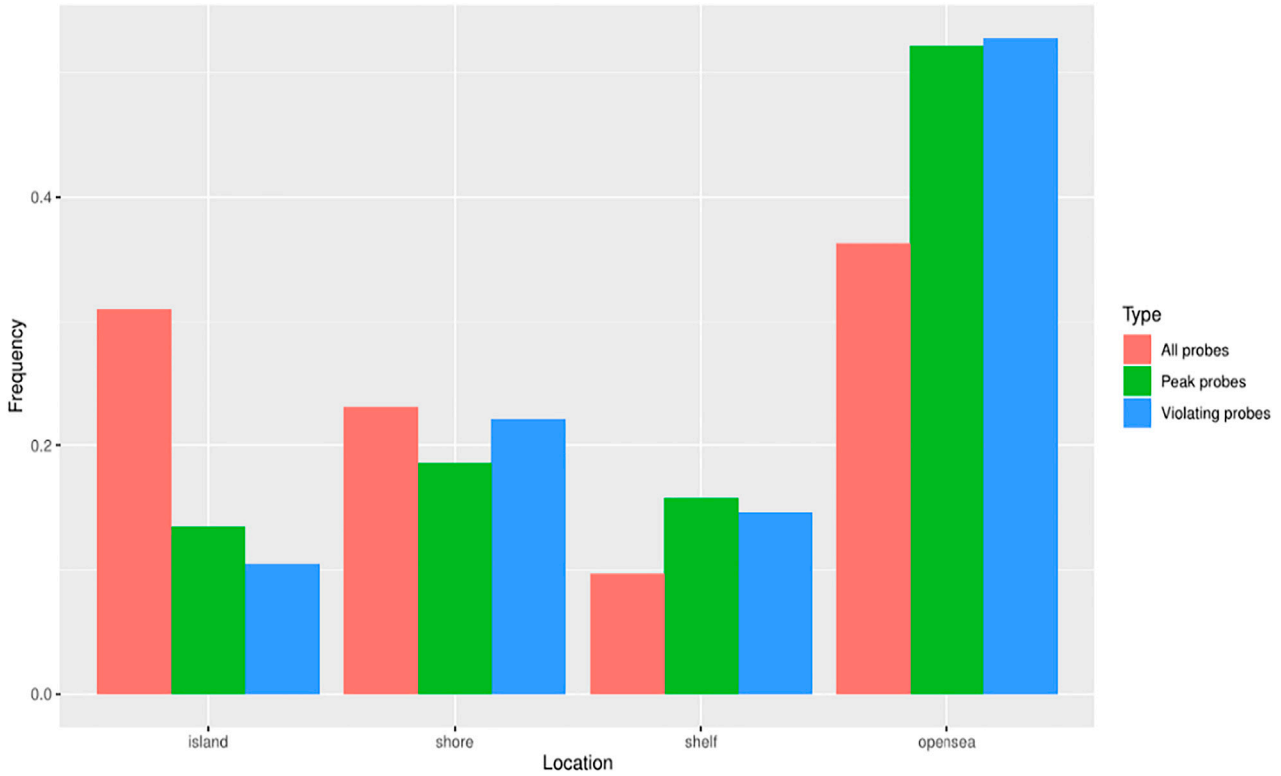

FIGURE 7 | Genomic loci classification of the probes. Violating and peak probes were less frequently located in CpG islands compared to all probes. Violating probes - probes with at least one discordant beta value. Peak probes - probes appearing in the peak of residuals below –0.6.

TABLE 4 | *p*-values obtained by chi-squared proportion tests on different types of discordant probes with the pool of all probes, stratified by the CpG region. All results are significant at $\alpha = 0.05$

Comparison with all probes	Islands	Shore	Shelf	Open sea
Violating probes	< 2.2e-16	9.479e-08	< 2.2e-16	< 2.2e-16
Peak probes	< 2.2e-16	1.726e-15	< 2.2e-16	< 2.2e-16

We also noted a prominent difference in guanine-cytosine (GC) content, and the discordant probes in the linear model had approximately 3% lower GC. One of the probes was discordant in 14 of 29 trio samples but had only a moderate GC content of 55%. Similarly, many of the probes with a higher error rate had lower GC values.

As mappability and GC content strongly differ along the genome, and presumably correlate with the presence of CpG islands, we investigated the location of discordant probes and tried to determine any preference for genomic loci relative to CpG islands. To avoid effect of overrepresentation of individual probes without the understanding of the underlying process, we counted each probe only once regardless of the number of occurrences in the investigated groups. Resorting to the standard four groups—CpG islands, shores, shelves, and open sea—we plotted and tested the proportion of groups for all probes (412,481), discordant probes (23,438), and the subset of probes giving the peak of residuals below –0.6 (peak probes, 4,535). We noted that the genomic location of both discordant groups (discordant and peak probes) was significantly different from the group of all probes (**Figure 7**; **Table 4**). These differences indicated that the discordant trios were most likely to be located in open sea regions, and least likely to be present in CpG islands.

DISCUSSION

Our present study reports several novel findings obtained through a comparative analysis of the methylation profile in buffy coat versus PMN and lymphocyte cell lines. First, the buffy coat methylation profile was representative of methylation patterns of derived cell lines. We characterized the genome-wide methylation profile of the buffy coat, PMN and the lymphocytic fractions drawn from the same individual in 29 normotensive pregnancies across >450,000 CpG sites in genes across the entire genome. We performed pairwise comparisons that yielded a number of probes that are differentially methylated, but with relatively small differences in beta values. We found a very small percentage of differentially methylated CpG sites when the buffy coat was compared to the PMN fraction (2.96%) and a greater percentage of differentially methylated CpG sites between PMN and lymphocytes (34.69%), consistent with the fact that the

PMN fraction is the main constituent of the buffy coat Second, differential methylation occurred in biological pathways that are specific for the derived cell lines, such as neutrophil degranulation and cytokine-mediated signaling pathways, consistent with the sensitivity of these cell-type specific pathways to perturbations during the cell separation process. Third, using a linear model we were able to identify approximately 29,000 probes for which the prediction of CpG methylation within the buffy coat is discordant from the prediction from constituent fractions. These discordant probes had a lower GC content, and the CpG sites involved also preferentially affected the open sea and shelf regions; discordant methylation seems to be an *in vitro* phenomenon and likely due to the separation process of the buffy coat.

To date, few studies have provided comparative analyses of different epigenetic profiles across different blood fractions in pregnancy. One notable example is a study of the cord blood, which showed that methylation in whole blood is reasonably comparable to buffy coat in a small number ($\underline{n}$ = 8) of paired samples (Dou et al., 2018). However, the concordance between special cell populations (such as lymphocytes or monocytes) with either whole blood or buffy coat was not studied. To address cell type composition of complex tissues, we have previously developed and characterized *in silico* epigenomic deconvolution methods (Onuchic et al., 2016; Decamps et al., 2020) that infer DNA methylation of constituent cell types by minimizing residuals.

We now extend residual analysis to address the complexity of the blood samples with their multiple cell types by providing a novel approach to analyzing and interpreting methylation profiles from the tissue of origin (whole blood, buffy coat) and derived cell lines (PMN and lymphocyte cell lines). Negative residuals in the overall linear model indicate that at least one of the fractions changed its state from unmethylated to methylated in derived cell lines (i.e., PMN and lymphocytes), while the positive residuals representing the opposite process, were few. Most residuals in the interval between −0.7 and 0.7 seem balanced, in accordance with the expected normal distribution as a result of unobserved variation. On the other hand, close to 50% of discordant probes are grouped in a clear peak below −0.8 and have no substantial positive counterpart, i.e., the same probe being methylated in the buffy coat, but unmethylated in derived cell line(s), indicating strong preference towards methylation in PMN and lymphocytes. This targeted DNA inactivation, preferentially targeting isolated CpGs in the open-sea regions, could be the result of the separation process, and the mechanical/chemical stress exerted on the cells removed from their normal medium.

While our study was performed on a relatively small sample size, a pairwise comparison of samples drawn from the same individual should limit the effects of potential confounders. We studied only normotensive pregnancies within 24 h prior to delivery, thus limiting the extrapolation of our results to other conditions with vastly different white blood cell composition or with selective methylation of a certain white blood cell fraction.

Our results have the potential to improve rigor and reproducibility of studies involving epigenomic profiling of buffy coat samples. For example, in the context of one of our previous studies, we identified a state of transient hypomethylation in normal early pregnancy compared with non-pregnancy (White et al., 2012). This hypomethylation would spontaneously revert after delivery. Our sample included patients close to delivery, suggesting a potential tendency towards global hypomethylation. DNA methylation can be affected by many factors including age (Bell et al., 2012), race, BMI, smoking, gestational diabetes (Wu et al., 2018), and preeclampsia (White et al., 2013). The patients in our study had healthy normotensive pregnancies, with a similar age range, a relatively homogeneous ethnicity, and free of major medical comorbidities that could affect DNA methylation. Some fetal DNA contamination was possible, but it likely represented a very small fraction (up to 6% of total measured DNA) (Bischoff, 2002) and, therefore, it was unlikely to have significantly changed our results. However, in our original study, we could not firmly establish the relation between the DNA methylation profiles in buffy coat samples and that of constituent cell types. Our current results help establish this relation, thus improving both the rigor and biological interpretability of our results. Moreover, our results will help integrate results obtained from buffy coat samples and those obtained from profiling of isolated constituent cell types. Finally, our results are not limited to studies of pregnancy and have implications for numerous other studies involving DNA methylation profiling of buffy coat samples and constituent cell types.

A potential limitation of this study is that we did not account for the effect of DNA extraction techniques. DNA was isolated in samples using the AutoGenFlex DNA purification kit for the buffy coat and the neutrophil fraction, and manual extraction of DNA was performed for the lymphocytic fraction. The use of different methods for DNA isolation may affect methylation results, although the methylation mark is considered quite stable, but this is currently minimally discussed in the literature (Hjorthaug et al., 2018). Blood sample processing techniques, such as using Ficoll density centrifugation, can also potentially confound methylation. Finally, we used the Illumina 450K array, which covers only ~2% of total CpGs within the human genome. The Illumina Infinium Human Methylation 450, however, controls for the confounding and takes SNPs into account when analyzing output data. Future directions include using a different sample cohort and methodology to confirm our results. We hope to reproduce our findings in a larger, independent sample, and in a different study population that would confirm the stability of the methylome in the buffy coat and its sub-fractions.

Despite these limitations, our results demonstrate that the buffy coat methylation profile is representative of the methylation patterns in white blood cell types in normal pregnancy obtained using Illumina Human Methylation 450 BeadChip. Small differences in the buffy coat composition may confound the methylation analysis at a very small number of CpG sites, but this is not likely to affect most results. Current methods to adjust for cellular heterogeneity, either by excluding these differentially methylated genes, or, better yet, adjusting methylation data to account for these differences in buffy coat composition, improve the robustness of methylome analysis in buffy coat. Overall, our

results support DNA methylation profiling of buffy coats as an acceptable approach for epigenomic profiling in pregnancy research and suggest that separation is likely only needed when studying lineage-specific diseases.

DATA AVAILABILITY STATEMENT

The datasets presented in this study can be found in an online repository. The name of the repository and accession link can be found below: OSF, https://osf.io/324ak/?view_only=5c1c7cf5b77a40d3bb29b7d9c418f763.

ETHICS STATEMENT

The studies involving human participants were reviewed and approved by Mayo Clinic Institutional Review Board. The patients/participants provided their written informed consent to participate in this study.

AUTHOR CONTRIBUTIONS

Conception and design of the work: RG, IV, OM, WW, LT, JC, AM, NM, VG; Acquisition, analysis or interpretation of data for the work: RG, IV, OM, WW, LT, JC, AM, NM, VG; Drafting the article: RG, IV, OM, WW, LT, CJ, AM, NM, VG; Revising article critically for important intellectual content: RG, IV, OM, WW, LT, JC, AM, NM, VG.

FUNDING

This work was supported by the National Institutes of Health R01-HL136348.

REFERENCES

Adalsteinsson, B. T., Gudnason, H., Aspelund, T., Harris, T. B., Launer, L. J., Eiriksdottir, G., et al. (2012). Heterogeneity in white Blood Cells Has Potential to Confound DNA Methylation Measurements. *PLoS One* 7 (10), e46705. doi:10.1371/journal.pone.0046705

Bell, J. T., Tsai, P.-C., Yang, T.-P., Pidsley, R., Nisbet, J., Glass, D., et al. (2012). Epigenome-wide Scans Identify Differentially Methylated Regions for Age and Age-Related Phenotypes in a Healthy Ageing Population. *Plos Genet.* 8 (4), e1002629. doi:10.1371/journal.pgen.1002629

Bischoff, F. Z. (2002). Cell-free Fetal DNA and Intact Fetal Cells in Maternal Blood Circulation: Implications for First and Second Trimester Non-invasive Prenatal Diagnosis. *Hum. Reprod. Update* 8 (6), 493–500. doi:10.1093/humupd/8.6.493

Decamps, C., Privé, F., Privé, F., Bacher, R., Jost, D., Waguet, A., et al. (2020). Guidelines for Cell-type Heterogeneity Quantification Based on a Comparative Analysis of Reference-free DNA Methylation Deconvolution Software. *BMC Bioinformatics* 21 (1), 16. doi:10.1186/s12859-019-3307-2

Doi, A., Park, I.-H., Wen, B., Murakami, P., Aryee, M. J., Irizarry, R., et al. (2009). Differential Methylation of Tissue- and Cancer-specific CpG Island Shores Distinguishes Human Induced Pluripotent Stem Cells, Embryonic Stem Cells and Fibroblasts. *Nat. Genet.* 41 (12), 1350–1353. doi:10.1038/ng.471

Dou, J., Schmidt, R. J., Benke, K. S., Newschaffer, C., Hertz-Picciotto, I., Croen, L. A., et al. (2018). Cord Blood Buffy Coat DNA Methylation Is Comparable to Whole Cord Blood Methylation. *Epigenetics* 13 (1), 108–116. doi:10.1080/15592294.2017.1417710

Geeleher, P., Hartnett, L., Egan, L. J., Golden, A., Raja Ali, R. A., and Seoighe, C. (2013). Gene set Analysis Is Severely Biased when Applied to Genome-wide Methylation Data. *Bioinformatics* 29 (15), 1851–1857. doi:10.1093/bioinformatics/btt311

Hellman, A., and Chess, A. (2007). Gene Body-specific Methylation on the Active X Chromosome. *Science* 315 (5815), 1141–1143. doi:10.1126/science.1136352

Hjorthaug, H. S., Gervin, K., Mowinckel, P., and Munthe-Kaas, M. C. (2018). Exploring the Influence from Whole Blood DNA Extraction Methods on Infinium 450K DNA Methylation. *PLoS One* 13 (12), e0208699. doi:10.1371/journal.pone.0208699

Hodges, E., Molaro, A., Dos Santos, C. O., Thekkat, P., Song, Q., Uren, P. J., et al. (2011). Directional DNA Methylation Changes and Complex Intermediate States Accompany Lineage Specificity in the Adult Hematopoietic Compartment. *Mol. Cell* 44 (1), 17–28. doi:10.1016/j.molcel.2011.08.026

Houseman, E. A., Kim, S., Kelsey, K. T., and Wiencke, J. K. (2015). DNA Methylation in Whole Blood: Uses and Challenges. *Curr. Envir Health Rpt* 2 (2), 145–154. doi:10.1007/s40572-015-0050-3

Järemo, P., Lindahl, T. L., Lennmarken, C., and Forsgren, H. (2000). The Use of Platelet Density and Volume Measurements to Estimate the Severity of Pre-eclampsia. *Eur. J. Clin. Invest.* 30 (12), 1113–1118. doi:10.1046/j.1365-2362.2000.00753.x

Jones, P. A. (2012). Functions of DNA Methylation: Islands, Start Sites, Gene Bodies and beyond. *Nat. Rev. Genet.* 13 (7), 484–492. doi:10.1038/nrg3230

Karimzadeh, M., Ernst, C., Kundaje, A., and Hoffman, M. M. (2018). Umap and Bismap: Quantifying Genome and Methylome Mappability. *Nucleic Acids Res.* 46 (20), e120. doi:10.1093/nar/gky677

Klutstein, M., Nejman, D., Greenfield, R., and Cedar, H. (2016). DNA Methylation in Cancer and Aging. *Cancer Res.* 76 (12), 3446–3450. doi:10.1158/0008-5472.can-15-3278

Kuss-Duerkop, S. K., Westrich, J. A., and Pyeon, D. (2018). DNA Tumor Virus Regulation of Host DNA Methylation and its Implications for Immune Evasion and Oncogenesis. *Viruses* 10 (2), 82. doi:10.3390/v10020082

Luppi, P., Haluszczak, C., Betters, D., Richard, C. A., Trucco, M., and DeLoia, J. A. (2002). Monocytes Are Progressively Activated in the Circulation of Pregnant Women. *J. Leukoc. Biol.* 72 (5), 874–884. doi:10.1189/jlb.72.5.874

Luppi, P., Haluszczak, C., Trucco, M., and Deloia, J. A. (2002). Normal Pregnancy Is Associated with Peripheral Leukocyte Activation. *Am. J. Reprod. Immunol.* 47 (2), 72–81. doi:10.1034/j.1600-0897.2002.1o041.x

Naccasha, N., Gervasi, M.-T., Chaiworapongsa, T., Berman, S., Yoon, B. H., Maymon, E., et al. (2001). Phenotypic and Metabolic Characteristics of Monocytes and Granulocytes in normal Pregnancy and Maternal Infection. *Am. J. Obstet. Gynecol.* 185 (5), 1118–1123. doi:10.1067/mob.2001.117682

Onuchic, V., Hartmaier, R. J., Boone, D. N., Samuels, M. L., Patel, R. Y., White, W. M., et al. (2016). Epigenomic Deconvolution of Breast Tumors Reveals Metabolic Coupling between Constituent Cell Types. *Cell Rep.* 17 (8), 2075–2086. doi:10.1016/j.celrep.2016.10.057

Peters, T. J., Buckley, M. J., Statham, A. L., Pidsley, R., Samaras, K., V Lord, R., et al. (2015). De Novo identification of Differentially Methylated Regions in the Human Genome. *Epigenetics & Chromatin* 8, 6. doi:10.1186/1756-8935-8-6

Phipson, B., Maksimovic, J., and Oshlack, A. (2016). missMethyl: an R Package for Analyzing Data from Illumina's HumanMethylation450 Platform. *Bioinformatics* 32 (2), 286–288. doi:10.1093/bioinformatics/btv560

Portela, A., and Esteller, M. (2010). Epigenetic Modifications and Human Disease. *Nat. Biotechnol.* 28 (10), 1057–1068. doi:10.1038/nbt.1685

Sacks, G., Sargent, I., and Redman, C. (1999). An Innate View of Human Pregnancy. *Immunol. Today* 20 (3), 114–118. doi:10.1016/s0167-5699(98)01393-0

Smyth, G. K. (2004). Linear Models and Empirical Bayes Methods for Assessing Differential Expression in Microarray Experiments. *Stat. Appl. Genet. Mol. Biol.* 3, 1–25. doi:10.2202/1544-6115.1027

Straussman, R., Nejman, D., Roberts, D., Steinfeld, I., Blum, B., Benvenisty, N., et al. (2009). Developmental Programming of CpG Island Methylation Profiles in the Human Genome. *Nat. Struct. Mol. Biol.* 16 (5), 564–571. doi:10.1038/nsmb.1594

White, W. M., Brost, B. C., Sun, Z., Rose, C., Craici, I., Wagner, S. J., et al. (2012). Normal Early Pregnancy: a Transient State of Epigenetic Change Favoring Hypomethylation. *Epigenetics* 7 (7), 729–734. doi:10.4161/epi.20388

White, W. M., Brost, B., Sun, Z., Rose, C., Craici, I., Wagner, S. J., et al. (2013). Genome-wide Methylation Profiling Demonstrates Hypermethylation in Maternal Leukocyte DNA in Preeclamptic Compared to Normotensive Pregnancies. *Hypertens. Pregnancy* 32 (3), 257–269. doi:10.3109/10641955.2013.796970

White, W. M., Sun, Z., Borowski, K. S., Brost, B. C., Davies, N. P., Rose, C. H., et al. (2016). Preeclampsia/Eclampsia Candidate Genes Show Altered Methylation in Maternal Leukocytes of Preeclamptic Women at the Time of Delivery. *Hypertens. Pregnancy* 35 (3), 394–404. doi:10.3109/10641955.2016.1162315

Wu, P., Farrell, W. E., Haworth, K. E., Emes, R. D., Kitchen, M. O., Glossop, J. R., et al. (2018). Maternal Genome-wide DNA Methylation Profiling in Gestational Diabetes Shows Distinctive Disease-Associated Changes Relative to Matched Healthy Pregnancies. *Epigenetics* 13 (2), 122–128. doi:10.1080/15592294.2016.1166321

Young, M. D., Wakefield, M. J., Smyth, G. K., and Oshlack, A. (2010). Gene Ontology Analysis for RNA-Seq: Accounting for Selection Bias. *Genome Biol.* 11 (2), R14. doi:10.1186/gb-2010-11-2-r14

Conflict of Interest: The authors declare that the research was conducted in the absence of any commercial or financial relationships that could be construed as a potential conflict of interest.

Publisher's Note: All claims expressed in this article are solely those of the authors and do not necessarily represent those of their affiliated organizations, or those of the publisher, the editors, and the reviewers. Any product that may be evaluated in this article, or claim that may be made by its manufacturer, is not guaranteed or endorsed by the publisher.

frontiers in Bioengineering and Biotechnology

REVIEW
published: 12 January 2022
doi: 10.3389/fbioe.2021.811417

Manipulating CD4+ T Cell Pathways to Prevent Preeclampsia

Eileen J. Murray[1], *Serena B. Gumusoglu*[1,2], *Donna A. Santillan*[1,3] *and Mark K. Santillan*[1,3,4,5,6]*

[1]Department of Obstetrics and Gynecology, University of Iowa Carver College of Medicine, Iowa City, IA, United States, [2]Department of Psychiatry, Iowa City, IA, United States, [3]Institute for Clinical and Translational Science, Iowa City, IA, United States, [4]Francois M. Abboud Cardiovascular Research Center, Iowa City, IA, United States, [5]Interdisciplinary Program in Molecular Medicine, Iowa City, IA, United States, [6]Center for Immunology, University of Iowa, Iowa City, IA, United States

Preeclampsia (PreE) is a placental disorder characterized by hypertension (HTN), proteinuria, and oxidative stress. Individuals with PreE and their children are at an increased risk of serious short- and long-term complications, such as cardiovascular disease, end-organ failure, HTN, neurodevelopmental disorders, and more. Currently, delivery is the only cure for PreE, which remains a leading cause of morbidity and mortality among pregnant individuals and neonates. There is evidence that an imbalance favoring a pro-inflammatory CD4+ T cell milieu is associated with the inadequate spiral artery remodeling and subsequent oxidative stress that prime PreE's clinical symptoms. Immunomodulatory therapies targeting CD4+ T cell mechanisms have been investigated for other immune-mediated inflammatory diseases, and the application of these prevention tactics to PreE is promising, as we review here. These immunomodulatory therapies may, among other things, decrease tumor necrosis factor alpha (TNF-α), cytolytic natural killer cells, reduce pro-inflammatory cytokine production [e.g. interleukin (IL)-17 and IL-6], stimulate regulatory T cells (Tregs), inhibit type 1 and 17 T helper cells, prevent inappropriate dendritic cell maturation, and induce anti-inflammatory cytokine action [e.g. IL-10, Interferon gamma (IFN-γ)]. We review therapies including neutralizing monoclonal antibodies against TNF-α, IL-17, IL-6, and CD28; statins; 17-hydroxyprogesterone caproate, a synthetic hormone; adoptive exogenous Treg therapy; and endothelin-1 pathway inhibitors. Rebalancing the maternal inflammatory milieu may allow for proper spiral artery invasion, placentation, and maternal tolerance of foreign fetal/paternal antigens, thereby combatting early PreE pathogenesis.

Keywords: preeclampsia, CD4+ T cells, prevention, treatment, early pregnancy

OPEN ACCESS

Edited by:
Vesna Garovic,
Mayo Clinic, United States

Reviewed by:
Staley Brod,
Medical College of Wisconsin, United States
Liyang Ma,
Albert Einstein College of Medicine, United States

***Correspondence:**
Mark K. Santillan
mark-santillan@uiowa.edu

Specialty section:
This article was submitted to Preclinical Cell and Gene Therapy, a section of the journal Frontiers in Bioengineering and Biotechnology

Received: *08 November 2021*
Accepted: *22 December 2021*
Published: *12 January 2022*

Citation:
Murray EJ, Gumusoglu SB, Santillan DA and Santillan MK (2022) Manipulating CD4+ T Cell Pathways to Prevent Preeclampsia. Front. Bioeng. Biotechnol. 9:811417. doi: 10.3389/fbioe.2021.811417

INTRODUCTION

Preeclampsia (PreE) is a multisystem hypertensive disorder that affects 5–7% of pregnancies and causes up to 18% of maternal deaths annually in the United States (Harmon et al., 2016; Robertson et al., 2019). This placental disorder is a leading cause of prematurity and low birth weight in babies and costs the US $2.18 billion annually (Harmon et al., 2016; Amaral et al., 2017; Cornelius et al., 2019; Robertson et al., 2019). While PreE often occurs in first pregnancies (4.1% of first pregnancies vs 1.7% in later pregnancies (Hernández-Díaz et al., 2009)), it has a significant rate of recurrence, with a risk of 14.7% following a PreE pregnancy and a risk of 31.9% following two prior PreE

pregnancies (Hernández-Díaz et al., 2009). Additionally, PreE is associated with long-term adverse health outcomes, especially in high-risk individuals and their children (Mostello et al., 2008). Despite documentation of the disease and its health implications dating back to almost 400 BCE (Before the Common Era) by Hippocrates, the underlying mechanism(s) and pathophysiology remain poorly understood (Burton et al., 2019). Consequently, prophylactics are limited to lifestyle modification and aspirin, while treatment is limited to delivery (Committee on Practice Bulletins-Obstetrics, 2020). Though early induction of pregnancy is often required when PreE threatens maternal health, there is evidence of significant health consequences following premature (Behrman and Butler, 2007). For example, neonatal respiratory morbidity has been evaluated at 4.4 times greater in pre-term infants than in at-term infants (Khashu et al., 2009).

Preventing PreE and its sequelae involves more than simply lowering maternal blood pressure (Amador et al., 2014; Redman, 1991); novel, molecularly-directed therapeutics are required. Many emerging therapeutic mechanisms of interest are immune in nature, as we review here. Clinical and preclinic studies have demonstrated that successful immunomodulation may prevent and/or treat the root immunologic causes of PreE and other inflammatory diseases. This review will examine therapeutic approaches involving modulation of CD4+ T cell mechanisms and their application to PreE.

PREECLAMPSIA DIAGNOSIS AND MANAGEMENT

According to American College of Obstetrics and Gynecology (ACOG) guidelines, which aligns with the International Society for the Study of Hypertension (ISSHP) guidelines, the clinical diagnosis of PreE, which is made only after the 20th week of gestation, requires pregnancy-specific hypertension (>140/90 2 separate occasions at least 4 h apart) and one of the following: proteinuria; low platelets; diseased liver, kidney, or lung; or new-onset headaches or visual problems. PreE with severe features is further diagnosed if systolic and diastolic blood pressure exceed 160 and 110 mmHg, respectively; central nervous system dysfunction (e.g., photophobia, severe headache) occurs; or in instances of thrombocytopenia or hepatic, renal, or pulmonary signs (Brown et al., 2018; Committee on Practice Bulletins-Obstetrics, 2020). When PreE complicates preexisting HTN (seen in 20–50% of pregnancies with chronic HTN), it is considered superimposed (Brown et al., 2018; Committee on Practice Bulletins-Obstetrics, 2020). PreE has a large spectrum of clinical presentations, and may present in individuals with or without existing hypertension, metabolic disease, obesity, genetic variants, or environmental risk factors (Wallis et al., 2008). Additionally, PreE is a highly clinically heterogeneous diagnosis, with clinical presentations that can include more canonically pro-inflammatory phenotypes, as well as more metabolic or endocrine phenotypes, as have been defined in molecular studies (Leavey et al., 2015). The clinical diagnosis and management of PreE is therefore highly complex, requiring significant expertise, experience, and sound judgement.

PreE, both with and without severe features, results in chronic immune activation, endothelial dysfunction, and often intrauterine growth restriction and fetal growth restriction (FGR). PreE risk factors include chronic HTN, chronic inflammatory medical conditions, obesity, family or personal history, genetic predispositions (e.g. mutations in RGS2) (Perschbacher et al., 2020), primiparity or new paternity (Li and Wi, 2000; Saftlas et al., 2003; Duckitt and Harrington, 2005), and low paternal exposure due to barrier contraceptives or a short interval between first coitus and conception (Duckitt and Harrington, 2005; Kho et al., 2009). Though PreE may progress even beyond delivery of the placenta, its initiation is often associated with early placentation processes.

PREECLAMPSIA RESULTS IN SERIOUS SHORT- AND LONG-TERM HEALTH COMPLICATIONS

Both the immediate and long-term health impacts of PreE are significant. PreE is responsible for over 70,000 maternal and 500,000 fetal/neonatal deaths globally (Duley, 2009). Serious immediate maternal morbidities are associated with PreE and include stroke; HTN; shock; seizure (eclampsia); acute respiratory syndrome; coagulopathy; elevated liver enzymes and low platelets (HELLP) syndrome; renal, pancreatic, or liver failure; and pulmonary edema (Duley, 2009; Amaral et al., 2017; Mayrink et al., 2018; Committee on Practice Bulletins-Obstetrics, 2020).

Individuals with a history of PreE are at particularly increased risk of serious cardiovascular complications after placental delivery, including HTN, myocardial infarction, stroke, venous thromboembolism, pulmonary edema, acute respiratory syndrome, intraventricular hemorrhage, sepsis, and bronchopulmonary dysplasia, and more (Mayrink et al., 2018; Committee on Practice Bulletins-Obstetrics, 2020). In fact, the 2011 American Heart Association guidelines for prevention of cardiovascular disease (CVD) in women equates PreE to chronic HTN, diabetes mellitus (DM), and obesity in terms of risk for future CVD (Roger et al., 2011). One in five patients develop HTN within 7 years of PreE, compared to only 2% after uncomplicated pregnancies (Bellamy et al., 2007).

Fetal mortality is also significantly increased with PreE (Santillan et al., 2009), and babies born to PreE pregnancies have increased risk for FGR and preterm birth risk (Duley, 2009). Additionally, children of PreE pregnancies have an increased risk of neurodevelopmental or behavioral conditions and CVD as they grow up, on top of the immediate risks of prematurity (Amaral et al., 2017; Gumusoglu et al., 2020).

PREECLAMPSIA PHARMACOTHERAPY

Pharmacologic treatments for PreE or its prevention are lacking, and management of PreE is focused on symptom alleviation and maintenance of the pregnancy until 37 weeks or sooner if there are more severe signs of PreE. After 37 weeks, removal of the placenta resolves PreE in most cases: only 18.4% of postpartum

PreE occurs in patients with an antecedent diagnosis of PreE (Al-Safi et al., 2011).

Prevention of PreE and associated morbidities is currently limited to aspirin. A recent meta-analysis of 45 randomized trials revealed that, when initiated before 16 weeks, a low dose of aspirin (LDA) significantly reduced PreE (risk ratio, RR, 0.47; confidence interval, CI 0.43–0.75), severe PreE (RR, 0.47; CI, 0.26–0.83), and FGR (RR, 0.56; CI, 0.44–0.70) (Roberge et al., 2017; Roberge et al., 2018). However, a LDA initiated after 16 weeks of gestation was not associated with reduced risk of severe PreE (RR, 0.85; CI, 0.64–1.14) or FGR (RR, 0.95; CI, 0.86–1.05), and only with a small reduction in PreE risk (RR, 0.81; CI, 0.66–0.99) (Roberge et al., 2017; Roberge et al., 2018). Therefore, LDA therapy is unlikely to significantly curtail global PreE-associated morbidity and mortality rates.

Another common PreE pharmacotherapy, magnesium sulfate, only prevents eclamptic seizures, which are rare. Similarly, PreE treatment with antihypertensives does not reverse disease processes (Duley et al., 2010). Some antihypertensives are even contraindicated in pregnancy, per the US Food and Drug Administration (FDA) category X labeling, including angiotensin-converting enzyme (ACE) inhibitors and angiotensin II receptor blockers (ARB) due to potential teratogenic and fetotoxic effects (Redman, 2011). Given these limitations, novel classes of PreE pharmacotherapy are required. An emerging area of study is the immunologic prevention of PreE, which is based largely on CD4+ T cell mechanisms.

CD4+ T CELLS IN PREGNANCY AND PREECLAMPSIA

As has been expertly reviewed elsewhere, CD4+ T cells and their immune products play a critical role in regulating normal reproductive processes. For instance, proper T cell responses govern early placentation, fertilization, and embryogenic processes, including angiogenic and patterning cascades (Trowsdale and Betz, 2006; Ingman and Jones, 2008; Howerton and Bale, 2012; Krishnan et al., 2013; Göhner et al., 2017). At the maternal-fetal interface, CD4+ T cells regulate dendritic cell maturation, NK cell cytolytic behavior, and the behavior of a host of cell types (e.g., placental trophoblasts, vascular endothelium, etc.) via release of pro- and anti-inflammatory cytokines and chemokines. However, these normative immune cell processes may go awry, increasing risk for PreE, as we detail in the present review. Therapeutic approaches for modulating CD4+ T cell polarization towards increased type 2 helper CD4+ T cells (Th2) and regulatory T cells (Tregs) are thus promising for PreE given pro-inflammation during early placental morphogenesis is a pathogenic risk factor for PreE. Altered immunology is a pervasive problem in PreE, beginning as early as conception (Robertson et al., 2019). Advanced modeling and analytic methods offer some promise for the detection of high-risk pregnancies (Fischer and Voss, 2014). Targeting high-risk pregnancies and then ameliorating this immunologic imbalance early in disease progression may prevent subsequent oxidative stress and poor placentation processes. If applied to high-risk pregnancies, early prevention may reverse or slow PreE pathogeneses before symptoms arise.

CD4+ T cells are a common denominator in the immunologic mechanisms underlying PreE, linking multiple pathways that may be targeted by intervention. Furthermore, therapies affecting dendritic cells (DCs), natural killer (NK) cells, B cells, neutrophils, and other immune cells ultimately impact upstream the CD4+ T cell counterparts. Preclinical data in animal models of PreE, as well as human studies in other immune-mediated diseases characterized by chronic inflammation, reveal multiple effective therapeutic approaches to manipulating CD4+ T cell mechanisms to restore a healthy balance. Further developing these therapies for use in PreE will provide options to minimize PreE's global health burden.

TWO STAGE MODEL OF PREECLAMPSIA

Redman in 1991 described the Two Stage Model which is a traditional explanation of the development of PreE (Redman, 1991). This model consists of two stages: pre-clinical and clinical (Redman, 1991; Redman et al., 1999; Staff, 2019). Stage 1 is defined by poor placentation and altered syncytiotrophoblast function in the outermost placental layer, which is made of epithelial cells that invade the wall of the uterus during placentation. During this stage, there is an excessive pro-inflammatory immune response due to failed maternal immune tolerance, which leads to inappropriate uterine spiral artery remodeling, placental hypoperfusion, hypoxia, and oxidative stress. Stage 2 is characterized by clinical symptoms (e.g., HTN and proteinuria), which arise from biological stressors that occur during stage 1 (e.g.,syncytiotrophoblast microvillous fragmentation, hypoxic damage, oxidative stress) (Redman, 2013).

The pre-clinical stage 1 of PreE occurs through approximately week 20 of gestation (Redman and Sargent, 2010), during which shallow cytotrophoblast (cells which differentiate into syncytiotrophoblasts and other placental cells) migrate towards the uterine spiral arterioles. This invasion contributes to inadequate spiral artery remodeling in early pregnancy. Without proper invasion and arterial remodeling, there is pulsatile high-pressure blood flow in the placental arteries and therefore placental oxidative stress and poor supplementation of the intervillous space (Burton et al., 2009). Placental ischemia is associated with reperfusion, apoptosis, macromolecule release [e.g. placental (PLGF) and vascular endothelial (VEGF) growth factors] into maternal circulation, and finally promotion of intravascular inflammatory response factors and free radicals associated with maternal vascular dysfunction (Mayrink et al., 2018). These changes include increased endothelin-1 (ET-1), antiangiogenic factor soluble Fms-like Tyrosine Kinase-1 (sFlt-1), agonistic autoantibodies to angiotensin II type 1 receptor (AT1-AA), and decreased nitric oxide (NO). The combination of these vasoconstrictive factors further prompts increased levels of pro-inflammatory immune cells and cytokines (Borzychowski et al., 2006; Harmon et al., 2016; Amaral et al., 2017; Staff, 2019; Aneman et al., 2020). Furthermore, increased pro-inflammatory

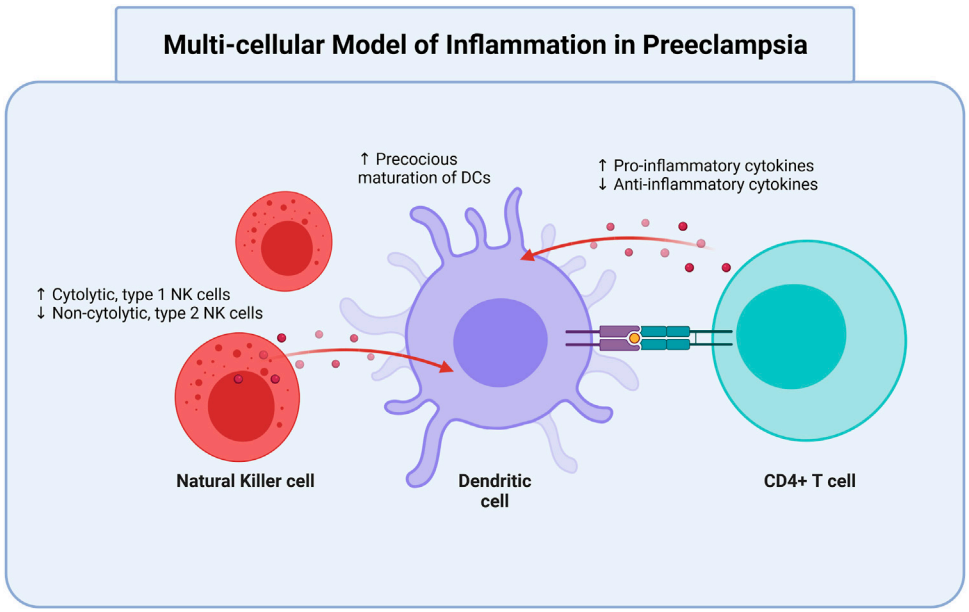

FIGURE 1 | Dendritic cells are modulated by T cells and NK cells in preeclampsia. Oxidative and vascular stress contribute to preeclamptic conditions. In preeclampsia, there is an increase of cytolytic, type 1 NK cells and precocious maturation of DCs, as well as increased production of pro-inflammatory cytokines. There is a simultaneous decrease in non-cytolytic, type 2 NK cells and anti-inflammatory cytokines. All three cell types interact to aggravate the elevated pro-inflammatory status that contributes to and occurs in preeclampsia. NK, natural killer; DC, dendritic cells. Created with https://biorender.com.

type 1 helper CD4+ T cells (Th1) and type 17 helper CD4+ T cells (Th17) is met with decreased anti-inflammatory Th2 and Tregs. a multi-cellular model of inflammation in PreE best illustrates the imbalanced cellular interactions that contribute to PreE pathogenesis (**Figure 1**).

The second stage of PreE is the clinical manifestation of systemic maternal disease. Stage 2 occurs during the second half of pregnancy and is defined by placental hypoxia and oxidative stress, clinical HTN, and proteinuria secondary to vascular inflammatory dysfunction and spiral artery insufficiency (Redman, 1991; Burton et al., 2019; Staff, 2019). While a discrete factor linking stage 1 to stage 2 is unknown, maternal immunological response to the fetus is one possible explanation. Targeting immune mechanisms in PreE therefore provides an opportunity to prevent clinical disease progression from the outset.

IMMUNOLOGY OF PREECLAMPSIA

Though PreE development is impacted by multiple factors and pathways, immunologic mechanisms offer promise for prevention because of the early and pervasive impacts of inflammation in PreE. An abnormal immune response and high Th1/17:Th2/Treg ratio is "central and causal" to PreE, as has been expertly reviewed elsewhere (Redman et al., 1999; Sargent et al., 2006; Saito et al., 2007; Sasaki et al., 2007; Robertson et al., 2019). The immune response leading to PreE may start as early as conception, as contact with paternally-derived transplantation antigens during coitus and conception primes Treg activation (Robertson et al., 2019). Proposedly, discrimination of paternal/fetal cells as non-self by the uterine immune system mounts an inflammatory offense that contributes to the broader pro-inflammatory immune imbalance in PreE (Robertson et al., 2019).

In healthy pregnancies, a pro-inflammatory CD4+ T cell response promotes trophoblast invasion, subsequent placentation, and an anti-inflammatory response, thus inducing local maternal tolerance for the semi-allogeneic fetus and placenta (Scroggins et al., 2018; Burton et al., 2019; Robertson et al., 2019; Staff, 2019; Aneman et al., 2020). During initial placentation, Tregs are at their most prevalent (Harmon et al., 2016). Tregs are partially responsible for shifting the decidual milieu from pro-to anti-inflammatory, thereby promoting immune tolerance in gestation (Robertson et al., 2019).

A carefully regulated, dynamic balance between pro- and anti-inflammatory factors is critical to multiple pregnancy processes. For instance, while an anti-inflammatory response is necessary to allow trophoblast cells to reach and invade the endometrium (Harmon et al., 2016), regulated pro-inflammation is essential to recruit NK cells and macrophages to the decidua to facilitate deep cytotrophoblast invasion into myometrial segments during maternal vascular remodeling (Redman and Sargent, 2005). Adequate spiral uterine remodeling in healthy pregnancy promotes low resistance blood flow via the placental intervillous space, which supplies the fetus with oxygen and nutrients (Aneman et al., 2020), when the pregnancy requires an enhanced circulatory capacity during the second trimester (Redman and Sargent, 2005). Overall, balanced immunity is important for successful placentation, vascular remodeling, and maternal-fetal tolerance.

In PreE, a mild systemic inflammatory response that presents in healthy pregnancies is over-intensified (Borzychowski et al., 2006; Saito et al., 2007; Staff, 2019). There is a shift away from anti-inflammatory cells and cytokines [e.g., Treg, Th2, interleukin (IL)-10, and IL-4] towards pro-inflammatory ones (e.g., Th1, Th17, and IL-4) (Borzychowski et al., 2006; Cornelius, 2018). An elevated Th1:Th2 ratio involves increased secretion of pro-inflammatory cytokines, such as tumor necrosis factor alpha (TNF-α), IL-6, and IL-17 (Harmon et al., 2016; Scroggins et al., 2018). An overactivated systemic inflammatory response then leads to an increase in antiangiogenic factors and placental insufficiency. Underlying mechanisms for this include excess placental oxidative stress and vascular damage, production of angiotensin II AT -1 receptor and sFlt-1 auto-antibodies, and decreased VEGF and PLGF (Gathiram and Moodley, 2016).

Decreased Tregs and increased Th17 CD4+ T cell subtypes may be specifically involved in the pathophysiology of PreE (Cornelius et al., 2015). Many pregnant individuals with PreE have fewer and less functionally competent Treg cells, and a decrease in Treg cells may be proportional to PreE severity (Robertson et al., 2019). The multi-cellular model of inflammation in PreE, demonstrating interactions between DCs, CD4+ T cells, and NK cells (**Figure 1**). Ultimately, inappropriate activation and subsequent pro- and anti-inflammatory response dysregulation contributes to improper maternal vascular remodeling and shallow trophoblast invasion, as well as endothelial and placental dysfunction in PreE (Harmon et al., 2016; Cornelius, 2018; Aneman et al., 2020).

The mechanisms driving inflammation in PreE are incompletely understood. One possibility is maladaptation to fetal/paternal alloantigens and a lingering immune attack against foreign fetal/paternal antigens (Redman and Sargent, 2010). Changing paternity may increase the risk of PreE by 30%, which supports the allogenic response hypothesis of PreE (Li and Wi, 2000; Redman and Sargent, 2010). Work by Saftlas et al., 2003 demonstrated a protective effect of previous fetal loss due to PreE against subsequent PreE, but only when the same partners are involved in a subsequent pregnancy. Furthermore, the more pre-conceptual exposure to semen, the lower the risk of PreE (Redman and Sargent, 2010). When the same partner is involved, the risk of PreE appears to be higher with a shorter interval between first coitus and conception (Kho et al., 2009). Together, these studies suggest that the chronicity of maternal immune exposure to paternal antigens modulates preeclampsia risk, further demonstrating the potential utility of immunomodulatory preeclampsia therapeutic.

Specifically, therapeutics that guide CD4+ T cell polarization may serve as promising tools in preventing oxidative stress and poor placentation upstream of clinical PreE manifestation. As we review here, preclinical data in similar immune mediated diseases—and in models of PreE itself—demonstrate the potential efficacy of CD4+ T cell modulators in PreE prevention.

CD4+ T CELL PATHWAYS ARE THERAPEUTIC TARGETS IN MULTIPLE INFLAMMATORY DISEASES

Preclinical studies demonstrate disease reduction following adoptive exogenous Treg therapy, intrinsic Treg expansion, and decreased pro-inflammatory cytokines via various approaches. Several clinical studies and approved therapies involve CD4+ T cell pathway manipulations across multiple immune-mediated, inflammatory diseases. These diseases include rheumatoid arthritis (RA), Crohn's disease (CD) and inflammatory bowel disease (IBD), atherosclerosis (AS), DM, pulmonary arterial hypertension (PAH), and systemic lupus erythematosus (SLE). The following therapy target candidates and their respective effects are summarized in **Table 1** and in **Figures 2**, **3**, **4**.

Neutralizing TNF-α

One possible target for CD4+ T cell modulation is TNF-α, which is secreted by Th1 and Th17 cells. TNF-α levels can be two to three times higher in PreE than in normotensive pregnancies (Harmon et al., 2016; Rambaldi et al., 2019) and have been linked to gestational HTN, endothelial dysfunction, and poor obstetric outcomes (Small et al., 2016). Though crucial for correct implantation and placentation (Yuan et al., 2015), TNF-α is attributed to IL-10-dependant inhibition of CD4+ T cell expansion (Alijotas-Reig et al., 2017), preventing a healthy pro- and anti-inflammatory CD4+ T cell balance. Additionally, TNF-α indirectly causes vasoconstriction after initiating systemic pro-inflammatory and pro-apoptotic signaling cascades that increase reactive oxygen species (ROS) and contribute to placental oxidative stress (Redman et al., 1999). Inhibiting TNF-α using anti-TNF-α neutralizing monoclonal antibodies (mAbs) promotes the proliferation of Tregs while suppressing effector T (Teff) cells (Xiao et al., 2021).

Guidelines from the FDA indicate that anti-TNF-α treatments are category B drugs (i.e. drugs that have failed to demonstrated risk to the fetus but for which no well-controlled studies exist in pregnant women) (Raja et al., 2012). The British Association of Dermatologists recommends the use of TNF-α inhibitors on a case-by-case basis in pregnancy (Johansen et al., 2018), and the European Crohn's and Colitis Organization has found that TNF-α inhibitors may be used safely until the third trimester (Johansen et al., 2018). Because of its presumed safety, anti-TNF-α may be a viable PreE therapy to increase Treg cell populations and rebalance the Th1/Th17:Treg/Th2 ratio in PreE.

Therapeutics targeting TNF-α have also been used in other inflammatory diseases to combat immune dysregulation. For instance, anti-TNF-α neutralizing mAbs are approved for use in RA, AS, and IBD. These drugs include etanercept (Aronson, 2006), infliximad (Wall et al., 1999), certolizumab pegol (Weber-Schöndorfer et al., 2015; J. Egan and Maaser, 2009), golimumab (Taylor et al., 2015), and adalimumab (Taylor et al., 2015; Jafri and Ormiston, 2017; Xiao et al., 2021).

Work in PreE animal models further suggests the utility of TNF-α therapeutics in clinical PreE. For instance, the TNF-α ligand trap etanercept prevents HTN and decreases ROS-induced vascular dysfunction in the reduced uterine perfusion pressure (RUPP) rat model of PreE. Etanercept also rescues vascular pathology in the deoxycorticosterone acetate (DOCA) high-salt diet neurogenic rodent HTN model (DOCA-salt) (Guzik et al., 2007; Basting and Lazartigues, 2017), which exhibits a similar immune state to PreE (i.e. excessive pro-inflammation and

TABLE 1 | Immunomodulation offers promise for preeclampsia (PreE) prevention. This table describes potential preeclampsia prevention targets, the directionality of target abnormality in PreE, drugs that modulate the targets, and the effects of each drug on PreE-related biological processes. Treg, regulatory T cell; NK, natural killer; DC, dendritic cell; CTLA-4, cytotoxic T lymphocyte-associated antigen-4; IVIg, intravenous immunoglobulin G; ET_A, endothelin-1 receptor A; anti, antibody; CoPPIX, cobalt protoporphyrin; HO-1, heme oxygenase 1, mAbs, monoclonal antibodies; Th, Helper T cell; Treg, regulatory T cell; IL, interleukin; IFN-γ, interferon gamma; TNF-α, tumor necrosis factor alphasFlt-1, soluble Fms-like Tyrosine Kinase-1; PLGF, placental growth factor; VEGF, vascular endothelial growth factor; IL-17RC mouse IL-17 receptor C; 17-OHPC, 17-hydroxyprogesterone caproate; NK2, non-cytolytic, type 2 Natural Killer cells; NK1, cytolytic, type 1 Natural Killer cells; TLR5, toll like receptor five; AT1-AA, Angiotensin II Type 1 Receptor Agonistic Autoantibody.

Target	Change in targets in preeclampsia	Drug	Drug effect on preeclampsia mechanisms	Citation
TNF-α	Increase	anti-TNF-α neutralizing mAb	Less pro-inflammatory T cell differentiation via DC maturation and IL-10-dependant inhibition of CD4+ T cell expansion	Yuan et al. (2015), Alijotas-Reig et al. (2017)
			Decreased vasoconstriction, coagulation, vascular permeability, and microvascular leakage	LaMarca et al. (2005), Kaplanski et al. (1997)
			Decreased endothelial dysfunction; trophoblastic apoptosis inactivation	Alexander et al. (2001), Huppertz and Kingdom (2004), Chen et al. (2010), Ibrahim et al. (2017)
CD28	Decrease	CD28 superagonist TGN1412/TAB08	Treg promotion Reduced pro-inflammatory response Reduced cytolytic NK cell activation during placental invasion	Tabares et al. (2014) Ibrahim et al. (2017) Ibrahim et al. (2017)
IL-10	Decrease	IL-10 administration	Promote macrophage maturation to anti-inflammatory M2	Harmon et al. (2015)
Treg	Decrease	adoptive transfer	Promote mast cell repair of the placental and vascular defects	Maganto-García et al. (2011), Matrougui et al. (2011), Woidacki et al. (2015)
			Reduced oxidative stress	Jafri and Ormiston (2017), Dall'Era et al. (2019), Chen et al. (2010)
IL-6	Increase	anti-TLR-5 anti-IL-6	Increased anti-inflammation	Narazaki et al. (2017) Tousoulis et al. (2016), Narazaki et al. (2017), Trivedi and Adams (2018)
IL-17	Increase	anti-IL-17	Prevents offspring neurodevelopmental defects	Amador et al. (2014), Reed et al. (2020)
			Improved vascularization; decreased AT1-AA and oxidative stress	Amador et al. (2014)
		ET_A antagonists	Downregulated mature DCs; decreased vascular permeability and vasoconstriction	Alexander et al. (2001); Tanaka et al. (2014); Morris et al. (2016)
		IL-17RC	Improved vascularization; decreased IL-17 activation of cytolytic NK cells and decreased pro-inflammation	Cornelius et al. (2013); Travis et al. (2020)
		Spironolactone	Decreased Th17 activation and increased FoxP3-dependent Treg differentiation	Amador et al. (2014)
			Improved placentation via competitive binding of aldosterone	Birukov et al. (2019)
HMG-CoA reductase		Statins	Improved placentation; reduced sFlt-1; increased pro-survival/antiapoptotic factors; upregulated PLGF and VEGF	Youssef et al. (2002); Kumasawa et al. (2011); McDonnold et al. (2014); Esteve-Valverde et al. (2018); 82
Cytolytic NK cells	Increase	17-OHPC CD28 mAbs	Decreased pro-inflammation Decrease IL-6/IL-2-mediated activation of cytolytic NK cells	Gupta and Roman (2012); Elfarra et al. (2020) Ibrahim et al. (2017)
DCs	skewed towards pro-inflammatory	CTLA-4 CoPPIX-mediated HO-1 induction IVIg	Decreased DC maturation and subsequent pro-inflammatory T cell and cytolytic NK cell activations	Gu et al. (2012) Bayry et al. (2003)

inadequate anti-inflammation) (Guzik et al., 2007). Similar effects have been reported in animal models of PAH and systemic HTN (Jafri and Ormiston, 2017).

These animal models of PreE have some limitations. For instance, the RUPP rat model features placental ischemia, which occurs only in the end stage of PreE. However, the RUPP model also mirrors increased Th1, Th17, and other PreE-associated molecular changes such as increased ET-1, AT1-AA, ROS, and TNF-α, as well as critical disease phenotypes (i.e., HTN, endothelial dysfunction) (Ibrahim et al., 2017). However, given that it is an end-stage model, RUPP is limited in its capacity to represent early PreE pathogenesis, where immune based therapies may be most useful. Despite this limitation, the results in RA, AS, IBD, and PreE animal models suggest the effectiveness of anti-TNF-α treatments

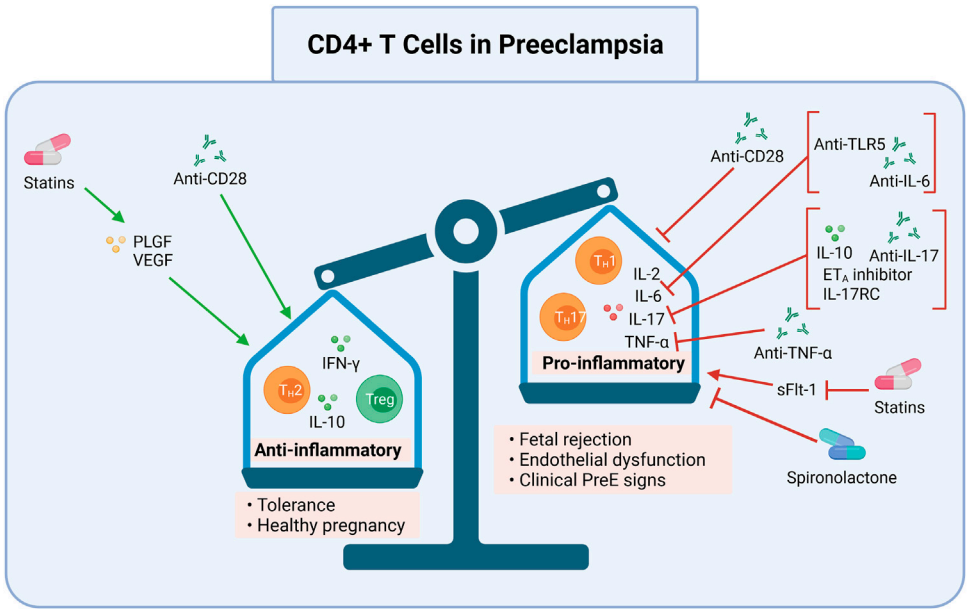

FIGURE 2 | CD4+ T cell pro-inflammation and processes may be targeted in preeclampsia. Induction of anti-inflammatory CD4+ T cells (Th2s) and Tregs, and inhibition of pro-inflammatory CD4+ T cells (Th17s, TH1s) may be one pathway for preeclampsia treatment and prevention. Collectively, modulation of these processes may ameliorate the overly pro-inflammatory immune response in preeclampsia. Shifting the ratio of pro-to anti-inflammatory CD4+ T cells may prevent preeclampsia by allowing proper placentation and reducing resultant oxidative stress. This can be done by 1) promoting an anti-inflammatory milieu (Th2, Treg, IFN-γ, IL-10) with anti-CD28, statins that induce PLGF and VEGF, or 2) inhibiting a pro-inflammatory milieu (Th1, Th17, IL-2, IL-6, IL-17, and TNF-α) with anti-CD28 or spironolactone, or inhibiting sFlt-1using statins. Specific cytokines may also be inhibited, such as IL-6 by anti-TLR5 or anti-IL-6; IL-17 by IL-10, ET_A inhibitors, IL-17RC, and anti-IL-17; or TNF-α by anti-TNF-α. The anti-inflammatory CD4+ T cell response may result in tolerance and a healthy pregnancy while the pro-inflammatory CD4+ T cell response may lead to fetal rejection, endothelial dysfunction, and clinical preeclampsia signs. DC, dendritic cells; mAbs, monoclonal antibodies; Th, Helper T cell; Treg, regulatory T cell; IL, interleukin; IFN-γ, interferon gamma; TNF-α, tumor necrosis factor alpha; anti, antibody; ET_A, endothelin-1 receptor A; sFlt-1, soluble Fms-like Tyrosine Kinase-1; PLGF, placental growth factor; VEGF, vascular endothelial growth factor; IL-17RC mouse IL-17 receptor C; TLR5, toll like receptor 5. Created with https://biorender.com.

for treating pro-inflammation in PreE, warranting further exploration.

TNF-A AND ENDOTHELIN-1/ ENDOTHELIN-1 RECEPTOR A

TNF-α is thought to exacerbate PreE by activating vasoconstrictive endothelial cells and increasing coagulation, vascular permeability, microvascular leakage, and trophoblastic apoptosis (Kaplanski et al., 1997; Huppertz and Kingdom, 2004). Resultant cellular debris activate endothelial cells via ET-1/ET-1 receptor A (ET_A) pathway activation, causing dysfunction and eliciting further pro-inflammatory activation, vasoconstriction, and HTN (Raghupathy, 2013; Morris et al., 2016). TNF-α also stimulates ET-1 production by endothelial cells, which is elevated in the RUPP rat model (Alexander et al., 2001). Three ET_A antagonists (ambrisentan, bosentan, and macitentan) that inhibit vasoconstriction to prevent HTN and slow disease progression are currently approved for the treatment of PAH because of their effects on IL-17 (National Institute of Diabetes and Digestive and Kidney Diseases, 2012).

IL-17 processes also interact with ET signaling. Despite modulating IL-17 production by Th17 cells, ET/ET_A does not appear to directly mediate Th17 differentiation (Tanaka et al., 2014). Instead, effector T cell differentiation is promoted by DC maturation, which is in turn associated with increased ET-1 (Tanaka et al., 2014). Incubation with ET_A receptor antagonists inhibit DC maturation, thus downregulating mature DC stimulation of cells including Th1 and cytotoxic NK cells (Guruli et al., 2004; Tanaka et al., 2014). In both *in vitro* and *in vivo* mouse models, ET_A receptor blockade reduces IL-17 production following Th17 activation, which is discussed later in this review. These reductions in IL-17 release and Th17 activation are associated with significantly decreased risk for HTN, HELLP syndrome, and renal dysfunction following ischemic injury (Alexander et al., 2001; Morris et al., 2016; Boesen, 2018). By neutralizing TNF-α, there may be fewer cellular debris in circulation and in the placenta, thus blunting ET-1/ET_A pathway activation and limiting pro-inflammation, HTN, and renal dysfunction. Together, this may lead to less TNF-α-mediated vasoconstriction, vascular permeability, and apoptosis (**Figure 2**).

CD28 ANTIBODIES

Another cytokine-specific antibody manipulation of interest for the treatment of PreE is the superagonistic monoclonal antibody

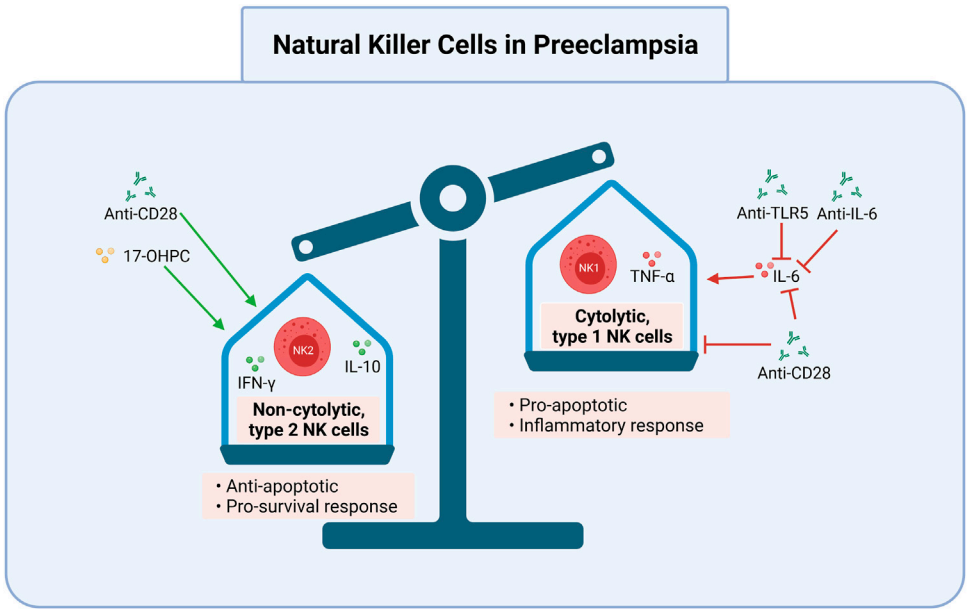

FIGURE 3 | Cytolytic NK cells may be targeted in preeclampsia. Induction of non-cytolytic NK cells and inhibition of cytolytic NK cells is one potential avenue for the treatment and prevention of preeclampsia. Anti-TLR5, anti-IL-6, and anti-CD28 inhibit IL-6's activation of pro-apoptotic cytolytic type 1 NK cells. Anti-CD28 also directly inhibits type 1 NK cells, and promotes non-cytolytic, type 2 NK cells and the anti-apoptotic cytokines IL-10 and IFN-γ. 17-OHPC works similarly to promote type 2 NK cells. Together, these reduce the cytolytic NK cell response, which can lead to improper placentation and subsequent preeclampsia. 17-OHPC, 17-hydroxyprogesterone caproate; anti, antibody; IFN-γ, interferon gamma; NK2, non-cytolytic, type 2 Natural Killer cells; IL, interleukin; NK1, cytolytic, type 1 Natural Killer cells; TNF-α, tumor necrosis factor alpha; TLR5, toll like receptor 5. Created with https://biorender.com.

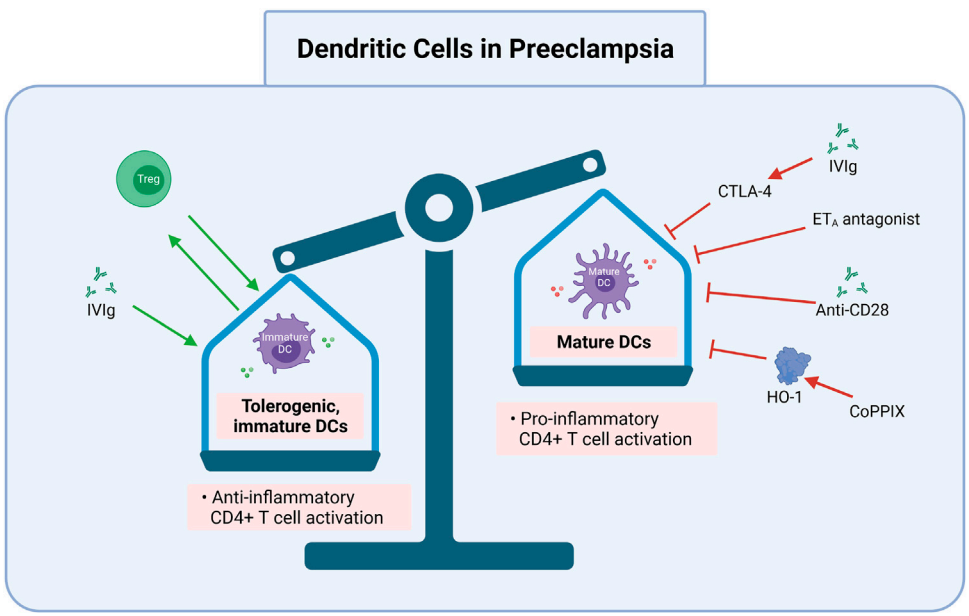

FIGURE 4 | DC cells maturation and function may be targeted in preeclampsia. Inhibition of mature CDs and induction of tolerogenic, immature DCs is one promising route for preeclampsia treatment and prevention. Targets to achieve this include exogenous Treg transfer, IVIgs to promote tolerogenic DCs (e.g., via CTLA-4), CoPPIX induced HO-1 activation, and ET_A antagonists. IVIg via CTLA-4, anti-CD28, ET_A antagonists, and CoPPIX via HO-1 inhibit mature DC function, which can be pro-inflammatory to CD4+ T cells. Treg, regulatory T cell; DC, dendritic cell; CTLA-4, cytotoxic T lymphocyte-associated antigen-4; IVIg, intravenous immunoglobulin G; ET_A, endothelin-1 receptor A; anti, antibody; CoPPIX, cobalt protoporphyrin; HO-1, heme oxygenase 1. Created with https://biorender.com.

(SA) against CD28. Recently, testing of anti-CD28 monoclonal antibodies (mAbs) has been studied in PAH as a Treg stimulator because CD28 is a potent Treg activator and decreases pro-inflammatory cytokine secretion (Tabares et al., 2014). In the PreE RUPP rat model, SA mAb administration stimulated Treg cell proliferation, increasing the percent of Treg cells relative to those seen in normal pregnancy and reducing the clinical signs of PreE in response to placental ischemia (Ibrahim et al., 2017). Additionally, IL-6 and IL-2 levels, which promote Th1 proliferation and activate NK cells, were decreased to control levels in the RUPP model after SA mAb treatment (Ibrahim et al., 2017). Stimulation of cytolytic NK cells increased apoptosis and debris, aggravating the pro-inflammatory response further. NP controls maintained balanced cytokine and Treg levels, normal BP, and delivered pups of a healthy weight (Ibrahim et al., 2017). A reduction without complete inhibition is notable because maintaining appropriate pro-inflammation is essential for proper placental invasion (Sargent et al., 2006). SA mAb administration also normalizes fetal weight in RUPP offspring, highlighting the PreE-relevant benefits of Treg and NK cell stimulation. These findings offer insights into antibody-based tactics that manipulate CD4+ T (**Figure 2**) and NK cell mechanisms (**Figure 3**).

IL-10 ADMINISTRATION AND INDUCTION

IL-10, which is produced by macrophages, Tregs, and regulatory NK cells, is an immunosuppressive cytokine necessary for appropriate differentiation of decidual macrophages and subsequent immune activation in trophoblast invasion and tissue remodeling (Heyward et al., 2017). Decreased IL-10 is associated with PreE and other inflammatory diseases, as IL-10 impedes macrophage differentiation and effectively suppresses pro-inflammation triggered by fetal/paternal antigens (**Figures 2–4**) (Lutsenko et al., 2014; Harmon et al., 2016; Heyward et al., 2017).

Animal models of PreE offer some insights into a potential role for IL-10 in PreE pathogenesis. For instance, in the BPH/5 inbred murine model of early PreE, IL-10 is spontaneously decreased. This model also develops early impaired invasion and placentation phenotypes and exhibits deficient spiral artery remodeling (Hoffmann et al., 2008). Decreased IL-10 in the BPH/5 model results from suppression of decidual macrophages and inadequate immune activation in response to fetal antigens (Davisson et al., 2002).

While the BPH/5 model represents early PreE phenotypes, the RUPP model, which recapitulates later pathoetiologic changes in PreE, demonstrates a potential therapeutic role for IL-10 supplementation in PreE. Administering IL-10 in the RUPP model leads to a partial rescue of HTN (Harmon et al., 2015). Moreover, IL-10 delivery via osmotic mini pumps in the RUPP model significantly lowers circulating Th1, Th17, and placental ROS, increases Treg cell differentiation, and normalizes TNF-α levels (**Figure 2**) (Harmon et al., 2015). This demonstrates that IL-10 agonism may help to prevent PreE pathogenesis via immune mechanisms. Given that IL-10-producing macrophages are decreased in PreE, together with data from the BPH/5 and RUPP models, suggests that IL-10 supplementation may be one PreE therapeutic avenue.

In addition to its utility in PreE, IL-10 supplementation and induction are possible prophylaxis and treatment options for a variety of additional pro-inflammatory diseases. For example, in adjuvant arthritis mice models for RA, IL-10 inducers or IL-10 producing cells (e.g., Th2, Tregs) attenuated clinical phenotypes and normalized IL-10 levels after 28 days of administration (Lutsenko et al., 2014). In another pro-inflammatory disorder, osteoarthritis, increased IL-10 expression significantly decreased pain in a dog model, supporting the benefits of IL-10 prophylactics for inflammatory conditions (Uzieliene et al., 2021). IL-10 also prevents PAH via suppressed antigen presentation by macrophages and DCs, blunted pro-inflammatory cytokine release, and activated Treg cells (Lai et al. (2011); Jafri and Ormiston, 2017). Incubating naïve CD4+ T cells with IL-10-producing DCs also promotes Treg cell differentiation (Harmon et al., 2015), which is decreased in PreE. Collectively, these results demonstrate that IL-10 may be a novel, effective modulator of pro-inflammatory phenotypes and disease pathogenesis across multiple conditions.

TRANSFER OF TREGS TO PROMOTE ANTI-INFLAMMATION

Transfer of Treg cells is a direct means by which to increase Treg levels. T-cell-based immunomodulation strategies are advancing quickly in the treatment of blood and tumor malignancies, as well as other immune-mediated diseases. The use of donor and engineered Tregs to combat immune dysregulation is also being studied in IBD (Graham and Xavier, 2020; Xiao et al., 2021), DM (Bluestone et al., 2015), PAH, SLE (Dall'Era et al., 2019; Shan et al., 2020), and in rodent models of PreE (Jafri and Ormiston, 2017). Collectively, these studies demonstrate that Treg adoptive transfer is effective in promoting anti-inflammation and restoring a healthy ratio of Treg/Th2:Th1/Th17, and is not associated with significant adverse effects (Ou et al., 2018). Preclinical trials have likewise demonstrated that adoptive transfer of CD4+CD25 + Treg cells into rats with PAH reduces HTN to immunocompetent control rat levels (Jafri and Ormiston, 2017). The first adoptive Treg cell therapy was used in a patient with SLE in 2019, yielding increased Treg cell activation and decreased Th1-mediated pro-inflammation (Dall'Era et al., 2019). Moreover, a phase I trial in type 1 diabetes demonstrated that a single Treg infusion was safe, well tolerated, and led to enhanced suppressive activity due to Treg and IL-2 expansion and 1 year of Teff cytokine depletion (Bluestone et al., 2015).

As in the clinical literature, studies of Treg cellular infusion in rodent models of hypertensive disease with Treg cell infusion also demonstrate mitigated inflammatory pathology. Mouse models of HTN demonstrate a protective effect when Treg cells are adopted from healthy pregnancies to hypertensive ones. More specifically, Treg cell transfer from healthy controls to HTN mice promotes mast cell repair of placental and vascular defects and reduces BP (Maganto-García et al., 2011; Matrougui et al., 2011;

Woidacki et al., 2015). However, lowering BP does not necessarily prevent PreE. For instance, in the RUPP rat model of PreE, while transfer of Tregs from a healthy pregnant rat into RUPP rats prior to uterine artery occlusion, which is used to model PreE placental ischemia, rescued multiple PreE endophenotypes (BP, growth restriction, vasoactive factors, pro-inflammation, placental oxidative stress) (Cornelius et al., 2015; Harmon et al., 2016; Jafri and Ormiston, 2017; Cornelius, 2018; Robertson et al., 2019). Yet, it did not fetal morbidity (Cornelius et al., 2015). The prophylactic potential of Treg transfer in PreE is mostly reliant on a direct increase in anti-inflammatory CD4+ T cell levels (i.e., Th2 and Treg) upon treatment (**Figure 2**).

Adoptive Treg cell transfer remains a promising area of study because it may mitigate gestational immune dysregulation at the outset, before PreE pathology progresses. While preclinical work has demonstrated the promise of adoptive Treg cell transfer for the treatment of PreE, more research is needed to better understand the side effects, underlying mechanisms, and application of this approach to human disease.

DECREASING IL-6 LEVELS

IL-6 contributes to pro-inflammation in PreE by inducing Th17 and cytotoxic T cell differentiation and inhibiting immunosuppressive Tregs and Th2 (Redman et al., 1999). Decreasing IL-6 via anti-IL-6 mAbs or toll-like receptor (TLR) five inhibitors may reduce pro-inflammation (Narazaki et al., 2017) (**Figure 2**), thereby modulating PreE pathogenesis. IL-6 inhibitors [e.g., anti-IL-6 receptor mAbs (e.g., sarilumab, tocilizumab) and anti-IL-6 mAbs (i.e., siltuximab)] may direct the expansion of inexperienced CD4+ T cells away from inflammatory Th1 and Th17 subtypes (Narazaki et al., 2017; Xiao et al., 2021). Clinical studies support the successful use of immunomodulation to modulate IL-6, as in IBD (Trivedi and Adams, 2018), RA (Narazaki et al., 2017), and AS (Tousoulis et al., 2016; Ridker et al., 2017). Various mAbs and TLR five antibodies have been used to achieve IL-6 regulation. The administration of these antibodies reduces IL-6 and lowers cardiovascular risk (Ridker et al., 2017). Applying similar IL-6-reduction strategies to the treatment of PreE may drive differentiation and proliferation of naïve CD4+ T cells towards an anti-inflammatory Treg and Th2 cell fate rather than a pro-inflammatory Th1 and Th17 one.

BLOCKING IL-17 AND DECREASING TH17

Another potential inflammatory target for the treatment of PreE is Th17, levels of which are increased in the disease. Suppression of Th17 via IL-17 recombinant receptor administration decreases HTN, oxidative stress, and AT1-AA production (Cornelius et al., 2013). A recent study utilizing chronic administration of recombinant mouse IL-17 receptor C (IL-17RC), a soluble receptor that blocks IL-17, to RUPP rats reported normalized total placental and cytolytic NK cells, decreased circulating IL-17, decreased circulating and placental Th17s, and decreased TNF-α, as well as decreased mean arterial pressure (MAP) (Travis et al., 2020). Additionally, repeated acute administrations of IL-17RC diminished Th17 proliferation (Travis et al., 2020). These studies reveal the potential efficacy of IL-17RC for treating IL-17-mediated pro-inflammation in PreE.

In the DOCA-salt neurogenic rodent model of HTN, Th17, and IL-17 levels are elevated as they are in PreE (Amador et al., 2014; Basting and Lazartigues, 2017). When given to DOCA-salt rats, Spironolactone competitively binds aldosterone and prevents Th17 activation, normalizing IL-17 levels and inducing Treg differentiation by increasing forkhead box P3 transcription (Amador et al., 2014). Administration of anti-IL-17 antibodies in the DOCA-salt model ameliorated HTN, oxidative stress, and fibrosis, likely by decreasing Th17 polarization (Amador et al., 2014). Similarly, in the HELLP rodent model of PreE, decreasing IL-17 by blocking the ET_A receptor preferentially reduced Th17 differentiation and lowered BP (Morris et al., 2016). Furthermore, Th17s may promote NK activation via IL-17 induction (Travis et al., 2020), though the exact mechanism underlying this remains unclear. By targeting Th17 or blocking IL-17 in PreE, pro-inflammatory cytokine production and NK cell activation may be decreased, resulting in less cytotoxic activity and thereby decreased pro-inflammation (**Figure 2**).

PRAVASTATIN

Recently, statins have attracted interest as targets for PreE prevention due to their potent anti-inflammatory effects. Statins are 3-hydroxy-3-methylglutaryl coenzyme A (HMG-CoA) reductase inhibitors that are approved by the FDA for cholesterol reduction, though they are currently contraindicated for use in pregnancy. The clinical PRINCE [pravastatin inflammation/reduced C-reactive protein (CRP) evaluation] trial confirmed that pravastatin has anti-inflammatory effects in primary and secondary prevention settings in addition to its lipid-lowering effects (Albert et al., 2001). Given these results, statins began to be considered for the treatment of pro-inflammatory diseases such as DM (van de Ree et al., 2003), metabolic syndrome (Bulcão et al., 2007), atherosclerosis (S. Antonopoulos et al., 2012), and multiple sclerosis (Youssef et al., 2002). Multiple trials have demonstrated reduced CRP and circulating pro-inflammatory cytokines with statins. *In vivo* studies have further shown specifically that administration of statins induces Th2 cytokines (including IL-4, IL-5, IL-10, and TGF-β) and suppresses Th1 cytokines (including IL-2, IL-12, TNF-α, and IFN-γ) (Youssef et al., 2002; Esteve-Valverde et al., 2018). Applying this to PreE may help balance the elevated Th1: Th2 ratio characteristic of the disease.

Despite being contraindicated for use in pregnancy, a recent study in DBA/2-mated CBA/J mice, a well-studied spontaneous abortion and fetal growth restriction mouse model (Redecha et al., 2009), demonstrated that pravastatin effectively rescued placental dysfunction and prevented fetal resorptions (Redecha et al., 2009). Another small study in a novel lentiviral vector-mediated placental sFlt-1 expression mouse model of PreE

reported decreased blood pressure and proteinuria with daily pravastatin (Kumasawa et al., 2011). Several studies in pregnant mice demonstrated reduced sFlt-1 levels and reduced hypoxia, significantly increased pro-survival/antiapoptotic factors, and upregulated PLGF and VEGF-A after treatment with adenovirus-carrying sFlt-1 and statins (McDonnold et al., 2014; Saad et al., 2014; Saad et al., 2016).

Reduced sFlt-1 expression is another potential intervention strategy for PreE, which can increase PLGF and VEGF. Additionally, the use of T-NPsisFLT1 or PEG-PLA nanoparticles as sFLT1 siRNA placenta specific delivery systems can decrease sFlt-1 in pregnant CD1 mice and silencing sFlt-1 in this way is being studied as a method to ameliorate PreE in similar manners to statins (Li et al., 2020). Furthermore, a 2016 pilot randomized controlled trial assessing the use of pravastatin in PreE found no safety risks (Costantine et al., 2016), while another recent study reported lower rates of PreE and preterm delivery in high-risk individuals treated with pravastatin (Costantine et al., 2021). These results, in conjunction with the known immunomodulatory effects of statins (**Figure 2**), justify further immune research into pravastatin's use in PreE prevention and therapy.

17-HYDROXYPROGESTERONE CAPROATE

Another potential avenue for immunologic treatment of PreE is targeting cytolytic placental NK cells early in gestation to decrease Th1/17 and increase Treg/Th2 cells. Within circulation and in the placenta in PreE, non-cytolytic, type 2 NK cells are decreased while cytolytic, type 1 NK cells are increased (Fukui et al., 2012), increasing apoptosis and therefore the production of debris. Elfarra *et al.* tested 17-hydroxyprogesterone caproate (17-OHPC) in the RUPP rat model of PreE (Elfarra et al., 2020) and found that the synthetic hormone, which is commonly used to prevent preterm delivery in healthy pregnancies, has anti-inflammatory and vasodilatory effects (Dodd et al., 2013). Because the naturally occurring hormone progesterone reduces cytotoxic NK cell activity in the uterus (Dosiou and Giudice, 2005; Elfarra et al., 2020), 17-OHPC may act similarly (Elfarra et al., 2020).

In the RUPP model, 17-OHPC normalized HTN and pup weight, decreased fetal demise rates, reduced uterine artery resistance, and increased circulating and placental Th2 cells while suppressing pro-inflammatory CD4+ T cells and cytokines to restore immune balance (Elfarra et al., 2020). Circulating Th2 cells were significantly increased in RUPP rats with 17-OHPC treatment (Elfarra et al., 2020). Furthermore, cytolytic NK cells were also decreased significantly with 17-OHPC administration, and the administration was associated with attenuated hypertension in response to placental ischemia (Elfarra et al., 2020). While there is limited data on 17-OHPC prevention of PreE, phenotypes were decreased in the RUPP model (e.g., decreased total and cytolytic placental NK cells, attenuation of pro-inflammatory T cells and cytokines, decreased HTN and fetal weight), which is likely attributable to suppressed inflammation and increased placental Th2. Together, these data on Th2-NK cell dynamics suggest that hormone strategies are another potential CD4+ T cell-based PreE prevention mechanism (**Figure 2**).

TREG CELL STIMULATION VIA NK CELLS AND DCS

Suppressing Teff cells and manipulating NK and DC pathways are additional methods for the treatment of AS, PAH, and SLE (Xiao et al., 2021). PreE pregnancies have increased populations of cytolytic, type 1 NK cells, which also exhibit enhanced cytolytic activation (Fukui et al., 2012; Sargent et al., 2007). These cytolytic NK cells secrete increased levels of TNF-α (Fukui et al., 2012), which contribute to PreE pathogenesis. Conversely, however, non-cytolytic, type 2 NK cells also stimulate Treg proliferation by releasing interferon gamma (IFN-γ) (Fukui et al., 2012). Therefore, normalizing NK levels may provide another route for PreE prevention. While the dynamics and direct interactions between NK cells, DCs, and resultant Treg stimulation require further interrogation, some promising manipulations inhibit cytotoxic NK cells and others prevent DCs from presenting self-antigens (Bayry et al., 2003; Gu et al., 2012; Elfarra et al., 2020).

DCs and other antigen presenting cells (APCs) also contribute to immune dysregulation by presenting fetal antigens and stimulating pro-inflammatory Th1 and Th17 cells at the maternal-fetal interface. It is likely that modulation of abundant decidual NK cells and DCs via interactions with T cells and their cytokine/chemokine products, may be one avenue for PreE treatment and prevention. In fact, decidual NK cells are a potential target for early pregnancy pathology and immune dysregulation, for example in recurrent miscarriage or implantation deficits (Tao et al., 2021). However, the precise interactions between CD4+ T cells and decidual NK cells at the maternal-fetal interface requires further elucidation.

For example, IL-10 and TGF-β (produced by Tregs), as well as Treg surface molecules such as inhibitory receptor cytotoxic T lymphocyte-associated antigen-4 (CTLA-4) inhibit DC function and maturation (**Figure 4**). This is likely because CTLA-4 binds to CD80/CD86 and blocks the activation of naïve T cells by DCs (Gu et al., 2012). DCs mediate either immune rejection or tolerance because they direct T cell alloresponses towards pro- or anti-inflammatory subtypes (Mashreghi et al., 2008). Stimulating the production or adoptive transfer of immature DCs can be manipulated for prevention use to prevent downstream activation of pro-inflammatory T cells (**Figure 1**) or cytolytic NK cells (**Figure 4**). CTLA-4, IL-10, and TGF-β and their subsequent inhibition of DC function are associated with increased Treg numbers and decreased pro-inflammatory responses in AS (Dietrich et al., 2012; Foks et al., 2015; Ou et al., 2018). The immunological similarities between AS and PreE suggest that DC inhibition decreases pro-inflammatory Th1 and Th17 differentiation, preventing PreE pathogenesis.

Another DC modulator is cobalt protoporphyrin induced heme oxygenase 1 (HO-1), which is currently used to protect against

inflammatory liver failure and ischemia reperfusion injury after transplant procedures. This is because HO-1 has potent anti-inflammatory properties; it attenuates the expression of various proinflammatory genes, such as TNF-α, IL-1, and -6 by mononuclear phagocytes and downregulates leukocytes adhesion in response to oxidative stress (Mashreghi et al., 2008; Vijayan et al., 2010). Similarly, intravenous immunoglobulin G administration is used as a therapy for many immune-mediated conditions, transplantation, and systemic inflammatory diseases (e.g., SLE, Guillain-Barre syndrome, RA, and more) because it inhibits DC maturation, increases anti-inflammatory IL-10, and down-regulates pro-inflammatory T cells (Bayry et al., 2003) (**Figure 4**). These approaches, which decrease NK cell numbers and blunt DC maturation, may demonstrate similar effectiveness in restoring a proper immune balance in PreE and therefore deserve further exploration.

DISCUSSION

A healthy pregnancy requires a balance of pro- and anti-inflammatory immune factors to accomplish proper placentation and protect the pregnant person from invading pathogens, while also establishing tolerance to fetal antigens. Growing evidence indicates that PreE pathology is in part attributed to an altered immune response; namely elevated pro-inflammatory Th1/Th17 and reduced anti-inflammatory Treg/Th2, along with their respective cytokines (Redman et al., 1999; Redman and Sargent, 2010). A dysregulated inflammatory response is associated with poor invasion and inadequate remodeling of the uterine spiral arteries during stage one of the classic Two Stage model of PreE (Redman, 1991; Redman et al., 1999). There is subsequent placental oxidative stress and hypoxia, and Stage 2 follows, prompting further pro-inflammation and ultimately the clinical manifestations of PreE (HTN, proteinuria, and end-organ damage) (Redman et al., 1999; Committee on Practice Bulletins-Obstetrics, 2020). Though the exact mechanism driving this immune shift is not fully understood, there is compelling evidence that maladaptation to fetal/paternal alloantigens is to blame. Immune modulation is thus a prime goal of successful PreE prophylactics (Li and Wi, 2000; Kho et al., 2009; Redman and Sargent, 2010).

Immunomodulation in other immune-mediated diseases to improve the immunosuppressive capacity of Tregs and decrease Th1/Th17 activation may offer viable strategies for the treatment and prevention of PreE. Specifically, immunomodulators targeting CD4+ T cell mechanisms are emerging as potential drugs of interest for PreE. Together, the studies and findings reviewed here point to a promising role for modulation of Tregs, Th1, and Th17 cells, in particular by specific cytokine inducers or suppressors. Existing classes of drugs (e.g., statins, spironolactone) may also be harnessed to achieve cytokine/chemokine modulation and thereby CD4+ T cell attenuation to treat and prevent PreE. The weight of the evidence also demonstrates that specific modulators (e.g., anti-IL-17) may be less effective than more global immunomodulatory agents (e.g., anti-CD28) in reducing the burden of pro-inflammatory CD4+ T cells in PreE pathogenesis.

Application of approved therapies for other immune-mediated diseases to the treatment of PreE has likewise yielded promising results. While most studies aim to normalize immune dysregulation by stimulating Treg cells and inhibiting Th1 and Th17 cells via cytokine induction or suppression of their downstream activation by mature DC or apoptotic debris (due to NK cells), adoptive transfer of Treg cells, or neutralization of pro-inflammatory cytokines via antibody-based drugs also offers promise. Furthermore, Treg therapies have gained popularity for use in combatting inflammatory and immune diseases. Over 50 total registered clinical trials using Tregs occurred in 2019: 12 for autoimmune diseases, 23 for hematopoietic stem cell transplantation or graft-versus-host disease, and 16 for solid organ transplantation (Ferreira et al., 2019). PreE pregnancies have striking commonalities to these disease categories. Because the immunological mechanisms underlying PreE are likely present very early in pregnancy, targeting CD4+ T cell pathways provides a possible and very promising avenue for PreE prevention, as this review demonstrates. Ultimately, by normalizing the maternal response to fetal antigens and the broader immune state (e.g. restoring the proper Th1/17:Treg/Th2 cell ratio), PreE pathogenesis may be interrupted.

Despite some successes, the application of specific immunomodulatory tactics to PreE is currently limited due to poor chemical stability, high cost, regulatory restrictions, and poor patient compliance with repeated dosing protocols (Xiao et al., 2021). However, existing work in other pro-inflammatory disorders offer important insights into the treatment of PreE, a devastating disease that impacts nearly 6.6 million pregnancies globally each year (Duley, 2009). It is essential that research continue to develop and assess improved or novel approaches to treating and preventing the immunology of PreE.

AUTHOR CONTRIBUTIONS

All authors listed have made a substantial, direct, and intellectual contribution to the work and approved it for publication.

FUNDING

The authors wish to acknowledge the funding sources including the University of Iowa Premed Student Summer Research Program, National Institutes of Health (This study was supported by the National Institutes of Health (R01HD089940, T32MH01911328), and the American Heart Association (18SCG34350001). Data reported in this publication received research support and financial support from the National Center for Advancing Translational Sciences of the National Institutes of Health (UL1TR002537, UL1TR002537-S1). The funders play no role in study design, collection/analysis/interpretation of data, writing of this manuscript, and the decision to submit the manuscript.

REFERENCES

Committee on Practice Bulletins-Obstetrics (2020), Gestational Hypertension and Preeclampsia: ACOG Practice Bulletin Summary, Number 222. *Obstet. Gynecol.* 135, 1492, 1495. doi:10.1097/AOG.0000000000003892

Al-Safi, Z., Imudia, A. N., Filetti, L. C., Hobson, D. T., Bahado-Singh, R. O., and Awonuga, A. O. (2011). Delayed Postpartum Preeclampsia and Eclampsia. *Obstet. Gynecol.* 118, 1102–1107. doi:10.1097/aog.0b013e318231934c

Albert, M. A., Danielson, E., Rifai, N., Ridker, P. M., and for the Prince Investigators, f. t. P. (2001). Effect of Statin Therapy on C-Reactive Protein Levels. *JAMA* 286, 64–70. doi:10.1001/jama.286.1.64

Alexander, B. T., Rinewalt, A. N., Cockrell, K. L., Massey, M. B., Bennett, W. A., and Granger, J. P. (2001). Endothelin Type a Receptor Blockade Attenuates the Hypertension in Response to Chronic Reductions in Uterine Perfusion Pressure. *Hypertension* 37, 485–489. doi:10.1161/01.hyp.37.2.485

Alijotas-Reig, J., Esteve-Valverde, E., Ferrer-Oliveras, R., Llurba, E., and Gris, J. M. (2017). Tumor Necrosis Factor-Alpha and Pregnancy: Focus on Biologics. An Updated and Comprehensive Review. *Clinic Rev. Allerg Immunol.* 53, 40–53. doi:10.1007/s12016-016-8596-x

Amador, C. A., Barrientos, V., Peña, J., Herrada, A. A., González, M., Valdés, S., et al. (2014). Spironolactone Decreases DOCA-Salt-Induced Organ Damage by Blocking the Activation of T Helper 17 and the Downregulation of Regulatory T Lymphocytes. *Hypertension* 63, 797–803. doi:10.1161/HYPERTENSIONAHA.113.02883

Amaral, L. M., Wallace, K., Owens, M., and LaMarca, B. (2017). Pathophysiology and Current Clinical Management of Preeclampsia. *Curr. Hypertens. Rep.* 19, 61. doi:10.1007/s11906-017-0757-7

Aneman, I., Pienaar, D., Suvakov, S., Simic, T. P., Garovic, V. D., and McClements, L. (2020). Mechanisms of Key Innate Immune Cells in Early- and Late-Onset Preeclampsia. *Front. Immunol.* 11, 1864. doi:10.3389/fimmu.2020.01864

Basting, T., and Lazartigues, E. (2017). DOCA-salt Hypertension: an Update. *Curr. Hypertens. Rep.* 19, 32. doi:10.1007/s11906-017-0731-4

B. Institute of Medicine Committee on Understanding Premature (2007). "O. Assuring Healthy," in *Preterm Birth: Causes, Consequences, and Prevention*. Editors R. E. Behrman and A. S. Butler (Washington (DC): National Academies Press (US)Copyright © 2007, National Academy of Sciences.).

Bayry, J., Lacroix-Desmazes, S., Carbonneil, C., Misra, N., Donkova, V., Pashov, A., et al. (2003). Inhibition of Maturation and Function of Dendritic Cells by Intravenous Immunoglobulin. *Blood* 101, 758–765. doi:10.1182/blood-2002-05-1447

Bellamy, L., Casas, J.-P., Hingorani, A. D., and Williams, D. J. (2007). Pre-eclampsia and Risk of Cardiovascular Disease and Cancer in Later Life: Systematic Review and Meta-Analysis. *Bmj* 335, 974. doi:10.1136/bmj.39335.385301.be

Birukov, A., Andersen, L. B., Herse, F., Rakova, N., Kitlen, G., Kyhl, H. B., et al. (2019). Aldosterone, Salt, and Potassium Intakes as Predictors of Pregnancy Outcome, Including Preeclampsia. *Hypertension* 74, 391–398. doi:10.1161/HYPERTENSIONAHA.119.12924

Bluestone, J. A., Buckner, J. H., Fitch, M., Gitelman, S. E., Gupta, S., Hellerstein, M. K., et al. (2015). Type 1 Diabetes Immunotherapy Using Polyclonal Regulatory T Cells. *Sci. Transl Med.* 7, 315ra189. doi:10.1126/scitranslmed.aad4134

Boesen, E. I. (2018). ETA Receptor Activation Contributes to T Cell Accumulation in the Kidney Following Ischemia-Reperfusion Injury. *Physiol. Rep.* 6, e13865. doi:10.14814/phy2.13865

Borzychowski, A. M., Sargent, I. L., and Redman, C. W. G. (2006). Inflammation and Pre-eclampsia. *Semin. Fetal Neonatal Med.* 11, 309–316. doi:10.1016/j.siny.2006.04.001

Brown, M. A., Magee, L. A., Kenny, L. C., Karumanchi, S. A., McCarthy, F. P., Saito, S., et al. (2018). Hypertensive Disorders of Pregnancy. *Hypertension* 72, 24–43. doi:10.1161/hypertensionaha.117.10803

Bulcão, C., Ribeiro-Filho, F. F., Sañudo, A., and Roberta Ferreira, S. G. (2007). Effects of Simvastatin and Metformin on Inflammation and Insulin Resistance in Individuals with Mild Metabolic Syndrome. *Am. J. Cardiovasc. Drugs : Drugs devices, other interventions* 7, 219–224.

Burton, G. J., Redman, C. W., Roberts, J. M., and Moffett, A. (2019). Pre-eclampsia: Pathophysiology and Clinical Implications. *Bmj* 366, l2381. doi:10.1136/bmj.l2381

Burton, G. J., Woods, A. W., Jauniaux, E., and Kingdom, J. C. P. (2009). Rheological and Physiological Consequences of Conversion of the Maternal Spiral Arteries for Uteroplacental Blood Flow during Human Pregnancy. *Placenta* 30, 473–482. doi:10.1016/j.placenta.2009.02.009

Chen, L. M., Liu, B., Zhao, H. B., Stone, P., Chen, Q., and Chamley, L. (2010). IL-6, TNFα and TGFβ Promote Nonapoptotic Trophoblast Deportation and Subsequently Causes Endothelial Cell Activation. *Placenta* 31, 75–80. doi:10.1016/j.placenta.2009.11.005

Cornelius, D. C., Hogg, J. P., Scott, J., Wallace, K., Herse, F., Moseley, J., et al. (2013). Administration of Interleukin-17 Soluble Receptor C Suppresses TH17 Cells, Oxidative Stress, and Hypertension in Response to Placental Ischemia during Pregnancy. *Hypertension* 62, 1068–1073. doi:10.1161/HYPERTENSIONAHA.113.01514

Cornelius, D. C. (2018). Preeclampsia: From Inflammation to Immunoregulation. *Clin. Med. Insights Blood Disord.* 11, 1179545x17752325. doi:10.1177/1179545X17752325

Cornelius, D. C., Amaral, L. M., Harmon, A., Wallace, K., Thomas, A. J., Campbell, N., et al. (2015). An Increased Population of Regulatory T Cells Improves the Pathophysiology of Placental Ischemia in a Rat Model of Preeclampsia. *Am. J. Physiology-Regulatory, Integr. Comp. Physiol.* 309, R884–R891. doi:10.1152/ajpregu.00154.2015

Cornelius, D. C., Cottrell, J., Amaral, L. M., and LaMarca, B. (2019). Inflammatory Mediators: a Causal Link to Hypertension during Preeclampsia. *Br. J. Pharmacol.* 176, 1914–1921. doi:10.1111/bph.14466

Costantine, M. M., Cleary, K., Hebert, M. F., Ahmed, M. S., Brown, L. M., Ren, Z., et al. (2016). Safety and Pharmacokinetics of Pravastatin Used for the Prevention of Preeclampsia in High-Risk Pregnant Women: a Pilot Randomized Controlled Trial. *Am. J. Obstet. Gynecol.* 214, 720.e721–e17.e717. doi:10.1016/j.ajog.2015.12.038

Costantine, M. M., West, H., Wisner, K. L., Caritis, S., Clark, S., Venkataramanan, R., et al. (2021). A Randomized Pilot Clinical Trial of Pravastatin versus Placebo in Pregnant Patients at High Risk of Preeclampsia. *Am. J. Obstet. Gynecol.* 225 (6), 666.e1–666.e15. doi:10.1016/j.ajog.2021.05.018

Dall'Era, M., Pauli, M. L., Remedios, K., Taravati, K., Sandova, P. M., Putnam, A. L., et al. (2019). Adoptive Treg Cell Therapy in a Patient with Systemic Lupus Erythematosus. *Arthritis Rheumatol.* 71, 431–440. doi:10.1002/art.40737

Davisson, R. L., Hoffmann, D. S., Butz, G. M., Aldape, G., Schlager, G., Merrill, D. C., et al. (2002). Discovery of a Spontaneous Genetic Mouse Model of Preeclampsia. *Hypertension* 39, 337–342. doi:10.1161/hy02t2.102904

Dietrich, T., Hucko, T., Schneemann, C., Neumann, M., Menrad, A., Willuda, J., et al. (2012). Local Delivery of IL-2 Reduces Atherosclerosis via Expansion of Regulatory T Cells. *Atherosclerosis* 220, 329–336. doi:10.1016/j.atherosclerosis.2011.09.050

Dodd, J. M., Jones, L., Flenady, V., Cincotta, R., and Crowther, C. A. (2013). Prenatal Administration of Progesterone for Preventing Preterm Birth in Women Considered to Be at Risk of Preterm Birth. *Cochrane database Syst. Rev.*, Cd004947. doi:10.1002/14651858.cd004947.pub3

Dosiou, C., and Giudice, L. C. (2005). Natural Killer Cells in Pregnancy and Recurrent Pregnancy Loss: Endocrine and Immunologic Perspectives. *Endocr. Rev.* 26, 44–62. doi:10.1210/er.2003-0021

Duckitt, K., and Harrington, D. (2005). Risk Factors for Pre-eclampsia at Antenatal Booking: Systematic Review of Controlled Studies. *Bmj* 330, 565. doi:10.1136/bmj.38380.674340.e0

Duley, L., Gülmezoglu, A. M., Henderson-Smart, D. J., and Chou, D. (2010). Magnesium Sulphate and Other Anticonvulsants for Women with Pre-eclampsia. *Cochrane Database Syst. Rev.* 2010, Cd000025. doi:10.1002/14651858.CD000025.pub2

Duley, L. (2009). The Global Impact of Pre-eclampsia and Eclampsia. *Semin. Perinatology* 33, 130–137. doi:10.1053/j.semperi.2009.02.010

Elfarra, J. T., Cottrell, J. N., Cornelius, D. C., Cunningham, M. W., Faulkner, J. L., Ibrahim, T., et al. (2020). 17-Hydroxyprogesterone Caproate Improves T Cells and NK Cells in Response to Placental Ischemia; New Mechanisms of Action for an Old Drug. *Pregnancy Hypertens.* 19, 226–232. doi:10.1016/j.preghy.2019.11.005

Esteve-Valverde, E., Ferrer-Oliveras, R., Gil-Aliberas, N., Baraldès-Farré, A., Llurba, E., and Alijotas-Reig, J. (2018). Pravastatin for Preventing and Treating Preeclampsia: A Systematic Review. *Obstetrical Gynecol. Surv.* 73, 40–55. doi:10.1097/ogx.0000000000000522

Ferreira, L. M. R., Muller, Y. D., Bluestone, J. A., and Tang, Q. (2019). Next-generation Regulatory T Cell Therapy. *Nat. Rev. Drug Discov.* 18, 749–769. doi:10.1038/s41573-019-0041-4

Fischer, C., and Voss, A. (2014). Three-Dimensional Segmented PoincarÃ Plot Analyses SPPA3 Investigates Cardiovascular and Cardiorespiratory Couplings in Hypertensive Pregnancy Disorders. *Front. Bioeng. Biotechnol.* 2, 51. doi:10.3389/fbioe.2014.00051

Foks, A. C., Lichtman, A. H., and Kuiper, J. (2015). Treating Atherosclerosis with Regulatory T Cells. *Atvb* 35, 280–287. doi:10.1161/atvbaha.114.303568

Fukui, A., Yokota, M., Funamizu, A., Nakamua, R., Fukuhara, R., Yamada, K., et al. (2012). Changes of NK Cells in Preeclampsia. *Am. J. Reprod. Immunol.* 67, 278–286. doi:10.1111/j.1600-0897.2012.01120.x

Gathiram, P., and Moodley, J. (2016). Pre-eclampsia: its Pathogenesis and Pathophysiolgy. *Cvja* 27, 71–78. doi:10.5830/cvja-2016-009

Göhner, C., Plösch, T., and Faas, M. M. (2017). Immune-modulatory Effects of Syncytiotrophoblast Extracellular Vesicles in Pregnancy and Preeclampsia. *Placenta* 60 (Suppl. 1), S41–S51. doi:10.1016/j.placenta.2017.06.004

Graham, D. B., and Xavier, R. J. (2020). Pathway Paradigms Revealed from the Genetics of Inflammatory Bowel Disease. *Nature* 578, 527–539. doi:10.1038/s41586-020-2025-2

Gu, P., Fang Gao, J., D'Souza, C. A., Kowalczyk, A., Chou, K.-Y., and Zhang, L. (2012). Trogocytosis of CD80 and CD86 by Induced Regulatory T Cells. *Cell Mol Immunol* 9, 136–146. doi:10.1038/cmi.2011.62

Gumusoglu, S. B., Chilukuri, A. S. S., Santillan, D. A., Santillan, M. K., and Stevens, H. E. (2020). Neurodevelopmental Outcomes of Prenatal Preeclampsia Exposure. *Trends Neurosciences* 43, 253–268. doi:10.1016/j.tins.2020.02.003

Gupta, S., and Roman, A. S. (2012). 17-α Hydroxyprogesterone Caproate for the Prevention of Preterm Birth. *Womens Health (Lond Engl.* 8, 21–30. doi:10.2217/whe.11.78

Guruli, G., Pflug, B. R., Pecher, S., Makarenkova, V., Shurin, M. R., and Nelson, J. B. (2004). Function and Survival of Dendritic Cells Depend on Endothelin-1 and Endothelin Receptor Autocrine Loops. *Blood* 104, 2107–2115. doi:10.1182/blood-2003-10-3559

Guzik, T. J., Hoch, N. E., Brown, K. A., McCann, L. A., Rahman, A., Dikalov, S., et al. (2007). Role of the T Cell in the Genesis of Angiotensin II-Induced Hypertension and Vascular Dysfunction. *J. Exp. Med.* 204, 2449–2460. doi:10.1084/jem.20070657

Harmon, A. C., Cornelius, D. C., Amaral, L. M., Faulkner, J. L., Cunningham, M. W., Wallace, K., et al. (2016). The Role of Inflammation in the Pathology of Preeclampsia. *Clin. Sci. (Lond)* 130, 409–419. doi:10.1042/cs20150702

Harmon, A., Cornelius, D., Amaral, L., Paige, A., Herse, F., Ibrahim, T., et al. (2015). IL-10 Supplementation Increases Tregs and Decreases Hypertension in the RUPP Rat Model of Preeclampsia. *Hypertens. Pregnancy* 34, 291–306. doi:10.3109/10641955.2015.1032054

Hernández-Díaz, S., Toh, S., and Cnattingius, S. (2009). Risk of Pre-eclampsia in First and Subsequent Pregnancies: Prospective Cohort Study. *BMJ (Clinical research ed.)* 338, b2255.

Heyward, C. Y., Sones, J. L., Lob, H. E., Yuen, L. C., Abbott, K. E., Huang, W., et al. (2017). The Decidua of Preeclamptic-like BPH/5 Mice Exhibits an Exaggerated Inflammatory Response during Early Pregnancy. *J. Reprod. Immunol.* 120, 27–33. doi:10.1016/j.jri.2017.04.002

Hoffmann, D. S., Weydert, C. J., Lazartigues, E., Kutschke, W. J., Kienzle, M. F., Leach, J. E., et al. (2008). Chronic Tempol Prevents Hypertension, Proteinuria, and Poor Feto-Placental Outcomes in BPH/5 Mouse Model of Preeclampsia. *Hypertension* 51, 1058–1065. doi:10.1161/HYPERTENSIONAHA.107.107219

Howerton, C. L., and Bale, T. L. (2012). Prenatal Programing: at the Intersection of Maternal Stress and Immune Activation. *Horm. Behav.* 62, 237–242. doi:10.1016/j.yhbeh.2012.03.007

Huppertz, B., and Kingdom, J. C. P. (2004). Apoptosis in the Trophoblast-Role of Apoptosis in Placental Morphogenesis. *J. Soc. Gynecol. Investig.* 11, 353–362. doi:10.1016/j.jsgi.2004.06.002

Ibrahim, T., Przybyl, L., Harmon, A. C., Amaral, L. M., Faulkner, J. L., Cornelius, D. C., et al. (2017). Proliferation of Endogenous Regulatory T Cells Improve the Pathophysiology Associated with Placental Ischaemia of Pregnancy. *Am. J. Reprod. Immunol.* 78, e12724. doi:10.1111/aji.12724

Ingman, W. V., and Jones, R. L. (2008). Cytokine Knockouts in Reproduction: the Use of Gene Ablation to Dissect Roles of Cytokines in Reproductive Biology. *Hum. Reprod. Update* 14, 179–192. doi:10.1093/humupd/dmm042

Jafri, S., and Ormiston, M. L. (2017). Immune Regulation of Systemic Hypertension, Pulmonary Arterial Hypertension, and Preeclampsia: Shared Disease Mechanisms and Translational Opportunities. *Am. J. Physiology-Regulatory, Integr. Comp. Physiol.* 313, R693–r705. doi:10.1152/ajpregu.00259.2017

Egan, J. L., and Maaser, C. (2009). "Inflammatory Bowel Diseases," in *Pharmacology and Therapeutics*. Editor S. A. Waldman (Philadelphia: W.B. Saunders), 487–503. doi:10.1016/b978-1-4160-3291-5.50037-8

J. K. Aronson (Editor) (2006). *Meyler's Side Effects of Drugs: The International Encyclopedia of Adverse Drug Reactions and Interactions*. Fifteenth Edition (Amsterdam: Elsevier), 1279–1282.

Johansen, C. B., Jimenez-Solem, E., Haerskjold, A., Sand, F. L., and Thomsen, S. F. (2018). The Use and Safety of TNF Inhibitors during Pregnancy in Women with Psoriasis: A Review. *Int. J. Mol. Sci.* 19. doi:10.3390/ijms19051349

Kaplanski, G., Fabrigoule, M., Boulay, V., Dinarello, C. A., Bongrand, P., Kaplanski, S., et al. (1997). Thrombin Induces Endothelial Type II Activation *In Vitro*: IL-1 and TNF-alpha-independent IL-8 Secretion and E-Selectin Expression. *J. Immunol.* 158, 5435–5441.

Khashu, M., Narayanan, M., Bhargava, S., and Osiovich, H. (2009). Perinatal Outcomes Associated with Preterm Birth at 33 to 36 Weeks' Gestation: A Population-Based Cohort Study. *Pediatrics* 123, 109–113. doi:10.1542/peds.2007-3743

Kho, E. M., McCowan, L. M. E., North, R. A., Roberts, C. T., Chan, E., Black, M. A., et al. (2009). Duration of Sexual Relationship and its Effect on Preeclampsia and Small for Gestational Age Perinatal Outcome. *J. Reprod. Immunol.* 82, 66–73. doi:10.1016/j.jri.2009.04.011

Krishnan, L., Nguyen, T., and McComb, S. (2013). From Mice to Women: the Conundrum of Immunity to Infection during Pregnancy. *J. Reprod. Immunol.* 97, 62–73. doi:10.1016/j.jri.2012.10.015

Kumasawa, K., Ikawa, M., Kidoya, H., Hasuwa, H., Saito-Fujita, T., Morioka, Y., et al. (2011). Pravastatin Induces Placental Growth Factor (PGF) and Ameliorates Preeclampsia in a Mouse Model. *Proc. Natl. Acad. Sci.* 108, 1451–1455. doi:10.1073/pnas.1011293108

Lai, Z., Kalkunte, S., and Sharma, S. (2011). A Critical Role of Interleukin-10 in Modulating Hypoxia-Induced Preeclampsia-like Disease in Mice. *Hypertension* 57, 505–514. doi:10.1161/Hypertensionaha.110.163329

LaMarca, B. B., Cockrell, K., Sullivan, E., Bennett, W., and Granger, J. P. (2005). Role of Endothelin in Mediating Tumor Necrosis Factor-Induced Hypertension in Pregnant Rats. *Hypertension* 46, 82–86. doi:10.1161/01.HYP.0000169152.59854.36

Leavey, K., Bainbridge, S. A., and Cox, B. J. (2015). Large Scale Aggregate Microarray Analysis Reveals Three Distinct Molecular Subclasses of Human Preeclampsia. *PloS one* 10, e0116508. doi:10.1371/journal.pone.0116508

Li, D.-K., and Wi, S. (2000). Changing Paternity and the Risk of Preeclampsia/eclampsia in the Subsequent Pregnancy. *Am. J. Epidemiol.* 151, 57–62. doi:10.1093/oxfordjournals.aje.a010122

Li, L., Yang, H., Chen, P., Xin, T., Zhou, Q., Wei, D., et al. (2020). Trophoblast-Targeted Nanomedicine Modulates Placental sFLT1 for Preeclampsia Treatment. *Front. Bioeng. Biotechnol.* 8, 64. doi:10.3389/fbioe.2020.00064

Lutsenko, E. D., Bondarovich, N. A., and Gol'tsev, A. N. (2014). Content of IL-10 and CD4+CD210+ Cells in Mice with Adjuvant Arthritis before and after Treatment with Cryopreserved Placental Cells. *Bull. Exp. Biol. Med.* 157, 673–676. doi:10.1007/s10517-014-2641-7

Maganto-García, E., Bu, D-X., Tarrio, M. L., Alcaide, P., Newton, G., Griffin, G. K., et al. (2011). Foxp3$^+$-Inducible Regulatory T Cells Suppress Endothelial Activation and Leukocyte Recruitment. *J. Immunol.* 187, 3521–3529. doi:10.4049/jimmunol.1003947

Mashreghi, M.-F., Klemz, R., Knosalla, I. S., Gerstmayer, B., Janssen, U., Buelow, R., et al. (2008). Inhibition of Dendritic Cell Maturation and Function Is Independent of Heme Oxygenase 1 but Requires the Activation of STAT3. *J. Immunol.* 180, 7919–7930. doi:10.4049/jimmunol.180.12.7919

Matrougui, K., Zakaria, A. E., Kassan, M., Choi, S., Nair, D., Gonzalez-Villalobos, R. A., et al. (2011). Natural Regulatory T Cells Control Coronary Arteriolar Endothelial Dysfunction in Hypertensive Mice. *Am. J. Pathol.* 178, 434–441. doi:10.1016/j.ajpath.2010.11.034

Mayrink, J., Costa, M. L., and Cecatti, J. G. (2018). Preeclampsia in 2018: Revisiting Concepts, Physiopathology, and Prediction. *ScientificWorldJournal* 2018, 6268276. doi:10.1155/2018/6268276

McDonnold, M., Tamayo, E., Kechichian, T., Gamble, P., Longo, M., Hankins, G. D., et al. (2014). The Effect of Prenatal Pravastatin Treatment on Altered Fetal Programming of Postnatal Growth and Metabolic Function in a Preeclampsia-like Murine Model. *Am. J. Obstet. Gynecol.* 210, 542–547. doi:10.1016/j.ajog.2014.01.010

Morris, R., Spencer, S.-K., Kyle, P. B., Williams, J. M., Harris, A. s., Owens, M. Y., et al. (2016). Hypertension in an Animal Model of HELLP Syndrome Is Associated with Activation of Endothelin 1. *Reprod. Sci.* 23, 42–50. doi:10.1177/1933719115592707

Mostello, D., Kallogjeri, D., Tungsiripat, R., and Leet, T. (2008). Recurrence of Preeclampsia: Effects of Gestational Age at Delivery of the First Pregnancy, Body Mass index, Paternity, and Interval between Births. *Am. J. Obstet. Gynecol.* 199, 55–57. doi:10.1016/j.ajog.2007.11.058

Narazaki, M., Tanaka, T., and Kishimoto, T. (2017). The Role and Therapeutic Targeting of IL-6 in Rheumatoid Arthritis. *Expert Rev. Clin. Immunol.* 13, 535–551. doi:10.1080/1744666x.2017.1295850

National Institute of Diabetes and Digestive and Kidney Diseases, LiverTox: Clinical and Research Information on Drug-Induced Liver Injury [Internet], Bethesda (MD), 2012).

Ou, H.-x., Guo, B.-b., Liu, Q., Li, Y.-k., Yang, Z., Feng, W.-j., et al. (2018). Regulatory T Cells as a New Therapeutic Target for Atherosclerosis. *Acta Pharmacol. Sin* 39, 1249–1258. doi:10.1038/aps.2017.140

Perschbacher, K. J., Deng, G., Sandgren, J. A., Walsh, J. W., Witcher, P. C., Sapouckey, S. A., et al. (2020). Reduced mRNA Expression of RGS2 (Regulator of G Protein Signaling-2) in the Placenta Is Associated with Human Preeclampsia and Sufficient to Cause Features of the Disorder in Mice. *Hypertension* 75, 569–579. doi:10.1161/HYPERTENSIONAHA.119.14056

Raghupathy, R. (2013). Cytokines as Key Players in the Pathophysiology of Preeclampsia. *Med. Princ Pract.* 22 Suppl 1 (Suppl. 1), 8–19. doi:10.1159/000354200

Raja, H., Matteson, E. L., Michet, C. J., Smith, J. R., and Pulido, J. S. (2012). Safety of Tumor Necrosis Factor Inhibitors during Pregnancy and Breastfeeding. *Trans. Vis. Sci. Tech.* 1, 6. doi:10.1167/tvst.1.2.6

Rambaldi, M. P., Weiner, E., Mecacci, F., Bar, J., and Petraglia, F. (2019). Immunomodulation and Preeclampsia. *Best Pract. Res. Clin. Obstet. Gynaecol.* 60, 87–96. doi:10.1016/j.bpobgyn.2019.06.005

Redecha, P., van Rooijen, N., Torry, D., and Girardi, G. (2009). Pravastatin Prevents Miscarriages in Mice: Role of Tissue Factor in Placental and Fetal Injury. *Blood* 113, 4101–4109. doi:10.1182/blood-2008-12-194258

Redman, C. W. G. (2011). Hypertension in Pregnancy: the NICE Guidelines. *Heart* 97, 1967–1969. doi:10.1136/heartjnl-2011-300949

Redman, C. W. G. (1991). Pre-eclampsia and the Placenta. *Placenta* 12, 301–308. doi:10.1016/0143-4004(91)90339-h

Redman, C. W. G., Sacks, G. P., and Sargent, I. L. (1999). Preeclampsia: An Excessive Maternal Inflammatory Response to Pregnancy. *Am. J. Obstet. Gynecol.* 180, 499–506. doi:10.1016/s0002-9378(99)70239-5

Redman, C. W. G., and Sargent, I. L. (2010). Immunology of Pre-eclampsia. *Am. J. Reprod. Immunol.* 63, 534–543. doi:10.1111/j.1600-0897.2010.00831.x

Redman, C. W. G. (2013). Stress Responses and Pre-eclampsia. *Pregnancy Hypertens. Int. J. Women's Cardiovasc. Health* 3, 57. doi:10.1016/j.preghy.2013.04.003

Redman, C. W., and Sargent, I. L. (2005). Latest Advances in Understanding Preeclampsia. *Science* 308, 1592–1594. doi:10.1126/science.1111726

Reed, M. D., Yim, Y. S., Wimmer, R. D., Kim, H., Ryu, C., Welch, G. M., et al. (2020). IL-17a Promotes Sociability in Mouse Models of Neurodevelopmental Disorders. *Nature* 577, 249–253. doi:10.1038/s41586-019-1843-6

Ridker, P. M., Everett, B. M., Thuren, T., MacFadyen, J. G., Chang, W. H., Ballantyne, C., et al. (2017). Antiinflammatory Therapy with Canakinumab for Atherosclerotic Disease. *N. Engl. J. Med.* 377, 1119–1131. doi:10.1056/nejmoa1707914

Roberge, S., Bujold, E., and Nicolaides, K. H. (2018). Aspirin for the Prevention of Preterm and Term Preeclampsia: Systematic Review and Metaanalysis. *Am. J. Obstet. Gynecol.* 218, 287–293. doi:10.1016/j.ajog.2017.11.561

Roberge, S., Nicolaides, K., Demers, S., Hyett, J., Chaillet, N., and Bujold, E. (2017). The Role of Aspirin Dose on the Prevention of Preeclampsia and Fetal Growth Restriction: Systematic Review and Meta-Analysis. *Am. J. Obstet. Gynecol.* 216, 110–120. doi:10.1016/j.ajog.2016.09.076

Robertson, S. A., Green, E. S., Care, A. S., Moldenhauer, L. M., Prins, J. R., Hull, M. L., et al. (2019). Therapeutic Potential of Regulatory T Cells in Preeclampsia-Opportunities and Challenges. *Front. Immunol.* 10, 478. doi:10.3389/fimmu.2019.00478

Roger, V. L., Go, A. S., Lloyd-Jones, D. M., Adams, R. J., Berry, J. D., Brown, T. M., et al. (2011). Heart Disease and Stroke Statistics--2011 Update: a Report from the American Heart Association. *Circulation* 123, e18–e209. doi:10.1161/CIR.0b013e3182009701

Saad, A. F., Diken, Z. M., Kechichian, T. B., Clark, S. M., Olson, G. L., Saade, G. R., et al. (2016). Pravastatin Effects on Placental Prosurvival Molecular Pathways in a Mouse Model of Preeclampsia. *Reprod. Sci.* 23, 1593–1599. doi:10.1177/1933719116648218

Saad, A. F., Kechichian, T., Yin, H., Sbrana, E., Longo, M., Wen, M., et al. (2014). Effects of Pravastatin on Angiogenic and Placental Hypoxic Imbalance in a Mouse Model of Preeclampsia. *Reprod. Sci.* 21, 138–145. doi:10.1177/1933719113492207

Saftlas, A. F., Levine, R. J., Klebanoff, M. A., Martz, K. L., Ewell, G. M., and Morris, C. D. (2003). Abortion, Changed Paternity, and Risk of Preeclampsia in Nulliparous Women. *Am. J. Epidemiol.* 157, 1108–1114. doi:10.1093/aje/kwg101

Saito, S., Sakai, M., Sasaki, Y., Nakashima, A., and Shiozaki, A. (2007). Inadequate Tolerance Induction May Induce Pre-eclampsia. *J. Reprod. Immunol.* 76, 30–39. doi:10.1016/j.jri.2007.08.002

Santillan, M. K., Santillan, D. A., Sigmund, C. D., and Hunter, S. K. (2009). From Molecules to Medicine: a Future Cure for Preeclampsia? *Drug News Perspect.* 22, 531–541. doi:10.1358/dnp.2009.22.9.1437961

S. Antonopoulos, A., Margaritis, M., Lee, R., Channon, K., and Antoniades, C. (2012). Statins as Anti-inflammatory Agents in Atherogenesis: Molecular Mechanisms and Lessons from the Recent Clinical Trials. *Cpd* 18, 1519–1530. doi:10.2174/138161212799504803

Sargent, I. L., Borzychowski, A. M., and Redman, C. W. G. (2007). NK Cells and Pre-eclampsia. *J. Reprod. Immunol.* 76, 40–44. doi:10.1016/j.jri.2007.03.009

Sargent, I. L., Borzychowski, A. M., and Redman, C. W. (2006). Immunoregulation in normal Pregnancy and Pre-eclampsia: an Overview. *Reprod. Biomed. Online* 13, 680–686. doi:10.1016/s1472-6483(10)60659-1

Sasaki, Y., Darmochwal-Kolarz, D., Suzuki, D., Sakai, M., Ito, M., Shima, T., et al. (2007). Proportion of Peripheral Blood and Decidual CD4+ CD25bright Regulatory T Cells in Pre-eclampsia. *Clin. Exp. Immunol.* 149, 139–145. doi:10.1111/j.1365-2249.2007.03397.x

Scroggins, S. M., Santillan, D. A., Lund, J. M., Sandgren, J. A., Krotz, L. K., Hamilton, W. S., et al. (2018). Elevated Vasopressin in Pregnant Mice Induces T-Helper Subset Alterations Consistent with Human Preeclampsia. *Clin. Sci. (Lond)* 132, 419–436. doi:10.1042/cs20171059

Shan, J., Jin, H., and Xu, Y. (2020). T Cell Metabolism: A New Perspective on Th17/Treg Cell Imbalance in Systemic Lupus Erythematosus. *Front. Immunol.* 11, 1027. doi:10.3389/fimmu.2020.01027

Small, H. Y., Nosalski, R., Morgan, H., Beattie, E., Guzik, T. J., Graham, D., et al. (2016). Role of Tumor Necrosis Factor-α and Natural Killer Cells in Uterine Artery Function and Pregnancy Outcome in the Stroke-Prone Spontaneously Hypertensive Rat. *Hypertension* 68, 1298–1307. doi:10.1161/HYPERTENSIONAHA.116.07933

Staff, A. C. (2019). The Two-Stage Placental Model of Preeclampsia: An Update. *J. Reprod. Immunol.* 134-135, 1–10. doi:10.1016/j.jri.2019.07.004

Tabares, P., Berr, S., Römer, P. S., Chuvpilo, S., Matskevich, A. A., Tyrsin, D., et al. (2014). Human Regulatory T Cells Are Selectively Activated by Low-dose Application of the CD28 Superagonist TGN1412/TAB08. *Eur. J. Immunol.* 44, 1225–1236. doi:10.1002/eji.201343967

Tanaka, K., Yoshioka, K., Tatsumi, K., Kimura, S., and Kasuya, Y. (2014). Endothelin Regulates Function of IL-17-producing T Cell Subset. *Life Sci.* 118, 244–247. doi:10.1016/j.lfs.2014.01.084

Tao, Y., Li, Y-H., Zhang, D., Xu, L., Chen, J-J., Sang, Y-F., et al. (2021). Decidual CXCR4(+) CD56(bright) NK Cells as a Novel NK Subset in Maternal-Foetal Immune Tolerance to Alleviate Early Pregnancy Failure. *Clin. Transl Med.* 11, e540. doi:10.1002/ctm2.540

Taylor, P. C. (2015). "Tumor Necrosis Factor-Blocking Therapies," in *Rheumatology*. Editors M. C. Hochberg, A. J. Silman, J. S. Smolen, M. E. Weinblatt, and M. H. Weisman. Sixth Edition (Philadelphia: Mosby), 492–510. doi:10.1016/b978-0-323-09138-1.00063-2

Tousoulis, D., Oikonomou, E., Economou, E. K., Crea, F., and Kaski, J. C. (2016). Inflammatory Cytokines in Atherosclerosis: Current Therapeutic Approaches. *Eur. Heart J.* 37, 1723–1732. doi:10.1093/eurheartj/ehv759

Travis, O. K., White, D., Baik, C., Giachelli, C., Thompson, W., Stubbs, C., et al. (2020). Interleukin-17 Signaling Mediates Cytolytic Natural Killer Cell Activation in Response to Placental Ischemia. *Am. J. Physiology-Regulatory, Integr. Comp. Physiol.* 318, R1036–r1046. doi:10.1152/ajpregu.00285.2019

Trivedi, P. J., and Adams, D. H. (2018). Chemokines and Chemokine Receptors as Therapeutic Targets in Inflammatory Bowel Disease; Pitfalls and Promise. *J. Crohn's Colitis* 12, S641–S652. doi:10.1093/ecco-jcc/jjx145

Trowsdale, J., and Betz, A. G. (2006). Mother's Little Helpers: Mechanisms of Maternal-Fetal Tolerance. *Nat. Immunol.* 7, 241–246. doi:10.1038/ni1317

Uzieliene, I., Kalvaityte, U., Bernotiene, E., and Mobasheri, A. (2021). Non-viral Gene Therapy for Osteoarthritis. *Front. Bioeng. Biotechnol.* 8, 618399. doi:10.3389/fbioe.2020.618399

van de Ree, M. A., Huisman, M. V., Princen, H. M. G., Meinders, A. E., and Kluft, C. (2003). Strong Decrease of High Sensitivity C-Reactive Protein with High-Dose Atorvastatin in Patients with Type 2 Diabetes Mellitus. *Atherosclerosis* 166, 129–135. doi:10.1016/s0021-9150(02)00316-7

Vijayan, V., Mueller, S., Baumgart-Vogt, E., and Immenschuh, S. (2010). Heme Oxygenase-1 as a Therapeutic Target in Inflammatory Disorders of the Gastrointestinal Tract. *Wjg* 16, 3112–3119. doi:10.3748/wjg.v16.i25.3112

Wall, G. C., Heyneman, C., and Pfanner, T. P. (1999). Medical Options for Treating Crohn's Disease in Adults: Focus on Antitumor Necrosis Factor-α Chimeric Monoclonal Antibody. *Pharmacotherapy* 19, 1138–1152. doi:10.1592/phco.19.15.1138.30574

Wallis, A. B., Saftlas, A. F., Hsia, J., and Atrash, H. K. (2008). Secular Trends in the Rates of Preeclampsia, Eclampsia, and Gestational Hypertension, United States, 1987-2004. *Am. J. Hypertens.* 21, 521–526. doi:10.1038/ajh.2008.20

Weber-Schöndorfer, C. (2015). in *Drugs during Pregnancy and Lactation*. Editors C. Schaefer, P. Peters, and R. K. Miller. Third Edition (San Diego: Academic Press), 341–372.

Woidacki, K., Meyer, N., Schumacher, A., Goldschmidt, A., Maurer, M., and Zenclussen, A. C. (2015). Transfer of Regulatory T Cells into Abortion-Prone Mice Promotes the Expansion of Uterine Mast Cells and Normalizes Early Pregnancy Angiogenesis. *Sci. Rep.* 5, 13938. doi:10.1038/srep13938

Xiao, Q., Li, X., Li, Y., Wu, Z., Xu, C., Chen, Z., et al. (2021). Biological Drug and Drug Delivery-Mediated Immunotherapy. *Acta Pharmaceutica Sinica. B* 11, 941–960. doi:10.1016/j.apsb.2020.12.018

Youssef, S., Stüve, O., Patarroyo, J. C., Ruiz, P. J., Radosevich, J. L., Hur, E. M., et al. (2002). The HMG-CoA Reductase Inhibitor, Atorvastatin, Promotes a Th2 Bias and Reverses Paralysis in central Nervous System Autoimmune Disease. *Nature* 420, 78–84. doi:10.1038/nature01158

Yuan, J., Li, J., Huang, S.-Y., and Sun, X. (2015). Characterization of the Subsets of Human NKT-like Cells and the Expression of Th1/Th2 Cytokines in Patients with Unexplained Recurrent Spontaneous Abortion. *J. Reprod. Immunol.* 110, 81–88. doi:10.1016/j.jri.2015.05.001

Conflict of Interest: The authors declare that the research was conducted in the absence of any commercial or financial relationships that could be construed as a potential conflict of interest.

Publisher's Note: All claims expressed in this article are solely those of the authors and do not necessarily represent those of their affiliated organizations, or those of the publisher, the editors and the reviewers. Any product that may be evaluated in this article, or claim that may be made by its manufacturer, is not guaranteed or endorsed by the publisher.

frontiers in Bioengineering and Biotechnology

SYSTEMATIC REVIEW
published: 19 January 2022
doi: 10.3389/fbioe.2021.780389

Using Machine Learning to Predict Complications in Pregnancy: A Systematic Review

Ayleen Bertini[1,2], *Rodrigo Salas*[3,4,5], *Steren Chabert*[3,4,5], *Luis Sobrevia*[6,7,8,9,10,11] *and Fabián Pardo*[1,6,12]*

[1]Metabolic Diseases Research Laboratory (MDRL), Interdisciplinary Center for Research in Territorial Health of the Aconcagua Valley (CIISTe Aconcagua), Center for Biomedical Research (CIB), Universidad de Valparaíso, Valparaiso, Chile, [2]PhD Program Doctorado en Ciencias e Ingeniería para La Salud, Faculty of Medicine, Universidad de Valparaíso, Valparaiso, Chile, [3]School of Biomedical Engineering, Faculty of Engineering, Universidad de Valparaíso, Valparaiso, Chile, [4]Centro de Investigación y Desarrollo en INGeniería en Salud – CINGS, Universidad de Valparaíso, Valparaiso, Chile, [5]Instituto Milenio Intelligent Healthcare Engineering, Valparaíso, Chile, [6]Cellular and Molecular Physiology Laboratory (CMPL), Division of Obstetrics and Gynaecology, School of Medicine, Faculty of Medicine, Pontificia Universidad Católica de Chile, Santiago, Chile, [7]Department of Physiology, Faculty of Pharmacy, Universidad de Sevilla, Seville, Spain, [8]University of Queensland Centre for Clinical Research (UQCCR), Faculty of Medicine and Biomedical Sciences, University of Queensland, Herston, QLD, Australia, [9]Department of Pathology and Medical Biology, University of Groningen, University Medical Center Groningen, Groningen, Netherlands, [10]Medical School (Faculty of Medicine), São Paulo State University (UNESP), São Paulo, Brazil, [11]Tecnologico de Monterrey, Eutra, The Institute for Obesity Research, School of Medicine and Health Sciences, Monterrey, Mexico, [12]School of Medicine, Campus San Felipe, Faculty of Medicine, Universidad de Valparaíso, San Felipe, Chile

OPEN ACCESS

Edited by:
Lana McClements, University of Technology Sydney, Australia

Reviewed by:
Mugdha V. Joglekar, Western Sydney University, Australia
Anandwardhan Hardikar, Western Sydney University, Australia

***Correspondence:**
Fabián Pardo
fabian.pardo@uv.cl

Specialty section:
This article was submitted to Preclinical Cell and Gene Therapy, a section of the journal Frontiers in Bioengineering and Biotechnology

Received: *21 September 2021*
Accepted: *10 December 2021*
Published: *19 January 2022*

Citation:
Bertini A, Salas R, Chabert S, Sobrevia L and Pardo F (2022) Using Machine Learning to Predict Complications in Pregnancy: A Systematic Review. Front. Bioeng. Biotechnol. 9:780389. doi: 10.3389/fbioe.2021.780389

Introduction: Artificial intelligence is widely used in medical field, and machine learning has been increasingly used in health care, prediction, and diagnosis and as a method of determining priority. Machine learning methods have been features of several tools in the fields of obstetrics and childcare. This present review aims to summarize the machine learning techniques to predict perinatal complications.

Objective: To identify the applicability and performance of machine learning methods used to identify pregnancy complications.

Methods: A total of 98 articles were obtained with the keywords "machine learning," "deep learning," "artificial intelligence," and accordingly as they related to perinatal complications ("complications in pregnancy," "pregnancy complications") from three scientific databases: PubMed, Scopus, and Web of Science. These were managed on the Mendeley platform and classified using the PRISMA method.

Results: A total of 31 articles were selected after elimination according to inclusion and exclusion criteria. The features used to predict perinatal complications were primarily electronic medical records (48%), medical images (29%), and biological markers (19%), while 4% were based on other types of features, such as sensors and fetal heart rate. The main perinatal complications considered in the application of machine learning thus far are pre-eclampsia and prematurity. In the 31 studies, a total of sixteen complications were predicted. The main precision metric used is the AUC. The machine learning methods with the best results were the prediction of prematurity from medical images using the support vector machine technique, with an accuracy of 95.7%, and the prediction of neonatal mortality with the XGBoost technique, with 99.7% accuracy.

Conclusion: It is important to continue promoting this area of research and promote solutions with multicenter clinical applicability through machine learning to reduce perinatal complications. This systematic review contributes significantly to the specialized literature on artificial intelligence and women's health.

Keywords: perinatal complications, machine learning, pregnancy, artificial intelligence, predictive tool, prediction model

INTRODUCTION

While most pregnancies and births are uneventful, all pregnancies are at risk. About 15% of all pregnant women will develop a life-threatening complication that requires specialized care, and some will require major obstetric intervention to survive (WHO, 2019). According to the World Health Organization (WHO), around 800 women die every day around the world from preventable causes related to the inherent risks of pregnancy. About 295,000 women died during and following pregnancy and childbirth in 2017. The vast majority of these deaths (94%) occurred in low-resource settings, and most could have been prevented (WHO, 2019).

Several maternal factors influence the appearance of perinatal complications. It is recognized that the first trimester of pregnancy is the best stage to predict and prevent perinatal complications. For example, it is known that increasing obesity in women of childbearing age leads to increased risk of perinatal complications such as gestational diabetes, large for gestational age (LGA), fetal macrosomia, and hypertensive syndromes in pregnancy (Denison et al., 2010; Mariona, 2016; Edwards and Wright, 2020). On the other hand, developed countries tend to see decreased birth rates over the years, leading to advanced gestational ages, predisposing women to adverse pregnancy outcomes (Laopaiboon et al., 2014).

Artificial intelligence (AI) technologies have been developed to analyze a wide range of health data, including patient data from multibiotic approaches, as well as clinical, behavioral, environmental, and drug data, and from various data included in the biomedical literature (Hinton, 2018). AI can help professionals in making decisions, reducing medical errors, improving accuracy in the interpretation of various diagnoses, and thereby reducing the workload to which they are exposed (Makary and Daniel, 2016). Machine learning (ML) is the subfield of computer science and a branch of AI. These techniques provide the ability to infer meaningful connections between data items from various data sets that would otherwise be difficult to correlate (Darcy et al., 2016; Obermeyer and Emanuel, 2016). Due to the large quantity and complex nature of medical information, ML is recognized as a promising method for supporting diagnosis or predicting clinical outcomes (Bottaci et al., 1997; Frizzell et al., 2017).

There are different types of data used for health learning models, including electronic medical records, medical images, biochemical parameters, and biological markers (Ahmed et al., 2020). The type of data that is used depends on what one tries to diagnose through ML.

Most of these decision support systems remain complex black boxes, which means that their internal logic is hidden from the clinical team who cannot fully understand the rationale behind their predictions. Interpretability is important before any health-care team can increase reliance on ML systems (Carvalho et al., 2019). Therefore, the research community has focused on developing both interpretable models and explanatory methods in recent years.

In general, the ML models are validated using the train–test split or the cross-validation schemes. Models are usually initially fitted to a training data set (Sohil et al., 2021), a set of examples used to fit the model parameters. Model fitting may include both variable selection and parameter estimation (Ripley, 1996). The test data set is a data set that is used to provide an unbiased evaluation of a final model fit on the training data set (Brownlee, 2017). Cross-validation is a statistical method for evaluating and comparing learning algorithms by dividing the data into k-folds, where each fold is separated into two segments: one used to learn or train a model and one used to validate the model. In typical cross-validation, the training and validation sets must be crossed in successive rounds so that each data point has a chance to be validated (Refaeilzadeh et al., 2009). Deciding the sizes and strategies for partitioning data sets into training, test, and validation sets depend mainly on the problem and available data. The performance metrics of the ML model are related to the ability of a test to determine if a health diagnosis is effective. Some of the commonly used metrics are accuracy (number of correctly classified assessments over the total number of assessments), precision, sensitivity and specificity, predictive values, probability ratios, and the area under the ROC curve (Šimundić, 2009). To evaluate the success of an ML system when predicting a medical diagnosis, these must be taken into account. It is relevant to note that the area under the curve (AUC) is one of the main performance metrics used in prediction systems; however, metrics such as precision are recommended to complement the results.

Recent studies have described how AI has been involved in areas like gynecology and obstetrics (Iftikhar et al., 2020; Cecula, 2021); however, the effect of all ML techniques on the prediction of perinatal complications has not been reviewed. Thus, we decided to carry out this review to present and synthesize different ML-based models, highlighting the main input characteristics used for training, output results, performance metrics in prediction, and contribution to decision-making related to perinatal complications associated with non-congenital risk factors in pregnant women.

METHODS

This systematic review was carried out following the guidelines for systematic reviews and meta-analysis (PRISMA) (Urrútia and Bonfill, 2010) (**Supplementary Table S1**).

TABLE 1 | Search expressions used in the systematic review.

Data base	Search expression	Year of publication
PubMed Web of Science Scopus	["Machine learning" (Mesh)] AND "Pregnancy Complications" (Mesh) NOT ("postpartum") ("Machine learning" OR "Deep learning" AND ("complications in pregnancy" OR "pregnancy complications" OR "perinatal complications") NOT ("postpartum")	2015–2020

Information Sources and Search Strategy

Full and original articles related to ML techniques on complications during pregnancy published in English from 2015 to 2020 were searched on PubMed, Web of Science, and Scopus databases. Search terms were chosen and searches performed in an iterative process, initially using word headings associated with ML, such as "machine learning," "deep learning," "artificial intelligence," and related to perinatal complications, such as "complications in pregnancy" and "pregnancy complications," and excluding articles related to postpartum and congenital complications. For PubMed, the MESH terms were used to include associated synonyms in the search, and for Scopus and Web of Science, the terms of interest mentioned before with Boolean operators were used (**Table 1**). The search and final collection of articles were 98 articles, of which 20 were excluded by duplication.

Eligibility Criteria

The included criteria for the articles searched were 1) English original articles, 2) access to full text, 3) studies based on humans, 4) studies using machine learning methods to predict complications in pregnancy, and 5) complications during pregnancy and at term in the mother and the newborn. The exclusion criteria applied were 1) systematic reviews, meta-analysis, and bibliographic reviews; 2) articles that included postpartum complications; 3) maternal congenital disease that increases the risk of perinatal complications; and 4) fetal congenital diseases. Articles were added manually according to the aforementioned criteria.

Article Screening

All articles found were uploaded to the Mendeley desktop platform, where they were saved in a dedicated folder for the present systematic review. After eliminating the duplicate articles, a total of 78 articles remained. Then 16 articles were excluded by title, 18 were excluded by criteria, and 19 were excluded after reading. Finally, 31 articles for the review were selected. The selected articles were classified by the ML model used, type of features used, outputs, and performance metrics, in order to estimate which methods are the most accurate in the context of predicting perinatal complications.

Risk of Bias

The 31 articles were subjected to the CASP checklist, which contains 11 questions to help evaluate a clinical prediction rule (CASP, 2017). Study quality was scored according to the CASP critical score: if the criterion was met entirely = 2 points; criterion partially met = 1 point; and criterion not applicable/not met/not mentioned = 0. Finally, study quality was ranked: a total score of 22 = high quality; 16–21 = moderate quality; and ≤15 = low quality.

Data Synthesis and Visualization

To optimize the visualization of the results obtained in the systematic review, several tables were made according to the terms addressed in the search, showing complications that the models seek to predict, input characteristics for the training of the ML model, the type of ML used, and its validation and performance metrics.

RESULTS

Study Characteristics

To apply the PRISMA method, the articles have been classified according to the criteria mentioned before: title, abstract, and the full article. A total of 84 articles were found, of which 52 were excluded because they did not meet the search criteria of interest. Of these, 16 were eliminated by title, 18 after reading the abstract, and 19 after reading the entire article, leaving 31 articles to analyze (**Figure 1** and **Supplementary Table S2**). The type of studies in the manuscripts analyzed were mainly cohort (87.2%) and retrospective (96.8%). The populations studied were primarily from Asia and Europe (both 32.3%), followed by North and South America (22.5 and 6.5%, respectively). An increased rate of studies was observed during 2019 (35.5%) (**Table 2**). The features mainly used to predict perinatal complications are electronic medical records (48%) and then medical images (29%), biological markers (19%), and 4% are based on another type of feature, in this case, sensors (Moreira et al., 2016a) and fetal heart rate (Zhao et al., 2019). Two studies contemplate two features: electronic medical records and medical images (Nair, 2018; Lipschuetz et al., 2020).

According to the CASP checklist, one article met the total score and was classified as a high-quality article (Gao et al., 2019). The rest of the items were classified as moderate quality and none as low quality according to the evaluation criteria (average total score = 18–19). It is essential to mention that the "non-compliance" items were not being mentioned or not applicable to the study. The item asking whether the sample was randomized in 15 articles does not apply since analyzed retrospective electronic health records or images. Regarding using a comparison group, 12 reports do not apply due to retrospective data and data management for the prediction model (**Supplementary Figure S1**).

Features Studied

The choice of informative, discriminatory, and independent characteristics is crucial to achieving effective algorithms for recognizing, classifying, and regression patterns. Thus, the four types of features analyzed in the articles were electronic medical

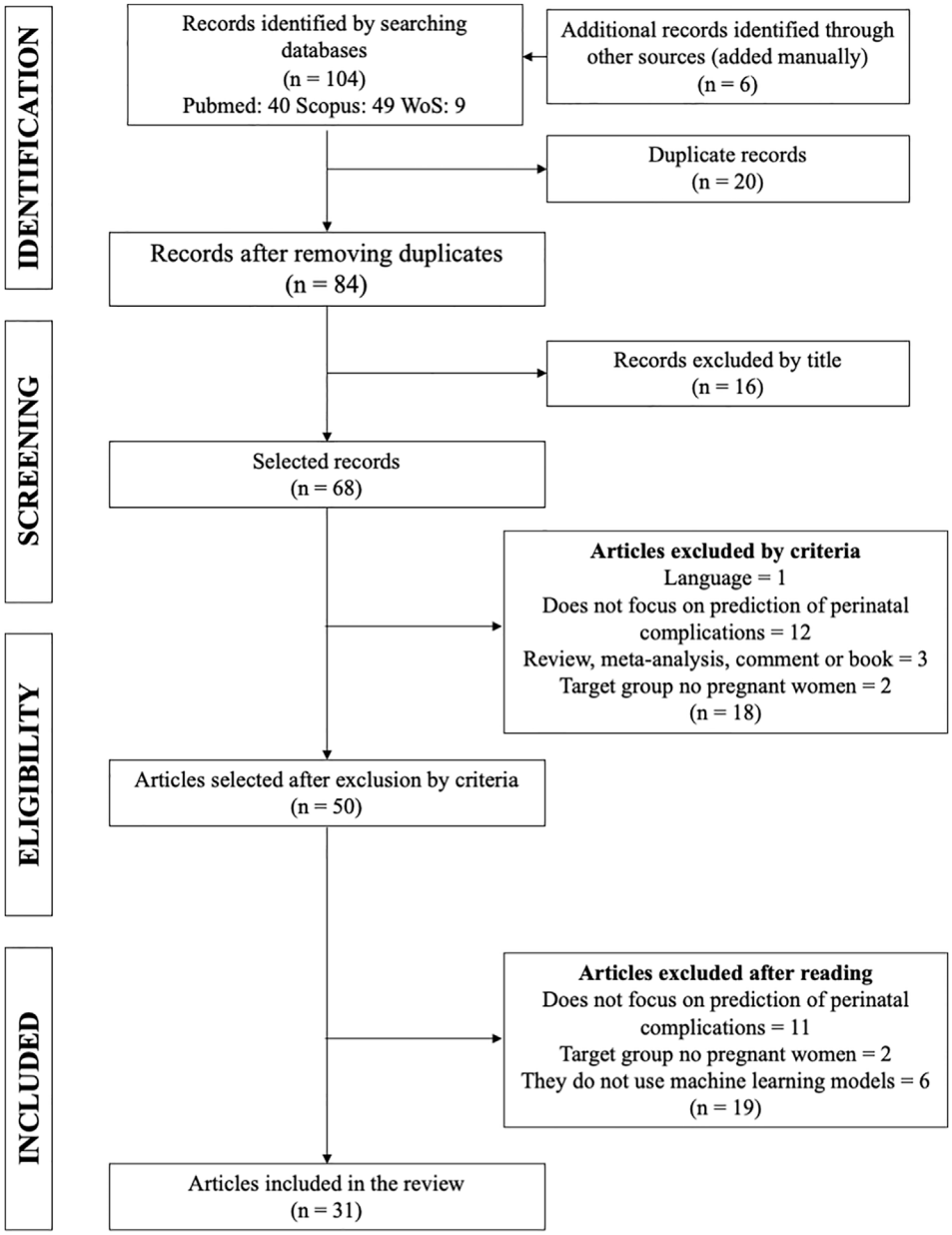

FIGURE 1 | Process for selecting articles for the systematic review (PRISMA). One hundred four articles were found. Sixteen articles were excluded by title, 18 were excluded by criteria, and 19 were excluded after reading. Finally, 31 articles for the review were selected.

TABLE 2 | Main characteristics of selected articles.

Type of study	Temporality	Geographic location of the study group	Year of publication
Cohort (87.2%)	Retrospective (96.8%)	Asia (32.3%)	2015 (3.2%)
Control case (6.4%)	Prospective (3.2%)	Europe (32.3%)	2016 (9.6%)
Exploratory (3.2%)		North America (22.5%)	2017 (12.9%)
Cross section (3.2%)		South America (6.5%)	2018 (19.4%)
		Africa (3.2%)	2019 (35.5%)
		Oceania (3.2%)	2020 (19.4%)

TABLE 3 | Perinatal complications predicted through ML models using electronic medical records.

Electronic medical records									
Ref	**Time of data collection**	**Number of records**	**Outcome**	**Validation technique**	**ML methods**	**Performance metrics**			
						AUC	**Sen. (%)**	**Spec. (%)**	**Acc. (%)**
Lipschuetz et al. (2020)	During pregnancy with term delivery	9,888	TOLAC failure risk	10-fold cross-validation and deletion of a portion of the data	Gradient increasing machines	0.793	—	—	—
			-High		RF	0.756	—	—	—
			-Medium		RF	0.782	—	—	—
			-Low		AdaBoost set	0.784	—	—	—
Hamilton et al. (2020)	<22 gw	100	Severe neonatal mortality v/s no severe neonatal mortality	10 replicates of 10-fold cross-validation and on the one standard error rule	Decision tree	0.853	79.7	80.9	75.6
					SVM	0.851	79.1	79.6	77.4
					Generalized additive model	0.850	80.6	81.8	75.0
					Simple neural network	0.848	78.5	80.7	73.3
Artzi et al. (2020)	<20 gw	588,622	High-risk GDM v/s low-risk GDM	Cross-validation on the training set, and resampling from the validation	Gradient augmentation machine built with decision tree base learners	0.850	—	—	—
Jhee et al. (2019)	Early second trimester to 34 gw	1,006	Pre-eclampsia v/s no pre-eclampsia	Training (70%) validation set (30%)	Logistic regression	—	70.3	—	86.2
					Decision tree	—	64.8	—	87.4
					Naive Bayes	—	50	—	89.9
					SVM	—	13.7	—	89.2
					RF	—	67.9	—	92.3
					Stochastic gradient augmentation method	—	60.3	—	97.3
Rittenhouse et al. (2019)	During pregnancy (not specified)	1,450	Premature v/s not premature[a]	k-fold cross-validation (with 10 folds)	Binary logistic regression model, RF classification, and generalized additive model	0.868	98.9	—	—
		—	Gestational age prediction	k-fold cross-validation (with 10 folds)	Combined continuous model of linear regression, RF, regression, and generalized additive models	0.878	90.2	—	—
Kuhle et al. (2018)	Pre-pregnancy at 26 gw	30,705	LGA v/s AGA	Test (20%) training (80%) and ten-fold cross-validation in the training data	RF	0.728	—	—	79.9
					Decision tree	0.718	—	—	79.4
					Elastic net	0.748	—	—	80.9
					Gradient increasing machines	0.748	—	—	80.5
					Logistic regression	0.745	—	—	81.3
					Neural network	0.746	—	—	81.2
			SGA v/s AGA	Test (20%) training (80%) and ten-fold cross-validation in the training data	RF	0.745	—	—	90.3
					Decision tree	0.713	—	—	80.1
					Elastic net	0.771	—	—	91.2
					Gradient increasing machines	0.766	—	—	91.1
					Logistic regression	0.771	—	—	91.2
					RF	0.772	—	—	91.4
Khatibi et al. (2019)	During pregnancy, before 37 gw	1,547,677	Non-premature delivery v/s premature	Training dataset	Set of decision trees, SVM and RF	0.68	—	—	81.0
Malacova et al. (2020)	During pregnancy (not specified)	952,813	Miscarriage v/s born alive	Dataset was randomly divided into 10 folds	Artificial neural networks: multilayer perceptron + radial base networks	—	80	94.1	90.9
Pan et al. (2017)	During pregnancy (not specified)	6,457	Adverse delivery v/s non-adverse delivery	10-fold cross-validation and repeated the cross-validation process with new folds 9 more times in the test set	Logistic regression	—	31.9	—	—
					Linear discriminant analysis	—	31.7	—	—
					RF	—	30.1	—	—
					Naive Bayes	—	29.2	—	—
Moreira et al., 2016b	During pregnancy (not specified)	25	Hypertensive disorder v/s without hypertensive disorder	10-fold cross-validation for decision trees	Decision tree J48	0.748	60	—	—
				5-fold cross-validation method	Naive Bayes	0.782	52	—	—

(Continued on following page)

TABLE 3 | (*Continued*) Perinatal complications predicted through ML models using electronic medical records.

Electronic medical records									
Ref	**Time of data collection**	**Number of records**	**Outcome**	**Validation technique**	**ML methods**	**Performance metrics**			
						AUC	**Sen. (%)**	**Spec. (%)**	**Acc. (%)**
Gao et al. (2019)	During pregnancy (not specified)	45,858	Severe maternal morbidity v/s no serious maternal morbidity	Train dataset and 10-fold stratified cross-validation	Logistic regression	0.937	76.5	—	—
Mailath-Pokorny et al. (2015)	Between 22 and 32 gw	617	Delivery prediction within 48 h of transfer v/s Before 32 gw	Validation set	Multivariate logistic regression	0.850	—	—	—
Shigemi et al. (2019)	Data from the first and last prenatal checkup	15,263	Macrosomia v/s No macrosomia	Training dataset (90%) and a validation dataset (10%)	Logistic regression	0.880	88	55	—
					RF	0.990	60	82	—
Paydar et al. (2017)	Before the first trimester	149	Live births v/s stillbirths	Test (70%) training (30%)	Logistic regression	0.834	40.5	99.7	94.7
					Decision tree	0.808	40.6	94.7	99.7
					RF	0.836	41.1	94.7	99.7
					XGBoost	0.842	45.3	94.7	99.7
					Artificial neural networks multilayer perceptron	0.840	43.5	94.7	99.7
			Spontaneous preterm birth		Multivariate logistic regression	0.670	—	—	—
Boland et al. (2017)	Each trimester of pregnancy	36,898	Pregnancies without congenital abnormality v/s pregnancies with congenital abnormality	Method of data validation is not identified	RF	—	—	—	88.9

Ref., references; ML, machine learning; AUC, area under curve; Sen, sensitivity; Spec, specificity; Acc, accuracy; TOLAC, trial of labor after caesarean, RF, random forest; gw, gestational weeks; SVM, support vector machine; GDM: gestational diabetes mellitus; LGA, large for gestational age; AGA, adequate for gestational age, SGA, mall for gestational age.
[a]*This study also uses biological markers.*

records (EMRs) (**Table 3**), medical images (recordings, ecotomographs, ultrasound, resonance, etc.) (**Table 4**), biological markers (**Table 5**), and others (sensors and fetal heart rate) (**Table 6**).

Perinatal Complications to Predict

These have been divided into 16 main prediction outputs: prematurity, pre-eclampsia, adverse delivery, size for gestational age, gestational diabetes mellitus, neonatal mortality, fetal acidemia, fetal hypoxia, placental accreta, pulmonary diseases, cesarean section, placental invasion, congenital anomaly, severe maternal morbidity, spontaneous abortion, and trial of labor after cesarean (TOLAC) failure (**Figure 2**). The main perinatal complications considered in the application of ML are prematurity (7 studies) and pre-eclampsia (6 studies).

Validation Methods

Validation methods are strategies that allow the estimation of the predictive capacity of ML models. Fifty-five percent use training tests and the cross-validation method as a validation method with greater reliability in results, while 41.8% use a single validation method and 3.2% do not use any validation method (neither training tests nor cross-validation).

ML Models and Performance Metrics

In the present review, 67.7% of the articles used AUC and 61.3% used the accuracy metric. Sensitivity was only evaluated in 61.3% of the studies. While all studies assess results with at least one performance metric, reports of predictive accuracy were often incomplete, with a total of 38.7% of studies reviewing at most two performance methods. According to the studies, none had a clinical application, they only functioned to establish precise prediction systems in the diagnosis of the different perinatal complications presented.

Twenty-one different ML methods were used to predict these 16 perinatal complications. Placental invasion is referred to as placental adhesive disorders observed in women with placenta previa or prior cesarean section that lead to complications such as perinatal hemorrhage and visceral injuries, where an early diagnosis is necessary for appropriate treatment (Sun et al., 2019). Excellent performance of placental invasion can be observed with an AUC and an accuracy of 0.980 and 95.2%, respectively, using the Tree-based Pipeline Optimization Tool (TPOT) (Sun et al., 2019). To predict fetal acidemia, using convolutional neural networks, an AUC and accuracy of 0.978 and 98.4% are achieved, respectively (Zhao et al., 2019). Only one study of the six attempting to diagnose pre-eclampsia had a performance considered as good, using the AdaBoost model, with an AUC of 0.964 and an accuracy of 89% (Munchel et al., 2020). The prediction of prematurity has excellent results in two studies; the one that uses SVM achieves an AUC of 0.952 and an accuracy of 95.7% (Sadi–Ahmed et al., 2017), and the study that uses stacked sparse autoencoder achieves an AUC of 0.900 and an accuracy

TABLE 4 | Perinatal complications predicted through ML models using medical images.

Medical Images									
Ref	**Time of data collection**	**Number of records**	**Outcome**	**Validation technique**	**ML methods**	**Performance metrics**			
						AUC	**Sen. (%)**	**Spec. (%)**	**Acc. (%)**
Sun et al. (2019)	After 24 gw	155	Placental invasion v/s placenta previa simple	Test (83%) Training (17%)	Genetic algorithm-based machine learning algorithm implemented in TPOT	0.980	100	88.5	95.2
Chen et al. (2019)	150 EHG in pregnancy (not specified) and 150 EHG in labor (24 h before delivery usually)	300	Premature v/s born of term	Test (67%) training (33%)	Stacked sparse autocoder	0.900	92	88	90
					Extreme learning machine	0.840	80	88	83
					SVM	0.850	88	82	85
Fergus et al. (2018)	>36 gw	552	Vaginal delivery v/s caesarean section	Test (80%) training (30%)	SVM RF and linear discriminant analysis of features	0.960	87	90	—
Borowska et al. (2018)	From 24 to 28 gw	20	Deliver after 7 days v/s deliver within 7 days	10-fold cross-validation	PCA + SVM	—	—	—	83.32
					RQA + SVM	—	—	—	79.3
Veeramani and Muthusamy (2016)	During pregnancy (not specified)	ni	Diagnosis of recurrent lung diseases in the newborn	Test Training	RVM	—	—	—	100
					Multilevel RVM	—	—	—	90
Romeo et al. (2019)	During pregnancy (not specified)	108	Delivery with placental accreta spectrum v/s delivery without placental accreta spectrum	Test (75%) training (25%) and a 10-fold cross-validation	RF	—	93.7	93.7	95.6
					K-nearest neighbor	—	97.5	98.7	98.1
					Naive Bayes	—	86.1	75	80.5
		—			Multilayer perceptron	—	92.4	83.8	88.6
Sadi-Ahmed et al. (2017)	Between the 27th and the 32nd gw	30	Premature vs. term	100 iterations of "holdout" cross-validation for training and test sets	SVM	0.952	98.4	93	95.7
Cömert et al. (2018)	During pregnancy (not specified)	552	Presence of fetal hypoxia v/s absence of fetal hypoxia	Test (90%) training (10%) and 10-fold cross-validation	Least squares support vector machines	—	63.5	65.9	65.4
Weber et al. (2018)	First prenatal visit	~2,700,000	Born preterm v/s born of term in white women v/s color	Test set and 5-fold cross-validation	Logistic Regression	0.625	56	62.5	—

Ref., references; ML, machine learning; AUC, area under curve; Sen, sensitivity; Spec, specificity; Acc, accuracy; gw, gestational weeks; TPOT, tree-based pipeline optimization tool; EHG, electrohysterograhic; SVM, support vector machine; PCA, principal components analysis; RQA, recurrence quantification analysis; RVM, relevance vector machine.

of 90% (Chen et al., 2019). For the prediction of neonatal mortality, through sociodemographic records using XGBoost, an AUC of 0.842 and an accuracy of 99.7% were obtained (Hamilton et al., 2020). Regarding the performance of the predictions included in the greatest number of studies, prematurity outperformed pre-eclampsia according to the AUC (**Table 7**).

It was decided to corroborate the performance of the methods based on deep learning. Only four studies used deep learning methods. They all had an excellent performance. For the prediction of fetal acidemia, a deep convolutional network was used with an AUC of 0.978 and an accuracy of 98.4% (Zhao et al., 2019). For the prediction of spontaneous abortion, multilayer perceptron and radial-based networks were used, with an accuracy of 90.9% (Paydar et al., 2017). And as mentioned above, for the prediction of pre-eclampsia, using biological markers and multilayer perceptron, an AUC of 0.908 was obtained (Nair, 2018). For the prediction of neonatal mortality, through sociodemographic records using XGBoost, an AUC of 0.842 and an accuracy of 99.7% were obtained (Hamilton et al., 2020) (**Table 8**).

Interpretable ML Models

The interpretability of ML models refers to the degree to which a human being can consistently predict the outcome of the model (Kim et al., 2016), which has been well accepted by the clinical team. In this systematic review, we found that 24% of the studies use AI-interpretable ML models. The ML methods that were the most used in the prediction of perinatal complications were the random forest, logistic regression, neural networks, and support vector machine (SVM).

Predictive Variables

Forty-eight percent of the studies explain the main characteristics of pregnant women that could be relevant to predict some conditions. Characteristics and antecedents such as gestational diabetes, cardiovascular disease, underlying diseases, and the age of the mother, as well as the presence of chronic arterial hypertension, are considered high-ranking features for the prediction of premature births; and the father's nationality is very important to differentiate the provider-initiated spontaneous preterm births (Khatibi et al., 2019).

TABLE 5 | Perinatal complications predicted through ML models using biological markers.

Biological Markers									
Ref	**Time of data collection**	**Numbers of records**	**Outcome**	**Validation technique**	**ML methods**	**Performance metrics**			
						AUC	**Sen. (%)**	**Spec. (%)**	**Acc. (%)**
Guo et al. (2020)*	For GDM <18 gw	2,199	GDM	Training and validation	Logistic regression	0.732	—	—	72.6
	For PE		PE			0.813	—	—	81.5
	<20gw		MA			0.766	71	82.3	80.0
	For MA and FGR, 12–28 gw		FGR			0.775	—	—	79.5
Liu et al. (2019)	>20 gw	77	PE v/s control	Test and training	SVM	0.958	95	66.7	—
Nair (2018)	>20 gw	38	PE v/s control	Test (85%) training (15%)	Artificial neural networks multilayer perception	0.908	—	—	—
Yoffe et al. (2019)	First trimester of gestation	43	GDM v/s without GDM[a]	Trained and evaluated the datasets via a leave-one-out cross-validation	Logistic regression	0.740	88	40	76
					RF	0.810	94	40	81
					AdaBoost	0.770	94	60	86
Munchel et al. (2020)	Between 12 and 37 gw	113	Severe PE v/s without PE	Dataset trained with 10-fold stratified cross-validation	AdaBoost	0.964	88	92	89

Ref., references; ML, machine learning; AUC, area under curve; Sen, sensitivity; Spec, specificity; Acc, accuracy; GDM, gestational diabetes mellitus; gw, gestational weeks; PE, pre-eclampsia; MA, macrosomia; FGR, fetal growth restriction; SVM, support vector machine.
[a]*This study also uses electronic medical records.*

TABLE 6 | Perinatal complications predicted through ML models using sensors and fetal heart rate.

Other features									
Ref.	**Time of data collection**	**Numbers of records**	**Outcome**	**Validation technique**	**ML methods**	**Performance metrics**			
						AUC	**Sen. (%)**	**Spec. (%)**	**Acc. (%)**
Moreira et al., 2016a	During pregnancy (not specified)	25	Complication in hypertensive disorder v/s without complication in hypertensive disorder[a]	Leave-one-out method of cross-validation	Naive Bayes	0.687	42.3	94.4	80
Zhao et al. (2019)	Intrapartum	552	Presence v/s absence of fetal acidemia[b]	Training set and 10-fold cross-validation	Deep convolutional neural network	0.978	98.2	94.9	98.4

Ref., references; ML, machine learning; AUC, area under curve; Sen, sensitivity; Spec, specificity; Acc, accuracy.
[a]*Sensors.*
[b]*Fetal heart rate.*

On the other hand, important predictors to determine the likelihood of a newborn to be small for gestational age (SGA) were smoking, a particular amount of gestational weight gain, and low–birth weight newborn. The body mass index (BMI) before pregnancy, gestational weight gain, and a macrosomic newborn in a previous delivery were the strongest predictors to determine large for gestational age (LGA) newborns (Kuhle et al., 2018). To predict fetal macrosomia, the determining variables were age ≥30, multiparity, 12 kg of total weight gain during pregnancy, abdominal circumference >95 cm (at the last perinatal checkup), and a gestation period over 39 weeks (Shigemi et al., 2019).

In order to predict pre-eclampsia, the most influential variables were systolic blood pressure, serum levels of ureic nitrogen and creatinine, platelet count, serum potassium level, leukocyte count, blood glucose level, serum calcium, and proteinuria levels in the early second trimester (Jhee et al., 2019). Interestingly, high pre-pregnancy BMI and previous preterm births (Pan et al., 2017) were able to predict whether pregnant women will have an adverse pregnancy outcome (preterm, low birth weight, neonatal/infant death, stay in the neonatal intensive care unit) and indicate the main risk characteristics.

Furthermore, in order to predict TOLAC, the determining factors in the prediction model were parity, age, vaginal birth with cesarean section in the past, gestational weeks, minimum gestation week in previous deliveries, the weight of the newborn from the previous delivery, dilation, and head position (Lipschuetz et al., 2020). To predict pregnancy complications associated with placental alterations (pre-eclampsia, GDM, fetal growth restriction, macrosomia), maternal age, BMI, newborn weight, and the results of adverse events in previous pregnancies were the most influential characteristics in the study (Guo et al., 2020).

To predict gestational age at delivery (if the newborn will be preterm) variables such as the date of the mother's last

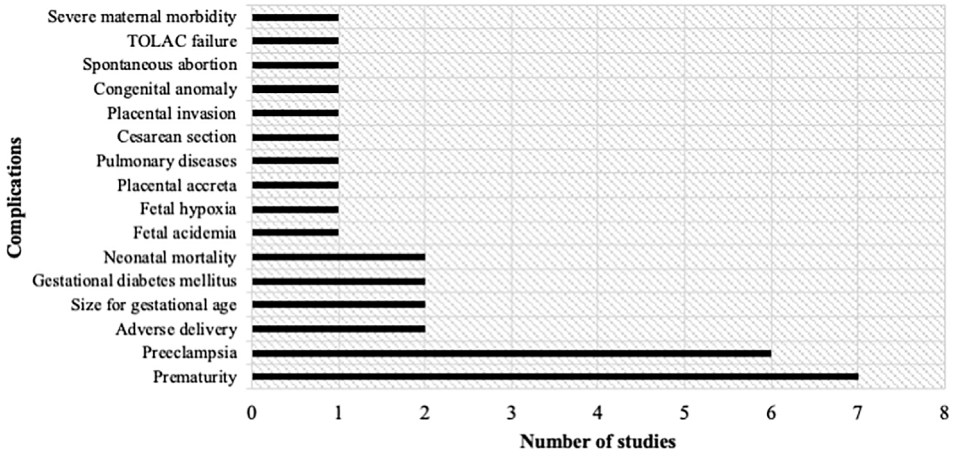

FIGURE 2 | Number of studies according to the complication to be predicted. Sixteen complications were identified: Prematurity, pre-eclampsia, adverse delivery, size for gestational age, gestational diabetes mellitus, neonatal mortality, fetal acidemia, fetal hypoxia, placental accreta, pulmonary diseases, cesarean section, placental invasion, congenital anomaly, spontaneous abortion and trial of labor after cesarean (TOLAC) failure, and severe maternal morbidity.

TABLE 7 | Models with best performance according to AUC and accuracy.

Prediction	Input characteristics	ML model	Performance	No of pregnant women
Placental invasion	Magnetic resonance	TPOT	AUC: 0.980 – Acc: 95.2%	100–1,000
Fetal academia	Maternal sociodemographic characteristics	Neural networks	AUC: 0.978 – Acc: 98.4%	100–1,000
Pre-eclampsia	Biological marker	AdaBoost	AUC: 0.964 – Acc: 89%	<100
Prematurity	EHG recordings	SVM	AUC: 0.952 – Acc. 95.7%	100–1,000
Prematurity	EHG recordings	Stacked sparse autocoder	AUC 0.900 – Acc: 90%	100–1,000
Neonatal mortality	Maternal sociodemographic characteristics	XGBoost	AUC: 0.842 – Acc: 99.7%	>10,000

ML, machine learning; TPOT, tree-based pipeline optimization tool; AUC, area under curve; Acc, accuracy; EHG, electrohysterogram; SVM, support vector machine.

TABLE 8 | Models and precision based on deep learning.

Prediction	Input characteristics	Deep learning model	Performance	N° of pregnant women
Fetal acidemia	Maternal and newborn sociodemographic characteristics	Deep convolutional network	AUC: 0.978, Acc: 98.4%	100 - 1,000
Spontaneous abortion	Maternal sociodemographic characteristics	Multilayer Perceptron and radial-based networks	Acc: 90.9%	100 - 1,000
Pre-eclampsia	Biological markers	Multilayer Perceptron	AUC: 0.908	<100
Neonatal mortality	Maternal sociodemographic characteristics	Multilayer Perceptron	AUC: 0.84 - Acc: 99.7%	>100,000

AUC, area under curve; Acc, accuracy.

menstruation, birth weight, delivery of twins, maternal height, hypertension during labor and HIV serological status were decisive in the ML model (Rittenhouse et al., 2019). To determine preterm birth, the presence of premature rupture of membranes and/or vaginal bleeding, ultrasound cervical length, gestation week, fetal fibronectin, and serum C-reactive protein were the determining variables (Mailath-Pokorny et al., 2015). In another study, prediction of preterm birth considered the most relevant variables to be maternal age, whether the mother was black, Hispanic, Asian, born in the United States, delivered by herself or assisted by a physician, presence of diabetes mellitus, chronic arterial hypertension, thyroid dysfunction, asthma, previous stillbirth, fetal weight loss, *in vitro* fertilization, nulliparity, being a smoker during the first trimester, and BMI (Weber et al., 2018).

Stillbirth can potentially be identified prenatally considering the combination of current pregnancy complications, congenital anomalies, maternal characteristics, and medical history (Malacova et al., 2020). Determining factors for the prediction of fetal acidemia were maternal age, gestational age, pH, extracellular fluid deficit, pCO2, base excess, APGAR 1 and 5 min, parity, gestational diabetes, birth weight, child sex, and the type of delivery (Zhao et al., 2019).

TABLE 9 | Main predictive variables for predicting perinatal complications

Prediction	Predictive variables	Machine learning model	Performance	
			AUC	Acc
Premature birth	Gestational diabetes Cardiovascular disease Underlying diseases Maternal age Chronic arterial hypertension	Set of decision trees, SVM and RF	0.680	81%
SGA	Smoking	RF	0.728	79.9%
	A particular values of gestational weight gain	DT	0.718	79.4%
	Low–birth weight newborn	Elastic net	0.748	80.9%
		Gradient increasing machines	0.748	80.5%
		Logistic regression	0.745	81.3%
		Neural network	0.746	81.2%
LGA	Pre-pregnancy BMI	RF	0.745	90.3%
	Gestational weight gain	DT	0.713	80.1%
	Macrosomic newborn in a previous delivery	Elastic net	0.771	91.2%
		Gradient increasing machines	0.766	91.1%
		Logistic regression	0.771	91.2%
		Neural network	0.772	91.4%
Fetal Macrosomia	Greater than 30 years-old	Logistic regression	0.888	ni
	Multiparity A 12 kg total weight gain in pregnancy Abdominal circumference > 95 cm (at last perinatal checkup) Gestation age > 39 weeks	RF	0.990	ni
Pre-eclampsia	At second trimester	Logistic regression	ni	86.2%
	Systolic blood pressure	DT	ni	87.4%
	Serum levels of ureic nitrogen	Naive Bayes	ni	89.9%
	Creatinine in the blood	SVM	ni	89.2%
	Platelet count, serum potassium level	RF	ni	92.3%
	Leukocyte count Blood glucose level Serum calcium and urinary protein levels	Stochastic gradient augmentation method	ni	97.3%
Adverse delivery (preterm, low birth weight, neonatal/infant death, stay in the neonatal intensive care unit) v/s non-adverse delivery	High pre-pregnancy BMI	Logistic regression	ni[a]	ni[a]
		Linear discriminant analysis	ni[a]	ni[a]
	Previous preterm births	Random forest	ni[a]	ni[a]
		Naive Bayes	ni[a]	ni[a]
TOLAC Failure Risk	Parity	Gradient increasing machines	0.793	ni
	Age	RF	0.756	ni
	Vaginal birth with cesarean section in the past Gestational week	RF	0.782	ni
	Minimum gestation week in previous deliveries The weight of the newborn from the previous delivery Dilation and head position	AdaBoost set	0.784	ni
Gestational age (if the newborn will be preterm)	Hypertension during labor HIV serological status	Binary logistic regression model, random forest classification, and generalized additive model	0.868	98.9%
Delivery prediction within 48 h of transfer v/s before 32 weeks gestation	Presence of premature rupture of membranes Vaginal bleeding Ultrasound cervical length Gestation week Fetal fibronectin and serum C-reactive protein	Multivariate logistic regression	0.850	ni
Spontaneous preterm birth	Maternal age Black woman Hispanic woman Asian Mother born in the United States Paid delivery by herself or physician Diabetes mellitus	Multivariate logistic regression	0.670	ni

(Continued on following page)

TABLE 9 | (*Continued*) Main predictive variables for predicting perinatal complications

Prediction	Predictive variables	Machine learning model	Performance	
			AUC	Acc
	Chronic arterial hypertension Thyroid dysfunction Asthma Previous stillbirth Fetal weight loss *In vitro* fertilization Nulliparity Pregnant smoker during the first trimester BMI			
Stillbirth	Current pregnancy complications	Logistic regression	0.834	94.7%
	Congenital anomalies	Decision tree	0.808	99.7%
	Maternal characteristics	Random forest	0.836	99.7%
	Medical history	XGBoost	0.842	99.7%
		Artificial neural networks multilayer perceptron	0.840	99.7%
Prediction of complications in pregnancy: pre-eclampsia, GDM, restriction of fetal growth, macrosomia	Maternal age BMI Newborn weight Results of adverse events in previous pregnancies	Logistic regression	0.770	78.6%
Severe maternal morbidity	Ventilator dependence Intubation Critical care Acute respiratory failure Ventilation Trauma and postoperative pulmonary failure Fluid and electrolyte disorder Systemic inflammatory response syndrome Acidosis and septicemia	Logistic regression	0.937	ni
Fetal acidemia	Maternal age Gestational age pH Extracellular fluid deficit pC O 2 Base excess APGAR 1 min, and 5 min Parity Gestational diabetes Birth weight Child sex Type of delivery	Deep convolutional neural network	0.978	98.4%

AUC, area under the curve; Acc., accuracy; SVM, support vector machines; RF, random forest; SGA, small for gestational age; DT, decision tree; LGA, large for gestational age; BMI, body index mass; TOLAC, trial of labor of after cesarean; HIV, human immunodeficiency virus; GDM, gestational diabetes mellitus; ni, not informed.

[a]*This study does not specify either AUC or accuracy. The only performance metric used is sensitivity; logistic regression: 31.9%, linear discriminant analysis: 31.7%, random forest: 30.1%, naive Bayes: 29.2%.*

In the case of the prediction of severe maternal morbidity, the following characteristics were determining factors: ventilator dependence, intubation, critical care, acute respiratory failure, ventilation, trauma and postoperative pulmonary failure, fluid and electrolyte disorder, systemic inflammatory response syndrome, acidosis, and septicemia (Gao et al., 2019).

Clinical Applicability of ML Systems

According to the studies, none had clinical application; they only served to establish precise prediction systems to diagnose the perinatal complications presented.

DISCUSSION

Input Variables on Machine Learning

Machine learning plays a vital role and offers solutions with many applications, for example, image detection, data mining, natural language processing, and disease diagnosis (Maity and Das, 2017). This systematic review provides a study of different ML techniques for the diagnosis of different perinatal complications and frames a contribution to women's health. A total of sixteen perinatal complications predicted by various ML models were detected, among which the most studied were prematurity and pre-eclampsia.

ML can significantly improve health care; however, it is necessary to consider the disadvantages of AI in health. Ethical dilemmas need to be addressed and the potential for human biases when creating computer algorithms (Ho et al., 2019). Health-care predictions can vary based on race, genetics, gender, and other characteristics, which could lead to the overestimation or underestimation of patient risk factors if not considered. When it comes to AI analysis in health care, it will be the physician's responsibility to ensure that AI algorithms are developed and applied appropriately (Jordan and Mitchell, 2015).

In the present systematic review, the main data collection method was the use of electronic medical records. ML techniques can establish patterns from a data set based on electronic medical records (EMRs). Pattern recognition from these records supports in predicting and making decisions for diagnosis and treatment planning (Johnson et al., 2016). The application of EMR-based ML methods can be combined with other sources of large medical data, such as genomics, and medical imaging, which through predictive algorithms could improve clinical diagnosis and treatment systems, when used as complementary information (Barak-Corren et al., 2017). EMR data usually include demographics data, diagnoses, biochemical markers, vital signs, clinical notes, prescriptions, and procedures, which are generally easy to obtain and reduce transfer errors when handling large amounts of information. Previously, several studies have described medical diagnosis prediction tools mediated EMRs (McCoy et al., 2015; Osborn et al., 2015; Nguyen et al., 2017; Rajkomar et al., 2018); furthermore, in the present systematic review, 48% of the features for the diagnosis prediction model to perinatal complications came from EMRs, of which the most used features were sociodemographic maternal characteristics. Thus, this tool can predict perinatal complications common in a given population, contributing to the overall improvement of perinatal public health.

Perinatal complications as Output Variables

Output variables were usually binary outputs (with complication or without complication). However, some studies quantified the risk, for example, the risk of TOLAC was classified as high, medium, or low (Lipschuetz et al., 2020), and in studies of gestational diabetes, one article quantified it as high risk or low risk (Cömert et al., 2018). The most frequently predicted perinatal complications in ML models were prematurity and pre-eclampsia. According to the literature, the high rate of preterm birth is a public health problem, since these newborns suffer substantial morbidity and mortality in the neonatal period, which translates to high medical costs (McCormick et al., 2011). Pre-eclampsia is a pregnancy disorder characterized by the new onset of hypertension after 20 weeks gestation and organ damage with underlying causes being endothelial dysfunction (ACOG (American College of Obstetricians and Gynecologists), 2020; Carrasco-Wong et al., 2021; Roberts, 1998). It is the leading cause of maternal and neonatal mortality and morbidity (Salsoso et al., 2017; Fondjo et al., 2019). Thus, prediction of the risk for developing pre-eclampsia can be performed in the first half of pregnancy.

Performance of the Machine Learning Methods

Diagnostic accuracy is the ability of a test to discriminate between the target condition and health. This discriminative potential can be quantified by several performance tools, such as sensitivity and specificity, AUC, accuracy metric, and other measurements (Šimundić, 2009). While all studies assess results with at least one performance metric and just 38.7% assess at least two performance methods, reports of predictive accuracy were often incomplete. With this observation, it is imperative to show the same performance tools on the different prediction models to evaluate accuracy compared between them.

In this systematic review, several ML methods were used. One of the better performances was obtained by the Tree-based Pipeline Optimization Tool (TPOT) to predict placental invasion (Sun et al., 2019), which was previously used in the investigation of novel characteristics in data science, providing optimization of the studied parameters (Le et al., 2020). Another excellent performance observed was the convolutional neural network (CNN) to predict fetal acidemia (Zhao et al., 2019). The CNN has gained much attention from attempts made at harnessing its power to automatically learn intrinsic patterns from data, which can avoid time-consuming manual functions engineering, and capture hidden intrinsic patterns more effectively (Oquab et al., 2014). Moreover, in the health-care field, CNN has been shown to capture more hidden data patterns and learn high-level abstraction in problem-solving (Zhang et al., 2017).

It is essential to mention that it is difficult to reach a consensus on the best method for predicting perinatal complications, since not all of them had the same input variables, type of records, and a number of samples. However, the best performance metrics observed were the prediction model of prematurity from medical images using the SVM technique with an accuracy of 95.7% and the prediction of neonatal mortality using the XGBoost technique with an accuracy of 99.7%. SVM has shown simplicity and flexibility to address several classification problems and also offers balanced predictive performance even in studies where sample sizes may be limited (Alkhaleefah and Wu, 2018). The XGBoost technique is a very effective and widely used ML method that data scientists use to achieve state-of-the-art results in many ML challenges (Wang et al., 2020).

Interpretability of Machine Learning

Despite the recognition of the value of ML in medical care, impediments persist for its greater acceptance within medical teams (Holzinger et al., 2019). A fundamental impediment relates to the nature of the black box, or "opacity," of many ML algorithms. The term refers to a system in which only the inputs and outputs are observable, while the question of what is transforming the inputs into the outputs cannot be fully understood (Molnar, 2019). Therefore, new techniques have been developed to facilitate the understanding of the internal functioning of the model, granting interpretability, which seeks to provide transparency to the black box (Freitas, 2014; Doshi-Velez et al., 2017; Lipton, 2018), so that the end-user can understand the model and may even improve the ML system (Freitas, 2014). The

improvement in the precision of the prediction will depend on the interpretability of the model to be used. This means that with ML interpretability, clinical staff could know which variables are involved in the prediction of a diagnosis.

Regarding the predictive variables, while most of them agreed with current knowledge, it was also shown that ML models contributed new variables of relevance, which would be interesting to observe in controlled clinical studies (**Table 9**). For example, pre-eclampsia was found to be predictable based on systemic blood pressure, platelet count, and urinary protein levels as influential variables, with lesser influence found from glucose levels, leukocytes count, serum calcium, and potassium levels (Jhee et al., 2019). Other innovative variables of interest found using ML in the prediction of perinatal complications were newborn sex for the prediction of fetal acidemia (Liu et al., 2019), and father's nationality and mother's age for the prediction of provider-initiated spontaneous preterm delivery (Malacova et al., 2020). Nevertheless, some prediction models lack variable measurements, making them impossible to apply in a clinical setting. For example, "weight gain" is mentioned as a predictor for SGA and LGA, but the article does not specify whether it was inadequate or excessive (Kuhle et al., 2018). It is also stated that the underlying disease of the mother influences the delivery initiated by the provider; however, it is not detailed which underlying disease is considered in this association (Khatibi et al., 2019). Also, some studies describe obvious associations, such as low birth weight is associated with SGA, or fetal macrosomia is associated with LGA (Kuhle et al., 2018). pH was also a predictor of fetal acidemia, which is logical since this condition is associated with pH changes (Zhao et al., 2019). Since the engineering team behind these investigations emphasizes these characteristics in the results, without taking this obviousness into account, it is imperative to include clinical experts on women's health into AI and data science teams.

Only 6.4% of the studies were case–control studies, while the vast majority were cohort studies. This may limit the use of these results in clinical practice (Salazar et al., 2019). Only one study was multicenter for predicting neonatal morbidity (Khatibi et al., 2019), representing higher quality evidence. Among the best performing studies, it is noteworthy that most had less than 1,000 patients, and only one based on XGBoost to predict neonatal mortality had over 10,000 patients. This may be risky since the sample size may not be representative for a given geographic group, representing one of the limitations of ML in health (Vayena et al., 2018). Also, another significant limitation of the present systematic review is that all studies included have different baselines, variable inputs, and separate complications (endpoints) assessed in their prediction, making it difficult to compare them.

It is essential to mention that all the studies reviewed have not been applied in a clinical phase; however, the majority mention that to optimize the results obtained, and the models should be used in hospitals or health services that care for pregnant women. Future prospective studies and additional population studies are needed to assess the clinical utility of the model for the real world (Liu et al., 2019; Malacova et al., 2020).

Few systematic reviews have addressed the use of AI in pregnancy. The first one describes how AI has been applied to evaluate maternal health during the entire pregnancy process and helped to understand the effects of pharmacological treatments during this stage (Davidson & Boland, 2020). The second systematic review concluded that using ML algorithms is better than using multivariable logistic regression for prognostic prediction studies in pregnancy care, focusing mainly on decision-making for the medical team (Sufriyana et al., 2020). Furthermore, the third one performed exclusively on neonatal mortality reported that ML models can accurately predict neonatal death (Mangold et al., 2021). Last, the use of modern bioinformatics methods analyzing ML models as non-invasive measures of heart rate variability to monitor newborns and infants was reported (Chiera et al., 2020). Although this body of evidence does not focus on predicting pregnancy complications, it encourages the clinical use of IA to support women's health during pregnancy.

CONCLUSION

In conclusion, the main advantage of interpretable ML applications is that the output is not subjective, due to the fact that it is based on real-world data and results and identifies the most critical variables for clinicians. It is important to continue promoting this field of research in ML in order to obtain solutions with multicenter clinical applicability reduce perinatal complications. AI has the overall potential to revolutionize women's health care by providing more accurate diagnosis, easing the workload of physicians, lowering health-care costs, and providing benchmark analysis for tests with substantial interpretation differences between specialists. This systematic review contributes significantly to the specialized literature on AI and women's health.

DATA AVAILABILITY STATEMENT

The original contributions presented in the study are included in the article/**Supplementary Material**, further inquiries can be directed to the corresponding author.

AUTHOR CONTRIBUTIONS

AB provided the principal idea, searched for information, and wrote the manuscript. RS provided the full support of the machine learning approach (search and discussion). SC provided the support on PRISMA technique and for machine learning applied on health. LS provided the support on the discussion on clinical approach on pregnancy complications. FP was the organizer of the manuscript and provided support on the discussion on machine learning, clinical approach, and pregnancy complications.

FUNDING

Supported by project PUENTE, UVA20993, Universidad de Valparaiso, Chile, the Fondo Nacional de Desarrollo Científico

y Tecnológico (FONDECYT) (grant number 1190316), Chile, and International Sabbaticals (LS) (University Medical Centre Groningen, University of Groningen, The Netherlands) from the Vicerectorate of Academic Affairs, Academic Development Office of the Pontificia Universidad Católica de Chile. The work of RS and SC was partially funded by ANID, Chile–Millennium Science Initiative Program—ICN2021_004. LS is part of The Diamater Study Group, Sao Paulo Research Foundation-FAPESP, São Paulo (grant number FAPESP 2016/01743–5), Brazil. AB holds a fellowship from "Beca de Doctorado FIB—UV 2021" from Universidad de Valparaíso.

SUPPLEMENTARY MATERIAL

The Supplementary Material for this article can be found online at: https://www.frontiersin.org/articles/10.3389/fbioe.2021.780389/full#supplementary-material

Supplementary Figure S1 | CASP prediction rule score of each article for bias review.The score for every study included in the systematic review. The maximum score is 22.

Supplementary Table S1 | Checklist for compliance with the review based on the PRISMA.

Supplementary Table S2 | List of selected items.

REFERENCES

ACOG (American College of Obstetricians and Gynecologists) (2020). Gestational Hypertension and Preeclampsia: ACOG Practice Bulletin, Number 222. *Obstet. Gynecol.* 135, e237–e260. doi:10.1097/AOG.0000000000003891

Ahmed, Z., Mohamed, K., Zeeshan, S., and Dong, X. (2020). Artificial Intelligence with Multi-Functional Machine Learning Platform Development for Better Healthcare and Precision Medicine. *Database (Oxford)* 2020, baaa010. doi:10.1093/database/baaa010

Alkhaleefah, M., and Wu, C.-C. (2018). "A Hybrid CNN and RBF-Based SVM Approach for Breast Cancer Classification in Mammograms,"in 2018 IEEE International Conference on Systems, Man, and Cybernetics (SMC), Miyazaki, Japan, 7-10 Oct. 2018, 894–899. doi:10.1109/SMC.2018.00159

Artzi, N. S., Shilo, S., Hadar, E., Rossman, H., Barbash-Hazan, S., Ben-Haroush, A., et al. (2020). Prediction of Gestational Diabetes Based on Nationwide Electronic Health Records. *Nat. Med.* 26, 71–76. doi:10.1038/s41591-019-0724-8

Barak-Corren, Y., Castro, V. M., Javitt, S., Hoffnagle, A. G., Dai, Y., Perlis, R. H., et al. (2017). Predicting Suicidal Behavior from Longitudinal Electronic Health Records. *Ajp* 174, 154–162. doi:10.1176/appi.ajp.2016.16010077

Boland, M. R., Polubriaginof, F., and Tatonetti, N. P. (2017). Development of A Machine Learning Algorithm to Classify Drugs of Unknown Fetal Effect. *Sci. Rep.* 7, 12839. doi:10.1038/s41598-017-12943-x

Borowska, M., Brzozowska, E., Kuć, P., Oczeretko, E., Mosdorf, R., and Laudański, P. (2018). Identification of Preterm Birth Based on RQA Analysis of Electrohysterograms. *Comp. Methods Programs Biomed.* 153, 227–236. doi:10.1016/j.cmpb.2017.10.018

Bottaci, L., Drew, P. J., Hartley, J. E., Hadfield, M. B., Farouk, R., Lee, P. W., et al. (1997). Artificial Neural Networks Applied to Outcome Prediction for Colorectal Cancer Patients in Separate Institutions. *The Lancet* 350, 469–472. doi:10.1016/S0140-6736(96)11196-X

Brownlee, J. (2017). What Is the Difference between Test and Validation Datasets. Available at: https://www.machinelearningmastery.com/difference-test-validation-datasets/(Accessed November 20, 2021).

Carrasco-Wong, I., Aguilera-Olguín, M., Escalona-Rivano, R., Chiarello, D. I., Barragán-Zúñiga, L. J., Sosa-Macías, M., et al. (2021). Syncytiotrophoblast Stress in Early Onset Preeclampsia: The Issues Perpetuating the Syndrome. *Placenta* 113, 57–66. doi:10.1016/j.placenta.2021.05.002

Carvalho, D. V., Pereira, E. M., and Cardoso, J. S. (2019). Machine Learning Interpretability: A Survey on Methods and Metrics. *Electronics* 8, 832. doi:10.3390/electronics8080832

CASP Clinical Prediction Rule Checklist (2017). *Critical Appraisal Skills Programme*. Oxford, UK: Oxford Centre for Triple Value Healthcare. Available at: https://casp-uk.net/wp-content/uploads/2018/01/CASP-Clinical-Prediction-Rule-Checklist_2018.pdf (Accessed November 12, 2021).

Cecula, P. (2021). Artificial Intelligence: The Current State of Affairs for AI in Pregnancy and Labour. *J. Gynecol. Obstet. Hum. Reprod.* 50, 102048. doi:10.1016/j.jogoh.2020.102048

Chen, L., Hao, Y., and Hu, X. (2019). Detection of Preterm Birth in Electrohysterogram Signals Based on Wavelet Transform and Stacked Sparse Autoencoder. *PLoS One* 14, e0214712. doi:10.1371/journal.pone.0214712

Chiera, M., Cerritelli, F., Casini, A., Barsotti, N., Boschiero, D., Cavigioli, F., et al. (2020). Heart Rate Variability in the Perinatal Period: A Critical and Conceptual Review. *Front. Neurosci.* 14, 561186. doi:10.3389/fnins.2020.561186

Cömert, Z., Kocamaz, A. F., and Subha, V. (2018). Prognostic Model Based on Image-Based Time-Frequency Features and Genetic Algorithm for Fetal Hypoxia Assessment. *Comput. Biol. Med.* 99, 85–97. doi:10.1016/j.compbiomed.2018.06.003

Darcy, A. M., Louie, A. K., and Roberts, L. W. (2016). Machine Learning and the Profession of Medicine. *JAMA* 315, 551–552. doi:10.1001/jama.2015.18421

Davidson, L., and Boland, M. R. (2020). Enabling Pregnant Women and Their Physicians to Make Informed Medication Decisions Using Artificial Intelligence. *J. Pharmacokinet. Pharmacodyn.* 47, 305–318. doi:10.1007/s10928-020-09685-1

Denison, F. C., Roberts, K. A., Barr, S. M., and Norman, J. E. (2010). Obesity, Pregnancy, Inflammation, and Vascular Function. *Reproduction* 140, 373–385. doi:10.1530/REP-10-0074

Doshi-Velez, F., Kortz, M., Budish, R., Bavitz, C., Gershman, S. J., O'Brien, D., et al. (2017). Accountability of AI under the Law: The Role of Explanation. *SSRN J.* arXiv. doi:10.2139/ssrn.3064761

Edwards, P., and Wright, G. (2020). Obesity in Pregnancy. *Obstet. Gynaecol. Reprod. Med.* 30, 315–320. doi:10.1016/j.ogrm.2020.07.003

Fergus, P., Selvaraj, M., and Chalmers, C. (2018). Machine Learning Ensemble Modelling to Classify Caesarean Section and Vaginal Delivery Types Using Cardiotocography Traces. *Comput. Biol. Med.* 93, 7–16. doi:10.1016/j.compbiomed.2017.12.002

Fondjo, L. A., Boamah, V. E., Fierti, A., Gyesi, D., and Owiredu, E.-W. (2019). Knowledge of Preeclampsia and its Associated Factors Among Pregnant Women: A Possible Link to Reduce Related Adverse Outcomes. *BMC Pregnancy Childbirth* 19, 456. doi:10.1186/s12884-019-2623-x

Freitas, A. A. (2014). Comprehensible Classification Models. *SIGKDD Explor. Newsl.* 15, 1–10. doi:10.1145/2594473.2594475

Frizzell, J. D., Liang, L., Schulte, P. J., Yancy, C. W., Heidenreich, P. A., Hernandez, A. F., et al. (2017). Prediction of 30-Day All-Cause Readmissions in Patients Hospitalized for Heart Failure. *JAMA Cardiol.* 2, 204–209. doi:10.1001/jamacardio.2016.3956

Gao, C., Osmundson, S., Yan, X., Edwards, D. V., Malin, B. A., and Chen, Y. (2019). Learning to Identify Severe Maternal Morbidity from Electronic Health Records. *Stud. Health Technol. Inform.* 264, 143–147. doi:10.3233/SHTI190200

Guo, Z., Yang, F., Zhang, J., Zhang, Z., Li, K., Tian, Q., et al. (2020). Whole-Genome Promoter Profiling of Plasma DNA Exhibits Diagnostic Value for Placenta-Origin Pregnancy Complications. *Adv. Sci.* 7, 1901819. doi:10.1002/advs.201901819

Hamilton, E. F., Dyachenko, A., Ciampi, A., Maurel, K., Warrick, P. A., and Garite, T. J. (2020). Estimating Risk of Severe Neonatal Morbidity in Preterm Births under 32 Weeks of Gestation. *J. Maternal-Fetal Neonatal Med.* 33, 73–80. doi:10.1080/14767058.2018.1487395

Hinton, G. (2018). Deep Learning-A Technology with the Potential to Transform Health Care. *JAMA* 320, 1101–1102. doi:10.1001/jama.2018.11100

Ho, C. W. L., Soon, D., Caals, K., and Kapur, J. (2019). Governance of Automated Image Analysis and Artificial Intelligence Analytics in Healthcare. *Clin. Radiol.* 74, 329–337. doi:10.1016/j.crad.2019.02.005

Holzinger, A., Langs, G., Denk, H., Zatloukal, K., and Müller, H. (2019). Causability and Explainability of Artificial Intelligence in Medicine. *Wires Data Mining Knowl Discov.* 9, e1312. doi:10.1002/widm.1312

Iftikhar, P. M., Kuijpers, M. V., Khayyat, A., Iftikhar, A., and DeGouvia De Sa, M. (2020). Artificial Intelligence: A New Paradigm in Obstetrics and Gynecology Research and Clinical Practice. *Cureus* 12, e7124. doi:10.7759/cureus.7124

Jhee, J. H., Lee, S., Park, Y., Lee, S. E., Kim, Y. A., Kang, S.-W., et al. (2019). Prediction Model Development of Late-Onset Preeclampsia Using Machine Learning-Based Methods. *PLoS ONE* 14, e0221202. doi:10.1371/journal.pone.0221202

Johnson, A. E. W., Ghassemi, M. M., Nemati, S., Niehaus, K. E., Clifton, D., and Clifford, G. D. (2016). Machine Learning and Decision Support in Critical Care. *Proc. IEEE* 104, 444–466. doi:10.1109/JPROC.2015.2501978

Jordan, M. I., and Mitchell, T. M. (2015). Machine Learning: Trends, Perspectives, and Prospects. *Science* 349, 255–260. doi:10.1126/science.aaa8415

Khatibi, T., Kheyrikoochaksarayee, N., and Sepehri, M. M. (2019). Analysis of Big Data for Prediction of Provider-Initiated Preterm Birth and Spontaneous Premature Deliveries and Ranking the Predictive Features. *Arch. Gynecol. Obstet.* 300, 1565–1582. doi:10.1007/s00404-019-05325-3

Kim, B., Khanna, R., and Koyejo, O. (2016). "Examples Are Not Enough, Learn to Criticize! Criticism for Interpretability," in Proceedings of the 30th International Conference on Neural Information Processing Systems, 2288–2296.

Kuhle, S., Maguire, B., Zhang, H., Hamilton, D., Allen, A. C., Joseph, K. S., et al. (2018). Comparison of Logistic Regression with Machine Learning Methods for the Prediction of Fetal Growth Abnormalities: a Retrospective Cohort Study. *BMC Pregnancy Childbirth* 18, 333. doi:10.1186/s12884-018-1971-2

Laopaiboon, M., Lumbiganon, P., Intarut, N., Mori, R., Ganchimeg, T., Vogel, J., et al. (2014). Advanced Maternal Age and Pregnancy Outcomes: a Multicountry Assessment. *Bjog: Int. J. Obstet. Gy* 121, 49–56. doi:10.1111/1471-0528.12659

Le, T. T., Fu, W., and Moore, J. H. (2020). Scaling Tree-Based Automated Machine Learning to Biomedical Big Data with a Feature Set Selector. *Bioinformatics* 36, 250–256. doi:10.1093/bioinformatics/btz470

Lipschuetz, M., Guedalia, J., Rottenstreich, A., Novoselsky Persky, M., Cohen, S. M., Kabiri, D., et al. (2020). Prediction of Vaginal Birth after Cesarean Deliveries Using Machine Learning. *Am. J. Obstet. Gynecol.* 222, e1–613.e12. doi:10.1016/j.ajog.2019.12.267

Lipton, Z. C. (2018). The Mythos of Model Interpretability. *Commun. ACM* 61, 36–43. doi:10.1145/3233231

Liu, K., Fu, Q., Liu, Y., and Wang, C. (2019). An Integrative Bioinformatics Analysis of Microarray Data for Identifying Hub Genes as Diagnostic Biomarkers of Preeclampsia. *Biosci. Rep.* 39, BSR20190187. doi:10.1042/BSR20190187

Mailath-Pokorny, M., Polterauer, S., Kohl, M., Kueronyai, V., Worda, K., Heinze, G., et al. (2015). Individualized Assessment of Preterm Birth Risk Using Two Modified Prediction Models. *Eur. J. Obstet. Gynecol. Reprod. Biol.* 186, 42–48. doi:10.1016/j.ejogrb.2014.12.010

Maity, N. G., and Das, S. (2017). "Machine Learning for Improved Diagnosis and Prognosis in Healthcare," in 2017 IEEE Aerospace Conference, Big Sky, MT, USA, 4-11 March 2017, 1–9. doi:10.1109/AERO.2017.7943950

Makary, M. A., and Daniel, M. (2016). Medical Error-The Third Leading Cause of Death in the US. *BMJ* 353, i2139. doi:10.1136/bmj.i2139

Malacova, E., Tippaya, S., Bailey, H. D., Chai, K., Farrant, B. M., Gebremedhin, A. T., et al. (2020). Stillbirth Risk Prediction Using Machine Learning for a Large Cohort of Births from Western Australia, 1980-2015. *Sci. Rep.* 10, 5354. doi:10.1038/s41598-020-62210-9

Mangold, C., Zoretic, S., Thallapureddy, K., Moreira, A., Chorath, K., and Moreira, A. (2021). Machine Learning Models for Predicting Neonatal Mortality: A Systematic Review. *Neonatology* 118, 394–405. doi:10.1159/000516891

Mariona, F. G. (2016). Perspectives in Obesity and Pregnancy. *Womens Health (Lond Engl.* 12, 523–532. doi:10.1177/1745505716686101

McCormick, M. C., Litt, J. S., Smith, V. C., and Zupancic, J. A. F. (2011). Prematurity: An Overview and Public Health Implications. *Annu. Rev. Public Health* 32, 367–379. doi:10.1146/annurev-publhealth-090810-182459

McCoy, T. H., Castro, V. M., Rosenfield, H. R., Cagan, A., Kohane, I. S., and Perlis, R. H. (2015). A Clinical Perspective on the Relevance of Research Domain Criteria in Electronic Health Records. *Ajp* 172, 316–320. doi:10.1176/appi.ajp.2014.14091177

Molnar, C. (2019). *Interpretable Machine Learning. A Guide for Making Black Box Models Explainable*. Konstanz, Alemania: Leanpub.

Moreira, M. W. L., Rodrigues, J. J. P. C., Oliveira, A. M. B., Saleem, K., and Neto, A. (2016b). "Performance Evaluation of Predictive Classifiers for Pregnancy Care," in 2016 IEEE Global Communications Conference (GLOBECOM), Washington, DC, USA, 4-8 Dec. 2016. doi:10.1109/GLOCOM.2016.7842136

Moreira, M. W. L., Rodrigues, J. J. P. C., Oliveira, A. M. B., and Saleem, K. (2016a). "Smart mobile System for Pregnancy Care Using Body Sensors," in 2016 International Conference on Selected Topics in Mobile & Wireless Networking (MoWNeT), Cairo, Egypt, 11-13 April 2016. doi:10.1109/MoWNet.2016.7496609

Munchel, S., Rohrback, S., Randise-Hinchliff, C., Kinnings, S., Deshmukh, S., Alla, N., et al. (2020). Circulating Transcripts in Maternal Blood Reflect a Molecular Signature of Early-Onset Preeclampsia. *Sci. Transl. Med.* 12, eaaz0131. doi:10.1126/scitranslmed.aaz0131

Nair, T. M. (2018). Statistical and Artificial Neural Network-Based Analysis to Understand Complexity and Heterogeneity in Preeclampsia. *Comput. Biol. Chem.* 75, 222–230. doi:10.1016/j.compbiolchem.2018.05.011

Nguyen, P., Tran, T., Wickramasinghe, N., and Venkatesh, S. (2017). $\mathtt{Deepr}$: A Convolutional Net for Medical Records. *IEEE J. Biomed. Health Inform.* 21, 22–30. doi:10.1109/JBHI.2016.2633963

Obermeyer, Z., and Emanuel, E. J. (2016). Predicting the Future - Big Data, Machine Learning, and Clinical Medicine. *N. Engl. J. Med.* 375, 1216–1219. doi:10.1056/NEJMp1606181

Oquab, M., Bottou, L., Laptev, I., and Sivic, J. (2014). "Learning and Transferring Mid-level Image Representations Using Convolutional Neural Networks," in Proceedings of the IEEE Computer Society Conference on Computer Vision and Pattern Recognition. doi:10.1109/CVPR.2014.222

Osborn, D. P. J., Hardoon, S., Omar, R. Z., Holt, R. I. G., King, M., Larsen, J., et al. (2015). Cardiovascular Risk Prediction Models for People with Severe Mental Illness. *JAMA Psychiatry* 72, 143–151. doi:10.1001/jamapsychiatry.2014.2133

Pan, I., Nolan, L. B., Brown, R. R., Khan, R., Van Der Boor, P., Harris, D. G., et al. (2017). Machine Learning for Social Services: A Study of Prenatal Case Management in Illinois. *Am. J. Public Health* 107, 938–944. doi:10.2105/AJPH.2017.303711

Paydar, K., Niakan Kalhori, S. R., Akbarian, M., and Sheikhtaheri, A. (2017). A Clinical Decision Support System for Prediction of Pregnancy Outcome in Pregnant Women with Systemic Lupus Erythematosus. *Int. J. Med. Inform.* 97, 239–246. doi:10.1016/j.ijmedinf.2016.10.018

Rajkomar, A., Oren, E., Chen, K., Dai, A. M., Hajaj, N., Hardt, M., et al. (2018). Scalable and Accurate Deep Learning with Electronic Health Records. *Npj Digital Med.* 1, 18. doi:10.1038/s41746-018-0029-1

Refaeilzadeh, P., Tang, L., and Liu, H. (2009). "Cross-Validation," in *Encyclopedia of Database Systems*. Arizona: Springer Science Business Media, LLC. 532–538. doi:10.1007/978-0-387-39940-9_565

Ripley, B. D. (1996). *Pattern Recognition and Neural Networks*. Cambridge, UK: Cambridge University Press.

Rittenhouse, K. J., Vwalika, B., Keil, A., Winston, J., Stoner, M., Price, J. T., et al. (2019). Improving Preterm Newborn Identification in Low-Resource Settings with Machine Learning. *PLoS One* 14, e0198919. doi:10.1371/journal.pone.0198919

Roberts, J. (1998). Endothelial Dysfunction in Preeclampsia. *Semin. Reprod. Med.* 16, 5–15. doi:10.1055/s-2007-1016248

Romeo, V., Ricciardi, C., Cuocolo, R., Stanzione, A., Verde, F., Sarno, L., et al. (2019). Machine Learning Analysis of MRI-Derived Texture Features to Predict Placenta Accreta Spectrum in Patients with Placenta Previa. *Magn. Reson. Imaging* 64, 71–76. doi:10.1016/j.mri.2019.05.017

Sadi-Ahmed, N., Kacha, B., Taleb, H., and Kedir-Talha, M. (2017). Relevant Features Selection for Automatic Prediction of Preterm Deliveries from Pregnancy ElectroHysterograhic (EHG) Records. *J. Med. Syst.* 41, 204. doi:10.1007/s10916-017-0847-8

Salazar, F. P., Manterola, C., Quiroz, S. G., García, M. N., Otzen, H. T., Mora, V. M., et al. (2019). Estudios de Cohortes. 1a Parte. Descripción, Metodología y Aplicaciones. *Rev. Cirugia* 71, 482–493. doi:10.35687/s2452-45492019005431

Salsoso, R., Farías, M., Gutiérrez, J., Pardo, F., Chiarello, D. I., Toledo, F., et al. (2017). Adenosine and Preeclampsia. *Mol. Aspects Med.* 55, 126–139. doi:10.1016/j.mam.2016.12.003

Shigemi, D., Yamaguchi, S., Aso, S., and Yasunaga, H. (2019). Predictive Model for Macrosomia Using Maternal Parameters without Sonography Information. *J. Maternal-Fetal Neonatal Med.* 32, 3859–3863. doi:10.1080/14767058.2018.1484090

Šimundić, A.-M. (2009). Measures of Diagnostic Accuracy: Basic Definitions. *EJIFCC* 19, 203–211.

Sohil, F., Sohali, M. U., and Shabbir, J. (2021). An Introduction to Statistical Learning with Applications in R. *Statistical Theory and Related Fields*. New York, NY: Taylor and Francis Group. doi:10.1080/24754269.2021.1980261

Sufriyana, H., Husnayain, A., Chen, Y.-L., Kuo, C.-Y., Singh, O., Yeh, T.-Y., et al. (2020). Comparison of Multivariable Logistic Regression and Other Machine Learning Algorithms for Prognostic Prediction Studies in Pregnancy Care: Systematic Review and Meta-Analysis. *JMIR Med. Inform.* 8, e16503. doi:10.2196/16503

Sun, H., Qu, H., Chen, L., Wang, W., Liao, Y., Zou, L., et al. (2019). Identification of Suspicious Invasive Placentation Based on Clinical MRI Data Using Textural Features and Automated Machine Learning. *Eur. Radiol.* 29, 6152–6162. doi:10.1007/s00330-019-06372-9

Urrútia, G., and Bonfill, X. (2010). Declaración PRISMA: una propuesta para mejorar la publicación de revisiones sistemáticas y metaanálisis. *Medicina Clínica* 135, 507–511. doi:10.1016/j.medcli.2010.01.015

Vayena, E., Blasimme, A., and Cohen, I. G. (2018). Machine Learning in Medicine: Addressing Ethical Challenges. *Plos Med.* 15, e1002689. doi:10.1371/journal.pmed.1002689

Veeramani, S. K., and Muthusamy, E. (2016). Detection of Abnormalities in Ultrasound Lung Image Using Multi-Level RVM Classification. *J. Maternal-Fetal Neonatal Med.* 29, 1–9. doi:10.3109/14767058.2015.1064888

Wang, C., Deng, C., and Wang, S. (2020). Imbalance-XGBoost: Leveraging Weighted and Focal Losses for Binary Label-Imbalanced Classification with XGBoost. *Pattern Recognition Lett.* 136, 190–197. doi:10.1016/j.patrec.2020.05.035

Weber, A., Darmstadt, G. L., Gruber, S., Foeller, M. E., Carmichael, S. L., Stevenson, D. K., et al. (2018). Application of Machine-Learning to Predict Early Spontaneous Preterm Birth Among Nulliparous Non-hispanic Black and white Women. *Ann. Epidemiol.* 28, 783–789. doi:10.1016/j.annepidem.2018.08.008

WHO (2019). *Trends in Maternal Mortality: 2000 to 2017: Estimates by WHO, UNICEF, UNFPA, World Bank Group and the United Nations Population Division*. Geneva: World Health Organization. WHO, UNICEF, UNFPA, World Bank Group and the United Nations Population Division.

Yoffe, L., Polsky, A., Gilam, A., Raff, C., Mecacci, F., Ognibene, A., et al. (2019). Early Diagnosis of Gestational Diabetes Mellitus Using Circulating microRNAs. *Eur. Jour. Endocrinol.* 181, 565–577. doi:10.1530/EJE-19-0206

Zhang, Q., Zhou, D., and Zeng, X. (2017). HeartID: A Multiresolution Convolutional Neural Network for ECG-Based Biometric Human Identification in Smart Health Applications. *IEEE Access* 5, 11805–11816. doi:10.1109/ACCESS.2017.2707460

Zhao, Z., Deng, Y., Zhang, Y., Zhang, Y., Zhang, X., and Shao, L. (2019). DeepFHR: Intelligent Prediction of Fetal Acidemia Using Fetal Heart Rate Signals Based on Convolutional Neural Network. *BMC Med. Inform. Decis. Mak.* 19, 286. doi:10.1186/s12911-019-1007-5

Conflict of Interest: The authors declare that the research was conducted in the absence of any commercial or financial relationships that could be construed as a potential conflict of interest.

Publisher's Note: All claims expressed in this article are solely those of the authors and do not necessarily represent those of their affiliated organizations, or those of the publisher, the editors, and the reviewers. Any product that may be evaluated in this article, or claim that may be made by its manufacturer, is not guaranteed or endorsed by the publisher.

frontiers in Bioengineering and Biotechnology

ORIGINAL RESEARCH
published: 28 January 2022
doi: 10.3389/fbioe.2022.819593

Dendrimer-Based N-Acetyl Cysteine Maternal Therapy Ameliorates Placental Inflammation *via* Maintenance of M1/M2 Macrophage Recruitment

*Yang Liu[1†], Quan Na[1†], Jin Liu[1], Anguo Liu[1], Akosua Oppong[1], Ji Yeon Lee[1], Anna Chudnovets[1], Jun Lei[1], Rishi Sharma[2], Sujatha Kannan[3], Rangaramanujam M. Kannan[2] and Irina Burd[1]**

[1]Integrated Research Center for Fetal Medicine, Department of Gynecology and Obstetrics, Johns Hopkins University School of Medicine, Baltimore, MD, United States, [2]Center for Nanomedicine, Department of Ophthalmology, Johns Hopkins University School of Medicine, Baltimore, MD, United States, [3]Department of Anesthesiology and Critical Care Medicine, Johns Hopkins University School of Medicine, Baltimore, MD, United States

OPEN ACCESS

Edited by:
Vesna Garovic,
Mayo Clinic, United States

Reviewed by:
Martin Mueller,
University Hospital Bern, Switzerland
Jun-chang Guan,
Bengbu Medical College, China

***Correspondence:**
Irina Burd
Iburd@jhmi.edu

[†]These authors have contributed equally to this work

Specialty section:
This article was submitted to Preclinical Cell and Gene Therapy, a section of the journal Frontiers in Bioengineering and Biotechnology

Received: 21 November 2021
Accepted: 03 January 2022
Published: 28 January 2022

Citation:
Liu Y, Na Q, Liu J, Liu A, Oppong A, Lee JY, Chudnovets A, Lei J, Sharma R, Kannan S, Kannan RM and Burd I (2022) Dendrimer-Based N-Acetyl Cysteine Maternal Therapy Ameliorates Placental Inflammation via Maintenance of M1/M2 Macrophage Recruitment. Front. Bioeng. Biotechnol. 10:819593. doi: 10.3389/fbioe.2022.819593

Intrauterine inflammation (IUI) is the primary cause of spontaneous preterm birth and predisposes neonates to long-term sequelae, including adverse neurological outcomes. N-acetyl-L-cysteine (NAC) is the amino acid L-cysteine derivative and a precursor to the antioxidant glutathione (GSH). NAC is commonly used clinically as an antioxidant with anti-inflammatory properties. Poor bioavailability and high protein binding of NAC necessitates the use of high doses resulting in side effects including nausea, vomiting, and gastric disruptions. Therefore, dendrimer-based therapy can specifically target the drug to the cells involved in inflammation, reducing side effects with efficacy at much lower doses than the free drug. Towards development of the new therapies for the treatment of maternal inflammation, we successfully administered dendrimer-based N-Acetyl Cysteine (DNAC) in an animal model of IUI to reduce preterm birth and perinatal inflammatory response. This study explored the associated immune mechanisms of DNAC treatment on placental macrophages following IUI, especially on M1/M2 type macrophage polarization. Our results demonstrated that intraperitoneal maternal DNAC administration significantly reduced the pro-inflammatory cytokine mRNA of *Il1β* and *Nos2*, and decreased $CD45^+$ leukocyte infiltration in the placenta following IUI. Furthermore, we found that DNAC altered placental immune profile by stimulating macrophages to change to the M2 phenotype while decreasing the M1 phenotype, thus suppressing the inflammatory responses in the placenta. Our study provides evidence for DNAC therapy to alleviate IUI *via* the maintenance of macrophage M1/M2 imbalance in the placenta.

Keywords: macrophage, M1/M2, placental inflammation, maternal therapy, DNAC

INTRODUCTION

Intrauterine inflammation (IUI) is the primary cause of spontaneous preterm birth and predisposes neonates to long-term sequelae, including adverse neurological outcomes, and accounting for approximately 35% of neonatal deaths in 2017 (Chawanpaiboon et al., 2019; Hug et al., 2019). The pro-inflammatory cytokines induced by IUI lead to fetal inflammatory response syndrome (FIRS), which results in these neonatal complications (Romero et al., 2005; Burd et al., 2012; Cappelletti et al., 2016). There is currently a lack of treatment options for spontaneous preterm birth, and new avenues for treatment should not only address spontaneous preterm birth but also pediatric outcomes.

Pro-inflammatory stimulation causes changes in the maternal immune system and placental microenvironment, a process in which placental macrophages may play an important role. The macrophage is the primary cell in the acute inflammatory response. Generally, macrophages are categorized into two main phenotypes based on their function (Wang et al., 2019; Yunna et al., 2020); M1 macrophages are pro-inflammatory, while M2 macrophages are anti-inflammatory (An et al., 2017). In normal pregnancy, maternal decidual and fetal placental macrophages (also known as Hoffbauer cells) are maintained in an anti-inflammatory state to achieve immune tolerance of the fetus (Bolton and Bilbo, 2014).

N-acetyl-*L*-cysteine (NAC) is the amino acid L-cysteine derivative and a precursor to the antioxidant glutathione (GSH). NAC is commonly used clinically as an antioxidant with anti-inflammatory properties (Smilkstein et al., 1988). A clinical study found that oral NAC administration can reduce recurrent preterm labor in patients with a history of bacterial vaginosis (Shahin et al., 2009). In another double-blinded trial, in which NAC was used as a neuroprotective agent in the case of maternal chorioamnionitis, administration of NAC improved maternal inflammatory cytokines (Jenkins et al., 2016). However, side effects from the necessary high dosage, include nausea, vomiting, and gastric disruptions (Copersino et al., 2006; Shahin et al., 2009). Therefore, dendrimer-based therapy has been used to decrease the dose necessary to contain the inflammation.

Dendrimers (~ 4 nm) are emerging as a promising strategy for targeted intracellular drug delivery. We have previously shown that dendrimer-drug conjugates specifically target activated macrophages and microglia in pre-clinical models of inflammation (Nance et al., 2016; Zhang et al., 2016; Nance et al., 2017; Nemeth et al., 2017). Dendrimer-drug conjugates offer many advantages over free drugs, including sustained/targeted delivery for improved efficacy and reduced drug side effects. We have also shown that polyamidoamine (PAMAM) dendrimers when conjugated to NAC (DNAC) specifically delivers NAC intracellularly into activated microglia/macrophages in the brain and is more effective than the free drug (Niño et al., 2018; Turk et al., 2018; Zhang et al., 2020). In an animal model of IUI, DNAC reduces preterm birth and perinatal inflammatory response (Lei et al., 2017). However, the mechanisms of action of DNAC in placenta have not been studied.

In this study, we sought to identify the immune mechanisms of DNAC in the placenta following IUI. We hypothesized that maternally administered DNAC reduces placental inflammation following IUI, through the maintenance of immune response, especially on macrophage recruitment and M1/M2 phenotypes and polarization.

MATERIALS AND METHODS

Animal Preparation and Experimental Groups

All animal care and treatment procedures were approved by the Animal Care and Use Committee of Johns Hopkins University Hopkins-IACUC Protocol No. MO14M326. CD-1 pregnant dams from Charles River were used for this study. Pregnant dams were subjected to a well-established model of IUI as per a previously described protocol on embryonic day 17 (E17) (Burd et al., 2010; Elovitz et al., 2011; Dada et al., 2014; Lei et al., 2017; Lei et al., 2018; Liu et al., 2021; Na et al., 2021). Briefly, mice were anesthetized with isoflurane (Baxter # NDC 10019-360-60) before undergoing a mini-laparotomy. After dressing the abdominal area, a 1.5-cm midline incision was performed in the lower abdominal wall. Mice were randomized to intrauterine injections of either lipopolysaccharide (LPS), a model of IUI, or phosphate-buffered saline (PBS) at E17. The dose of 25 μg of LPS (*E. coli* O55:B5, Sigma-Aldrich, St Louis, MO, United States, n = 150) in 100 μl PBS or vehicle only (PBS, n = 38) was injected between the first and second embryos of the lower right uterine horn. Routine laparotomy closure was performed, and dams were returned to cages individually. One hour after surgery, dams were randomly allocated to additional treatments: DNAC or PBS. 10 mg/kg DNAC (Sigma-Aldrich) in 100 μL PBS was injected intraperitoneally (IP), PBS was injected IP as vehicle. In total, four groups were utilized: PBS + PBS (n = 20), LPS + PBS (n = 96), LPS + DNAC (n = 54) and PBS + DNAC (n = 18). Pregnant mice were sacrificed 3, 6 or 12 h after the LPS injection to collect tissue samples of placenta for biochemical and histological analysis. Placentas were from the first four gestational sacs of the right uterine horn.

Flow Cytometry

Placentas were harvested from the first gestational sacs in the right uterine horn, which is the most adjacent to the injection point, after 3, 6 or 12 h of surgery, respectively (**Figure 1A**). The decidual zone was further removed from the placenta. Single cells were prepared from placentas by manual and enzymatic (collagenase D, Roche, Indianapolis, IN, United States) digestion and then passed through a 70-μm nylon mesh (BD Falcon cell strainer). Red blood cell lysis (ACK lysing buffer, ThermoFisher Scientific) and total cell counts were performed prior to surface staining. Isolated cells were stained with surface markers, at 1:100 concentration, in fluorescence activated cell sorting (FACS) buffer with 1 mM EDTA (Quality Biological, Gaithersburg, MD, United States) for 30 min at 4°C in the dark. OneComp eBeads (eBioscience) were used for compensation.

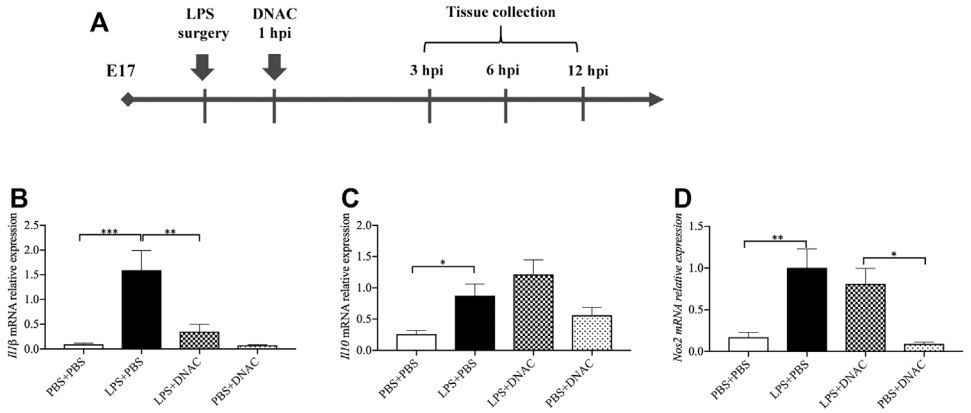

FIGURE 1 | Measurements of inflammatory cytokine expression at mRNA level in placenta following exposure to intrauterine inflammation and maternal Dendrimer-based N-Acetyl Cysteine (DNAC) treatment. **(A)** Study Strategy. At embryonic (E) day 17, pregnant CD-1 mice underwent a mini-laparotomy in the lower abdomen for intrauterine injection of lipopolysaccharide (LPS). One hour later, dams received intraperitoneally injection of DNAC or phosphate-buffered saline (PBS). At 6 h post injection (hpi) dams were sacrificed. Placentas were harvested from each dam and quantitative polymerase chain reaction (QPCR) was performed to evaluate the effect of DNAC treatment. The mRNA levels of *Il1β* **(B)**, *Il10* **(C)** and *Nos2* **(D)** were statically compared between groups. PBS + PBS, $n = 8$; LPS + PBS, $n = 8$; LPS + DNAC, $n = 7$; PBS + DNAC, $n = 6$. $^{*}p < 0.05$ $^{**}p < 0.01$ $^{***}p < 0.001$. Data were reported as Mean ± SEM.

TABLE 1 | Antibody selection.

Antibody	Clone	Manufacture
Mouse anti-CD45	30-F11	BD
Mouse anti-CD11b	M1/70	BD
Mouse anti-F4/80	MF48028	ThermoFisher Scientific
Mouse anti-CD163	MR6F3	ThermoFisher Scientific

Antibodies and corresponding isotype are listed in **Table 1**. Data were acquired on an Attune™ NxT Acoustic Focusing Cytometer (ThermoFisher Scientific Invitrogen™, 2017) and analyzed with FlowJo version 10.1 (FlowJo, LLC, Ashland, OR, United States). Seven-color flow cytometry was used to identify $CD45^+$ leukocytes and macrophage populations. Debris and doublets were excluded by sequential gating on forward scatter height versus forward scatter area. They were then gate on $CD45^+$ to identify all $CD45^+$ leukocytes, gated on $CD11b^+$ $F4/80^+$ from $CD45^+$ cells to identify placental macrophages, and gated on $CD11b^+$ $F4/80^+$ $CD163^+$ to identify M2 placental macrophages.

RNA Extraction and Quantitative Polymerase Chain Reaction

After euthanizing the mice 6 h after the LPS or PBS injection, quantitative polymerase chain reactions (qPCR) were completed based on protocols described in the previous study. Placentas were isolated from the first through fourth gestational sacs of the right uterine horn and fresh frozen on dry ice, followed by long-term storage at −80°C. Initially for each placental specimen, 2 μg of RNA was used for complementary 3) DNA synthesis in a 40 μL reaction, using Bio-Rad iScript™ cDNA Synthesis Kit (Bio-Rad, Cat. No. 170-8891). The primers for actin (Assay ID Mm. PT. 39a.22214843.g), interleukin (IL)-1β (Mm.Pt.58.44004828), IL-10 (Mm.Pt.58.13531087) and Nos2 (Mm.Pt.58.43705194) were obtained from Integrated DNA Technologies. The primer for 18S (Cat. No. 4310893E) was obtained from Applied Biosystems (Thermo Fisher Scientific).

Histochemistry and Immunohistochemistry

Six hours after LPS or PBS injection, fresh placentas were dissected and fixed in 4% paraformaldehyde (PFA) (Affymetrix Inc.) for histology. Tissue was then immersed in 30% sucrose (Sigma-Aldrich). Using Leica CM1950 cryostat (Leica Biosystems Inc.), the specimens were cut at 5 μm thickness and mounted on positively charged slides (Fischer Scientific). Placentas were cut transversally. For immunohistochemistry (IHC), slides were incubated in PBS solution containing 0.05% Triton X-100 (Sigma-Aldrich) and 5% normal goat serum (Invitrogen) for 30 min. Placental tissues were incubated with the M1 macrophage marker mouse anti-iNOS antibody (1:50, Abcam), and the M2 macrophage maker rabbit anti-CD163 antibody (1:200, Abcam) at 4°C overnight. Donkey anti-mouse Alexa Fluor 568 fluorescent and donkey anti-rabbit Alexa Fluor 488 fluorescent (1:500, Life Technologies) were secondary antibodies. DAPI (4′,6-diamino-2-phenylindole, Roche) was used to counterstain nuclei at a concentration of 1:5,000. All images analyzed were obtained from Zeiss AxioPlan 2 Microscope System. Placental data were obtained at the middle level. Analyses were performed with ImageJ by evaluators blinded to group identification.

Statistical Analyses

Data were analyzed using Chi-Square test and continuous variables using a One-way ANOVA with Tukey post-HSD test or Kruskal-Wallis test with Bonferroni-Dunn correction. Continuous data were tested for normality, and outliers were

identified using Grubb's test. When outliers were identified in data following normal distribution, they were excluded from the analysis. Statistical significance was set at $p < 0.05$, with consideration to multiple comparisons. Data analyses were performed with GraphPad Prism version 8 (GraphPad Software).

RESULTS

Preparation and Characterization of Dendrimer-NAC Conjugate

As described previously, we successfully prepared, characterized, and validated the DNAC conjugate and the drug release mechanism for DNAC(Kurtoglu et al., 2009; Kannan et al., 2012; Mishra et al., 2014; Lei et al., 2017). Briefly, we used Fmoc protection/deprotection chemistry to functionalize hydroxyl - terminated generation-4 poly amidoamino (PAMAM) dendrimer with reactive amine groups, and then used suitable thiol-reactive pyridyldithio propionates to react with NAC to get DNAC conjugates. ^{1}H NMR and high-pressure liquid chromatography (HPLC) were used to verified conjugate purity. Each dendrimer-conjugated contains 20 molecules of NAC to get a drug payload of ~ 15 wt%. The DNAC conjugate is readily soluble in water, saline or PBS (pH 7.4). This indicated that the use of a disulfide linker enabled rapid release of NAC from the conjugate, but only when it was exposed to intracellular GSH-rich environment. We previously shown that DNAC localizes only to the site of inflammation and the component and conjugate are safe for maternal administration (Lei et al., 2017).

Maternal Administration of DNAC Altered Cytokines Produced Following IUI Exposure

Firstly, we found that DNAC treatment does not affect dam weight, fetal weight and placental weight (data not shown). Then, we performed quantitative reverse transcription PCR (RT-qPCR) to measure the expression of pro-inflammatory mediators, interleukin (IL) -1β and nitrous oxide systems (Nos) 2, and anti-inflammatory mediator, Il-10, in the placenta of E17 at 6 h after PBS or PBS LPS exposure. The mRNA expression of *Il1β*, *Nos2* and *Il10* in the placenta were significantly increased in LPS + PBS group compared to PBS + PBS group (**Figures 1B–D**, $p < 0.05$), which was similar to our previous study (Na et al., 2021). Maternal administration of DNAC significantly decreased the pro-inflammatory cytokines mRNA of *Il1β*, *Nos2* in LPS + DNAC group compared to LPS + PBS group (**Figures 1B,D**, $p < 0.05$). This is seen in conjunction with an increase in the expression of anti-inflammatory mediator, *Il10,* in LPS + DNAC group compared to LPS + PBS group (**Figure 1C**). Treatment of the surgical control with DNAC (PBS + DNAC group) did not show any significant difference from the vehicle group (**Figures 1B–D**).

Maternal Administration of DNAC Prevented CD45^{+} Leukocytes Infiltration in the Placenta Following IUI

Following the observation that maternal DNAC regulates cytokines expression in the placenta, we performed flow cytometry to analyze CD45^{+} leukocytes infiltration in the placenta at E17 (**Figure 2A**). At 3hpi and 6hpi, CD45^{+} leukocyte infiltrates in the placenta were significantly increased in LPS + PBS group compared to PBS + PBS group, while maternal treatment of DNAC significantly decreased CD45 $^{+}$ leukocytes infiltration in LPS + DNAC group compared to LPS + PBS group (**Figure 2B**, $p < 0.05$). Similarly, as our prior study demonstrated, CD45^{+} leukocyte infiltration in placenta increased with LPS-exposure at 6hpi of E17 (Lei et al., 2017; Liu et al., 2021). At 12hpi, CD45 $^{+}$ leukocytes infiltration in the placenta did not show any significant difference between groups (**Figure 2B**).

Maternal Administration of DNAC Suppressed M1 and Increased M2 Macrophages Recruitment to the Placenta Following IUI

Our previous research has shown that placental macrophages are the primary cells producing IL-1β, iNOS and IL-10 (Na et al., 2021). M1 macrophages express CD80, CD86, CCR7 and CD40, while M2 macrophages express CD163 and CD206 on the cell surface (Sinha et al., 2005; Xu et al., 2006; Tardito et al., 2019; Heusinkveld et al., 2011; Rocher et al., 2012). We found that maternal DNAC treatment significantly decreased the leukocytes infiltration in placenta following exposure to LPS. We further used flow cytometry to analyze macrophage frequency for the placenta 6 h after PBS or LPS exposure at E17 (**Figures 3A,B**). The number of placental macrophages increased significantly with LPS exposure at 6hpi (**Figure 3C**, $p < 0.05$), which match our prior data (Na et al., 2021). Maternal treatment with DNAC did not lead to a significant change in macrophage numbers when compared to the untreated LPS groups. However, upon further assessment of the subtypes of macrophages by flow cytometry, we found that M1 phenotype macrophages increased significantly and M2 phenotype macrophages decreased significantly in LPS + PBS group compared to PBS + PBS group (**Figures 3D,E**, $p < 0.05$). Furthermore, maternal DNAC significantly decreased the M1 phenotype and increased the M2 phenotype macrophages in the LPS + DNAC group when compared to LPS + PBS group (**Figures 3D,E**, $p < 0.05$).

DNAC Treatment Alleviated M1 Macrophages and Increased M2 Macrophages Infiltration in Placenta Following IUI

We further performed IHC staining for iNOS and CD163 in placental tissue 6 h after PBS or LPS exposure at E17 (**Figure 4A**). IHC staining for iNOS demonstrated significant increased in iNOS expression in the LPS + PBS group compared to PBS + PBS, while maternal treatment with DNAC decreased iNOS expression

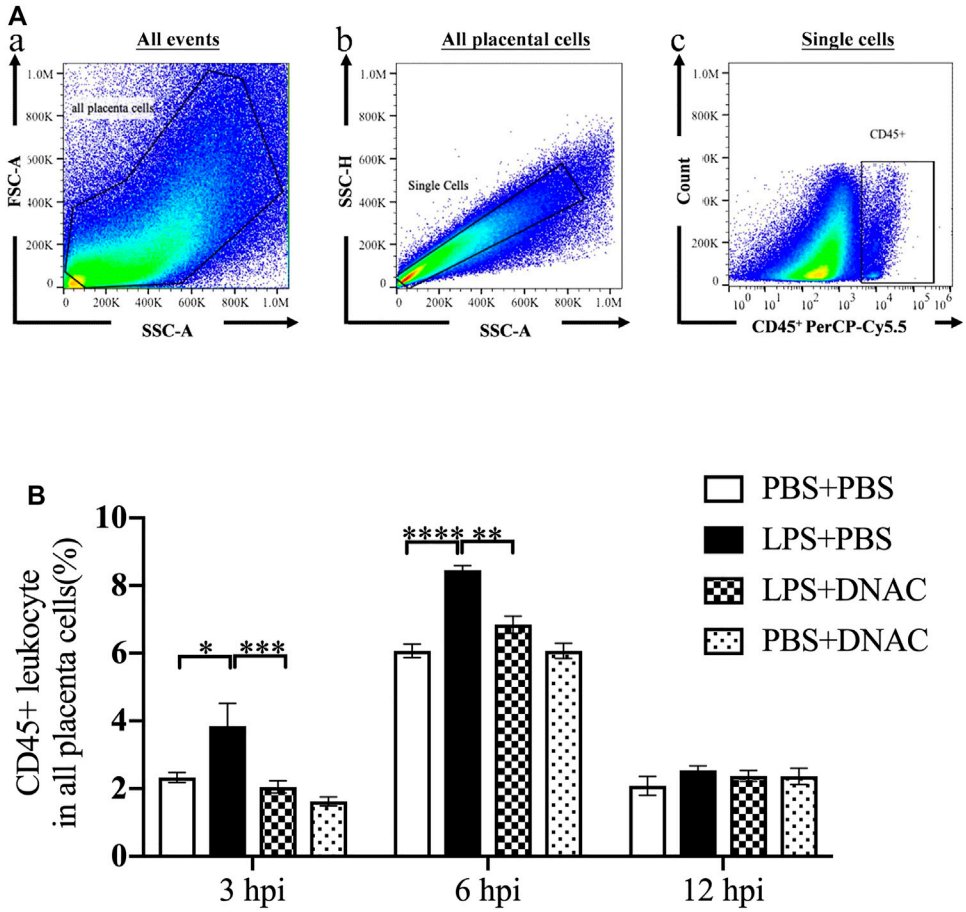

FIGURE 2 | Placenta leukocytes infiltration following exposure to intrauterine inflammation and maternal Dendrimer-based N-Acetyl Cysteine (DNAC) treatment. Lipopolysaccharide (LPS) or phosphate-buffered saline (PBS) was injected intrauterine at embryonic day 17 (E17). DNAC was injected intraperitoneally 1 h post inflammation (hpi). Placentas were collected at 3, 6 and 12 hpi. **(A)** a. All captured placental cells were distinguished based on properties of side scatter area (SSC-A) versus forward scatter area (FSC-A) generally, by using polygon/rectangular/oval gates. b. Debris and doublets were excluded by gating on side scatter height (SSC-H) versus SSC-A to further delaminate singlets. c. Placental leukocytes were gated sequentially on CD45 $^{+}$ versus SSC-A properties. **(B)** The ratio of $CD45^{+}$ leukocytes infiltrated in the placenta were statically compared between groups. PBS + PBS, $n = 16$; LPS + PBS, $n = 16$; LPS + DNAC, $n = 15$; PBS + DNAC, $n = 12$. $^{*}p < 0.05$ $^{**}p < 0.01$ $^{***}p < 0.001$ $^{****}p < 0.0001$. Data were reported as Mean ± SEM.

when compared to LPS + PBS (**Figure 4B**, $p < 0.05$). IHC staining for CD163 demonstrated decreased CD163 expression in LPS + PBS group compared to the PBS + PBS group, while maternal administration with DNAC significantly increased CD163 expression in LPS + DNAC group compared to LPS + PBS group (**Figure 4C**, $p < 0.05$). No significant differences were seen in iNOS or CD163 staining between PBS + PBS and PBS + DNAC groups (**Figures 4B,C**).

DISCUSSION

We investigated the effect of maternal DNAC therapy towards ameliorating placental inflammation through macrophage recruitment and polarization *via* M1/M2, following IUI. We found that DNAC decreased $CD45^{+}$ leukocytes infiltration in the placenta following IUI. DNAC altered placental immune profile, which stimulated macrophages to polarize to the M2 phenotype while decreasing the M1 phenotype, thus suppressing the inflammatory responses in the placenta. Specifically, our results demonstrated that maternal DNAC significantly reduced the pro-inflammatory cytokines *Il1β* and *Nos2* following IUI.

Hydroxyl dendrimer nanoparticles have several structural benefits, including reduced toxicity and interactions with proteins due to its hydroxyl end groups and near-neutral charge, specific targeting and uptake by "activated" macrophages, rapid cell entry, and rapid elimination of dendrimer through the kidney with minimal uptake in off-target organs (Menjoge et al., 2010; Magro et al., 2020). We explored the mechanism of action of maternal DNAC on placental inflammation treatment. D-NAC conjugates were stable at physiological conditions and without releasing NAC throughout 24 ~ 72 h (Kurtoglu et al., 2009; Kannan et al., 2012; Nance et al., 2017). Our data provided evidence that maternal treatment with a low dose of dendrimer-conjugated NAC

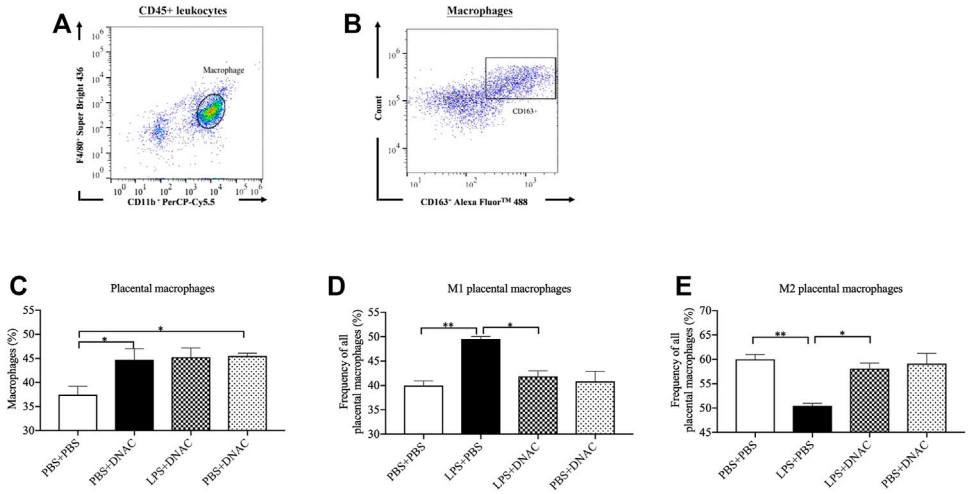

FIGURE 3 | Placenta M1 and M2 phenotype macrophage polarization following exposure to intrauterine inflammation and maternal dendrimer-based N-Acetyl Cysteine (DNAC) treatment. At embryonic (E) day 17, pregnant CD-1 mice underwent a mini-laparotomy in the lower abdomen for intrauterine injection of lipopolysaccharide (LPS). One hour later, dams received intraperitoneally injection of DNAC or phosphate-buffered saline (PBS). Placentas were collected at 6 hpi after LPS or PBS injection. **(A)** The placental macrophages were further identified by F4/80+ and CD11b + properties on placental leukocytes. **(B)** M2 macrophages was identified by CD163+ and side scatter sequentially on $CD45^+$ $CD11b^+$ $F4/80^+$ macrophages. The ratios of total macrophages **(C)**, M1 **(D)** and M2 **(E)** macrophages infiltrated in the placenta were statically compared between groups. PBS + PBS, $n = 8$; LPS + PBS, $n = 8$; LPS + DNAC, $n = 7$; PBS + DNAC, $n = 6$. $^*p < 0.05$; $^{**}p < 0.01$. Data were reported as Mean ± SEM.

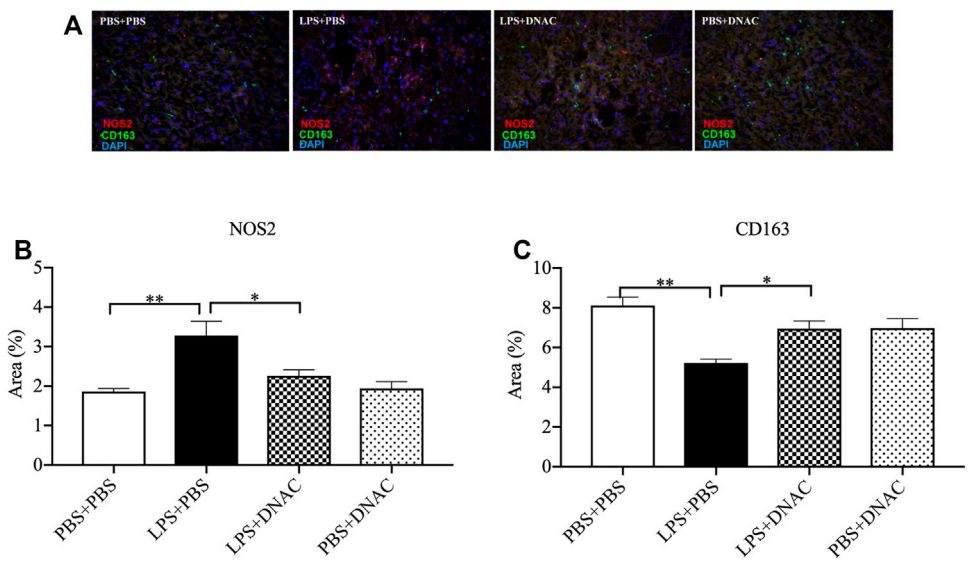

FIGURE 4 | Immunohistochemical staining (IHC) of M1 and M2 macrophages in the placenta following exposure to intrauterine inflammation and maternal dendrimer-based N-Acetyl Cysteine (DNAC) treatment. At embryonic (E) day 17, pregnant CD-1 mice underwent a mini-laparotomy in the lower abdomen for intrauterine injection of lipopolysaccharide (LPS). One hour later, dams received intraperitoneally injection of DNAC or phosphate-buffered saline (PBS). Placentas were collected at 6 hpi after LPS or PBS injection. Placentas were stained with anti-NOS2 (red, a marker for M1 macrophages) and anti-CD163 (green, a marker for M2 macrophage) antibodies. DAPI (blue) staining identified the nuclei. **(A)** Representative image of IHC. NOS2+ **(B)** and CD163+ **(C)**cells were quantified in the labyrinth of the placenta and were statically compared between groups. Images are ×40 magnification, and scale bars represent 50 μm $n = 5$ for each group. $^*p < 0.05$ $^{**}p < 0.01$. Data were reported as Mean ± SEM.

(DNAC-10 mg/kg of NAC) inhibits $CD45^+$ leukocytes infiltration in the placenta at 3hpi and 6hpi. These data and the previously published data support the role of DNAC in enhancing anti-inflammatory response in the placenta following IUI.

Inducible nitric oxide synthase (iNOS) is a crucial enzyme in the inflammatory response of macrophages and is a source of nitric oxide (NO) that effectively induces inflammatory stimulation (MacMicking et al., 1997). IL-1β elevated by inflammation during pregnancy is one factor that causes immunological, histological, and biochemical changes in the placenta (Tsimis et al., 2017; Lee et al., 2019a; Novak et al., 2019) and damaged fetal brain (Chudnovets et al., 2020). In this study, we identified that DNAC treatment suppressed the LPS-induced production of pro-inflammatory cytokines (iNOS and IL-1β). In our previously study, we provide evidence that DNAC suppresses inflammatory response in the placenta through decreased IL-6 and tumor necrosis factor (TNF)-α following IUI. Maternal intrauterine infection associated with increased levels of pro-inflammatory cytokines (IL-6, TNF-α, IL-1β) is the most important cause of preterm birth and neonatal neurological disorders (Duggan et al., 2001; Goepfert et al., 2004; Girard et al., 2010). These results suggested that low dose of DNAC improved maternal and placental inflammatory status by dampening the pro-inflammatory pathway caused by IUI.

Successful pregnancy depends on regulating dynamic and highly regulated immunologic processes (Mor et al., 2011), especially the placenta, in which macrophages play a critical role. Macrophages are involved in all states of all pregnancy, and the M1/M2 dynamics appropriate balance (Zhang et al., 2017). M1 polarized macrophages are more effective in clearing antigens and converting T cell responses into T helper-1 (Th1) immune responses. In contrast, M2 subsets have immunosuppressive capabilities that help tissue remodeling and promote T helper- 2 (Th2) or antibody-mediated immune response (Mantovani et al., 2004; Varin and Gordon, 2009; Zhang et al., 2017). M1 macrophage phenotype markers iNOs and CXCL10 are related to pro-inflammatory cytokines (IL-1β, IL-6), M2 macrophage phenotype markers MR2 and TREM2 are related to anti-inflammatory cytokines (IL-4, IL- 10). In our study, LPS increased IL-1β mRNA expression and M1 macrophages infiltration in the placenta, these data match our previous studies (Na et al., 2021). Furthermore, we found that DNAC prevents M1 macrophage and cytokinesis iNOs and IL-1□ expression. Nevertheless, in our studies, DNAC decreased M1 macrophages and increased M2 macrophage infiltration in the placenta following IUI. These data further provide evidence that DNAC maintains M1/M2 to anti-inflammation in the placenta.

In both humans and mice, immune cells are critical to maintaining tissue homeostasis, defending against infection, and contributing to labor initiation. The maternal-fetal interface supports multiple cellular immune systems comprising adaptive immune T cells and homeostatic innate immune cells such as macrophages. T cells have been shown to participate in placental pathological inflammation during pregnancy (Lee et al., 2011; Arenas-Hernandez et al., 2019; Liu et al., 2021). We proved that DNAC prevents $CD3^+$/$CD45^+$ cells increased by LPS-induced placental inflammations, but free NAC treatment does not. DNAC decreased $CD8^+$ T-cell infiltrates in LPS-induced inflammation. Macrophages interact with T cells to regulate T cell activation and infiltration in target organs (Chellan et al., 2013). These findings concluded that DNAC initiates innate (T cells) and acquired immunity (macrophages) to play pivotal roles in protecting placenta inflammation flowing IUI.

Placental macrophage infiltration following IUI has a strong correlation with fetal microglia activation (Na et al., 2021). Based on these results, we believed that DNAC administration prevented the macrophage polarization in placental inflammatory load, which indirectly benefits fetal neuroinflammation. As demonstrated in our previous studies, DNAC improved neurobehavioral profiles and decreased microglial activation in offspring (Lei et al., 2017).

Clinically, prevention and treatment options are limited, especially in human preterm deliveries. Most therapies focus on antibiotics, considering the association between inflammation and premature labor in humans. Other new treatment strategies for PTB include progesterone (Almutairi et al., 2021; Frey et al., 2021), tocolytics (Zheng et al., 2017; Jameson and Bernstein, 2019), anti-inflammatory agents (Chin et al., 2016; Xu et al., 2016; Gorasiya et al., 2018; Lee et al., 2019b) and high throughput screening (Le et al., 2020) for PTB prophylaxes (Zierden et al., 2021). In additional to the novel drugs, new drug delivery systems such as nanomedicine-based systems, help the drugs with more targeted and sustained approach. In our previous study, we checked the component and conjugate safety of DNAC. Most clinical therapies for preterm birth focus mainly on the maternal side and have limited benefits for the fetus. In this study, we found that DNAC treatment does not affect dam weight, fetal weight and placental weight. Besides, our previous study demonstrated that dendrimer-conjugated treatment decreased IUI-induced preterm birth rate, reduced placenta and fetal brain inflammation, and improved fetal neuroinflammation in offspring (Lei et al., 2017). This study further provide evidence that DNAC has advantages in preventing placental inflammation following IUI.

In summary, we provide evidence that DNAC regulates the polarization of placenta macrophages into M1 macrophages and induces the polarization of placenta macrophages into M2 macrophages, thus suppressing the placental inflammatory responses caused by intrauterine inflammation. Our results suggest a novel mechanism for DNAC to prevent intrauterine inflammation in placenta immune activation. DNAC shows potential as an experimental treatment for preventing inflammation-related perinatal period in clinical trials.

DATA AVAILABILITY STATEMENT

The original contributions presented in the study are included in the article/Supplementary Material, further inquiries can be directed to the corresponding author.

ETHICS STATEMENT

The animal study was reviewed and approved by Animal Care and Use Committee of Johns Hopkins University Hopkins.

AUTHOR CONTRIBUTIONS

YL, QN, IB, SK, and RK conceived of the study and experimental questions, RS, SK, RK made the conjugate, IB, QN, AC, JLe, and AL performed experiments and collected samples, JLi and JYL processed samples, YL and JLe analyzed and graphed data, YL, QN, AO, and IB wrote the manuscript, all authors reviewed, edited, and approved the final submission.

FUNDING

This work was supported by Johns Hopkins Intergraded Center for Fetal Medicine (I.B.) and Sheikh Abdullah Bugshan Fund (I.B.).

REFERENCES

Almutairi, A. R., Aljohani, H. I., and Al-Fadel, N. S. (2021). 17-Alpha-Hydroxyprogesterone vs. Placebo for Preventing of Recurrent Preterm Birth: A Systematic Review and Meta-Analysis of Randomized Trials. *Front. Med.* 8, 764855. doi:10.3389/fmed.2021.764855

An, Y., Shi, X., Tang, X., Wang, Y., Shen, F., Zhang, Q., et al. (2017). Aflatoxin B1 Induces Reactive Oxygen Species-Mediated Autophagy and Extracellular Trap Formation in Macrophages. *Front. Cel. Infect. Microbiol.* 7, 53. doi:10.3389/fcimb.2017.00053

Arenas-Hernandez, M., Romero, R., Xu, Y., Panaitescu, B., Garcia-Flores, V., Miller, D., et al. (2019). Effector and Activated T Cells Induce Preterm Labor and Birth that Is Prevented by Treatment with Progesterone. *J.I.* 202, 2585–2608. doi:10.4049/jimmunol.1801350

Bolton, J. L., and Bilbo, S. D. (2014). Developmental Programming of Brain and Behavior by Perinatal Diet: Focus on Inflammatory Mechanisms. *Dialogues Clin. Neurosci.* 16, 307–320. doi:10.31887/DCNS.2014.16.3/jbolton

Burd, I., Balakrishnan, B., and Kannan, S. (2012). Models of Fetal Brain Injury, Intrauterine Inflammation, and Preterm Birth. *Am. J. Reprod. Immunol.* 67, 287–294. doi:10.1111/j.1600-0897.2012.01110.x

Burd, I., Bentz, A. I., Chai, J., Gonzalez, J., Monnerie, H., Le Roux, P. D., et al. (2010). Inflammation-induced Preterm Birth Alters Neuronal Morphology in the Mouse Fetal Brain. *J. Neurosci. Res.* 88, 1872–1881. doi:10.1002/jnr.22368

Cappelletti, M., Della Bella, S., Ferrazzi, E., Mavilio, D., and Divanovic, S. (2016). Inflammation and Preterm Birth. *J. Leukoc. Biol.* 99, 67–78. doi:10.1189/jlb.3mr0615-272rr

Chawanpaiboon, S., Vogel, J. P., Moller, A.-B., Lumbiganon, P., Petzold, M., Hogan, D., et al. (2019). Global, Regional, and National Estimates of Levels of Preterm Birth in 2014: a Systematic Review and Modelling Analysis. *Lancet Glob. Health* 7, e37–e46. doi:10.1016/s2214-109x(18)30451-0

Chellan, B., Koroleva, E. P., Sontag, T. J., Tumanov, A. V., Fu, Y.-X., Getz, G. S., et al. (2013). LIGHT/TNFSR14 Can Regulate Hepatic Lipase Expression by Hepatocytes Independent of T Cells and Kupffer Cells. *PLoS One* 8, e54719. doi:10.1371/journal.pone.0054719

Chin, P. Y., Dorian, C. L., Hutchinson, M. R., Olson, D. M., Rice, K. C., Moldenhauer, L. M., et al. (2016). Novel Toll-like Receptor-4 Antagonist (+)-naloxone Protects Mice from Inflammation-Induced Preterm Birth. *Sci. Rep.* 6, 36112. doi:10.1038/srep36112

Chudnovets, A., Lei, J., Na, Q., Dong, J., Narasimhan, H., Klein, S. L., et al. (2020). Dose-dependent Structural and Immunological Changes in the Placenta and Fetal Brain in Response to Systemic Inflammation during Pregnancy. *Am. J. Reprod. Immunol.* 84, e13248. doi:10.1111/aji.13248

Copersino, M. L., Boyd, S. J., Tashkin, D. P., Huestis, M. A., Heishman, S. J., Dermand, J. C., et al. (2006). Quitting Among Non-treatment-seeking Marijuana Users: Reasons and Changes in Other Substance Use. *Am. J. Addict.* 15, 297–302. doi:10.1080/10550490600754341

Dada, T., Rosenzweig, J. M., Al Shammary, M., Firdaus, W., Al Rebh, S., Borbiev, T., et al. (2014). Mouse Model of Intrauterine Inflammation: Sex-specific Differences in Long-Term Neurologic and Immune Sequelae. *Brain Behav. Immun.* 38, 142–150. doi:10.1016/j.bbi.2014.01.014

Duggan, P., Maalouf, E., Watts, T., Sullivan, M., Counsell, S., Allsop, J., et al. (2001). Intrauterine T-Cell Activation and Increased Proinflammatory Cytokine Concentrations in Preterm Infants with Cerebral Lesions. *The Lancet* 358, 1699–1700. doi:10.1016/s0140-6736(01)06723-x

Elovitz, M. A., Brown, A. G., Breen, K., Anton, L., Maubert, M., and Burd, I. (2011). Intrauterine Inflammation, Insufficient to Induce Parturition, Still Evokes Fetal and Neonatal Brain Injury. *Int. J. Dev. Neurosci.* 29, 663–671. doi:10.1016/j.ijdevneu.2011.02.011

Frey, H. A., Finneran, M. M., Hade, E. M., Waickman, C., Lynch, C. D., Iams, J. D., et al. (2021). A Comparison of Vaginal and Intramuscular Progesterone for the Prevention of Recurrent Preterm Birth. *Am. J. Perinatol* [Epub ahead of print]. doi:10.1055/s-0041-1740010

Girard, S., Tremblay, L., Lepage, M., and Sébire, G. (2010). IL-1 Receptor Antagonist Protects against Placental and Neurodevelopmental Defects Induced by Maternal Inflammation. *J.I.* 184, 3997–4005. doi:10.4049/jimmunol.0903349

Goepfert, A. R., Andrews, W. W., Carlo, W., Ramsey, P. S., Cliver, S. P., Goldenberg, R. L., et al. (2004). Umbilical Cord Plasma Interleukin-6 Concentrations in Preterm Infants and Risk of Neonatal Morbidity. *Am. J. Obstet. Gynecol.* 191, 1375–1381. doi:10.1016/j.ajog.2004.06.086

Gorasiya, S., Mushi, J., Pekson, R., Yoganathan, S., and Reznik, S. E. (2018). Repurposing N,N-Dimethylacetamide (DMA), a Pharmaceutical Excipient, as a Prototype Novel Anti-inflammatory Agent for the Prevention And/or Treatment of Preterm Birth. *Cpd* 24, 989–992. doi:10.2174/1381612824666180130121706

Heusinkveld, M., de Vos van Steenwijk, P. J., Goedemans, R., Ramwadhdoebe, T. H., Gorter, A., Welters, M. J. P., et al. (2011). M2 Macrophages Induced by Prostaglandin E2and IL-6 from Cervical Carcinoma Are Switched to Activated M1 Macrophages by CD4+Th1 Cells. *J.I.* 187, 1157–1165. doi:10.4049/jimmunol.1100889

Hug, L., Alexander, M., You, D., and Alkema, L.UN Inter-agency Group for Child Mortality Estimation (2019). National, Regional, and Global Levels and Trends in Neonatal Mortality between 1990 and 2017, with Scenario-Based Projections to 2030: a Systematic Analysis. *Lancet Glob. Health* 7, e710–e720. doi:10.1016/s2214-109x(19)30163-9

Jameson, R. A., and Bernstein, H. B. (2019). Magnesium Sulfate and Novel Therapies to Promote Neuroprotection. *Clin. Perinatology* 46, 187–201. doi:10.1016/j.clp.2019.02.008

Jenkins, D. D., Wiest, D. B., Mulvihill, D. M., Hlavacek, A. M., Majstoravich, S. J., Brown, T. R., et al. (2016). Fetal and Neonatal Effects of N-Acetylcysteine when Used for Neuroprotection in Maternal Chorioamnionitis. *J. Pediatr.* 168, 67–76. doi:10.1016/j.jpeds.2015.09.076

Kannan, S., Dai, H., Navath, R. S., Balakrishnan, B., Jyoti, A., Janisse, J., et al. (2012). Dendrimer-based Postnatal Therapy for Neuroinflammation and Cerebral Palsy in a Rabbit Model. *Sci. Transl Med.* 4, 130ra46. doi:10.1126/scitranslmed.3003162

Kurtoglu, Y. E., Navath, R. S., Wang, B., Kannan, S., Romero, R., and Kannan, R. M. (2009). Poly(amidoamine) Dendrimer-Drug Conjugates with Disulfide Linkages for Intracellular Drug Delivery. *Biomaterials* 30, 2112–2121. doi:10.1016/j.biomaterials.2008.12.054

Le, B. L., Iwatani, S., Wong, R. J., Stevenson, D. K., and Sirota, M. (2020). Computational Discovery of Therapeutic Candidates for Preventing Preterm Birth. *JCI Insight* 5, e133761. doi:10.1172/jci.insight.133761

Lee, J., Romero, R., Dong, Z., Xu, Y., Qureshi, F., Jacques, S., et al. (2011). Unexplained Fetal Death Has a Biological Signature of Maternal Anti-fetal Rejection: Chronic Chorioamnionitis and Alloimmune Anti-human Leucocyte Antigen Antibodies. *Histopathology* 59, 928–938. doi:10.1111/j.1365-2559.2011.04038.x

Lee, J. Y., Song, H., Dash, O., Park, M., Shin, N. E., McLane, M. W., et al. (2019). Administration of Melatonin for Prevention of Preterm Birth and Fetal Brain Injury Associated with Premature Birth in a Mouse Model. *Am. J. Reprod. Immunol.* 82, e13151. doi:10.1111/aji.13151

Lee, J. Y., Shin, N. E., Na, Q., Dong, J., Chudnovets, A., Li, S., et al. (2019). Exposure to Systemic and Intrauterine Inflammation Leads to Decreased Pup Survival via Different Placental Mechanisms. *J. Reprod. Immunol.* 133, 52–62. doi:10.1016/j.jri.2019.06.004

Lei, J., Rosenzweig, J. M., Mishra, M. K., Alshehri, W., Brancusi, F., McLane, M., et al. (2017). Maternal Dendrimer-Based Therapy for Inflammation-Induced Preterm Birth and Perinatal Brain Injury. *Sci. Rep.* 7, 6106. doi:10.1038/s41598-017-06113-2

Lei, J., Xie, L., Zhao, H., Gard, C., Clemens, J. L., McLane, M. W., et al. (2018). Maternal CD8+T-Cell Depletion Alleviates Intrauterine Inflammation-Induced Perinatal Brain Injury. *Am. J. Reprod. Immunol.* 79, e12798. doi:10.1111/aji.12798

Liu, J., Liu, Y., Panda, S., Liu, A., Lei, J., and Burd, I. (2021). Type 1 Cytotoxic T Cells Increase in Placenta after Intrauterine Inflammation. *Front. Immunol.* 12, 718563. doi:10.3389/fimmu.2021.718563

MacMicking, J., Xie, Q.-w., and Nathan, C. (1997). Nitric Oxide and Macrophage Function. *Annu. Rev. Immunol.* 15, 323–350. doi:10.1146/annurev.immunol.15.1.323

Magro, M., Venerando, A., Macone, A., Canettieri, G., Agostinelli, E., and Vianello, F. (2020). Nanotechnology-Based Strategies to Develop New Anticancer Therapies. *Biomolecules* 10, 735. doi:10.3390/biom10050735

Mantovani, A., Sica, A., Sozzani, S., Allavena, P., Vecchi, A., and Locati, M. (2004). The Chemokine System in Diverse Forms of Macrophage Activation and Polarization. *Trends Immunol.* 25, 677–686. doi:10.1016/j.it.2004.09.015

Menjoge, A. R., Kannan, R. M., and Tomalia, D. A. (2010). Dendrimer-based Drug and Imaging Conjugates: Design Considerations for Nanomedical Applications. *Drug Discov. Today* 15, 171–185. doi:10.1016/j.drudis.2010.01.009

Mishra, M. K., Beaty, C. A., Lesniak, W. G., Kambhampati, S. P., Zhang, F., Wilson, M. A., et al. (2014). Dendrimer Brain Uptake and Targeted Therapy for Brain Injury in a Large Animal Model of Hypothermic Circulatory Arrest. *ACS Nano* 8, 2134–2147. doi:10.1021/nn404872e

Mor, G., Cardenas, I., Abrahams, V., and Guller, S. (2011). Inflammation and Pregnancy: the Role of the Immune System at the Implantation Site. *Ann. Ny Acad. Sci.* 1221, 80–87. doi:10.1111/j.1749-6632.2010.05938.x

Na, Q., Chudnovets, A., Liu, J., Lee, J. Y., Dong, J., Shin, N., et al. (2021). Placental Macrophages Demonstrate Sex-specific Response to Intrauterine Inflammation and May Serve as a Marker of Perinatal Neuroinflammation. *J. Reprod. Immunol.* 147, 103360. doi:10.1016/j.jri.2021.103360

Nance, E., Kambhampati, S. P., Smith, E. S., Zhang, Z., Zhang, F., Singh, S., et al. (2017). Dendrimer-mediated Delivery of N-Acetyl Cysteine to Microglia in a Mouse Model of Rett Syndrome. *J. Neuroinflammation* 14, 252. doi:10.1186/s12974-017-1004-5

Nance, E., Zhang, F., Mishra, M. K., Zhang, Z., Kambhampati, S. P., Kannan, R. M., et al. (2016). Nanoscale Effects in Dendrimer-Mediated Targeting of Neuroinflammation. *Biomaterials* 101, 96–107. doi:10.1016/j.biomaterials.2016.05.044

Nemeth, C. L., Drummond, G. T., Mishra, M. K., Zhang, F., Carr, P., Garcia, M. S., et al. (2017). Uptake of Dendrimer-Drug by Different Cell Types in the hippocampus after Hypoxic-Ischemic Insult in Neonatal Mice: Effects of Injury, Microglial Activation and Hypothermia. *Nanomedicine: Nanotechnology, Biol. Med.* 13, 2359–2369. doi:10.1016/j.nano.2017.06.014

Niño, D. F., Zhou, Q., Yamaguchi, Y., Martin, L. Y., Wang, S., Fulton, W. B., et al. (2018). Cognitive Impairments Induced by Necrotizing Enterocolitis Can Be Prevented by Inhibiting Microglial Activation in Mouse Brain. *Sci. Transl Med.* 10, eaan0237. doi:10.1126/scitranslmed.aan0237

Novak, C. M., Lee, J. Y., Ozen, M., Tsimis, M. E., Kucirka, L. M., McLane, M. W., et al. (2019). Increased Placental T Cell Trafficking Results in Adverse Neurobehavioral Outcomes in Offspring Exposed to Sub-chronic Maternal Inflammation. *Brain Behav. Immun.* 75, 129–136. doi:10.1016/j.bbi.2018.09.025

Rocher, C., Singla, R., Singal, P. K., Parthasarathy, S., and Singla, D. K. (2012). Bone Morphogenetic Protein 7 Polarizes THP-1 Cells into M2 Macrophages. *Can. J. Physiol. Pharmacol.* 90, 947–951. doi:10.1139/y2012-102

Romero, R., Erez, O., and Espinoza, J. (2005). Intrauterine Infection, Preterm Labor, and Cytokines. *J. Soc. Gynecol. Investig.* 12, 463–465. doi:10.1016/j.jsgi.2005.09.001

Shahin, A. Y., Hassanin, I. M. A., Ismail, A. M., Kruessel, J. S., and Hirchenhain, J. (2009). Effect of Oral N-Acetyl Cysteine on Recurrent Preterm Labor Following Treatment for Bacterial Vaginosis. *Int. J. Gynecol. Obstet.* 104, 44–48. doi:10.1016/j.ijgo.2008.08.026

Sinha, P., Clements, V. K., and Ostrand-Rosenberg, S. (2005). Interleukin-13-regulated M2 Macrophages in Combination with Myeloid Suppressor Cells Block Immune Surveillance against Metastasis. *Cancer Res.* 65, 11743–11751. doi:10.1158/0008-5472.can-05-0045

Smilkstein, M. J., Knapp, G. L., Kulig, K. W., and Rumack, B. H. (1988). Efficacy of Oral N-Acetylcysteine in the Treatment of Acetaminophen Overdose. *N. Engl. J. Med.* 319, 1557–1562. doi:10.1056/nejm198812153192401

Tardito, S., Martinelli, G., Soldano, S., Paolino, S., Pacini, G., Patane, M., et al. (2019). Macrophage M1/M2 Polarization and Rheumatoid Arthritis: A Systematic Review. *Autoimmun. Rev.* 18, 102397. doi:10.1016/j.autrev.2019.102397

Tsimis, M. E., Lei, J., Rosenzweig, J. M., Arif, H., Shabi, Y., Alshehri, W., et al. (2017). P2X7 Receptor Blockade Prevents Preterm Birth and Perinatal Brain Injury in a Mouse Model of Intrauterine Inflammation†. *Biol. Reprod.* 97, 230–239. doi:10.1093/biolre/iox081

Turk, B. R., Nemeth, C. L., Marx, J. S., Tiffany, C., Jones, R., Theisen, B., et al. (2018). Dendrimer-N-acetyl-L-cysteine Modulates Monophagocytic Response in Adrenoleukodystrophy. *Ann. Neurol.* 84, 452–462. doi:10.1002/ana.25303

Varin, A., and Gordon, S. (2009). Alternative Activation of Macrophages: Immune Function and Cellular Biology. *Immunobiology* 214, 630–641. doi:10.1016/j.imbio.2008.11.009

Wang, Y., Smith, W., Hao, D., He, B., and Kong, L. (2019). M1 and M2 Macrophage Polarization and Potentially Therapeutic Naturally Occurring Compounds. *Int. Immunopharmacology* 70, 459–466. doi:10.1016/j.intimp.2019.02.050

Xu, W., Roos, A., Schlagwein, N., Woltman, A. M., Daha, M. R., and van Kooten, C. (2006). IL-10-producing Macrophages Preferentially clear Early Apoptotic Cells. *Blood* 107, 4930–4937. doi:10.1182/blood-2005-10-4144

Xu, Y., Romero, R., Miller, D., Kadam, L., Mial, T. N., Plazyo, O., et al. (2016). An M1-like Macrophage Polarization in Decidual Tissue during Spontaneous Preterm Labor that Is Attenuated by Rosiglitazone Treatment. *J.I.* 196, 2476–2491. doi:10.4049/jimmunol.1502055

Yunna, C., Mengru, H., Lei, W., and Weidong, C. (2020). Macrophage M1/M2 Polarization. *Eur. J. Pharmacol.* 877, 173090. doi:10.1016/j.ejphar.2020.173090

Zhang, F., Nance, E., Zhang, Z., Jasty, V., Kambhampati, S. P., Mishra, M. K., et al. (2016). Surface Functionality Affects the Biodistribution and Microglia-Targeting of Intra-amniotically Delivered Dendrimers. *J. Controlled Release* 237, 61–70. doi:10.1016/j.jconrel.2016.06.046

Zhang, Y.-H., He, M., Wang, Y., and Liao, A.-H. (2017). Modulators of the Balance between M1 and M2 Macrophages during Pregnancy. *Front. Immunol.* 8, 120. doi:10.3389/fimmu.2017.00120

Zhang, Z., Lin, Y.-A., Kim, S.-Y., Su, L., Liu, J., Kannan, R. M., et al. (2020). Systemic Dendrimer-Drug Nanomedicines for Long-Term Treatment of Mild-Moderate Cerebral Palsy in a Rabbit Model. *J. Neuroinflammation* 17, 319. doi:10.1186/s12974-020-01984-1

Zheng, K., Lu, P., Delpapa, E., Bellve, K., Deng, R., Condon, J. C., et al. (2017). Bitter Taste Receptors as Targets for Tocolytics in Preterm Labor Therapy. *FASEB j.* 31, 4037–4052. doi:10.1096/fj.201601323rr

Zierden, H. C., Shapiro, R. L., DeLong, K., Carter, D. M., and Ensign, L. M. (2021). Next Generation Strategies for Preventing Preterm Birth. *Adv. Drug Deliv. Rev.* 174, 190–209. doi:10.1016/j.addr.2021.04.021

Conflict of Interest: Authors RMK and SK have awarded and pending patents relating to hydroxyl dendrimer targeting of reactive microglia. RMK and SK are co-founders and have financial interests in Ashvattha Therapeutics, Inc.

The remaining authors declare that the research was conducted in the absence of any commercial or financial relationships that could be construed as a potential conflict of interest.

Publisher's Note: All claims expressed in this article are solely those of the authors and do not necessarily represent those of their affiliated organizations, or those of the publisher, the editors and the reviewers. Any product that may be evaluated in this article, orclaim that may be made by its manufacturer, is not guaranteed or endorsed by the publisher.

frontiers in Bioengineering and Biotechnology

OPINION
published: 10 February 2022
doi: 10.3389/fbioe.2022.819183

New Approaches and Biomarker Candidates for the Early Detection of Ovarian Cancer

K. R. Hossain[1†], *J. D. Escobar Bermeo*[1,2†], *K. Warton*[3] *and S. M. Valenzuela*[1,2*]

[1]*School of Life Sciences, Faculty of Science, University of Technology Sydney, Sydney, NSW, Australia,* [2]*ARC Research Hub for Integrated Device for End-user Analysis at Low-levels (IDEAL), Faculty of Science, University of Technology Sydney, Sydney, NSW, Australia,* [3]*School of Women's and Children's Health, Faculty of Medicine and Health, University of New South Wales, South Wales, NSW, Australia*

Keywords: ovarian cancer, CLIC proteins, exosomes, diagnostics, biomarkers

OVARIAN CANCER

Ovarian cancer (OC) is a disease that most often affects post-menopausal women who present abdominal discomfort and bloating over a few months prior to detection. The majority of patients are diagnosed at advanced stages of the disease as the early stages are commonly asymptomatic (Jayson et al., 2014). According to Global Cancer Statistics 2020, OC is the seventh most common cancer in women worldwide accounting for around 314,000 new cases (3.4% of all new cancer cases in females) annually (Sung et al., 2021). In 2021 it established itself as the ninth most commonly diagnosed cancer amongst Australian women with 1720 new cases and 1,042 reported deaths (www.canceraustralia.gov.au). Prognosis is significantly determined by the stage of diagnosis where survival for stages I, II, III and IV is 73–92%, 45–55%, 21% and <6%, respectively[1], underscoring the need for better early detection of ovarian cancer.

There are four main types of OC: epithelial, Germ cell, sex chord and stromal, with each having different epidemiological statistics, and with epithelial ovarian cancer (EOC) accounting for approximately 90% of all cases (Smith et al., 2006). In EOC there are histological subtypes, though most patients have high-grade serous ovarian cancer, a disease characterised by p53 gene abnormalities (Köbel, 2010). Some high grade serous ovarian cancers are caused by deleterious mutations of BRCA1 and BRCA2 genes, while others arise from a combination of somatic mutations (Network, 2011). The most common and effective management of the disease is a combination of surgery with chemotherapy. Surgical removal of cancer mass almost always occurs after diagnosis however, this is not always feasible when the cancer is very advanced. Furthermore, although surgery has proven effective in early stages of the disease, most patients diagnosed at advanced stages will go on to develop many iterations of recurrent disease (Jayson et al., 2014).

Cancer Antigen-125 (CA-125) and trans-vaginal imaging are currently routinely used as part of ovarian cancer diagnosis. Blood level of CA-125 is the most widely used serum biomarker, but it lacks the sensitivity or specificity to be used alone as a screening test (Jayson et al., 2014). It is also not useful for early diagnosis as CA-125 expression levels are too low for accurate detection and there are also several other conditions including endometriosis (Nisenblat et al., 2016), gall bladder (Wang, 2014) and liver cancer (Devarbhavi et al., 2002) where CA-125 levels are elevated, leading to false positive results. Likewise, it is often difficult to detect small early-stage tumors with trans-vaginal imaging. Hence, diagnosis often involves invasive techniques like laporascopy and tissue biopsies. It is therefore clear that early diagnosis of ovarian cancer requires improved screening tests that can be performed easily and inexpensively, as well as achieving high sensitivity and specificity.

[1]UK, C.R. Cancer Research UK, 2013.

OPEN ACCESS

Edited by:
Dunja Aksentijevic, Queen Mary University of London, United Kingdom

Reviewed by:
Assaf Zinger, Technion Israel Institute of Technology, Israel
Manisha Sachan, Motilal Nehru National Institute of Technology Allahabad, India

****Correspondence:***
S. M. Valenzuela
Stella.Valenzuela@uts.edu.au

[†]These authors have contributed equally to this work

Specialty section:
This article was submitted to Preclinical Cell and Gene Therapy, a section of the journal Frontiers in Bioengineering and Biotechnology

Received: *21 November 2021*
Accepted: *24 January 2022*
Published: *10 February 2022*

Citation:
Hossain KR, Escobar Bermeo J, Warton K and Valenzuela SM (2022) New Approaches and Biomarker Candidates for the Early Detection of Ovarian Cancer. Front. Bioeng. Biotechnol. 10:819183. doi: 10.3389/fbioe.2022.819183

NEW ADVANCES IN THE SCREENING OF OVARIAN CANCER

Several different approaches have been proposed to combat the shortcomings of current techniques. Studies focused on smaller molecules, such as circulating miRNA and cell-free DNA (cf-DNA) have gained significant attention in recent times (Jørgensen, 2013; Ling et al., 2013; Peng and Croce, 2016). These molecules have emerged as promising cancer biomarkers suited for improved non/minimally invasive diagnostic, prognostic and therapeutic applications. Multiple miRNAs associated with ovarian cancer, such as the Let-7 family miRNAs, together with a variety of miRNA assays including RT-qPCR, microarrays and RNA sequencing have been reported as potential screening techniques (Banno et al., 2014; Deb et al., 2018; Aziz et al., 2020). As of 2021 there were over 250 miRNAs associated with ovarian cancers on the online database miRCancer, and depending on the cellular context, their up or down regulation was shown to be involved in disease progression (Xie et al., 2013). Despite demonstrating good analytical performance, a lack of reproducibility and the high costs associated with miRNA profiling mean their development remains a work in progress [for in-depth discussion of these challenges, see reviews (Tiberio et al., 2015; Witwer, 2015)]. In response to these issues, the research focus has expanded to include alternate approaches like the use of exosomes (EX) which are gaining increased interest in recent literature.

EXs are extracellular vesicles, ranging between 40 and 160 nm in size (Ruivo et al., 2017), released from the phospholipid membrane of the cell. These lipid bilayer-bound vehicles carry nucleic acids, proteins, and lipids to neighbouring or distant cells that influence a multitude of processes (Schey et al., 2015). Since EXs mimic the profile of the host cell from which they originate, it is not surprising that EXs released from cancer cells have been shown to aid in tumor progression including cellular proliferation, angiogenesis, migration, invasion, metastasis, and drug resistance (Tai et al., 2018). These properties make them suitable targets not only for novel therapeutics but also as specific markers for use in cancer diagnostics, prognosis, and even as chemotherapy drug-delivery systems. A recent review by Huda et al. (2021) highlighted several clinical applications and preclinical advancement outlining the importance of exosomes for use in targeted drug delivery, biomarker study, and vaccine development (Huda et al., 2021). A recent study by Zhao et al. (2016) reported the development of a microfluidic chip to isolate EXs expressing certain ovarian cancer biomarkers including CA-125 (Zhao et al., 2016). In addition, use of specific antibodies resulted in a greater number of exosomes being captured in patient samples, compared to healthy controls (Zhao et al., 2016). Although this study highlighted how exosomal CA-125 may be used to distinguish between healthy controls and cancer patients (Zhao et al., 2016), the associated drawbacks of CA-125 as a promising ovarian cancer biomarker for early detection remain a challenge.

It is now well established that the proteomic profile of EXs can act as a useful tool or biomarker for diagnosing various types of cancer (Nuzhat et al., 2017; Sharma et al., 2017; Kok and Yu, 2020; Croft et al., 2021). For example, a study by Klein-Scory et al. (2014) illustrated that EXs secreted from pancreatic cancer cells had a distinctive proteomic profile allowing for possible use as an early stage biomarker (Klein-Scory et al., 2014). Thus, it is seemingly reasonable to exploit the proteomic profile of exosomes from ovarian cancer cells to identify novel biomarkers. One such example is the Chloride Intracellular Ion Channels (CLIC) family of proteins which has been shown to be elevated in patients with ovarian cancer (Kobayashi et al., 2012).

CHLORIDE INTRACELLULAR ION CHANNELS AS BIOMARKERS FOR OVARIAN CANCER

The CLIC family in vertebrates consists of six evolutionarily conserved protein members (Littler et al., 2010). These proteins are unusual, existing in cells as both soluble and membrane bound proteins, where they demonstrate "moonlighting" activity, exhibiting two independent functions. In the membrane bound form, CLIC proteins act as ion channels (Valenzuela et al., 2013) while in the soluble form, they act as oxidoreductase enzymes, which are most likely involved in cell protective functions like detoxification and/or anti-oxidative roles (Al Khamici et al., 2015). Several studies have also shown CLIC proteins to have important extracellular activities (see review (Argenzio and Moolenaar, 2016)), with CLIC1, CLIC3 and CLIC4 found on endometrium/placenta cell exosomes (Zhao et al., 2016). CLICs are also known to be up-regulated in various types of cancers where they are primarily involved in cancer metastasis *via* exosomal and anti-apoptotic activities (GururajaRao et al., 2020). In a recent bioinformatics study of patient survival as a function of the relative mRNA levels, across several human cancers, the data clearly indicates both low or high CLIC expression levels, influence patient survival (GururajaRao et al., 2020). For example, high CLIC1 and CLIC3 mRNA expression were associated with advanced stages of liver cancer (Huang et al., 2021) while high CLIC4 mRNA expression correlates with poor patient survival in EOC (Singha et al., 2018). However, to better understand the therapeutic potential of these proteins, it is important to further deduce details regarding their tissue expression and release into blood.

Studies have shown two members of the CLIC protein family, CLIC1 and CLIC4, to be significantly upregulated in EOC patients compared to healthy controls (Tang et al., 2012; Tang et al., 2013; Ye et al., 2015; Singha et al., 2018; Yu et al., 2018), and shed into the blood of ovarian cancer patients (Tang et al., 2012; Tang et al., 2013). At the tissue level, combining CLIC1 and CLIC4 staining with CA-125, resulted in better sensitivity, compared to using CA-125 alone, hence a panel consisting of CLIC proteins and CA-125 may outperform individual biomarkers (Singha et al., 2018). Expression levels of CLIC1 and CLIC4 have also been implicated in patient survival, with elevated CLIC4 expression a negative indicator of patient survival in ovarian cancer (Singha et al., 2018). Knockdown of either CLIC4 or CLIC1 resulted in slower growth of ovarian cancer cells suggesting a role of CLICs in cell proliferation and cell migration (Singha et al., 2018). Furthermore, consistent with other reports,

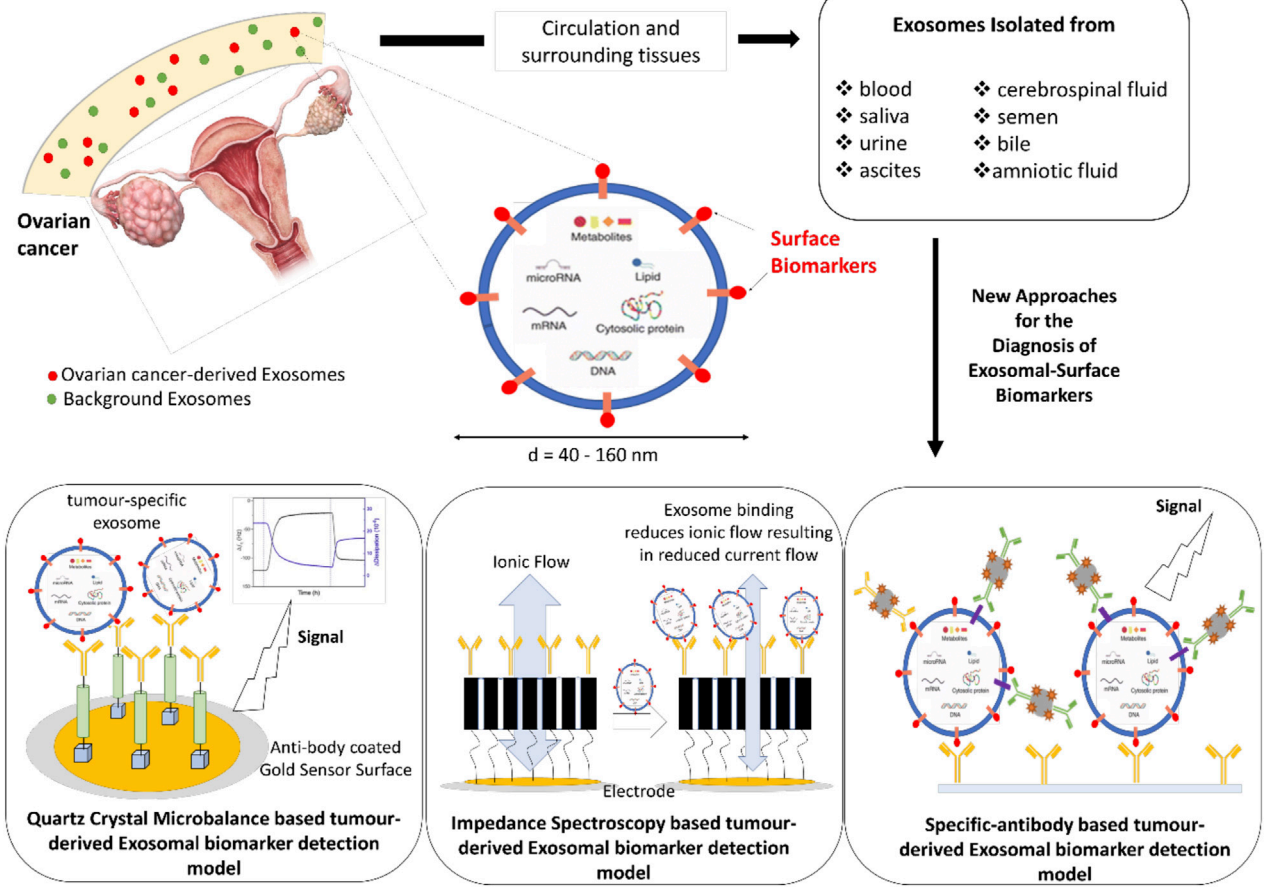

FIGURE 1 | Schematic representation of new diagnostic approaches for the detection of Exosomal-Surface Biomarkers.

these proteins have also been shown to play important roles in EOC progression across multiple EOC subtypes (Ye et al., 2015; Singha et al., 2018; Yu et al., 2018). Similarly, CLIC3 levels have been shown to be elevated in 90% of ovarian cancer patients, where upregulation of CLIC3 in breast cancer tissue was associated with increased cancer cell invasiveness (Hernandez-Fernaud et al., 2017). The fact that exosome associated CLICs display cancer-specific signatures for EOCs, allows for the coupling of CLIC expression with emerging technologies capable of detecting and profiling exosomes, leading to simple, non-invasive, early and specific detection of ovarian cancer.

DIAGNOSTIC APPROACHES FOR THE ANALYSIS OF EXOSOME ASSOCIATED CLICS AS BIOMARKERS FOR EARLY DETECTION OF OVARIAN CANCER

EXs have been successfully isolated from blood, urine, ascites, cerebrospinal fluid, amniotic fluid, semen, saliva, and bile (Colombo et al., 2014; Sullivan et al., 2017) thus providing an array of possibilities for their detection using several different techniques, with some examples as highlighted in **Figure 1**. Some of the currently available techniques that analyse EX proteins from different human body fluids, with or without EX isolation, include flow cytometry, protein microarray (EX Array), diagnostic magnetic resonance, nanoplasmonic sensing technology and microfluidics (Orozco and Lewis, 2010; Shao et al., 2012; Jørgensen, 2013; Im et al., 2014; Zhao et al., 2016; Sullivan et al., 2017). Recently, a number of studies have proposed exosomal proteins as diagnostic biomarkers of breast cancer (Rupp et al., 2011; Soung et al., 2017; Sullivan et al., 2017), where one such study showed EXs isolated using anti-CD24 and anti-EpCAM-coupled magnetic beads as potential breast cancer-specific markers (Rupp et al., 2011). An assay called "ExoScreen" available for the detection of colon cancer is based on the detection of cancer-specific circulating double-positive (CD146/CD9) EXs using photosensitive-beads, from as little as 5 μL of patient serum (Yoshioka et al., 2014). Numerous commercial kits are also available where specific EXs are isolated and analysed using microfluidic platforms for detecting different types of cancer (Contreras-Naranjo et al., 2017).

In the past several years, various electrochemical assays have been developed for the detection and characterisation of exosomes. One such development is an integrated magneto-

electrochemical sensor (iMEX) where antibody-coated-magnetic beads are used for EXs capture and labelling following detection via electrochemical sensing (Jeong et al., 2016). Doldan et al. have developed an electrochemical sandwich approach using gold electrodes prefunctionalised with specific antibodies for exosome determination (Doldán, 2016). Electrical impedance technology is another well-established technique, which over the last 30 years has gained increasing interest in its applications in medicine. Impedance biosensors are usually label free and do not depend on any specific enzyme for analyte detection. Instead, impedimetric biosensors rely on unique bioreceptors or tags, which when specifically bound to the biomarker, produce changes in an electric current that lead to detection and in some cases, quantification of the biomarkers (Leva-Bueno et al., 2020). Impedance spectroscopy with tethered membrane technology has also been used for *E. coli* and *Staphylococcus aureus* detection, where specific antibodies embedded in the membrane detect the presence of bacteria in different fluid samples (Tan et al., 2011). This technology has been adapted to detect prostate (Mishra et al., 2012) and skin (Braun et al., 2017) cancer specific biomarkers and has the potential to be reliable, specific and selective, while being inexpensive and fast. Similarly, the detection of disease-related biomarkers based on acoustic sensors has created global research interest, with biosensors based on the quartz crystal microbalance (QCM) exploited for cancer diagnosis. Commercial QCM systems have been utilised for detecting highly metastatic human breast cancer cells (Atay et al., 2016; Bakhshpour et al., 2019), while an aptamer-based QCM was applied for the detection of leukemia cells (Shan et al., 2014). QCM technology with different signal enhancing approaches has been employed for the detection of several cancer biomarkers such as the carcinoembryonic antigen (CEA) for colorectal cancer (Chi et al., 2020), potential cancer biomarker poly (ADP-ribose) polymerase-1 (PARP-1) (Yang et al., 2019) and even for the detection of volatile compounds like propanol, ethyl benzene, hexanal and decane which are under investigation as non-invasive lung cancer biomarkers (AthirahAwatif Abdul Rahman et al., 2019). Recently, Suther et al. (2020) highlighted the potential of a QCM with dissipation monitoring (QCM-D) system to detect exosomal-CD63 biomarker by exploiting their surface protein profile (Suthar et al., 2020). Thus, the QCM system has emerged as a robust biosensing platform which allows the detection and quantification of a wide range of biomolecules. This, together with their high sensitivity and short detection time, makes QCM based-biosensors attractive for the early detection of various cancer types and the routine monitoring of disease progression.

Achieving early detection of ovarian cancer remains the greatest hope for improved patient survival outcomes. Therefore, investigation of these novel tools and technologies for early ovarian cancer diagnosis is a high priority.

AUTHOR CONTRIBUTIONS

All authors listed have made a substantial, direct, and intellectual contribution to the work and approved it for publication.

ACKNOWLEDGMENTS

The authors thank the Australian Research Council (ARC) Industry Transformational Research Hub Scheme (Grant IH150100028 to SV) ARC website URL: http://www.arc.gov.au/. The funder had no role in study design or data collection and analysis.

REFERENCES

Al Khamici, H., Brown, L. J., Hossain, K. R., Hudson, A. L., Sinclair-Burton, A. A., Ng, J. P., et al. (2015). Members of the Chloride Intracellular Ion Channel Protein Family Demonstrate Glutaredoxin-like Enzymatic Activity. *PLOS ONE* 10 (1), e115699. doi:10.1371/journal.pone.0115699

Argenzio, E., and Moolenaar, W. H. (2016). Emerging Biological Roles of Cl–Intracellular Channel Proteins. *J. Cel Sci* 129 (22), 4165–4174. doi:10.1242/jcs.189795

Atay, S., Pişkin, K., Yılmaz, F., Çakır, C., Yavuz, H., and Denizli, A. (2016). Quartz crystal Microbalance Based Biosensors for Detecting Highly Metastatic Breast Cancer Cells via Their Transferrin Receptors. *Anal. Methods* 8, 153–161. doi:10.1039/c5ay02898a

Athirah Awatif Abdul Rahman, N., Hadi Ma'Radzi, A., and Zakaria, A. (2019). Fabrication of Quartz crystal Microbalance with Pegylated Lipopolymer for Detection of Non-invasive Lung Cancer Biomarker. *Mater. Today Proc.* 7 (2), 632–637. doi:10.1016/j.matpr.2018.12.054

Aziz, N. B., Mahmudunnabi, R. G., Umer, M., Sharma, S., Rashid, M. A., Alhamhoom, Y., et al. (2020). MicroRNAs in Ovarian Cancer and Recent Advances in the Development of microRNA-Based Biosensors. *Analyst* 145 (6), 2038–2057. doi:10.1039/c9an02263e

Bakhshpour, M., Piskin, A. K., Yavuz, H., and Denizli, A. (2019). Quartz crystal Microbalance Biosensor for Label-free MDA MB 231 Cancer Cell Detection via Notch-4 Receptor. *Talanta* 204, 840–845. doi:10.1016/j.talanta.2019.06.060

Banno, K., Yanokura, M., Iida, M., Adachi, M., Nakamura, K., Nogami, Y., et al. (2014). Application of microRNA in Diagnosis and Treatment of Ovarian Cancer. *Biomed. Res. Int.* 2014, 232817. doi:10.1155/2014/232817

Braun, R. P., Mangana, J., Goldinger, S., French, L., Dummer, R., and Marghoob, A. A. (2017). Electrical Impedance Spectroscopy in Skin Cancer Diagnosis. *Dermatol. Clin.* 35 (4), 489–493. doi:10.1016/j.det.2017.06.009

Chi, L., Xu, C., Li, S., Wang, X., Tang, D., and Xue, F. (2020). *In Situ* amplified QCM Immunoassay for Carcinoembryonic Antigen with Colorectal Cancer Using Horseradish Peroxidase Nanospheres and Enzymatic Biocatalytic Precipitation. *Analyst* 145 (18), 6111–6118. doi:10.1039/d0an01399d

Colombo, M., Raposo, G., and Théry, C. (2014). Biogenesis, Secretion, and Intercellular Interactions of Exosomes and Other Extracellular Vesicles. *Annu. Rev. Cel Dev. Biol.* 30, 255–289. doi:10.1146/annurev-cellbio-101512-122326

Contreras-Naranjo, J. C., Wu, H.-J., and Ugaz, V. M. (2017). Microfluidics for Exosome Isolation and Analysis: Enabling Liquid Biopsy for Personalized Medicine. *Lab. Chip* 17 (21), 3558–3577. doi:10.1039/c7lc00592j

Croft, P. K., Sharma, S., Godbole, N., Rice, G. E., and Salomon, C. (2021). Ovarian-Cancer-Associated Extracellular Vesicles: Microenvironmental Regulation and Potential Clinical Applications. *Cells* 10 (9). doi:10.3390/cells10092272

Deb, B., Uddin, A., and Chakraborty, S. (2018). miRNAs and Ovarian Cancer: An Overview. *J. Cel Physiol* 233, 3846–3854. doi:10.1002/jcp.26095

Devarbhavi, H., Kaese, D., Williams, A. W., Rakela, J., Klee, G. G., and Kamath, P. S. (2002). Cancer Antigen 125 in Patients with Chronic Liver Disease. *Mayo Clinic Proc.* 77 (6), 538–541. doi:10.4065/77.6.538

Doldán, X. (2016). Electrochemical Sandwich Immunosensor for Determination of Exosomes Based on Surface Marker-Mediated Signal Amplification. *Anal. Chem.* 88 (21), 10466–10473.

Gururaja Rao, S., Patel, N. J., and Singh, H. (2020). Intracellular Chloride Channels: Novel Biomarkers in Diseases. *Front. Physiol.* 11, 96. doi:10.3389/fphys.2020.00096

Hernandez-Fernaud, J. R., Ruengeler, E., Casazza, A., Neilson, L. J., Pulleine, E., Santi, A., et al. (2017). Secreted CLIC3 Drives Cancer Progression through its Glutathione-dependent Oxidoreductase Activity. *Nat. Commun.* 8 (1), 14206. doi:10.1038/ncomms14206

Huang, J. J., Lin, J., Chen, X., and Zhu, W. (2021). Identification of Chloride Intracellular Channels as Prognostic Factors Correlated with Immune Infiltration in Hepatocellular Carcinoma Using Bioinformatics Analysis. *Medicine (Baltimore)* 100 (45). doi:10.1097/md.0000000000027739

Huda, M. N., Nafiujjaman, M., Deaguero, I. G., Okonkwo, J., Hill, M. L., Kim, T., et al. (2021). Potential Use of Exosomes as Diagnostic Biomarkers and in Targeted Drug Delivery: Progress in Clinical and Preclinical Applications. *ACS Biomater. Sci. Eng.* 7 (6), 2106–2149. doi:10.1021/acsbiomaterials.1c00217

Im, H., Shao, H., Park, Y. I., Peterson, V. M., Castro, C. M., Weissleder, R., et al. (2014). Label-free Detection and Molecular Profiling of Exosomes with a Nano-Plasmonic Sensor. *Nat. Biotechnol.* 32 (5), 490–495. doi:10.1038/nbt.2886

Jayson, G. C., Kohn, E. C., Kitchener, H. C., and Ledermann, J. A. (2014). Ovarian Cancer. *The Lancet* 384 (9951), 1376–1388. doi:10.1016/s0140-6736(13)62146-7

Jeong, S., Park, J., Pathania, D., Castro, C. M., Weissleder, R., and Lee, H. (2016). Integrated Magneto-Electrochemical Sensor for Exosome Analysis. *ACS Nano* 10 (2), 1802–1809. doi:10.1021/acsnano.5b07584

Jørgensen, M. (2013). Extracellular Vesicle (EV) Array: Microarray Capturing of Exosomes and Other Extracellular Vesicles for Multiplexed Phenotyping. *J. Extracell Vesicles* 2.

Klein-Scory, S., Tehrani, M. M., Eilert-Micus, C., Adamczyk, K. A., Wojtalewicz, N., Schnölzer, M., et al. (2014). New Insights in the Composition of Extracellular Vesicles from Pancreatic Cancer Cells: Implications for Biomarkers and Functions. *Proteome Sci.* 12 (1), 50. doi:10.1186/s12953-014-0050-5

Kobayashi, E., Ueda, Y., Matsuzaki, S., Yokoyama, T., Kimura, T., Yoshino, K., et al. (2012). Biomarkers for Screening, Diagnosis, and Monitoring of Ovarian Cancer. *Cancer Epidemiol. Biomarkers Prev.* 21 (11), 1902–1912. doi:10.1158/1055-9965.epi-12-0646

Köbel, M. (2010). The Biological and Clinical Value of P53 Expression in Pelvic High-Grade Serous Carcinomas. *J. Pathol.* 222 (2), 191–198.

Kok, V. C., and Yu, C.-C. (2020). Cancer-Derived Exosomes: Their Role in Cancer Biology and Biomarker Development. *Ijn* Vol. 15, 8019–8036. doi:10.2147/ijn.s272378

Leva-Bueno, J., Peyman, S. A., and Millner, P. A. (2020). A Review on Impedimetric Immunosensors for Pathogen and Biomarker Detection. *Med. Microbiol. Immunol.* 209 (3), 343–362. doi:10.1007/s00430-020-00668-0

Ling, H., Fabbri, M., and Calin, G. A. (2013). MicroRNAs and Other Non-coding RNAs as Targets for Anticancer Drug Development. *Nat. Rev. Drug Discov.* 12 (11), 847–865. doi:10.1038/nrd4140

Littler, D. R., Harrop, S. J., Goodchild, S. C., Phang, J. M., Mynott, A. V., Jiang, L., et al. (2010). The enigma of the CLIC Proteins: Ion Channels, Redox Proteins, Enzymes, Scaffolding Proteins? *FEBS Lett.* 584 (10), 2093–2101. doi:10.1016/j.febslet.2010.01.027

Mishra, V., Bouayad, H., Schned, A., Heaney, J., and Halter, R. J. (2012). Electrical Impedance Spectroscopy for Prostate Cancer Diagnosis. *Annu. Int. Conf. IEEE Eng. Med. Biol. Soc.* 2012, 3258–3261. doi:10.1109/EMBC.2012.6346660

Network, T. C. G. A. R. (2011). Integrated Genomic Analyses of Ovarian Carcinoma. *Nature* 474 (7353), 609–615. doi:10.1038/nature10166

Nisenblat, V., Bossuyt, P. M., Shaikh, R., Farquhar, C., Jordan, V., Scheffers, C. S., et al. (2016). Blood Biomarkers for the Non-invasive Diagnosis of Endometriosis. *Cochrane Database Syst. Rev.* 2016 (5), CD012179. doi:10.1002/14651858.CD012179

Nuzhat, Z., Kinhal, V., Sharma, S., Rice, G. E., Joshi, V., and Salomon, C. (2017). Tumour-derived Exosomes as a Signature of Pancreatic Cancer - Liquid Biopsies as Indicators of Tumour Progression. *Oncotarget* 8 (10), 17279–17291. doi:10.18632/oncotarget.13973

Orozco, A. F., and Lewis, D. E. (2010). Flow Cytometric Analysis of Circulating Microparticles in Plasma. *Cytometry* 77A (6), 502–514. doi:10.1002/cyto.a.20886

Peng, Y., and Croce, C. M. (2016). The Role of MicroRNAs in Human Cancer. *Sig Transduct Target. Ther.* 1 (1), 15004. doi:10.1038/sigtrans.2015.4

Ruivo, C. F., Adem, B., Silva, M., and Melo, S. A. (2017). The Biology of Cancer Exosomes: Insights and New Perspectives. *Cancer Res.* 77 (23), 6480–6488. doi:10.1158/0008-5472.can-17-0994

Rupp, A.-K., Rupp, C., Keller, S., Brase, J. C., Ehehalt, R., Fogel, M., et al. (2011). Loss of EpCAM Expression in Breast Cancer Derived Serum Exosomes: Role of Proteolytic Cleavage. *Gynecol. Oncol.* 122 (2), 437–446. doi:10.1016/j.ygyno.2011.04.035

Schey, K. L., Luther, J. M., and Rose, K. L. (2015). Proteomics Characterization of Exosome Cargo. *Methods* 87, 75–82. doi:10.1016/j.ymeth.2015.03.018

Shan, W., Pan, Y., Fang, H., Guo, M., Nie, Z., Huang, Y., et al. (2014). An Aptamer-Based Quartz crystal Microbalance Biosensor for Sensitive and Selective Detection of Leukemia Cells Using Silver-Enhanced Gold Nanoparticle Label. *Talanta* 126, 130–135. doi:10.1016/j.talanta.2014.03.056

Shao, H., Chung, J., Balaj, L., Charest, A., Bigner, D. D., Carter, B. S., et al. (2012). Protein Typing of Circulating Microvesicles Allows Real-Time Monitoring of Glioblastoma Therapy. *Nat. Med.* 18 (12), 1835–1840. doi:10.1038/nm.2994

Sharma, S., Zuñiga, F., Rice, G. E., Perrin, L. C., Hooper, J. D., and Salomon, C. (2017). Tumor-derived Exosomes in Ovarian Cancer - Liquid Biopsies for Early Detection and Real-Time Monitoring of Cancer Progression. *Oncotarget* 8 (61), 104687–104703. doi:10.18632/oncotarget.22191

Singha, B., Harper, S. L., Goldman, A. R., Bitler, B. G., Aird, K. M., Borowsky, M. E., et al. (2018). CLIC1 and CLIC4 Complement CA125 as a Diagnostic Biomarker Panel for All Subtypes of Epithelial Ovarian Cancer. *Sci. Rep.* 8 (1), 14725. doi:10.1038/s41598-018-32885-2

Smith, H. O., Berwick, M., Verschraegen, C. F., Wiggins, C., Lansing, L., Muller, C. Y., et al. (2006). Incidence and Survival Rates for Female Malignant Germ Cell Tumors. *Obstet. Gynecol.* 107 (5), 1075–1085. doi:10.1097/01.aog.0000216004.22588.ce

Soung, Y. H., Ford, S., Zhang, V., and Chung, J. (2017). Exosomes in Cancer Diagnostics. *Cancers (Basel)* 9 (1). doi:10.3390/cancers9010008

Sullivan, R., Maresh, G., Zhang, X., Salomon, C., Hooper, J., Margolin, D., et al. (2017). The Emerging Roles of Extracellular Vesicles as Communication Vehicles within the Tumor Microenvironment and beyond. *Front. Endocrinol. (Lausanne)* 8, 194. doi:10.3389/fendo.2017.00194

Sung, H., Ferlay, J., Siegel, R. L., Laversanne, M., Soerjomataram, I., Jemal, A., et al. (2021). Global Cancer Statistics 2020: GLOBOCAN Estimates of Incidence and Mortality Worldwide for 36 Cancers in 185 Countries. *CA A. Cancer J. Clin.* 71 (3), 209–249. doi:10.3322/caac.21660

Suthar, J., Parsons, E. S., Hoogenboom, B. W., Williams, G. R., and Guldin, S. (2020). Acoustic Immunosensing of Exosomes Using a Quartz Crystal Microbalance with Dissipation Monitoring. *Anal. Chem.* 92 (5), 4082–4093. doi:10.1021/acs.analchem.9b05736

Tai, Y. L., Chen, K. C., Hsieh, J. T., and Shen, T. L. (2018). Exosomes in Cancer Development and Clinical Applications. *Cancer Sci.* 109 (8), 2364–2374. doi:10.1111/cas.13697

Tan, F., Leung, P. H. M., Liu, Z.-b., Zhang, Y., Xiao, L., Ye, W., et al. (2011). A PDMS Microfluidic Impedance Immunosensor for *E. coli* O157:H7 and *Staphylococcus aureus* Detection via Antibody-Immobilized Nanoporous Membrane. *Sensors Actuators B: Chem.* 159 (1), 328–335. doi:10.1016/j.snb.2011.06.074

Tang, H.-Y., Beer, L. A., Chang-Wong, T., Hammond, R., Gimotty, P., Coukos, G., et al. (2012). A Xenograft Mouse Model Coupled with In-Depth Plasma Proteome Analysis Facilitates Identification of Novel Serum Biomarkers for Human Ovarian Cancer. *J. Proteome Res.* 11 (2), 678–691. doi:10.1021/pr200603h

Tang, H.-Y., Beer, L. A., Tanyi, J. L., Zhang, R., Liu, Q., and Speicher, D. W. (2013). Protein Isoform-specific Validation Defines Multiple Chloride Intracellular Channel and Tropomyosin Isoforms as Serological Biomarkers of Ovarian Cancer. *J. Proteomics* 89, 165–178. doi:10.1016/j.jprot.2013.06.016

Tiberio, P., Callari, M., Angeloni, V., Daidone, M. G., and Appierto, V. (2015). Challenges in Using Circulating miRNAs as Cancer Biomarkers. *Biomed. Res. Int.* 2015, 731479. doi:10.1155/2015/731479

Valenzuela, S. M., Alkhamici, H., Brown, L. J., Almond, O. C., Goodchild, S. C., Carne, S., et al. (2013). Regulation of the Membrane Insertion and Conductance Activity of the Metamorphic Chloride Intracellular Channel Protein CLIC1 by Cholesterol. *PLoS ONE* 8 (2), e56948. doi:10.1371/journal.pone.0056948

Wang, Y.-F. (2014). Combined Detection Tumor Markers for Diagnosis and Prognosis of Gallbladder Cancer. *Wjg* 20 (14), 4085–4092. doi:10.3748/wjg.v20.i14.4085

Witwer, K. W. (2015). Circulating microRNA Biomarker Studies: Pitfalls and Potential Solutions. *Clin. Chem.* 61 (1), 56–63. doi:10.1373/clinchem.2014.221341

Xie, B., Ding, Q., Han, H., and Wu, D. (2013). miRCancer: a microRNA-Cancer Association Database Constructed by Text Mining on Literature. *Bioinformatics* 29 (5), 638–644. doi:10.1093/bioinformatics/btt014

Yang, H., Li, P., Wang, D., Liu, Y., Wei, W., Zhang, Y., et al. (2019). Quartz Crystal Microbalance Detection of Poly(ADP-Ribose) Polymerase-1 Based on Gold Nanorods Signal Amplification. *Anal. Chem.* 91 (17), 11038–11044. doi:10.1021/acs.analchem.9b01366

Ye, Y., Yin, M., Huang, B., Wang, Y., Li, X., and Lou, G. (2015). CLIC1 a Novel Biomarker of Intraperitoneal Metastasis in Serous Epithelial Ovarian Cancer. *Tumor Biol.* 36 (6), 4175–4179. doi:10.1007/s13277-015-3052-8

Yoshioka, Y., Kosaka, N., Konishi, Y., Ohta, H., Okamoto, H., Sonoda, H., et al. (2014). Ultra-sensitive Liquid Biopsy of Circulating Extracellular Vesicles Using ExoScreen. *Nat. Commun.* 5, 3591. doi:10.1038/ncomms4591

Yu, W., Cui, R., Qu, H., Liu, C., Deng, H., and Zhang, Z. (2018). Expression and prognostic value of CLIC1 in epithelial ovarian cancer. *Exp. Ther. Med.* 15 (6), 4943–4949. doi:10.3892/etm.2018.6000

Zhao, Z., Yang, Y., Zeng, Y., and He, M. (2016). A Microfluidic ExoSearch Chip for Multiplexed Exosome Detection towards Blood-Based Ovarian Cancer Diagnosis. *Lab. Chip* 16 (3), 489–496. doi:10.1039/c5lc01117e

Conflict of Interest: The authors declare that the research was conducted in the absence of any commercial or financial relationships that could be construed as a potential conflict of interest.

Publisher's Note: All claims expressed in this article are solely those of the authors and do not necessarily represent those of their affiliated organizations, or those of the publisher, the editors and the reviewers. Any product that may be evaluated in this article, or claim that may be made by its manufacturer, is not guaranteed or endorsed by the publisher.

frontiers in Bioengineering and Biotechnology

REVIEW
published: 10 February 2022
doi: 10.3389/fbioe.2022.836984

Three-Dimensional Modelling of Ovarian Cancer: From Cell Lines to Organoids for Discovery and Personalized Medicine

Christine Yee[1]*, *Kristie-Ann Dickson*[1], *Mohammed N. Muntasir*[1], *Yue Ma*[1] and *Deborah J. Marsh*[1,2]

[1]Translational Oncology Group, School of Life Sciences, Faculty of Science, University of Technology Sydney, Ultimo, NSW, Australia, [2]Northern Clinical School, Faculty of Medicine and Health, University of Sydney, Camperdown, NSW, Australia

Ovarian cancer has the highest mortality of all of the gynecological malignancies. There are several distinct histotypes of this malignancy characterized by specific molecular events and clinical behavior. These histotypes have differing responses to platinum-based drugs that have been the mainstay of therapy for ovarian cancer for decades. For histotypes that initially respond to a chemotherapeutic regime of carboplatin and paclitaxel such as high-grade serous ovarian cancer, the development of chemoresistance is common and underpins incurable disease. Recent discoveries have led to the clinical use of PARP (poly ADP ribose polymerase) inhibitors for ovarian cancers defective in homologous recombination repair, as well as the anti-angiogenic bevacizumab. While predictive molecular testing involving identification of a genomic scar and/or the presence of germline or somatic *BRCA1* or *BRCA2* mutation are in clinical use to inform the likely success of a PARP inhibitor, no similar tests are available to identify women likely to respond to bevacizumab. Functional tests to predict patient response to any drug are, in fact, essentially absent from clinical care. New drugs are needed to treat ovarian cancer. In this review, we discuss applications to address the currently unmet need of developing physiologically relevant *in vitro* and *ex vivo* models of ovarian cancer for fundamental discovery science, and personalized medicine approaches. Traditional two-dimensional (2D) *in vitro* cell culture of ovarian cancer lacks critical cell-to-cell interactions afforded by culture in three-dimensions. Additionally, modelling interactions with the tumor microenvironment, including the surface of organs in the peritoneal cavity that support metastatic growth of ovarian cancer, will improve the power of these models. Being able to reliably grow primary tumoroid cultures of ovarian cancer will improve the ability to recapitulate tumor heterogeneity. Three-dimensional (3D) modelling systems, from cell lines to organoid or tumoroid cultures, represent enhanced starting points from which improved translational outcomes for women with ovarian cancer will emerge.

Keywords: ovarian cancer, 3D cell culture, 3D bio-printing, organoids, tumoroid, drug screening, personalized medicine

OPEN ACCESS

Edited by:
Dunja Aksentijevic, Queen Mary University of London, United Kingdom

Reviewed by:
Ting-Yuan Tu, National Cheng Kung University, Taiwan
Hermann Frieboes, University of Louisville, United States

***Correspondence:**
Christine Yee
Christine.Yee@uts.edu.au

Specialty section:
This article was submitted to Preclinical Cell and Gene Therapy, a section of the journal Frontiers in Bioengineering and Biotechnology

Received: *16 December 2021*
Accepted: *19 January 2022*
Published: *10 February 2022*

Citation:
Yee C, Dickson K-A, Muntasir MN, Ma Y and Marsh DJ (2022) Three-Dimensional Modelling of Ovarian Cancer: From Cell Lines to Organoids for Discovery and Personalized Medicine. Front. Bioeng. Biotechnol. 10:836984. doi: 10.3389/fbioe.2022.836984

1 INTRODUCTION

Globally, ovarian cancer is the eighth most frequently diagnosed malignancy and cause of cancer-related death in women (Sung et al., 2021). The classification of ovarian cancer includes distinct histological subtypes with varied sites of origin underpinned by defining molecular events affecting tumor suppressors and oncogenes. These events drive specific patterns of clinical behavior characteristic of histotypes, including response to chemotherapeutic agents and molecular target drugs. Malignant histological subtypes arising from epithelial cells include high-grade serous ovarian cancer (HGSOC), ovarian clear cell carcinoma (OCCC), endometrioid ovarian cancer (EnOC), mucinous ovarian cancer (MOC), low-grade serous ovarian cancer (LGSOC) and malignant Brenner cell tumors (Shih Ie and Kurman, 2004; Kurman and Shih Ie, 2010). Ovarian carcinosarcomas (OCS), also known as malignant mixed mullerian tumors (MMMT), have epithelial and mesenchymal components (Harris et al., 2003). Ovarian sex-cord stromal tumors (SCST), the most common of which are granulosa cell tumors (GCT) along with the rarer Sertoli–Leydig cell tumors, are of stromal cell origin (Fuller et al., 2017). An extremely rare subtype of ovarian cancer primarily affecting women under 40 years of age is small cell carcinoma of the ovary, hypercalcemic type (SCCOHT), an ovarian rhabdoid tumor (Auguste et al., 2020).

Almost all HGSOC have a somatic *TP53* mutation and p53 immunohistochemistry is a surrogate marker for *TP53* mutation in these tumors (Bell, 2011; Cole et al., 2016; Köbel and Kang, 2021). *TP53* mutations are also observed in MOC (Köbel and Kang, 2021), ovarian carcinosarcomas (Trento et al., 2020) and less frequently in OCCC (Parra-Herran et al., 2019). *BRCA1* and *BRCA2* mutations occur in HGSOC, including in the germline of affected patients (Alsop et al., 2012), and rarely in patients with OCCC (De Pauw et al., 2021). *ARID1A* and *ARID1B* encode members of the SWI/SNF (SWItch/Sucrose Non-Fermentable) ATP-dependent chromatin remodeling complex important for interaction of this complex with DNA, both genes being mutated in OCCC and endometrioid ovarian cancers (McCluggage and Stewart, 2021). The SWI/SNF complex is also disrupted in the very rare SCCOHT with mutation of *SMARCA4* and epigenetic silencing of *SMARCA2* that encode catalytic subunits important for nucleosome sliding and eviction (Jelinic et al., 2016; Xue et al., 2021). OCCC and endometrioid carcinomas also have in common a disrupted PTEN-PI3K pathway with mutations observed in *PTEN* and *PIK3CA*, as well as mutations in *CTNNB1* (Kuo et al., 2009; Hollis et al., 2020). The RAS/MAPK pathway has been implicated in LGSOC, with mutations identified in *KRAS*, *NRAS,* and *BRAF* (Moujaber et al., 2021). Mutations in the RAS/MAPK pathway are also observed in EnOC (Hollis et al., 2020), OCCC (Kim et al., 2018), and MOC (Cheasley et al., 2021). Adult ovarian GCTs are characterized predominantly by mutation of *FOXL2*, and Sertoli-Leydig Cell Tumors (SLCTs) harbor mutations in *DICER1* (Fuller et al., 2017; De Paolis et al., 2021). Epithelial and stromal cell ovarian cancer histotypes and associated genes known to be mutated are summarized in **Figure 1**.

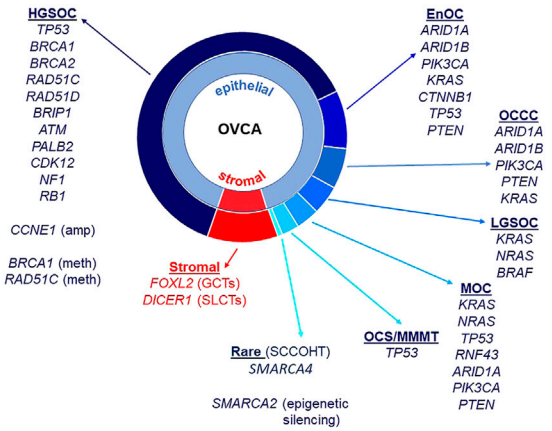

FIGURE 1 | Ovarian cancer histotypes and gene mutations. Epithelial ovarian cancers constitute approximately 90% of all malignant ovarian tumors and are made up of different histotypes: high-grade serous ovarian cancer (HGSOC), endometrioid ovarian cancer (EnOC), ovarian clear cell carcinoma (OCCC), low-grade serous ovarian cancer (LGSOC) and mucinous ovarian cancer (MOC). Ovarian carcinosarcomas (OCS)/malignant mixed mullerian tumors (MMMT) have epithelial and mesenchymal components. Stromal cell tumors include granulosa cell tumors (GCT, adult and juvenile) as well as Sertoli-Leydig cell tumors (SLCTs). Small cell carcinoma of the ovary, hypercalcemic type (SCCOHT) are a rare histotype. Gene mutations, copy number amplifications, methylation and other epigenetic silencing are noted against histotypes.

In addition to mutations, methylation of *BRCA1* is also observed in HGSOC, as is amplification of *CCNE1* (Bell, 2011; Patch et al., 2015). Along with defects in *BRCA1* and *BRCA2*, other genes that function in homologous recombination repair (HRR) are mutated in ovarian cancer, albeit at lower frequencies, including *RAD51C*, *RAD51D*, *BRIP1*, *PALB2,* and *ATM* (Pennington et al., 2014). Defects in HRR can lead to the presence of "genomic scars" caused by the cancer cell's inability to accurately repair sites of double strand breaks (DSBs). These include extensive loss of heterozygosity (LOH), large scale transitions (LST) and telomeric allelic imbalance (TAI) (Watkins et al., 2014; Chao et al., 2018; Nguyen et al., 2020). Tumors with defects in HRR are responsive to poly adenosine diphosphate-ribose polymerase inhibitors (PARPis), functioning in a synthetic lethal manner to inhibit repair of single strand breaks *via* the base excision repair pathway (Dedes et al., 2011). As a predictive DNA marker of defective HRR, genomic scars are helpful, but not all tumors with a genomic scar will respond to a PARPi. Reasons for this include reversion of a *BRCA* mutation, occurrence of a secondary mutation that restores wild-type function or changes in methylation patterns of an HRR gene that in effect functionally restores HRR but the genomic scar remains (Patch et al., 2015). Functional analyses, alongside molecular assays, are required to confirm the predicted response of women with ovarian cancer to PARPis such as the FDA-approved drugs olaparib, niraparib and rucaparib (Dickson et al., 2021; Lee et al., 2021; Valabrega et al., 2021).

Predicting which women will respond to a PARPi is particularly important given the unprecedented improvement

seen in Progression Free Survival (PFS) and Overall Survival (OS) for subsets of women administered these drugs, including as maintenance therapy (Audeh et al., 2010; Ledermann et al., 2012; Ledermann J. et al., 2014; Moore et al., 2018). Ovarian cancers with germline or somatic mutation of *BRCA1* or *BRCA2*, mutation of *RAD51C* or *RAD51D*, methylation of *BRCA1,* or high LOH have all been reported to respond to PARP inhibition (Audeh et al., 2010; Wang et al., 2012; Ledermann J. et al., 2014; Kondrashova et al., 2017; Swisher et al., 2017; Moore et al., 2018). Furthermore, loss of *RAD51C* methylation has recently been implicated as a mechanism of PARPi resistance (Nesic et al., 2021). The combination of molecular testing and functional analyses conducted in robust tumor or ascites models has the power to strongly predict whether a woman is likely to respond to a PARPi at each stage of her disease progression.

Unlike for PARPis, there are no clinically approved biomarkers to predict responses of women with ovarian cancer to the anti-angiogenic bevacizumab, although numerous studies have focused on this area (Buechel et al., 2021; Gao et al., 2021; Hsu et al., 2021). Given the advances seen in PFS and OS of some women receiving this monoclonal antibody that targets vascular endothelial growth factor (VEGF), development of functional assays to predict the likelihood that a woman will respond to bevacizumab would represent a major advance (Burger et al., 2011; Perren et al., 2011; Oza et al., 2015).

The majority of women with HGSOC will respond initially to carboplatin, although some tumors display innate platinum resistance (Davis et al., 2014). There are no robust markers to predict response to platinum drugs, including through the development of acquired chemoresistance, although defects in HRR in primary tumors have been associated with a more favorable response (Konstantinopoulos et al., 2010; Muggia and Safra, 2014). The use of platinum drugs in histotypes other than HGSOC must be questioned given frequent low response rates. Only 11–27% of OCCC respond initially to platinum therapy, dropping to only 1-2% response rates in recurrent disease (Sugiyama et al., 2000; Mabuchi et al., 2016; Tan et al., 2019). LGSOC also display a poor response to platinum drugs; however, the presence of activating mutations in mitogen-activated protein kinase (MAPK) pathway genes *KRAS*, *BRAF,* and *NRAS* has seen favorable responses in LGSOC with the MEK inhibitor trametinib (reviewed in Moujaber et al. (2021)).

The mutations and genomic variations described above offer opportunities to develop new molecular-based therapeutic strategies to treat ovarian cancer subtypes. Some molecular events, such as those described in the HRR pathway, are already being targeted clinically by FDA-approved PARPis. For both discovery science and translational approaches to predicting which women are likely to benefit from which therapies, robust models are needed that expand upon traditional 2D cell culture and pre-clinical models, and include both molecular profiling and functional analyses. In this review, we discuss methods of 3D modelling that are either currently being employed in ovarian cancer cell lines, primary or metastatic tumor tissue and ascites, or have the potential to be used into the future for these purposes.

2 THE MICROENVIRONMENT–CONSIDERATIONS WHEN MODELLING OVARIAN CANCER

2.1 Sites of Origin of Ovarian Cancer

There are numerous factors to examine when considering the microenvironment that supports the initiation, development and metastasis of ovarian cancer, not least being the very first microenvironment of these malignancies and that is the site of origin of the initial lesion. Many, perhaps most, HGSOC originate in the fallopian tube as Serous Tubal Intraepithelial Carcinomas (STICs), shedding onto the surface of the ovary and establishing a tumor (Crum et al., 2007; Karst et al., 2011; Perets and Drapkin, 2016; Zhang et al., 2019). This discovery has led to the generation of important models of non-cancerous fallopian tube epithelial cells transformed with c-Myc, H-Ras^{V12} or SV40 large T antigen (SV40 TAg) (Karst et al., 2011; Perets and Drapkin, 2016). These models complement those of normal ovarian surface epithelial (OSE) cells immortalized with factors including SV40 Tag, human telomerase (hTERT) and HPV-E6/E7 (Tsao et al., 1995; Davies et al., 2003; Kalli et al., 2004; Shin et al., 2018). OCCC and EnOC have been associated with endometriosis (Samartzis et al., 2020). While MOC has previously been reported as originating from metastatic deposits of primary tumors of the colon, stomach, pancreas and uterus, evidence now shows that these tumors do in fact arise in the ovary following a progression model commencing with benign and borderline precursor lesions (Ledermann J. A. et al., 2014; Cheasley et al., 2019). While constituting ~10% of all ovarian cancers, tumors arising in ovarian stromal cells have different considerations. In contrast to epithelial cell tumors, the sex cord stromal tumor GCT arise in granulosa cells that produce estrogen (Jamieson and Fuller, 2012). Knowledge of the sites of origin of ovarian tumors is imperative to ensure selection of models that best address both research questions and translational approaches.

2.2 The Ovarian Cancer Microenvironment and Metastatic Spread

The microenvironment of an ovarian cancer consists of both tumor and non-tumor cells, including immune cells. Patient-derived organoids or tumoroids retain cellular heterogeneity and immune cells, thus are able to more strongly recapitulate a three-dimensional (3D) tumor microenvironment *ex vivo* compared to homogeneous cell lines (Hill et al., 2018; Kopper et al., 2019). Ovarian tumoroid cultures have been established from both ascitic fluid and primary tumors, to date primarily from the more common HGSOC but also from LGSOC, MOC, OCCC, and EnOC (Hill et al., 2018; De Witte et al., 2020; Nanki et al., 2020). These models show great promise for conducting *ex vivo* drug assays to predict therapeutic response in the women from which they were established (De Witte et al., 2020; Maenhoudt et al., 2020; Nanki et al., 2020; Gorski et al., 2021).

Given the location of ovaries, there are no anatomical barriers preventing metastasis to organs in the pelvic cavity including the

TABLE 1 | Ovarian cancer cell line origin, *in vivo* growth and classifications.

Cell line	OvCa Histotype	Specimen site	Growth *in vivo* in mice	Commercial availability	References
CaOV-3	HGSOC[a,b,d]	Ovary tumor	Yes: IP; No: SC, IB	ATCC	Buick et al. (1985) [f]; Hernandez et al. (2016) [g]
CaOV-4	HGSOC[a,c,d]	Fallopian tube metastasis	Yes: SC, IP, IB	ATCC	Hernandez et al. (2016) [g]
COV318	HGSOC[a,d,e]	Ascites	No: SC, IP	ECACC	van den Berg-Bakker et al. (1993) [f]; De Haven Brandon et al. (2020) [g]
COV362**	HGSOC[a,d]	Pleural effusion	Yes: IP, forms ascites and IB; No: SC	ECACC	van den Berg-Bakker et al. (1993) [f]; De Haven Brandon et al. (2020) [g]
KURAMOCHI	HGSOC[a,b,d]	Ascites	Yes: SC; No: IP, IB	JCRB	Motoyama (1981) [f]; De Haven Brandon et al. (2020) [g]
OAW28	HGSOC[a,d]	Ascites	Unknown	ECACC	Wilson et al. (1996)
OV202	HGSOC	Primary tumor	Unknown	No	Conover et al. (1998) [f]
OVCAR-3	HGSOC[a,b,d,e]	Ascites	Yes: SC, IP	ATCC	Hamilton et al. (1983) [f]; Hernandez et al. (2016) [g], De Haven Brandon et al. (2020) [g]
OVCAR-4	HGSOC[a,d]	Ascites	Yes: SC, IP; No: IB	MERCK Millipore	Pirker et al. (1985) [f]; Hernandez et al. (2016) [g]; De Haven Brandon et al. (2020) [g]
OVKATE	HGSOC[a,d,e]	Solid metastasis	Yes: SC, IP	JCRB	Yanagibashi et al. (1997) [f,g]; Mitra et al. (2015b) [g]
OVSAHO	HGSOC[a,d,e]	Solid metastasis	Yes: SC; Yes: IP, forms ascites	JCRB	Yanagibashi et al. (1997) [f,g]; De Haven Brandon et al. (2020) [g]
PEO1	HGSOC[c]	Ascites	No	ECACC	Langdon et al. (1988) [f]; Hernandez et al. (2016) [g]
PEO4	HGSOC[c]	Ascites	No	ECACC	Langdon et al. (1988) [f], Hernandez et al. (2016) [g]
UWB1.289	HGSOC[c]	Ovary tumor	No: SC, IP	ATCC	DelloRusso et al. (2007) [f]; Mitra et al. (2015b) [g]
UWB1.289 + BRCA1	HGSOC[c]	Ovary tumor	Unknown	ATCC	DelloRusso et al. (2007) [f]
A2780*	EnOC[a,b,c,d]	Tumor tissue	Yes: SC and IP, forms ascites	ECACC	Behrens et al. (1987) [f]; Hernandez et al. (2016) [g]
TOV-112D	EnOC[b,d,e]	Ovary tumor	Yes: IP; No: SC	ATCC	Provencher et al. (2000) [f]; Hernandez et al. (2016) [g]
OVISE	OCCC[a,b,d,e]	Solid pelvic metastasis	Yes: SC; No: IP	JCRB	Gorai et al. (1995) [f]; Yanagibashi et al. (1997) [f,g]
OVMANA	OCCC[a,b,d,e]	Primary tumor	Yes: SC; No: IP	JCRB	Yanagibashi et al. (1997) [f,g]
OVTOKO	OCCC[a,b,d,e]	Solid splenic metastasis	Yes, SC; Yes: IP	JCRB	Gorai et al. (1995) [f]; Yanagibashi et al. (1997) [f,g]
RMG-I	OCCC[a,d,e]	Ascites	Yes: SC	JCRB	Nozawa et al. (1991) [f]; Kashiyama et al. (2014) [g]
TOV-21G	OCCC[a,b,d,e]	Ovary tumor	Yes: SC	ATCC	Provencher et al. (2000) [f]; Kashiyama et al. (2014) [g]
MCAS	MOC[b,e]	NS	Yes: SC	JCRB	Kidera et al. (1985) [f]; Sato et al. (2012) [g]
RMUG-S	MOC[d,e]	Ascites	Yes: SC, IP	JCRB	Sakayori et al. (1990) [f]; Sato et al. (2012) [g]; Matsuo et al. (2011) [g]
KGN	GCT	Tumor tissue	Unknown	RIKEN BRC	Nishi et al. (2001) [f]
COV434***	SCCOHT	Primary tumor	Unknown	No	van den Berg-Bakker et al. (1993) [f]; Karnezis et al. (2021)

Note: Cell lines identified with >50 publications via PUBMED, on 10/12/2021.

OvCa, Ovarian Cancer; NS, Not specified; ATCC, American Type Culture Collection; JCRB, Japanese Cancer Research Resources Bank; ECACC, European Collection of Authenticated Cell Cultures; RIKEN BRC, RIKEN, BioResource Center Cell Bank; SC, subcutaneous; IP, intraperitoneal; IB, intrabursal.

**Originally classified HGSOC,*

***Originally classified EnOC,*

****Originally classified as a GCT (Granulosa Cell Tumor),*

Recent classification of histotypes.

[a]*Domcke et al. (2013),*

[b]*Anglesio et al. (2013),*

[c]*Beauford et al. (2014),*

[d]*Barnes et al. (2021),*

[e]*Papp et al. (2018).*

[f]*Original histotype reference,*

[g]in vivo *tumour growth in mice reference.*

EnOC, Endometrioid Ovarian Cancer; OCCC, Ovarian Clear Cell Carcinoma; MOC, Mucinous Ovarian Cancer; HGSOC, High Grade Serous Ovarian Cancer; SCCOHT, Small Cell Carcinoma of the Ovary, Hypercalcemic Type.

uterus, bladder, rectum, and small intestine, as well as beyond the peritoneal cavity to organs such as the liver and lung (Motohara et al., 2019). Ovarian cancer cells detach from the primary tumor and are attracted to adipose-rich omental tissue. They disseminate by forming aggregates of multicellular spheroids that float in malignant ascitic fluid alongside fibroblasts, adipocytes, mesothelial, endothelial and inflammatory cells, as well as cell-free DNA, before "seeding" onto new microenvironments and establishing metastatic deposits (Ford et al., 2020). Given that many commercially available ovarian cancer cell lines are in fact established from ascites rather than primary tumors (**Table 1**, **Supplementary Tables S1,S2**) consideration should be given to including these cell types when establishing three dimensional models of ovarian cancer.

This is especially relevant for the study of ovarian cancer cell metastasis. An example of this is the organotypic model used by Ford and colleagues to determine the ability of ovarian cancer cell lines undergoing depletion of genes of interest to metastasize and adhere to omental-type tissue (Henry et al., 2017).

3 OVARIAN CANCER CELL LINE MODELS

To date, the majority of *in vitro* studies in ovarian cancer have relied on the use of 2D cell culture of immortalized cell lines derived from primary ovarian cancers, pleural effusion, ascitic fluid from the peritoneal cavity or a distant metastatic site. Many cell lines have been well characterized morphologically and molecularly and, when able to be tested, maintain unique features of their derivative sample. Several studies have attempted to determine "the best" ovarian cancer cell line models for investigators to use for both fundamental discovery science and translational projects (Anglesio et al., 2013; Domcke et al., 2013; Beaufort et al., 2014; Papp et al., 2018; Barnes et al., 2021). Comparison of the molecular profiles of ovarian cancer cell lines with that of primary tumors has led to the histotype reclassification of a number of frequently used ovarian cancer cell lines, including SK-OV-3 and A2780. Still, there remains conflicting reports in the field as to the accuracy of some ovarian cancer cell lines. We have summarized the current state of knowledge of site and histotype origin of a group of ovarian cancer cell line models, as well as models of normal cells representing sites of origin (**Table 1**, **Supplementary Tables S1–S3**).

With the exception of the PEO series of HGSOC, few ovarian cancer cell line models allow insight into the development and progression of ovarian cancer (Langdon et al., 1988). The PEO1 drug sensitive cell line has the pathogenic *BRCA2* mutation, c.5193C > G, derived after initial treatment with cisplatin, 5-Fluorouracil (5-FU) and chlorambucil. The PEO4 cell line represents malignant cells after the patient developed chemoresistance, having a secondary *BRCA2* reversion mutation which restores wild-type BRCA2 function. The PEO6 cell line was collected from the same patient before death (Langdon et al., 1988). Other ovarian cancer cell lines have been made resistant to cisplatin *in vitro*, including A2870/A2780CisR (Behrens et al., 1987), TYK-nu/TYK-nu.CP-r (Yoshiya et al., 1989) and CaOV3/CaOV3CisR (Joshi et al., 2021). The A2780/A2780VeliR lines were made resistant *in vitro* to the PARPi veliparib (Dickson et al., 2021). Still, often phenotypes such as drug response observed *in vitro* have been unable to mirror *in vivo* models, likely due to factors missing in the tumor microenvironment that are absent from homogeneous cell lines cultures such as stromal and immune cells (Beaufort et al., 2014).

Ovarian cancer cell lines show variable ability to grow in nude mice when implanted either subcutaneously (SC), intraperitoneally (IP) or intrabursally (Hernandez et al., 2016). Further, while some cell lines grow well in both SC and IP locations, others show a strong propensity to grow in one location only, suggesting a preference for a particular microenvironment. Ovarian cancer cell lines demonstrated to grow in mice are noted in **Table 1** and **Supplementary Tables S1,S2**.

4 MOUSE MODELS OF OVARIAN CANCER

Animal models continue to be the most physiologically relevant pre-clinical models to study disease pathogenesis and drug response, encompassing a whole-body system, including immune system, tumor microenvironment and vascularization. A number of non-mammalian models including fruit flies, the African clawed frog (*Xenopus*) and the laying hen, have been utilized for the study of ovarian cancer development (reviewed by (Johnson and Giles, 2013; Rosales-Nieves and González-Reyes, 2014; Bernardo et al., 2015; Tudrej et al., 2019)). The most widely used mammalian model is the mouse (*Mus musculus*), sharing 85 percent protein-encoding gene homology with humans (Makałowski et al., 1996), although concerns with translatability of disease mechanisms and drug responses between species remain. Further, the natural occurrence of ovarian cancer is low in the aging mouse, with rapid progression times contrasting with the development of human ovarian cancer (Sale and Orsulic, 2006). Nevertheless, genetically engineered mouse (GEM) models, syngeneic and patient-derived xenograft (PDX) models have enabled a greater understanding of ovarian cancer development and treatment responses.

4.1 GEM and Syngeneic Models

GEM models have enabled specific gene knockout to be modelled in a whole-body system, contributing to the understanding of individual and combinations of genes commonly mutated in ovarian cancer. Conditional knockout mice, using the Cre-lox system for cell type specificity, have been used to reproduce oncogenic mutations and HR defects to study ovarian cancer development and responses to clinically relevant treatments such as platin-based drugs and PARPis (Szabova et al., 2012; Perets et al., 2013; Szabova et al., 2014; Zhai et al., 2017). Extensive overviews of GEM models of ovarian cancer have been published in recent years, highlighting comparisons and translatability to the human condition (Stuckelberger and Drapkin, 2018; Maniati et al., 2020; Zakarya et al., 2020). Syngeneic mouse models transplant mouse cell lines into a recipient from the same genetic background, enabling the study of immune response, immunotherapies and tumor vascularization (Zhang et al., 2002; Yu et al., 2018). The murine ID8 ovarian cancer cell line (C57Bl/6 background) (Roby et al., 2000), has been used for a number of syngeneic mouse models, achieving primary ovarian tumors and ascites within 90 days (Greenaway et al., 2008). This model has also been used to study metastasis and immune infiltrates at the trocar site, where an incision is made into the abdomen for laparoscopic surgery (Wilkinson-Ryan et al., 2019). Injection with M0505 cells (derived from spontaneously transformed OSE of FVB/N mice) resulted in Pax8+ tumors with similar histology to human HGSOC (McCloskey et al., 2014). Generation of multiple fallopian tube epithelial cell lines with combinations of common mutations in HGSOC (*Tp53*, *Brca1*, *Brca2*, *Ccne1*,

Akt2, *Brd4*, *Smarca4*, *Kras*, *Myc*, *Nf1*, and *Pten*) using CRISPR/Cas9 recapitulated histopathological and clinical features observed in HGSOC patients, such as ascites and peritoneal metastases (Iyer et al., 2021). Overall, GEM and syngeneic models have proven their value for discovery studies and research into the origin of ovarian cancer.

4.2 Patient-Derived Xenograft Models

PDX models are the most useful *in vivo* model for testing response to targeted therapies of primary tumors attributed to their unique molecular profiles, to enable a precision medicine approach. The major advantage of using PDX models is the ability to reproduce histology of the human tumor (Colombo et al., 2015), although alterations in steroid hormone receptors and immune response genes have been reported, irrespective of the maintained mutational profile (Dong et al., 2016). Another advantage of PDX models is that they bypass the *in vitro* culture of tumor cells that may inadvertently drive phenotype divergence from the original tumor (Siolas and Hannon, 2013).

Limitations of primary tumor tissue implanted heterotypically into immunodeficient mice include the inability to recapitulate immune responses, site-specific tumor microenvironment interactions and lastly, that the tumor may not metastasize (Jin et al., 2010). The general methodology of producing PDX models requires multiple *in vivo* passages, leading to extended model creation times (Morton and Houghton, 2007). The reported engraftment rate can be variable and heavily influenced by ovarian cancer histotype; treatment history; stage and site of malignancy, with higher engraftment rates observed in non-epithelial histotypes (Wu et al., 2019). Platinum resistance has also been found to predict PDX engraftment success, with successful engraftment correlating with shorter PFS and OS of the derivative patient (Heo et al., 2017).

An extensive review of ovarian cancer PDX models by Scott et al. (2013), highlighted a number of gaps in the field related to variations in methodologies, genetic stability over multiple generations, representation of few ovarian cancer histotypes and the limitation of using immunocompromised mice as hosts. More recent developments have addressed some of these concerns, with higher rates of successful engraftment and propagation of rarer ovarian cancer histotypes such as LGSOC (De Thaye et al., 2020) and MOC (Ricci et al., 2020) as well as evaluation of drug responses for homologous recombination deficient (HRD) mutated ovarian cancers (George et al., 2017) and enabling the evaluation of immunotherapies through the use of humanized mouse models (Odunsi et al., 2020). Furthermore, the ability to label tumor cells with luciferin prior to transplantation has enabled tumor growth tracking *via* bioluminescence imaging (Liu et al., 2017).

5 3D *IN VITRO* OVARIAN CANCER MODELS

Two-dimensional (2D) growth of cancer cells as monolayers may fail to recapitulate aspects of the derivative cell behavior and morphology. Differential drug responses in 2D *versus* 3D cultures have been observed in many *in vitro* models of cancer, including ovarian cancers. Previously, high costs of materials, significant manual labor and low levels of reproducibility and matrix tunability rendered 3D culture models less favorable to 2D, irrespective of their higher physiological relevance (Jensen and Teng, 2020). Recent technological advances have enabled higher degrees of control over the creation of 3D cell cultures in areas including matrix stiffness and composition, spatial orientation and creation in an automated and high-throughput manner.

A number of different methodologies and techniques are being used in order to more efficiently create 3D cell culture models of cancer, including ovarian cancers. While there is still no "perfect" 3D *in vitro* model that can replace *in vivo* preclinical models, methodological advances are moving the field towards more accurate representations of human tumors, including in regards to drug response. Further, efforts towards creation of high-throughput *in vitro* and *ex vivo* models for drug screening have been a focus in recent years, and will eventually replace 2D cultures. An overview of techniques used to create 3D *in vitro* ovarian cancer models and their considerations is summarized in **Table 2**.

5.1 Scaffold-Free Models

5.1.1 Liquid Overlay Techniques

Liquid overlay techniques, such as the use of ultra-low attachment (ULA) plates or low-attachment coatings enable spheroid formation attributed to the hydrophilic properties of the neutrally charged polystyrene plastic or polymer coating, causing cells to adhere to each other rather than on a 2D surface. By preventing attachment to a surface, use of low attachment plates and coatings present a cost-effective and timely method for spheroid formation or maintenance of existing spheroid structures. Two methods have been used extensively for ovarian cancer spheroid culture to identify mechanisms of progression and various stages of disease, from primary tumor modelling to the generation of spheroids of metastatic ascites. The attachment and disaggregation of these spheroids on top of an ECM or in an immunodeficient mouse also allows assessment of the metastatic potential of the cancer.

5.1.1.1 Flat-Bottomed Ultra-Low Attachment Plates and Low Attachment Coatings

The use of flat-bottomed ULA plates (**Figure 2**) enables heterogenous multicellular aggregate formation from cell suspensions of adherent cells and can be used for short-term maintenance of primary ascites-derived spheroids. This method is often combined with secondary metastatic invasion assays involving the transfer of spheroids to regular tissue culture plastic plates or onto an extracellular matrix (ECM).

Culture of ovarian cancer cell lines in ULA plates as "ascitic" spheroids has been used as a model to investigate the efficacy of an oncolytic virus-based therapeutic on ovarian cancer metastasis (Tong et al., 2015). Patient-derived ovarian cancer ascites cells, when maintained on ULA plates, demonstrated epithelial-mesenchymal transition (EMT) during spheroid formation (Rafehi et al., 2016). Patient-derived solid-tumor and ascites-

TABLE 2 | Advantages and disadvantages of common 3D *in vitro* models of ovarian cancer.

Model type	Technique	Advantages	Disadvantages
Scaffold-free	Liquid overlay—Flat-bottom plates	Fast spheroid generation	Heterogenous spheroids No cell-ECM interactions
	Liquid overlay—Round-bottom plates	Fast spheroid generation May replicate necrotic core	May require Matrigel for cell-cell adhesion No cell-ECM interactions
	Hanging drop	High homogeneity Fast spheroid generation	Difficulties with media change, drug addition No cell-ECM interactions
Scaffold-based—Natural hydrogels	Matrigel	High biocompatibility Integrin interactions Commercially available Mimics basement membrane ECM Enables organoid propagation	Not human derived Limited control of mechanical properties Temperature dependent stability Batch-to-batch variation
	Collagen-I	High biocompatibility Enhances mesenchymal traits Variety of sources (animal, marine)	Not human derived Limited control of mechanical properties
	Alginate	High biocompatibility Low immunogenicity Can be combined with other biomaterials	Stiffness modulated by multivalent cations (possible cytotoxicity) No cell-ECM interaction
	Agarose and Agar	High biocompatibility	Innately inert for cell adhesion studies
Scaffold-based—Synthetic hydrogels	Polyethylene glycol (PEG)	Tunable stiffness Low batch-to-batch variation Able to be used as bioink for bioprinting	Requires biofunctionalization
	Gelatin methacryloyl (GelMA)	High biocompatibility Innate RGD and MMP cleavability	UV photocrosslinking may cause DNA damage
	Peptide-based e.g. RADA16-I	Defined nanofibers Highly engineerable Self-assembling	Low mechanical strength
Decellularized ECM		High biocompatibility Retention of native ECM and growth factors	Limited control of mechanical properties Donor heterogeneity
Organotypic omental mesothelial model		Modelling metastasis to omentum Organotypic co-culture	Reliance on primary cells (when used) No vasculature
Organoids		Maintenance of patient mutational profile and tumor histology Can be biobanked Can predict patient responses CRISPR-editable	No vasculature Loss of stromal and immune cells in longer-term culture Varied success rates
3D Bioprinting	Droplet	High-throughput High precision	High equipment cost Limited compatible bioinks
	Extrusion	Compatible with multiple ECM types	Low-throughput Potential for cell stress during extrusion process Low precision
Bioreactors	Rotating wall vessel	Mimic microgravity and transcoelomic metastases	Only spheroid culture
	Orbital shakers	Spheroid formation studies Maintenance of patient-derived explants	Only spheroid culture
	Compressive stress	Hydrostatic compression stress	Not commercially available
	Tumor-on-a-chip	Model shear stress on EMT Able to control drug or nutrient gradients	Short-term culture Potential variation between in-house fabricated devices

Note: ECM, extracellular matrix; MMP, matrix metalloproteinase; UV, ultraviolet; EMT, epithelial-mesenchymal transition.

derived ovarian cancer cell lines both form spheroids similar to those found in patient ascites when grown on ULA plates, and were shown to be self-renewing through serial passaging over a 6-month period (Yamawaki et al., 2021). Patient-derived spheroids were also more tumorigenic in immunodeficient mice, more stem-like and more invasive than their parental cell line (Liao et al., 2014). A direct comparison of cisplatin and paclitaxel sensitive and resistant A2780 cells grown as 2D monolayers

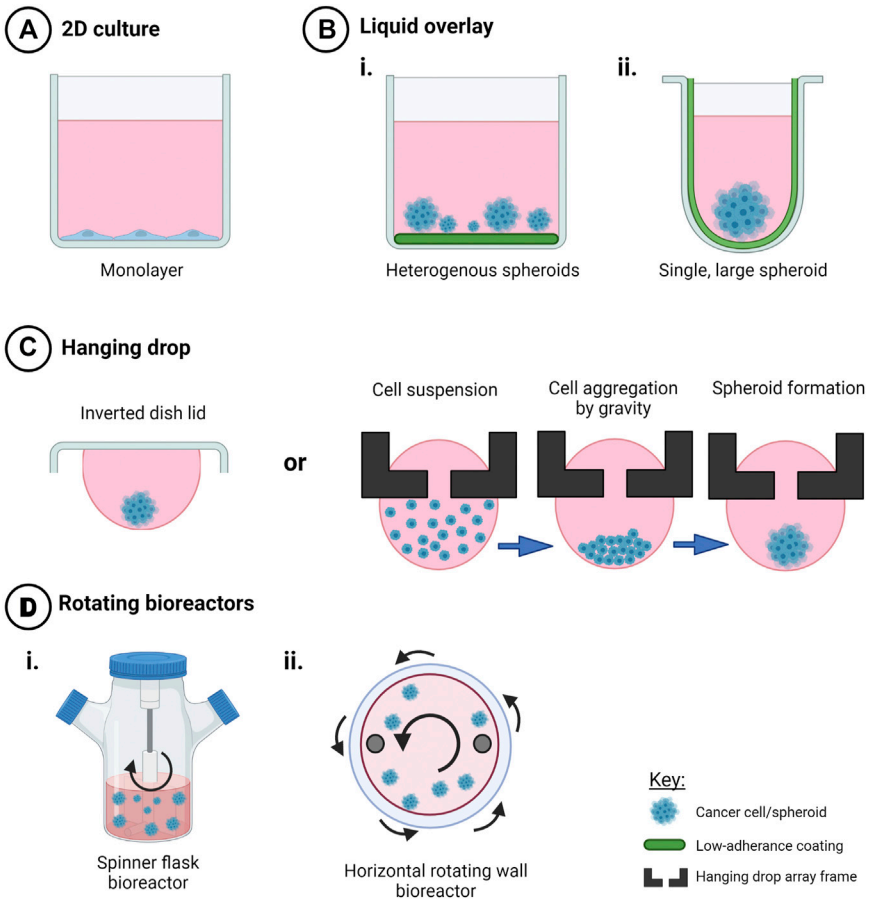

FIGURE 2 | Techniques to create scaffold-free 3D *in vitro* cancer models. Creation of 3D cell models in the absence of scaffolds promotes cell-cell interactions in three dimensions that mediate cell behavior and drug response when compared to **(A)** 2D monolayers. Use of **(B)** liquid overlay techniques with i) flat or ii) round-bottomed ULA plates **(C)**, hanging drop techniques and **(D)** rotating bioreactors such as i) spinner flasks and ii) horizontal rotating vessels have been used as time and cost-effective spheroid creation methods or to investigate drug response and other factors that my influence ovarian cancer progression, such as fluid shear stress and hypoxia. Created with Biorender.com.

versus 3D aggregates formed in ULA plates, identified gene expression changes attributed to conformation that may lead to drug resistance (Nowacka et al., 2021).

Poly(2-hydroxyethyl methacrylate), known as poly-HEMA, is a non-ionic polymer coating that discourages the formation of ECM and creates a low-adhesion environment that favors spheroid formation (Ivascu and Kubbies, 2006). A poly-HEMA coating in culture flasks has been used for the production of 3D heterotypic models of normal ovary and to study early ovarian cancer development (Lawrenson et al., 2012). Ovarian cancer cell lines grown under poly-HEMA conditions in the presence of activated platelet releasate, formed spheroids faster and were more resistant to the chemotherapeutic agents cisplatin, carboplatin and paclitaxel (Casagrande et al., 2021).

While flat-bottomed, ULA plates and non-adherent coatings present a cost-effective method for production and maintenance of ovarian cancer spheroids, these methods result in heterogenous spheroid morphologies which may impact on downstream analysis, reproducibility and drug response. As such, we suggest that this method is best suited for investigations into drivers of spontaneous spheroid formation.

5.1.1.2 Round-Bottomed ULA Plates

The use of round-bottomed ULA plates (**Figure 2**) facilitates single spheroid formation by gravity, and is often supplemented with ~2% Matrigel to fast track cell aggregations over periods of time less than 72 h. This method allows high consistency between replicates from a cell line or patient sample, as well as facilitating the ability to section and morphologically analyze biologically-relevant structures. Formation of single large spheroids (>500 µm diameter) enables the formation of a hypoxic core, and drug, oxygen and metabolite gradients that mimic solid tumor physiology (Vinci et al., 2012; Heredia-Soto et al., 2018).

The use of round-bottomed, ULA plates have assisted in the identification of Nectin-4 as essential for adhesion events in early spheroid formation of HGSOC cell lines, and as potential targets to improve chemotherapeutic sensitivity (Boylan et al., 2020). Pre-formed OVCAR-8 spheroids grown in round-bottomed ULA plates and further embedded as single spheroids in Matrigel,

developed vascularization after subcutaneous transplantation into athymic nude mice, enabling the evaluation of therapeutics such as the anti-angiogenic bevacizumab and the nano-drug Doxil® (Singh et al., 2020).

This method of spheroid formation has been utilized for speed, reproducibility and commercial availability, although spheroid morphology and overall size may differ due to intrinsic cell line-related characteristics. In a comparison of hanging drop arrays, liquid overlay on ULA plates and liquid overlay on ULA plates with a nutator device to produce three dimensional agitation, both the hanging drop and ULA plates with agitation demonstrated higher cellular compaction, higher ECM content and increased resistance to cisplatin compared with cultures on liquid overlaid ULA plates only (Raghavan et al., 2016). Addition of agitation may improve the comparability to other scaffold-free spheroid formation techniques, although this is yet to be tested on primary ovarian cancer cells.

5.1.2 Hanging Drop Techniques

Hanging drop cultures rely on surface tension and gravity to form homogenous, multicellular spheroid/aggregate cultures without the need for specialized equipment (**Figure 2**). Suspended cells in media are seeded either on the lid of a culture dish or in hang drop vessels, gather at the base of the droplet by gravity, aggregate by cell-cell integrin bridges and further mature by cell-mediated contraction to form compact spheroids within days (Sodek et al., 2009).

The hanging drop technique has been used in numerous studies investigating ovarian cancer morphology and phenotypes. The simplicity of the model has enabled it to act as a "low-stiffness" model as compared to traditional polystyrene plastic culture dishes (Mieulet et al., 2021). An advantage of this technique, particularly for low-volume primary tumor samples, is the formation of spheroids within days with high viability. Further, cell numbers as low as 10 cells per droplet will form spheroids that are uniform in both volume and circularity, amenable to many downstream analyses including high throughput analysis of drug responses (Raghavan et al., 2015).

The use of the hanging drop technique has led to the identification of mechanisms that promote ovarian cancer progression, chemoresistance and recurrence. A study of six ovarian cancer cell lines found a positive relationship between EMT status, spindle-like morphology and compactness of the formed spheroid, with more mesenchymal ovarian cancer cells exhibiting greater invasive and chemoresistant phenotypes (Sodek et al., 2009). Serial passaging of OVCAR-3 and ascites-derived spheroids in the hang drop system showed increasing stemness, proliferation, resistance to cisplatin and tumorigenicity *in vivo* with passage age (Ward Rashidi et al., 2019). Using a high-throughput 384-well hang drop array culture, increasing spheroid size and cell count was associated with resistance to cisplatin in A2780 and OVCAR-3 cells, which has impact particularly in ascitic spheroids escaping chemotherapeutic treatment (Raghavan et al., 2015). The stem-like changes and chemoresistance observed in this simple, multicellular spheroid model that would not be observed in traditional 2D cultures, emphasizes the importance of three-dimensional cell-cell interactions when modelling drug response. 3D heterotypic multicellular tumor spheroids generated by the hanging-drop technique using the cell lines HEY or SK-OV-3 in co-culture with the mouse fibroblast line NIH3T3, were used to identify off-target effects of drugs targeting cancer cells relative to neighboring stromal cells (Weydert et al., 2020).

While simple in design, using the hanging drop technique for spheroid creation has logistical issues with media replacements, drug addition, evaporation and downstream analysis of individual spheroids per hanging drop (Kunz-Schughart et al., 2004; Mehta et al., 2012). These models are therefore limited to short-term culture and require frequent attention. Improvements to the efficiency and reproducibility of this method include development of hanging drop arrays for use with liquid handling robotics and single cell seeding in nanoliter-sized wells in a microchip format (Raghavan et al., 2015; Ganguli et al., 2021). Creation of an open-source, 3D printable multi-purpose hanging drop "dripper" for use with standard tissue culture plates enables metastasis and migration assays as well as co-cultures of cells within the same plate (Zhao L. et al., 2019).

5.2 Scaffold-Based Hydrogel Models

Inclusion of scaffolds in 3D multicellular *in vitro* models of ovarian cancer adds another level of model complexity, allowing for the recreation of the physical and mechanical tumor microenvironment that can influence ovarian cancer cell behavior. Several methodologies pertaining to the use of scaffolds relevant to ovarian cancer are described here and in **Figure 3**.

5.2.1 Natural Scaffolds

Naturally derived ECM hydrogels such as Matrigel, collagens, alginate, and agarose have been favored in 3D cell culture models due to their history of high biocompatibility with various cell types, including ovarian cancer cell lines and tumor organoids, although they are limited in their mechanical tunability and composition consistency.

5.2.1.1 Matrigel

Matrigel, derived from the murine Engelbreth-Holm-Swarm (EHS) sarcoma, has been used for over 40 years as a mimic for the basement membrane and a structural support for many cell types (Orkin et al., 1977). The major constituents of this ECM are laminins, collagen IV, entactin, and the heparin sulfate proteoglycan perlecan (Hughes et al., 2010), though ratios often differ by batch, raising the need for caution when interpreting results of cells cultured in Matrigel (Vukicevic et al., 1992). Matrigel or EHS matrix may also contain collagens I, XVIII, VI, and III, alongside growth factors and enzymes such as TGF-β, FGF, and matrix metalloproteinases (MMPs) (Hughes et al., 2010).

Matrigel has been widely used for *in vitro* ovarian cancer models as the ECM components overlap with those found *in vivo*. As a matrix, Matrigel has been utilized for the assessment of *in vitro* ovarian cancer cell invasion by cell penetration through Matrigel-coated transwell inserts (Woo et al., 2007; Fujisawa et al., 2012; Hallas-Potts et al., 2019). Metastatic outgrowth of

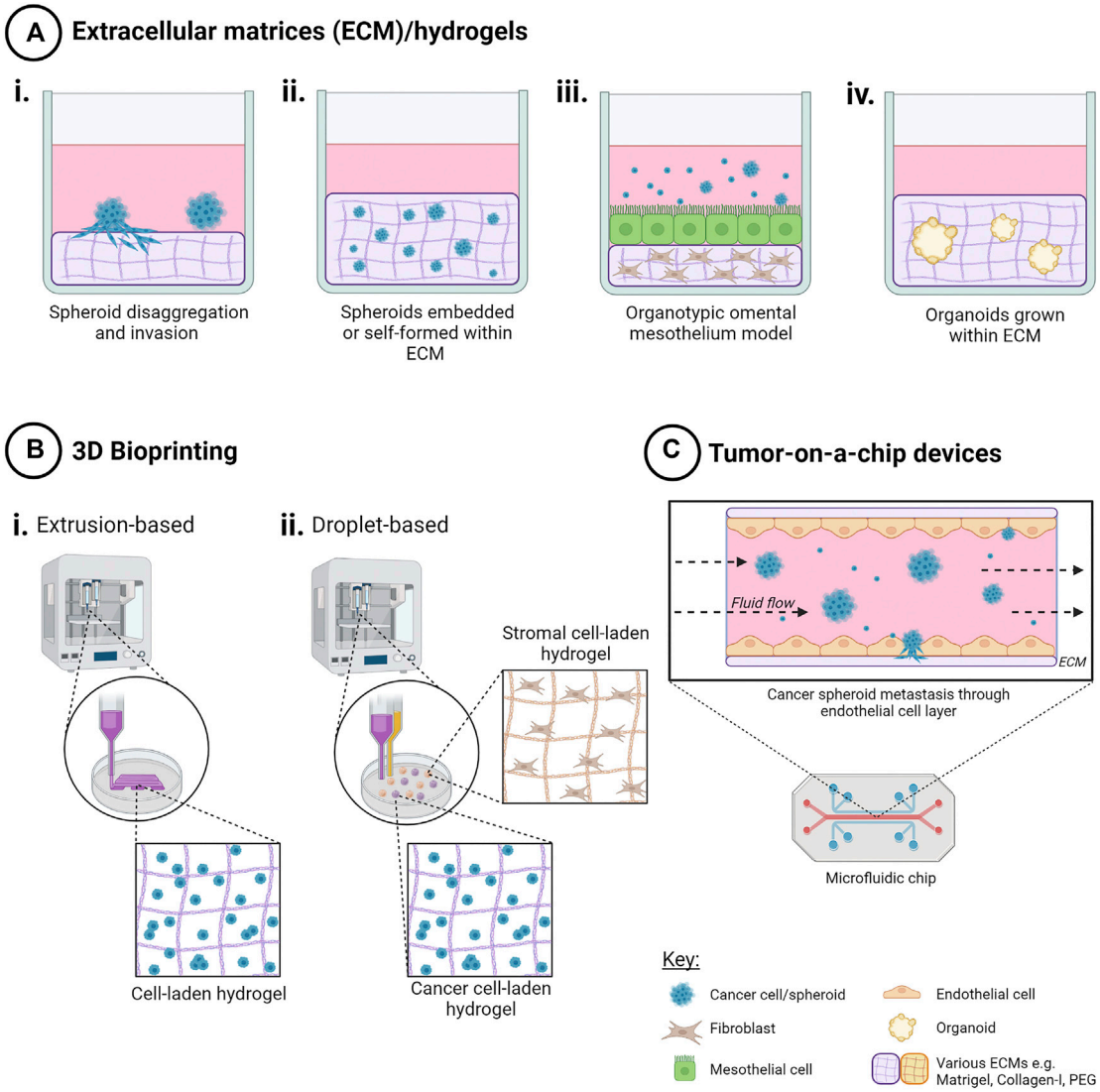

FIGURE 3 | Techniques to create 3D *in vitro* cancer models using scaffolds. Addition of extracellular matrix (ECM) as scaffolds for 3D cell cultures enables both cell-cell and cell-ECM interactions for a more physiologically relevant 3D cancer cell model. Methods include **(A)** ECM/hydrogels with cancer cells i) on top of, or ii) encapsulated within an ECM, iii) organotypic omental co-culture model and iv) organoid propagation. **(B)** 3D bioprinting techniques such as i) extrusion-based bioprinting enables creation of 3D cell-laden models in hydrogels in a layer-by-layer manner, and ii) droplet-based bioprinting enabling high-throughput creation of 3D cell models in hydrogels with higher spatial control for more complex co-culture. **(C)** Tumor-on-a-chip microfluidic devices have been used to model the effects of fluid shear stress, as well as simulating nutrient, gas and drug gradients, for ascites metastasis modelling. Created with Biorender.com.

ovarian cancer spheroids embedded within Matrigel has also been assessed (Sodek et al., 2008). Numerous ovarian cancer cell lines have been reported to require encapsulation within Matrigel or prior growth in Matrigel for successful seeding as *in vivo* tumors into athymic nude mice (Mullen et al., 1996). Growth of ovarian cancer cells on top of a Matrigel bed has been used to model seeding of metastatic ovarian cancer onto the peritoneum, resulting in ovarian cancer nodules in the absence of vascularization, and modelling chemoresistant metastases in the presence of a hypoxic core (Evans et al., 2011). At a 2-2.5% concentration in culture media, Matrigel has been utilized to promote efficient formation of dense, single spheroids of a number of cancer cell types, including ovarian, over 24 h in poly-HEMA treated, non-adherent, round-bottom plates for high-throughput toxicity studies (Ivascu and Kubbies, 2006). Further, Matrigel has been used as a scaffold to propagate primary cell types associated with ovarian cancer such as mesothelial cells and fibroblasts (Kenny et al., 2007), as well as to establish ovarian cancer tumoroids from patient biopsies that maintain key characteristics of the primary tumor (Maenhoudt and Vankelecom, 2021).

Aside from commercial availability and high biocompatibility with a wide range of cell types, there continues to be concerns regarding the use of Matrigel in a

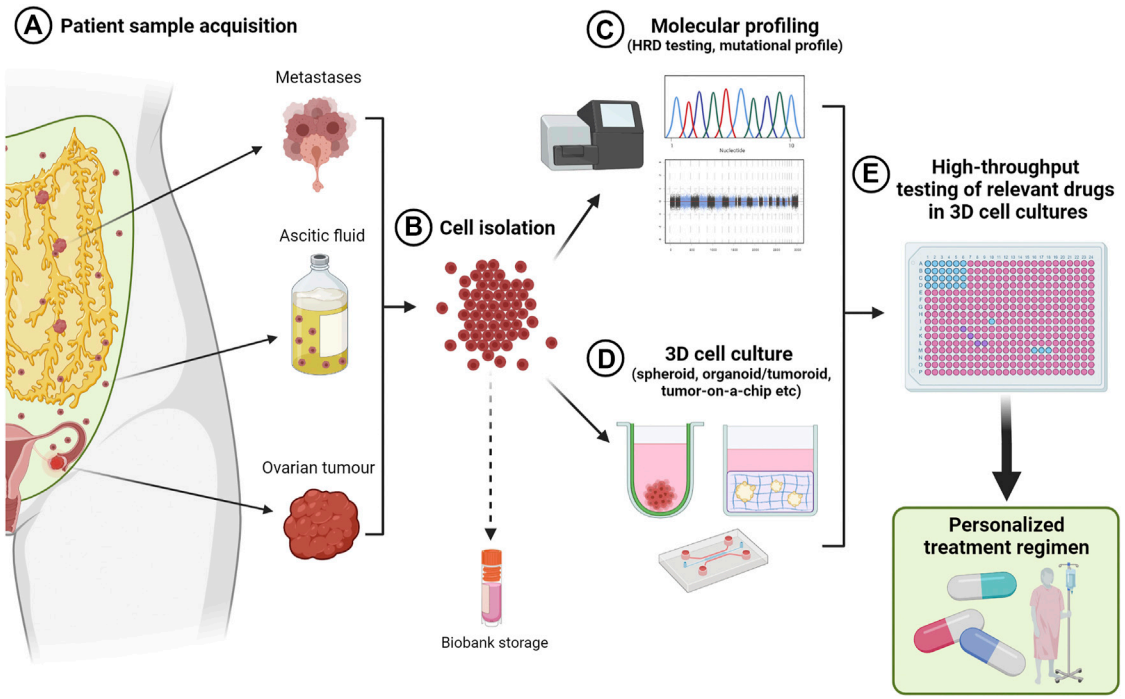

FIGURE 4 | A bench-to-bedside approach using 3D cell cultures to fast track personalized therapies for ovarian cancers. Utilization of **(A)** samples from multiple patient tumor sites, **(B)** isolation of cancer cells *ex vivo* for **(C)** molecular profiling and **(D)** propagation as 3D cell cultures can identify clues regarding a patient's unique tumor phenotype. Based on these findings, **(E)** a high-throughput drug screen of molecularly relevant drugs in 3D cell cultures can be employed to predict drug efficacy and utilized to guide a personalized medicine approach. Created with Biorender.com.

number of areas, including: batch-to-batch variation, potential for xenogeneic contaminants derived from mouse on human cells, inefficient cell retrieval requiring temperature reversal to 4°C, potential DNA/RNA contamination from the matrix, and matrix autofluorescence that reduces signal-to-noise ratio when imaging fluorescently stained cells *in situ* (Graf and Boppart, 2010; Hughes et al., 2010). The reported average modulus value of Matrigel was found to be approximately 450 Pa (Soofi et al., 2009), which remains below the average stiffness of human or mouse ovary or omentum (Alkhouli et al., 2013; Mckenzie et al., 2018; Hopkins et al., 2021). Further, the polymerization temperature for Matrigel of 22–37°C, mediated by entactin interaction with laminins and collagen IV, also limits its bioprintability in the absence of temperature-controlled environments or as a hybrid bioink (Fan et al., 2016).

Overall, Matrigel continues to be one of the most versatile ECMs for *in vitro* modelling of ovarian cancer cells. Synthetic alternatives are becoming more prominent but have yet to meet the standards of enabling the propagation of patient-derived spheroids and organoids as well as having mechanical properties to enable bio-printing for highly reproducible and high-throughput ovarian cancer model development. Until this time, Matrigel's major advantages lie with its rich ECM composition for biocompatibility with a wide range of cell types, including for ovarian cancers.

5.2.1.2 Collagens

Collagens are the most abundant ECM proteins in the body and are also the most widely used ECM for *in vitro* cell cultures due to high biocompatibility and commercial availability. Collagens provide structural support and facilitate cell adhesion, proliferation, differentiation and migration both *in vivo* and *in vitro*. Made up of 28 identified collagen types, the low antigenicity of collagen has enabled cross-species compatibility and in turn, availability from a variety of biological sources, including rat, bovine, porcine, and recombinant human (Lynn et al., 2004; Yang et al., 2004). Excessive macrofibrillar collagen-I produced by resident fibroblasts has been implicated in the promotion of cancer progression, metastatic and chemoresistant tumor microenvironments (Gurler et al., 2015). Crosslinking of collagen that increases stromal stiffness has also been implicated in chemoresistance (Sterzyńska et al., 2018). While there have been anti-cancer therapeutic strategies developed to enhance the efficiency of chemotherapy (Zhao Y. et al., 2019), collagen is abundant in both pathophysiological and normophysiological states and therefore, anti-collagen therapies require a targeted method of delivery (Xu et al., 2019).

Collagens, particularly collagen-I, have been used extensively in 3D ovarian cancer spheroid and organotypic cultures. OVCAR-5 spheroids plated on a collagen-I coating, were observed to readily disaggregate with increasing collagen concentration, compared to laminin or collagen-IV coatings, thus highlighting its properties as a promoter of cancer cell adhesion and invasion (Burleson et al., 2004). Rat-tail collagen-I has been used as the ECM to support primary mesothelial and fibroblast cells in an omental model of ovarian cancer metastasis (Kenny et al., 2007). Encapsulation of human ovarian cancer cell lines derived from primary tumors in collagen-I hydrogels showed enhanced mesenchymal traits, invasiveness and drug resistance (Liu et al., 2018). Microfibrillar collagen-VI, in addition to collagen-I, has also been reported to promote platinum resistance, cancer cell survival and HGSOC relapse both *in vivo* and *ex vivo* in collagen hydrogels (Pietilä et al., 2021). Collagen-XI has been implicated in tumor aggressiveness and poor clinical outcome of patients with ovarian cancer (Wu et al., 2014), although it has not been used as a scaffold for 3D ovarian cancer cultures. Marine collagen sources, such as from jellyfish species, have been found to have high amino acid similarity to collagen-I from mammals, showing similar *in vitro* cell behavior responses to traditional collagen-I matrices, and as such, are being investigated as a more sustainable collagen source (Paradiso et al., 2019).

5.2.1.3 Alginate

Alginate is a natural polysaccharide derived from the brown algae *Phaeophycota*. Features such as high biocompatibility, biodegradability, low immunogenicity, and low cost have been the drivers behind its use in tissue engineering and drug delivery studies (Gombotz and Wee, 1998). Control of the degree of gelation, and in turn stiffness, can be modulated by multivalent cations including Ca^{2+}, Fe^{3+}, or Sr^{2+} for crosslinking. These cations can also mediate individual biofunctional properties such as cell attachment or absorption of serum proteins (Machida-Sano et al., 2009). However, proteins are unable to interact with the matrix, and as such ECM-cell signaling is lacking in alginate models and is considered a more synthetic ECM that can be biofunctionalized by the addition of peptides (Rowley et al., 1999). Further, certain cations may also induce cytotoxicity and may differ in stability.

While more studies have used alginate as a drug delivery system, alginate and alginate mixes, such as chitosan-alginate, have also been used as 3D hydrogel scaffolds for the enrichment of a cancer stem cell (CSC) phenotype in prostate, breast and hepatocellular carcinomas (Florczyk et al., 2016). Alginate encapsulation has been used as a method for *ex vivo* culture of murine ovary slices for the investigation of ovarian surface epithelial changes that may drive cancer development (King et al., 2011). Many reports have also combined alginate with other ECMs, both natural and synthetic, to create more biofunctionalized scaffolds to support a variety of ovarian cell types. Shin and colleagues combined alginate, for its biocompatible properties, with marine collagen and agarose to create a hydrogel that supported the growth of A2780 endometrioid ovarian cancer cells (Shin et al., 2016). A double network of alginate and polyethylene glycol (PEG)-based hydrogels was shown to increase doxorubicin resistance and CSC markers in SK-OV-3 cells compared to 2D cultures (Zhou et al., 2020). SK-OV-3 cells grown in these scaffolds were also reported to be more tumorigenic in a triple immunodeficient mouse model NCG (NOD-*Prkdc*^{em26Cd52}*Il2rg*^{em26Cd22}/NjuCrl) (Zhou et al., 2020).

5.2.1.4 Agarose and Agar

Agarose is a natural linear polysaccharide derived from the marine red algae *Rhodophyceae*, made from repeating monomeric units of agarobiose (Zarrintaj et al., 2018). In comparison, agar, famously used for microbiological growth purposes, is comprised of a heterogenous mixture of agarobiose and agaropectin. Their features of high biocompatibility, commercial availability, ability to adjust stiffness with concentration and reversible polymerization enabled the use of agar and agarose as *in vitro* and *in vivo* cell scaffolds that mimic soft tissue stiffness (Varoni et al., 2012). Whilst normally inert to cell interaction, agarose can be bioengineered to integrate biofunctional peptides that supports cell adhesion and cell viability (Yamada et al., 2020).

The use of soft agar to determine tumorgenicity and invasiveness of cancer cell lines has been employed for more than 50 years (Shin et al., 1975). Early work utilized soft agar assays where clusters of cancer cells from malignant effusions from ovarian cancer patients were propagated as clones on an agar base and responded to the anti-cancer drugs cisplatin and 5-FU in a similar manner to their derivative patient (Ozols et al., 1980). Agarose, as a hydrogel for ovarian cancer cells, has been used to show physiological cancer characteristics such as elevated expression of HIF-1α, VEGF-A, profibrogenic MMP-2 and -9 when compared to 2D SK-OV-3 monolayers (Xu et al., 2014). In contrast, an agarose coating was used as a non-adherent surface on which the liquid overlay technique of spheroid formation was used. HEY and OVHS1 ovarian cancer cells grown by liquid overlay technique with an agarose low-attachment base, formed spheroids more readily than the normal ovarian cell line IOSE29, and further, showed metastatic features such as disaggregation and MMP activation when transferred onto an ECM (Shield et al., 2007).

5.2.2 Synthetic ECM Hydrogel Scaffolds

Synthetic ECMs are becoming a more popular *in vitro* ECM option compared to gold standard EHS-derived ECMs, due to a higher degree of control over properties such as stiffness, pore size and biofunctionalization.

5.2.2.1 PEG-Based Hydrogels

Hydrogels based on bioinert polyethylene glycol (PEG) have been widely utilized for *in vitro* 3D models for their ability to customize biofunctionalization by peptides and hydrogel stiffness control. The inclusion of MMP-degradable crosslinkers also enables more physiological proteolytic ECM remodeling by cancer cells (Lutolf et al., 2003). A 4-arm PEG-maleimide based hydrogel was designed to recreate the omentum ECM with GFOGER (collagen-I), PHSRN-RGD (fibronectin), RGD (fibronectin,

vitronectin, collagen-VI), and DGEA (collagen-IV) biofunctionalization peptide motifs, adjusting stiffness to a physiological level of ~2.9 kPa for omental tissue and incorporating MMP-degradable crosslinkers (Brooks et al., 2019). This hydrogel supported cell growth and viability of SK-OV-3 multicellular spheroids that were pre-made in non-adherent polydimethylsiloxane (PDMS)-coated grids and spheroids from patient-derived ascites, with paclitaxel and doxorubicin treatments mimicking the drug responses seen in patients. PEG-crosslinked poly(methyl vinyl ether-*alt*-maleic acid) or PEMM/alginate network hydrogels induced EMT, a CSC-like phenotype and chemoresistance in encapsulated SK-OV-3 spheroids, driven by hydrogel stiffness, porosity and cation of choice for crosslinking (Zhou et al., 2020). This pro-metastatic phenotype was confirmed when hydrogels were implanted into immunodeficient mice. An extension of this work by the same authors showed higher RGD (arginine-glycine-aspartic acid) concentrations encouraged spheroid cell dispersion and drug sensitivity, whereas hydrogels with lower RGD concentrations had preserved cell aggregations with CSC-like changes and drug resistance when grown on PEMM hydrogel discs with varying RGD concentrations (Zhou et al., 2021). When taken together to account for mechanical properties, lower stiffness hydrogels with low RGD levels promoted a CSC-like phenotype with drug resistance. While this study highlighted the importance of cell-ECM interactions in drug resistance, the hydrogels studied were of a stiffness much higher than *in vivo* physiological conditions ranging from 60–240 kPa.

5.2.2.2 Gelatin Methacryloyl

GelMA is a semi-synthetic bioengineered, biocompatible material with high batch-to-batch consistency, control of mechanophysical properties, innate RGD responsive peptide motifs and ability to be cleaved by MMPs, having been designed as an alternative to Matrigel (Zhu et al., 2019). GelMA requires modification with a photocrosslinker (typically UV or visible light responsive) for efficient polymerization and to prevent degradation. Visible light, as expected, promotes higher cell viability and lower free radical damage compared to UV light when using GelMA (Noshadi et al., 2017). Addition of Laminin-411 and hyaluronic acid to GelMA hydrogels of 3.4 kPa stiffness enabled ovarian cancer spheroid formation, proliferation and chemoresistance to paclitaxel (Kaemmerer et al., 2014). GelMA hydrogel models also showed similar tumorigenic responses when transplanted into NOD/SCID mice. Interestingly, peripheral blood mononuclear cells or PBMCs grown on GelMA hydrogels showed suppressed pro-inflammatory responses to stimulation with lipopolysaccharide (LPS), particularly in the presence of tumor necrosis factor (TNF), whereby cellular TNF mRNA levels were elevated, but soluble TNF was bound to the hydrogel (Donaldson et al., 2018). This study highlighted the need to consider the immunogenic properties of biomaterials to match hydrogel models for their appropriate application, and may have implications on future 3D *in vitro* immunotherapy models. In the 3D bioprinting field, ovarian cancer cell lines have to date only been used to test printability of GelMA with extrusion based bioprinting, prior to testing its biocompatibility with murine oocytes (Wu et al., 2021).

5.2.2.3 Peptide-Based Hydrogels

Self-assembling peptide-based hydrogels are increasingly being used as a biomimetic material for 3D *in vitro* culture for their engineerability, ability to form well-defined nanofibers with natural amino acid constituents and absence of animal-derived contaminants (Yang et al., 2020). RADA16-I peptide-based hydrogels performed as well as Matrigel and Collagen-I based hydrogels in terms of cell viability, adhesion, migration and drug resistance of encapsulated A2780 and SK-OV-3 ovarian cancer cells (Yang and Zhao, 2011). A disadvantage of some peptide-based hydrogels is their low mechanical strength, where hydrogels with encapsulated cells are able to be disrupted easily by mechanical forces such as pipetting (Song et al., 2020). A study by Hedegaard and colleagues utilized peptide amphiphile-based hydrogels with elastin mimetics, fibronectin, keratin, RGDS (arginine-glycine-aspartic acid-serine) motif for cell adhesion and GHK (glycine-histidine-lysine) motif for pro-angiogenic signaling with encapsulated OVCAR-4 cells in monoculture as well as in co-culture with HUVECs and human mesenchymal stem cells (Hedegaard et al., 2020). Tumor spheroids grown in this hydrogel were comparable in morphology, viability and drug response compared to those grown in GelMA and Matrigel. Importantly, this model is one of the first to incorporate peptides to promote angiogenesis, addressing one of the major missing components of 3D *in vitro* cell culture models.

5.2.3 Decellularized Ovary ECM

Decellularized extracellular matrices (dECM) are the natural matrices from an organ that have been void of all native cellular components, preserving the biological and mechanical properties of the original ECM. These ECMs can be used to seed new cells in an organ's native conformation in the absence of an immune response, as well as can be lyophilized and reconstituted to form hydrogels. To date, there have been no reports of using decellularized ovary ECM for the study of ovarian cancers. However, the use of ovarian dECMs might benefit 3D *in vitro* ovarian models, due to the preservation of ECM proteins and growth factors found in the native ovary. A handful of studies have shown high biocompatibility with ovarian cell types grown in reconstituted dECM hydrogels and scaffolds. A mixture of sodium alginate with decellularized murine ovarian tissue supported *in vitro* follicle survival (Nikniaz et al., 2021). Preliminary studies of hydrogels derived from decellularized porcine ovarian ECM highlighted the effect of ECM stiffness on ovarian follicle development, with stiffer matrices reducing oocyte viability and triggering premature follicle release (Buckenmeyer et al., 2016), though this effect has not been investigated with ovarian cancer cells. There are nevertheless some concerns surrounding the use of dECMs, namely donor batch differences, retention of native genetic material such as DNA, and the harsh decellularization process that may result in a loss of critical downstream biological interactions with cells (Mendibil et al., 2020).

5.2.4 Organotypic Omental Mesothelial Model

Three-dimensional organotypic models of the human mesothelium (**Figure 3**) have been utilized for the study of early metastasis to the omentum and interactions with the tumor microenvironment (Kenny et al., 2007). Taking a layered approach to reproduce the architecture of the omentum as observed from histological staining of omental biopsies, this model consists of primary human fibroblasts with ECM, rat-tail collagen-I and human fibronectin, as a base, layered with primary human mesothelial cells. Ovarian cancer cells or ascites-derived spheroids can be added to investigate cell attachment and invasion into the omentum. Using this model, Kenny and colleagues identified MMP-2 mediated cleavage of fibronectin and vitronectin produced by mesothelial cells as an early response to omental metastasis (Kenny et al., 2009). Another study identified mir-193b downregulation as a driver of omental metastasis with this mesothelial model (Mitra et al., 2015a). Further, Henry and colleagues described the dynamic roles of the receptor tyrosine kinases ROR1 and ROR2 in different omental cell types that promote cancer cell adhesion in early metastasis (Henry et al., 2017). This model has also been adapted for high throughput drug screening of potential inhibitors of adhesion and invasion. Though the mesothelial models had fewer efficacious drug hits than traditional 2D models, similar drug responses were observed *in vivo* in PDX models (Kenny et al., 2014; Lal-Nag et al., 2017). This organotypic model was also more cost and time-efficient with similar results to *in vivo* models, when testing micellar-based nanoparticle therapies to prevent early metastasis (Lu et al., 2019). To add complexity to the static organotypic mesothelial model, it has been incorporated into a microfluidics device, enabling the study of hydrodynamic forces of ascites fluid flow on spheroid attachment and metastasis.

The use of the organotypic mesothelial model has been reviewed in depth and a standardized protocol published to enable reproducibility between research groups across the world (Peters et al., 2015; Watters et al., 2018). While this co-culture model has been quite successful, as a scalable, 3D pre-clinical model of ovarian cancer metastases, it lacks vasculature, as well as immune cells and cells from adipose tissue.

5.2.5 3D Ovarian Cancer Co-Cultures

In order to best recapitulate the TME of ovarian cancers, the addition of cancer-associated cells types including stromal, immune, mesenchymal, mesothelial, and endothelial cells, to ovarian cancer cells *in vitro* enables the heterotypic cell-to-cell crosstalk that may influence chemoresistance, angiogenesis, and metastasis. Two-dimensional co-cultures, while enabling intercellular contact and cross-talk, cannot mimic the multidimensional cell interactions. Three-dimensional co-cultures, particularly when combined with ECM scaffolds, are *in vitro*, biomimetic models that may better represent the *in vivo* situation and more accurately predict cellular responses in a patient. While not an exhaustive list, recently published 2D and 3D ovarian cancer co-cultures models are summarized in **Table 3**.

There are two major co-culture methodologies: indirect and direct contact models. Indirect contact co-cultures, such as by the use of transwells or conditioned media, mimic cellular signaling in the absence of physical cellular contact, and enable simple segregation of cell types for ease of downstream analyses of individual cell population behavior. Direct contact co-cultures enable the study of physical interaction of several cell types and their influence on cell behavior as an "organ-like" model. Two-dimensional culture studies showed ovarian cancer cell lines in contact with normal omental fibroblasts could drive activation to a cancer-associated fibroblast (CAF) phenotype associated with TGF-β1 secretion (Cai et al., 2012).

In 3D multicellular spheroid cultures, addition of fibroblasts, mesenchymal stem cells, or endothelial cells have been shown to enhance spheroid size, chemoresistance and a stem-like phenotype compared to 3D monocultures (Hedegaard et al., 2020; Tofani et al., 2021). Co-cultures of ovarian cancer cells and macrophages have identified positive feedback loops that drive stemness, chemoresistance and spheroid formation in cancer cells and M2 polarization of macrophages (Long et al., 2018; Ning et al., 2018; Raghavan et al., 2019). Three-dimensional co-culture systems of ovarian cancers and mesothelial cells, including the organotypic omental mesothelium model (described in **Section 5.2.4**) have also enabled the study of mechanisms driving peritoneal and omental metastasis (Iwanicki et al., 2011; Henry et al., 2017; Shishido et al., 2018; Loessner et al., 2019).

The number of studies utilizing 3D co-cultures of ovarian cancers at the time of this publication was limited but is growing. It is clear that with increasing model complexity through addition of multiple patient-derived cell types in conjunction with physiologically relevant ECM mimics, that the most biologically appropriate and predictive *in vitro* models will be discovered. Integration of organoids with endothelial cells could enable more biologically appropriate, predictive studies of anti-angiogenic drugs such as bevicizumab in the presence of ovarian cancers with specific mutations. Further, utilization of microfluidics devices for emulation of fluid flow and the addition of immune cells types enable the creation of a more accurate biomimetic TME.

5.2.6 Organoids

Patient-derived organoids are becoming an important and powerful pre-clinical model for personalized medicine (**Figure 3**). While primary patient-derived samples are the gold standard for prediction of treatment response, long-term culture of these samples in 2D often leads to phenotypic changes and differential responses to drug treatments (Kapałczyńska et al., 2018). Cryopreservation of patient-derived organoids allows for biobanking of unique samples for genotype/phenotype matching with future samples from the same patient as their cancer progresses to inform treatment decision making.

In comparison to xenograft models, organoid or tumoroid cultures require significantly shorter times for development from small starting samples, have a higher success rate and accurately reproduce the genetic and phenotypic features of the derivative tumor, allowing for personalized medicine strategies (Hidalgo

TABLE 3 | Indirect and direct *in vitro* ovarian cancer co-culture models.

Co-culture type	Co-culture model	Model format	References
Indirect/non-contact	Cancer-stroma	SK-OV-3 + FP-96 fibroblasts (transwell insert)	Medeiros et al. (2019) [a]
		OVCAR-5 + MRC-5 fibroblasts (bioprinted onto Matrigel)	Xu et al. (2011)
	Cancer-immune (macrophage)	SK-OV-3, HEY, HO8910, A2780 in Matrigel (transwell insert) + Primary macrophages	Yi et al. (2020)
		SK-OV-3 spheres (transwell insert) + THP-1 macrophages	Ning et al. (2018)
		SK-OV-3 + THP-1 macrophages (transwell insert)	Wang et al. (2013) [a]
	Cancer-endothelial	SK-OV-3, OVCAR-3 + HUVECs on Matrigel (transwell insert)	Yuan et al. (2021) [a]
		"NICO-1" transwell system—Primary OvCa stem cell spheroids (ascites, ULA plate) + HUEhT-1 endothelial cells on Matrigel	Miyagawa et al. (2020)
	Cancer-MSC	OvCa cell lines + MSC (adipocyte, bone marrow, umbilical cord) conditioned media	Khalil et al. (2019) [a]
Direct/ contact	Cancer-stroma	SK-OV-3 on top of WI38 fibroblasts in Matrigel	Lau et al. (2017)
		HEY or SK-OV-3 + NIH3T3 cells in hanging drop	Weydert et al. (2020)
		A2780 + Human ovarian fibroblast cell line in a microfluidic chip	Flont et al. (2020)
		SK-OV-3 + mesenchymal cells (MUC-9) or fibroblasts (CCD27-Sk) in ULA plates	Tofani et al. (2021)
	Cancer-immune (macrophage)	ID8 cells on top of Matrigel + TAMs from mouse ascites	Long et al. (2018)
		OVCAR-3 + PBMCs in hanging drop	Raghavan et al. (2019)
	Cancer-adipocyte	ID8 cells on top of primary mouse adipocytes in Matrigel	John et al. (2019)
	Cancer-mesothelial	OVCA433 spheroids (created on poly-HEMA coating) on top of immortalized human lung mesothelial cells or MeT-5A mesothelial cells	Iwanicki et al. (2011)
		CAOV-3 or A2780 + Primary mesothelial cell or MeT-5A mesothelial cell spheroids on poly-HEMA coated plates	Shishido et al. (2018)
		OV-MZ-6 + MeT-5A mesothelial cells in PEG hydrogel	Loessner et al. (2019)
	Organotypic omental mesothelial model	OvCa cell line + Primary mesothelial cells + Primary omental fibroblasts	Kenny et al. (2009); Kenny et al. (2007); Mitra et al. (2015a); Henry et al. (2017); Lu et al. (2019); Li et al. (2017); Peters et al. (2015)
	Multicellular models	OVCAR-4 + HUVEC + hMSC in peptide-based hydrogels	Hedegaard et al. (2020)
		Patient explant orbital rotational cultures (epithelial cells, fibroblasts, tumor-infiltrating immune cells)	Abreu et al. (2020)
		Early passage HGSOC organoids (maintained immune cells)	Hill et al. (2018)

[a]*Cancer cells grown in 2D*

MSC, Mesenchymal stem cell; HUVEC, Human umbilical vein endothelial cell; CSC, Cancer Stem Cell; OvCa, Ovarian Cancer; TAM, tumor-associated macrophages; PBMC, primary blood mononuclear cell; PEG, polyethlyene glycol.

et al., 2014). Nanki and colleagues were able to propagate primary ovarian tumor organoids from a variety of histological subtypes including HGSOC, OCCC, and EnOC with an 80% success rate and maintenance of their original tumor mutational profiles (Nanki et al., 2020). The analysis of ovarian tumor organoids derived from multiple tumor sites within the same patient showed differential drug sensitivities, emphasizing the need to account for intrapatient tumor heterogeneity (De Witte et al., 2020). When grown in a modified Matrigel bilayer, organoids from MOCs could reproduce behaviors of their derivative cancer, such as production of mucin and a cystic morphology (Maru et al., 2019).

While there is growing evidence that ovarian cancer organoids/tumoroids are becoming the new benchmark for pre-clinical models compared to traditional 2D methods, varying success rates have been reported, particularly attributed to the heterogeneity of these cancers, and propagation success has been highly dependent on starting sample volume and sample handling. In contrast to traditional organoid culture methods that utilize Wnt to maintain stem-like properties, Wnt pathway induction resulted in tumoroid growth arrest in HGSOC organoids, however was able to be rescued by BMP signaling (Hoffmann et al., 2020). The opposite was observed in fallopian tube organoids whereby shRNA downregulation of tumor suppressor genes *TP53*, *PTEN,* and *RB*, showed stem-like changes occurring early in tumor development. Work by Maenhoudt and colleagues identified that the addition of neuregulin-1 (NRG1) to culture medium can increase the proliferation time of primary organoid cultures from fresh and cryopreserved HGSOC and LGSOC, particularly in slower-growing cultures (Maenhoudt et al., 2020). In contrast, it has been noted that organoid propagation methods tend to be selective and result in a cell population that may not be representative of the original tumor heterogeneity and in turn, treatment response, particularly in patients who have undergone previous neoadjuvant therapy (Hill et al., 2018). Therefore, care must be taken in interpretation of data and use of the correct modelling systems. Improvements in methodologies to maintain the heterogenous phenotype that exists in patient tumors are needed, such as propagation of organoids from different regions of the same tumor (Maru et al., 2019). Furthermore, the standardization of protocols and materials for organoid culture between laboratories around the world will lead to vast

improvements in reproducibility and reliability of this technique into the future.

As the initial triggers for the development of ovarian cancer is still being debated, organoids from normal ovarian tissue have also been utilized in studies of tumor development. Organoid cultures from high-risk women with germline mutations in *BRCA1* or *BRCA2* have been developed for research into early tumor development (Kopper et al., 2019). Kopper and colleagues have performed gene editing in normal non-tumor organoids established from fallopian tube or ovarian epithelium using CRISPR-Cas9 gene editing for modelling *TP53* mutations, and determined that HRD ovarian cancer organoids with fewer RAD51 loci were more sensitive to the PARPi niraparib, analogous to responses observed *in vivo* (Kopper et al., 2019). An extension of this work has similarly used CRISPR-Cas9 genome editing to introduce common HGSOC gene defects into mouse oviduct and OSE cell organoids, showing that both organoid types could become carcinogenic and that drug sensitivities in HGSOC patients may be cell lineage-dependent (Lõhmussaar et al., 2020).

5.3 Bioprinting of 3D OC Models

Three dimensional bioprinting presents an automated solution that combines both ECM components and high-throughput creation of ovarian cancer models in a spatially-controlled manner (**Figure 3**). As a relatively new approach to 3D cell model creation, the number of published studies is limited for ovarian cancer.

Droplet-based bioprinting systems enable the precise and agile fabrication of microtissue cultures by overlaying drops of biomaterial. Used mainly for deposition of scaffolds, this layer-by-layer technique has also been used for addition of drugs, growth factors and living cells. Xu and colleagues have used a droplet-based system to bioprint OVCAR-5 cells and MRF-5 normal fibroblasts on top of a Matrigel scaffold in a controlled spatial distribution for investigation of feedback mechanisms between tumor and stromal cells (Xu et al., 2011). While there are no publications to date utilizing drop-on-demand inkjet bioprinting, laser-assisted bioprinting or stereolithography with ovarian cancer cells, these are promising techniques that could enable high-throughput 3D ovarian cancer cell model development that would seamlessly integrate with existing high-throughput drug screening technologies (Mazzocchi et al., 2019).

Extrusion based bioprinting has been employed to fabricate a 3D bioprinted ovary that successfully supported oocyte growth using a GelMA-based bioink (Wu et al., 2021). While this study focused on oocyte maturation *ex vivo*, ovarian cancer cell lines were utilized during optimization of bioink biocompatibility, showing high cell viability during and after the extrusion process. Unfortunately, this was not translatable in primary murine oocytes, suggestive of the delicate nature of primary-derived cells with this technique.

An important factor of 3D bioprinting is the printability of the matrix to be deposited. The material properties of Matrigel and other natural matrices are limited in their printability as bioinks due to temperature sensitivities and pre-determined stiffnesses, highlighting the flexibility of synthetic matrices that can be modified to best mimic *in vivo* conditions. In contrast, synthetic matrices are limited by their biocompatibility but can be biofunctionalized with peptides and full-length ECM proteins. Overall, 3D bioprinting and automation has great potential as a future staple for *in vitro* and *ex vivo* studies driving drug development and discovery for all cancer types.

5.4 Bioreactors

Bioreactors have largely been used to study the effects of fluid flow as a physiological mechanical stimulus on cell behavior. In the context of ovarian cancers, mechanotransduction and shear stress from ascites fluid build-up and flow in the peritoneum have been shown to drive ovarian cancer metastasis. Tumor-on-a-chip microfluidics systems have been used to model peritoneal metastases as well as vasculature in solid tumors.

5.4.1 Rotating Wall Vessels and Orbital Shakers

Rotating wall vessel bioreactors or rotary cell culture systems (**Figure 2**) utilize low shear, low turbulence biomechanical forces to influence cell differentiation and aggregation in three dimensions as a suspension (Schwarz et al., 1992). Originally designed to mimic microgravity, this technique has been important for studies of transcoelomic ovarian cancer metastases (Shield et al., 2009). Microgravity, as a biomechanical force, has been reported to reduce metastatic markers, change cell metabolism and chemosensitivity in a variety of cancer cell lines, though the *in vivo* effect is unknown (Takeda et al., 2009; Vidyasekar et al., 2015). LN1 cells, derived from a mixed Mullerian tumor, were grown in a horizontally-oriented high aspect rotating vessel (HARV) with microcarrier beads as a scaffold to investigate the potential for metastatic growth as spheroids or aggregates (Becker et al., 1993). This study also showed that there is growth selection for certain cell types from a mixed population in 3D compared to 2D. Further work confirmed the production of chondroitin sulphate in the 3D culture similar to that observed in the *in vivo* tumor; however, this was not observed in 2D culture (Goodwin et al., 1997; Grun et al., 2009). These spheroids also showed varying degree of oncogene expression not seen in 2D, although the variation was likely due to the mixed populations present. Low passage primary ovarian and endometrial cancer cell lines propagated as multicellular spheroids in a rotating cell culture system, showed similar histological markers to the primary tumor with differentially expressed markers including prohibitin, VDAC1 and annexin 4 identified in 2D *versus* 3D culture methods (Grun et al., 2009).

Orbital shakers, traditionally used for bacterial cultures, have also been employed to investigate fluid shear stress on ovarian cancer spheroid formation. Masiello and colleagues adapted the orbital shaker to rotate at physiologically relevant speeds and utilized typical culture dishes to investigate the effects of rotational speeds, cell density and well size on spheroid formation (Masiello et al., 2018). This study resulted in more rounded and consistent spheroid formation, amenable to the analyses of functional endpoints. Patient-derived explants of

multiple ovarian cancer histotypes have been propagated for up to 30 days in orbital shakers, resulting in maintenance of tumor architectures, epithelial, fibroblasts and immune cells, as well as ECM (Abreu et al., 2020). Studies using these rotational techniques have contributed to the understanding of shear stress on ovarian cancer metastasis, drivers of spheroid formation in ascites and long-term propagation of ovarian cancer cells.

5.4.2 Compressive Stress Bioreactors

The majority of bioreactor-based models for ovarian cancer have been used for the study of fluid shear stress pressures on cancer invasion and proliferation. Investigation into compressive stress to model external compressive stimuli such as ascites accumulation that increases hydrostatic pressure as a driver of metastasis is a relatively new approach and its effect on treatment is still unknown. Novak and colleagues created a custom bioreactor to mimic the hydrostatic compression pressures on ovarian cancer metastasis from the primary tumor (Novak et al., 2020). This was modelled by the HGSOC cell line OVSAHO that was encapsulated in an agarose-collagen-I hydrogel on top of a membrane where air can be pumped to mimic the compressive forces from ascites fluid build-up in both a static and cyclic manner. This work identified CDC42 as a driver of chemoresistance and proliferation under compressive stimuli. Recently, Onal and colleagues developed a microfluidic platform with micro-pistons that enable the application of dynamic compression to the system, for investigations of cyclic and pressure-controlled compressive stress on SK-OV-3 cell damage (Onal et al., 2021). While this study used ovarian cancer cells as a monolayer, the authors iterate that their platform can be easily modified to include hydrogel ECM and spheroid models.

5.4.3 Tumor-on-a-Chip Microfluidic Systems

Tumor-on-a-chip devices utilize microfluidics to simulate effects of vascular flow in solid tumors and more specifically in the context of ovarian cancer, mimicking the hydrodynamics that influence ascitic seeding in the peritoneum and contributing to metastases (**Figure 3**). Microfluidic devices consist of networks of microchannels where fluids including cell media with cells, or media with drugs or cytokines can be injected and evacuated in an automated manner, enabling nutrient and gas exchange. Microchannels may be laden with matrix and/or cells to mimic a lumen. Culture within a microfluidic system is often short-term and high-throughput.

Tumor-on-a-chip microfluidic systems have been used to model various aspects of ovarian cancer progression, both as solid primary tumors and drivers of cell survival in metastases. Microfluidic chips have been used to model 3D tumor nodule development in the peritoneum by ascitic spheroids, showing that the flow stream was a factor that drove OVCAR-5 cell attachment to Matrigel-laden walls *via* EMT (Rizvi et al., 2013). Using the same system, SK-OV-3 spheroids were flowed through a poly-HEMA-coated chamber to investigate the effects of shear stress on EMT status changes in cancer spheroids, similarly showing that perfusion promoted spheroid viability and stemness (Ip et al., 2016). These findings were further validated when transplanted into nude mice as xenografts, with perfused spheroids forming larger subcutaneous tumors that were found to be chemoresistant, regulated by the PI3K/AKT signaling pathway. Microfluidic chips have also been used to investigate platelet extravasion in the presence of both primary endothelial cell and ovarian cancer cells, whereby platelets were found to induce cancer cell mediated disruption of the endothelial layer (Saha et al., 2020). This disruption was partially rescued by addition of atorvastatin, a statin drug used for preservation of endothelial junctions, with results reproduced using primary HGSOC cells with prior atorvastatin treatment *in vivo*. Induction of inflammatory cytokines such as MCP-1 and TNF also mirrored the pro-inflammatory vascular microenvironment observed in the vicinity of ovarian tumors *in vivo* and inferred some regulation of cancer progression.

Advantages of microfluidic chip systems include the ability to utilize small amounts of starting material, homogenous creation of large numbers of spheroids, portable sizing, and the potential to control drug or chemokine gradients with integration of multiple wells or chips. An orthogonal microfluidic chip developed for seeding into PDMS-based microwells, was superior to standard low-attachment plates and Matrigel seeding in cell viability and maintenance of patient-derived epithelial ovarian cancer cell phenotypes, even when starting with low starting cell numbers (Dadgar et al., 2020). The multi-well microfluidic chip also enabled simpler cytotoxicity measurements by imaging analyses when compared to Matrigel methods, and allowed simultaneous drug gradients in a single microfluidic chip. A direct comparison of spheroid formation and carboplatin sensitivity in four ovarian cancer cell lines in either PDMS-based microfluidic devices with microwells, ULA plates or hanging drop showed microfluidic devices created more homogeneous spheroids with similar carboplatin sensitivities to ULA-plate derived spheroids (Patra et al., 2020). Microfluidic systems have also been used to study macrophage recruitment by ovarian cancer cells *via* integration of chemokine concentration gradients to mimic macrophage infiltration into the tumor with both HGSOC cell lines and patient-derived xenografts (Scott et al., 2021). The study showed correlation between macrophage recruitment and tumor invasiveness and results were replicated in *in vivo* PDX models, with future work looking to identify correlations between macrophage infiltration and chemoresistance.

While microfluidic devices have great potential as more physiological and reproducible 3D *in vitro* models of ovarian cancer, there are still a number of drawbacks to this new technology, namely in costing. There is also a high level of variability between studies due to the majority of devices being fabricated in-house to meet specific researchers' needs, though commercially available options ranging from single to multichannel perfusion systems are becoming increasingly obtainable, that assists with method standardization.

6 3D *IN VITRO* OVARIAN CANCER MODELS FOR PERSONALIZED MEDICINE

The concept of a personalized medicine approach where specific treatments are tailored for individuals, is the overarching goal of cancer therapy. As already discussed, ovarian cancer is in fact an umbrella term for multiple histotypes, with differing sites of origin, different genetic and epigenetic events and survival rates. Further, ethnicity and different occurrence rates of histotypes between ethnicities adds another layer of complexity (Peres et al., 2018). Given these variables, homogenous, immortalized 2D cell lines as *in vitro* models of ovarian cancer only address few of these variables at a single given timepoint of the disease and in a defined microenvironment dissimilar to the *in vivo* situation. Therefore, there is a need for more representative *in vitro* and *ex vivo* models of ovarian cancer for a more personalized prediction of therapeutic efficacy.

There is growing evidence that 2D cultures are more divergent and 3D cultures are better models to reproduce and predict patient drug responses. Patient-derived spheroids grown in 384-well ULA plates derived from primary debulking surgery formed over 24 h and after a further 72 h of growth predicted patient response to first-line adjuvant chemotherapies with 89% accuracy (Shuford et al., 2019). A study by Jabs and colleagues documented that primary ovarian cancers cells grown as organoids had HRD scores, growth and drug cytotoxicity more strongly correlated with the original tumor compared to monolayer cultures, indicative that 3D tumoroid cultures are better mimics of patient tumor behavior (Jabs et al., 2017). Further, numerous studies have shown the utility of ovarian cancer organoids of various histotypes for drug screening, with maintenance of mutational profiles and accurate reproduction of treatment responses when challenged with FDA-approved clinically utilized drugs (Kopper et al., 2019; Maenhoudt et al., 2020; Nanki et al., 2020).

For the prediction of drug response, HGSOC tumor organoids from primary and interval debulking surgeries showed histological concordance with the original tumor and reliably predicted carboplatin sensitivity and resistance (Gorski et al., 2021). RNA sequencing of these tumoroids identified cell-specific pathways that may contribute to carboplatin sensitivity or resistance, and has potential for use in stratification of patients, to guide treatment strategies before clinical recurrence (Gorski et al., 2021). High-throughput development of patient-derived ovarian cancer organoids grown in a ring-shaped geometry of Matrigel, was able to identify responses to 240 kinase inhibitor compounds within a week of cell isolation (Phan et al., 2019). The ring-shaped geometry is particularly advantageous as it eliminates the need for sample transfer or tumoroid dissociation, and can utilize very small starting cell numbers. Further, tumoroids grown by this method were able to maintain heterogeneity with distinct cytomorphologies from mixed type carcinomas. This method could enable rapid screening and identification of clinically actionable drugs as well as identify clinical trial eligibility. Hill and colleagues employed organoids from HGSOC for DNA repair profiling and were able to predict the therapeutic sensitivity in patients to PARP inhibitors. This valuable study highlights the use of organoids as a tool to guide treatment decisions that may have the most benefit (Hill et al., 2018).

7 FUTURE PERSPECTIVES

Given the high mortality and recurrence rate of ovarian cancers, there is a clear need for more physiologically relevant models that can accurately predict the likelihood that a patient will respond to a particular therapy, both at diagnosis and relapse in order to guide therapeutic strategy. These models will need to be constructed across all of the ovarian cancer histotypes, including those that are very rare, and generate results in a timeframe that facilitates rapid and targeted translation to patients. A vision for the future would encompass automated functional assays of ovarian tumoroids including tumor proliferation, metastatic spread, spheroid formation and cell death that routinely complement molecular studies to provide strong predictions of patient response to new molecular targeted therapies such as described in **Figure 4**. Furthermore, discovery-based science that will identify new drugs to treat ovarian cancer, will also be conducted in models that more strongly mimic *in vivo* condition. These studies will not only identify new therapies, but also diagnostic and prognostic markers.

The field of 3D bioprinting, currently in its infancy, is rapidly emerging as an answer to the manual, low throughput methods of creating 3D cell models, including organoids and tumoroids. In the future, the challenges of including common components missing in most 3D *in vitro* models today of ovarian cancer such as incorporation of vasculature, immune cells and hydrostatic forces will be met as models are created to best recapitulate the patient environment and to better inform the clinical management of women with ovarian cancer.

AUTHOR CONTRIBUTIONS

CY and DJM contributed to all aspects of the article and led the team efforts. CY and K-AD created the tables, and all authors (CY, K-AD, MNM, YM, and DJM) collected the literature, provided revision suggestions, reviewed and commented on the manuscript.

FUNDING

CY was supported by grants to DJM: Medical Research Future Fund (APP1199620) and Cancer Council NSW (2019/TPG1002).

SUPPLEMENTARY MATERIAL

The Supplementary Material for this article can be found online at: https://www.frontiersin.org/articles/10.3389/fbioe.2022.836984/full#supplementary-material

REFERENCES

Abreu, S., Silva, F., Mendes, R., Mendes, T. F., Teixeira, M., Santo, V. E., et al. (2020). Patient-derived Ovarian Cancer Explants: Preserved Viability and Histopathological Features in Long-Term Agitation-Based Cultures. *Sci. Rep.* 10 (1), 1. doi:10.1038/s41598-020-76291-z

Alkhouli, N., Mansfield, J., Green, E., Bell, J., Knight, B., Liversedge, N., et al. (2013). The Mechanical Properties of Human Adipose Tissues and Their Relationships to the Structure and Composition of the Extracellular Matrix. *Am. J. Physiology-Endocrinology Metab.* 305 (12), E1427–E1435. doi:10.1152/ajpendo.00111.2013

Alsop, K., Fereday, S., Meldrum, C., deFazio, A., Emmanuel, C., George, J., et al. (2012). BRCAMutation Frequency and Patterns of Treatment Response inBRCAMutation-Positive Women with Ovarian Cancer: A Report from the Australian Ovarian Cancer Study Group. *Jco* 30 (21), 2654–2663. doi:10.1200/jco.2011.39.8545

Anglesio, M. S., Wiegand, K. C., Melnyk, N., Chow, C., Salamanca, C., Prentice, L. M., et al. (2013). Type-specific Cell Line Models for Type-specific Ovarian Cancer Research. *PLoS One* 8 (9), e72162. doi:10.1371/journal.pone.0072162

Audeh, M. W., Carmichael, J., Penson, R. T., Friedlander, M., Powell, B., Bell-McGuinn, K. M., et al. (2010). Oral poly(ADP-Ribose) Polymerase Inhibitor Olaparib in Patients with BRCA1 or BRCA2 Mutations and Recurrent Ovarian Cancer: a Proof-Of-Concept Trial. *The Lancet* 376 (9737), 245–251. doi:10.1016/s0140-6736(10)60893-8

Auguste, A., Blanc-Durand, F., Deloger, M., Le Formal, A., Bareja, R., Wilkes, D. C., et al. (2020). Small Cell Carcinoma of the Ovary, Hypercalcemic Type (SCCOHT) beyond SMARCA4 Mutations: A Comprehensive Genomic Analysis. *Cells* 9 (6), 1496. doi:10.3390/cells9061496

Barnes, B. M., Nelson, L., Tighe, A., Burghel, G. J., Lin, I.-H., Desai, S., et al. (2021). Distinct Transcriptional Programs Stratify Ovarian Cancer Cell Lines into the Five Major Histological Subtypes. *Genome Med.* 13 (1), 140. doi:10.1186/s13073-021-00952-5

Beaufort, C. M., Helmijr, J. C. A., Piskorz, A. M., Hoogstraat, M., Ruigrok-Ritstier, K., Besselink, N., et al. (2014). Ovarian Cancer Cell Line Panel (OCCP): Clinical Importance of *In Vitro* Morphological Subtypes. *PLoS ONE* 9 (9), e103988. doi:10.1371/journal.pone.0103988

Becker, J. L., Prewett, T. L., Spaulding, G. F., and Goodwin, T. J. (1993). Three-dimensional Growth and Differentiation of Ovarian Tumor Cell Line in High Aspect Rotating-wall Vessel: Morphologic and Embryologic Considerations. *J. Cel. Biochem.* 51 (3), 283–289. doi:10.1002/jcb.240510307

Behrens, B. C., Hamilton, T. C., Masuda, H., Grotzinger, K. R., Whang-Peng, J., Louie, K. G., et al. (1987). Characterization of a cis-Diamminedichloroplatinum(II)-resistant Human Ovarian Cancer Cell Line and its Use in Evaluation of Platinum Analogues. *Cancer Res.* 47 (2), 414–418.

Bell, D. (2011). Integrated Genomic Analyses of Ovarian Carcinoma. *Nature* 474, 609–615. doi:10.1038/nature10166

Bernardo, A. D. M., Thorsteinsdóttir, S., and Mummery, C. L. (2015). Advantages of the Avian Model for Human Ovarian Cancer. *Mol. Clin. Oncol.* 3 (6), 1191–1198. doi:10.3892/mco.2015.619

Boylan, K. L. M., Manion, R. D., Shah, H., Skubitz, K. M., and Skubitz, A. P. N. (2020). Inhibition of Ovarian Cancer Cell Spheroid Formation by Synthetic Peptides Derived from Nectin-4. *Ijms* 21 (13), 4637. doi:10.3390/ijms21134637

Brooks, E. A., Gencoglu, M. F., Corbett, D. C., Stevens, K. R., and Peyton, S. R. (2019). An Omentum-Inspired 3D PEG Hydrogel for Identifying ECM-Drivers of Drug Resistant Ovarian Cancer. *APL Bioeng.* 3 (2), 026106. doi:10.1063/1.5091713

Buechel, M. E., Enserro, D., Burger, R. A., Brady, M. F., Wade, K., Secord, A. A., et al. (2021). Correlation of Imaging and Plasma Based Biomarkers to Predict Response to Bevacizumab in Epithelial Ovarian Cancer (EOC). *Gynecol. Oncol.* 161 (2), 382–388. doi:10.1016/j.ygyno.2021.02.032

Buick, R. N., Pullano, R., and Trent, J. M. (1985). Comparative Properties of Five Human Ovarian Adenocarcinoma Cell Lines. *Cancer Res.* 45 (8), 3668–3676.

Burger, R. A., Brady, M. F., Bookman, M. A., Fleming, G. F., Monk, B. J., Huang, H., et al. (2011). Incorporation of Bevacizumab in the Primary Treatment of Ovarian Cancer. *N. Engl. J. Med.* 365 (26), 2473–2483. doi:10.1056/NEJMoa1104390

Burleson, K. M., Casey, R. C., Skubitz, K. M., Pambuccian, S. E., Oegema, T. R., and Skubitz, A. P. N. (2004). Ovarian Carcinoma Ascites Spheroids Adhere to Extracellular Matrix Components and Mesothelial Cell Monolayers. *Gynecol. Oncol.* 93 (1), 170–181. doi:10.1016/j.ygyno.2003.12.034

Cai, J., Tang, H., Xu, L., Wang, X., Yang, C., Ruan, S., et al. (2012). Fibroblasts in Omentum Activated by Tumor Cells Promote Ovarian Cancer Growth, Adhesion and Invasiveness. *Carcinogenesis* 33 (1), 20–29. doi:10.1093/carcin/bgr230

Casagrande, N., Borghese, C., Agostini, F., Durante, C., Mazzucato, M., Colombatti, A., et al. (2021). In Ovarian Cancer Multicellular Spheroids, Platelet Releasate Promotes Growth, Expansion of ALDH+ and CD133+ Cancer Stem Cells, and Protection against the Cytotoxic Effects of Cisplatin, Carboplatin and Paclitaxel. *Ijms* 22 (6), 3019. doi:10.3390/ijms22063019

Chao, A., Lai, C.-H., Wang, T.-H., Jung, S.-M., Lee, Y.-S., Chang, W.-Y., et al. (2018). Genomic Scar Signatures Associated with Homologous Recombination Deficiency Predict Adverse Clinical Outcomes in Patients with Ovarian clear Cell Carcinoma. *J. Mol. Med.* 96 (6), 527–536. doi:10.1007/s00109-018-1643-8

Cheasley, D., Nigam, A., Zethoven, M., Hunter, S., Etemadmoghadam, D., Semple, T., et al. (2021). Genomic Analysis of Low-grade Serous Ovarian Carcinoma to Identify Key Drivers and Therapeutic Vulnerabilities. *J. Pathol.* 253 (1), 41–54. doi:10.1002/path.5545

Cheasley, D., Wakefield, M. J., Ryland, G. L., Allan, P. E., Alsop, K., Amarasinghe, K. C., et al. (2019). The Molecular Origin and Taxonomy of Mucinous Ovarian Carcinoma. *Nat. Commun.* 10 (1), 3935. doi:10.1038/s41467-019-11862-x

Cole, A. J., Dwight, T., Gill, A. J., Dickson, K.-A., Zhu, Y., Clarkson, A., et al. (2016). Assessing Mutant P53 in Primary High-Grade Serous Ovarian Cancer Using Immunohistochemistry and Massively Parallel Sequencing. *Sci. Rep.* 6, 26191. doi:10.1038/srep26191

Colombo, P.-E., du Manoir, S., Orsetti, B., Bras-Gonçalves, R., Lambros, M. B., MacKay, A., et al. (2015). Ovarian Carcinoma Patient Derived Xenografts Reproduce Their Tumor of Origin and Preserve an Oligoclonal Structure. *Oncotarget* 6 (29), 28327–28340. doi:10.18632/oncotarget.5069

Conover, C. A., Hartmann, L. C., Bradley, S., Stalboerger, P., Klee, G. G., Kalli, K. R., et al. (1998). Biological Characterization of Human Epithelial Ovarian Carcinoma Cells in Primary Culture: the Insulin-like Growth Factor System. *Exp. Cell Res.* 238 (2), 439–449. doi:10.1006/excr.1997.3861

Crum, C. P., Drapkin, R., Kindelberger, D., Medeiros, F., Miron, A., and Lee, Y. (2007). Lessons from BRCA: the Tubal Fimbria Emerges as an Origin for Pelvic Serous Cancer. *Clin. Med. Res.* 5 (1), 35–44. doi:10.3121/cmr.2007.702

Dadgar, N., Gonzalez-Suarez, A. M., Fattahi, P., Hou, X., Weroha, J. S., Gaspar-Maia, A., et al. (2020). A Microfluidic Platform for Cultivating Ovarian Cancer Spheroids and Testing Their Responses to Chemotherapies. *Microsyst Nanoeng* 6 (1), 1. doi:10.1038/s41378-020-00201-6

Davies, B., Steele, I. A., Edmondson, R. J., Zwolinski, S. A., Saretzki, G., von Zglinicki, T., et al. (2003). Immortalisation of Human Ovarian Surface Epithelium with Telomerase and Temperature-Senstitive SV40 Large T Antigen. *Exp. Cell Res.* 288 (2), 390–402. doi:10.1016/s0014-4827(03)00218-0

Davis, A., Tinker, A. V., and Friedlander, M. (2014). "Platinum Resistant" Ovarian Cancer: What Is it, Who to Treat and How to Measure Benefit? *Gynecol. Oncol.* 133 (3), 624–631. doi:10.1016/j.ygyno.2014.02.038

De Haven Brandon, A., Box, G., Hallsworth, A., Court, W., Matthews, N., Herodek, B., et al. (2020). Identification of Ovarian High-Grade Serous Carcinoma Cell Lines that Show Estrogen-Sensitive Growth as Xenografts in Immunocompromised Mice. *Sci. Rep.* 10 (1), 1. doi:10.1038/s41598-020-67533-1

De Paolis, E., Paragliola, R. M., and Concolino, P. (2021). Spectrum of DICER1 Germline Pathogenic Variants in Ovarian Sertoli-Leydig Cell Tumor. *Jcm* 10 (9), 1845. doi:10.3390/jcm10091845

De Pauw, A., Naert, E., Van de Vijver, K., Philippe, T., Vandecasteele, K., and Denys, H. (2021). A Clearer View on Ovarian Clear Cell Carcinoma. *Acta Clinica Belgica* 17, 1–13. doi:10.1080/17843286.2021.1964051

De Thaye, E., Van de Vijver, K., Van der Meulen, J., Taminau, J., Wagemans, G., Denys, H., et al. (2020). Establishment and Characterization of a Cell Line and Patient-Derived Xenograft (PDX) from Peritoneal Metastasis of Low-Grade Serous Ovarian Carcinoma. *Sci. Rep.* 10 (1), 6688. doi:10.1038/s41598-020-63738-6

De Witte, C. J., Espejo Valle-Inclan, J., Hami, N., Lõhmussaar, K., Kopper, O., Vreuls, C. P. H., et al. (2020). Patient-Derived Ovarian Cancer Organoids Mimic Clinical Response and Exhibit Heterogeneous Inter- and Intrapatient Drug Responses. *Cell Rep.* 31 (11), 107762. doi:10.1016/j.celrep.2020.107762

Dedes, K. J., Wilkerson, P. M., Wetterskog, D., Weigelt, B., Ashworth, A., and Reis-Filho, J. S. (2011). Synthetic Lethality of PARP Inhibition in Cancers lackingBRCA1andBRCA2mutations. *Cell Cycle* 10 (8), 1192–1199. doi:10.4161/cc.10.8.15273

DelloRusso, C., Welcsh, P. L., Wang, W., Garcia, R. L., King, M.-C., and Swisher, E. M. (2007). Functional Characterization of a Novel BRCA1-Null Ovarian Cancer Cell Line in Response to Ionizing Radiation. *Mol. Cancer Res.* 5 (1), 35–45. doi:10.1158/1541-7786.Mcr-06-0234

Dickson, K.-A., Xie, T., Evenhuis, C., Ma, Y., and Marsh, D. J. (2021). PARP Inhibitors Display Differential Efficacy in Models of BRCA Mutant High-Grade Serous Ovarian Cancer. *Ijms* 22 (16), 8506. doi:10.3390/ijms22168506

Domcke, S., Sinha, R., Levine, D. A., Sander, C., and Schultz, N. (2013). Evaluating Cell Lines as Tumour Models by Comparison of Genomic Profiles. *Nat. Commun.* 4, 2126. doi:10.1038/ncomms3126

Donaldson, A. R., Tanase, C. E., Awuah, D., Vasanthi Bathrinarayanan, P., Hall, L., Nikkhah, M., et al. (2018). Photocrosslinkable Gelatin Hydrogels Modulate the Production of the Major Pro-inflammatory Cytokine, TNF-α, by Human Mononuclear Cells. *Front. Bioeng. Biotechnol.* 6 (116), 1. doi:10.3389/fbioe.2018.00116

Dong, R., Qiang, W., Guo, H., Xu, X., Kim, J. J., Mazar, A., et al. (2016). Histologic and Molecular Analysis of Patient Derived Xenografts of High-Grade Serous Ovarian Carcinoma. *J. Hematol. Oncol.* 9 (1), 92. doi:10.1186/s13045-016-0318-6

Evans, C. L., Abu-Yousif, A. O., Park, Y. J., Klein, O. J., Celli, J. P., Rizvi, I., et al. (2011). Killing Hypoxic Cell Populations in a 3D Tumor Model with EtNBS-PDT. *PLoS ONE* 6 (8), e23434. doi:10.1371/journal.pone.0023434

Fan, R., Piou, M., Darling, E., Cormier, D., Sun, J., and Wan, J. (2016). Bio-printing Cell-Laden Matrigel-Agarose Constructs. *J. Biomater. Appl.* 31 (5), 684–692. doi:10.1177/0885328216669238

Flont, M., Jastrzębska, E., and Brzózka, Z. (2020). A Multilayered Cancer-On-A-Chip Model to Analyze the Effectiveness of New-Generation Photosensitizers. *Analyst* 145 (21), 6937–6947. doi:10.1039/D0AN00911C

Florczyk, S. J., Kievit, F. M., Wang, K., Erickson, A. E., Ellenbogen, R. G., and Zhang, M. (2016). 3D Porous Chitosan-Alginate Scaffolds Promote Proliferation and Enrichment of Cancer Stem-like Cells. *J. Mater. Chem. B* 4 (38), 6326–6334. doi:10.1039/C6TB01713D

Ford, C. E., Werner, B., Hacker, N. F., and Warton, K. (2020). The Untapped Potential of Ascites in Ovarian Cancer Research and Treatment. *Br. J. Cancer* 123 (1), 9–16. doi:10.1038/s41416-020-0875-x

Fujisawa, T., Joshi, B. H., and Puri, R. K. (2012). IL-13 Regulates Cancer Invasion and Metastasis through IL-13Rα2 via ERK/AP-1 Pathway in Mouse Model of Human Ovarian Cancer. *Int. J. Cancer* 131 (2), 344–356. doi:10.1002/ijc.26366

Fuller, P. J., Leung, D., and Chu, S. (2017). Genetics and Genomics of Ovarian Sex Cord-Stromal Tumors. *Clin. Genet.* 91 (2), 285–291. doi:10.1111/cge.12917

Ganguli, A., Mostafa, A., Saavedra, C., Kim, Y., Le, P., Faramarzi, V., et al. (2021). Three-dimensional Microscale Hanging Drop Arrays with Geometric Control for Drug Screening and Live Tissue Imaging. *Sci. Adv.* 7 (17), eabc1323. doi:10.1126/sciadv.abc1323

Gao, J., Li, F., Liu, Z., Huang, M., Chen, H., Liao, G., et al. (2021). Multiple Genetic Variants Predict the Progression-free Survival of Bevacizumab Plus Chemotherapy in Advanced Ovarian Cancer. *Medicine (Baltimore)* 100 (35), e27130. doi:10.1097/md.0000000000027130

George, E., Kim, H., Krepler, C., Wenz, B., Makvandi, M., Tanyi, J. L., et al. (2017). A Patient-Derived-Xenograft Platform to Study BRCA-Deficient Ovarian Cancers. *JCI Insight* 2 (1), 1. doi:10.1172/jci.insight.89760

Gombotz, W., and Wee, S. (1998). Protein Release from Alginate Matrices. *Adv. Drug Deliv. Rev.* 31 (3), 267–285. doi:10.1016/S0169-409X(97)00124-5

Goodwin, T. J., Prewett, T. L., Spaulding, G. F., and Becker, J. L. (1997). Three-dimensional Culture of a Mixed Mullerian Tumor of the Ovary: Expression of *In Vivo* Characteristics. In Vitro *Cell.Dev.Biol.-Animal* 33 (5), 366–374. doi:10.1007/s11626-997-0007-4

Gorai, I., Nakazawa, T., Miyagi, E., Hirahara, F., Nagashima, Y., and Minaguchi, H. (1995). Establishment and Characterization of Two Human Ovarian clear Cell Adenocarcinoma Lines from Metastatic Lesions with Different Properties. *Gynecol. Oncol.* 57 (1), 33–46. doi:10.1006/gyno.1995.1097

Gorski, J. W., Zhang, Z., McCorkle, J. R., DeJohn, J. M., Wang, C., Miller, R. W., et al. (2021). Utilizing Patient-Derived Epithelial Ovarian Cancer Tumor Organoids to Predict Carboplatin Resistance. *Biomedicines* 9 (8), 1021. doi:10.3390/biomedicines9081021

Graf, B. W., and Boppart, S. A. (2010). Imaging and Analysis of Three-Dimensional Cell Culture Models. *Methods Mol. Biol. (Clifton, N.J.)* 591, 211–227. doi:10.1007/978-1-60761-404-3_13

Greenaway, J., Moorehead, R., Shaw, P., and Petrik, J. (2008). Epithelial-stromal Interaction Increases Cell Proliferation, Survival and Tumorigenicity in a Mouse Model of Human Epithelial Ovarian Cancer. *Gynecol. Oncol.* 108 (2), 385–394. doi:10.1016/j.ygyno.2007.10.035

Grun, B., Benjamin, E., Sinclair, J., Timms, J. F., Jacobs, I. J., Gayther, S. A., et al. (2009). Three-dimensionalin Vitrocell Biology Models of Ovarian and Endometrial Cancer. *Cell Prolif.* 42 (2), 219–228. doi:10.1111/j.1365-2184.2008.00579.x

Gurler, H., Yu, Y., Choi, J., Kajdacsy-Balla, A., and Barbolina, M. (2015). Three-Dimensional Collagen Type I Matrix Up-Regulates Nuclear Isoforms of the Microtubule Associated Protein Tau Implicated in Resistance to Paclitaxel Therapy in Ovarian Carcinoma. *Ijms* 16 (2), 3419–3433. doi:10.3390/ijms16023419

Hallas-Potts, A., Dawson, J. C., and Herrington, C. S. (2019). Ovarian Cancer Cell Lines Derived from Non-serous Carcinomas Migrate and Invade More Aggressively Than Those Derived from High-Grade Serous Carcinomas. *Sci. Rep.* 9 (1), 1. doi:10.1038/s41598-019-41941-4

Hamilton, T. C., Young, R. C., McKoy, W. M., Grotzinger, K. R., Green, J. A., Chu, E. W., et al. (1983). Characterization of a Human Ovarian Carcinoma Cell Line (NIH:OVCAR-3) with Androgen and Estrogen Receptors. *Cancer Res.* 43 (11), 5379–5389.

Harris, M. A., Delap, L. M., Sengupta, P. S., Wilkinson, P. M., Welch, R. S., Swindell, R., et al. (2003). Carcinosarcoma of the Ovary. *Br. J. Cancer* 88 (5), 654–657. doi:10.1038/sj.bjc.6600770

Hedegaard, C. L., Redondo-Gómez, C., Tan, B. Y., Ng, K. W., Loessner, D., and Mata, A. (2020). Peptide-protein Coassembling Matrices as a Biomimetic 3D Model of Ovarian Cancer. *Sci. Adv.* 6 (40), eabb3298. doi:10.1126/sciadv.abb3298

Henry, C., Hacker, N., and Ford, C. (2017). Silencing ROR1 and ROR2 Inhibits Invasion and Adhesion in an Organotypic Model of Ovarian Cancer Metastasis. *Oncotarget* 8 (68), 112727–112738. doi:10.18632/oncotarget.22559

Heo, E. J., Cho, Y. J., Cho, W. C., Hong, J. E., Jeon, H.-K., Oh, D.-Y., et al. (2017). Patient-Derived Xenograft Models of Epithelial Ovarian Cancer for Preclinical Studies. *Cancer Res. Treat.* 49 (4), 915–926. doi:10.4143/crt.2016.322

Heredia-Soto, V., Redondo, A., Berjón, A., Miguel-Martín, M., Díaz, E., Crespo, R., et al. (2018). High-throughput 3-dimensional Culture of Epithelial Ovarian Cancer Cells as Preclinical Model of Disease. *Oncotarget* 9 (31), 21893–21903. doi:10.18632/oncotarget.25098

Hernandez, L., Kim, M. K., Lyle, L. T., Bunch, K. P., House, C. D., Ning, F., et al. (2016). Characterization of Ovarian Cancer Cell Lines as *In Vivo* Models for Preclinical Studies. *Gynecol. Oncol.* 142 (2), 332–340. doi:10.1016/j.ygyno.2016.05.028

Hidalgo, M., Amant, F., Biankin, A. V., Budinská, E., Byrne, A. T., Caldas, C., et al. (2014). Patient-derived Xenograft Models: an Emerging Platform for Translational Cancer Research. *Cancer Discov.* 4 (9), 998–1013. doi:10.1158/2159-8290.Cd-14-0001

Hill, S. J., Decker, B., Roberts, E. A., Horowitz, N. S., Muto, M. G., Worley, M. J., Jr., et al. (2018). Prediction of DNA Repair Inhibitor Response in Short-Term Patient-Derived Ovarian Cancer Organoids. *Cancer Discov.* 8 (11), 1404–1421. doi:10.1158/2159-8290.Cd-18-0474

Hoffmann, K., Berger, H., Kulbe, H., Thillainadarasan, S., Mollenkopf, H. J., Zemojtel, T., et al. (2020). Stable Expansion of High-grade Serous Ovarian Cancer Organoids Requires a low-Wnt Environment. *Embo J.* 39 (6), 1. doi:10.15252/embj.2019104013

Hollis, R. L., Thomson, J. P., Stanley, B., Churchman, M., Meynert, A. M., Rye, T., et al. (2020). Molecular Stratification of Endometrioid Ovarian Carcinoma Predicts Clinical Outcome. *Nat. Commun.* 11 (1), 4995. doi:10.1038/s41467-020-18819-5

Hopkins, T. I. R., Bemmer, V. L., Franks, S., Dunlop, C., Hardy, K., and Dunlop, I. E. (2021). Micromechanical Mapping of the Intact Ovary interior Reveals Contrasting Mechanical Roles for Follicles and Stroma. *Biomaterials* 277, 121099. doi:10.1016/j.biomaterials.2021.121099

Hsu, P.-C., Chao, T.-K., Chou, Y.-C., Yu, M.-H., Wang, Y.-C., Lin, Y.-H., et al. (2021). AIM2 Inflammasome in Tumor Cells as a Biomarker for Predicting the Treatment Response to Antiangiogenic Therapy in Epithelial Ovarian Cancer Patients. *Jcm* 10 (19), 4529. doi:10.3390/jcm10194529

Hughes, C. S., Postovit, L. M., and Lajoie, G. A. (2010). Matrigel: a Complex Protein Mixture Required for Optimal Growth of Cell Culture. *Proteomics* 10 (9), 1886–1890. doi:10.1002/pmic.200900758

Ip, C. K. M., Li, S.-S., Tang, M. Y. H., Sy, S. K. H., Ren, Y., Shum, H. C., et al. (2016). Stemness and Chemoresistance in Epithelial Ovarian Carcinoma Cells under Shear Stress. *Sci. Rep.* 6 (1), 26788. doi:10.1038/srep26788

Ivascu, A., and Kubbies, M. (2006). Rapid Generation of Single-Tumor Spheroids for High-Throughput Cell Function and Toxicity Analysis. *J. Biomol. Screen.* 11 (8), 922–932. doi:10.1177/1087057106292763

Iwanicki, M. P., Davidowitz, R. A., Ng, M. R., Besser, A., Muranen, T., Merritt, M., et al. (2011). Ovarian Cancer Spheroids Use Myosin-Generated Force to Clear the Mesothelium. *Cancer Discov.* 1 (2), 144–157. doi:10.1158/2159-8274.cd-11-0010

Iyer, S., Zhang, S., Yucel, S., Horn, H., Smith, S. G., Reinhardt, F., et al. (2021). Genetically Defined Syngeneic Mouse Models of Ovarian Cancer as Tools for the Discovery of Combination Immunotherapy. *Cancer Discov.* 11 (2), 384–407. doi:10.1158/2159-8290.CD-20-0818

Jabs, J., Zickgraf, F. M., Park, J., Wagner, S., Jiang, X., Jechow, K., et al. (2017). Screening Drug Effects in Patient-derived Cancer Cells Links Organoid Responses to Genome Alterations. *Mol. Syst. Biol.* 13 (11), 955. doi:10.15252/msb.20177697

Jamieson, S., and Fuller, P. J. (2012). Molecular Pathogenesis of Granulosa Cell Tumors of the Ovary. *Endocr. Rev.* 33 (1), 109–144. doi:10.1210/er.2011-0014

Jelinic, P., Schlappe, B. A., Conlon, N., Tseng, J., Olvera, N., Dao, F., et al. (2016). Concomitant Loss of SMARCA2 and SMARCA4 Expression in Small Cell Carcinoma of the Ovary, Hypercalcemic Type. *Mod. Pathol.* 29 (1), 60–66. doi:10.1038/modpathol.2015.129

Jensen, C., and Teng, Y. (2020). Is it Time to Start Transitioning from 2D to 3D Cell Culture? *Front. Mol. Biosci.* 7 (33), 1. doi:10.3389/fmolb.2020.00033

Jin, K., Teng, L., Shen, Y., He, K., Xu, Z., and Li, G. (2010). Patient-derived Human Tumour Tissue Xenografts in Immunodeficient Mice: a Systematic Review. *Clin. Transl Oncol.* 12 (7), 473–480. doi:10.1007/s12094-010-0540-6

John, B., Naczki, C., Patel, C., Ghoneum, A., Qasem, S., Salih, Z., et al. (2019). Regulation of the Bi-directional Cross-Talk between Ovarian Cancer Cells and Adipocytes by SPARC. *Oncogene* 38 (22), 4366–4383. doi:10.1038/s41388-019-0728-3

Johnson, P. A., and Giles, J. R. (2013). The Hen as a Model of Ovarian Cancer. *Nat. Rev. Cancer* 13 (6), 432–436. doi:10.1038/nrc3535

Joshi, N., Liu, D., Dickson, K.-A., Marsh, D. J., Ford, C. E., and Stenzel, M. H. (2021). An Organotypic Model of High-Grade Serous Ovarian Cancer to Test the Anti-metastatic Potential of ROR2 Targeted Polyion Complex Nanoparticles. *J. Mater. Chem. B* 9 (44), 9123–9135. doi:10.1039/d1tb01837j

Kaemmerer, E., Melchels, F. P. W., Holzapfel, B. M., Meckel, T., Hutmacher, D. W., and Loessner, D. (2014). Gelatine Methacrylamide-Based Hydrogels: An Alternative Three-Dimensional Cancer Cell Culture System. *Acta Biomater.* 10 (6), 2551–2562. doi:10.1016/j.actbio.2014.02.035

Kalli, K. R., Chen, B.-K., Bale, L. K., Gernand, E., Overgaard, M. T., Oxvig, C., et al. (2004). Pregnancy-associated Plasma Protein-A (PAPP-A) Expression and Insulin-like Growth Factor Binding Protein-4 Protease Activity in normal and Malignant Ovarian Surface Epithelial Cells. *Int. J. Cancer* 110 (5), 633–640. doi:10.1002/ijc.20185

Kapałczyńska, M., Kolenda, T., Przybyła, W., Zajączkowska, M., Teresiak, A., Filas, V., et al. (2018). 2D and 3D Cell Cultures - a Comparison of Different Types of Cancer Cell Cultures. *aoms* 14 (4), 910–919. doi:10.5114/aoms.2016.63743

Karnezis, A. N., Chen, S. Y., Chow, C., Yang, W., Hendricks, W. P. D., Ramos, P., et al. (2021). Re-assigning the Histologic Identities of COV434 and TOV-112D Ovarian Cancer Cell Lines. *Gynecol. Oncol.* 160 (2), 568–578. doi:10.1016/j.ygyno.2020.12.004

Karst, A. M., Levanon, K., and Drapkin, R. (2011). Modeling High-Grade Serous Ovarian Carcinogenesis from the Fallopian Tube. *Proc. Natl. Acad. Sci.* 108 (18), 7547–7552. doi:10.1073/pnas.1017300108

Kashiyama, T., Oda, K., Ikeda, Y., Shiose, Y., Hirota, Y., Inaba, K., et al. (2014). Antitumor Activity and Induction of TP53-dependent Apoptosis toward Ovarian clear Cell Adenocarcinoma by the Dual PI3K/mTOR Inhibitor DS-7423. *PLoS ONE* 9 (2), e87220. doi:10.1371/journal.pone.0087220

Kenny, H. A., Chiang, C.-Y., White, E. A., Schryver, E. M., Habis, M., Romero, I. L., et al. (2014). Mesothelial Cells Promote Early Ovarian Cancer Metastasis through Fibronectin Secretion. *J. Clin. Invest.* 124 (10), 4614–4628. doi:10.1172/jci74778

Kenny, H. A., Dogan, S., Zillhardt, M., Mitra, A. A., Yamada, S. D., Krausz, T., et al. (2009). "Organotypic Models of Metastasis: A Three-Dimensional Culture Mimicking the Human Peritoneum and Omentum for the Study of the Early Steps of Ovarian Cancer Metastasis," in *Cancer Treatment and Research* (US: Springer), 335–351. doi:10.1007/978-0-387-98094-2_16

Kenny, H. A., Krausz, T., Yamada, S. D., and Lengyel, E. (2007). Use of a Novel 3D Culture Model to Elucidate the Role of Mesothelial Cells, Fibroblasts and Extra-cellular Matrices on Adhesion and Invasion of Ovarian Cancer Cells to the Omentum. *Int. J. Cancer* 121 (7), 1463–1472. doi:10.1002/ijc.22874

Khalil, C., Moussa, M., Azar, A., Tawk, J., Habbouche, J., Salameh, R., et al. (2019). Anti-proliferative Effects of Mesenchymal Stem Cells (MSCs) Derived from Multiple Sources on Ovarian Cancer Cell Lines: an *In-Vitro* Experimental Study. *J. Ovarian Res.* 12 (1), 70. doi:10.1186/s13048-019-0546-9

Kidera, Y., Yoshimura, T., Ohkuma, Y., Iwasaka, T., and Sugimori, H. (1985). Establishment and Characterization of a Cell Line Derived from Mucinous Cystadenocarcinoma of Human Ovary. *Nihon Sanka Fujinka Gakkai Zasshi* 37 (9), 1820–1824.

Kim, S. I., Lee, J. W., Lee, M., Kim, H. S., Chung, H. H., Kim, J.-W., et al. (2018). Genomic Landscape of Ovarian clear Cell Carcinoma via Whole Exome Sequencing. *Gynecol. Oncol.* 148 (2), 375–382. doi:10.1016/j.ygyno.2017.12.005

King, S. M., Quartuccio, S., Hilliard, T. S., Inoue, K., and Burdette, J. E. (2011). Alginate Hydrogels for Three-Dimensional Organ Culture of Ovaries and Oviducts. *JoVE* 52, 1. doi:10.3791/2804

Köbel, M., and Kang, E. Y. (2021). The Many Uses of P53 Immunohistochemistry in Gynecological Pathology: Proceedings of the ISGyP Companion Society Session at the 2020 USCAP Annual9 Meeting. *Int. J. Gynecol. Pathol.* 40 (1), 32–40. doi:10.1097/pgp.0000000000000725

Kondrashova, O., Nguyen, M., Shield-Artin, K., Tinker, A. V., Teng, N. N. H., Harrell, M. I., et al. (2017). Secondary Somatic Mutations Restoring RAD51C and RAD51D Associated with Acquired Resistance to the PARP Inhibitor Rucaparib in High-Grade Ovarian Carcinoma. *Cancer Discov.* 7 (9), 984–998. doi:10.1158/2159-8290.Cd-17-0419

Konstantinopoulos, P. A., Spentzos, D., Karlan, B. Y., Taniguchi, T., Fountzilas, E., Francoeur, N., et al. (2010). Gene Expression Profile ofBRCAness that Correlates with Responsiveness to Chemotherapy and with Outcome in Patients with Epithelial Ovarian Cancer. *Jco* 28 (22), 3555–3561. doi:10.1200/jco.2009.27.5719

Kopper, O., de Witte, C. J., Lõhmussaar, K., Valle-Inclan, J. E., Hami, N., Kester, L., et al. (2019). An Organoid Platform for Ovarian Cancer Captures Intra- and Interpatient Heterogeneity. *Nat. Med.* 25 (5), 838–849. doi:10.1038/s41591-019-0422-6

Kuo, K.-T., Mao, T.-L., Jones, S., Veras, E., Ayhan, A., Wang, T.-L., et al. (2009). Frequent Activating Mutations of PIK3CA in Ovarian clear Cell Carcinoma. *Am. J. Pathol.* 174 (5), 1597–1601. doi:10.2353/ajpath.2009.081000

Kunz-Schughart, L. A., Freyer, J. P., Hofstaedter, F., and Ebner, R. (2004). The Use of 3-D Cultures for High-Throughput Screening: The Multicellular Spheroid Model. *J. Biomol. Screen.* 9 (4), 273–285. doi:10.1177/1087057104265040

Kurman, R. J., and Shih, I.-M. (2010). The Origin and Pathogenesis of Epithelial Ovarian Cancer: a Proposed Unifying Theory. *Am. J. Surg. Pathol.* 34 (3), 433–443. doi:10.1097/PAS.0b013e3181cf3d79

Lal-Nag, M., McGee, L., Guha, R., Lengyel, E., Kenny, H. A., and Ferrer, M. (2017). A High-Throughput Screening Model of the Tumor Microenvironment for Ovarian Cancer Cell Growth. *SLAS DISCOVERY: Advancing Sci. Drug Discov.* 22 (5), 494–506. doi:10.1177/2472555216687082

Langdon, S. P., Lawrie, S. S., Hay, F. G., Hawkes, M. M., McDonald, A., Hayward, I. P., et al. (1988). Characterization and Properties of Nine Human Ovarian Adenocarcinoma Cell Lines. *Cancer Res.* 48 (21), 6166–6172.

Lau, T.-S., Chan, L. K.-Y., Wong, E. C.-H., Hui, C. W.-C., Sneddon, K., Cheung, T.-H., et al. (2017). A Loop of Cancer-Stroma-Cancer Interaction Promotes Peritoneal Metastasis of Ovarian Cancer via TNFα-Tgfα-EGFR. *Oncogene* 36 (25), 3576–3587. doi:10.1038/onc.2016.509

Lawrenson, K., Grun, B., and Gayther, S. A. (2012). Heterotypic Three-Dimensional *In Vitro* Modeling of Stromal-Epithelial Interactions during Ovarian Cancer Initiation and Progression. *JoVE* 66, e4206. doi:10.3791/4206

Ledermann, J. A., Luvero, D., Shafer, A., O'Connor, D., Mangili, G., Friedlander, M., et al. (2014b). Gynecologic Cancer InterGroup (GCIG) Consensus Review for Mucinous Ovarian Carcinoma. *Int. J. Gynecol. Cancer* 24 (9), S14–S19. doi:10.1097/igc.0000000000000296

Ledermann, J., Harter, P., Gourley, C., Friedlander, M., Vergote, I., Rustin, G., et al. (2014a). Olaparib Maintenance Therapy in Patients with Platinum-Sensitive Relapsed Serous Ovarian Cancer: a Preplanned Retrospective Analysis of Outcomes by BRCA Status in a Randomised Phase 2 Trial. *Lancet Oncol.* 15 (8), 852–861. doi:10.1016/s1470-2045(14)70228-1

Ledermann, J., Harter, P., Gourley, C., Friedlander, M., Vergote, I., Rustin, G., et al. (2012). Olaparib Maintenance Therapy in Platinum-Sensitive Relapsed Ovarian Cancer. *N. Engl. J. Med.* 366 (15), 1382–1392. doi:10.1056/NEJMoa1105535

Lee, C. K., Friedlander, M. L., Tjokrowidjaja, A., Ledermann, J. A., Coleman, R. L., Mirza, M. R., et al. (2021). Molecular and Clinical Predictors of Improvement in Progression-free Survival with Maintenance PARP Inhibitor Therapy in Women with Platinum-sensitive, Recurrent Ovarian Cancer: A Meta-analysis. *Cancer* 127 (14), 2432–2441. doi:10.1002/cncr.33517

Li, S.-S., Ip, C. K. M., Tang, M. Y. H., Sy, S. K. H., Yung, S., Chan, T.-M., et al. (2017). Modeling Ovarian Cancer Multicellular Spheroid Behavior in a Dynamic 3D Peritoneal Microdevice. *JoVE* 120, 55337. doi:10.3791/55337

Liao, J., Qian, F., Tchabo, N., Mhawech-Fauceglia, P., Beck, A., Qian, Z., et al. (2014). Ovarian Cancer Spheroid Cells with Stem Cell-like Properties Contribute to Tumor Generation, Metastasis and Chemotherapy Resistance through Hypoxia-Resistant Metabolism. *PLoS ONE* 9 (1), e84941. doi:10.1371/journal.pone.0084941

Liu, J. F., Palakurthi, S., Zeng, Q., Zhou, S., Ivanova, E., Huang, W., et al. (2017). Establishment of Patient-Derived Tumor Xenograft Models of Epithelial Ovarian Cancer for Preclinical Evaluation of Novel Therapeutics. *Clin. Cancer Res.* 23 (5), 1263–1273. doi:10.1158/1078-0432.Ccr-16-1237

Liu, M., Zhang, X., Long, C., Xu, H., Cheng, X., Chang, J., et al. (2018). Collagen-based Three-Dimensional Culture Microenvironment Promotes Epithelial to Mesenchymal Transition and Drug Resistance of Human Ovarian Cancerin Vitro. *RSC Adv.* 8 (16), 8910–8919. doi:10.1039/C7RA13742G

Loessner, D., Rockstroh, A., Shokoohmand, A., Holzapfel, B. M., Wagner, F., Baldwin, J., et al. (2019). A 3D Tumor Microenvironment Regulates Cell Proliferation, Peritoneal Growth and Expression Patterns. *Biomaterials* 190-191, 63–75. doi:10.1016/j.biomaterials.2018.10.014

Lõhmussaar, K., Kopper, O., Korving, J., Begthel, H., Vreuls, C. P. H., Van Es, J. H., et al. (2020). Assessing the Origin of High-Grade Serous Ovarian Cancer Using CRISPR-Modification of Mouse Organoids. *Nat. Commun.* 11 (1), 1. doi:10.1038/s41467-020-16432-0

Long, L., Yin, M., and Min, W. (2018). 3D Co-culture System of Tumor-Associated Macrophages and Ovarian Cancer Cells. *Bio-protocol* 8 (8), e2815. doi:10.21769/BioProtoc.2815

Lu, M., Henry, C. E., Lai, H., Khine, Y. Y., Ford, C. E., and Stenzel, M. H. (2019). A New 3D Organotypic Model of Ovarian Cancer to Help Evaluate the Antimetastatic Activity of RAPTA-C Conjugated Micelles. *Biomater. Sci.* 7 (4), 1652–1660. doi:10.1039/c8bm01326h

Lutolf, M. P., Lauer-Fields, J. L., Schmoekel, H. G., Metters, A. T., Weber, F. E., Fields, G. B., et al. (2003). Synthetic Matrix Metalloproteinase-Sensitive Hydrogels for the Conduction of Tissue Regeneration: Engineering Cell-Invasion Characteristics. *Proc. Natl. Acad. Sci.* 100 (9), 5413–5418. doi:10.1073/pnas.0737381100

Lynn, A. K., Yannas, I. V., and Bonfield, W. (2004). Antigenicity and Immunogenicity of Collagen. *J. Biomed. Mater. Res.* 71B (2), 343–354. doi:10.1002/jbm.b.30096

Mabuchi, S., Sugiyama, T., and Kimura, T. (2016). Clear Cell Carcinoma of the Ovary: Molecular Insights and Future Therapeutic Perspectives. *J. Gynecol. Oncol.* 27 (3), e31. doi:10.3802/jgo.2016.27.e31

Machida-Sano, I., Matsuda, Y., and Namiki, H. (2009). In Vitroadhesion of Human Dermal Fibroblasts on Iron Cross-Linked Alginate Films. *Biomed. Mater.* 4, 025008. doi:10.1088/1748-6041/4/2/025008

Maenhoudt, N., Defraye, C., Boretto, M., Jan, Z., Heremans, R., Boeckx, B., et al. (2020). Developing Organoids from Ovarian Cancer as Experimental and Preclinical Models. *Stem Cell Rep.* 14 (4), 717–729. doi:10.1016/j.stemcr.2020.03.004

Maenhoudt, N., and Vankelecom, H. (2021). Protocol for Establishing Organoids from Human Ovarian Cancer Biopsies. *STAR Protoc.* 2 (2), 100429. doi:10.1016/j.xpro.2021.100429

Makałowski, W., Zhang, J., and Boguski, M. S. (1996). Comparative Analysis of 1196 Orthologous Mouse and Human Full-Length mRNA and Protein Sequences. *Genome Res.* 6 (9), 846–857. doi:10.1101/gr.6.9.846

Maniati, E., Berlato, C., Gopinathan, G., Heath, O., Kotantaki, P., Lakhani, A., et al. (2020). Mouse Ovarian Cancer Models Recapitulate the Human Tumor Microenvironment and Patient Response to Treatment. *Cell Rep.* 30 (2), 525–540. e527. doi:10.1016/j.celrep.2019.12.034

Maru, Y., Tanaka, N., Itami, M., and Hippo, Y. (2019). Efficient Use of Patient-Derived Organoids as a Preclinical Model for Gynecologic Tumors. *Gynecol. Oncol.* 154 (1), 189–198. doi:10.1016/j.ygyno.2019.05.005

Masiello, T., Dhall, A., Hemachandra, L., Tokranova, N., Melendez, J., and Castracane, J. (2018). A Dynamic Culture Method to Produce Ovarian Cancer Spheroids under Physiologically-Relevant Shear Stress. *Cells* 7 (12), 277. doi:10.3390/cells7120277

Matsuo, K., Nishimura, M., Bottsford-Miller, J. N., Huang, J., Komurov, K., Armaiz-Pena, G. N., et al. (2011). Targeting SRC in Mucinous Ovarian Carcinoma. *Clin. Cancer Res.* 17 (16), 5367–5378. doi:10.1158/1078-0432.Ccr-10-3176

Mazzocchi, A., Soker, S., and Skardal, A. (2019). 3D Bioprinting for High-Throughput Screening: Drug Screening, Disease Modeling, and Precision Medicine Applications. *Appl. Phys. Rev.* 6 (1), 011302. doi:10.1063/1.5056188

McCloskey, C. W., Goldberg, R. L., Carter, L. E., Gamwell, L. F., Al-Hujaily, E. M., Collins, O., et al. (2014). A New Spontaneously Transformed Syngeneic Model of High-Grade Serous Ovarian Cancer with a Tumor-Initiating Cell Population. *Front. Oncol.* 4 (53), 1. doi:10.3389/fonc.2014.00053

McCluggage, W. G., and Stewart, C. J. R. (2021). SWI/SNF-deficient Malignancies of the Female Genital Tract. *Semin. Diagn. Pathol.* 38 (3), 199–211. doi:10.1053/j.semdp.2020.08.003

Mckenzie, A. J., Hicks, S. R., Svec, K. V., Naughton, H., Edmunds, Z. L., and Howe, A. K. (2018). The Mechanical Microenvironment Regulates Ovarian Cancer Cell Morphology, Migration, and Spheroid Disaggregation. *Sci. Rep.* 8 (1), 1. doi:10.1038/s41598-018-25589-0

Medeiros, M., Ribeiro, A. O., Lupi, L. A., Romualdo, G. R., Pinhal, D., Chuffa, L. G. d. A., et al. (2019). Mimicking the Tumor Microenvironment: Fibroblasts Reduce miR-29b Expression and Increase the Motility of Ovarian Cancer Cells in a Co-culture Model. *Biochem. Biophysical Res. Commun.* 516 (1), 96–101. doi:10.1016/j.bbrc.2019.06.001

Mehta, G., Hsiao, A. Y., Ingram, M., Luker, G. D., and Takayama, S. (2012). Opportunities and Challenges for Use of Tumor Spheroids as Models to Test Drug Delivery and Efficacy. *J. Control. Release* 164 (2), 192–204. doi:10.1016/j.jconrel.2012.04.045

Mendibil, U., Ruiz-Hernandez, R., Retegi-Carrion, S., Garcia-Urquia, N., Olalde-Graells, B., and Abarrategi, A. (2020). Tissue-Specific Decellularization Methods: Rationale and Strategies to Achieve Regenerative Compounds. *Ijms* 21 (15), 5447. doi:10.3390/ijms21155447

Michael, B., Yong-Hyun, S., Aleksandar, R., and Bryan, B. (2016). The Effect of ECM Stiffness on Ovarian Follicle Development. *Front. Bioeng. Biotechnol.* 4, 1. doi:10.3389/conf.FBIOE.2016.01.00303

Mieulet, V., Garnier, C., Kieffer, Y., Guilbert, T., Nemati, F., Marangoni, E., et al. (2021). Stiffness Increases with Myofibroblast Content and Collagen Density in Mesenchymal High Grade Serous Ovarian Cancer. *Sci. Rep.* 11 (1), 1. doi:10.1038/s41598-021-83685-0

Mitra, A. K., Chiang, C. Y., Tiwari, P., Tomar, S., Watters, K. M., Peter, M. E., et al. (2015a). Microenvironment-induced Downregulation of miR-193b Drives Ovarian Cancer Metastasis. *Oncogene* 34 (48), 5923–5932. doi:10.1038/onc.2015.43

Mitra, A. K., Davis, D. A., Tomar, S., Roy, L., Gurler, H., Xie, J., et al. (2015b). *In Vivo* tumor Growth of High-Grade Serous Ovarian Cancer Cell Lines. *Gynecol. Oncol.* 138 (2), 372–377. doi:10.1016/j.ygyno.2015.05.040

Miyagawa, Y., Nagasaka, K., Yamawaki, K., Mori, Y., Ishiguro, T., Hashimoto, K., et al. (2020). Evaluating the Angiogenetic Properties of Ovarian Cancer Stem-

like Cells Using the Three-Dimensional Co-culture System, NICO-1. *JoVE* 166, 1. doi:10.3791/61751

Moore, K., Colombo, N., Scambia, G., Kim, B.-G., Oaknin, A., Friedlander, M., et al. (2018). Maintenance Olaparib in Patients with Newly Diagnosed Advanced Ovarian Cancer. *N. Engl. J. Med.* 379 (26), 2495–2505. doi:10.1056/NEJMoa1810858

Morton, C. L., and Houghton, P. J. (2007). Establishment of Human Tumor Xenografts in Immunodeficient Mice. *Nat. Protoc.* 2 (2), 247–250. doi:10.1038/nprot.2007.25

Motohara, T., Masuda, K., Morotti, M., Zheng, Y., El-Sahhar, S., Chong, K. Y., et al. (2019). An Evolving story of the Metastatic Voyage of Ovarian Cancer Cells: Cellular and Molecular Orchestration of the Adipose-Rich Metastatic Microenvironment. *Oncogene* 38 (16), 2885–2898. doi:10.1038/s41388-018-0637-x

Motoyama, T. (1981). Biological Characterization Including Sensitivity to Mitomycin C of Cultured Human Ovarian Cancers (Author's Transl). *Nihon Sanka Fujinka Gakkai Zasshi* 33 (8), 1197–1204.

Moujaber, T., Balleine, R. L., Gao, B., Madsen, I., Harnett, P. R., and DeFazio, A. (2022). New Therapeutic Opportunities for Women with Low-Grade Serous Ovarian Cancer. *Endocr. Relat. Cancer* 29 (1), R1–r16. doi:10.1530/erc-21-0191

Muggia, F., and Safra, T. (2014). 'BRCAness' and its Implications for Platinum Action in Gynecologic Cancer. *Anticancer Res.* 34 (2), 551–556.

Mullen, P., Ritchie, A., Langdon, S. P., and Miller, W. R. (1996). Effect of Matrigel on the Tumorigenicity of Human Breast and Ovarian Carcinoma Cell Lines. *Intl J. Cancer* 67 (6), 816–820. doi:10.1002/(sici)1097-0215(19960917)67:6<816:aid-ijc10>3.0.co;2-#

Nanki, Y., Chiyoda, T., Hirasawa, A., Ookubo, A., Itoh, M., Ueno, M., et al. (2020). Patient-derived Ovarian Cancer Organoids Capture the Genomic Profiles of Primary Tumours Applicable for Drug Sensitivity and Resistance Testing. *Sci. Rep.* 10 (1), 1. doi:10.1038/s41598-020-69488-9

Nesic, K., Kondrashova, O., Hurley, R. M., McGehee, C. D., Vandenberg, C. J., Ho, G.-Y., et al. (2021). Acquired RAD51C Promoter Methylation Loss Causes PARP Inhibitor Resistance in High-Grade Serous Ovarian Carcinoma. *Cancer Res.* 81 (18), 4709–4722. doi:10.1158/0008-5472.Can-21-0774

Nguyen, L., W. M. Martens, J., Van Hoeck, A., and Cuppen, E. (2020). Pan-cancer Landscape of Homologous Recombination Deficiency. *Nat. Commun.* 11 (1), 5584. doi:10.1038/s41467-020-19406-4

Nikniaz, H., Zandieh, Z., Nouri, M., Daei-farshbaf, N., Aflatoonian, R., Gholipourmalekabadi, M., et al. (2021). Comparing Various Protocols of Human and Bovine Ovarian Tissue Decellularization to Prepare Extracellular Matrix-Alginate Scaffold for Better Follicle Development *In Vitro*. *BMC Biotechnol.* 21 (1), 8. doi:10.1186/s12896-020-00658-3

Ning, Y., Cui, Y., Li, X., Cao, X., Chen, A., Xu, C., et al. (2018). Co-culture of Ovarian Cancer Stem-like Cells with Macrophages Induced SKOV3 Cells Stemness via IL-8/STAT3 Signaling. *Biomed. Pharmacother.* 103, 262–271. doi:10.1016/j.biopha.2018.04.022

Nishi, Y., Yanase, T., Mu, Y.-M., Oba, K., Ichino, I., Saito, M., et al. (2001). Establishment and Characterization of a Steroidogenic Human Granulosa-like Tumor Cell Line, KGN, that Expresses Functional Follicle-Stimulating Hormone Receptor. *Endocrinology* 142 (1), 437–445. doi:10.1210/endo.142.1.7862

Noshadi, I., Hong, S., Sullivan, K. E., Shirzaei Sani, E., Portillo-Lara, R., Tamayol, A., et al. (2017). *In Vitro* and *In Vivo* Analysis of Visible Light Crosslinkable Gelatin Methacryloyl (GelMA) Hydrogels. *Biomater. Sci.* 5 (10), 2093–2105. doi:10.1039/c7bm00110j

Novak, C. M., Horst, E. N., Lin, E., and Mehta, G. (2020). Compressive Stimulation Enhances Ovarian Cancer Proliferation, Invasion, Chemoresistance, and Mechanotransduction via CDC42 in a 3D Bioreactor. *Cancers* 12 (6), 1521. doi:10.3390/cancers12061521

Nowacka, M., Sterzynska, K., Andrzejewska, M., Nowicki, M., and Januchowski, R. (2021). Drug Resistance Evaluation in Novel 3D *In Vitro* Model. *Biomed. Pharmacother.* 138, 111536. doi:10.1016/j.biopha.2021.111536

Nozawa, S., Yajima, M., Sasaki, H., Tsukazaki, K., Aoki, D., Sakayori, M., et al. (1991). A New CA125-like Antigen (CA602) Recognized by Two Monoclonal Antibodies against a Newly Established Ovarian clear Cell Carcinoma Cell Line (RMG-II). *Jpn. J. Cancer Res.* 82 (7), 854–861. doi:10.1111/j.1349-7006.1991.tb02713.x

Odunsi, A., McGray, A. J. R., Miliotto, A., Zhang, Y., Wang, J., Abiola, A., et al. (2020). Fidelity of Human Ovarian Cancer Patient-Derived Xenografts in a Partially Humanized Mouse Model for Preclinical Testing of Immunotherapies. *J. Immunother. Cancer* 8 (2), e001237. doi:10.1136/jitc-2020-001237

Onal, S., Alkaisi, M. M., and Nock, V. (2021). A Flexible Microdevice for Mechanical Cell Stimulation and Compression in Microfluidic Settings. *Front. Phys.* 9 (280), 1. doi:10.3389/fphy.2021.654918

Orkin, R. W., Gehron, P., McGoodwin, E. B., Martin, G. R., Valentine, T., and Swarm, R. (1977). A Murine Tumor Producing a Matrix of Basement Membrane. *J. Exp. Med.* 145 (1), 204–220. doi:10.1084/jem.145.1.204

Oza, A. M., Cook, A. D., Pfisterer, J., Embleton, A., Ledermann, J. A., Pujade-Lauraine, E., et al. (2015). Standard Chemotherapy with or without Bevacizumab for Women with Newly Diagnosed Ovarian Cancer (ICON7): Overall Survival Results of a Phase 3 Randomised Trial. *Lancet Oncol.* 16 (8), 928–936. doi:10.1016/s1470-2045(15)00086-8

Ozols, R. F., Willson, J. K., Grotzinger, K. R., and Young, R. C. (1980). Cloning of Human Ovarian Cancer Cells in Soft agar from Malignant and Peritoneal Washings. *Cancer Res.* 40 (8), 2743–2747.

Papp, E., Hallberg, D., Konecny, G. E., Bruhm, D. C., Adleff, V., Noë, M., et al. (2018). Integrated Genomic, Epigenomic, and Expression Analyses of Ovarian Cancer Cell Lines. *Cell Rep.* 25 (9), 2617–2633. doi:10.1016/j.celrep.2018.10.096

Paradiso, F., Fitzgerald, J., Yao, S., Barry, F., Taraballi, F., Gonzalez, D., et al. (2019). Marine Collagen Substrates for 2D and 3D Ovarian Cancer Cell Systems. *Front. Bioeng. Biotechnol.* 7, 1. doi:10.3389/fbioe.2019.00343

Parra-Herran, C., Bassiouny, D., Lerner-Ellis, J., Olkhov-Mitsel, E., Ismiil, N., Hogen, L., et al. (2019). p53, Mismatch Repair Protein, and POLE Abnormalities in Ovarian Clear Cell Carcinoma. *Am. J. Surg. Pathol.* 43 (12), 1591–1599. doi:10.1097/pas.0000000000001328

Patch, A.-M., Christie, E. L., Christie, E. L., Etemadmoghadam, D., Garsed, D. W., George, J., et al. (2015). Whole-genome Characterization of Chemoresistant Ovarian Cancer. *Nature* 521 (7553), 489–494. doi:10.1038/nature14410

Patra, B., Lateef, M. A., Brodeur, M. N., Fleury, H., Carmona, E., Péant, B., et al. (2020). Carboplatin Sensitivity in Epithelial Ovarian Cancer Cell Lines: The Impact of Model Systems. *PLoS ONE* 15 (12), e0244549. doi:10.1371/journal.pone.0244549

Pennington, K. P., Walsh, T., Harrell, M. I., Lee, M. K., Pennil, C. C., Rendi, M. H., et al. (2014). Germline and Somatic Mutations in Homologous Recombination Genes Predict Platinum Response and Survival in Ovarian, Fallopian Tube, and Peritoneal Carcinomas. *Clin. Cancer Res.* 20 (3), 764–775. doi:10.1158/1078-0432.Ccr-13-2287

Peres, L. C., Risch, H., Terry, K. L., Webb, P. M., Goodman, M. T., Wu, A. H., et al. (2018). Racial/ethnic Differences in the Epidemiology of Ovarian Cancer: a Pooled Analysis of 12 Case-Control Studies. *Int. J. Epidemiol.* 47 (2), 460–472. doi:10.1093/ije/dyx252

Perets, R., and Drapkin, R. (2016). It's Totally Tubular. . .Riding the New Wave of Ovarian Cancer Research. *Cancer Res.* 76 (1), 10–17. doi:10.1158/0008-5472.Can-15-1382

Perets, R., Wyant, G. A., Muto, K. W., Bijron, J. G., Poole, B. B., Chin, K. T., et al. (2013). Transformation of the Fallopian Tube Secretory Epithelium Leads to High-Grade Serous Ovarian Cancer in Brca;Tp53;Pten Models. *Cancer Cell* 24 (6), 751–765. doi:10.1016/j.ccr.2013.10.013

Perren, T. J., Swart, A. M., Pfisterer, J., Ledermann, J. A., Pujade-Lauraine, E., Kristensen, G., et al. (2011). A Phase 3 Trial of Bevacizumab in Ovarian Cancer. *N. Engl. J. Med.* 365 (26), 2484–2496. doi:10.1056/NEJMoa1103799

Peters, P. N., Schryver, E. M., Lengyel, E., and Kenny, H. (2015). Modeling the Early Steps of Ovarian Cancer Dissemination in an Organotypic Culture of the Human Peritoneal Cavity. *JoVE* 106, e53541. doi:10.3791/53541

Phan, N., Hong, J. J., Tofig, B., Mapua, M., Elashoff, D., Moatamed, N. A., et al. (2019). A Simple High-Throughput Approach Identifies Actionable Drug Sensitivities in Patient-Derived Tumor Organoids. *Commun. Biol.* 2 (1), 78. doi:10.1038/s42003-019-0305-x

Pietilä, E. A., Gonzalez-Molina, J., Moyano-Galceran, L., Jamalzadeh, S., Zhang, K., Lehtinen, L., et al. (2021). Co-evolution of Matrisome and Adaptive Adhesion Dynamics Drives Ovarian Cancer Chemoresistance. *Nat. Commun.* 12 (1), 1. doi:10.1038/s41467-021-24009-8

Pirker, R., FitzGerald, D. J., Hamilton, T. C., Ozols, R. F., Laird, W., Frankel, A. E., et al. (1985). Characterization of Immunotoxins Active against Ovarian Cancer Cell Lines. *J. Clin. Invest.* 76 (3), 1261–1267. doi:10.1172/JCI112082

Provencher, D. M., Lounis, H., Champoux, L., Tétrault, M., Manderson, E. N., Wang, J. C., et al. (2000). Characterization of Four Novel Epithelial Ovarian Cancer Cell Lines. In Vitro *Cell Dev Biol Anim* 36 (6), 357–361. doi:10.1290/1071-2690(2000)036<0357:Cofneo>2.0.Co;2

Rafehi, S., Valdes, Y. R., Bertrand, M., Mcgee, J., Préfontaine, M., Sugimoto, A., et al. (2016). TGFβ Signaling Regulates Epithelial-Mesenchymal Plasticity in Ovarian Cancer Ascites-Derived Spheroids. *Endocrine-Related Cancer* 23 (3), 147–159. doi:10.1530/erc-15-0383

Raghavan, S., Mehta, P., Horst, E. N., Ward, M. R., Rowley, K. R., and Mehta, G. (2016). Comparative Analysis of Tumor Spheroid Generation Techniques for Differential *In Vitro* Drug Toxicity. *Oncotarget* 7 (13), 16948–16961. doi:10.18632/oncotarget.7659

Raghavan, S., Mehta, P., Xie, Y., Lei, Y. L., and Mehta, G. (2019). Ovarian Cancer Stem Cells and Macrophages Reciprocally Interact through the WNT Pathway to Promote Pro-tumoral and Malignant Phenotypes in 3D Engineered Microenvironments. *J. Immunotherapy Cancer* 7 (1), 1. doi:10.1186/s40425-019-0666-1

Raghavan, S., Ward, M. R., Rowley, K. R., Wold, R. M., Takayama, S., Buckanovich, R. J., et al. (2015). Formation of Stable Small Cell Number Three-Dimensional Ovarian Cancer Spheroids Using Hanging Drop Arrays for Preclinical Drug Sensitivity Assays. *Gynecol. Oncol.* 138 (1), 181–189. doi:10.1016/j.ygyno.2015.04.014

Ricci, F., Guffanti, F., Affatato, R., Brunelli, L., Roberta, P., Fruscio, R., et al. (2020). Establishment of Patient-Derived Tumor Xenograft Models of Mucinous Ovarian Cancer. *Am. J. Cancer Res.* 10 (2), 572–580.

Rizvi, I., Gurkan, U. A., Tasoglu, S., Alagic, N., Celli, J. P., Mensah, L. B., et al. (2013). Flow Induces Epithelial-Mesenchymal Transition, Cellular Heterogeneity and Biomarker Modulation in 3D Ovarian Cancer Nodules. *Proc. Natl. Acad. Sci.* 110 (22), E1974–E1983. doi:10.1073/pnas.1216989110

Roby, K. F., Taylor, C. C., Sweetwood, J. P., Cheng, Y., Pace, J. L., Tawfik, O., et al. (2000). Development of a Syngeneic Mouse Model for Events Related to Ovarian Cancer. *Carcinogenesis* 21 (4), 585–591. doi:10.1093/carcin/21.4.585

Rosales-Nieves, A. E., and González-Reyes, A. (2014). Genetics and Mechanisms of Ovarian Cancer: Parallels between Drosophila and Humans. *Semin. Cell Dev. Biol.* 28, 104–109. doi:10.1016/j.semcdb.2014.03.031

Rowley, J. A., Madlambayan, G., and Mooney, D. J. (1999). Alginate Hydrogels as Synthetic Extracellular Matrix Materials. *Biomaterials* 20 (1), 45–53. doi:10.1016/s0142-9612(98)00107-0

Saga, Y., Saga, Y., Mizukami, H., Wang, D., Fujiwara, H., Takei, Y., et al. (2012). Cetuximab Inhibits the Growth of Mucinous Ovarian Carcinoma Tumor Cells Lacking KRAS Gene Mutations. *Oncol. Rep.* 27 (5), 1336–1340. doi:10.3892/or.2012.1626

Saha, B., Mathur, T., Handley, K. F., Hu, W., Afshar-Kharghan, V., Sood, A. K., et al. (2020). OvCa-Chip Microsystem Recreates Vascular Endothelium-Mediated Platelet Extravasation in Ovarian Cancer. *Blood Adv.* 4 (14), 3329–3342. doi:10.1182/bloodadvances.2020001632

Sakayori, M., Nozawa, S., Udagawa, Y., Chin, K., Lee, S. G., Sakuma, T., et al. (1990). Biological Properties of Two Newly Established Cell Lines (RMUG-S, RMUG-L) from a Human Ovarian Mucinous Cystadenocarcinoma. *Hum. Cell* 3 (1), 52–56.

Šale, S., and Orsulic, S. (2006). Models of Ovarian Cancer Metastasis: Murine Models. *Drug Discov. Today Dis. Models* 3 (2), 149–154. doi:10.1016/j.ddmod.2006.05.006

Samartzis, E. P., Labidi-Galy, S. I., Moschetta, M., Uccello, M., Kalaitzopoulos, D. R., Perez-Fidalgo, J. A., et al. (2020). Endometriosis-associated Ovarian Carcinomas: Insights into Pathogenesis, Diagnostics, and Therapeutic Targets-A Narrative Review. *Ann. Transl Med.* 8 (24), 1712. doi:10.21037/atm-20-3022a

Schwarz, R. P., Goodwin, T. J., and Wolf, D. A. (1992). Cell Culture for Three-Dimensional Modeling in Rotating-wall Vessels: an Application of Simulated Microgravity. *J. Tissue Cult. Methods* 14 (2), 51–57. doi:10.1007/bf01404744

Scott, A. L., Ayoola, O., and Zervantonakis, I. K. (2021). Abstract PO042: Microfluidic Modeling of Tumor-Macrophage Signaling in Ovarian Cancer. *Cancer Res.* 81 (5), PO042. doi:10.1158/1538-7445.TME21-PO042

Scott, C. L., Becker, M. A., Haluska, P., and Samimi, G. (2013). Patient-derived Xenograft Models to Improve Targeted Therapy in Epithelial Ovarian Cancer Treatment. *Front. Oncol.* 3, 295. doi:10.3389/fonc.2013.00295

Shield, K., Ackland, M. L., Ahmed, N., and Rice, G. E. (2009). Multicellular Spheroids in Ovarian Cancer Metastases: Biology and Pathology. *Gynecol. Oncol.* 113 (1), 143–148. doi:10.1016/j.ygyno.2008.11.032

Shield, K., Riley, C., Quinn, M. A., Rice, G. E., Ackland, M. L., and Ahmed, N. (2007). α2β1 Integrin Affects Metastatic Potential of Ovarian Carcinoma Spheroids by Supporting Disaggregation and Proteolysis. *J. Carcinog* 6, 11. doi:10.1186/1477-3163-6-11

Shih, I.-M., and Kurman, R. J. (2004). Ovarian Tumorigenesis. *Am. J. Pathol.* 164 (5), 1511–1518. doi:10.1016/s0002-9440(10)63708-x

Shin, H.-Y., Yang, W., Lee, E.-j., Han, G. H., Cho, H., Chay, D. B., et al. (2018). Establishment of Five Immortalized Human Ovarian Surface Epithelial Cell Lines via SV40 T Antigen or HPV E6/E7 Expression. *PLoS ONE* 13 (10), e0205297. doi:10.1371/journal.pone.0205297

Shin, S. I., Freedman, V. H., Risser, R., and Pollack, R. (1975). Tumorigenicity of Virus-Transformed Cells in Nude Mice Is Correlated Specifically with anchorage Independent Growth *In Vitro*. *Proc. Natl. Acad. Sci.* 72 (11), 4435–4439. doi:10.1073/pnas.72.11.4435

Shin, S., Ikram, M., Subhan, F., Kang, H. Y., Lim, Y., Lee, R., et al. (2016). Alginate-marine Collagen-Agarose Composite Hydrogels as Matrices for Biomimetic 3D Cell Spheroid Formation. *RSC Adv.* 6 (52), 46952–46965. doi:10.1039/c6ra01937d

Shishido, A., Mori, S., Yokoyama, Y., Hamada, Y., Minami, K., Qian, Y., et al. (2018). Mesothelial Cells Facilitate Cancer Stem like properties in spheroids of ovarian cancer cells. *Oncol. Rep.* 40 (4), 2105–2114. doi:10.3892/or.2018.6605

Shuford, S., Wilhelm, C., Rayner, M., Elrod, A., Millard, M., Mattingly, C., et al. (2019). Prospective Validation of an *Ex Vivo*, Patient-Derived 3D Spheroid Model for Response Predictions in Newly Diagnosed Ovarian Cancer. *Sci. Rep.* 9 (1), 11153. doi:10.1038/s41598-019-47578-7

Singh, M. S., Goldsmith, M., Thakur, K., Chatterjee, S., Landesman-Milo, D., Levy, T., et al. (2020). An Ovarian Spheroid Based Tumor Model that Represents Vascularized Tumors and Enables the Investigation of Nanomedicine Therapeutics. *Nanoscale* 12 (3), 1894–1903. doi:10.1039/c9nr09572a

Siolas, D., and Hannon, G. J. (2013). Patient-derived Tumor Xenografts: Transforming Clinical Samples into Mouse Models. *Cancer Res.* 73 (17), 5315–5319. doi:10.1158/0008-5472.CAN-13-1069

Sodek, K. L., Brown, T. J., and Ringuette, M. J. (2008). Collagen I but Not Matrigel Matrices Provide an MMP-dependent Barrier to Ovarian Cancer Cell Penetration. *BMC Cancer* 8 (1), 223. doi:10.1186/1471-2407-8-223

Sodek, K. L., Ringuette, M. J., and Brown, T. J. (2009). Compact Spheroid Formation by Ovarian Cancer Cells Is Associated with Contractile Behavior and an Invasive Phenotype. *Int. J. Cancer* 124 (9), 2060–2070. doi:10.1002/ijc.24188

Song, H., Cai, G.-H., Liang, J., Ao, D.-S., Wang, H., and Yang, Z.-H. (2020). Three-dimensional Culture and Clinical Drug Responses of a Highly Metastatic Human Ovarian Cancer HO-8910PM Cells in Nanofibrous Microenvironments of Three Hydrogel Biomaterials. *J. Nanobiotechnol* 18 (1), 1. doi:10.1186/s12951-020-00646-x

Soofi, S. S., Last, J. A., Liliensiek, S. J., Nealey, P. F., and Murphy, C. J. (2009). The Elastic Modulus of Matrigel as Determined by Atomic Force Microscopy. *J. Struct. Biol.* 167 (3), 216–219. doi:10.1016/j.jsb.2009.05.005

Sterzyńska, K., Klejewski, A., Wojtowicz, K., Świerczewska, M., Nowacka, M., Kaźmierczak, D., et al. (2018). Mutual Expression of ALDH1A1, LOX, and Collagens in Ovarian Cancer Cell Lines as Combined CSCs- and ECM-Related Models of Drug Resistance Development. *Ijms* 20 (1), 54. doi:10.3390/ijms20010054

Stuckelberger, S., and Drapkin, R. (2018). Precious GEMMs: Emergence of Faithful Models for Ovarian Cancer Research. *J. Pathol.* 245 (2), 129–131. doi:10.1002/path.5065

Sugiyama, T., Kamura, T., Kigawa, J., Terakawa, N., Kikuchi, Y., Kita, T., et al. (2000). Clinical Characteristics of clear Cell Carcinoma of the Ovary. *Cancer* 88 (11), 2584–2589. doi:10.1002/1097-0142(20000601)88:11<2584:aid-cncr22>3.0.co;2-5

Sung, H., Ferlay, J., Siegel, R. L., Laversanne, M., Soerjomataram, I., Jemal, A., et al. (2021). Global Cancer Statistics 2020: GLOBOCAN Estimates of Incidence and

Mortality Worldwide for 36 Cancers in 185 Countries. *CA A. Cancer J. Clin.* 71 (3), 209–249. doi:10.3322/caac.21660

Swisher, E. M., Lin, K. K., Oza, A. M., Scott, C. L., Giordano, H., Sun, J., et al. (2017). Rucaparib in Relapsed, Platinum-Sensitive High-Grade Ovarian Carcinoma (ARIEL2 Part 1): an International, Multicentre, Open-Label, Phase 2 Trial. *Lancet Oncol.* 18 (1), 75–87. doi:10.1016/s1470-2045(16)30559-9

Szabova, L., Bupp, S., Kamal, M., Householder, D. B., Hernandez, L., Schlomer, J. J., et al. (2014). Pathway-Specific Engineered Mouse Allograft Models Functionally Recapitulate Human Serous Epithelial Ovarian Cancer. *PLoS ONE* 9 (4), e95649. doi:10.1371/journal.pone.0095649

Szabova, L., Yin, C., Bupp, S., Guerin, T. M., Schlomer, J. J., Householder, D. B., et al. (2012). Perturbation of Rb, P53, and Brca1 or Brca2 Cooperate in Inducing Metastatic Serous Epithelial Ovarian Cancer. *Cancer Res.* 72 (16), 4141–4153. doi:10.1158/0008-5472.CAN-11-3834

Takeda, M., Magaki, T., Okazaki, T., Kawahara, Y., Manabe, T., Yuge, L., et al. (2009). Effects of Simulated Microgravity on Proliferation and Chemosensitivity in Malignant Glioma Cells. *Neurosci. Lett.* 463 (1), 54–59. doi:10.1016/j.neulet.2009.07.045

Tan, T. Z., Ye, J., Yee, C. V., Lim, D., Ngoi, N. Y. L., Tan, D. S. P., et al. (2019). Analysis of Gene Expression Signatures Identifies Prognostic and Functionally Distinct Ovarian clear Cell Carcinoma Subtypes. *EBioMedicine* 50, 203–210. doi:10.1016/j.ebiom.2019.11.017

Tofani, L. B., Sousa, L. O., Luiz, M. T., Abriata, J. P., Marchetti, J. M., Leopoldino, A. M., et al. (2021). Generation of a Three-Dimensional *In Vitro* Ovarian Cancer Co-culture Model for Drug Screening Assays. *J. Pharm. Sci.* 110 (7), 2629–2636. doi:10.1016/j.xphs.2021.04.003

Tong, J. G., Valdes, Y. R., Barrett, J. W., Bell, J. C., Stojdl, D., McFadden, G., et al. (2015). Evidence for Differential Viral Oncolytic Efficacy in an *In Vitro* Model of Epithelial Ovarian Cancer Metastasis. *Mol. Ther. - Oncolytics* 2, 15013. doi:10.1038/mto.2015.13

Trento, M., Munari, G., Carraro, V., Lanza, C., Salmaso, R., Pizzi, S., et al. (2020). Mutational and Immunophenotypic Profiling of a Series of 8 Tubo-Ovarian Carcinosarcomas Revealed a Monoclonal Origin of the Disease. *Int. J. Gynecol. Pathol.* 39 (4), 305–312. doi:10.1097/pgp.0000000000000645

Tsao, S.-W., Mok, S. C., Fey, E. G., Fletcher, J. A., Wan, T. S. K., Chew, E.-C., et al. (1995). Characterization of Human Ovarian Surface Epithelial Cells Immortalized by Human Papilloma Viral Oncogenes (HPV-E6e7 ORFs). *Exp. Cell Res.* 218 (2), 499–507. doi:10.1006/excr.1995.1184

Tudrej, P., Kujawa, K. A., Cortez, A. J., and Lisowska, K. M. (2019). Characteristics of *In Vivo* Model Systems for Ovarian Cancer Studies. *Diagnostics* 9 (3), 120. doi:10.3390/diagnostics9030120

Valabrega, G., Scotto, G., Tuninetti, V., Pani, A., and Scaglione, F. (2021). Differences in PARP Inhibitors for the Treatment of Ovarian Cancer: Mechanisms of Action, Pharmacology, Safety, and Efficacy. *Ijms* 22 (8), 4203. doi:10.3390/ijms22084203

van den Berg-Bakker, C. A. M., Hagemeijer, A., Franken-Postma, E. M., Smit, V. T. H. B. M., Kuppen, P. J. K., Claasen, H. H. V. R., et al. (1993). Establishment and Characterization of 7 Ovarian Carcinoma Cell Lines and One Granulosa Tumor Cell Line: Growth Features and Cytogenetics. *Int. J. Cancer* 53 (4), 613–620. doi:10.1002/ijc.2910530415

Varoni, E., Tschon, M., Palazzo, B., Nitti, P., Martini, L., and Rimondini, L. (2012). Agarose Gel as Biomaterial or Scaffold for Implantation Surgery: Characterization, Histological and Histomorphometric Study on Soft Tissue Response. *Connect. Tissue Res.* 53 (6), 548–554. doi:10.3109/03008207.2012.712583

Vidyasekar, P., Shyamsunder, P., Arun, R., Santhakumar, R., Kapadia, N. K., Kumar, R., et al. (2015). Genome Wide Expression Profiling of Cancer Cell Lines Cultured in Microgravity Reveals Significant Dysregulation of Cell Cycle and MicroRNA Gene Networks. *PLoS ONE* 10 (8), e0135958. doi:10.1371/journal.pone.0135958

Vinci, M., Gowan, S., Boxall, F., Patterson, L., Zimmermann, M., Court, W., et al. (2012). Advances in Establishment and Analysis of Three-Dimensional Tumor Spheroid-Based Functional Assays for Target Validation and Drug Evaluation. *BMC Biol.* 10 (1), 29. doi:10.1186/1741-7007-10-29

Vukicevic, S., Kleinman, H. K., Luyten, F. P., Roberts, A. B., Roche, N. S., and Reddi, A. H. (1992). Identification of Multiple Active Growth Factors in Basement Membrane Matrigel Suggests Caution in Interpretation of Cellular Activity Related to Extracellular Matrix Components. *Exp. Cell Res.* 202 (1), 1–8. doi:10.1016/0014-4827(92)90397-q

Wang, X., Zhao, X., Wang, K., Wu, L., and Duan, T. (2013). Interaction of Monocytes/macrophages with Ovarian Cancer Cells Promotes Angiogenesisin Vitro. *Cancer Sci.* 104 (4), 516–523. doi:10.1111/cas.12110

Wang, Z. C., Birkbak, N. J., Culhane, A. C., Drapkin, R., Fatima, A., Tian, R., et al. (2012). Profiles of Genomic Instability in High-Grade Serous Ovarian Cancer Predict Treatment Outcome. *Clin. Cancer Res.* 18 (20), 5806–5815. doi:10.1158/1078-0432.Ccr-12-0857

Ward Rashidi, M. R., Mehta, P., Bregenzer, M., Raghavan, S., Fleck, E. M., Horst, E. N., et al. (2019). Engineered 3D Model of Cancer Stem Cell Enrichment and Chemoresistance. *Neoplasia* 21 (8), 822–836. doi:10.1016/j.neo.2019.06.005

Watkins, J. A., Irshad, S., Grigoriadis, A., and Tutt, A. N. (2014). Genomic Scars as Biomarkers of Homologous Recombination Deficiency and Drug Response in Breast and Ovarian Cancers. *Breast Cancer Res.* 16 (3), 211. doi:10.1186/bcr3670

Watters, K. M., Bajwa, P., and Kenny, H. A. (2018). Organotypic 3D Models of the Ovarian Cancer Tumor Microenvironment. *Cancers* 10 (8), 265. doi:10.3390/cancers10080265

Weydert, Z., Lal-Nag, M., Mathews-Greiner, L., Thiel, C., Cordes, H., Küpfer, L., et al. (2020). A 3D Heterotypic Multicellular Tumor Spheroid Assay Platform to Discriminate Drug Effects on Stroma versus Cancer Cells. *SLAS DISCOVERY: Advancing Sci. Drug Discov.* 25 (3), 265–276. doi:10.1177/2472555219880194

Wilkinson-Ryan, I., Pham, M. M., Sergent, P., Tafe, L. J., and Berwin, B. L. (2019). A Syngeneic Mouse Model of Epithelial Ovarian Cancer Port Site Metastases. *Translational Oncol.* 12 (1), 62–68. doi:10.1016/j.tranon.2018.08.020

Wilson, A., Dent, M., Pejovic, T., Hubbold, L., and Radford, H. (1996). Characterisation of Seven Human Ovarian Tumour Cell Lines. *Br. J. Cancer* 74 (5), 722–727. doi:10.1038/bjc.1996.428

Woo, M. M. M., Salamanca, C. M., Minor, A., and Auersperg, N. (2007). An Improved Assay to Quantitate the Invasiveness of Cells in Modified Boyden chambers. In Vitro *Cell.Dev.Biol.-Animal* 43 (1), 7–9. doi:10.1007/s11626-006-9002-4

Wu, J., Zheng, Y., Tian, Q., Yao, M., and Yi, X. (2019). Establishment of Patient-derived Xenograft Model in Ovarian Cancer and its Influence Factors Analysis. *J. Obstet. Gynaecol. Res.* 45 (10), 2062–2073. doi:10.1111/jog.14054

Wu, T., Gao, Y. Y., Su, J., Tang, X. N., Chen, Q., Ma, L. W., et al. (2021). Three-dimensional Bioprinting of Artificial Ovaries by an Extrusion-Based Method Using Gelatin-Methacryloyl Bioink. *Climacteric* 17, 1–9. doi:10.1080/13697137.2021.1921726

Wu, Y.-H., Chang, T.-H., Huang, Y.-F., Huang, H.-D., and Chou, C.-Y. (2014). COL11A1 Promotes Tumor Progression and Predicts Poor Clinical Outcome in Ovarian Cancer. *Oncogene* 33 (26), 3432–3440. doi:10.1038/onc.2013.307

Xu, F., Celli, J., Rizvi, I., Moon, S., Hasan, T., and Demirci, U. (2011). A Three-Dimensional *In Vitro* Ovarian Cancer Coculture Model Using a High-Throughput Cell Patterning Platform. *Biotechnol. J.* 6 (2), 204–212. doi:10.1002/biot.201000340

Xu, G., Yin, F., Wu, H., Hu, X., Zheng, L., and Zhao, J. (2014). *In Vitro* ovarian Cancer Model Based on Three-Dimensional Agarose Hydrogel. *J. Tissue Eng.* 5 (0), 204173141352043. doi:10.1177/2041731413520438

Xu, S., Xu, H., Wang, W., Li, S., Li, H., Li, T., et al. (2019). The Role of Collagen in Cancer: from Bench to Bedside. *J. Transl Med.* 17 (1), 309. doi:10.1186/s12967-019-2058-1

Xue, Y., Morris, J. L., Yang, K., Fu, Z., Zhu, X., Johnson, F., et al. (2021). SMARCA4/2 Loss Inhibits Chemotherapy-Induced Apoptosis by Restricting IP3R3-Mediated Ca2+ Flux to Mitochondria. *Nat. Commun.* 12 (1), 5404. doi:10.1038/s41467-021-25260-9

Yamada, Y., Yoshida, C., Hamada, K., Kikkawa, Y., and Nomizu, M. (2020). Development of Three-Dimensional Cell Culture Scaffolds Using Laminin Peptide-Conjugated Agarose Microgels. *Biomacromolecules* 21 (9), 3765–3771. doi:10.1021/acs.biomac.0c00871

Yamawaki, K., Mori, Y., Sakai, H., Kanda, Y., Shiokawa, D., Ueda, H., et al. (2021). Integrative Analyses of Gene Expression and Chemosensitivity of Patient-Derived Ovarian Cancer Spheroids Link G6PD-Driven Redox Metabolism to Cisplatin Chemoresistance. *Cancer Lett.* 521, 29–38. doi:10.1016/j.canlet.2021.08.018

Yanagibashi, T., Gorai, I., Nakazawa, T., Miyagi, E., Hirahara, F., Kitamura, H., et al. (1997). Complexity of Expression of the Intermediate Filaments of Six New Human Ovarian Carcinoma Cell Lines: New Expression of Cytokeratin 20. *Br. J. Cancer* 76 (7), 829–835. doi:10.1038/bjc.1997.471

Yang, C., Hillas, P. J., Baez, J. A., Nokelainen, M., Balan, J., Tang, J., et al. (2004). The Application of Recombinant Human Collagen in Tissue Engineering. *BioDrugs* 18 (2), 103–119. doi:10.2165/00063030-200418020-00004

Yang, Z., Xu, H., and Zhao, X. (2020). Designer Self-Assembling Peptide Hydrogels to Engineer 3D Cell Microenvironments for Cell Constructs Formation and Precise Oncology Remodeling in Ovarian Cancer. *Adv. Sci.* 7 (9), 1903718. doi:10.1002/advs.201903718

Yang, Z., and Zhao, X. (2011). A 3D Model of Ovarian Cancer Cell Lines on Peptide Nanofiber Scaffold to Explore the Cell–Scaffold Interaction and Chemotherapeutic Resistance of Anticancer Drugs. *Ijn* 6, 303–310. doi:10.2147/IJN.S15279

Yi, J., Lin, Y., Yicong, W., Chengyan, L., Shulin, Z., and Wenjun, C. (2020). Effect of Macrophages on Biological Function of Ovarian Cancer Cells in Tumor Microenvironment *In Vitro*. *Arch. Gynecol. Obstet.* 302 (4), 1009–1017. doi:10.1007/s00404-020-05719-8

Yoshiya, N., Adachi, S., Misawa, Y., Yuzawa, H., Honda, T., Kanazawa, K., et al. (1989). Isolation of Cisplatin-Resistant Subline from Human Ovarian Cancer Cell Line and Analysis of its Cell-Biological Characteristics. *Nihon Sanka Fujinka Gakkai Zasshi* 41 (1), 7–14.

Yu, J. W., Bhattacharya, S., Yanamandra, N., Kilian, D., Shi, H., Yadavilli, S., et al. (2018). Tumor-immune Profiling of Murine Syngeneic Tumor Models as a Framework to Guide Mechanistic Studies and Predict Therapy Response in Distinct Tumor Microenvironments. *PLoS ONE* 13 (11), e0206223. doi:10.1371/journal.pone.0206223

Yuan, J., Yi, K., and Yang, L. (2021). LncRNA NEAT1 Promotes Proliferation of Ovarian Cancer Cells and Angiogenesis of Co-incubated Human Umbilical Vein Endothelial Cells by Regulating FGF9 through Sponging miR-365. *Medicine (Baltimore)* 100 (3), e23423. doi:10.1097/md.0000000000023423

Zakarya, R., Howell, V. M., and Colvin, E. K. (2020). Modelling Epithelial Ovarian Cancer in Mice: Classical and Emerging Approaches. *Ijms* 21 (13), 4806. doi:10.3390/ijms21134806

Zarrintaj, P., Manouchehri, S., Ahmadi, Z., Saeb, M. R., Urbanska, A. M., Kaplan, D. L., et al. (2018). Agarose-based Biomaterials for Tissue Engineering. *Carbohydr. Polym.* 187, 66–84. doi:10.1016/j.carbpol.2018.01.060

Zhai, Y., Wu, R., Kuick, R., Sessine, M. S., Schulman, S., Green, M., et al. (2017). High-grade Serous Carcinomas Arise in the Mouse Oviduct via Defects Linked to the Human Disease. *J. Pathol.* 243 (1), 16–25. doi:10.1002/path.4927

Zhang, L., Yang, N., Conejo Garcia, J.-R., Mohamed, A., Benencia, F., Rubin, S. C., et al. (2002). Generation of a Syngeneic Mouse Model to Study the Effects of Vascular Endothelial Growth Factor in Ovarian Carcinoma. *Am. J. Pathol.* 161 (6), 2295–2309. doi:10.1016/s0002-9440(10)64505-1

Zhang, S., Dolgalev, I., Zhang, T., Ran, H., Levine, D. A., and Neel, B. G. (2019). Both fallopian Tube and Ovarian Surface Epithelium Are Cells-Of-Origin for High-Grade Serous Ovarian Carcinoma. *Nat. Commun.* 10 (1), 5367. doi:10.1038/s41467-019-13116-2

Zhao, L., Xiu, J., Liu, Y., Zhang, T., Pan, W., Zheng, X., et al. (2019a). A 3D Printed Hanging Drop Dripper for Tumor Spheroids Analysis without Recovery. *Sci. Rep.* 9 (1), 1. doi:10.1038/s41598-019-56241-0

Zhao, Y., Cao, J., Melamed, A., Worley, M., Gockley, A., Jones, D., et al. (2019b). Losartan Treatment Enhances Chemotherapy Efficacy and Reduces Ascites in Ovarian Cancer Models by Normalizing the Tumor Stroma. *Proc. Natl. Acad. Sci. USA* 116 (6), 2210–2219. doi:10.1073/pnas.1818357116

Zhou, N., Ma, X., Bernaerts, K. V., Ren, P., Hu, W., and Zhang, T. (2020). Expansion of Ovarian Cancer Stem-like Cells in Poly(ethylene Glycol)-Cross-Linked Poly(methyl Vinyl Ether-Alt-Maleic Acid) and Alginate Double-Network Hydrogels. *ACS Biomater. Sci. Eng.* 6 (6), 3310–3326. doi:10.1021/acsbiomaterials.9b01967

Zhou, N., Ma, X., Hu, W., Ren, P., Zhao, Y., and Zhang, T. (2021). Effect of RGD Content in Poly(ethylene Glycol)-Crosslinked Poly(methyl Vinyl Ether-Alt-Maleic Acid) Hydrogels on the Expansion of Ovarian Cancer Stem-like Cells. *Mater. Sci. Eng. C* 118, 111477. doi:10.1016/j.msec.2020.111477

Zhu, M., Wang, Y., Ferracci, G., Zheng, J., Cho, N.-J., and Lee, B. H. (2019). Gelatin Methacryloyl and its Hydrogels with an Exceptional Degree of Controllability and Batch-To-Batch Consistency. *Sci. Rep.* 9 (1), 1. doi:10.1038/s41598-019-42186-x

Conflict of Interest: The authors declare that the research was conducted in the absence of any commercial or financial relationships that could be construed as a potential conflict of interest.

Publisher's Note: All claims expressed in this article are solely those of the authors and do not necessarily represent those of their affiliated organizations, or those of the publisher, the editors, and the reviewers. Any product that may be evaluated in this article, or claim that may be made by its manufacturer, is not guaranteed or endorsed by the publisher.

frontiers in Bioengineering and Biotechnology

SYSTEMATIC REVIEW
published: 03 March 2022
doi: 10.3389/fbioe.2022.819697

Impact of Remote Monitoring Technologies for Assisting Patients With Gestational Diabetes Mellitus: A Systematic Review

Ayleen Bertini[1,2], Bárbara Gárate[3], Fabián Pardo[1,4], Julie Pelicand[1,4], Luis Sobrevia[5,6,7,8,9,10,11], Romina Torres[12], Steren Chabert[3,13,14] and Rodrigo Salas[3,13,14]**

[1]Metabolic Diseases Research Laboratory (MDRL), Interdisciplinary Center for Research in Territorial Health of the Aconcagua Valley (CIISTe Aconcagua), Center for Biomedical Research, Universidad de Valparaíso, Valparaíso, Chile, [2]Programa de Doctorado en Ciencias e Ingeniería para La Salud, Faculty of Medicine, Universidad de Valparaíso, Valparaíso, Chile, [3]School of Biomedical Engineering, Faculty of Engineering, Universidad de Valparaíso, Valparaíso, Chile, [4]School of Medicine, Campus San Felipe, Faculty of Medicine, Universidad de Valparaíso, Valparaíso, Chile, [5]Cellular and Molecular Physiology Laboratory (CMPL), Department of Obstetrics, Division of Obstetrics and Gynaecology, School of Medicine, Faculty of Medicine, Pontificia Universidad Católica de Chile, Santiago, Chile, [6]Department of Physiology, Faculty of Pharmacy, Universidad de Sevilla, Seville, Spain, [7]University of Queensland Centre for Clinical Research (UQCCR), Faculty of Medicine and Biomedical Sciences, University of Queensland, Herston, QLD, Australia, [8]Medical School (Faculty of Medicine), Sao Paulo State University (UNESP), São Paulo, Brazil, [9]Department of Pathology and Medical Biology, University of Groningen, Groningen, Netherlands, [10]University Medical Center Groningen (UMCG), Groningen, Netherlands, [11]Tecnologico de Monterrey, Eutra, The Institute for Obesity Research, School of Medicine and Health Sciences, Monterrey, Mexico, [12]Faculty of Engineering, Universidad Andres Bello, Viña Del Mar, Chile, [13]Millennium Institute for Intelligent Healthcare Engineering, Valparaíso, Chile, [14]Centro de Investigación y Desarrollo en INGeniería en Salud—CINGS, Universidad de Valparaíso, Valparaíso, Chile

OPEN ACCESS

Edited by:
Lana McClements, University of Technology Sydney, Australia

Reviewed by:
Laura Burattini, Marche Polytechnic University, Italy
Pranay Goel, Indian Institute of Science Education and Research, India

***Correspondence:**
Rodrigo Salas
rodrigo.salas@uv.cl
Ayleen Bertini
ayleen.bertini@uv.cl

Specialty section:
This article was submitted to Preclinical Cell and Gene Therapy, a section of the journal Frontiers in Bioengineering and Biotechnology

Received: *22 November 2021*
Accepted: *31 January 2022*
Published: *03 March 2022*

Citation:
Bertini A, Gárate B, Pardo F, Pelicand J, Sobrevia L, Torres R, Chabert S and Salas R (2022) Impact of Remote Monitoring Technologies for Assisting Patients With Gestational Diabetes Mellitus: A Systematic Review. Front. Bioeng. Biotechnol. 10:819697. doi: 10.3389/fbioe.2022.819697

Introduction: In Chile, 1 in 8 pregnant women of middle socioeconomic level has gestational diabetes mellitus (GDM), and in general, 5–10% of women with GDM develop type 2 diabetes after giving birth. Recently, various technological tools have emerged to assist patients with GDM to meet glycemic goals and facilitate constant glucose monitoring, making these tasks more straightforward and comfortable.

Objective: To evaluate the impact of remote monitoring technologies in assisting patients with GDM to achieve glycemic goals, and know the respective advantages and disadvantages when it comes to reducing risk during pregnancy, both for the mother and her child.

Methods: A total of 188 articles were obtained with the keywords "gestational diabetes mellitus," "GDM," "gestational diabetes," added to the evaluation levels associated with "glucose level," "glycemia," "glycemic index," "blood sugar," and the technological proposal to evaluate with "glucometerm" "mobile application," "mobile applications," "technological tools," "telemedicine," "technovigilance," "wearable" published during the period 2016–2021, excluding postpartum studies, from three scientific databases: PUBMED, Scopus and Web of Science. These were managed in the Mendeley platform and classified using the PRISMA method.

Results: A total of 28 articles were selected after elimination according to inclusion and exclusion criteria. The main measurement was glycemia and 4 medical devices were found (glucometer: conventional, with an infrared port, with Bluetooth, Smart type and

continuous glucose monitor), which together with digital technology allow specific functions through 2 identified digital platforms (mobile applications and online systems). In four articles, the postprandial glucose was lower in the Tele-GDM groups than in the control group. Benefits such as improved glycemic control, increased satisfaction and acceptability, maternal confidence, decreased gestational weight gain, knowledge of GDM, and other relevant aspects were observed. There were also positive comments regarding the optimization of the medical team's time.

Conclusion: The present review offers the opportunity to know about the respective advantages and disadvantages of remote monitoring technologies when it comes to reducing risk during pregnancy. GDM centered technology may help to evaluate outcomes and tailor personalized solutions to contribute to women's health. More studies are needed to know the impact on a healthcare system.

Keywords: remote monitoring, telemedicine, gestational diabetes (GDM), technovigilance, mobile applications

INTRODUCTION

Gestational diabetes mellitus (GDM) is diagnosed when glycemia increases during pregnancy without any previous history (American Diabetes Association, 2020). GDM is currently the most common medical complication of pregnancy and the prevalence of undiagnosed hyperglycemia and even overt diabetes in young women is increasing (McIntyre et al., 2019). In Chile, 1 in 8 pregnant women of middle socioeconomic status has GDM (Garmendia et al., 2020), and 5–10% of women with GDM develop type 2 diabetes after delivery, maintaining a linear growth (Auvinen et al., 2020).

Maternal overweight and obesity (Shin and Sond, 2014), late age at childbearing (Anna et al., 2008), previous history of GDM, family history of type 2 diabetes mellitus, and ethnicity are the main risk factors for GDM (McIntyre et al., 2019). Diagnosis is usually made by an oral glucose tolerance test (OGTT), although in some parts of the world a non-fasting glucose challenge test (GCT) is used to screen for those women who require a full OGTT (McIntyre and Moses, 2020).

In Chile, the diagnosis of diabetes during the first trimester of pregnancy is based on the same criteria used for the general population (World Health Organization, 2006; ADA, 2014). 1) Common symptoms related to diabetes (polydipsia, polyuria, polyphagia and low weight) and a glycemia at any time of the day greater or equal than 200 mg/dl, unrelated to the time elapsed since last meal. 2) Fasting glycemia greater than or equal to 126 mg/dl. Confirm with a second glycemia ≥126 mg/dl, on a different day. 3) Glycemia greater than or equal to 200 mg/dl 2 h after a 75 g glucose load during an OGTT (Ministerio de Salud, 2014).

GDM in the health care system has tripled over a 14-years period, which could be explained by changes in the trend of risk factors during this period (Garmendia et al., 2020), such as the increased prevalence of obesity, along with later fertility which has been associated with higher risk gestation. All this results in an increased burden of care and demand for specialized services (Ministerio de Salud, 2014). For proper management of GDM during pregnancy, it is important to meet the glycemic goals, so patients must achieve constant monitoring, at least once a day, and maybe more, depending on the severity of the glycemia alteration in pregnancy, and they must also comply with dietary treatment and an exercise plan suggested by a specialist (Ministerio de Salud, 2014; McIntyre and Moses, 2020).

The goal of treatment of a woman with GDM is to achieve optimal metabolic control from the time of conception and throughout pregnancy, with fasting and postprandial euglycemia levels, and to screen for and treat any intercurrent pathology (Jovanovic et al., 2005). In Chile, the glycemic target is to maintain fasting glycemia levels between 60 and 90 mg/dl and <140 mg/dl, 1 h postprandial and <120 mg/dl, 2 h postprandial and HbA1c <6% (Ministerio de Salud, 2014).

Keeping a constant and orderly manual record can be complex and cumbersome, considering current lifestyles: women with more than one child often work full or part-time in addition to being homemakers. Thus, to facilitate the constant monitoring of glucose levels or to keep a caloric record of the diet suggested by a specialist, several technological tools have emerged that will make this type of task simpler and more comfortable. This is where the term Telemonitoring or E-Health comes into play, which has made it possible to simplify self-care by empowering the patients themselves to manage their health, while keeping health personnel informed and facilitating access to timely medical care (Lemelin et al., 2020).

The main objective of the review is to evaluate the impact of current technologies and methods of assisting patients with GDM to achieve glycemic goals, and know the respective advantages and disadvantages of these technologies when it comes to reducing risk during pregnancy, both for the mother and her child.

METHODOLOGY

This systematic review was carried out following the guidelines for systematic reviews and meta-analysis (PRISMA) (Urrútia and Bonfill, 2010). To access the literature of interest in a database, in this case, Web of

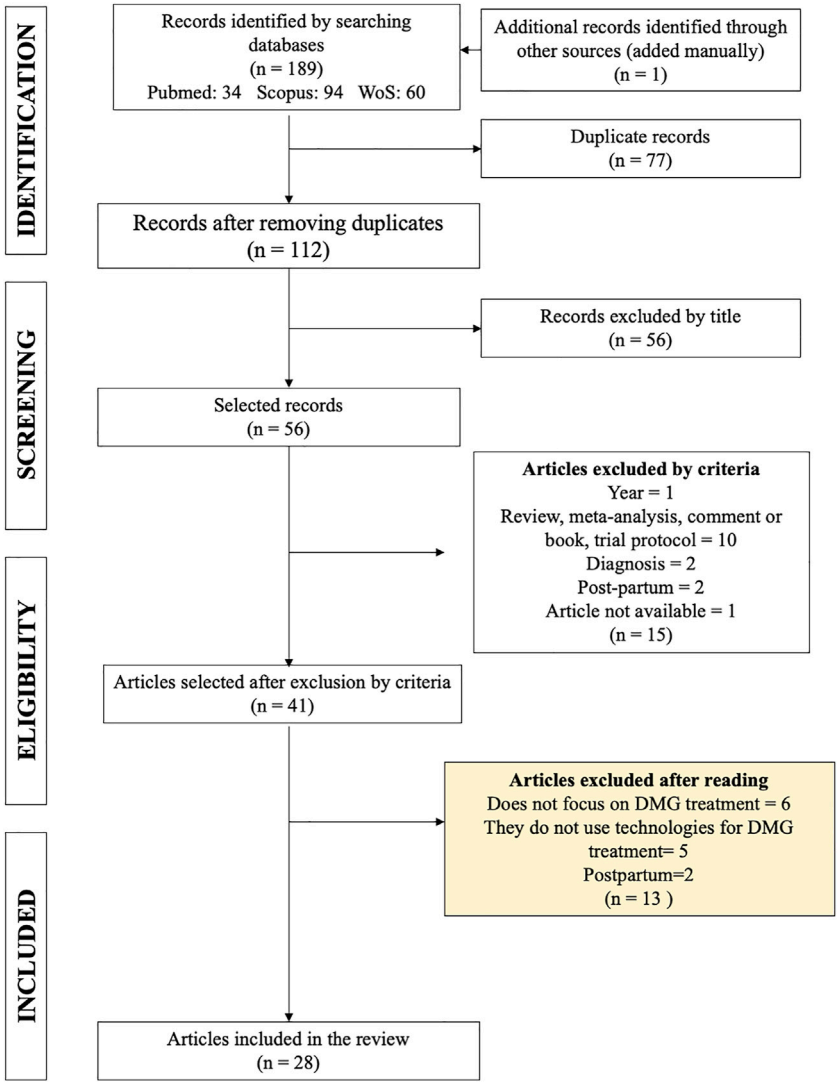

FIGURE 1 | PRISMA diagram for the articles selection process.

Science, Scopus and Pubmed, it was necessary to identify the search criteria. The following were established as inclusion criteria: Articles related to current technologies for remote monitoring of GDM and parameters and variables related to blood glucose control and treatment compliance monitoring, articles published between 2016 and 2021. As exclusion criteria were established: publications referring to the post-natal/postpartum period, articles related to other types of diabetes, articles related to the diagnosis of GDM, articles related to Pregestational Diabetes Mellitus (PGD), articles from Systematic Reviews and Meta-analyses, articles involving technologies that have not been tested in patients with GDM and articles related to technologies for the use of clinical staff. It should be noted that articles related to GDM treatments and therapies were not excluded from the selection, since a topic of interest in the review is remote monitoring of compliance with these. In addition, there was no exclusion of articles according to the number of study cases, nor will there be exclusion according to the age range of the subjects. After establishing the databases and search criteria, it was important to consider the keywords we used to perform the Boolean expression that gave us the related articles in the databases. To perform the search in the databases, it was necessary to form the optimal search expression that completely covers the topics of interest of the subject to be investigated. Synonyms for gestational diabetes, glycemic levels, and technology or monitoring were chosen among the keywords.

Once the articles that were considered for the review were determined (according to the inclusion/exclusion criteria), the articles were categorized by the type of technology used for remote monitoring of GDM, monitoring parameters, accuracy

TABLE 1 | Main characteristics of selected articles.

Approach of study	Temporality	Geographic location of the study group	Year of publication
Quantitative (85.7%)	Retrospective (21.4%)	Asia (32.1%)	2016 (7.2%)
Qualitative (10.7%)	Prospective (75%)	Europe (46.4%)	2017 (14.3%)
Mixed (3.6%)	Mixed (3.6%)	North America (14.3%)	2018 (35.6%)
		Oceania (7.2%)s	2019 (14.3%)
			2020 (14.3%)
			2021 (14.3%)

according to the studies, and by the advantages and disadvantages of the different methods, to estimate which ones might be more practical for patients with GDM.

RESULTS

Result Selection

The search in the aforementioned databases resulted in a total of 188 articles, and one article was added manually as it met the inclusion criteria (**Figure 1**), of which 77 were eliminated as duplicates, leaving 112 publications for analysis. After eliminating duplicate entries, the titles were read. From this reading, it was deemed necessary to exclude a further 56 articles with titles too far from the topic of interest. Among the reasons for exclusion of articles by title were: meta-analysis, not using technology, focused on prediction or diagnosis of GDM, studies on mice, not focused on GDM or including the word "postpartum."

The articles (abstracts) were then analyzed using the list of inclusion and exclusion criteria defined in the Methodology section. As a result, 15 articles that did not meet the guidelines were eliminated: 1 for being outside the stipulated time range; 2 for being concerned with the postpartum period; 2 for focusing on the diagnosis of GDM; 10 articles for being systematic reviews, meta-analyses, commentaries, chapters of books or trial protocols. One article was eliminated because it was not available on any platform. At this point, 41 articles were available for further reading.

Finally, the articles were read, and the decision was made to exclude a further 13 articles. Six of these did not focus on GDM, five did not use technologies for the treatment of GDM and two articles focused on postpartum measurements. In the end, 28 articles were selected for the systematic review (**Supplementary Table S1**).

Characteristics of the Selected Studies

Based on the results presented above, we proceeded to analyze each article individually to gather as much information as possible (**Table 1**).

Most of the studies were quantitative (24 studies) and prospective (9 studies). Regarding the location of the study group of pregnant women, they were mainly concentrated in Europe (13 studies) and Asia (9 studies). It is important to note that there were no studies that focused on pregnant women in Latin America, the Caribbean, or in Africa. As for the year of publication, the largest number of studies that met the inclusion criteria were published in 2018. Only two studies that met the inclusion criteria were published in 2016.

Of the total number of articles, 18 of these conducted two study groups or "case controls" where one group did not have the technology intervention for control of GDM and the other did. A total of 9 studies chose only to evaluate the technology tool prospectively, where there is only one study group of intervened pregnant women. One study divides the patients into 3 study groups, separating patients without GDM and with GDM, and separating the latter into those intervened using the technology tool and those not intervened (**Figure 2**).

Measurement Parameters

The measurements included in the technology (application) used in the studies include the following characteristics: glycemia (26 articles), bodyweight measurement (7 articles), blood pressure (4 articles), insulin dose (3 articles), number of measurements (2 articles), meals (8 articles), ketonuria (2 articles), physical activity level (7 articles), anxiety and/or depression levels (1 article), medications (1 article), satisfaction levels and quality of life (2 articles). The article that included the technology with the most evaluations included 6 measures: glycemia, weight, blood pressure, ketonuria, physical activity, and satisfaction and quality of life levels (Peleg et al., 2017).

Medical Devices

Regarding the medical equipment used for glucose monitoring, 11 articles did not specify which one they used or focused on blood results at the beginning and end of the evaluations (Harrison et al., 2017; Johnson and Berry, 2018; Miremberg et al., 2018; Rasekaba et al., 2018; Skar et al., 2018; Triberti et al., 2018; Yang et al., 2018; Kim et al., 2019; Kim et al., 2021; Tian et al., 2021; Varnfield et al., 2021) The most commonly used glucometer was with BlueTooth: This type of glucometer transfers information to the technological device using a Bluetooth integrated into the device. It is necessary that the technological device also have BlueTooth (in this case the most used was a smartphone). It is important to note that, at the time of transferring information, the glucometer should be at a recommended safe distance of 10 m from the technological device. This medical device was used in 6 articles (22.2%) of the total number of articles chosen (Borgen et al., 2017; Peleg et al., 2017; Rigla et al., 2018; Albert et al., 2020; Lemelin et al., 2020; Seo et al., 2020). As for the Smart glucometer, this device measures glycemia just like a conventional glucometer, but must be connected directly by inserting its 3.5 mm jack into the

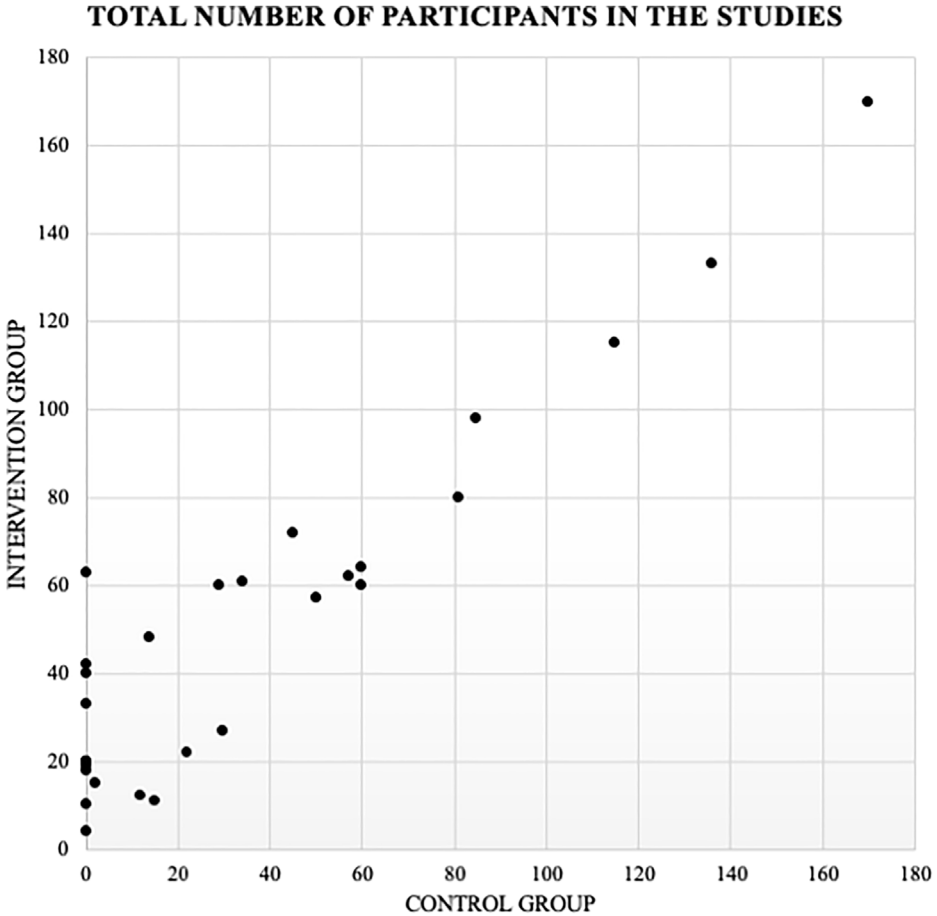

FIGURE 2 | Graphical representation of the distribution of the number of participants. Intervention (with technological intervention for the treatment of GDM) v/s Control (without technological intervention for the treatment of GDM).

headphone jack of the smartphone. Using the corresponding mobile application, it is possible to perform the measurement and transfer the data to the clinical staff for later review. Three articles (11%) used this medical device (Al-ofi et al., 2019; Guo et al., 2019; Yew et al., 2021). Two articles used a glucometer with an infrared port (Caballero-Ruiz et al., 2016; Caballero-Ruiz et al., 2017), which emits the information to a device reader, which is connected to a computer that will automatically receive the information. This information, after being received by the computer, is uploaded to the platform. It should be noted that the glucometer should be at a distance of 10 cm and the infrared ports facing the front. The continuous glucose monitor requires the insertion of a glucose sensor under the skin, which will receive information that will be continuously transmitted from the patient to the digital platform through the technological device. This medical device was used in two articles (Pustozerov et al., 2018; Pustozerov and Popova, 2018). All studies had moderately invasive methods to achieve glycemic control. Conventional glucometers, smart, Bluetooth and infrared, require blood sampling by the user at certain times depending on each study. The continuous glucose monitor, which goes through the skin, however, does not require the user to be aware of the schedules; she only has to wear it. As for the studies that did not use a glucose monitor, they measured blood glycemia and the other parameters, which implies at least two blood samples per study.

Technology and Digital Platform

The digital technologies used for GDM monitoring were smartphones, computers and tablets. A total of 14 articles used only a smartphone, 4 articles used a smartphone and computer, 5 articles used a smartphone, computer and tablet, 4 articles used only a computer and one article used a basic phone. The use of these technologies depends on the digital platform used for the telemonitoring of MGD. The articles that used mobile applications relied on smartphones for data collection (Bromuri et al., 2016; Borgen et al., 2017; Harrison et al., 2017; Mackillop et al., 2018; Miremberg et al., 2018; Rigla et al., 2018; Skar et al., 2018; Triberti et al., 2018; Yang et al., 2018; Al-ofi et al., 2019; Guo et al., 2019; Seo et al., 2020; Tian et al., 2021; Varnfield et al., 2021), the articles that used online systems used computers for data collection (Caballero-Ruiz et al., 2016; Caballero-Ruiz et al., 2017; Kim et al., 2019; Wernimont et al., 2020), and the articles that used multiplatform systems used

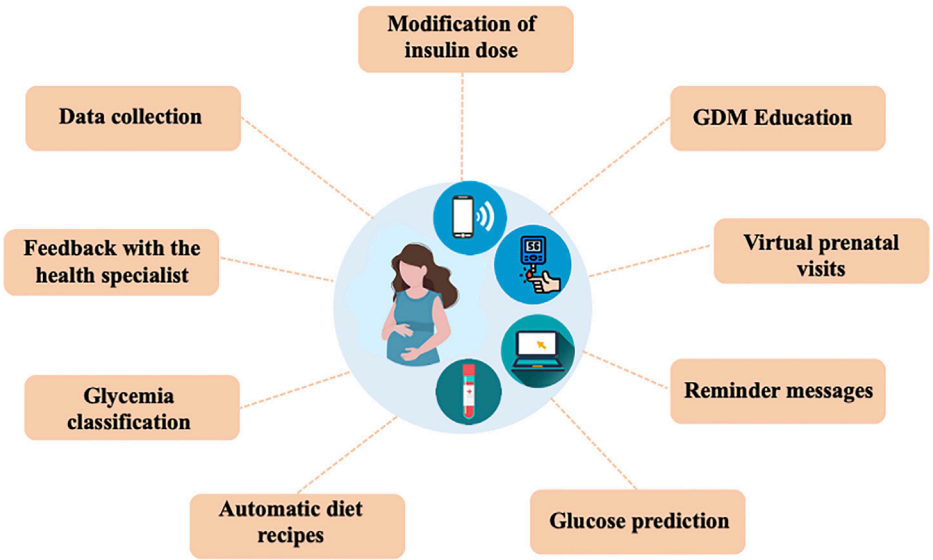

FIGURE 3 | The technological applications were mainly focused on the objective of improving glycemic control and supporting pregnant women in understanding GDM. Nine functions were selected that were common in the applied technologies.

smartphones and computers (Peleg et al., 2017; Albert et al., 2020; Kim et al., 2021; Yew et al., 2021), and four of these also used tablets (Pustozerov et al., 2018; Pustozerov and Popova, 2018; Rasekaba et al., 2018; Alqudah et al., 2019; Lemelin et al., 2020). Only one article did not specify its system used, however, they relied on smartphone data collection (Johnson and Berry, 2018).

Functions of the Technology for Monitoring GMD

In the selected articles, the technological applications were mainly focused on the objective of improving glycemic control and supporting pregnant women in understanding GDM. Nine functions were selected that were common in the applied technologies: data collection, feedback with the specialist, glycemia classification, automatic feeding recipes, education in GDM, virtual prenatal visits, reminder messages, glycemia prediction and live modification of insulin doses (**Figure 3**).

Data Collection

This function allows the patient to record all values that are requested by the clinical staff. Some are downloaded automatically and others need to be recorded manually. This function is enabled in 81.5% (22 articles) of the total, which is the most repeated (Bromuri et al., 2016; Borgen et al., 2017; Harrison et al., 2017; Peleg et al., 2017; Mackillop et al., 2018; Miremberg et al., 2018; Pustozerov et al., 2018; Pustozerov and Popova, 2018; Rasekaba et al., 2018; Rigla et al., 2018; Triberti et al., 2018; Yang et al., 2018; Al-ofi et al., 2019; Guo et al., 2019; Kim et al., 2019; Albert et al., 2020; Lemelin et al., 2020; Seo et al., 2020; Wernimont et al., 2020; Kim et al., 2021; Varnfield et al., 2021; Yew et al., 2021).

Feedback With the Health Specialist

Feedback refers to the communication that exists between the patient and the clinical staff, either through telephone calls, video calls, or text messages. Thirty-seven percent of the articles (10 articles) have this function (Caballero-Ruiz et al., 2017; Peleg et al., 2017; Miremberg et al., 2018; Pustozerov and Popova, 2018; Rasekaba et al., 2018; Triberti et al., 2018; Al-ofi et al., 2019; Albert et al., 2020; Lemelin et al., 2020; Varnfield et al., 2021). In most cases, it goes along with data collection.

Glycemia Classification

This type of function allows the patient to automatically associate the appropriate meal and time of measurement (preprandial or postprandial) to each incomplete glucose data downloaded from a glucometer. Five articles (19%) presented this function (Caballero-Ruiz et al., 2016; Borgen et al., 2017; Skar et al., 2018; Seo et al., 2020; Yew et al., 2021).

Automatic Diet Recipes

This function delivers automatically personalized diets based on the data recorded by the patients. Like the glycemia classification, this function is present in five articles (19%) (Borgen et al., 2017; Caballero-Ruiz et al., 2017; Skar et al., 2018; Seo et al., 2020; Yew et al., 2021).

GDM Education

Through messages or information uploaded to the platform, additional data on diets, exercises, medications, etc. are delivered to treat GDM. Educational information on GDM is presented in 44.4% (12 articles) (Borgen et al., 2017; Johnson and Berry, 2018; Mackillop et al., 2018; Skar et al., 2018; Triberti et al., 2018; Yang et al., 2018; Guo et al., 2019;

TABLE 2 | Results of glycemic control in pregnant women with GDM.

Autor	Control group (n)	Intervetion group (n)	Technology used	Intervention Time	Glycemic control results	Other results
Al-Ofi et al. (2019)	30	27	Smart glucometer + Smartphone + Mobile Application	From week 24 to week 28 the pregnant women began to use the technology (4 weeks). The comparison tests were measured between gestational weeks 38 to 40 (2 weeks)	PPG 2 h is significantly lower in the intervention group (p = 0.002) Fasting glycemia and HbA1c were not significantly different	Most of the pregnant women in the intervention group had adequate gestational weight gain. The weight at the end of pregnancy in the intervention group was significantly lower (p = 0.03)
Guo, et al. (2019)	60	64	Smart glucometer + Smartphone + Mobile Application	13 weeks	HbA1c before delivery (%) 5.3 ± 0.3 (C) v/s 4.7 ± 0.2 (I) (p < 0.001) Off-target fasting glucose measurement (%) 8.3 ± 0.6 (C) v/s 4.6 ± 0.4 (I) (p < 0.001) Off-target 2 h post-prandial glucose measurement (%) 14.7 ± 0.8 (C) v/s 7.9 ± 0.7 (I) (p < 0.001)	Weight gain after treatment (kg) 4.8 ± 0.7 v/s 3.2 ± 0.8 (p < 0.001)
Yang et al. (2018)	50	57	Smartphone + Mobile Application	From week 24–28 until term (approximately 13 weeks)	FBG (mmol/l) 5.31 ± 1.29 (C) v/s 4.31 ± 0.75 (I) (p = 0.000) 1 h PBG 7.75 ± 2.08 (C) v/s 7.71 ± 0.73 (I) (p = 0.780) 2 h PBG 6.94 ± 2.47 (C) v/s 5.76 ± 0.67 (I) (p = 0.000)	Preterm delivery was significantly less likely in group A than in group B (p < 0.05)
Miremberg et al. (2018)	60	60	Smartphone + Mobile Application	From week 24–28 until term (approximately 13 weeks)	Mean blood glucose (mg/dl) vs. 112.6 ± 7.4 (C) v/s 105.1 ± 8.6 (I)(p < 0.001)Off-target fasting glucose measurement (%) 8.4 ± 0.6 (C) v/s 4.7 ± 0.4 (I) (p < 0.001)Off-target 1 h post-prandial glucose measurement (%) 14.3 ± 0.8 (C) v/s 7.7 ± 0.8 (I) (p < 0.001) Rate of pregnancies requiring insulin treatment 30.0 (C) v/s 13.3 (I) (p = 0.044)	—
Kim et al. (2021)	62	57	Computer/Smartphone + Multiplatform application	12 weeks	Fasting flucose (mg/L) 103 ± 15.6 (C) v/s 92 ± 6.8 (p = 0.031) HbA1c (%)5.6 ± 0.3 (C) v/s 5.4 ± 0.3 (I) (p = 0.019)	Body weight (kg) 68.2 ± 17.1 kg (C) v/s 61.5 ± 8.6 (I) (p = 0.007) Body fat (%) 37.4 ± 5.9 (C) ± 32 ± 5.1 (I) (p=<0.001) Diabetes knowledge 0.62 ± 0.9 (C) v/s 0.64 ± 0.9 (I) (p = 0.558) Dietary habits 3.8 ± 0.4 (C) v/s 4 ± 0.3 (I) (p < 0.001) Health Promoting Lifestyle Profile Total Score 2.64 ± 0.38 (C) v/s 2.82 ± 0.3 (I) (p < 0.001)
Kim et al. (2019)	22	22	Computer + Web system	12 weeks	HbA1c (%) 5.3 ± 0.2 (C) v/s 5.0 ± 0.2 (I) (p = 0.001) Glycated albumin (%) 11.0 ± 1.4 (C) v/s 10.8 ± 1.2 (I) (p = 0.776) Fasting glucose (mg/dl) 80.9 ± 8.4 (C) v/s 78.8 ± 8.4 (I) (p = 0.075)	Anxiety in the experimental group decreased by 5.1 points but increased by 1.0 points in the control group (p = 0.048). Depression increased in both groups

(Continued on following page)

TABLE 2 | (*Continued*) Results of glycemic control in pregnant women with GDM.

Autor	Control group (n)	Intervetion group (n)	Technology used	Intervention Time	Glycemic control results	Other results
					1 h PBG (mg/dl) 117.2 ± 22.2 (C) v/s 129.5 ± 19.9 (I) (p = 0.489)	
Seo et al. (2020)	0	4	Glucometer Bluetooth + Smartphone + Mobile application	From week 24–28 until 32—36 weeks (approximately 8 weeks)	Fasting glucose (mg/dl) 104.5 (C) v/s 94.75 (I) 2 h PBG (mg/dl) 223.25 (C) v/s 150.5 (I)	Alteration in the intake of some nutrients: 1. Reduced consumption of: Calories, proteins, fats, Vitamin A, Vitamin C, Thiamine, Riboflavin, Calcium, animal and vegetable iron 2. Increased consumption of: Carbohydrates
Wernimont et al. (2020)	45	72	Glucometer smart and standard glucometer (control) + Computer + Web system	From the first prenatal visit until delivery (approximately 34 weeks)	At delivery, women using the cellular glucometer had an average HbA1c of 6.0% compared with an average HbA1c of 6.8% for those women using a standard glucometer. The average decrease in HbA1c from baseline visit to delivery was significantly greater for women using the cellular glucometer (-2.6 ± 1.7%) compared with those using a standard glucometer (-1.4 ± 1.4%)	—

Albert et al., 2020; Seo et al., 2020; Kim et al., 2021; Tian et al., 2021; Yew et al., 2021).

Virtual Prenatal Visits

This intervention makes it possible to alternate the usual clinical visits to the clinic with virtual visits from the patient's home. This function is enabled in three articles (Harrison et al., 2017; Mackillop et al., 2018; Kim et al., 2019).

Reminder Messages

Patients are reminded to perform the corresponding glucose measurements using text messages. This function is found in 7 articles (Borgen et al., 2017; Johnson and Berry, 2018; Skar et al., 2018; Seo et al., 2020; Kim et al., 2021; Tian et al., 2021; Yew et al., 2021).

Glucose Prediction

This function allows the prediction of the glucose value without the patient having to measure with the glucometer, all this thanks to the nutritional information recorded by the patient. This function can be found in one article (Pustozerov et al., 2018).

Modification of Insulin Dose

The system has automatic responses or responses mediated by health professionals every time the patient needs to modify her insulin doses according to the glycemia measurement. This function is found in two articles (Albert et al., 2020; Yew et al., 2021).

Glycemic Results

Regarding glycemic results as such, in general, the technological interventions had positive results in the control of GDM. The articles that measured fasting glycemia decreased in the intervention group, in contrast to the control group in four articles (Yang et al., 2018; Guo et al., 2019; Seo et al., 2020; Kim et al., 2021). As for the articles that measured postprandial glycemia, this decreased significantly in four articles that evaluated this measurement (Miremberg et al., 2018; Yang et al., 2018; Al-ofi et al., 2019; Seo et al., 2020). Other studies evaluated glycosylated hemoglobin levels, all of which showed a decrease in this parameter in the experimental group (with technological intervention) versus the non-experimental group (Guo et al., 2019; Kim et al., 2019; Wernimont et al., 2020; Kim et al., 2021) (**Table 2**).

All glycemic outcomes had significant improvements in the intervention groups with the use of GDM monitoring technologies. In addition to glycemic outcomes, there were positive results in terms of lower weight gain during pregnancy (Al-ofi et al., 2019; Guo et al., 2019; Kim et al., 2021), decreased complications at delivery, body fat, dietary habits and Health Promoting Lifestyle Profile Total Score (Kim et al., 2021). Anxiety decreased in the experimental

group, but depression increased in both groups (Kim et al., 2019). The consumption of certain nutrients was affected in one of the studies that sought glycemic control through a mobile application (Seo et al., 2020) (**Table 2**).

Other Results Associated With the Maternal Perception of the Technologies Used for the Control of GDM

User satisfaction and Acceptability

Some of the conclusions of the articles were: Multi-platform system with Bluetooth glucometer monitoring improved user satisfaction (Peleg et al., 2017). In another study, many participants appreciated the ease of access (not having to keep a paper diary), ease of use, and convenience of the mobile application. They liked being able to monitor their blood glycemia values, the application's ability to connect them quickly, and being able to get answers from their physician (Varnfield et al., 2021). In another study they state that as telemedicine becomes increasingly common in healthcare, user feedback will be essential to tailoring, communicating, and supporting the acceptance and success of these programs (Harrison et al., 2017). In another study, remote glycemia monitoring in women with GDM was shown to be safe. Although glycemic control and maternal and neonatal outcomes were similar, women preferred this model of care (Mackillop et al., 2018). In another study, more than a third of patients gave a cross-platform app with continuous glucose monitoring the maximum score of 10 points for its usefulness in monitoring the disease. At the same time, the convenience of the app received high ratings, with an average value of 8 (Pustozerov and Popova, 2018). Patients who used the system based on a mobile app and Bluetooth glucometer monitoring, according to a survey at the end of the study, reflect a high degree of satisfaction (Rigla et al., 2018). In another study where patients with DM2 and GDM used an app to record glycemic values, they generally adhered satisfactorily to the use of the application (Triberti et al., 2018). In a qualitative study reviewing the perception of mHealth solutions for diabetes in pregnancy, most of these women are willing to self-manage their condition from home and be monitored remotely by a healthcare team (Alqudah et al., 2019).

Increased Awareness and Motivation

For many of the women in the study where a mobile app was used, self-monitoring of blood glucose values, including an overview and real-time feedback, was the most important aspect of the app for increasing self-awareness and motivation (Skar et al., 2018). As a conclusion of the study, it is mentioned that there is still much room for improvement in the usability of the multiplatform application associated with continuous glucose monitoring, especially when it comes to perceiving patient motivation (Pustozerov and Popova, 2018).

Other Psychological Variables

Patients' spiritual growth, level of interpersonal relationships and stress management improved significantly ($p < 0.001$) with the use of the cross-platform application-based system (Kim et al., 2021). In another study, anxiety in the experimental group, which used the web system, decreased by 5.1 points and increased by 1.0 points in the control group ($p = 0.048$). Depression increased in both groups (Kim et al., 2019). However, contrary to this result, in another randomized controlled trial, the intervention (multiplatform application) did not increase anxiety or depression (Yew et al., 2021). In another study, patients rated the sense of security provided by the system based on a multiplatform application with Bluetooth glucometer monitoring (Peleg et al., 2017).

Other Results Associated With the Medical Team Perception of the Technologies Used for the Control of GDM

Medical Team Satisfaction and Acceptability

The Bluetooth glucometer-based multiplatform system improved medical team satisfaction (Peleg et al., 2017). Physicians showed high levels of satisfaction with the mobile application (Varnfield et al., 2021).

Optimization of Patient Management

Some conclusions from the articles were: The medical team agreed that the multi-platform application and Bluetooth glucometer monitoring facilitated the glycemic management of patients (Peleg et al., 2017). The cross-platform glucometer app can be an excellent tool to avoid unnecessary hospital visits while maintaining better quality medical care and reducing physician workload in the management of GDM (Albert et al., 2020). In another study, all physicians either strongly agreed or agreed that the mobile application improved their efficiency in caring for their patients (Varnfield et al., 2021). In another study, the telemedicine system for GDM intervention did not change health care utilization or clinical outcomes compared to usual care (Rasekaba et al., 2018).

Improved Glycemic Control Remotely From the Patient

Some conclusions from the articles were: The use of the multiplatform application and Bluetooth glucometer monitoring resulted in high patient compliance with self-measurement. And physicians agreed that it facilitated patient management (Peleg et al., 2017). In the Smartphone group, there were more glucose measurements, and these measurements were significantly lower compared to the control group (Miremberg et al., 2018). The time needed to achieve optimal glycemic control was significantly shorter for participants in the intervention group using the web-based system than for those using usual care alone. Along with this, women in the intervention group required fewer insulin titrations than controls (Rasekaba et al., 2018). In another study where patients with DM2 and GDM used a mobile app to record glycemic values, there were no significant differences in the recording of glycemia between the two groups (Triberti et al., 2018). With the use of a mobile

application, patients in the study showed greater compliance in glucose measurements (Rigla et al., 2018).

Time Spent by Clinicians in Patient Assessment and Evaluation

One article showed an 88.6% reduction in face-to-face visits and a 27.4% reduction in time spent by clinicians evaluating patients in the intervention group that used a multiplatform application with Bluetooth glucometer monitoring. The system detected all situations requiring therapeutic adjustment, generating safe recommendations (Albert et al., 2020). The use of a web System reduced personal visits, as well as the time physicians spend evaluating patients, this improves physicians' efficiency in overcoming their increasing workload (Caballero-Ruiz et al., 2017). It was seen in another study that the *telehomecare* intervention group (THC) had an average of 1.5 versus 3.3 more medical visits than the control group. It increased 10 times more group nursing interventions compared to the control group, promoting greater GDM education. The results of this study show a significant decrease in medical visits and total health care costs for women in the THC group (Lemelin et al., 2020).

Some Problems or Adverse Study Results

Glucose Measurement

Some patients experienced discharge problems with the glucose meter (Albert et al., 2020). In another study, many women experienced technical problems in using the application. Several had problems with the automatic transfer of blood glucose values to the application, and many stopped using the application to record blood glucose values because of this (Skar et al., 2018).

Lack of Commitment of Medical Personnel to the Application

The pregnant women stated that the health professionals had little knowledge about the application and that they could not help them when they had problems with the application. Women also reported that their health professionals seemed to have little interest in the application and that they seemed more comfortable looking at blood glucose values on paper, which is standard procedure in the treatment of GDM. Some women stopped using the application to record blood glucose values because their health professionals only looked at their books with the recorded levels and not the application. The lack of support from their health professionals generated some frustration (Skar et al., 2018).

Frustration and Misinformation From the Patient

In a qualitative study of system use, some patients admitted that they sometimes "cheated" to get better values and feedback comments. One patient reported waiting 10 min to take her blood sugar to see if the value was lower. In addition, this same app generated some frustration and stress in the users. They stated that it is stressful to think about blood glucose values all the time, and it is frustrating to think if they are out of range. These negative feelings were associated with women who had problems controlling their blood glucose values. Of the women who had to use insulin, none used the application to monitor their blood glucose values, as they saw it as a burden (Skar et al., 2018).

DISCUSSION

The systematic review conducted provides valuable information to be able to apply telemedicine to pregnant women with GDM. Moreover, it may lay the groundwork for revising technological monitoring of other diseases in pregnancy. One of the strengths of this work was the robust and rigorous search strategy used to find the selected articles since we searched for content in 3 popular repositories that store a large number of current scientific papers, and the methodology explicates in detail what we want to find. This work also allows us to identify which devices and technologies are currently being used and how they are being used (concerning measurements and functions), in addition to describing in detail the main conclusions of the studies; not only for glycemic control and treatment of GDM, but also other characteristics of the use of technological systems, such as user satisfaction, measurements of psychological variables in pregnant women, motivation for using said systems, perceptions of the medical team, optimization of care times, and others. It also includes the possible errors that may be involved in the use of these systems.

Most of the studies were prospective and case-control studies, which reflects good robustness in terms of the quality of the results. Ideally, this type of study should be multicenter to further support the results; however, its application can be difficult because they are systems or studies that require large financial resources.

An important detail to consider is that there are no records in Latin America, so a parallel search was performed and a Brazilian author was found with several publications, mainly on intelligent mobile systems for pregnancy care and prediction, and decision making systems. Both systems presented in the articles found showed high accuracy of 80%, in predicting hypertensive disorders, so they are good predictive methods, but in both articles concluded that more studies were needed [Moreira et al., 2016a; Moreira et al., 2016b (1)]. It is important to encourage this type of study in the population of pregnant women in Latin America because overweight and obesity is a major problem among women of reproductive age in Latin America and the Caribbean, where it is estimated that 70% of women between 20 and 49 years of age are overweight or obese, which are risk factors for GDM. According to the International Diabetes Federation, approximately 12% of live births in Latin America and the Caribbean may be affected by hyperglycemia during pregnancy (Organización Panamericana de la Salud. Hiperglucemia y embarazo en las Américas, 2016; WHO et al., 2019) which is why it is relevant to invite the authors to continue searching for technological strategies for monitoring GDM, based on the results observed in the present review.

It is important to consider that inadequate management of gestational diabetes can lead to various complications, including increased likelihood of a large-for-gestational-age newborn, cesarean section, increased fetal insulin levels, and neonatal fat levels (Coustan et al., 2010). Elevated glycosylated hemoglobin levels were also associated with preeclampsia and preterm delivery (Lowe et al., 2012). On the other hand, a higher maternal BMI, independent of maternal glycemia, is strongly associated with a higher frequency of pregnancy complications, particularly those related to excess fetal growth, adiposity and preeclampsia (Metzger, 2010). Therefore, it is relevant that technologies for the management of GDM should include intake control, weight control and energy and nutrient adequacy to control weight gain in pregnancy.

The categories used in the monitoring of GDM using a technological system coincided precisely with the models of prevention and treatment of GDM: healthy eating and carbohydrate counting (Yuen, 2015; Awuchi et al., 2020), exercise (Mottola, 2008; Bianchi et al., 2017) and lifestyle changes (Moholdt et al., 2020).

In the case of manual transfer of information with standard glucometers, a margin of error may occur at the time of transcribing the value to the digital platform. On the other hand, glucometers with an infrared port must have an additional device (a device reader) for direct transfer to occur. Continuous glucose monitoring (CGM) is becoming increasingly reliable and has demonstrated efficacy in terms of improving glycosylated hemoglobin, reducing hypoglycemia and improving time in the target glucose range. This system that provides immediate feedback to patients and decision support tools for patients and providers have demonstrated superior results compared to intermittent self-monitored blood glucose monitoring (Reddy et al., 2020). More information is needed to know whether the Smart glucometer offers the same reliability as a glucometer with Bluetooth. Just by chance, it is estimated that the most convenient glucometer for pregnant women would be the Bluetooth glucometer since the download is automatic and direct to the technology (as long as this technology has a BlueTooth connection).

There are several factors associated with which platform would be the most convenient. One of them is the need for an internet connection, for example, to access a web system it is necessary to be connected to the internet, while a mobile application may require a connection for a limited time. On the other hand, to be able to download a mobile application, it is necessary to have enough storage space in the digital technology, so it must be a lightweight application. Ideally, the platform should be available in both forms (web page and mobile application), many of the studies reviewed used multiplatform applications, which is the most advantageous concerning the usability of the technology (Delia et al., 2015).

In the selected articles, the technological applications were mainly focused on the objective of improving glycemic control and supporting pregnant women in understanding GDM. These functions are relevant and it is good that they are included in the monitoring of the GDM with the use of technologies. According to the literature, GDM can have serious effects if not adequately treated. An important part of the management of GDM involves patient education on diet, exercise, self-monitoring of blood glucose and self-administration of insulin (Evans and Patry, 2004). It is precisely these functions that the authors of the reviewed articles seek to implement in their systems. It is important to note that none of the selected articles has focused on evaluating the impact of a specific diet on gestational diabetes using these technologies. As future work, it will be of great relevance to analyze various types of diet, such as the effect of a very low-calorie diet through remote monitoring of gestational diabetes.

According to the results found, only 30% of the studies showed glycemic monitoring figures; of these, 100% showed improvements in the measurement parameters: fasting glycemia, postprandial 1 or 2 h, HbA1c, % of measurements outside the recommended range, etc. Even so, it can be concluded that the use of technologies in pregnant women with diabetes is promising; however, studies that continue to support their efficacy in a multicenter, randomized and controlled manner are lacking. It has been previously demonstrated in 11 systematic reviews and 15 meta-analyses, most focused on patients with type 1 diabetes (10 and 6, respectively), reported a reduction in glycosylated hemoglobin (HbA1c) levels from 0.17 to 0.70% after the use of diabetes monitoring systems. Among the control systems is conventional monitoring with traditional glucometer, continuous glucose monitoring, noninvasive glucose monitor, artificial pancreas, insulin pump with sensors and mobile technology or telemedicine (Kamusheva et al., 2021). In this review, we have focused mainly on mobile technology or telemedicine for diabetes monitoring in pregnancy, so the results contribute to this area.

The satisfaction of the patients and the medical team was demonstrated, which provides positive aspects to the use of technology in GDM. What patients highlighted the most was the short time required to use this type of service, in addition to the comfort they provide at the time of monitoring. This empowers patients for their health, increasing their security and confidence concerning their pregnancy condition since they know how they are currently and how to improve their quality of life for the benefit of themselves and their children. On the part of the medical team, what was most valued was the optimization of the time spent on education and monitoring, as well as the greater amount of data associated with glycemic control that they were able to obtain with the applications used.

Some limitations or negative aspects of the use of the technology were concerning glucose measurement, mainly associated with technical problems, though also with the users' feeling that the clinical staff was not sufficiently committed to the application, which caused them some frustration. Others were associated with the fact that the information using standard glucometers could be modified or altered, or that the pregnant women did not take their glycemia as specified according to the instructions, which could lead to untruthful information at the time of analysis. It was also observed that the use of technology could generate stress in pregnant women due to the excess of information to be processed (both in terms of content and measurement taking).

Limitations and Future Projections

As for weaknesses of this work, because it details in such a specific way what we want to find, with the inclusion criteria limiting the articles to those published in the last 6 years, there is a probability that texts were left out which could have provided more information regarding remote monitoring of GDM. Also, in the exclusion criteria, the post-natal period is left out, so it cannot be deduced whether the use of technologies decreases maternal or neonatal risks associated with this period in this work.

Regarding the limitations of this review, we recognize that there is no agreement on which is the most appropriate methodology for screening and diagnosis of GDM or standard treatment protocols, so patients may not be precisely comparable among all trials. On the other hand, although values associated with glycemia obtained in patients were found, there was no single or exclusive measurement parameter, which makes it impossible to compare quantitatively the technologies used in the selected articles. There is also no specific information on the digital technology used; only one article specifies the brand and model of the technology, so we do not know what storage space is required for use of the platform, or what operating system it is compatible with if it is a mobile application.

It is important to consider how all the information that can be collected by the digital platforms discussed above can help us. From this arises the definition of Big Data: data sets whose size is beyond the capacity of typical database software to capture, store, manage and analyze (Bahri et al., 2019). During the search of databases, an article emerged about a prototype data integration system from mobile apps and glucometers that aims to standardize the data and have it stored to assist clinicians in the diagnosis and treatment of GDM, but since it is a prototype, there is no information about the results (Pais et al., 2016). It is also necessary to make way for Artificial Intelligence technologies that help to predict glucose, such as the glucose prediction system mentioned in the article by (Pustozerov et al., 2018), as it would allow minimization of invasiveness that can result from the constant use of a glucometer several times a day, and thus improve the quality of life of patients. It would be interesting to optimize resources in medical care by using predictive models for insulin adjustment based on glycemia monitoring and to take it to a clinical context where its use can be validated and prototyped.

CONCLUSION

The objective of this systematic review was to determine the impact of current technologies, and recognize types and methods that assist patients with GDM. At the end of this work, it was concluded that monitoring technologies are safe and at no time did they worsen the glycemic status of pregnant women. However, a greater number of randomized controlled multi-center studies and clinical trials are needed, as well as a standardization of the measurements to be established to consider a given measurement "an improvement in glycemic control". There were benefits such as increased satisfaction and acceptability, maternal confidence, and knowledge of GDM and thus improvements in the quality of the health service delivered. There were also positive comments in terms of optimizing the time of the medical team. GDM centered technology may help to evaluate outcomes and tailor personalize solutions. Further studies are still needed to understand the efficacy and economic impact that could arise from the use of this type of intervention. The present review provides an opportunity to learn about the use of technology in GDM and contribute to women's health.

DATA AVAILABILITY STATEMENT

The original contributions presented in the study are included in the article/**Supplementary Material**, further inquiries can be directed to the corresponding author.

AUTHOR CONTRIBUTIONS

AB and BG provide the principal idea, search for information, and write the manuscript. FP was full the support on the clinical approach and Gestational Diabetes Mellitus (GDM). RT and SC were the full support for the Remote Technology for Health (search and discussion). SC was the support on PRISMA technique. LS and JP were the support on the discussion on clinical approach on GDM. RS was the organizer of the manuscript, support the discussion on technology for remote monitoring of GDM.

FUNDING

This work was partially founded by the following grants: Centro de Investigación y Desarrollo en Ingeniería en Salud, Universidad de Valparaíso, Chile. CIDIS-UV 14; ANID – Millennium Science Initiative Program ICN2021-004; Proyecto PUENTE, UVA20993; Fondo Nacional de Desarrollo Científico y Tecnológico (FONDECYT) (grant number 1190316 and 1221938), Chile; and International Sabbaticals (University Medical Centre Groningen, University of Groningen, The Netherlands) from the Vicerectorate of Academic Affairs, Academic Development Office of the Pontificia Universidad Católica de Chile.

SUPPLEMENTARY MATERIAL

The Supplementary Material for this article can be found online at: https://www.frontiersin.org/articles/10.3389/fbioe.2022.819697/full#supplementary-material

REFERENCES

Al-ofi, E. A., Mosli, H. H., Ghamri, K. A., and Ghazali, S. M. (2019). Management of Postprandial Hyperglycaemia and Weight Gain in Women with Gestational Diabetes Mellitus Using a Novel Telemonitoring System. *J. Int. Med. Res.* 47, 754–764. doi:10.1177/0300060518809872

Albert, L., Capel, I., García-Sáez, G., Martín-Redondo, P., Hernando, M. E., and Rigla, M. (2020). Managing Gestational Diabetes Mellitus Using a Smartphone Application with Artificial Intelligence (SineDie) during the COVID-19 Pandemic: Much More Than Just Telemedicine. *Diabetes Res. Clin. Pract.* 169, 108396. doi:10.1016/j.diabres.2020.108396

Alqudah, A., McMullan, P., Todd, A., O'Doherty, C., McVey, A., McConnell, M., et al. (2019). Service Evaluation of Diabetes Management during Pregnancy in a Regional Maternity Hospital: Potential Scope for Increased Self-Management and Remote Patient Monitoring through mHealth Solutions. *BMC Health Serv. Res.* 19, 662. doi:10.1186/s12913-019-4471-9

American Diabetes Association (2020). Classification and Diagnosis of Diabetes: Standards of Medical Care in Diabetes-2020. *Diabetes Care* 43, S14–S31. doi:10.2337/dc20-S002

American Diabetes Association (2014). Standards of Medical Care in Diabetes–2014. *Diabetes care* 37 Suppl 1, S14–S80. doi:10.2337/dc14-S014

Anna, V., van der Ploeg, H. P., Cheung, N. W., Huxley, R. R., and Bauman, A. E. (2008). Sociodemographic Correlates of the Increasing Trend in Prevalence of Gestational Diabetes Mellitus in a Large Population of Women between 1995 and 2005. *Diabetes Care* 31, 2288–2293. doi:10.2337/dc08-1038

Auvinen, A.-M., Luiro, K., Jokelainen, J., Järvelä, I., Knip, M., Auvinen, J., et al. (2020). Type 1 and Type 2 Diabetes after Gestational Diabetes: a 23 Year Cohort Study. *Diabetologia* 63, 2123–2128. doi:10.1007/s00125-020-05215-3

Awuchi, C. G., Echeta, C. K., and Igwe, V. S. (2020). Diabetes and the Nutrition and Diets for its Prevention and Treatment: A Systematic Review and Dietetic Perspective. *Health Sci. Res.* 6, 5–19.

Bahri, S., Zoghlami, N., Abed, M., and Tavares, J. M. R. S. (2019). BIG DATA for Healthcare: A Survey. *IEEE Access* 7, 7397–7408. doi:10.1109/access.2018.2889180

Bianchi, C., Battini, L., Aragona, M., Lencioni, C., Ottanelli, S., Romano, M., et al. (2017). Prescribing Exercise for Prevention and Treatment of Gestational Diabetes: Review of Suggested Recommendations. *Gynecol. Endocrinol.* 33, 254–260. doi:10.1080/09513590.2016.1266474

Borgen, I., Garnweidner-Holme, L. M., Jacobsen, A. F., Bjerkan, K., Fayyad, S., Joranger, P., et al. (2017). Smartphone Application for Women with Gestational Diabetes Mellitus: A Study Protocol for a Multicentre Randomised Controlled Trial. *BMJ Open* 7, e013117. doi:10.1136/bmjopen-2016-013117

Bromuri, S., Puricel, S., Schumann, R., Krampf, J., Ruiz, J., and Schumacher, M. (2016). An Expert Personal Health System to Monitor Patients Affected by Gestational Diabetes Mellitus: A Feasibility Study. *Ais* 8, 219–237. doi:10.3233/AIS-160365

Caballero-Ruiz, E., García-Sáez, G., Rigla, M., Villaplana, M., Pons, B., and Hernando, M. E. (2017). A Web-Based Clinical Decision Support System for Gestational Diabetes: Automatic Diet Prescription and Detection of Insulin Needs. *Int. J. Med. Inform.* 102, 35–49. doi:10.1016/j.ijmedinf.2017.02.014

Caballero-Ruiz, E., García-Sáez, G., Rigla, M., Villaplana, M., Pons, B., and Hernando, M. E. (2016). Automatic Classification of Glycaemia Measurements to Enhance Data Interpretation in an Expert System for Gestational Diabetes. *Exp. Sys. App.* 63, 386–396. doi:10.1016/j.eswa.2016.07.019

Coustan, D. R., Lowe, L. P., Metzger, B. E., and Dyer, A. R. (2010). The Hyperglycemia and Adverse Pregnancy Outcome (HAPO) Study: Paving the Way for New Diagnostic Criteria for Gestational Diabetes Mellitus. *Am. J. Obstet. Gynecol.* 202, 654–656. doi:10.1016/j.ajog.2010.04.006

Delia, L., Galdamez, N., Thomas, P., Corbalan, L., and Pesado, P. (2015). "Multi-platform mobile Application Development Análisis," in IEEE RCIS. Athens, Greece, May 13-15, 2015. doi:10.1109/RCIS.2015.7128878

Evans, E., and Patry, R. (2004). Management of Gestational Diabetes Mellitus and Pharmacists' Role in Patient Education. *Pharm* 61, 1460–1465. doi:10.1093/ajhp/61.14.1460

Garmendia, M. L., Mondschein, S., Montiel, B., and Kusanovic, J. P. (2020). Trends and Predictors of Gestational Diabetes Mellitus in Chile. *Int. J. Gynecol. Obstet.* 148, 210–218. doi:10.1002/ijgo.13023

Guo, H., Zhang, Y., Li, P., Zhou, P., Chen, L.-M., and Li, S.-Y. (2019). Evaluating the Effects of mobile Health Intervention on Weight Management, Glycemic Control and Pregnancy Outcomes in Patients with Gestational Diabetes Mellitus. *J. Endocrinol. Invest.* 42, 709–714. doi:10.1007/s40618-018-0975-0

Harrison, T. N., Sacks, D. A., Parry, C., Macias, M., Ling Grant, D. S., and Lawrence, J. M. (2017). Acceptability of Virtual Prenatal Visits for Women with Gestational Diabetes. *Women's Health Issues* 27, 351–355. doi:10.1016/j.whi.2016.12.009

Johnson, Q. B., and Berry, D. C. (2018). Impacting Diabetes Self-Management in Women with Gestational Diabetes Mellitus Using Short Messaging Reminders. *J. Am. Assoc. Nurse Pract.* 30, 320–326. doi:10.1097/JXX.0000000000000059

Jovanovic, L., Knopp, R. H., Kim, H., Cefalu, W. T., Zhu, X.-D., Lee, Y. J., et al. (2005). Elevated Pregnancy Losses at High and Low Extremes of Maternal Glucose in Early Normal and Diabetic Pregnancy. *Diabetes Care* 28, 1113–1117. doi:10.2337/diacare.28.5.1113

Kamusheva, M., Tachkov, K., Dimitrova, M., Mitkova, Z., García-Sáez, G., Hernando, M. E., et al. (2021). A Systematic Review of Collective Evidences Investigating the Effect of Diabetes Monitoring Systems and Their Application in Health Care. *Front. Endocrinol.* 12, 636959. doi:10.3389/fendo.2021.636959

Kim, S.-H., Kim, H. J., and Shin, G. (2021). Self-management mobile Virtual Reality Program for Women with Gestational Diabetes. *Int. J. Environ. Res. Public Health* 18, 1–12. doi:10.3390/ijerph18041539

Kim, Y.-S., Kim, H.-S., and Kim, Y.-L. (2019). Effects of a Web-Based Self-Management Program on the Behavior and Blood Glucose Levels of Women with Gestational Diabetes Mellitus. *Telemed. e-Health* 25, 407–414. doi:10.1089/tmj.2017.0332

Lemelin, A., Paré, G., Bernard, S., and Godbout, A. (2020). Demonstrated Cost-Effectiveness of a Telehomecare Program for Gestational Diabetes Mellitus Management. *Diabetes Tech. Ther.* 22, 195–202. doi:10.1089/dia.2019.0259

Lowe, L. P., Metzger, B. E., Dyer, A. R., Lowe, J., McCance, D. R., Lappin, T. R. J., et al. (2012). Hyperglycemia and Adverse Pregnancy Outcome (HAPO) Study: Associations of Maternal A1C and Glucose with Pregnancy Outcomes. *Diabetes Care* 35, 574–580. doi:10.2337/dc11-1687

Mackillop, L., Hirst, J. E., Bartlett, K. J., Birks, J. S., Clifton, L., Farmer, A. J., et al. (2018). Comparing the Efficacy of a Mobile Phone-Based Blood Glucose Management System with Standard Clinic Care in Women with Gestational Diabetes: Randomized Controlled Trial. *JMIR Mhealth Uhealth* 6, e71. doi:10.2196/mhealth.9512

McIntyre, H. D., Catalano, P., Zhang, C., Desoye, G., Mathiesen, E. R., and Damm, P. (2019). Gestational Diabetes Mellitus. *Nat. Rev. Dis. Primers* 5, 47–19. doi:10.1038/s41572-019-0098-8

McIntyre, H. D., and Moses, R. G. (2020). The Diagnosis and Management of Gestational Diabetes Mellitus in the Context of the COVID-19 Pandemic. *Diabetes Care* 43, 1433–1434. doi:10.2337/dci20-0026

Metzger, B. E. (2010). Hyperglycaemia and Adverse Pregnancy Outcome (HAPO) Study: Associations with Maternal Body Mass index. *BJOG* 117, 575–584. doi:10.1111/j.1471-0528.2009.02486.x

Ministerio de Salud (2014). *Guía Diabetes Y Embarazo*. Chile: Ministerio de Salud.

Miremberg, H., Ben-Ari, T., Betzer, T., Raphaeli, H., Gasnier, R., Barda, G., et al. (2018). The Impact of a Daily Smartphone-Based Feedback System Among Women with Gestational Diabetes on Compliance, Glycemic Control, Satisfaction, and Pregnancy Outcome: a Randomized Controlled Trial. *Am. J. Obstet. Gynecol.* 218, 453. doi:10.1016/j.ajog.2018.01.044

Moholdt, T., Hayman, M., Shorakae, S., Brown, W. J., and Harrison, C. L. (2020). The Role of Lifestyle Intervention in the Prevention and Treatment of Gestational Diabetes. *Semin. Reprod. Med.* 38, 398–406. doi:10.1055/s-0040-1722208

Moreira, M. W. L., Rodrigues, J. J. P. C., Oliveira, A. M. B., and Saleem, K. (2016b). "Smart mobile System for Pregnancy Care Using Body Sensors," in IEEE. MoWNeT, Cairo, Egypt, April 11-13, 2016. doi:10.1109/MoWNet.2016.7496609

Moreira, M. W. L., Rodrigues, J. J. P. C., Oliveira, A. M. B., Saleem, K., and Neto, A. (2016a). "Performance Evaluation of Predictive Classifiers for Pregnancy Care,"

in IEEE GLOBECOM, Washington, DC, USA, December 04-08, 2016. doi:10.1109/GLOCOM.2016.7842136

Mottola, M. F. (2008). The Role of Exercise in the Prevention and Treatment of Gestational Diabetes Mellitus. *Curr. Sports Med. Rep.* 6, 381–386. doi:10.1007/s11892-008-0053-7

Organización Panamericana de la Salud. Hiperglucemia y embarazo en las Américas (2016). *Informe final de la Conferencia Panamericana sobre Diabetes y Embarazo. Lima, Perú: 8–10 de septiembre de 2015)*. Washington, DC: Institutional Repository for Information Sharing.

Pais, S., Parry, D., Rush, E., and Rowan, J. (2016). Data Integration for mobile Wellness Apps to Support Treatment of GDM. *ACSW* 64, 1–7. doi:10.1145/2843043.2843382

Peleg, M., Shahar, Y., Quaglini, S., Broens, T., Budasu, R., Fung, N., et al. (2017). Assessment of a Personalized and Distributed Patient Guidance System. *Int. J. Med. Inform.* 101, 108–130. doi:10.1016/j.ijmedinf.2017.02.010

Pustozerov, E., and Popova, P. (2018). Mobile-based Decision Support System for Gestational Diabetes Mellitus. *USBEREIT* 2018, 45–48. doi:10.1109/USBEREIT.2018.8384546

Pustozerov, E., Popova, P., Tkachuk, A., Bolotko, Y., Yuldashev, Z., and Grineva, E. (2018). Development and Evaluation of a Mobile Personalized Blood Glucose Prediction System for Patients with Gestational Diabetes Mellitus. *JMIR. Mhealth Uhealth* 6, e6. doi:10.2196/mhealth.9236

Rasekaba, T. M., Furler, J., Young, D., Liew, D., Gray, K., Blackberry, I., et al. (2018). Using Technology to Support Care in Gestational Diabetes Mellitus: Quantitative Outcomes of an Exploratory Randomised Control Trial of Adjunct Telemedicine for Gestational Diabetes Mellitus (TeleGDM). *Diabetes Res. Clin. Pract.* 142, 276–285. doi:10.1016/j.diabres.2018.05.049

Reddy, N., Verma, N., Dungan, K., Feingold, K. R., Anawalt, B., Boyce, A., et al. (2020). *Monitoring Technologies – Continuous Glucose Monitoring, Mobile Technology, Biomarkers of Glycemic Control*. San Francisco, USA: Endotext.

Rigla, M., Martínez-Sarriegui, I., García-Sáez, G., Pons, B., and Hernando, M. E. (2018). Gestational Diabetes Management Using Smart Mobile Telemedicine. *J. Diabetes Sci. Technol.* 12 (12), 260–264. doi:10.1177/1932296817704442

Seo, Y., Kim, E. M., Choi, J. S., and Park, C.-Y. (2020). Using a Mobile-based Nutritional Intervention Application Improves Glycemic Control but Reduces the Intake of Some Nutrients in Patients with Gestational Diabetes Mellitus: A Case Series Study. *Clin. Nutr. Res.* 9, 73–79. doi:10.7762/cnr.2020.9.1.73

Shin, D., and Song, W. O. (2014). Prepregnancy Body Mass index Is an Independent Risk Factor for Gestational Hypertension, Gestational Diabetes, Preterm Labor, and Small- and Large-For-Gestational-Age Infants. *J. Maternal-Fetal Neonatal Med.* 28, 1679–1686. doi:10.3109/14767058.2014.964675

Skar, J. B., Garnweidner-Holme, L. M., Lukasse, M., and Terragni, L. (2018). Women's Experiences with Using a Smartphone App (The Pregnant+ App) to Manage Gestational Diabetes Mellitus in a Randomised Controlled Trial. *Midwifery* 58, 102–108. doi:10.1016/j.midw.2017.12.021

Tian, Y., Zhang, S., Huang, F., and Ma, L. (2021). Comparing the Efficacies of Telemedicine and Standard Prenatal Care on Blood Glucose Control in Women with Gestational Diabetes Mellitus: Randomized Controlled Trial. *JMIR Mhealth Uhealth* 9, e22881. doi:10.2196/22881

Triberti, S., Bigi, S., Rossi, M. G., Caretto, A., Laurenzi, A., Dozio, N., et al. (2018). The ActiveAgeing Mobile App for Diabetes Self-Management: First Adherence Data and Analysis of Patients' In-App Notes. *LNICST* 253, 129–138. doi:10.1007/978-3-030-01093-5_17

Urrútia, G., and Bonfill, X. (2010). Declaración PRISMA: una propuesta para mejorar la publicación de revisiones sistemáticas y metaanálisis. *Medicina Clínica* 135, 507–511. doi:10.1016/j.medcli.2010.01.015

Varnfield, M., Redd, C., Stoney, R. M., Higgins, L., Scolari, N., Warwick, R., et al. (2021). M♡THer, an mHealth System to Support Women with Gestational Diabetes Mellitus: Feasibility and Acceptability Study. *Diabetes Tech. Ther.* 23, 358–366. doi:10.1089/dia.2020.0509

Wernimont, S. A., Sheng, J. S., Fleener, D., Summers, K. M., Syrop, C., and Andrews, J. I. (2020). Cellular-Enabled Glucometers and Maternal Glucose Control: A Quality Improvement Initiative. *J. Diabetes Sci. Technol.* 14, 77–82. doi:10.1177/1932296819856360

WHO; UNICEF; UNFPA; World Bank; United nations population division (2019). *Trends in Maternal Mortality: 2000 to 2017: Estimates by WHO, UNICEF, UNFPA, World Bank Group and the United Nations Population Division*. Geneva: World Health Organization, UNICEF, UNFPA, World Bank, Group and the United Nations Population Division.

World Health Organization (2006). *Definition and Diagnosis of Diabetes Mellitus and Intermediate Hyperglycaemia*. Geneva: WHO.

Yang, P., Lo, W., He, Z.-l., and Xiao, X.-m. (2018). Medical Nutrition Treatment of Women with Gestational Diabetes Mellitus by a Telemedicine System Based on Smartphones. *J. Obstet. Gynaecol. Res.* 44, 1228–1234. doi:10.1111/jog.13669

Yew, T. W., Chi, C., Chan, S.-Y., van Dam, R. M., Lim, C. S., Foong, P. S., et al. (2021). A Randomized Controlled Trial to Evaluate the Effects of a Smartphone Application-Based Lifestyle Coaching Program on Gestational Weight Gain, Glycemic Control, and Maternal and Neonatal Outcomes in Women with Gestational Diabetes Mellitus: The SMART-GDM Study. *The SMART-GDM Diabetes Care* 44, 456–463. doi:10.2337/dc20-1216

Yuen, L. (2015). Gestational Diabetes Mellitus: Challenges for Different Ethnic Groups. *Wjd* 6, 1024–1032. doi:10.4239/wjd.v6.i8.1024

Conflict of Interest: The authors declare that the research was conducted in the absence of any commercial or financial relationships that could be construed as a potential conflict of interest.

Publisher's Note: All claims expressed in this article are solely those of the authors and do not necessarily represent those of their affiliated organizations, or those of the publisher, the editors and the reviewers. Any product that may be evaluated in this article, or claim that may be made by its manufacturer, is not guaranteed or endorsed by the publisher.

frontiers in Bioengineering and Biotechnology

ORIGINAL RESEARCH
published: 04 March 2022
doi: 10.3389/fbioe.2022.807139

Novel Technique for Confirmation of the Day of Ovulation and Prediction of Ovulation in Subsequent Cycles Using a Skin-Worn Sensor in a Population With Ovulatory Dysfunction: A Side-by-Side Comparison With Existing Basal Body Temperature Algorithm and Vaginal Core Body Temperature Algorithm

Hurst B. S.[1], *Davies K.*[2], *Milnes R. C.*[3]*, *Knowles T. G.*[4] and *Pirrie A.*[5]

[1]Carolinas Medical Center, Department of Assisted Reproduction, Charlotte, NC, United States, [2]Independent Fertility Nurse Consultant and Coach, Castle Bytham, United Kingdom, [3]Fertility Focus Inc. (Now viO HealthTech Inc.), Old Saybrook, CT, United States, [4]Faculty of Health Sciences, University of Bristol, Bristol, United Kingdom, [5]Fertility Focus Limited (now viO HealthTech Limited), Basepoint Business Centre, Warwick, United Kingdom

OPEN ACCESS

Edited by:
Vesna Garovic,
Mayo Clinic, United States

Reviewed by:
Rita Payan Carreira,
University of Evora, Portugal
Virginia Pensabene,
University of Leeds, United Kingdom

***Correspondence:**
Milnes R. C.
robert.milnes@fertility-focus.com

Specialty section:
This article was submitted to Preclinical Cell and Gene Therapy, a section of the journal Frontiers in Bioengineering and Biotechnology

Received: 01 November 2021
Accepted: 25 January 2022
Published: 04 March 2022

Citation:
B. S. H, K. D, R. C. M, T. G. K and A. P (2022) Novel Technique for Confirmation of the Day of Ovulation and Prediction of Ovulation in Subsequent Cycles Using a Skin-Worn Sensor in a Population With Ovulatory Dysfunction: A Side-by-Side Comparison With Existing Basal Body Temperature Algorithm and Vaginal Core Body Temperature Algorithm. Front. Bioeng. Biotechnol. 10:807139. doi: 10.3389/fbioe.2022.807139

Objective: Determine the accuracy of a novel technique for confirmation of the day of ovulation and prediction of ovulation in subsequent cycles for the purpose of conception using a skin-worn sensor in a population with ovulatory dysfunction.

Methods: A total of 80 participants recorded consecutive overnight temperatures using a skin-worn sensor at the same time as a commercially available vaginal sensor for a total of 205 reproductive cycles. The vaginal sensor and its associated algorithm were used to determine the day of ovulation, and the ovulation results obtained using the skin-worn sensor and its associated algorithm were assessed for comparative accuracy alongside a number of other statistical techniques, with a further assessment of the same skin-derived data by means of the "three over six" rule. A number of parameters were used to divide the data into separate comparative groups, and further secondary statistical analyses were performed.

Results: The skin-worn sensor and its associated algorithm (together labeled "SWS") were 66% accurate for determining the day of ovulation (±1 day) or the absence of ovulation and 90% accurate for determining the fertile window (ovulation day ±3 days) in the total study population in comparison to the results obtained from the vaginal sensor and its associated algorithm (together labeled "VS").

Conclusion: SWS is a useful tool for confirming the fertile window and absence of ovulation (anovulation) in a population with ovulatory dysfunction, both known and

determined by means of the timing of ovulation. The body site where the skin-worn sensor was worn (arm or wrist) did not appear to affect the accuracy. Prior diagnosis of known causes of ovulatory dysfunction appeared to affect the accuracy to a lesser extent than those cycles grouped into late ovulation and "early and normal ovulation" groups. SWS is a potentially useful tool for predicting ovulation in subsequent cycles, with greater accuracy obtained for the "normal ovulation" group.

Keywords: ovulation, skin temperature, core body temperature, basal body temperature, ovulatory dysfunction, fertile window, vaginal sensor, ovulation algorithm

1 INTRODUCTION

1.1 Clinical and Scientific Background

There are three main goals in the determination of ovulation for the purposes of improving the chances of conception: 1) to confirm the presence or absence of ovulation (anovulation) in a reproductive cycle, 2) to confirm the day on which ovulation occurred, and 3) to use this ovulation day in one reproductive cycle to predict the date of ovulation and the "fertile window" for the subsequent cycle in order to improve the chances of natural conception or timing of intervention. The fertile window is the span of time during a reproductive cycle when conception can take place. Based on the 5-day lifespan of sperm in the female reproductive tract and the up to 48-h lifespan of the unfertilized oocyte (egg), the window is largely deemed to run from 3 to 5 days prior to the day of ovulation up to 1–2 days after ovulation (Colombo and Masarotto, 2000).

The relationship between a temperature rise and ovulation, and the use of a charted single oral temperature recording taken first thing upon waking to retrospectively determine the presence and timing of ovulation was reported in the literature over 100 years ago (van de Velde, 1904; Harvey and Crockete, 1932; Tompkins, 1944). This methodology is generally referred to as basal body temperature (BBT), as it seeks to establish the consistent lowest (basal) temperature in a 24-h period from which to determine a rise. Body temperature is actually at its most stable and lowest during nighttime sleep, and the waking oral temperature was considered the best proxy for that nighttime temperature when the method was developed. The "three over six (TOS) rule" originally proposed by Barrett and Marshall (Barrett and Marshall, 1969) and as further developed (McCarthy and Rockette, 1983) is the most widely used current method for determining the presence and timing of ovulation with the BBT technique. The basic rule holds that ovulation has occurred if in any window in the cycle there is a sustained rise in temperature over 3 consecutive days, which is at least 0.3°C (0.54°F) higher than the previous 6 consecutive days. The day of ovulation is determined to be the day prior to the first of the 3 "high" temperatures. This method is in effect a simple time and mathematical-based algorithm. Traditional clinical thinking holds that the temperature rise is associated with the thermogenic effect of released progesterone and that progesterone starts being released after a follicle has ruptured during ovulation and the corpus luteum starts to form. Following this logic, clinicians have long believed a temperature rise can only take place *after* ovulation has occurred. Recent research calls this association into question and instead suggests that there is a progesterone rise of approximately 0.5 ng/ml prior to ovulation (Dozortsev and Diamond, 2020). Clinical publications have generally dismissed the use of other temperature curve characteristics such as the "nadir" (the lowest point of the curve) or "dip" prior to the rise for confirmation or prediction of ovulation (McCarthy and Rockette, 1983; Barron and Fehring, 2005). These are important considerations when assessing algorithmic techniques, which might assist us in better understanding both when a temperature rise has occurred and also more importantly when the temperature rise *is* occurring *as a cycle progresses*. The limitations of the BBT method, in particular for confirming the absence of ovulation, the exact day of ovulation, and for predicting a subsequent fertile window, have been widely reported (Lenton et al., 1977; Martinez et al., 1992; Barron and Fehring, 2005; Mazerolle et al., 2011). The method is especially problematic for women with ovulatory dysfunction for two reasons. Their temperature curves are generally more erratic, increasing the difficulty of interpreting charts and hence confirming 1) the presence or absence of ovulation and 2) the day of ovulation. The difficulty in the use of the ovulation day for predicting ovulation and the fertile window for a subsequent cycle—goal 3)—is compounded by the irregularity of their ovulation timing and or cycles, which makes it considerably less likely that ovulation will re-occur on the same day in a subsequent cycle even if it could be established accurately in the first place (Ayres-de-Campos et al., 1995).

1.2 Research Topic

In recent years, temperature sensors have been developed, which allow the gathering of multiple temperature measurements over a period of time from either the skin or within the vagina. These sensors upload data to a mobile device app either automatically or by user-initiated transfer. They potentially eliminate some of the inaccuracy associated with the waking oral measurement used in the BBT method in three ways. Firstly, they can be "worn" overnight—when the body temperature is at its most stable and lowest level. Secondly, by using an industrial temperature measurement component (thermistor), they can, in theory, record at a higher temperature resolution (enabling the steps between each temperature value to be better understood), and at a higher accuracy than an oral thermometer. Thirdly, they can be "worn" throughout the night, enabling multiple readings to be

taken—providing a better understanding of the most representative overnight temperature from which to calculate a temperature shift for each successive night. The sensors combined with the computing power of mobile devices make the application of algorithmic techniques much easier, both in determining the most representative overnight temperature and in understanding the temperature rise as the cycle progresses. Various publications have attempted to assess the accuracy of oral temperature (Freundl et al., 2003), skin temperature recorded on the top of the wrist (Goodale et al., 2019; Zhu et al., 2021), and vaginal temperature (Papaioannou et al., 2013a; Papaioannou et al., 2013b; Papaioannou et al., 2014; Regidor et al., 2018) for the determination of the date of ovulation by different statistical techniques, comparing the test method variously with ultrasound ovarian follicle measurements (to determine the date of ovulation by estimated date of follicle rupture), urinary luteinizing hormone (LH) results (to determine the date of ovulation as 24–48 h following two positive results), and BBT using the "TOS" rule. Although these comparator methods provide imperfect estimates of the date of ovulation, the results are nonetheless useful with a larger volume of cycles in determining the likelihood that the test method has provided a good understanding of the presence or absence of ovulation, and the day of ovulation. An estimate of percentage accuracy of each test method using data from the various statistical techniques employed by these publications has been made by the authors, by applying the principle of identifying true positives (TPs), true negatives (TNs), false positives (FPs), and false negatives (FNs) of the test method vs. the comparator method in the calculation (TP + TN)/(TP + TN + FP + FN). F score was also calculated to provide a comparison to studies where this was provided but the detailed results were not, using the calculation TP/TP + ½(FP + FN). The detailed results are recorded in **Supplementary Table S1**, and the details of the studies including comparator methods are recorded in **Supplementary Table S2**. The calculations based on these clinical papers as outlined in **Supplementary Table S1** show that oral temperature is up to 78% accurate in determining the fertile window rather than the day of ovulation with an F score of 0.88, skin temperature recorded on the top of the wrist provides an F score of 0.78 in determining the fertile window, and vaginal temperature is up to 99% accurate in determining the actual day of ovulation, with an F score of 0.99. The greater accuracy of the vaginal temperature method and its ability to determine the day of ovulation rather than the less stringent fertile window is understood to be a result of it providing a better proxy for true core body temperature without the external influences and signal "noise" that affect oral and skin temperature (Baker et al., 2020) and that core body temperature is likely to provide a more accurate reflection of the temperature rise associated with the release of progesterone (Coyne et al., 2000). It should be noted that clinical studies show that the accuracy of all these temperature methods can be improved by the inclusion of a secondary method of ovulation confirmation, and the combination of temperature with cervical mucus observation is particularly relevant (Frank-Herrmann et al., 2007), although not the subject of this paper.

1.3 Objectives

We aimed to determine the accuracy of a novel algorithm combined with a newly developed skin-worn-sensor (together with the "SWS": OvuFirst™—viO HealthTech Limited and Inc.). SWS determines the most representative overnight temperature, and then algorithmically confirms the presence or absence of ovulation and the date of ovulation. SWS was compared with the "TOS" rule for assessing the presence and timing of ovulation by eye on the same overnight representative data ("TOS"). SWS and TOS were then separately compared with an independent measurement of overnight vaginal temperature and its associated algorithm ("VS": OvuSense™ OvuCore, viO HealthTech Limited and Inc.). In these comparative analyses VS was treated as the "gold standard". SWS and VS were worn "side by side" by each participant with measurements taken each night of each recorded cycle except during menstruation and until ovulation was confirmed by both SWS and VS methods.

We aimed to compare the accuracy of the "Training Set" (an initial 93 cycles used to develop, test, and iterate the SWS algorithm) against the "Additional Set" (a further 112 cycles used for comparative testing after the Training Set was concluded). The methodology of these data sets shall be explained in the report.

We aimed to compare the accuracy of SWS for arm and wrist positioning modalities.

We aimed to separately compare SWS accuracy for four groups of reported prior diagnoses for the participants (Prior diagnosis of Polycystic Ovarian Syndrome ("PCOS"), "Hypothyroid," "PCOS and Hypothyroid," and "Confirmed No Diagnosis"), and the timing of ovulation.

We aimed to further examine the accuracy of TOS and SWS in predicting the date of ovulation in subsequent cycles compared with the actual VS confirmed day of ovulation for that subsequent cycle. By way of comparison and illustration of the potential difficulty in using prior cycle ovulation confirmation for prediction of ovulation in subsequent cycles, we aimed to examine the accuracy of VS in predicting the date of ovulation in subsequent cycles with the actual VS confirmed day of ovulation for those subsequent cycles.

2 METHODS

2.1 Study Population

The volunteers for the study were recruited from the current userbase of the VS product in the United States and the United Kingdom at the time of recruitment, self-selected by responding to an advert in the VS product user group and answering an initial questionnaire. The volunteers consented to use the SWS alongside the VS to enable the collection of side-by-side results and as such were a convenience sample from within the users of the product. No financial incentive was provided to participate in the study.

The volunteers were randomly assigned a recording skin site of "arm" or "wrist" for SWS with the intention of ensuring approximately 25% of the study population were assigned to the "wrist" site and sent a "one size fits all" wristband along with

TABLE 1 | Study population cycle comparison by number of years trying to conceive.

	0–1 year	1–2 years	2–3 years	3–4 years	4–5 years	5–6 years	6–7 years	>7 years	Not actively trying	Total
Number of cycles	14	64	39	20	22	12	22	4	8	205
Average cycle length	35.5	37.0	35.3	35.7	36.4	33.2	49.0	99.8	47.1	39.1
Median cycle length	33.5	32.0	30.0	32.0	30.0	31.5	29.5	43.5	40.0	32.0
Std Dev cycle length	15.6	17.3	15.8	16.4	17.2	11.3	59.2	119.4	25.6	30.1
Upper CI 95%	43.7	41.2	40.2	42.9	43.6	39.5	73.8	216.7	64.9	43.2
Lower CI 95%	27.3	32.8	30.3	28.5	29.2	26.8	24.3	−17.2	29.4	34.9
CI	8.2	4.2	5.0	7.2	7.2	6.4	24.7	117.0	17.7	4.1

their SWS sensor, with those assigned to the "arm" site being allocated one of three armband sizes according to their declared arm circumference: *Size D* 8 to <23 cm (7 to <9 in.); *Size F* 23 to <31 cm (9 to <12 in.); and *Size G* 31–38 cm (12–15 in.) and larger. Hence, there were four separate cohorts. Twenty volunteers received a wristband, 2 received armband *Size D*, 19 received armband *Size F*, and 46 received armband *Size G*. Note: although nominally each band size cohort (wrist, arm D, arm F, and arm G) should represent 25% of the total study population, it was clearly not possible to randomize the "arm" site group to the 3 armband sizes. Therefore, all those using an armband were treated as a single "skin site" group.

As part of the consent questionnaire, the volunteers were also asked to record existing prior diagnoses for "PCOS," "Hypothyroid," "PCOS and Hypothyroid," and "Confirmed No Diagnosis."

The 87 volunteers started the side-by-side recordings, of which 7 failed to eventually complete one registered full cycle of data (6 armband *Size F* and 1 armband *Size G*) and were excluded from the analysis. The remaining 80 volunteers recorded one or more cycles of side-by-side data. These 80 analysis participants recorded a total of 205 included cycles. They had an age range of 22–46 years at the start of the study, an average age of 32, and a median age of 32, with 95% CI 31.3–33.3. Fifty-three were from the United States, and 27 were from the United Kingdom.

As the study progressed, a "Training Set" of 93 cycles from 59 participants was used to develop, test, and iterate the SWS algorithm. Once the algorithm development was concluded, these data were set aside as a comparator for future recorded cycles. These 59 participants had an age range of 23–42 years at the start of the study, an average age of 33, and a median age of 33, with 95% CI 33.2–33.7. Thirty-nine Training Set participants were from the United States, and 20 were from the United Kingdom.

As users of the VS device, they were naturally biased towards a longer period of trying to conceive (TTC). For the 205 included cycles, the initial declared TTC time plus usage time for VS prior to the start of the study was calculated, with the demographic spread shown in **Table 1**.

The average cycle lengths for the 6–7 years group were increased by two cycles of 167 and 279 days in length, and the average cycle length for the >7 years group was increased by one cycle of 290 days in length. Although these long cycles might be regarded as outliers and excluded from similar analyses in previous studies, the authors felt it was important to fully reflect the study population results including long negative (anovulatory) cycles with temperature fluctuations, which might create FPs in the comparator methods, and the authors decided to therefore retain them for this analysis.

A Kruskal–Wallis test was performed to determine if median cycle length was significantly different for the nine time TTC groups.

The test revealed that the median cycle length was not significantly different ($H = 1.793$, $p = 0.877$), and hence, these groups were thus treated as one in all subsequent analyses.

2.2 Materials

The VS and SWS sensors are proprietary devices using off-the-shelf industrial components. Both comply with Thermometer Standards ASTM E1112 and ISO 80601-2-56:2017+A1:2020.

Independent laboratory testing of the production VS device in simulated physiological conditions was conducted for the purposes of the manufacturer's original FDA 510(k) submission in the United States and CE marking Technical File for certification as a class II medical device in Europe. This established a temperature measurement resolution (steps between each temperature value measured) of 0.003°C and an accuracy of 0.05°C for the VS. The SWS sensor uses an identical thermistor and circuitry to VS. SWS was tested in-house against VS under matching laboratory conditions to the original VS tests, and details were added to the regulatory Technical File for the product line in order to provide regulatory qualification for use in the study. A first production batch of the SWS sensor was produced.

The participants "wore" the SWS sensor under the armpit or on the underside of the wrist, and VS vaginally.

Data were downloaded from each sensor to a study version of the mobile device application each morning by the participants. Data were uploaded to an encrypted database, with a portal allowing the authors to assess the cycle results visually and with calculated results.

2.3 Algorithm Development

An initial "Training Set" of 93 cycles included in this study analysis was used to develop, test, and iterate the SWS algorithm. (Note: 2 additional cycles from 2 additional volunteers who produced positive results for VS were included for SWS development purposes originally but excluded from the study analysis due to having no confirmed cycle end date.)

The algorithm development examined three broad techniques with the representative overnight temperatures:

- a straight mathematical application of the "TOS" rule
- a moving average method that adds each new night's data to a "window" as the cycle progresses and drops the oldest night, enabling an assessment of temperature rise by means of the change from one window to the next window
- a "spring-loaded beam" method*, which uses all the previous recordings in the cycle with the aim of lowering the overall impact of sample noise (for example, due to changes in sensor position at its particular skin site, sensor contact, alcohol consumption, and sleep times), but maximizing the sensitivity to general trends. *Note: this is the authors' own nomenclature, which attempts to describe the way in which the algorithm works.

2.4 Data Analysis—Inclusion/Exclusion Criteria

Completed ovulatory and anovulatory cycles for which a cycle end date was logged by the participant with sufficient serial recordings for both sensors were included.

All cycles where a cycle end date was not logged by the participant were excluded.

2.5 Statistical Methods

Each cycle for each user was treated as an independent statistical unit as has been standard practice in clinical papers examining methods of determining ovulation in a study population.

Where confirmation of ovulation occurred by VS, the cycle was reported as a positive, and the VS reported date was deemed to be the date of ovulation. Where VS was unable to confirm ovulation, the cycle was reported as a negative (in other words anovulatory).

Two main methods were used for analyzing the resulting data and groups: a "Days Difference Method" and a "Threshold Method," as follows.

2.5.1 Days Difference Method

In order to provide an understanding of the statistical validity of the positive cycle results (those for which a day of ovulation was confirmed by VS) an analysis was conducted to show the difference between the day of ovulation as confirmed by TOS and SWS from the VS confirmed day of ovulation.

The analysis shows both the mean number of days difference (and therefore how far out the results are from VS) and also whether the results are biased towards earlier ovulation confirmation (negative days) or later ovulation confirmation (positive days) in the cycle for each of the TOS and SWS methods in comparison to VS.

Average Days difference (between TOS and SWS result compared with VS result) and the Standard Deviation of Days were calculated together with upper and lower 95% confidence bounds. An equal number of earlier and later days difference would of course produce a mean difference of zero; hence, it is important to assess the standard deviation alongside the mean days difference result to understand how far from the VS result each of the SW results was.

2.5.2 Threshold Method

Sensitivity, specificity, accuracy, positive predictive value (PPV), negative predictive value (NPV), and an F score were reported for each of the TOS and SWS methods compared with VS results for 2 windows: TP result within ±1 day of the VS result and a TP result within ±3 days of VS result. The ±1 day result was deemed to be a valid TP equivalent result to VS (as ovulation can in reality occur at any point within a 24-h period and a result is only available once in every 24-h period), and the ±3 days result was deemed to be a valid TP for the fertile window (3 days either side of the date of ovulation as determined by VS).

Results other than TPs were classified as follows:

FP = a positive (+ve) result outside of these windows; or SWS and/or TOS +ve, VS negative (−ve)

TN = concordance between TOS and/or SWS and VS that no ovulation took place

FN = SWS and/or TOS −ve, VS +ve

The following formulae were then used for calculations:

Sensitivity = TP/(TP + TN)

Specificity = TN/(FP + TN)

PPV = TP/(TP + FN)

NPV = TN/(TN + FN)

These calculations can be interpreted as follows.

The sensitivity shows the percentage of positive ovulations for TOS or SWS, which correctly matches with the VS positive results within the ±1 day and ±3 days thresholds. The specificity shows the percentage of absent ovulations (anovulatory cycles) for TOS or SWS, which correctly match with the VS negative (anovulatory) results. The PPV results show the percentage of detected ovulations TOS or SWS get right compared with VS within the ±1 day and ±3 days thresholds. The NPV is the percentage of absent ovulations (anovulatory cycles) TOS or SWS detect correctly compared with VS.

However, the most important overall results in developing SWS are measures of accuracy. The accuracy figure shows how many positive and absent ovulations (anovulatory results) TOS or SWS match the VS results and within the ±1 day and ±3 days thresholds for the ovulatory cycles. It is a good measure of accuracy for a binary diagnostic test when TPs and TNs are deemed to be most important. The F score provides a useful alternative measure of accuracy, which is calculated using the precision and recall of the test. The precision is the same as the PPV, and the recall is the same as sensitivity. The F score is more appropriate for unbalanced populations where FPs and FNs are felt to be more important.

The following formulae were used for these calculations:

Accuracy = (TP + TN)/(TP + FP + TN + FN)

F score = TP/TP + ½(FP + FN).

The upper and lower 95% CIs were calculated for the accuracy and F score results to provide the likely range of values around the population mean.

2.6 Data Group Analyses

2.6.1 Data Sets

From this initial data analysis carried out on the "Training Set," the final version of the "spring-loaded beam" algorithm

TABLE 2 | Cycle comparison by prior diagnosis group.

	PCOS	Hypothyroid	PCOS + Hypothyroid	Confirmed No Diagnosis
Number of cycles	106	7	6	53
Average cycle length	40.9	31.3	76.2	34.5
Median cycle length	32.0	32.0	35.0	29.0
Std Dev cycle length	30.1	4.0	104.8	16.6
Upper CI 95%	46.6	34.2	160.0	39.0
Lower CI 95%	35.2	28.3	−7.7	30.1

Note. PCOS, polycystic ovarian syndrome.

was chosen as the most accurate SWS method in comparison to VS and was fixed for the purposes of further testing. Participants were encouraged to continue side-by-side recordings using both the skin-worn and vaginal sensors, and some participants joined the study after the Training Set was frozen. The same analysis was then conducted for this "Additional Set" and then the "Combined Set" comprising all data to provide an overall assessment of the accuracy for the SWS as a marketable product.

The "Training Set" and "Additional Set" groups were tested for the significant difference by means of a Mann–Whitney test applied to the median cycle length.

The TOS and SWS methods themselves were then each tested for significant differences for their positive ovulation confirmation performance in comparison to VS between the "Training Set" and "Additional Set" groups. This was done by means of a Mann–Whitney test applied to the absolute Days Difference produced by the method outlined in **Section 2.5.1** between the TOS and VS confirmed day of ovulation and the SWS and VS confirmed day of ovulation, in each case ignoring the negative sign, as appropriate.

2.6.2 Skin Site Groups

A further analysis for "Arm" and "Wrist" groups was conducted. This analysis is labeled Skin Site. The Arm and Wrist groups were tested for the significant difference by means of a Mann–Whitney test applied to the median cycle length.

The TOS and SWS methods themselves were then each tested for significant differences for their positive ovulation confirmation performance in comparison to VS between the "Arm" and "Wrist" groups. This was done by means of a Mann–Whitney test applied to the absolute Days Difference produced by the method outlined in **Section 2.5.1** between the TOS and VS confirmed day of ovulation and the SWS and VS confirmed day of ovulation, in each case ignoring the negative sign, as appropriate.

2.6.3 Diagnosis and Ovulation Timing Groups

Seventy participants volunteered to provide information on their prior diagnoses at the start of the study and were grouped accordingly into the categories: "PCOS," "Hypothyroid," "PCOS and Hypothyroid," and "Confirmed No Diagnosis" diagnostic results. For the 172 included cycles from these 70 participants, the median cycle values were assessed as shown in **Table 2**.

A Kruskal–Wallis test revealed that the median cycle length was significantly different ($H = 7.676$, $p = 0.053$) between the four groups.

However, forty-three participants reported a prior diagnosis of PCOS, but only 2 reported hypothyroid diagnosis, and 4 reported both diagnoses. These smaller numbers produced anomalous results (e.g., both produced 100% accuracy for SWS in the ±3 days Threshold Analysis). As further described in the *Results* section, these four groups were therefore amalgamated into "Confirmed Prior Diagnosis" and "Confirmed No Diagnosis" groups and tested for the significant difference by means of a Mann–Whitney test applied to the median cycle length.

A further analysis was performed for VS confirmed positive results using the criteria of "Late Ovulation" as defined by all cycles, where the VS ovulation date was greater than 65% of the cycle length*. An analysis of "Early Ovulation" was also made using a <40% threshold, but only 6 cycles showed this characteristic. These cycles were therefore aggregated with those with ovulation confirmed between 40% and 65% of the cycle length in *Early + Normal Ovulation Timing* group for comparative purposes. This analysis is labeled "Diagnosis and Ovulation Timing." The "Early + Normal Ovulation Timing" and "Late Ovulation" groups were tested for the significant difference by means of a Mann–Whitney test applied to the median cycle length. *For example, day 20 ovulation in a 30-day cycle is 20/30 = 66.7% of the way through the cycle and therefore labeled as "late" for this analysis.

The TOS and SWS methods themselves were then each tested for significant difference for their positive ovulation confirmation performance in comparison to VS between each pair of groups: "Confirmed Prior Diagnosis" and "Confirmed No Diagnosis," and "Early + Normal Ovulation Timing" and "Late Ovulation." This was done by means of a Mann–Whitney test applied to the absolute Days Difference produced by the method outlined in **Section 2.5.1** between the TOS and VS confirmed day of ovulation and the SWS and VS confirmed day of ovulation (ignoring the negative sign, as appropriate).

2.6.4 Ovulation Prediction

Lastly, the analysis for the prediction of ovulation in a subsequent cycle was conducted. Only positive results are included (as predicting a negative result has no meaning in this context); hence, accuracy and specificity can be calculated by omitting TNs, along with PPV and F score using the calculations above.

TABLE 3 | Cycle comparison by data set groups.

	Combined set	Training set	Additional set
Total number of cycles	205	93	112
Average cycle length	39.1	44.8	34.3
Median cycle length	32.0	32.0	31.0
Std Dev cycle length	30.1	40.4	16.2
Upper CI 95%	43.2	53.0	37.3
Lower CI 95%	34.9	36.5	31.3
CI	4.1	8.2	3.0

The subsequent cycle ovulation prediction method has been adapted by VS and SWS algorithms and was applied manually to the data for TOS for the purposes of this study. The prediction method works as follows: when a user enters a new cycle start date, the median day of ovulation confirmation from the up to 12 previous ovulatory cycles (those for which an ovulation confirmation occurred) is used to predict the ovulation day for the cycle that has just started, with cycles containing no ovulation confirmation ignored. As the data are not continuous, the algorithm never picks a median ovulation day value that has not previously actually occurred, so in the case of an even number of previous ovulatory cycles, the higher of the two values which sit in the middle of the array is taken. This analysis is labeled "Subsequent Cycle Prediction."

As confirmation and prediction are separate algorithmic methods, the authors felt it was important that in order to judge how accurately TOS and SWS methods predict ovulation as confirmed by the VS result for a subsequent cycle, VS was also examined for its own ability to predict ovulation compared with its separate confirmed ovulation date for the subsequent cycle. Both TOS and SWS prediction compared with VS subsequent cycle confirmation and VS prediction compared with VS subsequent cycle confirmation are therefore included.

The TOS and SWS methods themselves were each tested for significant differences for their positive ovulation prediction performance in comparison to VS between each pair of groups: "Confirmed Prior Diagnosis" and "Confirmed No Diagnosis," and "Early + Normal Ovulation Timing" and "Late Ovulation." This was done by means of a Mann–Whitney test applied to the absolute Days Difference produced by the method outlined in **Section 2.5.1** between the TOS and VS predicted day of ovulation and the SWS and VS predicted day of ovulation (ignoring the negative sign, as appropriate).

3 RESULTS

3.1 Data Sets

As outlined in **Table 3**, median cycle lengths in the Training Set and Additional Set groups were 32 and 31 days, respectively. However, the distributions in the two groups for which cycle lengths could be determined differed significantly (Mann–Whitney U = 4,285.5, n1 = 93, n2 = 112, p = 0.0291), and therefore, for the purpose of this analysis, this may account for a difference in results between the two groups.

Table 4 presents the comparison of absolute days difference between the TOS and SWS methods compared with VS for the Training, Additional, and Combined Data Sets. Participants were able to belong to both of these groups, as the Additional Set represented a follow-on data gathering. The mean days difference for both methods is a negative number indicating that, on average, both TOS and SWS methods are confirming ovulation earlier in the cycle than VS. The Training Set was intended to provide optimal results against the VS method, which would then allow SWS to perform consistently in a larger data set as the SWS product use increases. Notwithstanding the statistical difference in cycle lengths shown by the Mann–Whitney test, it is clear from the standard deviation results that there is a wider spread in the day of ovulation results obtained by TOS and SWS compared with VS in the Additional Set than the Training Set, although the mean difference is actually closer to the SWS result in the Additional Set for both methods.

Table 5 presents the Threshold Method analysis for the Training Set and Additional Set data, with the Combined Set of both data presented to provide complete results for the ±1 day and ±3 days thresholds compared with VS results.

The ovulation confirmation performance of Days Difference distributions in the Training Set and Additional Set groups did not differ significantly for either TOS (p = 0.1948) or SWS (p = 0.3132), and therefore, despite the significant difference in median cycle lengths between the two groups, it is valid to compare the Days Difference and Threshold results for TOS and SWS between the two groups.

With an accuracy of 65%, SWS does not appear to be capable of accurate confirmation of the exact day of ovulation (when compared with the VS method), although it is shown by these data to be more sensitive than TOS (91% vs. 79%) for that ±1 day threshold. It should be noted that the accuracy of the TOS method is higher than that of the SWS for the ±1 day threshold but lower than that of the SWS for the ±3 days threshold. SWS has an accuracy of 90% and an F score of 0.93 for the Combined Group for the ±3 days threshold. The accuracy drops for ±3 days for the SWS method in the Additional Set. Given these populations are probably unbalanced, the F score may provide a better indicator of the TOS and SWS accuracy between the groups.

3.2 Skin Site

As outlined in **Table 6**, median cycle lengths in the Arm and Wrist groups were each 32 days. The distributions in the two groups did not differ significantly (Mann–Whitney U = 3,829.5, n1 = 153, n2 = 51, p = 0.7906). Median cycle lengths are therefore unlikely to account for any differences in results between the two groups.

Table 7 presents the comparison of absolute days difference between the TOS and SWS methods compared with VS for the Arm and Wrist Modalities. Each participant was only able to belong to one of these distinct groups. The TOS method appears to have a large negative mean days difference

TABLE 4 | Days difference between TOS and SWS confirmed day of ovulation for ovulatory cycles compared with VS positive cycles for data sets.

	Combined set		Training set		Additional set	
+ve VS cycles in each group	158		75		83	
Participants with +ve VS cycles in each group	70		51		43	
Method	TOS	SWS	TOS	SWS	TOS	SWS
Mean days difference compared with VS	−3.26	−1.51	−4.05	−1.29	−2.52	−1.71
Standard deviation days compared with VS	1.93	1.83	1.31	1.05	1.44	1.51
Upper CI 95%	−2.96	−1.23	−3.76	−1.06	−2.21	−1.39
Lower CI 95%	−3.56	−1.80	−4.35	−1.53	−2.83	−2.04

Note. A single participant was able to take part in both the Training Set and the Additional Set; hence, each participant was able to have one or more cycles, which contributed to both groups, and the total number of participants added together for those two groups in the table above is therefore more than the 70 total participants with positive cycles.

TABLE 5 | Threshold method results for TOS and SWS compared with VS for data sets.

	Combined set				Training set				Additional set			
+ve VS cycles	158				75				83			
−ve VS cycles	47				18				29			
Total cycles	205				93				112			
Participants	80				60				55			
Thresholds	±1 day		±3 days		±1 day		±3 days		±1 day		±3 days	
Method	TOS	SWS	TOS	SWS	TOS	SWS	TOS	SWS	TOS	SWS	TOS	SWS
TP	86	88	119	140	43	47	55	71	43	41	64	69
FP	53	63	20	11	23	26	11	2	30	37	9	9
TN	43	45	43	45	16	18	16	18	27	27	27	27
FN	23	9	23	9	11	2	11	2	12	7	12	7
Total cycles	205	205	205	205	93	93	93	93	112	112	112	112
Sensitivity	79%	91%	84%	94%	80%	96%	83%	97%	78%	85%	84%	91%
Specificity	45%	42%	68%	80%	41%	41%	59%	90%	47%	42%	75%	75%
PPV	62%	58%	86%	93%	65%	64%	83%	97%	59%	53%	88%	88%
NPV	65%	83%	65%	83%	59%	90%	59%	90%	69%	79%	69%	79%
Accuracy	62.9%	64.9%	79.0%	90.2%	63.4%	69.9%	76.3%	95.7%	62.5%	60.7%	81.3%	85.7%
Upper CI 95%	69.6%	71.4%	84.4%	93.9%	73.2%	79.0%	84.5%	98.8%	71.5%	69.8%	88.0%	91.6%
Lower CI 95%	55.9%	57.9%	72.8%	85.3%	52.8%	59.5%	66.4%	89.4%	52.9%	51.0%	72.8%	77.8%
F score	0.69	0.71	0.85	0.93	0.72	0.77	0.83	0.97	0.67	0.65	0.86	0.90
Upper CI 95%	0.77	0.79	0.90	0.97	0.83	0.87	0.91	1.00	0.78	0.77	0.93	0.95
Lower CI 95%	0.60	0.62	0.78	0.88	0.59	0.65	0.72	0.90	0.54	0.52	0.76	0.81

Note. A single participant was able to take part in both the Training Set and the Additional Set; hence, each participant was able to have one or more cycles, which contributed to both groups, and the total number of participants added together for those two groups in the table above is therefore more than the 80 total participants with positive and negative cycles. TP, true positive; FP, false positive; TN, true negative; FN, false negative; PPV, positive predictive value; NPV, negative predictive value.

TABLE 6 | Cycle comparison by skin site groups.

	Arm	Wrist
Number of cycles	154	51
Average cycle length	39.0	39.3
Median cycle length	32.0	32.0
Std Dev cycle length	28.0	36.1
Upper CI 95%	43.4	49.2
Lower CI 95%	34.5	29.4

compared with VS for the Arm Site in comparison to the SWS results for both Skin Site groups and the TOS Method for the Wrist Site Group.

Table 8 presents the Threshold Method analysis for the Arm and Wrist Skin Site groups.

The ovulation confirmation performance of Days Difference distributions in the Arm and Wrist groups did not differ significantly for either TOS ($p = 0.2647$) or SWS ($p = 0.0953$), and therefore Mann–Whitney tests on both median cycle length and absolute days difference would indicate that it is valid to compare the Days Difference and Threshold results for TOS and SWS between the two groups.

As with the Training and Additional Data Set results, SWS produces a higher accuracy for both groups than TOS. Given the lack of statistical significance between the two groups, it would appear that the Wrist Site provides a higher accuracy for SWS than the Arm Site in terms of both the accuracy and F score results (±3 days threshold accuracy 94% and F score 0.96 Wrist, accuracy 89% and F score 0.92 Arm).

3.3 Diagnosis and Ovulation Timing

Eight participants accounting for 33 cycles provided no data on prior Diagnosis and were excluded from the Diagnosis analysis. Forty-seven anovulatory cycles were excluded from the Ovulation Timing analysis.

TABLE 7 | Days difference between TOS and SWS confirmed day of ovulation for ovulatory cycles compared with VS positive cycles for skin site.

	Arm		Wrist	
+ve VS cycles in each group	118		40	
Participants with +ve VS cycles in each group	51		20	
Method	TOS	SWS	TOS	SWS
Mean days difference compared with VS	−3.78	−1.65	−1.69	−1.10
Standard deviation days compared with VS	1.70	1.66	0.94	0.79
Upper CI 95%	−3.47	−1.35	−1.40	−0.85
Lower CI 95%	−4.09	−1.95	−1.98	−1.35

TABLE 8 | Threshold method results for TOS and SWS compared with VS for skin site.

	Arm				Wrist			
+ve VS cycles	118				40			
−ve VS cycles	36				11			
Total cycles	154				51			
Participants	60				20			
Thresholds	±1 day		±3 days		±1 day		±3 days	
Method	TOS	SWS	TOS	SWS	TOS	SWS	TOS	SWS
TP	61	61	87	103	25	27	32	37
FP	41	52	15	10	12	11	5	1
TN	33	34	33	34	10	11	10	11
FN	19	7	19	7	4	2	4	2
Total cycles	154	154	154	154	51	51	51	51
Sensitivity	76%	90%	82%	94%	86%	93%	89%	95%
Specificity	45%	40%	69%	77%	45%	50%	67%	92%
PPV	60%	54%	85%	91%	68%	71%	86%	97%
NPV	63%	83%	63%	83%	71%	85%	71%	85%
Accuracy	61.0%	61.7%	77.9%	89.0%	68.6%	74.5%	82.4%	94.1%
Upper CI 95%	68.8%	69.4%	84.2%	93.4%	80.9%	85.7%	91.6%	98.8%
Lower CI 95%	52.9%	53.5%	70.5%	82.9%	54.1%	60.4%	69.1%	83.8%
F score	0.67	0.67	0.84	0.92	0.76	0.81	0.88	0.96
Upper CI 95%	0.77	0.77	0.90	0.97	0.89	0.92	0.96	1.00
Lower CI 95%	0.56	0.57	0.75	0.86	0.58	0.63	0.73	0.84

Note. TP, true positive; FP, false positive; TN, true negative; FN, false negative; PPV, positive predictive value; NPV, negative predictive value.

A total of 22 participants with Confirmed Prior Diagnosis recorded one or more ovulatory cycles with Late Ovulation, and a further 11 recorded only anovulatory cycles. A further 10 participants with Confirmed No Diagnosis or who did not provide an answer on prior diagnosis recorded one or more cycles with Late Ovulation, and a final additional 2 participants with Confirmed No Diagnosis or did not provide an answer on prior diagnosis recorded only anovulatory cycles. These total 45 participants could each be regarded as having potential ovulatory dysfunction. However, 17 participants with Confirmed Prior Diagnosis recorded only Early + Normal Ovulation Cycles, so although these participants might be expected to exhibit signs of ovulatory dysfunction, they were not shown to do so in this study. These participants accounted for 100 cycles with signs of ovulatory dysfunction (53 Late Ovulation and 47 anovulatory cycles), and a further 54 cycles with Short + Normal Ovulation Timing recorded by participants indicating a Confirmed Prior Diagnosis. With over half the 80 participants and just under half the 205 cycles in the study showing signs of ovulatory dysfunction, the population can be expected to record less accurate results than in a population with no diagnosis, or normal ovulation timing, i.e., those without expected ovulatory dysfunction. These analyses in this section seek to examine the differences between these groups.

The association between Diagnosis and Ovulation Timing cycles is shown in **Figure 1**, demonstrating that although Late Ovulation was more prevalent for 43% of those who declared a prior diagnosis of PCOS, it still occurred in over ¼ cycles for those who declared no prior diagnosis associated with ovulatory dysfunction. No comment can be made on the ovulation timing splits for the Hypothyroid and PCOS and Hypothyroid groups due to the small sample sizes.

Table 9 presents the cycle comparison for the Diagnosis and Ovulation Timing Groups.

Median cycle lengths in the Confirmed Prior Diagnosis and Confirmed No Diagnosis groups were 33 and 29 days, respectively. The distributions in the two groups differed significantly (Mann–Whitney U = 2,405.5, n1 = 119, n2 = 53, p = 0.0131), and therefore for the purpose of this analysis, the differences in results between the two groups may be a result of that statistical difference in median cycle lengths for the group populations.

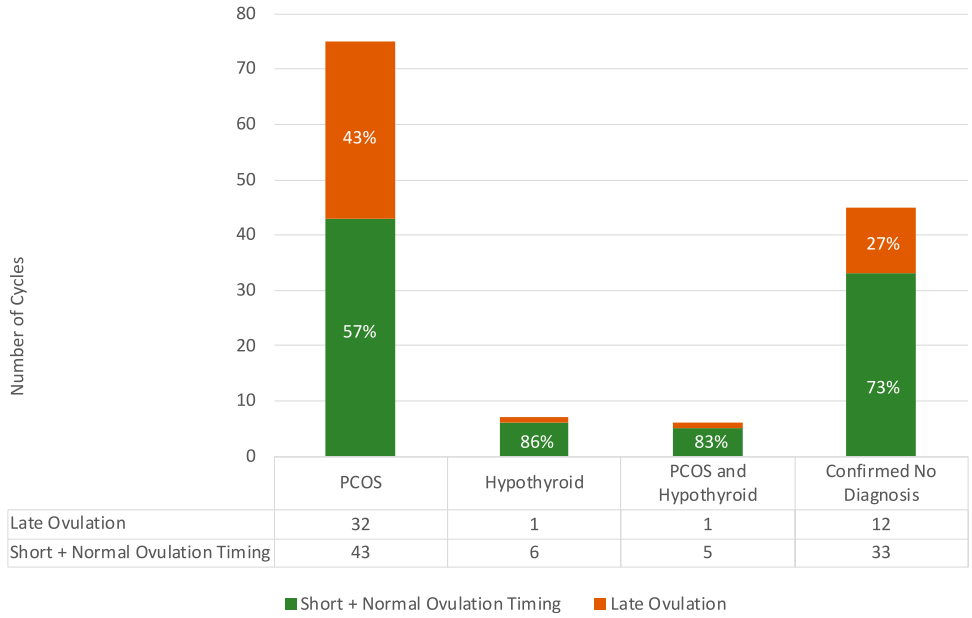

FIGURE 1 | Relationship between ovulation timing and confirmed diagnosis in the study population with numbers of cycles per category tabulated.

TABLE 9 | Cycle comparison by diagnosis and ovulation timing groups.

	Confirmed prior diagnosis	Confirmed No diagnosis	Late ovulation	Early + normal ovulation timing
Number of cycles	119	53	53	105
Average cycle length	42.1	34.5	38.5	34.4
Median cycle length	33.0	29.0	36.0	30.0
Std Dev cycle length	34.5	17.1	18.3	25.6
Upper CI 95%	48.3	39.1	43.4	39.3
Lower CI 95%	35.9	29.9	33.6	29.5
CI	6.2	4.6	4.9	4.9

TABLE 10 | Days difference between TOS and SWS confirmed day of ovulation for ovulatory cycles compared with VS positive cycles for diagnosis and ovulation timing groups.

	Confirmed prior diagnosis		Confirmed No diagnosis		Late ovulation		Early + normal ovulation timing	
+ve VS cycles in each group	88		45		53		105	
Participants with +VS cycles in each group	40		21		37		53	
Method	TOS	SWS	TOS	SWS	TOS	SWS	TOS	SWS
Mean days difference compared with VS	−2.98	−1.24	−3.45	−2.93	−7.09	−3.26	−1.28	−0.63
Standard deviation days compared with VS	1.35	1.45	0.98	0.73	0.84	1.02	1.75	1.53
Upper CI 95%	−2.69	−0.93	−3.17	−2.72	−6.87	−2.99	−0.95	−0.34
Lower CI 95%	−3.26	−1.54	−3.74	−3.15	−7.32	−3.54	−1.62	−0.92

Median cycle lengths in the Late Ovulation and Early + Normal Ovulation Timing groups were 36 and 30 days, respectively. The distributions in the two groups for which cycle lengths could be determined differed highly significantly (Mann–Whitney U = 1,470.5, n1 = 53, n2 = 105, $p < 0.001$), and therefore for the purpose of this analysis, the differences in results between the two groups may be a result of that statistical difference in median cycle lengths for the group populations.

Table 10 presents the comparison of absolute days difference between the TOS and SWS methods compared with VS for those participants for the Diagnosis and Ovulation Timing groups.

TABLE 11 | Threshold method results for TOS and SWS compared with VS for diagnosis and ovulation timing groups.

	Confirmed prior diagnosis				Confirmed No diagnosis				Late ovulation				Early + normal ovulation timing			
+ve VS cycles	88				45				53				105			
–ve VS cycles	31				8				0				0			
Total cycles	119				53				53				105			
Participants	50				22				37				53			
Thresholds	±1 day		±3 days		±1 day		±3 days		±1 day		±3 days		±1 day		±3 days	
Method	TOS	SWS	TOS	SWS	TOS	SWS	TOS	SWS	TOS	SWS	TOS	SWS	TOS	SWS	TOS	SWS
TP	49	48	64	76	24	27	36	41	28	31	39	46	58	57	80	94
FP	27	35	12	7	15	15	3	1	14	18	3	3	35	43	13	6
TN	28	30	28	30	8	8	8	8								
FN	15	6	15	6	6	3	6	3	11	4	11	4	12	5	12	5
Total cycles	119	119	119	119	53	53	53	53	53	53	53	53	105	105	105	105
Sensitivity	77%	89%	81%	93%	80%	90%	86%	93%	72%	89%	78%	92%	83%	92%	87%	95%
Specificity	51%	46%	70%	81%	35%	35%	73%	89%								
PPV	64%	58%	84%	92%	62%	64%	92%	98%	67%	63%	93%	94%	62%	57%	86%	94%
NPV	65%	83%	65%	83%	57%	73%	57%	73%								
Accuracy	64.7%	65.5%	77.3%	89.1%	60.4%	66.0%	83.0%	92.5%	52.8%	58.5%	73.6%	86.8%	55.2%	54.3%	76.2%	89.5%
Upper CI 95%	73.2%	74.0%	84.5%	94.1%	73.5%	78.5%	91.9%	97.9%	66.7%	71.9%	84.7%	94.5%	65.0%	64.0%	84.0%	94.7%
Lower CI 95%	55.4%	56.3%	68.7%	82.0%	46.0%	51.7%	70.2%	81.8%	38.6%	44.1%	59.7%	74.7%	45.2%	44.3%	66.9%	82.0%
F score	0.70	0.70	0.83	0.92	0.70	0.75	0.89	0.95	0.69	0.74	0.85	0.93	0.71	0.70	0.86	0.94
Upper CI 95%	0.80	0.81	0.90	0.97	0.84	0.88	0.97	0.99	0.83	0.86	0.94	0.98	0.81	0.80	0.93	0.98
Lower CI 95%	0.58	0.58	0.72	0.84	0.52	0.58	0.75	0.84	0.53	0.58	0.71	0.82	0.60	0.59	0.78	0.88

Note. TP, true positive; FP, false positive; TN, true negative; FN, false negative; PPV, positive predictive value; NPV, negative predictive value.

Each participant was only able to belong to one of the Confirmed Prior Diagnosis (by answering the study survey indicating PCOS, PCOS, and Hypothyroid, or Hypothyroid) or Confirmed No Diagnosis group. The spread of results as indicated by the standard deviation of days appears to be larger in the Confirmed Prior Diagnosis group. Despite the mean days difference being higher in the Confirmed No Diagnosis group, there appears to be a closer overall agreement between TOS and SWS with VS as indicated by the lower standard deviation of days.

For absolute days difference between the TOS and SWS methods compared with VS for the Late Ovulation and Early + Normal Ovulation Timing groups, each participant was able in theory to contribute cycles to both groups, so there is a degree of crossover between the population despite exhibiting different cycle characteristics in order to contribute to one or other group. The spread of results as indicated by the standard deviation of days appears to be lower in the Late Ovulation group, whereas the negative mean days difference is higher in this group, indicating closer overall agreement between TOS and SWS with VS for the Late Ovulation group but a larger overall shift to earlier ovulation confirmation by TOS and SWS.

Table 11 presents the Threshold Method analysis for the Diagnosis and Ovulation Timing groups.

The ovulation confirmation performance of Days Difference distributions in the Confirmed Prior Diagnosis and Confirmed No Diagnosis groups did not differ significantly for either TOS (p = 0.6518) or SWS (p = 0.3182), and therefore, despite the significant difference in median cycle lengths between the two groups, it is valid to compare the Days Difference and Threshold results for TOS and SWS between the two groups.

The ovulation confirmation performance of Days Difference distributions in the Late Ovulation and Confirmed Early + Normal Ovulation Timing groups did not differ significantly for either TOS (p = 1.9551) or SWS (p = 0.3601), and therefore, despite the significant difference in median cycle lengths between the two groups, it is valid to compare the Days Difference and Threshold results for TOS and SWS between the two groups.

The relative number of TN results in the Confirmed Prior Diagnosis group (24% of all cycles for TOS, 25% of all cycles for SWS) has resulted in a similar accuracy for the ±1 day threshold for this group (65% TOS, 66% SWS) compared with the Confirmed No Diagnosis group (60% TOS, 66% SWS) despite the difference in Standard Deviation days (SD) results for positive ovulations between the two groups as shown in **Table 10**. The relative number of FN results in the Confirmed No Diagnosis group (11% of all cycles for TOS and 6% of all cycles for SWS) accounts for the difference in the accuracy between the two methods for ±1 day threshold in the Confirmed No Diagnosis group. The accuracy for both groups is noticeably higher for SWS for the ±3 days Threshold.

No TN results are presented for the Ovulation Timing group analysis, as an ovulation confirmation has to take place in order to determine ovulation timing. FNs are still possible where the comparator method (TOS or SWS) provides a Negative result when VS showed a Positive result.

The relative number of FN results in the Late Ovulation group (21% of all cycles for TOS and 8% of all cycles for SWS) has created a disparity in the accuracy for the ±1 day threshold between TOS and SWS (53% TOS and 59% SWS) in comparison with the Standard Deviation days (SD) results for positive ovulations only of 0.84 TOS and 1.02 SWS. On the other hand, the same relative total FP and FN results in the Early and Normal Ovulation group (45% for both methods) have results in a similar accuracy with 55% TOS and 54% SWS for the ±1 day threshold vs. SD 1.75 TOS and 1.53 SWS. The accuracy

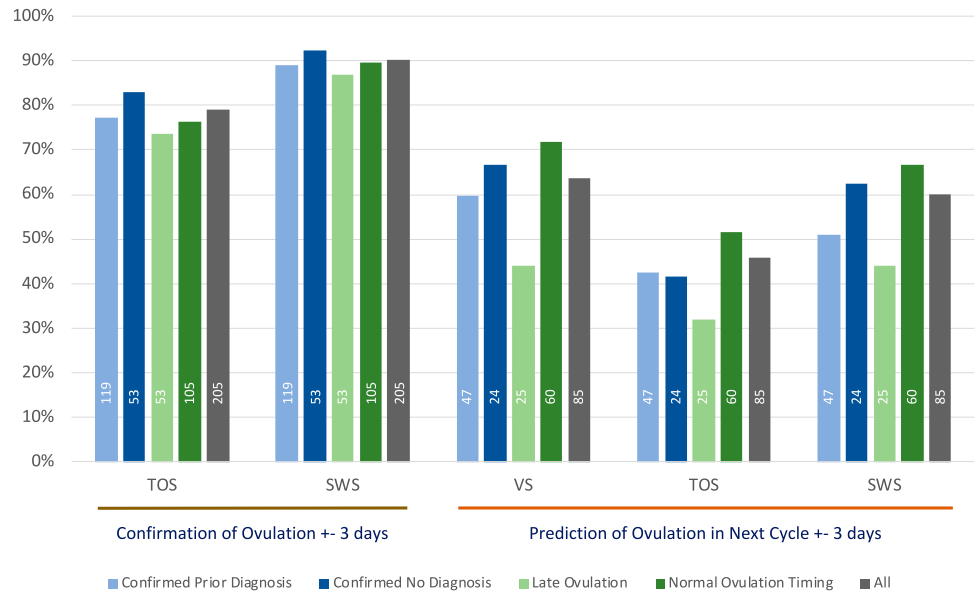

FIGURE 2 | The ±3 days % accuracy of confirmation of ovulation and prediction of ovulation in subsequent cycles using median day of ovulation prediction method, annotated with numbers of cycles contributing to each analysis.

for both groups is markedly higher for SWS for the ±3 days Threshold.

3.4 Subsequent Cycle Prediction

Thirty-seven participants had 85 serial positive cycles, which could be included in the prediction analysis.

The percentage accuracy for predicting ovulation in a subsequent cycle within ±3 days is shown in **Figure 2**. The figure repeats the confirmation accuracy as outlined earlier in **Section 3** and then shows the ability of each method to predict ovulation in each subsequent cycle with the algorithm technique detailed in **Section 2.6.4**. As VS is used as the gold standard in this study for confirmation, it is important to understand how well it is capable of predicting ovulation on the basis of its own data in prior cycles; hence, the prediction accuracy of VS compared with the separate VS subsequent cycle ovulation confirmation is included.

As outlined in **Section 3.3**, at least half the population in this study can be regarded as having a degree of ovulatory dysfunction. As for the expected lower accuracy with confirmation of ovulation, it would likewise be expected to produce lower accuracy for predicting ovulation by the method outlined in **Section 2.6.4**. The analyses in this section seek to further examine the groups that have signs of ovulatory dysfunction against those with no signs of ovulatory dysfunction.

The total number of cycles that contributed to each of the VS, TOS, and SWS methods for each group summarized in **Figure 2** is shown as a legend within each relevant bar.

Table 12 outlines the results for the days difference in the prediction of ovulation using VS (against itself), TOS, and SWS previous cycle data for data in the study when compared to the VS result for a subsequent cycle. The analysis includes all data, and then the data are separated for Diagnosis and Ovulation Timing groups.

The VS, TOS, and SWS methods for all data together have a high standard deviation for prediction, which is the result of very different actual ovulation results in subsequent cycles.

There is a noticeably higher days standard deviation for the Confirmed Prior Diagnosis group than the Confirmed No Diagnosis group.

There is a noticeably high standard deviation for the Late Ovulation group for all three methods.

Table 13 presents the Threshold Method analysis for the ovulation prediction based on previous cycles for all data, and Diagnosis and Ovulation Timing groups.

As VS confirmation can only be for a day of ovulation in a positive cycle, there are no TN results; hence, only sensitivity and PPV results are available. The result can still be an FN for a comparator method (TOS or SWS) if it is unable to predict a positive result because the median value for the day of ovulation in previous cycles cannot be calculated due to anovulatory results, but VS is capable of predicting ovulation based on previous cycle results. VS and SWS data produce similar accuracy and F scores, with both accuracy measures dragged down for TOS by the number of FNs.

The ovulation prediction performance of Days Difference distributions in the Confirmed Prior Diagnosis and Confirmed No Diagnosis groups did not differ significantly for VS ($p = 0.4534$), TOS ($p = 0.2778$), or SWS ($p = 0.5226$); and therefore, it is valid to compare the Days Difference and Threshold results for TOS and SWS between the two groups.

VS and SWS methods produce reduced accuracy for the Confirmed Prior Diagnosis group, which bears out the higher

TABLE 12 | Days difference between VS confirmed day of ovulation for ovulatory cycles compared with predicted day of ovulation by VS, TOS, and SWS using median day of ovulation prediction method for all data, and diagnosis and ovulation timing groups.

	All data			Confirmed prior diagnosis			Confirmed No diagnosis			Late ovulation			Early + normal ovulation timing		
+ve subsequent VS Cycles	85			47			24			25			60		
Participants with +ve subsequent cycles in each group	37			19			13			19			28		
Method	VS	TOS	SWS	VS	TOS	SWS	VS	TOS	SWS	VS	TOS	SWS	VS	TOS	SWS
Mean days difference compared with VS	−0.34	−1.74	−0.66	−0.34	−2.20	−0.94	−1.25	−1.85	−0.96	−4.80	−5.50	−4.88	1.52	−0.15	1.10
Standard deviation days compared with VS	7.22	7.20	7.43	9.00	9.03	9.27	4.46	4.35	4.76	11.06	11.07	11.36	3.52	4.15	3.92
Upper CI 95%	1.19	−0.21	0.92	2.23	0.38	1.71	0.53	−0.11	0.95	−0.46	−1.16	−0.43	2.41	0.90	2.09
Lower CI 95%	−1.88	−3.27	−2.24	−2.91	−4.78	−3.59	−3.03	−3.59	−2.86	−9.14	−9.84	−9.33	0.62	−1.20	0.11

TABLE 13 | Threshold method results for VS, TOS, and SWS ovulation prediction compared with VS subsequent cycle results using median day of ovulation prediction method for all data, and diagnosis and ovulation timing groups.

	All data			Confirmed prior diagnosis			Confirmed No diagnosis			Late ovulation			Early + normal ovulation timing		
+ve subsequent VS cycles	85			47			24			25			60		
Participants with +ve subsequent cycles in each group	37			19			13			19			28		
Threshold	±3 days			±3 days			±3 days			±3 days			±3 days		
Method	VS	TOS	SWS	VS	TOS	SWS	VS	TOS	SWS	VS	TOS	SWS	VS	TOS	SWS
TP	54	39	51	28	20	24	16	10	15	11	8	11	43	31	40
FP	31	35	34	19	20	23	8	10	9	14	14	14	17	21	20
TN	0	0	0	0	0	0	0	0	0	0	0	0	0	0	0
FN	0	11	0	0	7	0	0	4	0	0	3	0	0	8	0
Total cycles	85	85	85	47	47	47	24	24	24	25	25	25	60	60	60
Sensitivity	100%	78%	100%	100%	74%	100%	100%	71%	100%	100%	73%	100%	100%	79%	100%
PPV	64%	53%	60%	60%	50%	51%	67%	50%	63%	44%	36%	44%	72%	60%	67%
Accuracy	63.5%	45.9%	60.0%	59.6%	42.6%	51.1%	66.7%	41.7%	62.5%	44.0%	32.0%	44.0%	71.7%	51.7%	66.7%
Upper CI 95%	73.7%	57.0%	70.5%	73.6%	57.8%	65.9%	84.4%	63.4%	81.2%	65.1%	53.5%	65.1%	82.5%	64.8%	78.3%
Lower CI 95%	52.4%	35.0%	48.8%	44.3%	28.3%	36.1%	44.7%	22.1%	40.6%	24.4%	14.9%	24.4%	58.6%	38.4%	53.3%
F score	0.78	0.63	0.75	0.75	0.60	0.68	0.80	0.59	0.77	0.61	0.48	0.61	0.83	0.68	0.80
Upper CI 95%	0.87	0.75	0.85	0.87	0.76	0.82	0.94	0.82	0.93	0.83	0.74	0.83	0.92	0.81	0.90
Lower CI 95%	0.66	0.50	0.63	0.58	0.41	0.50	0.56	0.33	0.53	0.36	0.24	0.36	0.71	0.53	0.66

Note. TP, true positive; FP, false positive; TN, true negative; FN, false negative; PPV, positive predictive value; NPV, negative predictive value.

standard days deviation results for that group presented in **Table 12**, whereas the TOS method produced very similar accuracy between the two groups.

The ovulation prediction performance of Days Difference distributions in the Late Ovulation and Confirmed Early + Normal Ovulation Timing groups differed significantly for VS ($p = 0.006$) and TOS ($p = 0.0151$) but did not differ significantly for SWS ($p = 0.0817$), and therefore, although it may be valid to compare the Days Difference and Threshold results for TOS and SWS between the two groups for SWS, caution should be exercised in doing so for VS and TOS.

The accuracy and F scores are very low in the Late Ovulation group, although VS and SWS produce exactly the same results. VS produces the highest accuracy for the Early + Normal Ovulation Timing group, but the accuracy scores for TOS are lower.

4 DISCUSSION

4.1 Introduction

It should be remembered before discussing the results that by recording temperature intravaginally, VS is measuring a different temperature curve from SWS. The hypothesis for this study based on previous research (Papaioannou et al., 2013a; Papaioannou et al., 2013b; Papaioannou et al., 2014; Regidor et al., 2018) is that VS provides the most accurate representation of the thermogenic effect of progesterone released during ovulation and can hence be treated as a "gold standard" ovulation result for each side-by-side measured cycle for comparative purposes with the TOS and SWS methods.

In general, for all the group analyses, the high FN rate for TOS was largely the result of strict application of the method rules, with insufficient data points available to determine three high

values in a window of six consecutive days. The higher FP rate for the SWS method vs. TOS for ±1 day but a lower rate for ±3 days shows the "spring-loaded beam" algorithm employed by SWS is probably better at adjusting for the overall bi-phasic pattern around the ovulation window than for producing exact agreement with VS.

For all group analyses, the Days Difference Method mean days difference results show that TOS and SWS confirmations of ovulation are earlier in the cycle than VS. TOS results are generally earlier than SWS, but the standard deviation of most analyses show a lower variability between the TOS and SWS results than the mean days difference would suggest alone.

4.2 Data Set Results

As would be expected, the Training Data Set produced higher SWS accuracy for both ±1 day and ±3 days analyses. SWS outperforms TOS by all measures in comparison to the VS results, but the TOS accuracy was very similar for Training and Additional data sets, which may indicate that the SWS algorithm was "over-tuned" to the Training Set. As can also be expected, the F score measure varied less than the accuracy measure between the three sets.

It should be noted that the Mann–Whitney test revealed a significant difference between the Training Set and Additional Set groups (p = 0.0291), and this might indicate a greater span of median cycle lengths and hence cycle variability in the Additional Data Set group. This may be responsible for the poorer performance of the algorithm with the Additional Data Set group, although the individual Mann–Whitney tests on ovulation confirmation would indicate no significant difference in performance between the Training Set and Additional Set groups using either the TOS (p = 0.1948) or SWS (p = 0.3132) methods.

4.3 Skin Site Results

As discussed in the *Introduction*, few papers have established the accuracy of skin-based temperature measurement for the determination of the date of ovulation, and to the authors' knowledge by means of a literature search conducted for this paper, none to date has provided a comparative assessment of the same device in differing skin sites for this purpose, although a number of papers have attempted to establish the best approach to skin temperature monitoring as detailed in the literature review by MacRae et al. (MacRae et al., 2018).

Intuitively, by offering a greater skin contact surface area that is more shielded from ambient temperature, the arm site should provide a more consistent temperature result from night to night and therefore a more accurate measure of ovulation than measuring on the underside of the wrist. However, in this analysis, the Wrist site outperformed the Arm for accuracy as measured by the accuracy and F score. This may be due to better contact due to the wristband vs. the armband design or that the Wrist participants complied more closely with the protocol for wearing the sensor on the wrist. MacRae et al. (2018) pointed out that the more insulated the temperature sensor is from the ambient temperature (as is the case for the Arm site of SWS vs. the Wrist site), the higher the resulting measured temperature is likely to be, but it is likely these conditions remain relatively constant from night to night for an individual user and hence do no significantly affect a system where relative changes in temperature over time rather than absolute temperature is the key to functionality.

However, the smaller sample size in the Wrist group may have nonetheless biased the results in a way that did not affect median cycle length or proportion of +ve and −ve results, as there are noticeably fewer SWS FP and FN results (6% of cycles) for the Wrist group compared with the Arm group (11% of cycles) for the ±3 days threshold. Likewise, the TOS FP and FN results (6% of cycles) for the Wrist group compared with the Arm Group (22% of cycles) explain the larger discrepancy in its accuracy. Nonetheless, the lack of significant difference between the groups as shown by the Mann–Whitney test combined with the similar results between the modalities is encouraging, as it indicates that SWS can be made to work equally well on either the Wrist or Arm, within the precision of this study. It follows that by applying similar sensor construction and algorithm techniques, other systems could also be made to work as well for the underside of the wrist as well as the arm. Some existing products use the top side of the wrist for temperature measurement (Goodale et al., 2019; Zhu et al., 2021), and the results from this study cannot therefore be used to draw an inference of potential accuracy for those systems.

4.4 Diagnosis and Ovulation Timing Results

A number of clinically useful observations can be drawn from the analysis of prior Diagnosis and Ovulation Timing.

1) *For this study population*, 28% of participants who confirmed a prior diagnosis associated with ovulatory dysfunction (17 out of 61 participants) recorded cycles that only showed Early + Normal Ovulation Timing. This is an unexpected result and indicates some of the challenges in trying to understand what represents a "normal" patient.
2) Late Ovulation is prevalent in this study population, and given 25% of cycles recorded by participants indicating Confirmed No Diagnosis showed Late Ovulation, it is possible that ovulatory dysfunction goes undetected. This reflects previous clinical findings (Lenton et al., 1984) and explains perhaps why the use of prior cycle results for the prediction of ovulation in subsequent cycles is generally problematic.
3) Although the usefulness of knowing the exact date of ovulation in a prior cycle can be questioned, it is generally accepted that better knowledge of the fertile window provides a higher chance of conception and that the more accurately this is known, the higher the chance of conception (Wilcox et al., 1995; Dunson et al., 2002).
4) With an accuracy of 90% and F score of 0.93 for the ±3 days threshold, SWS appears to be a more accurate method for the confirmation of the fertile window than previously studied methods of oral temperature (Freundl et al., 2003) (accuracy 78%, F score 0.88) and skin temperature (Goodale et al., 2019; Zhu et al., 2021) (F score of 0.78) in determining the fertile window. However, comparison of these results with other

studies should be treated with caution, as it is carried out on a distinct user population with a distinct device and algorithm.

5) The detection of the absence of ovulation is perhaps one of the most important potential uses for temperature in monitoring fertility, but anovulatory cycles are often excluded from analysis in studies, as they reduce the amount of usable data for determining the date of ovulation. The study presented 47 anovulatory cycles in a total of 205 cycles. This significant number of anovulatory cycles provides a much better understanding of true accuracy, and SWS would appear to be capable of detecting anovulation when compared to VS results and by-eye cycle assessment.
6) There appears to be slightly lower accuracy in the confirmation of ovulation by SWS in the Confirmed Prior Diagnosis group (±3 days accuracy 89%, F score 0.92) than those with Confirmed No Diagnosis (accuracy 93%, F score 0.95). Although the groups were found to differ significantly in median cycle length ($p = 0.0131$), which may account for the difference, the ovulation confirmation performance of the methods themselves TOS ($p = 0.6518$) and SWS ($p = 0.3182$) did not differ significantly between the two groups, so the difference in the accuracy and F score is more likely to be a result of the performance of the methods in respect of negative results.
7) There appears to be a smaller difference in accuracy in the confirmation of ovulation by SWS for those with Late Ovulation (±3 days accuracy 87%, F score 0.93) vs. Early + Normal Ovulation Timing (accuracy 90%, F score 0.94), although again the groups differed significantly ($p < 0.001$). This would indicate SWS can be used effectively in a population with ovulatory dysfunction whether it is previously known or not. This is also a useful result given the drawbacks of BBT outlined by previous clinical literature (Lenton et al., 1977; Martinez et al., 1992; Ayres-de-Campos et al., 1995; Barron and Fehring, 2005; Mazerolle et al., 2011).

4.5 Prediction Results

With a ±3 days threshold accuracy result of 60.0% (CI 48.8%–70.5%), SWS provides a surprisingly similar prediction result to VS, which produces a ±3 days threshold prediction accuracy of 63.5% (CI 52.4%–73.7%) compared with its own confirmatory data for the next cycle. The F scores are similarly close: SWS 0.75 and VS 0.78.

The ±3 days prediction accuracy is improved for both methods: SWS = 66.7% (CI 53.3%–78.3%) and VS = 71.7% (CI 58.6%–82.5%) when Late Ovulation results are removed, so the identification of such cycles would appear to be helpful for women with ovulatory dysfunction when trying to conceive naturally. This conclusion may also lead to future algorithm improvements.

Nevertheless, real-time in-cycle prediction using current cycle data remains important for aiding conception and offers significant benefits over predictions based on prior cycle results. While urinary LH provides these in-cycle results, clinical publications have highlighted the inaccuracy of LH, particularly for those with ovulatory dysfunction (Lloyd and Coulam, 1989; Robinson et al., 1992; McGovern et al., 2004). The VS in-cycle method was developed to overcome this issue and has been reported upon previously (Papaioannou et al., 2014).

5 CONCLUSION

Although ovulatory dysfunction and luteal phase abnormalities may be causes of infertility or early pregnancy loss, clinical assessment of the luteal phase has proven challenging (Practice Committees of the American Society for Reproductive Medicine and the Society for Reproductive Endocrinology and Infertility, 2021). Luteal progesterone production is stimulated by LH pulses. The variability of serum progesterone levels from day to day and hour to hour limits the utility of measuring a single progesterone level to assess the overall adequacy of progesterone production during the luteal phase. Assessing multiple progesterone levels over several days and determining the area under the curve has been used to demonstrate luteal phase abnormalities, but this type of evaluation is not feasible in a clinical setting. Fertility may be impaired in women who experience a short luteal phase, but since urine LH tests are unreliable for some women, misinterpretation of the data or misdiagnosis may occur. The endometrium undergoes histologic and molecular changes throughout the postovulatory interval, but the reliability and reproducibility of endometrial biopsy have been questioned. To date, there is no universally accepted method to adequately assess the luteal phase.

Assessing the thermogenic effect of progesterone on core body temperature by VS or SWS provides a simple and reproducible method to confirm ovulation and assess the luteal phase. In this study, we have shown that VS and SWS are useful tools for confirming the fertile window and assessing for ovulation and anovulation for women's ovulatory dysfunction.

5.1 Contribution to the Field Statement

The number of female fertility monitoring tools available on the market has increased markedly over the past 5 years, mainly due to the advent of mobile devices, facilitating the development of personal period and fertility tracking applications. However, without accurate sensors and analysis algorithms, these have no way of confirming the presence or absence of ovulation. Where applications do use sensors, accuracy for predicting ovulation in a subsequent cycle has been generally poorly examined in the literature, in particular with respect to comparator methods. Indeed, a number of publications question using past cycles for predicting ovulation in subsequent cycles (Setton et al., 2016), given estimates of only approximately 21% accuracy (Johnson et al., 2018).

This paper examines a novel approach to confirmation of ovulation and prediction for subsequent cycles when compared to an established independent comparator method. It was of further interest to determine its value in a population with prior diagnoses known to cause ovulatory dysfunction, as well as its ability to diagnose possible ovulatory dysfunction in users with no prior diagnosis.

The conclusions are that temperature-based sensors increase the accuracy of ovulation determination over the use of historic data alone and therefore significantly benefit those trying to

conceive naturally. Furthermore, a more convenient skin-worn sensor, with appropriate data analysis, can be almost as useful as a vaginal sensor for real-time ovulation detection and as such is especially useful for women with irregular cycles.

Both kinds of sensors can also contribute to the screening for ovulatory dysfunction, even when it is less evident because cycle lengths appear to be in the expected range and as such better inform women struggling to conceive by helping them understand their cycles, reducing unnecessary uncertainty and stress, and providing practical advice on when to attempt conception.

5.2 Implications for Further Research

The "spring-loaded beam" temperature analysis method appears to provide a more accurate result than the "TOS" (Barrett and Marshall, 1969; McCarthy and Rockette, 1983) rule for determining when ovulation has taken place. It also is better at removing anomalous results produced by "TOS" where there is a clear bi-phasic temperature shift (by manual plotting and then by eye), but the hard mathematical rule cannot be applied as a result of too few data points, or data points lying outside of the "low" or "high" sets.

Furthermore, the "spring-loaded beam" method would be expected to have similar advantages for data obtained by other temperature measurements and hence improve the accuracy of results obtained by other temperature measurements, particularly oral temperature.

The SWS algorithm should now be reassessed in light of the Additional Set results.

It is unclear whether the median methodology for Prediction from prior cycle results is beneficial or in fact a hindrance to accuracy compared with a simpler method of (for instance) just using the most recent prior cycle result. The extension of the multiple serial cycles data set should assist with the creation and testing of further algorithmic predictive techniques.

Given the relative similarity in ovulation confirmation results between SWS and VS, using current cycle data to predict the onset of ovulation using an adapted algorithm might be possible with SWS. Adding to the current data set, in particular adding serial cycles with "normal" ovulation timing from women without known ovulatory dysfunction, would aid such a development. Equally, understanding whether a user of such a device ovulates late in their cycle and adjusting the algorithm to intelligently exclude or use those cycles through machine learning techniques could enhance the accuracy of prediction.

Additional confirmatory methods, in particular multiple LH and ultrasound follicular monitoring results, would greatly assist in establishing accuracy for a broader user population and demographic, of both Confirmation of the day of ovulation and Prediction of the ovulation day for a subsequent cycle and in the development of in-cycle prediction.

DATA AVAILABILITY STATEMENT

The original contributions presented in the study are included in the article/**Supplementary Material**, further inquiries can be directed to the corresponding author.

ETHICS STATEMENT

The studies involving human participants were reviewed and approved by the Atrium Health IRB 03-19-16E. The patients/participants provided their written informed consent to participate in this study.

AUTHOR CONTRIBUTIONS

HB has provided oversight for the original study protocol, IRB submission, clinical and scientific input, review of the data, and co-authorship of the paper. DK has conducted the analysis of the reproductive cycle data and results, provided clinical and scientific input in respect of the use of fertility awareness and "three over six" methodology, and provided co-authorship of the Introduction, Results, and Discussion sections. MR has conducted data compilation and data analysis and provided co-authorship of the paper. KT has advised on the statistical methodology used, reviewed the statistical analyses, and provided suggestions for modifications for the authorship of the paper. PA has conducted data compilation, algorithm methodology, and review and provided co-authorship of the *Discussion* section.

FUNDING

This research was financially supported by Fertility Focus Limited (now viO HealthTech Limited).

SUPPLEMENTARY MATERIAL

The Supplementary Material for this article can be found online at: https://www.frontiersin.org/articles/10.3389/fbioe.2022.807139/full#supplementary-material

REFERENCES

Ayres-de-Campos, D., Silva-Carvalho, J. L., Oliveira, C., Martins-da-Silva, I., Silva-Carvalho, J., and Pereira-Leite, L. (1995). Infertility: Inter-observer Agreement in Analysis of Basal Body Temperature Graphs from Infertile Women. *Hum. Reprod.* 10 (8), 2010–2016. doi:10.1093/oxfordjournals.humrep.a136227

Baker, F. C., Siboza, F., and Fuller, A. (2020). Temperature Regulation in Women: Effects of the Menstrual Cycle. *Temperature* 7 (3), 226–262. doi:10.1080/23328940.2020.1735927

Barrett, J. C., and Marshall, J. (1969). The Risk of conception on Different Days of the Menstrual Cycle. *Popul. Stud.* 23 (3), 455–461. doi:10.1080/00324728.1969.10405297

Barron, M. L., and Fehring, R. J. (2005). Basal Body Temperature Assessment. *MCN, Am. J. Maternal/Child Nurs.* 30 (5), 290–296. doi:10.1097/00005721-200509000-00004

Colombo, B., and Masarotto, G. (2000). Daily Fecundability: First Results from a New Data Base. *Demogr. Res.* 3, 39. doi:10.4054/demres.2000.3.5

Coyne, M. D., Kesick, C. M., Doherty, T. J., Kolka, M. A., and Stephenson, L. A. (2000). Circadian Rhythm Changes in Core Temperature over the Menstrual

Cycle: Method for Noninvasive Monitoring. *Am. J. Physiology-Regulatory, Integr. Comp. Physiol.* 279 (4), R1316–R1320. doi:10.1152/ajpregu.2000.279.4.R1316

Dozortsev, D. I., and Diamond, M. P. (2020). Luteinizing Hormone-independent Rise of Progesterone as the Physiological Trigger of the Ovulatory Gonadotropins Surge in the Human. *Fertil. Sterility* 114 (2), 191–199. doi:10.1016/j.fertnstert.2020.06.016

Dunson, D. B., Colombo, B., and Baird, D. D. (2002). Changes with Age in the Level and Duration of Fertility in the Menstrual Cycle. *Hum. Reprod.* 17 (5), 1399–1403. doi:10.1093/humrep/17.5.1399

Frank-Herrmann, P., Heil, J., Gnoth, C., Toledo, E., Baur, S., Pyper, C., et al. (2007). The Effectiveness of a Fertility Awareness Based Method to Avoid Pregnancy in Relation to a Couple's Sexual Behaviour during the fertile Time: a Prospective Longitudinal Study. *Hum. Reprod.* 22 (5), 1310–1319. doi:10.1093/humrep/dem003

Freundl, G., Godehardt, E., Kern, P. A., Frank-Herrmann, P., Koubenec, H. J., and Gnoth, Ch. (2003). Estimated Maximum Failure Rates of Cycle Monitors Using Daily conception Probabilities in the Menstrual Cycle. *Hum. Reprod.* 18 (12), 2628–2633. doi:10.1093/humrep/deg488

Goodale, B. M., Shilaih, M., Falco, L., Dammeier, F., Hamvas, G., and Leeners, B. (2019). Wearable Sensors Reveal Menses-Driven Changes in Physiology and Enable Prediction of the fertile Window: Observational Study. *J. Med. Internet Res.* 21 (4), e13404. doi:10.2196/13404

Harvey, O. L., and Crockete, H. E. (1932). Individual Differences in Temperature Changes of Women during the Course of the Menstrual Cycle. *Hum. Biol.* 4, 453–468.

Johnson, S., Marriott, L., and Zinaman, M. (2018). Can Apps and Calendar Methods Predict Ovulation with Accuracy? *Curr. Med. Res. Opin.* 34 (9), 1587–1594. doi:10.1080/03007995.2018.1475348

Lenton, E. A., Landgren, B.-M., and Sexton, L. (1984). Normal Variation in the Length of the Luteal Phase of the Menstrual Cycle: Identification of the Short Luteal Phase. *BJOG:An Int. J. O&G* 91 (7), 685–689. doi:10.1111/j.1471-0528.1984.tb04831.x

Lenton, E. A., Weston, G. A., and Cooke, I. D. (1977). Problems in Using Basal Body Temperature Recordings in an Infertility Clinic. *BMJ* 1, 803–805. doi:10.1136/bmj.1.6064.803

Lloyd, R., and Coulam, C. B. (1989). The Accuracy of Urinary Luteinizing Hormone Testing in Predicting Ovulation. *Am. J. Obstet. Gynecol.* 160 (6), 1370–1375. doi:10.1016/0002-9378(89)90857-0

MacRae, B. A., Annaheim, S., Spengler, C. M., and Rossi, R. M. (2018). Skin Temperature Measurement Using Contact Thermometry: A Systematic Review of Setup Variables and Their Effects on Measured Values. *Front. Physiol.* 9. doi:10.3389/fphys.2018.00029

Martinez, A. R., van Hooff, M. H. A., Schoute, E., van der Meer, M., Broekmans, F. J. M., and Hompes, P. G. A. (1992). The Reliability, Acceptability and Applications of Basal Body Temperature (BBT) Records in the Diagnosis and Treatment of Infertility. *Eur. J. Obstet. Gynecol. Reprod. Biol.* 47, 121–127. doi:10.1016/0028-2243(92)90041-v

Mazerolle, S. M., Ganio, M. S., Casa, D. J., Vingren, J., and Klau, J. (2011). Is Oral Temperature an Accurate Measurement of Deep Body Temperature? A Systematic Review. *A. Syst. Rev. J Athl Train* 46 (5), 566–573. doi:10.4085/1062-6050-46.5.566

McCarthy, J. J., Jr, and Rockette, H. E. (1983). A Comparison of Methods to Interpret the Basal Body Temperature graph**Supported in Part by Funds from the National Institute of Child Health and Human Development and the Office for Family Planning. *Fertil. Sterility* 39 (5), 640–646. doi:10.1016/s0015-0282(16)47059-7

McGovern, P. G., Myers, E. R., Silva, S., Coutifaris, C., Carson, S. A., Legro, R. S., et al. (2004). Absence of Secretory Endometrium after False-Positive home Urine Luteinizing Hormone Testing. *Fertil. Sterility* 82 (5), 1273–1277. doi:10.1016/j.fertnstert.2004.03.070

Papaioannou, S., Delkos, D., and Pardey, J. (2014). Abstract Book of the 30thESHRE Annual Meeting, Munich, Germany, 29 June - 2 July 2014. *Hum. Reprod.* 29, i1–i389. doi:10.1093/humrep/29.Supplement_1.1

Papaioannou, S., Al Wattar, B. H., Milnes, R. C., and Knowles, T. G. (2013). Quality index Assessment of Vaginal Temperature Based Fertility Prediction and Comparison with Luteinising Hormone Testing, Ultrasound Folliculometry and Other home Cycle Monitors. *Fertil. Sterility* 100 (3), S326–S327. doi:10.1016/j.fertnstert.2013.07.947

Papaioannou, S., Aslam, M., Al Wattar, B. H., Milnes, R. C., and Knowles, T. G. (2013). User's Acceptability of OvuSense: a Novel Vaginal Temperature Sensor for Prediction of the fertile Period. *J. Obstet. Gynaecol.* 33 (7), 705–709. doi:10.3109/01443615.2013.817984

Practice Committees of the American Society for Reproductive Medicine and the Society for Reproductive Endocrinology and Infertility (2021). Diagnosis and Treatment of Luteal Phase Deficiency: a Committee Opinion. *Fertil. Steril* 115, 1416–1423. doi:10.1016/j.fertnstert.2021.02.010

Regidor, P.-A., Kaczmarczyk, M., Schiweck, E., Goeckenjan-Festag, M., and Alexander, H. (2018). Identification and Prediction of the fertile Window with a New Web-Based Medical Device Using a Vaginal Biosensor for Measuring the Circadian and Circamensual Core Body Temperature. *Gynecol. Endocrinol.* 34 (3), 256–260. doi:10.1080/09513590.2017.1390737

Robinson, S., Rodin, D. A., Deacon, A., Wheeler, M. J., and Clayton, R. N. (1992). Which Hormone Tests for the Diagnosis of Polycystic Ovary Syndrome? *BJOG:An Int. J. O&G* 99 (3), 232–238. doi:10.1111/j.1471-0528.1992.tb14505.x

Setton, R., Tierney, C., and Tsai, T. (2016). The Accuracy of Web Sites and Cellular Phone Applications in Predicting the Fertile Window. *Obstet. Gynecol.* 128 (1), 58–63. doi:10.1097/AOG.0000000000001341

Tompkins, P. (1944). The Use of Basal Temperature Graphs in Determining the Date of Ovulation. *JAMA* 124 (11), 698–700. doi:10.1001/jama.1944.02850110022005

van de Velde, T. H. (1904). *Ueber den Zusammenhang zwischen Ovarialfunction, Wellenbewegung und Menstrualblutung*. Open Library OL20446827 OCLC/WorldCat14801387. Haarlem, De Erven F. Bohn Jena, Gustav Fischer.

Wilcox, A. J., Weinberg, C. R., and Baird, D. D. (1995). Timing of Sexual Intercourse in Relation to Ovulation - Effects on the Probability of Conception, Survival of the Pregnancy, and Sex of the Baby. *N. Engl. J. Med.* 333 (23), 1517–1521. doi:10.1056/NEJM199512073332301

Zhu, T. Y., Rothenbühler, M., Hamvas, G., Hofmann, A., Welter, J., Kahr, M., et al. (2021). The Accuracy of Wrist Skin Temperature in Detecting Ovulation Compared to Basal Body Temperature: Prospective Comparative Diagnostic Accuracy Study. *J. Med. Internet Res.* 23 (6), e20710. doi:10.2196/20710

Conflict of Interest: DK is an independent nurse consultant who consults on a part-time basis on behalf of Fertility Focus Limited (now viO HealthTech Limited) in addition to conducting other businesses. KT is a shareholder in Fertility Focus Limited (now viO HealthTech Limited) but has not been remunerated for participation in this research. MR and PA are paid employees and shareholders of Fertility Focus Inc. (now viO HealthTech Limited).

The remaining author declares that the research was conducted in the absence of any commercial or financial relationships that could be construed as a potential conflict of interest.

Publisher's Note: All claims expressed in this article are solely those of the authors and do not necessarily represent those of their affiliated organizations, or those of the publisher, the editors and the reviewers. Any product that may be evaluated in this article, or claim that may be made by its manufacturer, is not guaranteed or endorsed by the publisher.

frontiers | Frontiers in Bioengineering and Biotechnology

ORIGINAL RESEARCH
published: 12 April 2022
doi: 10.3389/fbioe.2022.786755

Comprehensive Metabolomic Profiling of Cord Blood and Placental Tissue in Surviving Monochorionic Twins Complicated by Twin-Twin Transfusion Syndrome With or Without Fetoscopic Laser Coagulation Surgery: A Retrospective Cohort Study

Tianjiao Liu[1,2†], Li Wen[1,2,3†], Shuai Huang[1,2,3†], Ting-li Han[2], Lan Zhang[1,2,3], Huijia Fu[4], Junnan Li[1,2,3], Chao Tong[1,2], Hongbo Qi[1,5]*, Richard Saffery[6,7], Philip N. Baker[8] and Mark D. Kilby[9,10]*

[1]State Key Laboratory of Maternal and Fetal Medicine of Chongqing Municipality, Chongqing, The First Affiliated Hospital of Chongqing Medical University, Chongqing, China, [2]International Collaborative Laboratory of Reproduction and Development, Ministry of Education, Chongqing Medical University, Chongqing, China, [3]Department of Obstetrics, The First Affiliated Hospital of Chongqing Medical University, Chongqing, China, [4]Department of Reproduction Health and Infertility, The First Affiliated Hospital of Chongqing Medical University, Chongqing, China, [5]Chongqing Women and Children's Health Center, Chongqing, China, [6]Cancer, Disease and Developmental Epigenetics, Murdoch Children's Research Institute, Parkville, VIC, Australia, [7]Department of Pediatrics, University of Melbourne, Parkville, VIC, Australia, [8]College of Life Sciences, University of Leicester, Leicester, United Kingdom, [9]Institute of Metabolism and System Research, University of Birmingham, Birmingham, United Kingdom, [10]Fetal Medicine Centre, Birmingham Women's and Children's Foundation Trust, Birmingham, United Kingdom

OPEN ACCESS

Edited by:
Lana McClements, University of Technology Sydney, Australia

Reviewed by:
Clarissa Lim Velayo, University of the Philippines Manila, Philippines
Dunja Aksentijevic, Queen Mary University of London, United Kingdom

***Correspondence:**
Chao Tong
chaotongcqmu@163.com
Hongbo Qi
qihongbo728@163.com

†These authors have contributed equally to this work

Specialty section:
This article was submitted to Preclinical Cell and Gene Therapy, a section of the journal Frontiers in Bioengineering and Biotechnology

Received: 30 September 2021
Accepted: 16 March 2022
Published: 12 April 2022

Citation:
Liu T, Wen L, Huang S, Han T-l, Zhang L, Fu H, Li J, Tong C, Qi H, Saffery R, Baker PN and Kilby MD (2022) Comprehensive Metabolomic Profiling of Cord Blood and Placental Tissue in Surviving Monochorionic Twins Complicated by Twin-Twin Transfusion Syndrome With or Without Fetoscopic Laser Coagulation Surgery: A Retrospective Cohort Study. Front. Bioeng. Biotechnol. 10:786755. doi: 10.3389/fbioe.2022.786755

Objectives: To investigate metabolomic perturbations caused by twin-twin transfusion syndrome, metabolic changes associated with fetoscopic laser coagulation in both placental tissue and cord plasma, and to investigate differential metabolites pertinent to varying fetal outcomes, including hemodynamic status, birth weight, and cardiac function, of live-born babies.

Methods: Placental tissue and cord plasma samples from normal term or uncomplicated preterm-born monochorionic twins and those complicated by twin-twin transfusion syndrome treated with or without fetoscopic laser coagulation were analyzed by high-performance liquid chromatography metabolomic profiling. Sixteen comparisons of different co-twin groups were performed. Partial least squares–discriminant analysis, metabolic pathway analysis, biomarker analysis, and Spearman's correlation analysis were conducted based on differential metabolites used to determine potential biomarkers in different comparisons and metabolites that are pertinent to neonatal birth weight and left ventricular ejection fraction.

Results: These metabolomic investigations showed that the cord plasma metabolome has a better performance in discriminating fetuses among different hemodynamic groups

than placental tissue. The metabolic alteration of twin-twin transfusion syndrome in these two types of samples centers on fatty acid and lipid metabolism. The fetoscopic laser coagulation procedure improves the metabolomic change brought by this syndrome, making the metabolomes of the treated group less distinguishable from those of the control and preterm birth groups. Certain compounds, especially lipids and lipid-like molecules, are noted to be potential biomarkers of this morbid disease and pertinent to neonatal birth weight and ejection fraction.

Conclusions: Fetoscopic laser coagulation can ameliorate the metabolomic alteration caused by twin-twin transfusion syndrome in placental tissue and cord plasma, which are involved mainly in fatty acid and lipid-like molecule metabolism. Certain lipids and lipid-like molecules are helpful in differentiating co-twins of different hemodynamic statuses and are significantly correlated with neonatal birth weight or ejection fraction.

Keywords: twin-twin transfusion syndrome, fetoscopic laser coagulation, metabolomics, cord plasma, placenta

INTRODUCTION

Perinatal mortality and morbidity are three to seven times higher in twin pregnancy than in singleton pregnancy (Hack et al., 2008). In monochorionic diamniotic (MCDA) twin pregnancies, which are prone to multiple concomitant complications such as twin-twin transfusion syndrome (TTTS), selective intrauterine growth retardation (sIUGR), severe weight discordance, and twin anemia-polycythemia sequence (TAPS), the perinatal mortality rate is even higher (11%) (Hack et al., 2008; Lewi et al., 2008); thus, more insights into this field are desperately needed. Among these complications, TTTS, mainly caused by unidirectional intertwin blood flow *via* placental arteriovenous anastomoses (AVA), is almost the most detrimental. It could result in severe hypovolemia and anemia in the donor fetus and serious hypertensive hemodynamic perturbation in the recipient twin's circulation, with subsequent myocardial hypertrophy and even cardiomegaly in the later stage (Stirnemann et al., 2010). TTTS complicates approximately 9–15% of MCDA pregnancies (Sebire et al., 2000; Lewi et al., 2008) and accounts for approximately half of the stillbirths in MCDA pregnancies (Lewi et al., 2008). For those with onset in the second trimester, if left untreated, this syndrome is highly fatal for each fetus (at least 90%) (Van Mieghem et al., 2009), and surviving fetuses are at high risk of suffering from many undesirable perinatal outcomes and sequelae, such as preterm births (PTBs) (Ong et al., 2006), severe cardiovascular anomalies (Michelfelder et al., 2015; Pruetz et al., 2015), neurological impairments (van Klink et al., 2016), renal dysfunction (Melhem et al., 2019), and fetal endocrinal dysregulation (Bajoria et al., 2002). If onset occurs in late pregnancy, a timely cesarean section is recommended to ensure the survival of both twins, though the aforementioned adverse outcomes may also occur (Simpson and Simpson, 2013).

Recent decades have witnessed the advent and advancement of invasive therapeutic techniques for curing TTTS (Senat et al., 2004; Ruano et al., 2013; Slaghekke et al., 2014). Fetoscopic laser coagulation (FLC) aims to photocoagulate the pathological AVA between co-twins on the surface of the monochorionic placenta and therefore restores hemodynamics in the circulation of both fetuses. With the survival rate of both co-twins approaching 70% and the noticeable reduction in the occurrence of neurodevelopmental morbidity and cardiac dysfunction (Senat et al., 2004; Ruano et al., 2013; Diehl et al., 2017), FLC has grossly outperformed serial amnioreduction in improving the prognosis of twins complicated by TTTS, making it the current first-line effective therapy for TTTS (Senat et al., 2004).

Metabolomics is the full-scale untargeted deciphering of the metabolic profile of biological samples. The metabolome, resulting from the interplay of genotype and the environment, can provide much critical and sensitive bioinformation on the pathophysiology of human disease and physiological activities. Given that the molecular mechanism that drives the occurrence of communicating AVA in the MCDA placenta is poorly understood and an animal model for the study of TTTS is lacking, metabolomics could be applied as a promising tool in TTTS research. However, notwithstanding the considerable merits of metabolomic studies, due to the low overall incidence of TTTS and the difficulty in retrieving biological samples, very little evidence has been reported to elucidate metabolomic disturbances in twins suffering from TTTS, not to mention those who underwent FLC procedures. In our analysis of maternal plasma, our laboratory previously found that TTTS-complicated pregnant women had an altered metabolome before 16 weeks of gestation, and these alterations included changes in fatty acids, Krebs cycle intermediates, and amino acids (Yang et al., 2021). Correspondingly, it was previously implied that the altered carbohydrate and fatty acid profile in the amniotic fluid of the TTTS-complicated recipient co-twin has a close association with FLC treatment, fetal cardiovascular dysfunction, and anomalies (Dunn et al., 2016). However, to date, the metabolomics of samples which are more relevant to the fetal circulation in TTTS with or without FLC surgery has rarely been reported.

In this research, we applied holistic metabolomic fingerprinting, by LC-MS (liquid chromatography–mass spectrometry), of placental tissue and umbilical cord blood

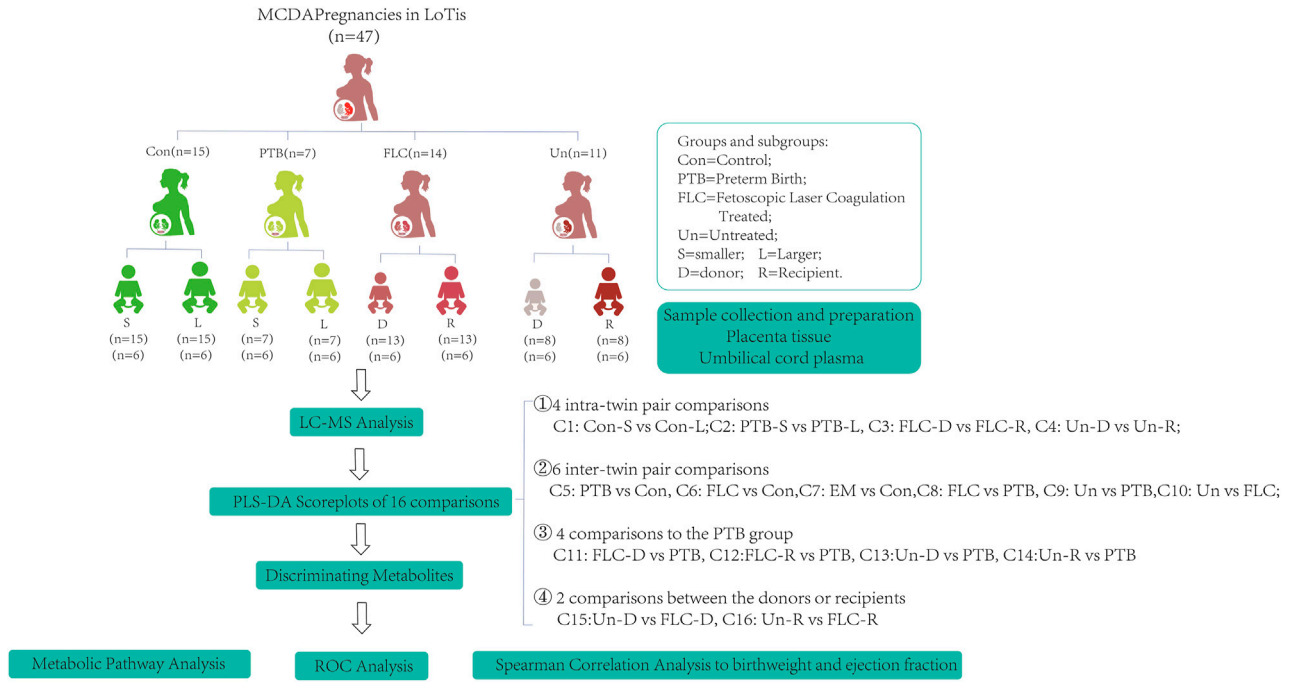

FIGURE 1 | Schematic diagram of the study design. The abbreviations are as follows: MCDA, monochorionic diamniotic; TTTS, twin-to-twin transfusion syndrome; Con, control; FLC, fetoscopic laser coagulation; Un, untreated; PTB, preterm birth; C, comparison; S, smaller twins; L, larger twins; D, donor twins; R, recipient twins.

plasma collected from normal MCDA pregnancies, apparently uncomplicated preterm-born MCDA twins, TTTS twins treated with FLC surgery, and TTTS pregnancies that were untreated due to the late onset of the syndrome to delineate the metabolomic alterations caused by TTTS and metabolic improvement conferred by the FLC operation and to identify significant metabolite correlations with the discrepancy in neonatal birth weight and ejection fraction within 2 days after birth.

MATERIALS AND METHODS

Participants

As shown in **Figure 1**, 15 normal MCDA twin pregnancies, 25 MCDA twin pregnancies complicated by TTTS (14 FLC-treated cases and 11 untreated cases), and seven preterm-born MCDA twin pregnancies were retrospectively selected from an ongoing twin cohort study conducted at the Department of Obstetrics at the First Affiliated Hospital of Chongqing Medical University. These groups are abbreviated as Con, PTB, FLC, and Un groups in this article, and the 16 comparisons between groups or co-twins are abbreviated as C1–C16 (**Figure 1**). The identification of chorionicity was conducted by ultrasonic monitoring at 11–14 weeks' gestational age and confirmed by postpartum examination. Thereafter, MCDA twin pregnancies were followed up by routine ultrasound monitoring every 2 weeks. According to the internationally recognized guidelines, TTTS was diagnosed when the following ultrasound criteria were met: the presence of oligohydramnios (defined as a maximal vertical pocket (MVP) <2 cm) in one amniotic sac and polyhydramnios (an MVP >8 cm before the 20th gestational week (GW) or >10 cm after the 20th GW) in the other sac (Simpson and Simpson, 2013). The staging of TTTS was conducted with the observance of the Quintero system based on sonographic findings (Quintero et al., 1999). TTTS neonates were categorized as larger (or recipient) co-twins and smaller (or donor) co-twins. Because most TTTS pregnancies are complicated by preterm delivery, we included preterm MCDA without apparent fetal complications. The cases in the untreated group had late but rapid onset (>28 weeks when diagnosed with TTTS), so they were promptly administered with dexamethasone, underwent cesarean section on the third day after diagnosis (**Supplementary Table S1**), and did not receive the FLC procedure due to safety concerns (Simpson and Simpson, 2013). Cases in the control MCDA twin group had appropriate fetal development and a delivery age beyond 37 GWs. The PTB and control groups were managed during the same time span as the TTTS group. All twin pregnancies in the present study were delivered by a cesarean section, and monochorionicity, integrity, and pathological AVA of the placenta were promptly checked by experienced midwives or obstetricians at delivery.

Fetoscopic Laser Coagulation and Postoperative Follow-Up

FLC surgeries were performed by two experienced operators from the Department of Obstetrics at the First Affiliated Hospital of Chongqing Medical University. The selective sequential FLC technique was adopted in most cases, and

an additional "Solomon" procedure was applied in the remaining cases, as described in some published reports (Senat et al., 2004; Morris et al., 2010; Slaghekke et al., 2014). The clinical information of the FLC-treated patients is presented in **Supplementary Table S1**. Postoperative ultrasound examinations for all participants were performed every week during follow-up. Dexamethasone was prophylactically administered at approximately 32 GWs for subjects with viable fetus (es) to promote fetal lung maturation. All viable pregnancies were advised to be delivered by cesarean section at the 34th to 36th GW if no undesirable complications occurred.

Echocardiography of Neonates

The echocardiographic monitoring of newborns in this study was performed within 2 days of birth and conducted according to previous studies and published clinical guidelines (Mertens et al., 2011; Tissot et al., 2018; Phad and Waal, 2020) by several experienced ultrasound specialists. LV endocardial tracing was performed semiautomatically using speckle tracking software. All parameters were measured three times and are shown as averages. LV-EF was calculated according to the following formula: EF (%) = SV/EDV × 100, where EF = ejection fraction, SV = stroke volume, and EDV = end-diastolic volume. The SV was calculated as the left ventricle EDV minus the left ventricle end-systolic volume (ESV).

Sample Collection and Metabolite Extraction

The umbilical cord plasma and placental tissue samples were immediately collected when the placenta was delivered. The demarcation of the monochorionic placenta was conducted according to the septum of the amniotic membrane and the distribution of different placental vasculatures in the co-twins. We collected placental tissues that were approximately 0.5 × 0.5 × 0.5 cm^3 adjacent to the individual insertion point of the umbilical cord from the fetal side. Placental tissue was instantly washed in precooled physiological saline to remove blood clots, blotted dry, and then frozen in liquid nitrogen for further use. Four milliliters of blood was drained from each umbilical vein and transferred into EDTA-coated blood collection tubes, which were later centrifuged at 3,000 rpm for 10 min at 4°C. The supernatant was aliquoted into cryopreservation tubes (Micronic, Holland) and then stored at −80°C prior to analysis. Fifty milligrams of pretreated placental tissue was mixed with 20 μl internal standard (fexofenadine hydrochloride, 50 μg/ml), 300 μl methanol, and a tiny iron bead in a 2-ml Eppendorf tube, sealed with a sealing membrane, and then homogenized in a tissue disruptor (QIAGEN®, TissueLyser II) for 5 min at 25 r/s. The supernatant was transferred into a new set of 1.5-ml Eppendorf tubes. A total volume of 100 μl cord plasma was vortex-mixed with 20 μl of the aforementioned internal standard for 15 s and then with 600 μl acetonitrile for 30 s. Each sample was centrifuged at 12,000 rpm for 15 min at 4°C, dried under a vacuum with a CentriVap® concentrator (Labconco, Kansas City, MO, United States) at room temperature for 7 h to induce metabolite stability, and cryopreserved at −80°C until further analysis.

Ultra-Performance Liquid Chromatography–Mass Spectrometry (UPLC-MS) Analysis

A metabolomic analysis of the placental tissue and umbilical cord plasma extracts was conducted, as previously described (Wen et al., 2019; Chen et al., 2020; Wu et al., 2021). Each placental tissue sample was reconstituted in 100 μl of acetonitrile water mixture (1:1, v/v), vortexed, and centrifuged at 12,000 rpm for 5 min, and then 100 μl of supernatant was injected into a loading vial for metabolomic fingerprinting. Similarly, each cord plasma sample was vortex-mixed with 100 μl of 10% methanol water (1:9, v/v) and centrifuged at 12,000 rpm for 5 min, and then 80 μl of supernatant was transferred into a loading vial. The identification of different metabolites in our samples was conducted using Progenesis QITM (Waters, Milford, MA, United States), a software that enables the performance of peak alignment, peak selection, deconvolution, and identification of metabolites against HMDB library databases. Only samples with a mass accuracy within ±5 ppm and overall score ≥36 were regarded as highly confident and kept for subsequent analysis.

Statistical and Metabolomic Analysis

Statistical analysis was performed using SPSS version 19 (IBM Inc., Armonk, NY, United States) and Prism version 8.0 (GraphPad Software Inc. San Diego, California, United States) for Windows. Student's t test was applied to compare data with normal distribution among different data sets. The intergroup comparisons of non-normally distributed continuous variables were performed by means of the non-parametric Mann–Whitney *U* test to investigate the statistical characteristics. Median values and 95% confidence intervals (CIs) are described. For categorical variables, the χ^2 test and Fisher's exact test were used when appropriate. A p value <0.05 was regarded as statistically significant. The score plots of partial least squares–discriminant analysis (PLS-DA) with leave-one-out cross validation, quantitative enrichment analysis (QEA), receiver operating characteristic (ROC) curve analysis, univariate non-parametric Wilcoxon signed-rank test, and Spearman rank correlation analysis were performed using the online metabolomic analysis software MetaboAnalyst 5.0 (www.MetaboAnalyst.ca). Differential metabolites of each comparison were clustered according to their chemical structures in the heat map generated by the R package ggplot2. A network of discriminating metabolites and corresponding pathways was constructed based on the KEGG database by implementing Metscape (Gao et al., 2010), a plug-in installed in Cytoscape version 3.8.2.

RESULTS

Participants Characteristics

Clinical Information About TTTS and FLC Surgery

Information related to TTTS and FLC, such as the gestational age, Quintero stage at diagnosis, surgery or delivery, and survival rates of FLC and EM groups, is presented in **Supplementary Table S1**. Notably, the gestational age (days) at diagnosis of TTTS in the EM group was much higher than that in the FLC-treated group (156.14 ± 24.24

vs 221.55 ± 23.65, $p < 0.001$), which may account for the larger proportion of FLC-treated cases diagnosed at earlier Quintero stages (7/14 at stage I in the FLC group vs 6/11 at stage III in the EM group). Within 2 days after the final diagnosis, FLC procedures were performed (at the 16th to 28th GWs) for the FLC group, according to published clinical guides (Middeldorp et al., 2007; Simpson and Simpson, 2013). For cases staged Quintero I in the FLC group, because of the short cervical length or severe maternal clinical manifestations, they also received FLC surgery, except for two cases in which the pregnancy was terminated by induced labor due to fetal cardiac anomalies, and the cases in the untreated group were delivered later than the 28th GW when diagnosed with TTTS; thus, it was not appropriate for them to undergo FLC procedures according to clinical guidelines, and they subsequently received cesarean section within 3 days after the TTTS diagnosis (Simpson and Simpson, 2013). There was no significant difference in the Quintero stage at diagnosis, gestational age at delivery, or survival rate in pregnancy between the FLC and Un groups. In addition, there was no significant difference in the amniotic deepest vertical pool in the recipients and donors of the FLC and Un groups at TTTS diagnosis (**Supplementary Table S2**) and in the larger and smaller co-twins between Con and PTB twin groups at the last ultrasound (**Supplementary Table S3**).

Maternal Clinical Characteristics

The maternal demographic and clinical features of each subgroup and the significance of every comparison are listed in **Supplementary Table S4**. Maternal age, employment status, body mass index (BMI) before pregnancy or delivery, primigravida, smoking before or during pregnancy, conceptional mode, gestational age at delivery, delivery approaches, and neonatal sex were described and showed no significant difference in any of those comparisons ($p > 0.05$). The gestational age of the control group was markedly higher than that of any other group ($p < 0.001$), while there was no significant difference in any comparisons among the PTB, FLC, and Un groups.

Neonatal Characteristics

Supplementary Table S5 presents the birth outcomes of each neonatal group in the present study. None of the comparisons showed a significant difference in placental weight or neonatal sex. Observably, the donor and recipient fetuses differed significantly in terms of birth weight, abdominal circumference, and amniotic fluid volume, while neither the body length nor head circumference significantly differed between the FLC and Un groups (C3 and C4). On the other hand, the inner group comparison of the Con and PTB groups did not demonstrate any significant differences in those variables (C1 and C2). The birth weight, body length, and head circumference of the Con group markedly outperformed those of the PTB, FLC, and Un groups (C5, C6, and C10). In addition, the abdominal circumference of the normal MCDA newborns was also higher than that of their FLC and Un counterparts (C5 and C6). Compared with the Con group, FLC (C7) and Un groups (C8) both showed a remarkably greater birth weight disparity and shorter body length and head circumference but presented no significant differences in parameters such as abdominal circumference, placenta weight, and newborn sex. Notably, the Un group had a significantly lower birth weight and greater discrepancy in amniotic fluid volume in C8, while the group of neonates who received FLC procedures did not differ from that in the PTB group in terms of these two variables, highlighting the greatly ameliorated birth outcomes of the FLC.

PLS-DA Analysis of Placental Metabolomes Between Different Co-twin Groups in the Control, PTB, FLC, and Un Groups

The present study included 86 placental tissue samples collected from both co-twins in different groups, as shown in **Figure 1**. The placental metabolomic difference within co-twin pairs, in comparisons 1–4, was first investigated. As shown in **Supplementary Figures S1A–D**, when the larger/recipient co-twins and smaller/donor co-twins in the control, FLC, and Un groups were compared, the PLS-DA score plots indicated that the metabolomes in the placental tissue in those comparisons could not be clustered separately, which implies subtle metabolomic discrepancies within co-twin pairs between C1, C3, and C4.

Given that the placental metabolomes between different co-twins within the Con, PTB, FLC, and Un groups demonstrated little difference, we collectively grouped the larger/recipient or smaller/donor co-twins in each group and conducted intergroup comparisons (C5–C10). The PLS-DA score plots of C6 (Control vs FLC, **Figure 2B**) and C8 (PTB vs FLC, **Figure 2D**) were not distinctly separated, which implies that there were no significant metabolomic differences between those two comparisons. In other words, the FLC procedure might significantly mitigate the metabolomic disturbance of TTTS in the FLC group placenta, thus making it less different from the control and gestational age-matched PTB groups. However, when the placental metabolome of untreated TTTS pregnancies was compared to that of the control group (C7, **Figure 2C**), PTB group (C9, **Figure 2E**), and FLC-treated group (C10, **Figure 2F**), the PLS-DA displayed strikingly significant differences, suggesting that TTTS caused notable metabolomic changes in the placenta. Intriguingly, the score plot for C5, namely, the control group versus the PTB group, also showed an obvious separation, which is in accordance with the findings of previous studies that fetal and maternal metabolomes vary temporarily according to the gestational age (Ernst et al., 2020; Liang et al., 2020). Therefore, we focused mainly on gestational age-matched comparisons in the following analysis and compared the metabolomes of FLC donors, FLC recipients, Un donors, and Un recipients to the total number of PTB neonates (C11–C14, **Supplementary Figures S1E–H**). In addition, the comparison between the donors or recipients with or without the FLC procedure was carried out (C15 and C16, **Supplementary Figures S1I,J**). These six comparisons demonstrated clear separation and great performance.

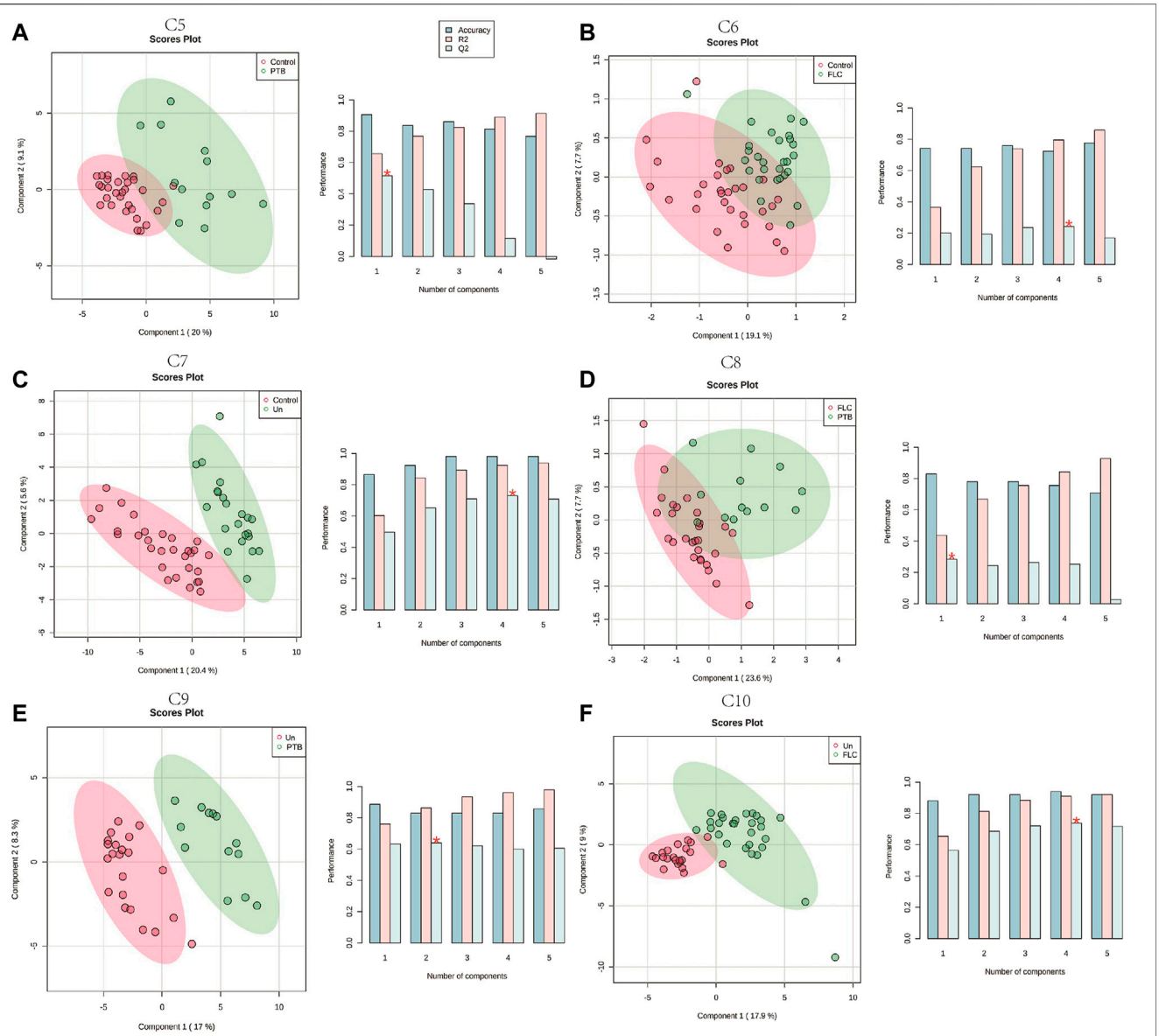

FIGURE 2 | Partial least squares–discriminant analysis (PLS-DA) of the placental metabolome in comparisons 5–10. The left plots in **(A–F)** are the PLS-DA score plots of the corresponding comparisons. Histograms on the right display the evaluation of prediction model performance *via* leave-one-out cross validations (LOOCV), in which R2 represents the model's explanatory ability of the data and Q2 reflects the predictive ability of the corresponding PLS-DA model.

PLS-DA Analysis of Umbilical Cord Plasma Metabolomes Between Different Co-twin Groups in the Control, PTB, FLC, and Un Groups

In total, 48 cord plasma samples (six samples per subgroup) were detected using LC-MS in this study, and PLS-DA for the aforementioned 16 comparisons was subsequently performed. Unlike the placental metabolomes, the cord plasma samples showed a better capability for distinguishing the metabolomes of the different co-twin groups, as they clearly separated the metabolomes in the PLS-DA score plots of different co-twins in all the Con, PTB, FLC, and Un groups (**Supplementary Figures S2A–D**). When the major group comparisons were conducted, the cord plasma sample displayed a very similar result to the placental tissue. Specifically, the C5 (Con vs PTB, **Supplementary Figure S2E**), C7 (Con vs Un, **Supplementary Figure S2G**), C9 (Un vs PTB, **Supplementary Figure S2I**), and C10 (Un vs FLC, **Supplementary Figure S2F**) distinctly differentiated the "divisor" and "dividend" groups in the corresponding comparisons, and C6 (Con vs FLC, **Supplementary Figure S2F**) and C8 (FLC vs PTB, **Supplementary Figure S2H**) demonstrated a less clear separation. These findings indicated that 1) the gestational age is likely to also have a significant impact on the umbilical cord plasma metabolome (appearing in C5), 2) TTTS leads to some apparent metabolomic alteration in the cord plasma of the Un group (appearing in C7 and C9), and 3) FLC surgery greatly mitigates the metabolomic profile of cord plasma of the

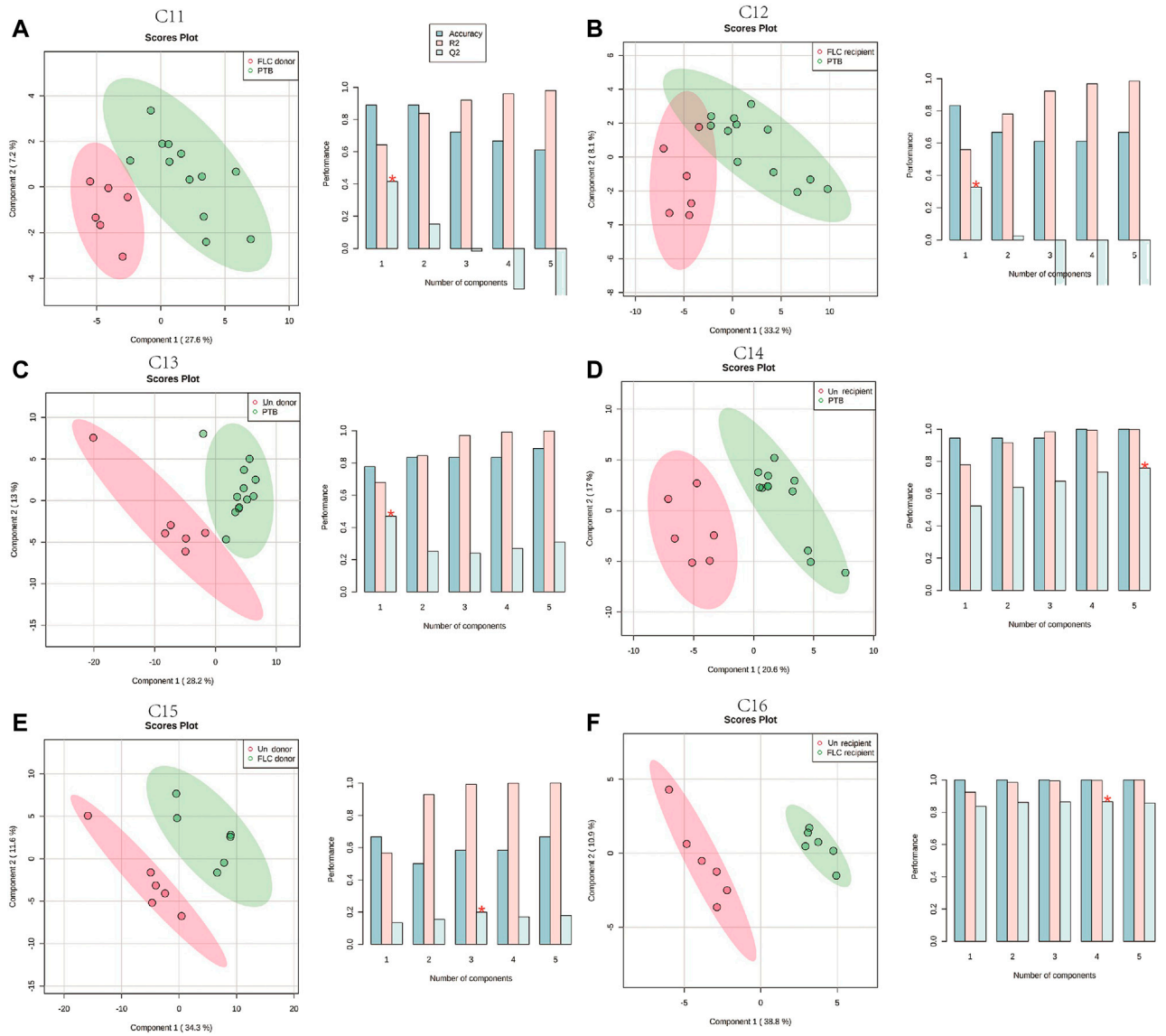

FIGURE 3 | Partial least squares–discriminant analysis (PLS-DA) of the umbilical cord plasma metabolome in comparisons 11–16. The left plots in **(A–F)** are the PLS-DA score plots of corresponding comparisons. Histograms on the right display the evaluation of prediction model performance *via* leave-one-out cross validations (LOOCV), in which R2 represents the model's explanatory ability of the data and Q2 reflects the predictive ability of the corresponding PLS-DA model.

FLC group (appearing in C6, C8, and C10). To avoid the confounding effect of gestational age and to differentiate the metabolomic difference of the donors and recipients in the FLC and Un groups, we carried out C11–C16, which presented good separation (shown in **Figure 3**), indicating the existence of distinguishable metabolomic profiles between these co-twin groups.

Pathway Analysis of Placental and Cord Plasma Metabolomes in the Comparisons of the Con, PTB, FLC, and Un Groups

In the PLS-DA, 55 discriminating metabolites were successfully matched with the corresponding compound superclass in the SMPDB (the Small Molecule Pathway Database, https://smpdb.ca/). There were 11 fatty acyls, 16 lipid- and lipid-like molecules, five organic acids, eight sterol lipids, and two sphingolipids found to be significantly different in C1–C10 in the placental metabolome (**Supplementary Figure S3A**). Regarding the umbilical cord plasma, 118 differential metabolites were matched with the corresponding superclass in the SMPDB. These discriminating metabolites in C1-C16 in the umbilical cord plasma metabolome are 48 lipid and lipid-like molecules, 17 fatty acids, 15 sterol lipids, 5 prenol lipids, 4 organic acids, and 4 nucleic acids (**Supplementary Figure 3B**).

We constructed a heat map of the significantly different metabolites (FC > 2, p value < 0.05, and FDR<0.1) in C1–C10

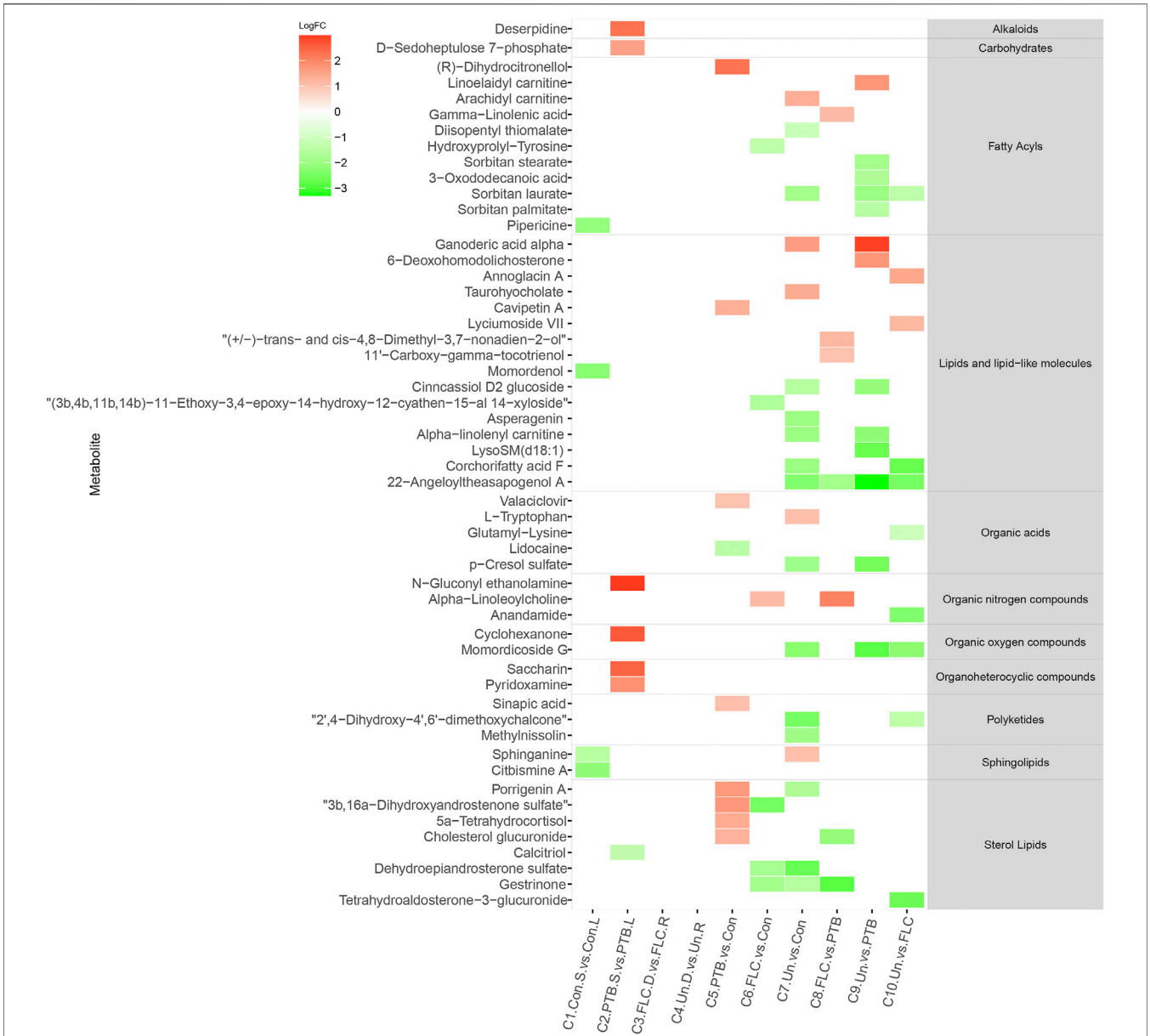

FIGURE 4 | Heat map demonstrating the discriminating metabolites of corresponding comparisons and compound superclass in placental tissue metabolomes. The $\log_2$ scale matched with gradually changed colors shows the relative abundance of a given placental metabolite. Only differential metabolites (*p* value < 0.05, q value < 0.1, and FC > 2) that can be identified in the SMPDB and HMDB databases are displayed. Blocks with red or green represent higher or lower expression than the denominator group. Abbreviations: con, control; PTB, preterm birth; FLC, fetoscopic laser coagulation; Un, untreated; T, total; S, small; L, large; D, donor; R, recipient.

in the placental metabolomes and C1–C16 in the umbilical cord plasma metabolome according to their LogFC values. As shown in **Figure 4**, the donor and recipient co-twins had few differential placental metabolites in the FLC and Un groups (C3 and C4), whereas the major group comparisons depicted striking metabolomic discrepancies. Compared to the PTB group, the Un group showed decrease in four lipid- and lipid-like molecules, four fatty acyls, and one organic acid. Furthermore, compared to the FLC group, the Un group had lower levels of one organic acid, one sterol lipid, one fatty acyl, and two lipids and lipid-like molecules. On the other hand, as shown in **Figure 5**, the cord plasma revealed many discriminating metabolites in the intragroup comparisons of the FLC (C3) and EM groups (C4). Notably, the cord plasma of donors in the Un group displayed an increased enrichment in the levels of many sterol lipids, lipids and lipid-like molecules, and fatty acyls compared to the EM recipients and the PTB group, and this was not found in the FLC donors.

To depict the latent pertinent correlation between the differential metabolites in comparisons of the placental

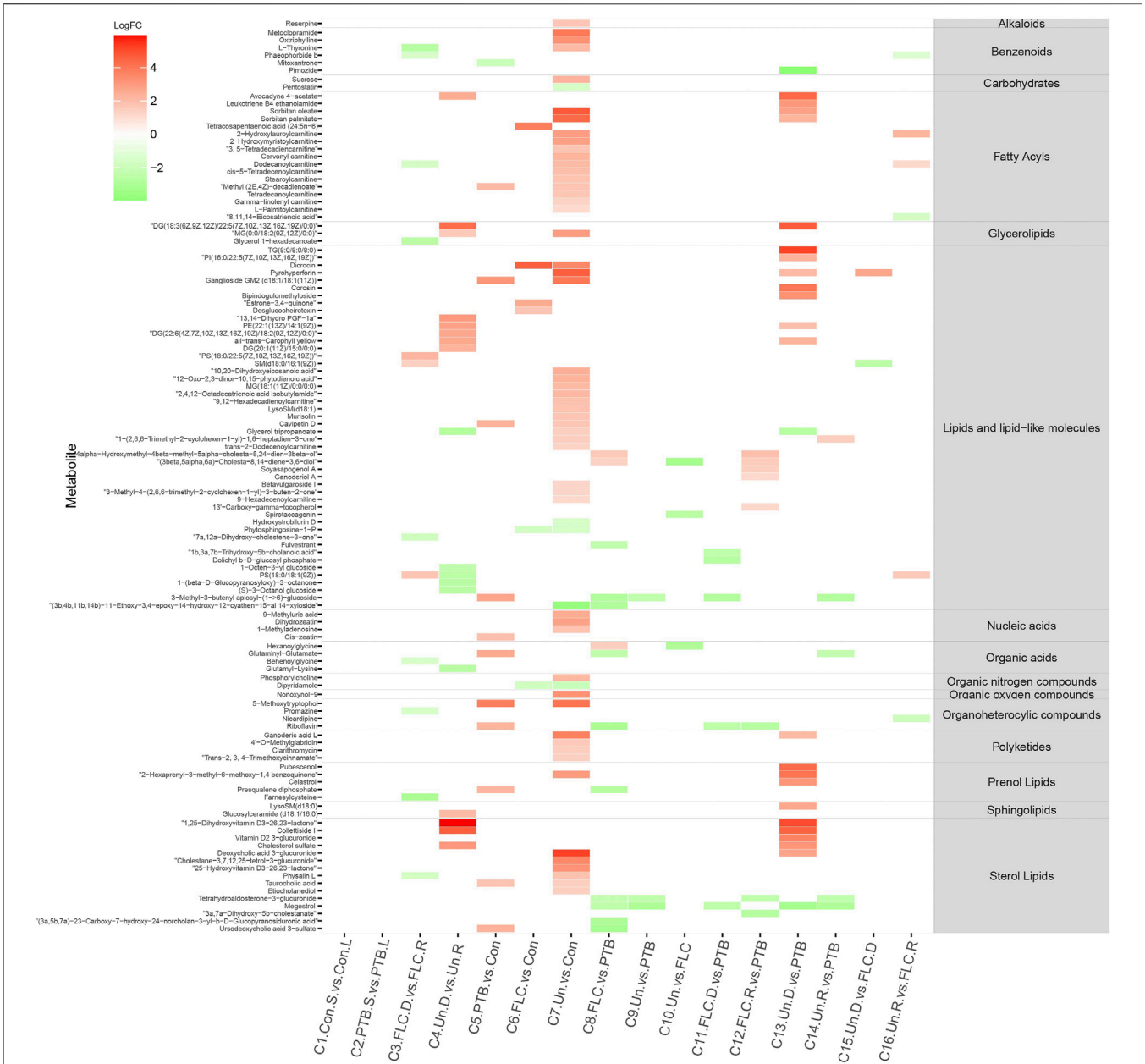

FIGURE 5 | Heat map demonstrating the discriminating metabolites of corresponding comparisons and compound superclass in umbilical cord plasma metabolomes. The $\log_2$ scale matched with gradually changed color shows the relative abundance of a given placental metabolite. Only differential metabolites (p value < 0.05, q value < 0.1, and FC > 2) that can be identified in the SMPDB database are displayed. Blocks with red or green represent higher or lower expression than the denominator group. Abbreviations: con, control; PTB, preterm birth; FLC, fetoscopic laser coagulation; Un, untreated; T, total; S, small; L, large; D, donor; R, recipient.

metabolome and umbilical cord plasma metabolome, metabolic networks were constructed (**Figure 6**). The levels of γ-linolenic acid, pregnenolone, dehydroepiandrosterone sulfate, and (8Z,11Z,14Z)-eicosatrienoic acid in the placental metabolome were significantly different among the multiple comparisons. Regarding the cord plasma metabolic network, the expression of phytosphingosine, tetracosahexaenoic acid, riboflavin, N1,N12-diacetylspermine, bilirubin, and biliverdin was found to be significantly different in many comparisons. Both networks shared similar annexes that center on sphingolipid, glycerophospholipid, linoleic acid, and steroid hormone metabolism.

Next, we conducted topological pathway analyses of each comparison of the placental and cord plasma metabolites. Based on the KEGG database, pertinent pathways of annotated discriminating metabolites (p value < 0.05, q value < 0.1, and FC >

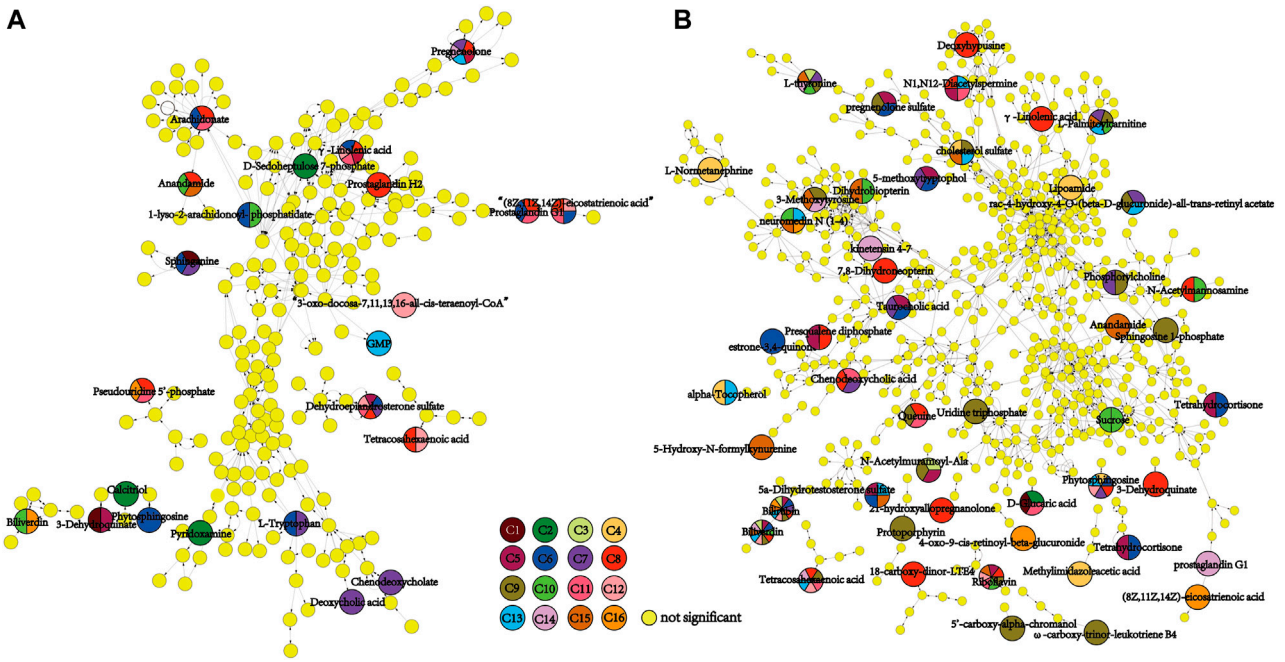

FIGURE 6 | Metabolomic network of discriminating metabolic pathways in the 16 comparisons of placental **(A)** and umbilical cord plasma **(B)** metabolomes. The small yellow dots represent the non-significant metabolites in the pertinent pathways, and the colored dots represent the differential metabolites of the color-matched comparisons. Dots with multiple colors indicate that statistical significance was observed in all color-matched comparisons involved.

2) in those comparisons are shown as bubbles in **Figures 7**, **8** and **Supplementary Figure S4**. In placental tissue, compared with the Con, PTB, and FLC groups, the Un group's metabolome differed in terms of sphingolipid, glycerophospholipid, steroid, and unsaturated fatty acid metabolism (**Figure 7**), which is consistent with the results of the major group comparisons in umbilical cord plasma (**Supplementary Figure S4**). In our separate investigation of the discriminatory metabolic pathway in the umbilical plasma of donors and recipients in the Un and FLC groups compared to the PTB group, similar alterations in the metabolic pathways were observed; however, both the donors and recipients in the FLC group had altered riboflavin metabolism, which was also evident in the comparison of Un-D to FLC-D (**Figure 8**).

Biomarker Analysis of Placental and Umbilical Cord Plasma Metabolites in Corresponding Comparisons

ROC curves for discriminating metabolites in each comparison of placental tissue and cord plasma were generated. **Figure 9** displays representative images with an area under the curve (AUC) > 0.9. For placental comparisons, CE (19:0) was found to have good performance in C9, C10, and C15. Umbilical cord plasma metabolome comparisons had unveiled more potential biomarkers in more comparisons: C3-PC (18:3 (9Z,12Z,15Z) (16:0), bilirubin, l-thyronine, biliverdin; C4 PC (18:2 (9Z,12Z)/16:0), PE (20:5 (5Z,8Z,14Z,17Z (/14:1 (9Z)), sorbitan palmitate, palmitoyglycine, LysoSm (d18:0), C5 dihydrocortisol; C8 riboflavin, glutaminyl-glutamate, and tetrahydroaldosterone-3-glucuronide.

Correlation Analysis of Discriminating Placental Metabolites to Neonatal Birth Weight and Ejection Fraction

We measured neonatal birth weight and LV-EF and correlated these parameters with placental differential metabolites in comparison 10 (Un vs FLC) *via* Spearman's analysis. Metabolites with a p-value < 0.05 are shown in **Table 1**. (9Z,12Z,14E)-16-Hydroxy-9,12,14-octadecatrienoic acid was negatively correlated with birth weight, while SM(d18:1/18:1 (9Z)) was positively correlated with birth weight. Regarding the ejection fraction, six negatively correlated discriminating metabolites, namely, PE (20:2 (11Z,14Z)/15:0), 2-arachiodonylglycerol, PG (18:2 (9Z,12Z)/20:3 (8Z,11Z,14Z), CE (19:0), PE (15:0/14:0), and DG (15:0/0:0/14:1n5), were displayed.

DISCUSSION

TTTS is a highly fatal complication for both fetuses in MCDA pregnancy if left untreated. In recent decades, there have been various improvements in curative methods for TTTS, among which the FLC procedure is the most celebrated and effective one in mitigating birth outcomes. Although it is widely accepted that the pathological communication between different co-twins' parts of the MCDA placenta *via* AVAs is the etiological basis

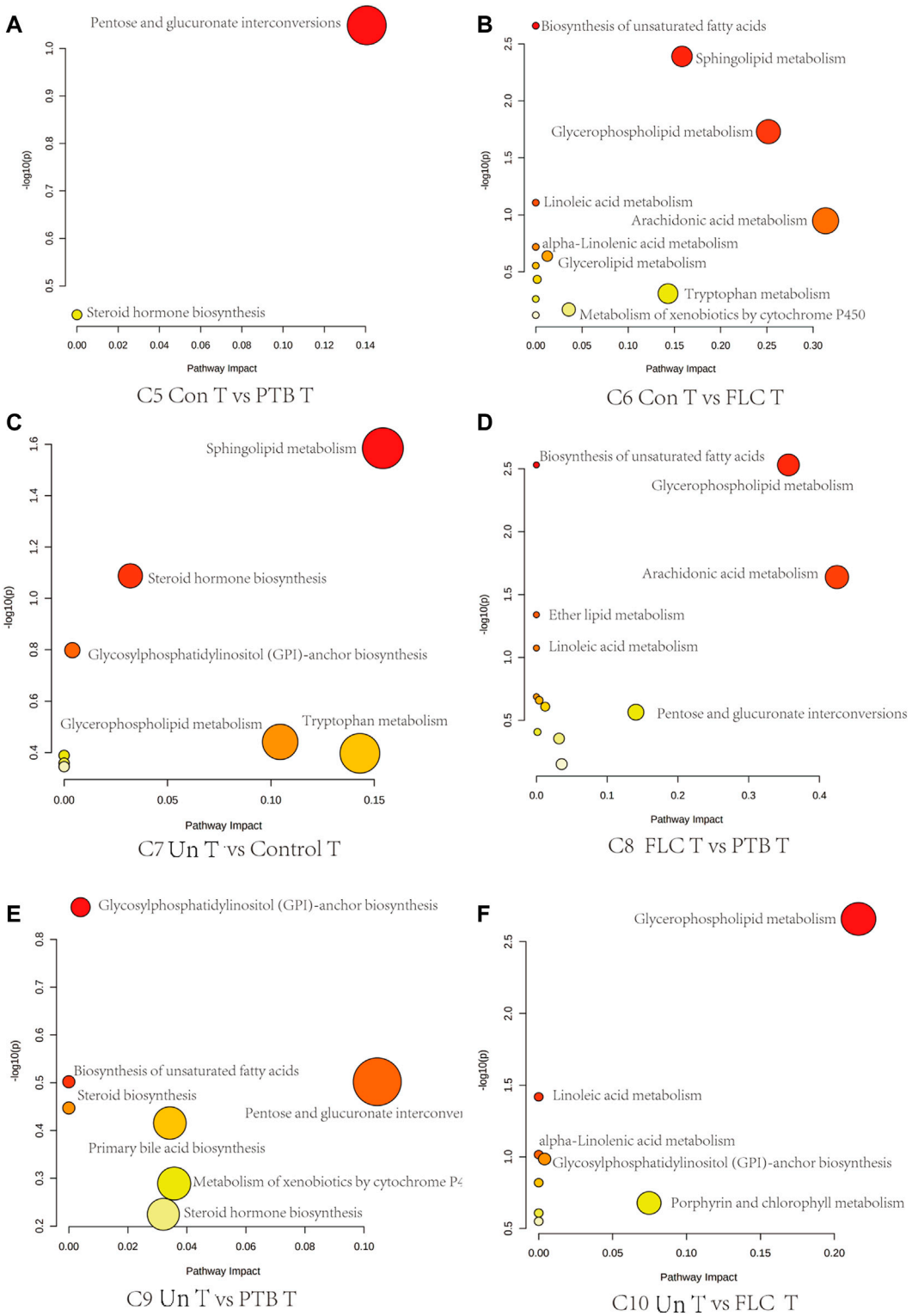

FIGURE 7 | Bubble plots demonstrate the results of quantitative enrichment analysis of comparisons 5–10 in the placental metabolome. The significant metabolic pathways in corresponding comparisons are shown as bubbles in each plot. Bubbles with red and larger size indicate that they are more significant according to their p-values and pathway impact. Abbreviations: C, comparison; Con, control; PTB, preterm birth; FLC, fetoscopic laser coagulation; Un, untreated; T, total; S, small; L, large; D, donor; R, recipient.

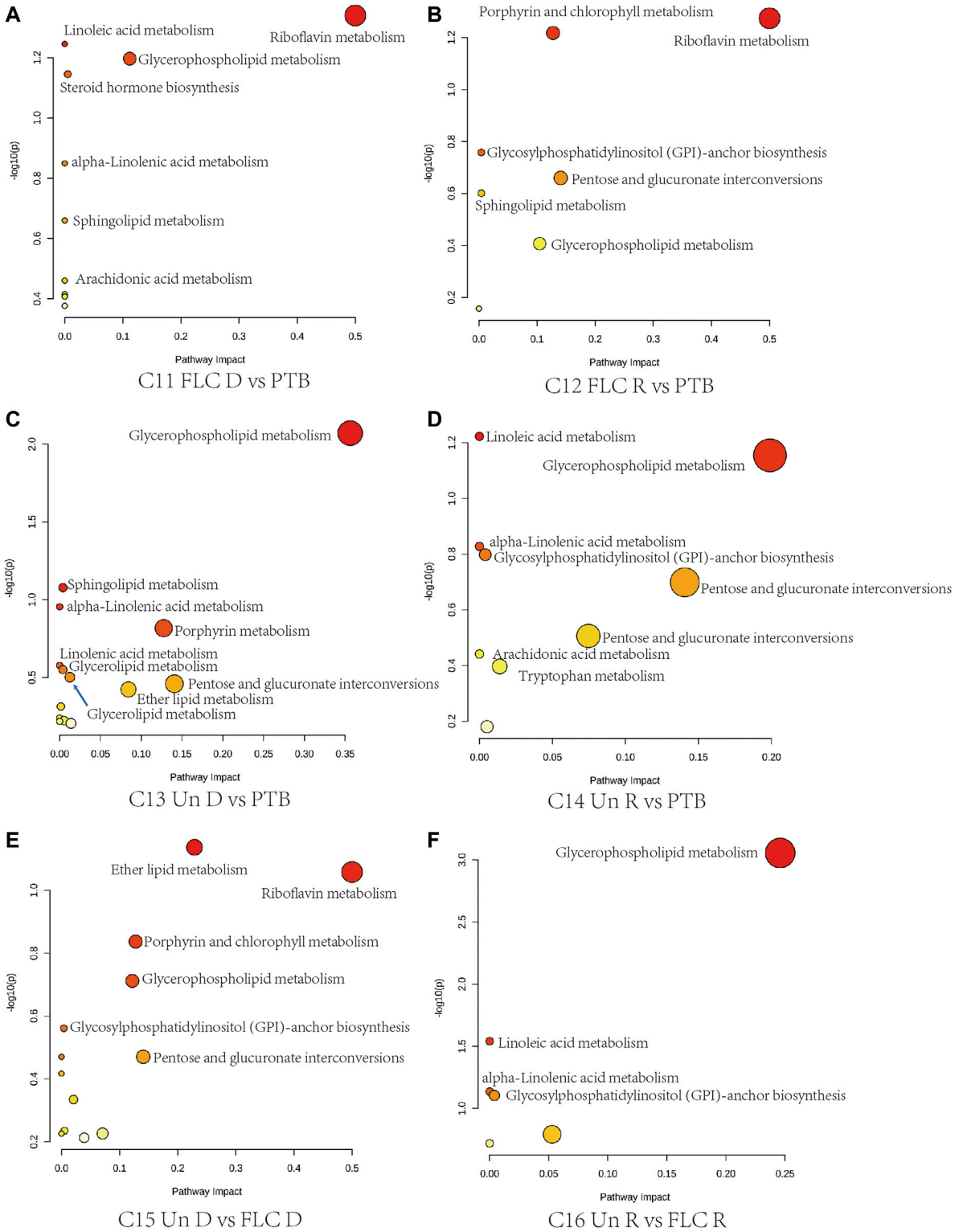

FIGURE 8 | Bubble plots demonstrate the results of quantitative enrichment analysis of comparisons 11–16 in the umbilical cord plasma metabolome. The metabolic pathways with the most significance in corresponding comparisons are shown as bubbles in each plot. Bubbles with red and larger size indicate that they are more significant according to their p-values and pathway impact. Abbreviations: C, comparison; Con, control; PTB, preterm birth; FLC, fetoscopic laser coagulation; Un, untreated; T, total; S, small; L, large; D, donor; R, recipient.

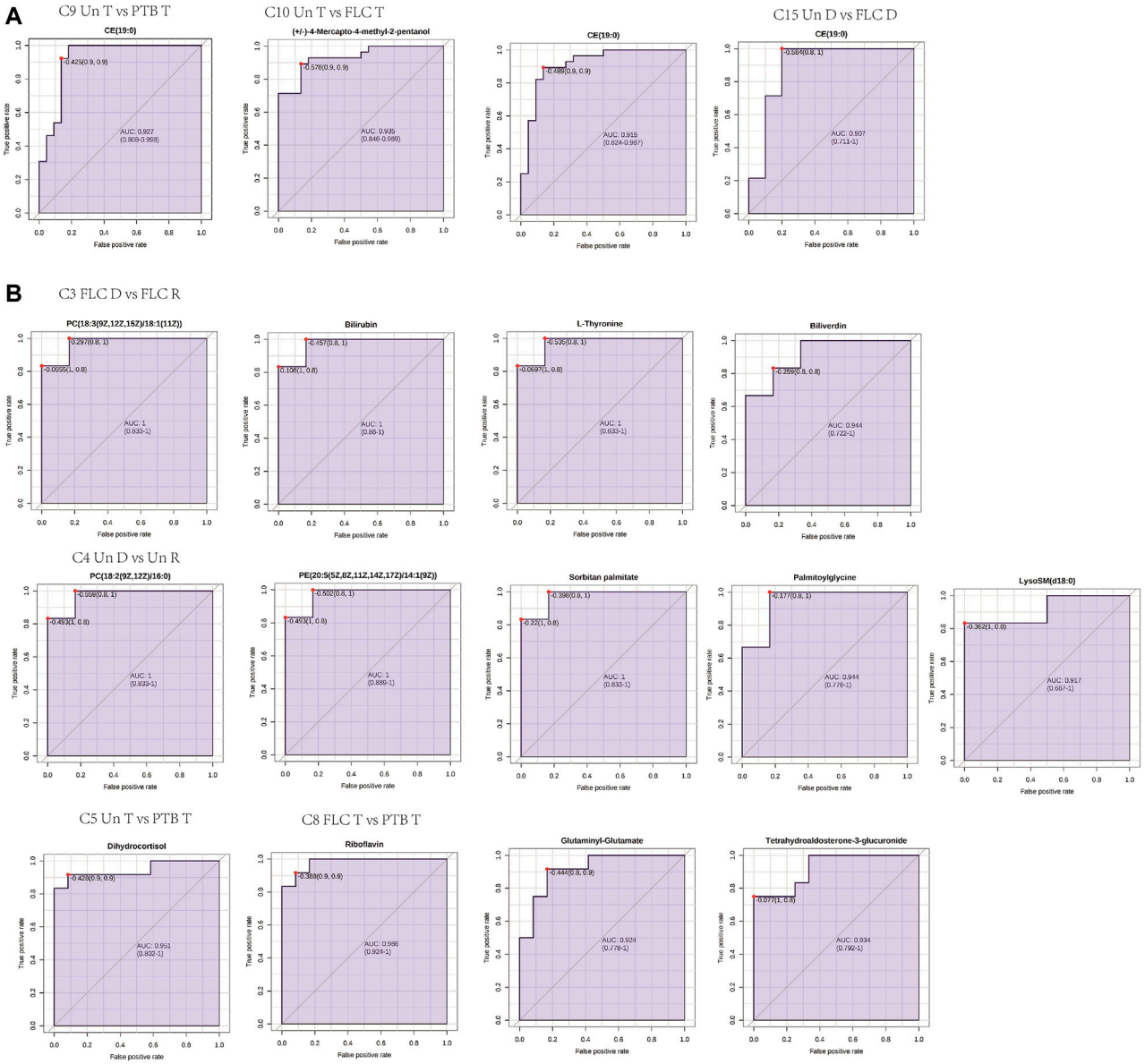

FIGURE 9 | Receiver operating characteristic (ROC) curves of representative metabolites (AUC > 0.9) for corresponding comparisons in placental **(A)** and umbilical cord metabolomes **(B)**. Abbreviations: C, comparison; PTB, preterm birth; FLC, fetoscopic laser coagulation; Un, untreated; T, total; D, donor; R, recipient.

TABLE 1 | Spearman's correlation analysis of placental differential metabolites with birth weight and cardiac function (ejection fraction).

Correlated parameters	Metabolite name	R	p-value
Birth weight	(9Z,12Z,14E)-16-Hydroxy-9,12,14-octadecatrienoic acid	–0.313	0.049
	SM(d18:1/18:1 (9Z))	0.338	0.014
Ejection fraction	PE (20:2 (11Z,14Z)/15:0)	–0.761	<0.001
	2-Arachidonylglycerol	–0.539	0.021
	PG (18:2 (9Z,12Z)/20:3 (8Z,11Z,14Z)	–0.528	0.024
	CE (19:0)	–0.640	0.004
	PE (15:0/14.0)	–0.582	0.011
	DG (15:0/0:0/14:1n5)	–0.545	0.019

for TTTS, the molecular mechanism that drives the sprouting and growth of AVAs remains ambiguous. Moreover, how FLC surgery improves the neonatal outcomes of newborns suffering from TTTS beyond the hemodynamic mechanism has rarely been reported.

By cross comparing the placental or umbilical cord plasma metabolomes of different co-twin groups, this research depicted a holistic metabolomic landscape of the placental tissue and umbilical cord plasma of TTTS pregnancies in the absence or presence of FLC procedures, revealing the different phenotypical metabolomic alterations in the donors and recipients of the Un group. We noticed that the FLC procedure greatly alleviated the metabolic disturbance for both co-twins and led to better neonatal outcomes, making their metabolomes less distinguishable from those of the control and PTB groups. FLC also mitigated birth weight discordance and improved the Apgar scores of FLC neonates. It was also demonstrated that intragroup comparisons of cord plasma metabolomes showed greater difference than the placental metabolomes, thus it can better differentiate the donors and recipients in the FLC and PTB groups. This finding, probably caused by the equalizing effect of vessel communication in the MCDA placenta, is consistent with our previous study on placental and cord plasma metabolomes of SIUGR (Wang et al., 2018).

The placental metabolomes also revealed that, compared with the control, PTB, and FLC groups, the untreated group had lower expression mainly of sterol lipids, fatty acyls, and lipids and lipid-like molecules, which are involved in sphingolipid metabolism, steroid hormone biosynthesis, glycerophospholipid metabolism, and biosynthesis of unsaturated fatty acids, among other metabolic processes. On the other hand, the cord plasma metabolomes indicated that the Un group also experienced perturbations in riboflavin metabolism and porphyrin metabolism compared to their counterparts in the FLC and PTB groups. Moreover, this study showed that among the placental metabolites, CE (19:0), a cholesteryl ester also known as cholesteryl nonadecanoic acid, has a strong diagnostic ability in distinguishing Un from PTB and FLC groups. In addition, glycerophospholipids such as PC (16:0/18:3 (9Z,12Z,15Z)), PC (18:2 (9Z,12Z)/16:0), PE (20:5 (5Z,8Z,14Z,17Z (/14:1 (9Z)), and sphingolipids such as LysoSm (d18:0) were all found to have high AUCs (>0.9) in discriminating donors and recipients in the Un or FLC group. By relating the differential metabolites with the birth weight and ejection fraction, we noticed that the cholesteryl ester CE (19:0) and glycerophospholipids including PE (15:0/14:0), PE (20:2 (11Z,14Z)/15:0), and PG (18:2 (9Z,12Z)/20:3 (8Z,11Z,14Z) were negatively correlated with ejection fraction and that SM (d18:1/18:1 (9Z)), a sphingolipid, was positively correlated with birth weight. Such a correlation between bound lipids and birth weight or neonatal echocardiographic measurements was also found in the cord plasma or amniotic fluid metabolome by many previous studies (Dunn et al., 2016; Hellmuth et al., 2017).

To date, evidence from previous studies that provides comprehensive insights into the metabolic aspects of TTTS has been exceedingly rare. Some studies have shed some light on certain types of metabolites or cytokines, such as iron, natriuretic peptides (Bajoria et al., 2002), circulating or placental angiogenic factors (Yinon et al., 2014; Chon et al., 2018), and amino acids (Bajoria et al., 2000). Until recently, by investigating the amniotic fluid metabolomes of the recipient co-twin of TTTS pregnancies that underwent FLC surgery, Dunn observed disrupted carbohydrate and fatty acid metabolism and found its correlation with fetal cardiovascular functions (Dunn et al., 2016). However, since the metabolites in the amniotic fluid could be secreted by the placenta or fetal organs and their secretion could be induced by trophoblast or vessel destruction in FLC surgery or amniodrainage, we still lack solid evidence to confirm the sources of these perturbed metabolites and their role in the pathogenesis of TTTS. Another newly published retrospective cohort study conducted by our team also reported disrupted amino acid and fatty acid metabolism in serum samples prospectively collected during the first gestational trimester of TTTS pregnancies (Yang et al., 2021).

However, there are no published articles on the holistic metabolomic profile of donor co-twins or recipient co-twins in TTTS-complicated umbilical cord plasma and placental tissue or the metabolic change brought by FLC surgery in those two types of samples. Kumazaki reported that the villi on the donor side of the TTTS-complicated monochorionic placenta have higher expression of pro-angiogenetic factors such as VEGF, Flt-1, and KDR (Kumazaki et al., 2002), implying that potential overactive angiogenesis may exist in the donor part of the TTTS placenta. Since the angiogenetic activity of endothelial cells mainly consumes energy substrates such as glucose, amino acids (AAs), and fatty acids (Bruning et al., 2018; Eelen et al., 2018), it would inevitably change the metabolomic profile of the TTTS placenta and even of the cord blood. For the fetus, the imbalanced circulation volume of both the donor and recipient co-twin, brought by the intertwining AVA, would also trigger the release or suppression of renin–angiotensin system (RAS) components and atrial natriuretic peptide (Mosquera et al., 2012), change the profile of fetal cardiac nutrients and oxygen supply for both co-twins (recipient heart receives too much blood, while donor gets deficient cardiac blood perfusion, nutrition, and oxygen supply), and cause cardiac anomalies in the recipients (hypervolemia leads to the hypertrophy and dilation of recipients' heart) (Galea et al., 2005). Alternatively, in another hypothetical scenario, the metabolomic disparity could be the consequence of the TTTS or, more specifically, the AVAs, as data from both our group and others show that the FLC procedure brought significant changes to or improvements in the relative concentrations of hundreds of metabolites in the amniotic fluid, placental tissue or umbilical cord plasma (Dunn et al., 2016). Therefore, the metabolic clues in such tissues or fluids are of great significance for the elucidation of the etiological and pathophysiological machinery of TTTS.

In the present study, disrupted fatty acid metabolism was observed in untreated TTTS fetuses' umbilical cord plasma and placental tissue, which is consistent with our previous finding in the later diagnosed TTTS maternal serum collected at early pregnancy (Yang et al., 2021). Compared with the FLC-treated group, the Un group had lower alpha-linolenic acid metabolism in placental metabolomes, and the recipients in the Un group also had less active biosynthesis of unsaturated fatty acids in the cord

plasma metabolome. Even after the FLC procedures, the placental metabolomes of the FLC group still showed downregulated expression of arachidonic acid and linoleic acid metabolism compared to the PTB group. Many previous studies have reported the essential role of fatty acids in angiogenetic activities and the correlation of many adverse birth outcomes with disturbed fatty acid metabolism (Yang et al., 2018). Fatty acids can be transported and metabolized by endothelial cells (Eelen et al., 2018) and trophoblasts (Lewis et al., 2018), providing substrates and ATP for angiogenesis (Basak and Duttaroy, 2013) and facilitating the proliferation of human umbilical vein smooth muscle cells (Li et al., 2013) and tube formation by trophoblasts in early gestation (Johnsen et al., 2011). Moreover, essential fatty acids can also function as precursors for producing vasoactive substances for the fetus and influence fetal insulin sensitivity and neurodevelopment (Lewis et al., 2018), which may account for the pathogenesis of neural sequelae and endocrinal dysfunction in TTTS fetuses. Furthermore, in the setting of TTTS, the increased overload in recipients could lead to fetal cardiac prematurity (Pruetz et al., 2015), which may change the myocardium metabolic preference from carbohydrates to fatty acids (Lopaschuk et al., 1992), thus consuming more fatty acids and leading to phenotypic metabolomic differences.

Our findings provide novel insights into the pathophysiology of TTTS: metabolomic disturbance may play a role in the development of pathological AVA in the MCDA placenta, and the altered metabolic profile might be relevant to cardiac anomalies. These findings may not only present new clues for improving diagnostic methods of TTTS pregnancies but also promote refinement for current therapeutic approaches and even inspire novel pharmacological intervention for cases in which the besting timing of FLC surgery is missed. To investigate the correlation of differential metabolites and neurological or cardiac sequelae in neonates complicated by TTTS, further follow-up of the neonates in this study is needed. Moreover, although this research has pointed out that altered fatty acid, lipid, and lipid-like molecule metabolism is involved in the pathogenesis of TTTS, how these metabolic pathways impact the sprouting and growth of AVA and the hemodynamics of co-twins during pregnancy still lacks a clear explanation; thus, prospective animal experiments are needed to provide *in vivo* evidence.

CONCLUSION

FLC surgery greatly mitigates the metabolomic disturbance brought by the TTTS in the placental tissue and cord plasma, which centers mainly on fatty acid and lipid-like molecule metabolism and thus makes the placental and cord plasma metabolomes of FLC-treated twins close to the control or PTB MCDA co-twins. Certain subsets of compounds, especially lipid derivatives, are helpful in differentiating co-twins with different hemodynamic statuses and are significantly correlated with birth weight or neonatal ejection fraction.

DATA AVAILABILITY STATEMENT

The raw data supporting the conclusions of this article will be made available by the authors, without undue reservation.

ETHICS STATEMENT

The studies involving human participants were reviewed and approved by the Ethical Committee of Chongqing Medical University. The patients/participants provided their written informed consent to participate in this study.

AUTHOR CONTRIBUTIONS

LW, CT and HQ designed the study. TL contributed to the sample collection, data analysis, and drafting of this research. SH and JL performed the FLC surgery. LZ and HF participated in the patient recruitment and data collection. T-lH performed part of the data analysis. RS, PB and MK gave their critical review and suggestion. All authors showed their approval for the publication of current study.

FUNDING

This study was funded by the National Natural Science Foundation of China (U21A20346, 82171662 and 82001580), the Chongqing Science and Technology Commission (cstc2019jcyj-msxmX0856, cstc2021ycjh-bgzxm0192), and the Chongqing Health Committee (2019GDRC012, 2020MSXM037).

ACKNOWLEDGMENTS

We are grateful to the families who participated in this study and all clinical staff involved in the study group.

SUPPLEMENTARY MATERIAL

The Supplementary Material for this article can be found online at: https://www.frontiersin.org/articles/10.3389/fbioe.2022.786755/full#supplementary-material

REFERENCES

Bajoria, R., Hancock, M., Ward, S., D'Souza, S. W., and Sooranna, S. R. (2000). Discordant Amino Acid Profiles in Monochorionic Twins with Twin-Twin Transfusion Syndrome. *Pediatr. Res.* 48 (6), 821–828. doi:10.1203/00006450-200012000-00020

Bajoria, R., Ward, S., and Chatterjee, R. (2002). Natriuretic Peptides in the Pathogenesis of Cardiac Dysfunction in the Recipient Fetus of Twin-Twin Transfusion Syndrome. *Am. J. Obstet. Gynecol.* 186 (1), 121–127. doi:10.1067/mob.2002.118845

Basak, S., and Duttaroy, A. K. (2013). Effects of Fatty Acids on Angiogenic Activity in the Placental Extravillious Trophoblast Cells. *Prostaglandins Leukot. Essent. Fatty Acids* 88 (2), 155–162. doi:10.1016/j.plefa.2012.10.001

Bruning, U., Morales-Rodriguez, F., Kalucka, J., Goveia, J., Taverna, F., Queiroz, K. C. S., et al. (2018). Impairment of Angiogenesis by Fatty Acid Synthase Inhibition Involves mTOR Malonylation. *Cel Metab.* 28 (6), 866–880. doi:10.1016/j.cmet.2018.07.019

Chen, J., Zhang, S., Chen, C., Jiang, X., Qiu, J., Qiu, Y., et al. (2020). Crosstalk of Gut Microbiota and Serum/hippocampus Metabolites in Neurobehavioral Impairments Induced by Zinc Oxide Nanoparticles. *Nanoscale* 12 (41), 21429–21439. doi:10.1039/d0nr04563b

Chon, A. H., Chavira, E. R., Wilson, M. L., Ingles, S. A., Llanes, A., and Chmait, R. H. (2018). The Impact of Laser Surgery on Angiogenic and Anti-angiogenic Factors in Twin-Twin Transfusion Syndrome: a Prospective Study. *J. Maternal Fetal Neonatal Med.* 31 (8), 1085–1091. doi:10.1080/14767058.2017.1309020

Diehl, W., Diemert, A., Grasso, D., Sehner, S., Wegscheider, K., and Hecher, K. (2017). Fetoscopic Laser Coagulation in 1020 Pregnancies with Twin-Twin Transfusion Syndrome Demonstrates Improvement in Double-Twin Survival Rate. *Ultrasound Obstet. Gynecol.* 50 (6), 728–735. doi:10.1002/uog.17520

Dunn, W. B., Allwood, J. W., Van Mieghem, T., Morris, R. K., Mackie, F. L., Fox, C. E., et al. (2016). Carbohydrate and Fatty Acid Perturbations in the Amniotic Fluid of the Recipient Twin of Pregnancies Complicated by Twin-Twin Transfusion Syndrome in Relation to Treatment and Fetal Cardiovascular Risk. *Placenta* 44, 6–12. doi:10.1016/j.placenta.2016.05.012

Eelen, G., de Zeeuw, P., Treps, L., Harjes, U., Wong, B. W., and Carmeliet, P. (2018). Endothelial Cell Metabolism. *Physiol. Rev.* 98 (1), 3–58. doi:10.1152/physrev.00001.2017

Ernst, M., Rogers, S., Lausten-Thomsen, U., Björkbom, A., Laursen, S. S., Courraud, J., et al. (2020). Gestational Age-dependent Development of the Neonatal Metabolome. *Pediatr. Res.* 89, 1396–1404. doi:10.1038/s41390-020-01149-z

Galea, P., Jain, V., and Fisk, N. M. (2005). Insights into the Pathophysiology of Twin-Twin Transfusion Syndrome. *Prenat. Diagn.* 25 (9), 777–785. doi:10.1002/pd.1264

Gao, J., Tarcea, V. G., Karnovsky, A., Mirel, B. R., Weymouth, T. E., Beecher, C. W., et al. (2010). Metscape: a Cytoscape Plug-In for Visualizing and Interpreting Metabolomic Data in the Context of Human Metabolic Networks. *Bioinformatics* 26 (7), 971–973. doi:10.1093/bioinformatics/btq048

Hack, K., Derks, J., Elias, S., Franx, A., Roos, E., Voerman, S., et al. (2008). Increased Perinatal Mortality and Morbidity in Monochorionic versus Dichorionic Twin Pregnancies: Clinical Implications of a Large Dutch Cohort Study. *BJOG* 115 (1), 58–67. doi:10.1111/j.1471-0528.2007.01556.x

Hellmuth, C., Uhl, O., Standl, M., Demmelmair, H., Heinrich, J., Koletzko, B., et al. (2017). Cord Blood Metabolome Is Highly Associated with Birth Weight, but Less Predictive for Later Weight Development. *Obes. Facts* 10 (2), 85–100. doi:10.1159/000453001

Johnsen, G. M., Basak, S., Weedon-Fekjær, M. S., Staff, A. C., and Duttaroy, A. K. (2011). Docosahexaenoic Acid Stimulates Tube Formation in First Trimester Trophoblast Cells, HTR8/SVneo. *Placenta* 32 (9), 626–632. doi:10.1016/j.placenta.2011.06.009

Kumazaki, K., Nakayama, M., Suehara, N., and Wada, Y. (2002). Expression of Vascular Endothelial Growth Factor, Placental Growth Factor, and Their Receptors Flt-1 and KDR in Human Placenta under Pathologic Conditions. *Hum. Pathol.* 33 (11), 1069–1077. doi:10.1053/hupa.2002.129420

Lewi, L., Jani, J., Blickstein, I., Huber, A., Gucciardo, L., Van Mieghem, T., et al. (2008). The Outcome of Monochorionic Diamniotic Twin Gestations in the Era of Invasive Fetal Therapy: a Prospective Cohort Study. *Am. J. Obstet. Gynecol.* 199 (5), 514. doi:10.1016/j.ajog.2008.03.050

Lewis, R. M., Wadsack, C., and Desoye, G. (2018). Placental Fatty Acid Transfer. *Curr. Opin. Clin. Nutr. Metab. Care* 21 (2), 78–82. doi:10.1097/mco.0000000000000443

Li, X.-P., Luo, T., Li, J., Fan, Y.-W., Liu, R., Hu, J.-N., et al. (2013). Linolelaidic Acid Induces a Stronger Proliferative Effect on Human Umbilical Vein Smooth Muscle Cells Compared to Elaidic Acid. *Lipids* 48 (4), 395–403. doi:10.1007/s11745-012-3754-2

Liang, L., Rasmussen, M.-L. H., Piening, B., Shen, X., Chen, S., Röst, H., et al. (2020). Metabolic Dynamics and Prediction of Gestational Age and Time to Delivery in Pregnant Women. *Cell* 181 (7), 1680–1692. doi:10.1016/j.cell.2020.05.002

Lopaschuk, G. D., Collins-Nakai, R. L., and Itoi, T. (1992). Developmental Changes in Energy Substrate Use by the Heart. *Cardiovasc. Res.* 26 (12), 1172–1180. doi:10.1093/cvr/26.12.1172

Melhem, N. Z., Ledermann, S., and Rees, L. (2019). Chronic Kidney Disease Following Twin-To-Twin Transfusion Syndrome-Long-Term Outcomes. *Pediatr. Nephrol.* 34 (5), 883–888. doi:10.1007/s00467-018-4176-z

Mertens, L., Seri, I., Marek, J., Arlettaz, R., Barker, P., McNamara, P., et al. (2011). Targeted Neonatal Echocardiography in the Neonatal Intensive Care Unit: Practice Guidelines and Recommendations for Training. *J. Am. Soc. Echocard.* 24 (10), 1057–1078. doi:10.1016/j.echo.2011.07.014

Michelfelder, E., Tan, X., Cnota, J., Divanovic, A., Statile, C., Lim, F.-Y., et al. (2015). Prevalence, Spectrum, and Outcome of Right Ventricular Outflow Tract Abnormalities in Twin-Twin Transfusion Syndrome: A Large, Single-center Experience. *Congenit. Heart Dis.* 10 (3), 209–218. doi:10.1111/chd.12215

Middeldorp, J., Lopriore, E., Sueters, M., Klumper, F., Kanhai, H., Vandenbussche, F., et al. (2007). Twin-to-twin Transfusion Syndrome after 26 Weeks of Gestation: Is There a Role for Fetoscopic Laser Surgery? *BJOG: Int. J. Obstet. Gynaecol.* 114 (6), 694–698. doi:10.1111/j.1471-0528.2007.01337.x

Morris, R., Selman, T., Harbidge, A., Martin, W., and Kilby, M. (2010). Fetoscopic Laser Coagulation for Severe Twin-To-Twin Transfusion Syndrome: Factors Influencing Perinatal Outcome, Learning Curve of the Procedure and Lessons for New Centres. *BJOG* 117 (11), 1350–1357. doi:10.1111/j.1471-0528.2010.02680.x

Mosquera, C., Miller, R. S., and Simpson, L. L. (2012). Twin-twin Transfusion Syndrome. *Semin. Perinatol.* 36 (3), 182–189. doi:10.1053/j.semperi.2012.02.006

Ong, S., Zamora, J., Khan, K., and Kilby, M. (2006). Prognosis for the Co-twin Following Single-Twin Death: a Systematic Review. *BJOG* 113 (9), 992–998. doi:10.1111/j.1471-0528.2006.01027.x

Phad, N., and Waal, K. (2020). Left Ventricular Ejection Fraction Using Manual and Semi-automated Biplane Method of Discs in Very Preterm Infants. *Echocardiography* 37 (8), 1265–1271. doi:10.1111/echo.14784

Pruetz, J. D., Schrager, S. M., Wang, T. V., Llanes, A., Chmait, R. H., and Vanderbilt, D. L. (2015). Blood Pressure Evaluation in Children Treated with Laser Surgery for Twin-Twin Transfusion Syndrome at 2-year Follow-Up. *Am. J. Obstet. Gynecol.* 213 (3), e1–417. doi:10.1016/j.ajog.2015.05.031

Quintero, R. A., Morales, W. J., Allen, M. H., Bornick, P. W., Johnson, P. K., and Kruger, M. (1999). Staging of Twin-Twin Transfusion Syndrome. *J. Perinatol.* 19 (8 Pt 1), 550–555. doi:10.1038/sj.jp.7200292

Ruano, R., Rodo, C., Peiro, J. L., Shamshirsaz, A. A., Haeri, S., Nomura, M. L., et al. (2013). Fetoscopic Laser Ablation of Placental Anastomoses in Twin-Twin Transfusion Syndrome Using 'Solomon Technique'. *Ultrasound Obstet. Gynecol.* 42 (4), 434. doi:10.1002/uog.12492

Sebire, N. J., Souka, A., Skentou, H., Geerts, L., and Nicolaides, K. H. (2000). Early Prediction of Severe Twin-To-Twin Transfusion Syndrome. *Hum. Reprod.* 15 (9), 2008–2010. doi:10.1093/humrep/15.9.2008

Senat, M.-V., Deprest, J., Boulvain, M., Paupe, A., Winer, N., and Ville, Y. (2004). Endoscopic Laser Surgery versus Serial Amnioreduction for Severe Twin-To-Twin Transfusion Syndrome. *N. Engl. J. Med.* 351 (2), 136–144. doi:10.1056/NEJMoa032597

Simpson, L. L., and Simpson, L. L. (2013). Twin-twin Transfusion Syndrome. *Am. J. Obstet. Gynecol.* 208 (1), 3–18. doi:10.1016/j.ajog.2012.10.880

Slaghekke, F., Lopriore, E., Lewi, L., Middeldorp, J. M., van Zwet, E. W., Weingertner, A.-S., et al. (2014). Fetoscopic Laser Coagulation of the Vascular Equator versus Selective Coagulation for Twin-To-Twin

Transfusion Syndrome: an Open-Label Randomised Controlled Trial. *Lancet* 383 (9935), 2144–2151. doi:10.1016/S0140-6736(13)62419-8

Stirnemann, J. J., Mougeot, M., Proulx, F., Nasr, B., Essaoui, M., Fouron, J. C., et al. (2010). Profiling Fetal Cardiac Function in Twinâ€"twin Transfusion Syndrome. *Ultrasound Obstet. Gynecol.* 35 (1), 19–27. doi:10.1002/uog.7488

Tissot, C., Singh, Y., and Sekarski, N. (2018). Echocardiographic Evaluation of Ventricular Function-For the Neonatologist and Pediatric Intensivist. *Front. Pediatr.* 6, 79. doi:10.3389/fped.2018.00079

van Klink, J. M. M., Koopman, H. M., Rijken, M., Middeldorp, J. M., Oepkes, D., and Lopriore, E. (2016). Long-Term Neurodevelopmental Outcome in Survivors of Twin-To-Twin Transfusion Syndrome. *Twin Res. Hum. Genet.* 19 (3), 255–261. doi:10.1017/thg.2016.26

Van Mieghem, T., Klaritsch, P., Doné, E., Gucciardo, L., Lewi, P., Verhaeghe, J., et al. (2009). Assessment of Fetal Cardiac Function before and after Therapy for Twin-To-Twin Transfusion Syndrome. *Am. J. Obstet. Gynecol.* 200 (4), e1–400. doi:10.1016/j.ajog.2009.01.051

Wang, L., Han, T.-L., Luo, X., Li, S., Young, T., Chen, C., et al. (2018). Metabolic Biomarkers of Monochorionic Twins Complicated with Selective Intrauterine Growth Restriction in Cord Plasma and Placental Tissue. *Sci. Rep.* 8 (1), 15914. doi:10.1038/s41598-018-33788-y

Wen, L., Wu, Y., Yang, Y., Han, T.-l., Wang, W., Fu, H., et al. (2019). Gestational Diabetes Mellitus Changes the Metabolomes of Human Colostrum, Transition Milk and Mature Milk. *Med. Sci. Monit.* 25, 6128–6152. doi:10.12659/MSM.915827

Wu, Y., Yu, J., Liu, X., Wang, W., Chen, Z., Qiao, J., et al. (2021). Gestational Diabetes Mellitus-Associated Changes in the Breast Milk Metabolome Alters the Neonatal Growth Trajectory. *Clin. Nutr.* 40 (6), 4043–4054. doi:10.1016/j.clnu.2021.02.014

Yang, X., Xu, P., Zhang, F., Zhang, L., Zheng, Y., Hu, M., et al. (2018). AMPK Hyper-Activation Alters Fatty Acids Metabolism and Impairs Invasiveness of Trophoblasts in Preeclampsia. *Cell Physiol. Biochem.* 49 (2), 578–594. doi:10.1159/000492995

Yang, Y., Wen, L., Han, T. l., Zhang, L., Fu, H., Gan, J., et al. (2021). Twin-twin Transfusion Syndrome is Associated with Alterations in the Metabolic Profile of Maternal Plasma in Early Gestation: a Pilot Study. *Prenatal Diagn.* 41, 1080–1088. doi:10.1002/pd.5933

Yinon, Y., Ben Meir, E., Berezowsky, A., Weisz, B., Schiff, E., Mazaki-Tovi, S., et al. (2014). Circulating Angiogenic Factors in Monochorionic Twin Pregnancies Complicated by Twin-To-Twin Transfusion Syndrome and Selective Intrauterine Growth Restriction. *Am. J. Obstet. Gynecol.* 210 (2), 141–147. doi:10.1016/j.ajog.2013.09.022

Conflict of Interest: The authors declare that the research was conducted in the absence of any commercial or financial relationships that could be construed as a potential conflict of interest.

Publisher's Note: All claims expressed in this article are solely those of the authors and do not necessarily represent those of their affiliated organizations, or those of the publisher, the editors, and the reviewers. Any product that may be evaluated in this article, or claim that may be made by its manufacturer, is not guaranteed or endorsed by the publisher.

frontiers | Frontiers in Bioengineering and Biotechnology

SYSTEMATIC REVIEW
published: 26 May 2022
doi: 10.3389/fbioe.2022.809528

Pre-Eclampsia Biomarkers for Women With Type 1 Diabetes Mellitus: A Comprehensive Review of Recent Literature

Katrina Z. Freimane[1], *Lauren Kerrigan*[1], *Kelly-Ann Eastwood*[2,3] *and Chris J. Watson*[1]*

[1]*Wellcome-Wolfson Institute for Experimental Medicine, Queen's University Belfast, Belfast, United Kingdom,* [2]*School of Medicine, Dentistry and Biomedical Sciences, Centre for Public Health, Queen's University Belfast, Belfast, United Kingdom,* [3]*Department of Fetal Medicine, St. Michael's Hospital, University Hospitals Bristol and Weston NHS Foundation Trust, Bristol, United Kingdom*

Background: Pre-eclampsia is a serious consideration for women with type 1 diabetes mellitus (T1DM) planning pregnancy. Risk stratification strategies, such as biomarkers measured in the first trimester of pregnancy, could help identify high-risk women. The literature on T1DM-specific pre-eclampsia biomarkers is expanding. We aimed to provide a narrative review of recently published evidence to identify the most promising biomarker candidates that could be targeted for clinical implementation in existing PE models.

Methods: A search using MeSH terms was carried out of Medline, EMBASE, Maternity and Infant Care, Web of Science, and Scopus for relevant papers published since 2015 inclusive and in English. The time limit was applied from the publication of the preceding systematic review in this field. Included studies had pre-eclampsia as a primary outcome, measured one or more serum, plasma or urine biomarkers at any time during pregnancy, and had a distinct group of women with T1DM who developed pre-eclampsia. Studies with pre-eclampsia as a composite outcome were not considered. No restrictions on study types were applied. A narrative synthesis approach was adopted for analysis.

Results: A total of 510 records were screened yielding 18 eligible studies relating to 32 different biomarkers. Higher first-trimester levels of HbA1c and urinary albumin were associated with an increased risk of pre-eclampsia development in women with T1DM. Urinary neutrophil gelatinase-associated lipocalin and adipokines were novel biomarkers showing moderate predictive ability before 15 gestational weeks. Two T1DM-specific pre-eclampsia prediction models were proposed, measuring adipokines or urinary neutrophil gelatinase-associated lipocalin together with easily attainable maternal clinical characteristics. Contradicting previous literature, pre-eclampsia risk in women with T1DM was correlated with vitamin D levels and atherogenic lipid profile in the context of haptoglobin phenotype 2-2. Pregnancy-associated plasma protein-A and soluble endoglin did not predict pre-eclampsia in women with T1DM, and soluble Fms-like tyrosine kinase 1 only predicted pre-eclampsia from the third trimester.

OPEN ACCESS

Edited by:
Vesna Garovic,
Mayo Clinic, United States

Reviewed by:
Martin Mueller,
University Hospital Bern, Switzerland
Reem El-Gendy,
University of Leeds, United Kingdom

****Correspondence:***
Chris J. Watson
chris.watson@qub.ac.uk

Specialty section:
This article was submitted to Preclinical Cell and Gene Therapy, a section of the journal Frontiers in Bioengineering and Biotechnology

Received: *05 November 2021*
Accepted: *21 April 2022*
Published: *26 May 2022*

Citation:
Freimane KZ, Kerrigan L, Eastwood K-A and Watson CJ (2022) Pre-Eclampsia Biomarkers for Women With Type 1 Diabetes Mellitus: A Comprehensive Review of Recent Literature. Front. Bioeng. Biotechnol. 10:809528. doi: 10.3389/fbioe.2022.809528

Conclusion: Maternally derived biomarkers reflecting glycemic control, insulin resistance and renal dysfunction performed better as PE predictors among women with T1DM than those derived from the placenta. These biomarkers could be trialed in current PE prediction algorithms to tailor them for women with T1DM.

Keywords: pre-eclampsia (PE), type 1 diabetes mellitus, biomarkers, pregnancy complications, pregestational diabetes, narrative review

INTRODUCTION

Pre-eclampsia (PE) is a hypertensive multisystem disorder of pregnancy that has been subject to intense research scrutiny. Its pathophysiology and factors dictating maternal susceptibility remain incompletely understood. The mortality and morbidity burden of PE is high, with women in low- and middle-income countries disproportionately affected (Say et al., 2014). Delivery remains the only definitive cure presenting a clinical dilemma where fetal maturity is balanced against maternal risks of continuing the pregnancy (National Institute for Health and Care Excellence (NICE), 2019). Women with pregestational type 1 diabetes mellitus (T1DM) have a five-fold risk of PE compared to the general population (Weissgerber and Mudd, 2015), with the risk even higher with pre-existing diabetic microvascular disease (Leguizamón et al., 2015).

Management of pregnancy with T1DM is challenging and resource-intensive. Current practice includes the initiation of aspirin prophylaxis from 12 weeks' gestation (National Institute for Health and Care Excellence (NICE), 2019; American College of Obstetrics and Gynecology (ACOG), 2018), although some cohorts of high-risk women have been resistant to aspirin therapy (Caritis et al., 1998; Villa et al., 2013; Rolnik et al., 2017a). No clinical trials have been carried out randomizing women with T1DM to aspirin or placebo prior to 12 weeks' gestation with an ongoing phase III randomized controlled trial by Finnegan et al. (2019) using placental dysfunction as a composite outcome. Prediction and risk stratification remain research priorities in this high-risk group and preventatives other than aspirin are yet to be found. Alleviation of the highly medicalized pregnancy course for women with T1DM is vital to improve patient satisfaction and optimize the use of healthcare resources, considerations relevant to an increasingly overwhelmed health service. A biomarker for PE specific to pregnancies complicated by T1DM has the potential to address this need.

Women with T1DM have been historically underrepresented in PE research (Weissgerber and Mudd, 2015), resulting in an unclear understanding of what accounts for the exaggerated PE risk in this group. No major advances have been made in this field since White's classification (White, 1949) and generalizing findings from studies of existing PE prediction models, such as the Fetal Medicine Foundation (FMF) algorithm, is problematic due to the small number of women with T1DM in the study population (Rolnik et al., 2017b). This is despite previous reports of PE biomarkers performing differently in pregnancies complicated by pregestational diabetes (Zen et al., 2019). Moreover, large clinical trials investigating PE biomarkers and risk prediction models often pool data from type 1 and type 2 diabetes mellitus groups together or exclude them completely (Agrawal et al., 2017; Guy et al., 2020; Serra et al., 2020). As a result, an important research gap remains in the development of predictive modalities for PE in women with T1DM. To date, only one comprehensive systematic review of T1DM-specific PE biomarkers has been carried out by Wotherspoon et al. (2016a), which did not recommend any individual biomarker for clinical implementation. We aim to provide a comprehensive review of recently published evidence of biomarker candidates for PE among women with T1DM that could be targeted for clinical implementation in existing PE prediction models.

METHODS

Electronic Database Search

A search was carried out using the electronic databases Medline, EMBASE, Maternity and Infant Care, Web of Science, and Scopus on 11 July 2020 (**Table 1**). Searches were limited to human studies published since 2015 inclusive to identify all relevant publications after the search carried out by Wotherspoon et al. on 16 January 2015 (Wotherspoon et al., 2016a). No limitations on study type were applied. All the articles included were available in English. The database-specific formatting of keywords was combined with the use of medical subject headings to maximize the number of results. Once all duplicates had been eliminated, articles were screened by title and abstract to identify those relevant for PE prediction in women with T1DM. Full-text manuscripts were obtained for the selected articles and assessed for inclusion in the review. To identify any omitted articles in the search, reference lists of the included articles were scanned and a broader search was carried out on Medline using only search terms relating to PE and T1DM (**Table 1**). Inclusion and exclusion criteria applied are outlined in **Supplementary Appendix S1**.

Data Extraction

A data extraction form was used to record key information about the design of each study including study type, cohort country of origin, number of women with T1DM, diabetes duration, age distribution, the prevalence of PE within the cohort and ethnicity distribution. For biomarker data, information was extracted using a data extraction form including the biomarkers used, measurement timeframe within gestation, main findings and measures of predictive potential used.

Data Analysis

Due to the heterogeneity of biomarkers used within the included studies, a meta-analysis could not be carried out and a narrative synthesis approach was adopted instead. An assessment of overlapping data between studies included in this review, and

TABLE 1 | Syntax used for searching electronic databases.

1.	Preeclampsia OR pre-eclampsia OR pregnancy-induced hypertension OR pregnancy induced hypertension OR hypertensive disorder of pregnancy OR toxaemia of pregnancy OR toxemia of pregnancy OR gestosis
2.	Pregnancy in diabetics OR pregravid diabetes OR pre-pregnancy diabetes OR pregestational diabetes OR diabetes mellitus OR type 1 diabetes OR type 1 diabetes mellitus OR type one diabetes OR type one diabetes mellitus OR insulin dependent diabetes mellitus OR IDDM OR T1DM OR juvenile diabetes OR juvenile-onset diabetes
3.	Biomarker OR biological marker OR biochemical marker OR molecular marker
4.	#1 AND #2 AND #3

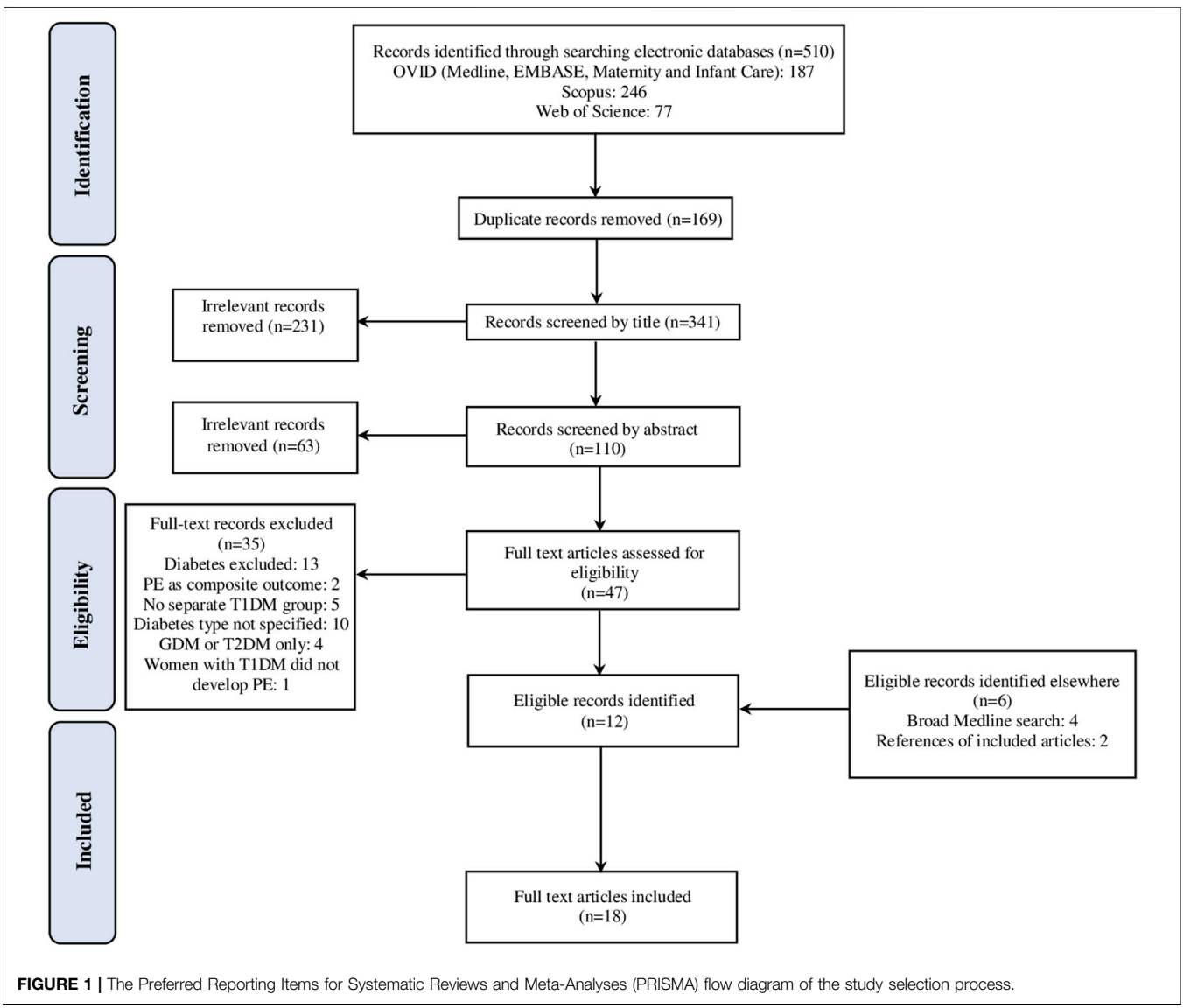

FIGURE 1 | The Preferred Reporting Items for Systematic Reviews and Meta-Analyses (PRISMA) flow diagram of the study selection process.

TABLE 2 | Study and population characteristics.

Author, year	Women with T1DM (n)	PE prevalence in T1DM, n (%)[a]	Duration of T1DM (years)[b]	Age distribution (years)[c]	Ethnicity	Country
Basu et al. (2015)	47	24 (35.9%)	T1DM + PE+: 16.8 ± 6.8 T1DM + PE–: 14.8 ± 7.0	T1DM + PE+: 28.5 ± 5.6 T1DM + PE–: 29.9 ± 3.8	86% Caucasian	Australia, United States, Norway[d]
Cavero-Redondo et al. (2018)	2559 (pooled)	11.0–28.6%	8.4–15.4	23.5–29.7	Not recorded	4 studies pertaining to 5 cohorts originating from Finland, the United Kingdom, Denmark, and Bulgaria
Gutaj et al. (2017)	165	16 (9.7%)	Control: 12 ± 7 Gestational HTN: 12 ± 8 PE+: 17 ± 7	Control: 29 ± 4 Gestational HTN: 29 ± 7 PE+: 27 ± 4	Caucasian	Poland
Kapustin et al. (2020)	100	25 (25%)	Not recorded	27.2–30.1	Not recorded	Russia
Kelly et al. (2017)	47	24 (35.9%)	T1DM + PE+: 16.8 ± 6.8 T1DM + PE–: 14.8 ± 7.0	T1DM + PE+: 28.5 ± 5.6 T1DM + PE–: 29.9 ± 3.8	86% Caucasian	Australia, the United States, and Norway[d]
Kelly et al. (2018)	47	23 (35.9%)	T1DM + PE+: 16.8 ± 6.8 T1DM + PE–: 14.8 ± 7.0	T1DM + PE+: 28.5 ± 5.6 T1DM + PE–: 29.9 ± 3.8	86% Caucasian	Australia, the United States, and Norway[d]
Kelly et al. (2019)	47	23 (35.9%)	T1DM + PE+: 16.8 ± 6.8 T1DM + PE–: 14.8 ± 7.0	T1DM + PE+: 28.5 ± 5.6 T1DM + PE–: 29.9 ± 3.8	86% Caucasian	Australia, the United States, and Norway[d]
Kelly et al. (2020)	47	24 (35.9%)	T1DM + PE+: 16.8 ± 6.8 T1DM + PE–: 14.8 ± 7.0	T1DM + PE+: 28.5 ± 5.6 T1DM + PE–: 29.9 ± 3.8	86% Caucasian	Australia, the United States, and Norway[d]
Klemetti et al. (2016)	1094	260 (23.7%)	White B: 4 (0–9) White C: 13 (2–19) White D: 22 (6–36) White R: 24 (11–36) White F: 20 (10–34)	White B: 31.5 ± 4.4 White C: 29.7 ± 5.4 White D: 30.8 ± 5.2 White R: 31.6 ± 4.4 White F: 30.0 ± 4.9	Not recorded	Finland
Lauszus and Fuglsang (2016)	97	32 (33%)	Normoalbuminuric: 12 ± 8 Microalbuminuric: 14 ± 8 Macroalbuminuric: 20 ± 5	Normoalbuminuric: 28 ± 4 Microalbuminuric: 27 ± 5 Macroalbuminuric: 30 ± 4	Not recorded	Denmark
Maresh et al. (2015)	725	120 (17%)	14.5 ± 8.2	29·5 ± 5.6	96.5% Caucasian 0.5% Black 1.5% Asian 1.5% Other/not known	United Kingdom[e]
Nielsen et al. (2018)	88	14 (16%)	T1DM + PE+: 16.2 ± 7.5 T1DM + PE–: 13.3 ± 8.9	T1DM + PE+: 29.5 ± 5.9 T1DM + PE–: 29.9 ± 4.5	Caucasian	Denmark
Perea et al. (2019)	77	14 (18%)	IAH: 19.4 ± 8.6 NAH: 16.1 ± 8.6	IAH: 33.7 ± 3.2 NAH: 34.4 ± 4.0	Caucasian	Spain
Tsiakkas et al. (2015)	228	11 (4.8%)	Not recorded	11 + 0 to 13 + 6 w: 31.1 (26.6–34.9) 19 + 0 to 24 + 6 w: 31.1 (26.6–34.8) 30 + 0 to 37 + 6 w: 31.1 (26.7–34.8)	72.5–73.1 Caucasian 17.7–19.2% Afro-Caribbean 3.7–4.5% South Asian 2.0–2.3% East Asian 2.2–2.5% Mixed	United Kingdom

(Continued on following page)

TABLE 2 | (*Continued*) Study and population characteristics.

Author, year	Women with T1DM (n)	PE prevalence in T1DM, n (%)[a]	Duration of T1DM (years)[b]	Age distribution (years)[c]	Ethnicity	Country
Vestgaard et al. (2017b)	198	16 (8%)	Preterm delivery: 15.0 (0.5–32.0) Term delivery: 15.0 (0.5–38.0)	Preterm delivery: 31 (19–39) Term delivery: 30 (21–43)	Caucasian	2 cohorts from Denmark
Vestgaard et al. (2017a)	11,518 (pooled)	9.3–33.5%	Not recorded	Not recorded	Not recorded	11 studies pertaining to 11 cohorts from Italy, Denmark, United Kingdom, Sweden, Finland, the United States, and United Kingdom
Wotherspoon et al. (2016b)	710	120 (17%)	14.5 ± 8.2	29·5 ± 5.6	96.5% Caucasian 0.5% Black 1.5% Asian 1.5% Other/not known	United Kingdom[e]
Xiang et al. (2018)	3239 (pooled)	8.5–30.8%	Not recorded	25–40	Not recorded	11 studies pertaining to 11 cohorts from Poland, Slovakia, Brazil, Finland, Italy, Denmark, the United States of America, United Kingdom, and Sweden

HTN, hypertension; IAH, impaired awareness of hypoglycemia; NAH, normal awareness of hypoglycemia; T1DM + PE+, women with T1DM who developed pre-eclampsia; T1DM + PE–, women with T1DM who did not develop pre-eclampsia; w, weeks; y, years.

[a]*PE prevalence within the T1DM, group of the cohort, given as a range for systematic reviews.*

[b]*Data given as mean ± SD, range or median (range).*

[c]*Data given as mean ± SD, mean, range, or mean (interquartile range).*

[d]*Studies by Basu et al. (2015), Kelly et al. (2017), Tsiakkas et al. (2015), Kelly et al. (2019), and Kelly et al. (2020) were based on participants from the same cohort.*

[e]*Studies by Maresh et al. (2015) and Wotherspoon et al. (2016b) were based on participants from the same cohort.*

Wotherspoon et al. (2016a) can be found in **Supplementary Appendix S2**.

RESULTS

Study Selection

A total of 510 records were identified which was reduced to 341 after the removal of duplicates and 47 after screening by title and abstract. Full-text articles were acquired for these and subsequently, 35 publications were excluded, with 18 remaining studies selected for inclusion in the final review. The process of article selection is detailed in a PRISMA diagram in **Figure 1**

Characteristics of Included Studies

A detailed summary of study and cohort characteristics can be found in **Table 2**. Of the 18 studies selected for the current review, three were systematic reviews (Vestgaard et al., 2017a; Cavero-Redondo et al., 2018; Xiang et al., 2018), six were case-control studies (Basu et al., 2015; Tsiakkas et al., 2015; Gutaj et al., 2017; Kelly et al., 2017; Kelly et al., 2018; Kelly et al., 2020) and nine were cohort studies (Maresh et al., 2015; Wotherspoon et al., 2016b; Klemetti et al., 2016; Lauszus and Fuglsang, 2016; Vestgaard et al., 2017b; Nielsen et al., 2018; Kelly et al., 2019; Perea et al., 2019; Kapustin et al., 2020). The number of women with T1DM in the cohorts ranged from 47 to 1,094, with Vestgaard et al. and Xiang et al. having pooled 11,518 and 3,239 participants with T1DM, respectively (Vestgaard et al., 2017a; Xiang et al., 2018). A total of 27 cohorts represented 11 European countries and Australia, the United States, Russia and Brazil. PE prevalence within cohorts ranged from 4.8% to 35.9%. There was heterogeneity in the timeframe of biomarker measurements, with 12 studies (Basu et al., 2015; Tsiakkas et al., 2015; Klemetti et al., 2016; Lauszus and Fuglsang, 2016; Gutaj et al., 2017; Kelly et al., 2017; Cavero-Redondo et al., 2018; Kelly et al., 2018; Nielsen et al., 2018; Kelly et al., 2019; Perea et al., 2019; Kelly et al., 2020) recording biomarker levels across all three trimesters of pregnancy, four studies (Maresh et al., 2015; Wotherspoon et al., 2016b; Vestgaard et al., 2017a; Vestgaard et al., 2017b) in any two trimesters and one study (Kapustin et al., 2020) taking measurements in the first trimester only. The timing of biomarker measurements was not specified in Xiang et al. (2018). Of the 32 different biomarkers identified, glycosylated hemoglobin, serum lipid-associated molecules and urinary protein were most commonly discussed with a smaller number of studies investigating adipokines or angiogenic factors. Several novel markers were described including vitamin D and urinary neutrophil gelatinase-associated lipocalin. A narrative synthesis of the main results of included studies is contained in **Table 3.**

Glycosylated Hemoglobin

The predictive potential of plasma glycated hemoglobin A1c (HbA1c) was examined in six studies (Maresh et al., 2015; Klemetti et al., 2016; Vestgaard et al., 2017a; Gutaj et al., 2017; Cavero-Redondo et al., 2018; Nielsen et al., 2018). PE risk was

TABLE 3 | Narrative synthesis of biomarkers for pre-eclampsia prediction in women with pregestational T1DM.

Study	Biomarkers	Measurements (w or w + days)[a]	Findings (T1DM + PE + vs. T1DM + PE-)	Predictive potential measure
Basu et al. (2015)	Copper, iron, manganese, selenium, zinc, HDL-c, LDL-c, triglycerides, and total cholesterol	V1: 12.3 ± 1.9 w V2: 21.6 ± 1.5 w V3: 31.5 ± 1.7 w	↑Zinc in T1 ↑Zinc:HDL in T1 ↑Copper:zinc and ↑Copper: HDL-c throughout gestation ↑HDL-c at baseline	—
Cavero-Redondo et al. (2018)	HbA1c	V1: T1 (7–12 w) V2: T2/T3 (22–36 w)	↑HbA1c at all visits	For 1% HbA1c ↑ OR = 1.37 in T1 OR = 1.67 in T2/T3
Gutaj et al. (2017)	HbA1c and triglycerides HDL-c LDL-c Total cholesterol	V1: <12 w V2: 20–24 w V3: 34–39 w	↑HbA1c at all visits ↑Triglycerides in T3	For ↑HbA1c OR = 1.38 in T1 OR = 2.76 in T2 OR = 2.42 in T3 For ↑triglycerides OR = 5.32 in T1 OR = 2.52 T2 OR = 2.28 in T3
Kapustin et al. (2020)	PAPP-A, β-hCG	11 + 0 w to 13+6 w	NSD	—
Kelly et al. (2017)	Leptin, adiponectin (total, HMW), FABP4, resistin, and RBP4	V1: 12.3 ± 1.9 w V2: 21.6 ± 1.5 w V3: 31.5 ± 1.7 w	↑Leptin:total adiponectin at V1 and V2 ↑Leptin:HMW adiponectin at V1 and V2 ↑FABP4 at V2 and V3 ↑Leptin, ↑FABP4:total adiponectin, and ↑FABP4: HMW adiponectin throughout pregnancy ↓Total adiponectin at V1 ↓HMW adiponectin at V1 and V2	Best prediction models using doubling of serum levels OR = 9.0, sensitivity 81%, specificity 80%, PPV 100%, NPV 69% for leptin in T1 OR 3.7, sensitivity 84%, specificity 68%, PPV 100%, NPV 56% for leptin:total adiponectin in T2 OR 25.1, sensitivity 71%, specificity 75%, PPV 100%, NPV 65% for FABP4 in T3
Kelly et al. (2018)	uNGALcc, pNGAL, creatinine, and KIM-1	V1: 12.3 ± 1.9 w V2: 21.6 ± 1.5 w V3: 31.5 ± 1.7 w	↑uNGALcc at V1 NSD in pNGAL NSD in urinary KIM-1 ↑eGFR at V1 but NSD after adjustment	↑uNGALcc (leukocyte-negative): sensitivity 75%, specificity 70%, PPV 32%, NPV 93% before 15 w
Kelly et al. (2019)	Hp, LDL-c, LDL particle concentration, ApoB, ApoA1, triglyceride:HDL-c, ApoB:ApoA1, sFlt-1, sEng, PlGF, and sFlt-1/PlGF	V1: 12.3 ± 1.9 w V2: 21.6 ± 1.5 w V3: 31.5 ± 1.7 w	↑sFlt-1, sFlt-1/PlGF at V3 ↓PlGF at V3 Within the Hp 2–2 only ↑LDL-c at V1 and V2 ↑LDL particle concentration, ↑ApoB, ↑Triglyceride:HDL-c, and ↑ApoB/ApoA1 at all visits ↓HDL-c, ApoA1, and large HDL particle concentrations at all visits	—
Kelly et al. (2020)	25(OH)D 1 $25(OH)_2D$ VDBP	V1: 12.3 ± 1.9 w V2: 21.6 ± 1.5 w V3: 31.5 ± 1.7 w	↑$1,25(OH)_2D$ at V2 (free, total, and bioavailable) and V3 (bioavailable and free) ↑$1,25(OH)_2D/25(OH)D$ at V3 ↑$1,25(OH)_2D$/VDBP at V2 and V3 ↓VDBP at V3	For every 1 pg/ml ↑ OR = 1.28 for 1,25(OH)2D at T2 OR = 1.18 for $1,25(OH)_2D$ at T3 For every unit ↑ OR = 2.71 for $1,25(OH)_2D$/VDBP at T2 OR = 2.53 for $1,25(OH)_2D$/VDBP at T3
Klemetti et al.(2016)	Macroalbuminuria, HbA1c	HbA1c V1: last value within 12 months before pregnancy; V2: first value in	Stepwise ↑ in White's class from B to F corresponded to ↑PE incidence HbA1c ≥ 7% in T1	For HbA1c ≥ 7%: OR = 1.92 in T1 For macroalbuminuria: OR = 8.65 in T1

(Continued on following page)

TABLE 3 | (*Continued*) Narrative synthesis of biomarkers for pre-eclampsia prediction in women with pregestational T1DM.

Study	Biomarkers	Measurements (w or w + days)[a]	Findings (T1DM + PE + vs. T1DM + PE-)	Predictive potential measure
		T1; V3: 18+0 w to 22+0 w; V4: last value before delivery Macroalbuminuria V1: 6–10 w; V2: 11–13 w; every 2-4 w during T2; every 1-2w during T3		
Lauszus and Fuglsang (2016)	IGF-1	V1: 14 w, V2: 18 w, V3: 22 w, V4: 26 w, V5: 30 w, V6: 32 w	NSD	—
Maresh et al. (2015)	HbA1c	V1: 26 w V2: 34 w	↑HbA1c at all visits	Compared to HbA1c <6.0% OR = 4.3 for 6.5–6.9%, OR = 4.6 for 7.0–7.4%, OR = 5.1 for ≥7.5% at 26 w OR = 3.0 for 6.5–6.9%, OR = 5.3 for 7.0–7.4%, OR = 6.8 for ≥7.5% at 34 w
Nielsen et al. (2018)	Urine PCR Plasma aldosterone	V1: 12 w, V2: 20 w, V3: 28 w, V4: 32 w, V5: 36 w	↑Urine PCR at V5 ↑Plasma aldosterone at V2	For ↑Urine ACR OR = 3.92 at 12 w, OR = 3.43 at 20 w, OR = 3.58 at 28 w, OR = 6.15 at 32 w, OR = 17.94 at 36 w, AUC = 0.91 at 36 w
	Urine ACR HbA1c		↑Urine ACR at all visits ↑HbA1c from V2 onwards	For ↑Urine PCR OR = 2.49 and AUC = 0.74 at 36 w For each 1% HbA1c↑ OR = 1.08 at 20 w, OR = 1.09 at 28 w, OR = 6.15 at 32 w, OR = 17.94 at 36 w
Perea et al. (2019)	Total cholesterol Triglycerides HDL-c	V1: 8–14 w V2: 22–28 w V3: 31–36 w	↑Triglycerides at V2	For each 10 mg/dl ↑Triglycerides: OR = 1.32 - -
Tsiakkas et al. (2015)	MoMs of serum PlGF	V1: 11 + 0 to 13 + 6 V2: 19 + 0 to 24 + 6 w V3: 30 + 0 to 34 + 6 w/35 + 0 to 37 + 6 w	↓PlGF MoM	—
Vestgaard et al. (2017b)	25(OH)D	V1: 8 (5–14 w) V2: 24 (32–36 w)	Non-significantly ↓25(OH)D at baseline	
Vestgaard et al. (2017a)	Microalbuminuria, macroalbuminuria, and HbA1c	<16–20 w	Presence of microalbuminuria, macroalbuminuria, and ↑HbA1c from T1	For microalbuminuria: OR = 3.8 and OR = 11.7 in T1 For macroalbuminuria: OR = 4.7–23.5 in T1
Wotherspoon et al. (2016b)	FABP4	V1: 14 w (8–22 w) V2: 26 w	↑FABP4 at V1 and V2 ↑FABP4 at 13 w	For each doubling of FABP4: OR = 1.4 at V1, OR = 1.6 at V2
Xiang et al. (2018)	Microalbuminuria and macroalbuminuria	Not recorded	Presence of microalbuminuria and macroalbuminuria	For microalbuminuria: OR = 4.19 For macroalbuminuria: OR = 7.19

ApoA1, apolipoprotein A1; ApoB, apolipoprotein B; HMW, high molecular weight; IGF-1, insulin-like growth factor 1; KIM-1, urinary kidney injury molecule-1; NSD, no significant difference; RBP4, retinol-binding protein 4; T1–T3, trimesters 1 to 3; V1–V6, visits 1 to 6; w, weeks.

[a]*Data given as mean ± SD, mean, or median (range).*

correlated to HbA1c ≥ 7% and >6% (Klemetti et al., 2016; Gutaj et al., 2017) cut-offs denoting "poor" glycemic control or 0.5% and 1% HbA1c increments (Maresh et al., 2015; Cavero-Redondo et al., 2018; Nielsen et al., 2018). With the exception of two studies (Hsu et al., 1996; Ekbom et al., 2001) included by Vestgaard et al. (2017a) in their systematic review, a positive association between rising HbA1c and PE was seen, although the odds ratios (OR) differed between studies and trimesters. For HbA1c cut-offs indicating poor glycemic control, ORs were 1.38–1.92 in the first trimester, 2.76 in the second trimester, and 2.42 in the third trimester (Klemetti et al., 2016; Gutaj et al., 2017). Comparatively, every 1% HbA1c increase produced OR = 1.37 in the first trimester, OR = 1.08–1.67 in the second trimester, and OR = 6.15–17.94 in the third trimester (Cavero-Redondo et al., 2018; Nielsen et al., 2018). In the second trimester, OR was 4.3 for HbA1c 6.5%–6.9% compared to OR of 4.6 for HbA1c 7.0–7.4%, and in the third trimester OR was 3.0 for HbA1c 6.5%–6.9% compared to OR of 5.3 for HbA1c 7.0%–7.4% and OR of 6.8 for HbA1c ≥ 7% (Maresh et al., 2015).

Urinary Protein

Five studies investigated some form of urinary protein (Klemetti et al., 2016; Vestgaard et al., 2017a; Kelly et al., 2018; Nielsen et al., 2018; Xiang et al., 2018). A strong association was shown between urinary albumin excretion and PE development, with a higher

risk demonstrated for women with macroalbuminuria rather than microalbuminuria. The presence of microalbuminuria prior to 16–20 weeks of gestation was associated with OR = 3.8 (Castiglioni et al., 2014) and 11.7 (Ekbom et al., 2001) for subsequent PE diagnosis in Vestgaard et al. (2017a). A pooled OR of 4.19 for microalbuminuria was calculated by Xiang et al. (2018), although the gestational age to which this applied was not specified. For macroalbuminuria, the pooled first trimester ORs were 7.19 (Klemetti et al., 2016) and 8.65 (Vestgaard et al., 2017a; Nielsen et al., 2018) which contrasted with the wide range of ORs (4.7–23.5) collated in Vestgaard et al. (2017a). Nielsen et al. (2018) investigated urine plasminogen/creatinine ratio (PCR) and urine albumin/creatinine ratio (ACR). The authors demonstrated an association between increased ACR and PE risk across the whole gestation, with ORs = 3.92 at 12 weeks and 3.43 at 20 weeks. However, a significant area under the curve (AUC) improvement for PE prediction using ACR compared to clinical variables was only found at 36 weeks. Urine PCR performed poorly, only showing an association with PE at 36 weeks.

A novel marker of renal cell injury, urinary neutrophil gelatinase-associated lipocalin (uNGALcc), was found to accurately predict PE from late first trimester (Kelly et al., 2018). Significantly raised uNGALcc was sustained in leukocyte-negative samples of women with subsequent PE diagnosis, which was important as NGAL is produced by activated neutrophils as well as damaged renal epithelium (Kelly et al., 2018). A model incorporating uNGALcc together with body mass index, HbA1c, and daily insulin dose had 75% sensitivity and 70% specificity for PE prediction prior to 15 weeks with a non-significant AUC improvement.

Lipid-Associated Molecules

Six studies examined circulating cholesterol, triglycerides, adipokines and lipoproteins (Basu et al., 2015; Wotherspoon et al., 2016b; Gutaj et al., 2017; Kelly et al., 2017; Kelly et al., 2019; Perea et al., 2019). Data regarding levels of high-density lipoprotein cholesterol (HDL-c), low-density lipoprotein cholesterol (LDL-c), total cholesterol and PE development were conflicting. Two studies (Gutaj et al., 2017; Perea et al., 2019) found no difference in the levels of either molecule between PE and normotensive groups, contrasting with Basu et al. (2015) who showed a significant first-trimester HDL-c fall in PE. Kelly et al. (2019) examined whether an atherogenic lipid profile in PE is confined to certain haptoglobin phenotypes (Hp) and found that increased LDL-c and decreased HDL-c across the whole gestation existed only in women with T1DM who had Hp 2-2. The triglyceride data were also inconsistent. Contrasting with Basu et al. (2015) who found no difference in triglyceride levels between women who developed PE and those who did not others demonstrated higher triglyceride levels in women who developed PE across all three trimesters (Gutaj et al., 2017; Perea et al., 2019). Kelly et al. (2019) did not find increased triglyceride levels in women with PE with Hp 2-2 although they did show an increased triglyceride:HDL-c ratio across the whole gestation. Additionally, Kelly et al. (2019) found significantly upregulated ApoA1 and ApoB:ApoA1 throughout pregnancy in women with the Hp2-2 phenotype who developed PE.

Two studies examined adipokines (Wotherspoon et al., 2016b; Kelly et al., 2017). Fatty acid-binding protein 4 (FABP4) was elevated across all trimesters with OR = 1.4 at 14 weeks, 1.6 at 26 weeks (Wotherspoon et al., 2016b) and 25.1 at 31.5 weeks (Kelly et al., 2017) respective to each doubling of serum FABP4. In addition, Kelly et al. (2017) used HbA1c, daily insulin dose and gestational age to develop trimester-specific PE prediction models incorporating adipokines. In a third-trimester model, FABP4 was 71% sensitive and 75% specific for subsequent PE development. In the same study leptin was upregulated throughout pregnancy in women subsequently diagnosed with PE, and total and high molecular weight forms of adiponectin were decreased in the first and second trimesters. A first-trimester prediction model using doubling of serum leptin had OR = 9.0, with 81% sensitivity and 80% specificity, and a second-trimester prediction model using doubling of serum leptin:total adiponectin ratio had OR = 3.7, with 84% sensitivity and 68% specificity. The AUC improvements were non-significant for all prediction models using adipokines (Kelly et al., 2017).

Other Plasma or Serum Biomarkers

Nine studies (Basu et al., 2015; Tsiakkas et al., 2015; Lauszus and Fuglsang, 2016; Vestgaard et al., 2017b; Kelly et al., 2018; Nielsen et al., 2018; Kelly et al., 2019; Kapustin et al., 2020; Kelly et al., 2020) examined other circulating molecules. Two studies (Tsiakkas et al., 2015; Kelly et al., 2019) investigated angiogenic factors soluble Fms-like tyrosine kinase 1 (sFlt-1), soluble endoglin (sEng) and placental growth factor (PlGF) in PE prediction among women with T1DM. PlGF was lower among women with T1DM developing PE (Tsiakkas et al., 2015) compared to normotensive women with T1DM but sEng was no different due to being consistently elevated in both groups. In the same study, sFlt-1, PlGF and sFlt-1/PlGF ratios were only predictive from the third trimester (Kelly et al., 2019). PAPP-A was found to be not different between groups of women with T1DM who developed PE or remained normotensive (Kapustin et al., 2020).

Two studies (Vestgaard et al., 2017b; Kelly et al., 2020) measured vitamin D in pregnant women with T1DM. Vitamin D deficiency was more common in T1DM groups in both studies but the predictive potential of vitamin D differed. The ORs were non-significant for the active form of vitamin D, 25(OH)D, in Vestgaard et al. (2017b) similar to Kapustin et al. (2020) However, Kapustin et al. (2020) were able to show significantly elevated levels of the precursor form of vitamin D, $1,25(OH)_2D$, and its ratio with vitamin D binding protein (VDBP) in second and third trimesters in PE groups. Every unit increase in $1,25(OH)_2D$:VDBP was correlated with OR = 2.71 in the second trimester and OR = 2.53 in the third trimester for later PE development.

DISCUSSION

Thirty-two different biomolecules spanning 5.5 years of published data were identified in this narrative review of PE biomarkers for women with T1DM. This compares to a similar

number of biomolecules reported in Wotherspoon et al. (2016a), however, the previous review covered 25 years of literature, suggesting an expansion of the research field. Previously, Wotherspoon et al. (2016a) opted not to nominate any single PE biomarker for clinical implementation indicating a need for further validation of existing data and for discovery of novel candidates. The combined body of evidence between this review and Wotherspoon et al. (2016a) suggests that maternally derived biomarkers, such as HbA1c, urinary albumin and adipokines, are the highest performing predictors of PE among women with T1DM, with placental biomarkers such as PAPP-A showing less capacity to predict PE development in this population. These findings are in line with the growing body of evidence that some PE phenotypes are caused primarily by pre-existing cardiovascular compromise rather than placental dysfunction (Thilaganathan and Kalafat, 2019), with diabetes being one of the major known cardiovascular risk factors. Modern PE screening approaches, such as the FMF (Poon et al., 2009), incorporate biophysical, biochemical and ultrasonographic maternal parameters. Although evaluating the application of each parameter to women with T1DM is beyond the scope of this review, we propose that our findings are used to focus the search for alternatives to the biochemical components of these models, such as PAPP-A. Using biomarkers with known predictive performance and pathophysiological basis of action in PE development within a T1DM context would allow tailoring of such models to this high-risk population.

Maternally Derived Biomarkers

The recent meta-analyses of HbA1c (Cavero-Redondo et al., 2018) and urinary albumin (Xiang et al., 2018) have validated previous observations (Wotherspoon et al., 2016a) in support of these biomarkers as predictors of PE among women with T1DM. Furthermore, HbA1c and urinary albumin are molecules whose upregulation in a high-risk PE state would be plausible, as they both directly relate to the current theories of the disease pathogenesis in this group. Hyperglycemia has a profoundly toxic effect on vascular function (Brownlee, 2001) and trophoblast viability (Inadera et al., 2010), with HbA1c reflecting a woman's glycemic control over 6–8 weeks (Inkster et al., 2006). Comparatively, kidney damage detectable as albuminuria is a diagnostic feature of PE in both women with diabetes and the general population (National Institute for Health and Care Excellence (NICE), 2019). In women with T1DM, the placental pathology in PE stresses the kidneys whose functional reserve might have already been reduced by diabetic kidney disease, with albumin sometimes detectable in their urine even before pregnancy (Azzoug and Chentli, 2016; Mathiesen, 2016). Therefore, it is not surprising that the level of microalbuminuria, macroalbuminuria and HbA1c would be correlated with PE risk among women with T1DM (Leguizamón et al., 2015; Cavero-Redondo et al., 2018; Xiang et al., 2018).

Among studies within this review, HbA1c was used both as an independent biomarker and as part of prediction models for PE. Bearing in mind the physiological caveat of falling levels as pregnancy progresses, which has precluded HbA1c use beyond the first trimester in current practice (American College of Obstetrics and Gynaecology (ACOG), 2018; National Institute for Health and Care Excellence (NICE), 2015), HbA1c might be better placed for use in support of other PE biomarkers not affected by such physiological flux. However, validation of the HbA1c and PE relationship in a meta-analysis and the characterization of this using HbA1c increments beyond the arbitrary "poor" or "good" glycemic control thresholds (Maresh et al., 2015; Cavero-Redondo et al., 2018) indicate that its full clinical potential in pregnancy complicated by T1DM might not be realised. The clinical applications of HbA1c measurements during pregnancy might even extend beyond PE prediction to stratify the long-term risk of microangiopathy after PE development, an association already shown in non-pregnant women with diabetes (Gorst et al., 2015). Considering that the increased risk of diabetic retinopathy (Lövestam-Adrian et al., 1997; Gordin et al., 2013) and nephropathy (Gordin et al., 2007) is well established after PE, an accurate biomarker stratifying this would be desirable. Comparably, drawing definitive conclusions about albuminuria use in PE prediction is problematic due to difficult data interpretation. Reasons for this include crude cut-offs in 24 h urinary albumin excretion that distinguish microalbuminuria from macroalbuminuria and the variety of definitions used for both across the studies identified. Better alternatives might be necessary to reflect kidney damage in PE. One alternative discussed is uNGALcc (Kelly et al., 2018), presenting a real-time indicator of pre-albuminuria kidney damage.

The role of insulin resistance and metabolic syndrome in the pathogenesis of PE among women with T1DM is another largely unexplored area, yet several biomarkers discussed in this review can be directly correlated with these states. Increased insulin resistance is a feature of normal pregnancy (Salzer et al., 2015), but excessive resistance has been linked to PE in both the general population (Wolf et al., 2002) and women with T1DM (Gutaj et al., 2015). The importance of insulin resistance in T1DM is becoming increasingly recognized (Kilpatrick et al., 2007), yet few studies have explored its role in PE pathogenesis in this group (Wender-Ozegowska et al., 2011). Adipokines such as leptin, adiponectin and FABP4, are released from metabolically active adipose tissue providing an indirect assessment of the degree of insulin resistance (Gutaj et al., 2015) and upregulation of these molecules has already been associated with PE in the general population (Haugen et al., 2006). Kelly et al. (2017) and Wotherspoon et al. (2016b) are the first to demonstrate a PE biomarker potential for adipokines among women with T1DM. Notably, as Kelly et al. (2017) recommended using a different adipokine for each trimester, the clinical implementation of these biomarkers might be logistically complex. Lipids, dysregulation of which is a known component of the metabolic syndrome together with insulin resistance (Kilpatrick et al., 2007), were also discussed in this review (Kilpatrick et al., 2007). There is uncertainy around the significance of abnormal lipid metabolism in women with T1DM who go on to develop PE, reflected in the inconsistent evidence seen within the current review and Wotherspoon et al. (2016a). Recommendations for use of atherogenic lipid profiles for PE prediction among women with T1DM by some authors contrasted with others finding no differences in triglyceride, HDL-c and LDL-c levels between hypertensive and normotensive groups. Interestingly, the recent findings of Kelly et al.

(2019) might explain such conflicting results with different haptoglobin phenotypes. Although contradicting previous studies that found no correlation (Weissgerber et al., 2013), Kelly et al. (2019) were able to showed a significant association between atherogenic dyslipidemia, haptoglobin phenotype 2-2 and PE among women with T1DM. Further investigation is warranted to validate these findings, and of the possibility of haptoglobin phenotype-specific PE biomarkers. Importantly, Hp 2-2 represents only half of the Caucasian T1DM population (Langlois and Delanghe, 1996; Kelly et al., 2019) with further variation likely among other ethnicities.

The newly significant association between rising vitamin D levels and PE in women with pre-existing T1DM was a major finding in this review, in contrast to what has been described previously among women with T1DM (Azar et al., 2011; Vestgaard et al., 2017b) and the evidence for low vitamin D levels among women with PE in the general population (Poniedziałek-Czajkowska and Mierzyński, 2021). This correlation was uncovered due to the different approach adopted by Kelly et al. (2020), measuring both active and precursor vitamin D forms in contrast to their predecessors, who only measured the active form (Azar et al., 2011; Vestgaard et al., 2017b). The findings of Kelly et al. (2020) suggest that other previously non-significant biomarker data could assume significance after methodological re-evaluation. It should be noted that the results of this study were limited by the small number of women included (n = 47) and the pathophysiological relevance of the elevated $1,25(OH)_2D$/VDBP ratio in women with T1DM with increased PE risk remains unclear. One explanation could be a compensatory increase of an antioxidant to combat the oxidative stress associated with placental and vascular dysfunction in PE (Kelly et al., 2020). The role of vitamin D supplementation in PE prevention is also notoriously inconclusive in the general population (Poniedziałek-Czajkowska and Mierzyński, 2021).

Placenta Derived Biomarkers

The lack of association between PAPP-A and PE in women with T1DM (Kapustin et al., 2020) was a notable negative finding in this review. Importantly, as Kapustin et al. (2020) measured PAPP-A at 11–13 + 6 weeks, similar to PAPP-A measurements in studies using the FMF (Thilaganathan and Kalafat, 2019), these results cannot be explained by differences in measurement timeframes. Given the key role of PAPP-A in the first trimester combined PE screening algorithm (Chaemsaithong et al., 2020), prediction models performing well in the general population might not predict PE as accurately among women with T1DM (Guy et al., 2020; Serra et al., 2020). This demonstrates a need to validate general population biomarkers in women with T1DM. The lack of such validation was previously noted by Wotherspoon et al. (2016a). Similarly, placental angiogenic markers were some of the poorest PE predictors discussed in this review (Wotherspoon et al., 2016a; Kelly et al., 2019). Despite the initial optimism surrounding angiogenic factor discovery (Levine et al., 2004), their accuracy has been called into question in the general population (Kleinrouweler et al., 2012), and a recent study of pregnant women with diabetes found that the sFlt-1/PlGF ratio was driven by PlGF in these pregnancies with little difference in sFlt-1 between the PE and normotensive groups (Zen et al., 2019). Therefore, only PlGF might hold a benefit for PE prediction in a system with T1DM.

Future Directions

Several knowledge gaps were identified that could be addressed by ongoing research efforts. First, the incomplete understanding of PE pathogenesis in women with T1DM is a research priority, as this continues to hinder the prediction and prevention efforts of this disease. The relative trend of maternally-derived PE biomarkers performing better among studies in this review could be a clue to the maternal origins of PE among women with T1DM, worthy of investigation. Moreover, the consistently elevated sEng in pregnant women with T1DM was an intriguing finding (Kelly et al., 2019) and could be an indicator of the maternal cardiovascular preponderance towards PE in the form of pre-existing systemic endothelial dysfunction with long-term T1DM. Elucidating reasons for differences in biomarker performance between groups of women with and without T1DM could also suggest pathophysiological pathways to target in studies investigating preventative approaches for PE beyond aspirin. No clinical trials have been carried out as of yet randomizing women with T1DM to aspirin or placebo.

Second, there was a notable lack of HbA1c studies considering a hypoglycemia risk assessment. Lower HbA1c levels at periconception are correlated with fewer subsequent hypoglycemia episodes (Garey et al., 2020) and Perea et al. (2019) observed a relationship between impaired hypoglycemia awareness, atherogenic dyslipidemia and PE, meriting further investigation. Another largely unexplored area relates to the relationship between PE and diabetic retinopathy. In their meta-analysis, Xiang et al. (2018) showed that presence of diabetic retinopathy increased the risk of PE, however, little other literature exists to explain why and whether there are any modalities reflecting diabetic retinopathy that could be used to predict PE. Indeed, considering that progression of diabetic retinopathy is an important pregnancy consideration in all women with T1DM (Rosenn et al., 1992) and the common pathological considerations between PE, diabetic retinopathy, and nephropathy in the maternal vasculature, this relationship could be important. Regarding methodology, an over-representation of Caucasian women was revealed among the included articles. As this could reduce the external validity of biomarker performance, studies testing their accuracy in other demographics should follow.

Strengths and Limitations

A particular strength of this review was its robust search strategy. Database searches were supplemented by hand-searching the references of included articles, minimizing the number of unidentified records. Defined inclusion and exclusion criteria were used (**Supplementary Appendix S1**), and 18 studies were reviewed in total, providing a detailed summary of the current

state of research on T1DM-specific PE biomarkers. The novelty of the data was verified by comparing similarities of included studies between this review and Wotherspoon et al. (2016a) (**Supplementary Appendix S2**). The inability to carry out a meta-analysis in this study was a limitation, attributable to biomarker heterogeneity. We also acknowledge that the included studies were not assessed for risk of bias. Additionally, it was noted that there was some overlap between patient cohorts used by some studies, however, as different biomarkers were investigated in each study, these were included as individual records. Finally, the electronic search was restricted to articles in English only.

CONCLUSION

The growing literature on PE biomarkers for women with T1DM has yielded exciting findings in recent years. This narrative review has demonstrated that maternally derived PE biomarkers reflecting glycemic control, insulin resistance and renal dysfunction might be better predictors of PE development among women with T1DM than placental biomarkers. Maternally derived biomarkers could be trialled in with current PE prediction models in the general population to devise an algorithm tailored to PE pathophysiology among women with T1DM. A further investigation of the maternal origins of PE in women with T1DM and reasons for differing biomarker performance might lead novel discoveries in this field.

DATA AVAILABILITY STATEMENT

The original contributions presented in the study are included in the article/**Supplementary Material**, further inquiries can be directed to the corresponding author.

AUTHOR CONTRIBUTIONS

KF, K-AE and CW contributed to the conception and design of the study. KF and LK performed the review. KF wrote the first draft of the manuscript. KF, LK, K-AE and CW wrote sections of the manuscript. All authors contributed to manuscript revision, read and approved the submitted version.

FUNDING

Funding from the Association of Clinical Pathologists was received by KF and from Queen's University Belfast was received by KF and CW. These organizations had no role in the design or conduct of this study.

ACKNOWLEDGMENTS

We would like to thank the Welcome Wolfson Institute for Experimental Medicine and especially the Watson Research group at Queen's University Belfast for their support and guidance. We would also like to thank the Association of Clinical Pathologists and Queen's University Belfast for the scholarships that allowed KF to undertake the MSc degree during which this research was carried out. The content of this manuscript has been submitted to Queen's University Belfast as part of the MSc thesis by KF.

SUPPLEMENTARY MATERIAL

The Supplementary Material for this article can be found online at: https://www.frontiersin.org/articles/10.3389/fbioe.2022.809528/full#supplementary-material

REFERENCES

Agrawal, S., Cerdeira, A. S., Redman, C., and Vatish, M. (2017). Meta-Analysis and Systematic Review to Assess the Role of Soluble FMS-like Tyrosine Kinase-1 and Placenta Growth Factor Ratio in Prediction of Preeclampsia: The SaPPPhirE Study. *Hypertension* 71 (2), 306–316. doi:10.1161/HYPERTENSIONAHA.117.10182

American College of Obstetrics & Gynaecology (ACOG) (2018). ACOG Practice Bulletin No. 201: Pregestational Diabetes Mellitus. *Obstet. Gynecol.* 132 (6), e228–e248. doi:10.1097/aog.0000000000002960

Azar, M., Basu, A., Jenkins, A. J., Nankervis, A. J., Hanssen, K. F., Scholz, H., et al. (2011). Serum Carotenoids and Fat-Soluble Vitamins in Women with Type 1 Diabetes and Preeclampsia. *Diabetes Care* 34 (6), 1258–1264. doi:10.2337/dc10-2145

Azzoug, S., and Chentli, F. (2016). Microangiopathy and Pregnancy. *J. Pak Med. Assoc.* 66 (9 Suppl. 1), S52–S55.

Basu, A., Yu, J. Y., Jenkins, A. J., Nankervis, A. J., Hanssen, K. F., Henriksen, T., et al. (2015). Trace Elements as Predictors of Preeclampsia in Type 1 Diabetic Pregnancy. *Nutr. Res.* 35 (5), 421–430. doi:10.1016/j.nutres.2015.04.004

Brownlee, M. (2001). Biochemistry and Molecular Cell Biology of Diabetic Complications. *Nature* 414 (6865), 813–820. doi:10.1038/414813a

Caritis, S., Sibai, B., Hauth, J., Lindheimer, M. D., Klebanoff, M., Thom, E., et al. (1998). Low-Dose Aspirin to Prevent Preeclampsia in Women at High Risk. *N. Engl. J. Med.* 338 (11), 701–705. doi:10.1056/nejm199803123381101

Castiglioni, M. T., Valsecchi, L., Cavoretto, P., Pirola, S., Di Piazza, L., Maggio, L., et al. (2014). The Risk of Preeclampsia beyond the First Pregnancy Among Women with Type 1 Diabetes Parity and Preeclampsia in Type 1 Diabetes. *Pregnancy Hypertens. Int. J. Women's Cardiovasc. Health* 4 (1), 34–40. doi:10.1016/j.preghy.2013.09.001

Cavero-Redondo, I., Martínez-Vizcaíno, V., Soriano-Cano, A., Martínez-Hortelano, J. A., Sanabria-Martínez, G., and Álvarez-Bueno, C. (2018). Glycated Haemoglobin A1c as a Predictor of Preeclampsia in Type 1 Diabetic Pregnant Women: A Systematic Review and Meta-Analysis. *Pregnancy Hypertens.* 14, 49–54. doi:10.1016/j.preghy.2018.04.004

Chaemsaithong, P., Sahota, D., and Poon, L. C. (2020). First Trimester Preeclampsia Screening and Prediction. *Am. J. Obstet. Gynecol.* 226, S1071. doi:10.1016/j.ajog.2020.07.020

Ekbom, P., Damm, P., Feldt-Rasmussen, B., Feldt-Rasmussen, U., Mølvig, J., and Mathiesen, E. R. (2001). Pregnancy Outcome in Type 1 Diabetic Women with Microalbuminuria. *Diabetes Care* 24 (10), 1739–1744. doi:10.2337/diacare.24.10.1739

Finnegan, C., Dicker, P., Fernandez, E., Tully, E., Higgins, M., Daly, S., et al. (2019). Investigating the Role of Early Low-Dose Aspirin in Diabetes: A Phase III Multicentre Double-Blinded Placebo-Controlled Randomised Trial of Aspirin Therapy Initiated in the First Trimester of Diabetes Pregnancy. *Contemp. Clin. Trials Commun.* 16, 100465. doi:10.1016/j.conctc.2019.100465

Garey, C., Lynn, J., Floreen Sabino, A., Hughes, A., and McAuliffe-Fogarty, A. (2020). Preeclampsia and Other Pregnancy Outcomes in Nulliparous Women

with Type 1 Diabetes: a Retrospective Survey. *Gynecol. Endocrinol.* 36, 982–985. doi:10.1080/09513590.2020.1749998

Gordin, D., Hiilesmaa, V., Fagerudd, J., Rönnback, M., Forsblom, C., Kaaja, R., et al. (2007). Pre-eclampsia but Not Pregnancy-Induced Hypertension Is a Risk Factor for Diabetic Nephropathy in Type 1 Diabetic Women. *Diabetologia* 50 (3), 516–522. doi:10.1007/s00125-006-0544-5

Gordin, D., Kaaja, R., Forsblom, C., Hiilesmaa, V., Teramo, K., and Groop, P.-H. (2013). Pre-eclampsia and Pregnancy-Induced Hypertension Are Associated with Severe Diabetic Retinopathy in Type 1 Diabetes Later in Life. *Acta Diabetol.* 50 (5), 781–787. doi:10.1007/s00592-012-0415-0

Gorst, C., Kwok, C. S., Aslam, S., Buchan, I., Kontopantelis, E., Myint, P. K., et al. (2015). Long-term Glycemic Variability and Risk of Adverse Outcomes: A Systematic Review and Meta-Analysis. *Diabetes Care* 38 (12), 2354–2369. doi:10.2337/dc15-1188

Gutaj, P., Sawicka-Gutaj, N., Brązert, M., and Wender-Ożegowska, E. (2015). Insulin Resistance in Pregnancy Complicated by Type 1 Diabetes Mellitus. Do We Know Enough? *Ginekol. Pol.* 86 (3), 219–223. doi:10.17772/gp/2065

Gutaj, P., Zawiejska, A., Mantaj, U., and Wender-Ożegowska, E. (2017). Determinants of Preeclampsia in Women with Type 1 Diabetes. *Acta Diabetol.* 54 (12), 1115–1121. doi:10.1007/s00592-017-1053-3

Guy, G. P., Leslie, K., Diaz Gomez, D., Forenc, K., Buck, E., Khalil, A., et al. (2020). Implementation of Routine First Trimester Combined Screening for Pre-eclampsia: a Clinical Effectiveness Study. *Bjog* 128, 149. doi:10.1111/1471-0528.16361

Haugen, F., Ranheim, T., Harsem, N. K., Lips, E., Staff, A. C., and Drevon, C. A. (2006). Increased Plasma Levels of Adipokines in Preeclampsia: Relationship to Placenta and Adipose Tissue Gene Expression. *Am. J. Physiology-Endocrinology Metabolism* 290 (2), E326–E333. doi:10.1152/ajpendo.00020.2005

Hsu, C. D., Tan, H. Y., Hong, S. F., Nickless, N. A., and Copel, J. A. (1996). Strategies for Reducing the Frequency of Preeclampsia in Pregnancies with Insulin-dependent Diabetes Mellitus. *Am. J. Perinatol.* 13 (5), 265–268. doi:10.1055/s-2007-994340

Inadera, H., Tachibana, S., Takasaki, I., Tatematsu, M., and Shimomura, A. (2010). Hyperglycemia Perturbs Biochemical Networks in Human Trophoblast BeWo Cells. *Endocr. J.* 57 (7), 567–577. doi:10.1507/endocrj.k10e-045

Inkster, M. E., Fahey, T. P., Donnan, P. T., Leese, G. P., Mires, G. J., and Murphy, D. J. (2006). Poor Glycated Haemoglobin Control and Adverse Pregnancy Outcomes in Type 1 and Type 2 Diabetes Mellitus: Systematic Review of Observational Studies. *BMC Pregnancy Childbirth* 6, 30. doi:10.1186/1471-2393-6-30

Kapustin, R. V., Kascheeva, T. K., Alekseenkova, E. N., and Shelaeva, E. V. (2020). Are the First-Trimester Levels of PAPP-A and Fb-hCG Predictors for Obstetrical Complications in Diabetic Pregnancy? *J. Maternal Fetal Neonatal Med.* 35, 1113. doi:10.1080/14767058.2020.1743658

Kelly, C. B., Wagner, C. L., Shary, J. R., Leyva, M. J., Yu, J. Y., Jenkins, A. J., et al. (2020). Vitamin D Metabolites and Binding Protein Predict Preeclampsia in Women with Type 1 Diabetes. *Nutrients* 12 (7), 2048. doi:10.3390/nu12072048

Kelly, C. B., Hookham, M. B., Yu, J. Y., Jenkins, A. J., Nankervis, A. J., Hanssen, K. F., et al. (2018). Subclinical First Trimester Renal Abnormalities Are Associated with Preeclampsia in Normoalbuminuric Women with Type 1 Diabetes. *Diabetes Care* 41 (1), 120–127. doi:10.2337/dc17-1635

Kelly, C. B., Hookham, M. B., Yu, J. Y., Lockhart, S. M., Du, M., Jenkins, A. J., et al. (2017). Circulating Adipokines Are Associated with Pre-eclampsia in Women with Type 1 Diabetes. *Diabetologia* 60 (12), 2514–2524. doi:10.1007/s00125-017-4415-z

Kelly, C. B., Yu, J. Y., Jenkins, A. J., Nankervis, A. J., Hanssen, K. F., Garg, S. K., et al. (2019). Haptoglobin Phenotype Modulates Lipoprotein-Associated Risk for Preeclampsia in Women with Type 1 Diabetes. *J. Clin. Endocrinol. Metab.* 104 (10), 4743–4755. doi:10.1210/jc.2019-00723

Kilpatrick, E. S., Rigby, A. S., and Atkin, S. L. (2007). Insulin Resistance, the Metabolic Syndrome, and Complication Risk in Type 1 Diabetes. *Diabetes Care* 30 (3), 707–712. doi:10.2337/dc06-1982

Kleinrouweler, C., Wiegerinck, M., Ris-Stalpers, C., Bossuyt, P., van der Post, J., von Dadelszen, P., et al. (2012). Accuracy of Circulating Placental Growth Factor, Vascular Endothelial Growth Factor, Soluble Fms-like Tyrosine Kinase 1 and Soluble Endoglin in the Prediction of Pre-eclampsia: a Systematic Review and Meta-Analysis. *Bjog* 119 (7), 778–787. doi:10.1111/j.1471-0528.2012.03311.x

Klemetti, M. M., Laivuori, H., Tikkanen, M., Nuutila, M., Hiilesmaa, V., and Teramo, K. (2016). White's Classification and Pregnancy Outcome in Women with Type 1 Diabetes: a Population-Based Cohort Study. *Diabetologia* 59 (1), 92–100. doi:10.1007/s00125-015-3787-1

Langlois, M. R., and Delanghe, J. R. (1996). Biological and Clinical Significance of Haptoglobin Polymorphism in Humans. *Clin. Chem.* 42 (10), 1589–1600. doi:10.1093/clinchem/42.10.1589

Lauszus, F. F., and Fuglsang, J. (2016). IGF-1 Is Associated with Fetal Growth and Preterm Delivery in Type 1 Diabetic Pregnancy. *Gynecol. Endocrinol.* 32 (6), 488–491. doi:10.3109/09513590.2015.1134477

Leguizamón, G., Trigubo, D., Pereira, J. I., Vera, M. F., and Fernández, J. A. (2015). Vascular Complications in the Diabetic Pregnancy. *Curr. Diab Rep.* 15 (4), 22. doi:10.1007/s11892-015-0586-5

Levine, R. J., Maynard, S. E., Qian, C., Lim, K.-H., England, L. J., Yu, K. F., et al. (2004). Circulating Angiogenic Factors and the Risk of Preeclampsia. *N. Engl. J. Med.* 350 (7), 672–683. doi:10.1056/nejmoa031884

Lövestam-Adrian, M., Agardh, C.-D., Åberg, A., and Agardh, E. (1997). Pre-eclampsia Is a Potent Risk Factor for Deterioration of Retinopathy during Pregnancy in Type 1 Diabetic Patients. *Diabet. Med.* 14 (12), 1059–1065. doi:10.1002/(sici)1096-9136(199712)14:12<1059::aid-dia505>3.0.co;2-8

Maresh, M. J. A., Holmes, V. A., Patterson, C. C., Young, I. S., Pearson, D. W. M., Walker, J. D., et al. (2015). Glycemic Targets in the Second and Third Trimester of Pregnancy for Women with Type 1 Diabetes. *Diabetes Care* 38 (1), 34–42. doi:10.2337/dc14-1755

Mathiesen, E. R. (2016). Pregnancy Outcomes in Women with Diabetes-Lessons Learned from Clinical Research: The 2015 Norbert Freinkel Award Lecture. *Diabetes Care* 39 (12), 2111–2117. doi:10.2337/dc16-1647

National Institue for Health and Care Excellence (NICE) (2019). *Hypertension in Pregnancy: Diagnosis and Management*. NICE.

National Institute for Health and Care Excellence (NICE) (2015). *Diabetes in Pregnancy: Management of Diabetes and its Complications from Preconception to the Postnatal Period*. NICE.

Nielsen, L. H., Jensen, B. L., Fuglsang, J., Andersen, L. L. T., Jensen, D. M., Jørgensen, J. S., et al. (2018). Urine Albumin Is a Superior Predictor of Preeclampsia Compared to Urine Plasminogen in Type I Diabetes Patients. *J. Am. Soc. Hypertens.* 12 (2), 97–107. doi:10.1016/j.jash.2017.12.003

Perea, V., Bertran, B., Bellart, J., Orois, A., Giménez, M., Conget, I., et al. (2019). Impaired Awareness of Hypoglycaemia: A New Risk Factor for Adverse Pregnancy Outcomes in Type 1 Diabetes. *Diabetes Metab. Res. Rev.* 35 (7), e3176. doi:10.1002/dmrr.3176

Poniedziałek-Czajkowska, E., and Mierzyński, R. (2021). Could Vitamin D Be Effective in Prevention of Preeclampsia? *Nutrients* 13 (11), 3854. doi:10.3390/nu13113854

Poon, L. C. Y., Kametas, N. A., Maiz, N., Akolekar, R., and Nicolaides, K. H. (2009). First-Trimester Prediction of Hypertensive Disorders in Pregnancy. *Hypertension* 53, 812–818. doi:10.1161/hypertensionaha.108.127977

Rolnik, D. L., O'Gorman, N., Roberge, S., Bujold, E., Hyett, J., Uzan, S., et al. (2017). Early Screening and Prevention of Preterm Pre-eclampsia with Aspirin: Time for Clinical Implementation. *Ultrasound Obstet. Gynecol.* 50 (5), 551–556. doi:10.1002/uog.18899

Rolnik, D. L., Wright, D., Poon, L. C., O'Gorman, N., Syngelaki, A., de Paco Matallana, C., et al. (2017). Aspirin versus Placebo in Pregnancies at High Risk for Preterm Preeclampsia. *N. Engl. J. Med.* 377, 613–622. doi:10.1056/nejmoa1704559

Rosenn, B., Miodovnik, M., Kranias, G., Khoury, J., Combs, C. A., Mimouni, F., et al. (1992). Progression of Diabetic Retinopathy in Pregnancy: Association with Hypertension in Pregnancy. *Am. J. Obstetrics Gynecol.* 166 (4), 1214–1218. doi:10.1016/s0002-9378(11)90608-5

Salzer, L., Tenenbaum-Gavish, K., and Hod, M. (2015). Metabolic Disorder of Pregnancy (Understanding Pathophysiology of Diabetes and Preeclampsia). *Best Pract. Res. Clin. Obstetrics Gynaecol.* 29 (3), 328–338. doi:10.1016/j.bpobgyn.2014.09.008

Say, L., Chou, D., Gemmill, A., Tunçalp, Ö., Moller, A.-B., Daniels, J., et al. (2014). Global Causes of Maternal Death: a WHO Systematic Analysis. *Lancet Glob. Health* 2 (6), e323–e333. doi:10.1016/s2214-109x(14)70227-x

Serra, B., Mendoza, M., Scazzocchio, E., Meler, E., Nolla, M., Sabrià, E., et al. (2020). A New Model for Screening for Early-Onset Preeclampsia. *Am. J. Obstet. Gynecol.* 222 (6), 608. doi:10.1016/j.ajog.2020.01.020

Thilaganathan, B., and Kalafat, E. (2019). Cardiovascular System in Preeclampsia and beyond. *Hypertension* 73, 522–531. doi:10.1161/hypertensionaha.118.11191

Tsiakkas, A., Duvdevani, N., Wright, A., Wright, D., and Nicolaides, K. H. (2015). Serum Placental Growth Factor in the Three Trimesters of Pregnancy: Effects of Maternal Characteristics and Medical History. *Ultrasound Obstet. Gynecol.* 45 (5), 591–598. doi:10.1002/uog.14811

Vestgaard, M., Secher, A. L., Ringholm, L., Jensen, J.-E. B., Damm, P., and Mathiesen, E. R. (2017). Vitamin D Insufficiency, Preterm Delivery and Preeclampsia in Women with Type 1 Diabetes - an Observational Study. *Acta Obstet. Gynecol. Scand.* 96 (10), 1197–1204. doi:10.1111/aogs.13180

Vestgaard, M., Sommer, M. C., Ringholm, L., Damm, P., and Mathiesen, E. R. (2017). Prediction of Preeclampsia in Type 1 Diabetes in Early Pregnancy by Clinical Predictors: a Systematic Review. *J. Maternal-Fetal Neonatal Med.* 31 (14), 1933–1939. doi:10.1080/14767058.2017.1331429

Villa, P., Kajantie, E., Räikkönen, K., Pesonen, A.-K., Hämäläinen, E., Vainio, M., et al. (2013). Aspirin in the Prevention of Pre-eclampsia in High-Risk Women: a Randomised Placebo-Controlled PREDO Trial and a Meta-Analysis of Randomised Trials. *Bjog* 120 (1), 64–74. doi:10.1111/j.1471-0528.2012.03493.x

Weissgerber, T., Gandley, R., Roberts, J., Patterson, C., Holmes, V., Young, I., et al. (2013). Haptoglobin Phenotype, Pre-eclampsia, and Response to Supplementation with Vitamins C and E in Pregnant Women with Type-1 Diabetes. *Bjog* 120 (10), 1192–1199. doi:10.1111/1471-0528.12288

Weissgerber, T. L., and Mudd, L. M. (2015). Preeclampsia and Diabetes. *Curr. Diab Rep.* 15 (3), 9. doi:10.1007/s11892-015-0579-4

Wender-Ozegowska, E., Zawiejska, A., Michalowska-Wender, G., Iciek, R., Wender, M., and Brazert, J. (2011). Metabolic Syndrome in Type 1 Diabetes Mellitus. Does it Have Any Impact on the Course of Pregnancy? *J. Physiol. Pharmacol.* 62 (5), 567–573.

White, P. (1949). Pregnancy Complicating Diabetes. *Am. J. Med.* 7 (5), 609–616. doi:10.1016/0002-9343(49)90382-4

Wolf, M., Sandler, L., Muñoz, K., Hsu, K., Ecker, J. L., and Thadhani, R. (2002). First Trimester Insulin Resistance and Subsequent Preeclampsia: a Prospective Study. *J. Clin. Endocrinol. Metab.* 87 (4), 1563–1568. doi:10.1210/jcem.87.4.8405

Wotherspoon, A. C., Holmes, V. A., Patterson, C. C., Young, I. S., and McCance, D. (2016). Serum FABP4 Predicts Preeclampsia in Pregnant Women with Type 1 Diabetes. *Diabetes* 65 (Suppl. 1), A352. doi:10.2337/dc16-0803

Wotherspoon, A. C., Young, I. S., McCance, D. R., and Holmes, V. A. (2016). Evaluation of Biomarkers for the Prediction of Pre-eclampsia in Women with Type 1 Diabetes Mellitus: A Systematic Review. *J. Diabetes its Complicat.* 30 (5), 958–966. doi:10.1016/j.jdiacomp.2016.02.001

Xiang, L.-J., Wang, Y., Lu, G.-Y., and Huang, Q. (2018). Association of the Presence of Microangiopathy with Adverse Pregnancy Outcome in Type 1 Diabetes: A Meta-Analysis. *Taiwan. J. Obstetrics Gynecol.* 57 (5), 659–664. doi:10.1016/j.tjog.2018.08.008

Zen, M., Padmanabhan, S., Zhang, K., Kirby, A., Cheung, N. W., Lee, V. W., et al. (2019). Urinary and Serum Angiogenic Markers in Women with Preexisting Diabetes during Pregnancy and Their Role in Preeclampsia Prediction. *Diabetes Care* 43 (1), 67–73. doi:10.2337/dc19-0967

Conflict of Interest: The authors declare that the research was conducted in the absence of any commercial or financial relationships that could be construed as a potential conflict of interest.

The handling editor declared a past co-authorship with several of the authors, KAE and CW.

Publisher's Note: All claims expressed in this article are solely those of the authors and do not necessarily represent those of their affiliated organizations, or those of the publisher, the editors, and the reviewers. Any product that may be evaluated in this article, or claim that may be made by its manufacturer, is not guaranteed or endorsed by the publisher.

Advantages of publishing in Frontiers

OPEN ACCESS
Articles are free to read for greatest visibility and readership

FAST PUBLICATION
Around 90 days from submission to decision

HIGH QUALITY PEER-REVIEW
Rigorous, collaborative, and constructive peer-review

TRANSPARENT PEER-REVIEW
Editors and reviewers acknowledged by name on published articles

Frontiers
Avenue du Tribunal-Fédéral 34
1005 Lausanne | Switzerland

Visit us: www.frontiersin.org
Contact us: frontiersin.org/about/contact

REPRODUCIBILITY OF RESEARCH
Support open data and methods to enhance research reproducibility

DIGITAL PUBLISHING
Articles designed for optimal readership across devices

FOLLOW US
@frontiersin

IMPACT METRICS
Advanced article metrics track visibility across digital media

EXTENSIVE PROMOTION
Marketing and promotion of impactful research

LOOP RESEARCH NETWORK
Our network increases your article's readership